VARIABILITY OF THE HORIZONTAL -TO-VERTICAL SPECTRAL RATIO (HVSR) METHOD IN URBAN AREAS

A Thesis

Presented to the Faculty of the Graduate School

at the University of Missouri-Columbia

In Partial Fulfillment

of the Requirements for the Degree

Master of Science in Civil Engineering

---

by

Braydon Smith

Dr. Brent Rosenblad P.E., Thesis Supervisor

December 2024

The undersigned, appointed by the dean of the Graduate School, have examined the thesis entitled

VARIABILITY OF THE HORIZONTAL -TO-VERTICAL SPECTRAL RATIO (HVSR) METHOD IN URBAN AREAS

presented by Braydon Smith

a candidate for the degree of Master of Science and Civil Engineering,

and hereby certify that, in their opinion, it is worthy of acceptance.

Professor Brent L. Rosenblad, P.E.

Professor John J. Bowders, P.E.

Professor J. Erik Loehr, P.E.

ACKNOWLEDGEMENTS

First and foremost, I would like to thank God and my entire family for the family for their unwavering love and support throughout my academic career. Their encouragement during the most challenging moments has been a constant source of strength, and I am deeply grateful for their belief in me. I couldn't have accomplished this feat without them by my side.

I cannot thank my advisor, Dr. Rosenblad, enough for everything he has done for me throughout my academic career. He is the one that fueled my interest in geotechnical engineering and continued to let it prosper. I would also like to thank him for believing I had what it took to complete a master's degree and this thesis. I would not have reached these accomplishments without his unwavering guidance, insightful feedback, and continuous encouragement throughout this research. His expertise and support were invaluable, and I am truly grateful for his patience and mentorship.

I would also like to extend my gratitude to the members of my thesis committee, Dr. Loehr and Dr. Bowders, for their time, constructive critiques, and thoughtful suggestions that significantly improved the quality of this thesis.

A special thank you to Dr. Fidalgo for the insight and support through the graduate school process, Dr. Salim for getting me interested in undergraduate engineering research, and all the staff and faculty at the University of Missouri-Columbia, particularly those in the Civil Engineering Department, for providing the resources and guidance completion of my undergraduate and master's degree. The opportunities to learn and collaborate with such dedicated professionals have been truly inspiring.

Lastly, I would like to thank my fellow graduate students, colleagues, and friends for their fellowship and support throughout this process. The numerous discussions, brainstorming sessions, and collaborative efforts made this journey not only more enjoyable but also more enriching.

This thesis is a testament to the collective efforts and support of all those mentioned, and I dedicate this work to them.

TABLE OF CONTENTS

TABLE OF FIGURES

TABLE OF TABLES

ABSTRACT

The Horizontal-to-Vertical Spectral Ratio (HVSR) method is widely employed in geotechnical investigations due to its non-intrusive approach for determining subsurface characteristics such as sediment thickness, bedrock depth, and seismic site response. The primary objective of this paper is to provide both quantitative and qualitative assessments of four potential factors influencing HVSR variability in urban environments: (1) in-situ instrumentation surface coupling (concrete vs. grass), (2) the effect of strong, nearby noise sources on in-situ instrumentation, (3) proximity to buildings, and (4) the influence of time-of-day with respect to building proximity. A total of 126 HVSR measurements across 16 locations at the University of Missouri-Columbia were analyzed, with an emphasis on influences on HVSR variability in urban environments.

The results show minimal variability between HVSR measurements conducted simultaneously on concrete and grass surfaces. This finding was in agreement with commonly used HVSR acquisition guidelines but contradicted more recent guidelines provided by an HVSR equipment manufacturer. Furthermore, data indicated that concrete surfaces exhibited greater variability in noisy environments, such as construction zones, possibly due to reduced attenuation of construction vibrations, whereas grass surfaces yielded more consistent measurements. Proximity to buildings was identified as a significant factor contributing to variability, with measurements taken within 50 feet of buildings typically producing low-quality HVSR results, likely due to building-induced vibrations. Time-of-day effects were found to be less significant, with ambient noise levels having a greater impact on measurement quality than noise from building occupancy itself.

HVSR frequency peaks identified from manual inspection methods improved result accuracy when compared to automated picking of the highest HVSR peak.

The study highlights the importance of considering site-specific conditions and incorporating human oversight in HVSR analysis, particularly in urban environments. Key findings include: (1) concrete is a reliable surface for HVSR measurements, indicating that data acquisition does not need to be exclusively conducted on grass, (2) acquisition near strong construction noise sources can yield accurate HVSR results, and does not necessarily need to be avoided, (3) maintaining a sufficient distance from buildings (preferably >50 ft) will reduce variability in HVSR results (4) manual identification of HVSR peaks can provide improved results over automated picks in difficult environments, and (5) measurements near building sites are best conducted during times when ambient noise levels are high. These insights contribute to the refinement of HVSR guidelines and enhance its application in urban geotechnical and geophysical investigations.

This study also contributes to the refinement of HVSR guidelines, offering recommendations for mitigating variability caused by urban factors and suggesting avenues for future research, including exploring the effects of building height, subsurface complexity, and azimuthal variability on HVSR measurements.

1. INTRODUCTION

1.1 Background

In recent decades, the introduction of non-invasive geophysical techniques like seismic refraction, electrical resistivity, and Ground Penetrating Radar (GPR) have enabled the investigation of subsurface conditions without soil disturbance in geotechnical engineering. These advancements in technology provide a more cost-effective means of assessing ground conditions, especially in challenging environments where boreholes or test pits might be impractical.

One such non-intrusive method, the Horizontal-to-Vertical Spectral Ratio (HVSR) method, has recently gained popularity throughout many different industries (e.g., engineering, geology, archeology) due to the method's lower costs than traditional methods (e.g., Standard Penetration Test (SPT), Cone Penetration Test (CPT), etc.), and its applicability in a wide range of terrains (e.g., remote and/or isolated locations, urban environments, etc.). The lower cost of the HVSR method is attributed to the minimal amount of equipment and ease of mobilization.

The HVSR method is a single-station geophysical technique utilizing a three-component seismometer without an active source to measure ambient ground motions in the horizontal and vertical directions. The HVSR method relies on the natural ambient vibrations of the Earth, at low frequencies (< 1Hz) and anthropic (human-made) vibrations at higher frequencies (> 1 Hz). The primary output of the HVSR method is an estimate of the resonance frequency of soil layers over rock. This can then be used to infer the thickness

of soil overlying bedrock, depth to bedrock, earthquake hazard, or assist in estimating the shear wave velocity of the subsurface.

Most studies implementing the HVSR method follow guidelines produced by **S**ite **E**ffect**S** assessment using **AM**bient **E**xcitations (SESAME, 2005). However, manufacturers of common HVSR equipment (e.g., the Tromino device used in this study, produced by MoHo Science and Technology) have established separate guidelines (MoHo S.R.L, 2020) based on a more recent publication (e.g., Chatelain et al., 2008) than the SESAME (2005) guidelines. Other studies have also proposed recommendations for the HVSR method (e.g., Koller et al., 2004; Castellaro and Mulargia, 2009; Molnar et al., 2022), which tend to align more closely with either the SESAME (2005) or MoHo S.R.L (2020) guidelines. In some respects, the guidelines and literature disagree with regard to recommendations for implementation of the HVSR method and some recommendations appear to be based on limited studies. A recent study by Chi (2022) demonstrated a great deal of variability in HVSR measurements at some locations. These findings highlight a need to better understand the factors contributing to variability in HVSR measurements.

1.2 Objective

The HVSR method is a powerful, non-invasive technique widely used in urban environments due to its non-invasive nature, ease of investigation, and relatively low cost. Despite its advantages, the method has limitations, as results can exhibit significant inconsistencies. Consequently, further research is necessary to refine and expand the guidelines for implementing the HVSR method in urban settings.

The primary objective of this paper is to provide qualitative and quantitative assessments of four potential influences on HVSR variability in urban environments

1) *In-situ instrumentation coupling through concrete versus grass*

SESAME (2005) guidelines suggest that data acquisition on concrete will not affect the HVSR results, which is in agreement with Koller et al. (2004) and Chatelain et al. (2008), while MoHo S.R.L (2020) guidelines advise to avoid HVSR acquisition on concrete, which is supported by Castellaro and Mulargia (2009) and Molnar et al. (2022). Research herein will assess these contradictory guidelines and provide a clear recommendation.

2) *In-situ instrumentation coupling through concrete versus grass with strong, nearby noise influence (i.e., construction activity)*

SESAME (2005) and MoHo S.R.L (2020) guidelines recommend that data acquisition be performed in a quiet environment (e.g., in the absence of construction machines, industrial machines, pumps, generators, etc.). These recommendations agree with literature from Koller et al. (2004), Chatelain et al. (2008), and Mihaylov et al. (2016). The study herein will further investigate these recommendations and their validity regarding varying in-situ instrument coupling conditions.

3) *Influence of proximity of HVSR measurements to buildings*

SESAME (2005) advised that recordings near structures should be avoided due to the strong influence the structures pose at lower frequencies, in agreement with Gallipoli et al. (2004) and Chatelain et al. (2008)). MoHo S.R.L (2020) does not provide any recommendations. The study herein will attempt to validate this recommendation by SESAME (2005) and provide additional insight in the effect of building offset distance on HVSR variability.

4) *Influence of time-of-day with building proximity*

Neither SESAME (2005) nor MoHo S.R.L (2020) provide recommendations on how time-of-day in conjunction with building proximity affect the HVSR method. Literature has observed that times of day can increase the amplitude of the HVSR curves and affect HVSR results (e.g., Guillier et al., 2007; Panou et al., 2005). It was hypothesized in this study that the quality of the HVSR measurement could be affected by the time-of-day that the measurement was performed, due to the effect of noise from building occupancy. The study herein will attempt to provide recommendations for the best time of day to acquire HVSR data if data acquisition must be conducted near a building.

1.3 Scope of Work

The following tasks were performed to complete the investigation herein: (1) conducted a literature review to determine current recommended testing procedures for the HVSR method and device guidelines, (2) identified testing sites (16 sites) to address the objectives of this study, (3) collected ambient noise data (126 acquisitions) at the selected sites, (4) processed the ambient noise data using the HVSR method, (5) and assessed the variability in the frequency where the maximum peak in HVSR is observed, termed the HVSR resonance frequency ($HVSR_{Res}$) using repeat measurements, (6) presented a discussion of assessment findings, and (7) provided recommendations based on the conclusions from the study.

1.4 Layout of the Thesis

This thesis comprises of seven chapters. Chapter 1 contains the introduction to the project. Chapter 2 contains the background and motivation for this investigation. Chapter 3 provides details on the collection and analysis of the ambient noise data, while the sites selected for the study are outlined in Chapter 4. Chapter 5 contains the results from the

analysis of the data due to the influence of in-situ coupling (concrete versus grass), the influence of in-situ coupling in the presence of a strong, near noise source (construction), the effect of the proximity to buildings, and the effect of the time-of-day of the measurement with building proximity. Presented in Chapter 6 is a discussion of the results. An overall summary of the findings, along with conclusions and recommendations, are included in Chapter 7.

2. BACKGROUND

2.1 Introduction

Presented in this chapter are brief overview of the HVSR method, followed by applications of the HVSR methods found throughout the literature. Finally, studies investigating HVSR variability and HVSR method guidelines are reviewed.

2.2 Overview of HVSR Method

The HVSR method, first introduced by Nogoshi and Igarashi (1971) and later advanced by Nakamura (1989), involves recording ambient ground vibrations with a three-component seismometer over specified durations, typically several minutes. These vibrations include low-frequency signals (< 1 Hz) mainly from naturally occurring sources, such as ocean waves and wind, and higher frequencies (> 1 Hz) typically due to human activities.

During HVSR processing, the recorded noise is segmented into specified time windows and filtered (Figure 1), before being transformed from the time to the frequency domain using the Fast Fourier Transform (FFT) to produce amplitude spectra for each of the three measurement directions, one vertical and two horizontal (Figure 2). In each amplitude spectra window, corresponding to the time record, the horizontal spectra (H) are divided by the vertical spectrum (V), resulting in two directional HVSR plots (Figure 3), which are later averaged from all individual windows to create a single representative average HVSR curve (Figure 4).

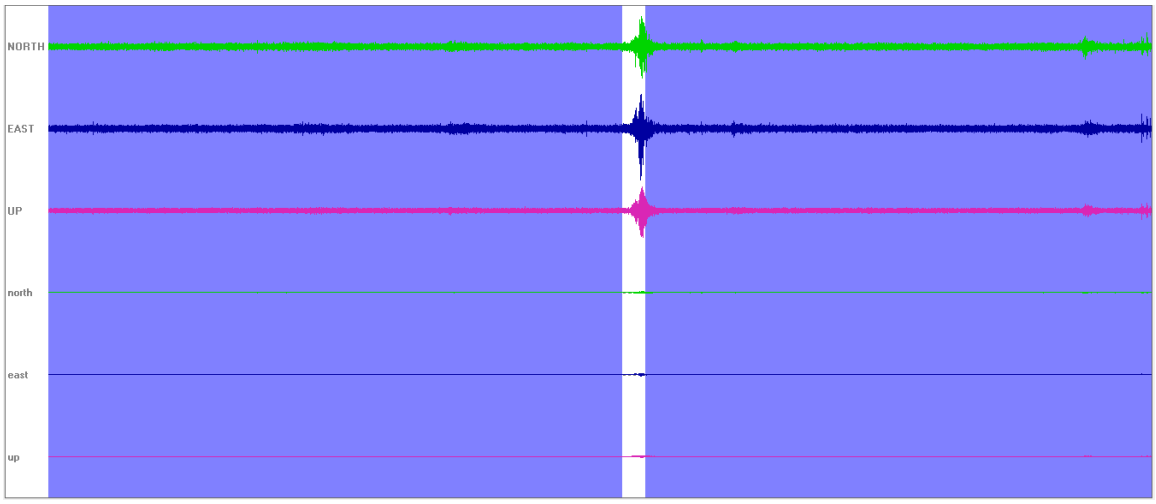

Figure 1: The HVSR ambient noise record showing the window selection and filtering of time record for one site (MIZ MiddleQuad Test 4 on Grass site). The unshaded portion of the time records indicates a time window that has been filtered out and omitted from the analysis.

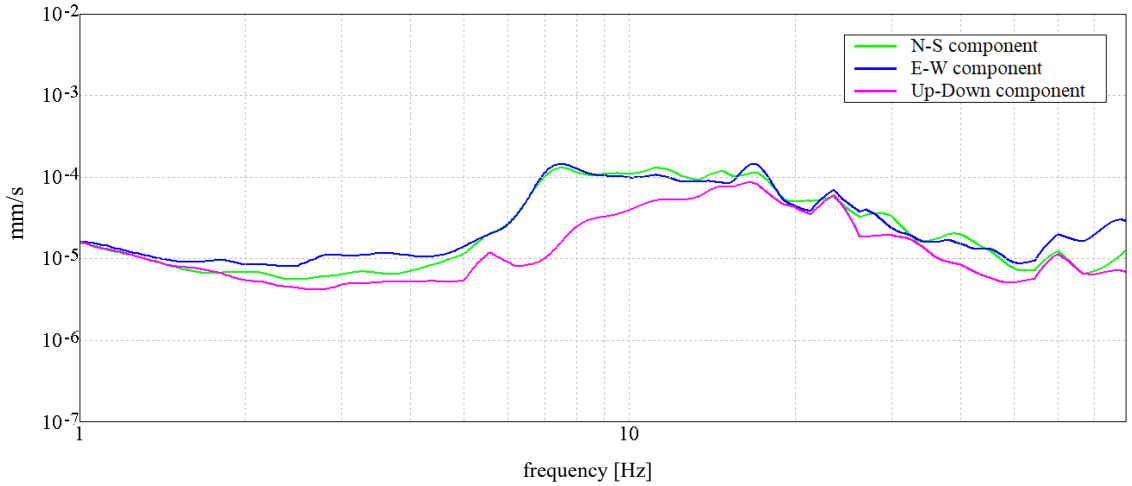

Figure 2: HVSR amplitude spectra plots produced by performing an FFT on the time records (MIZ MiddleQuad Test 4 on Grass site). The green line indicates the H spectrum from the instrumentation North orientation, the blue line indicates the H spectrum collected 90° from the North orientation, and the pink line indicates the V spectrum.

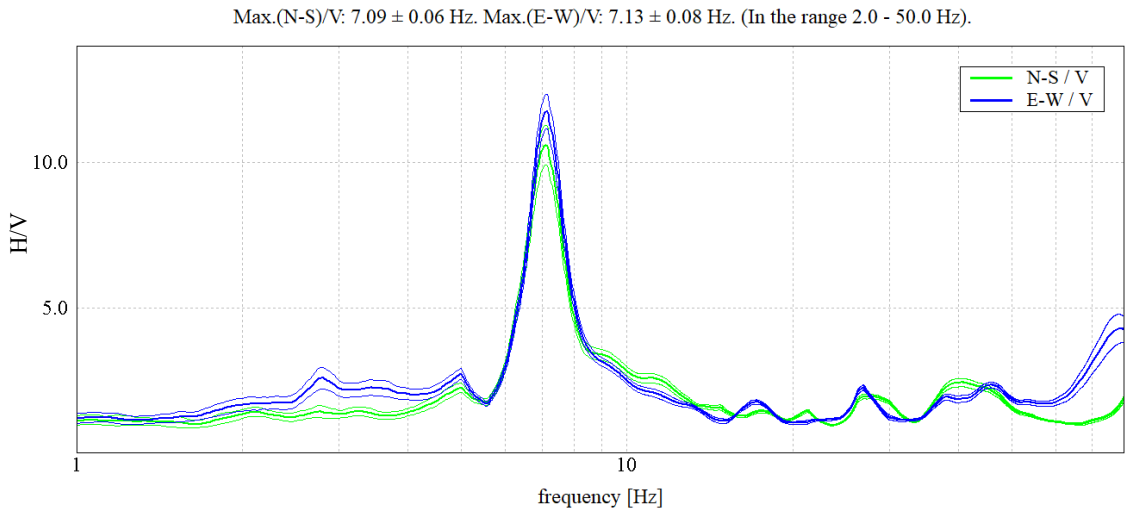

Figure 3: Two directional HVSR plot produced by taking the H spectra and dividing the V spectra. North-South (N-S) plot is represented by the green line and an East-West (E-W) plot is represented by the blue line (MIZ MiddleQuad Test 4 on Grass site).

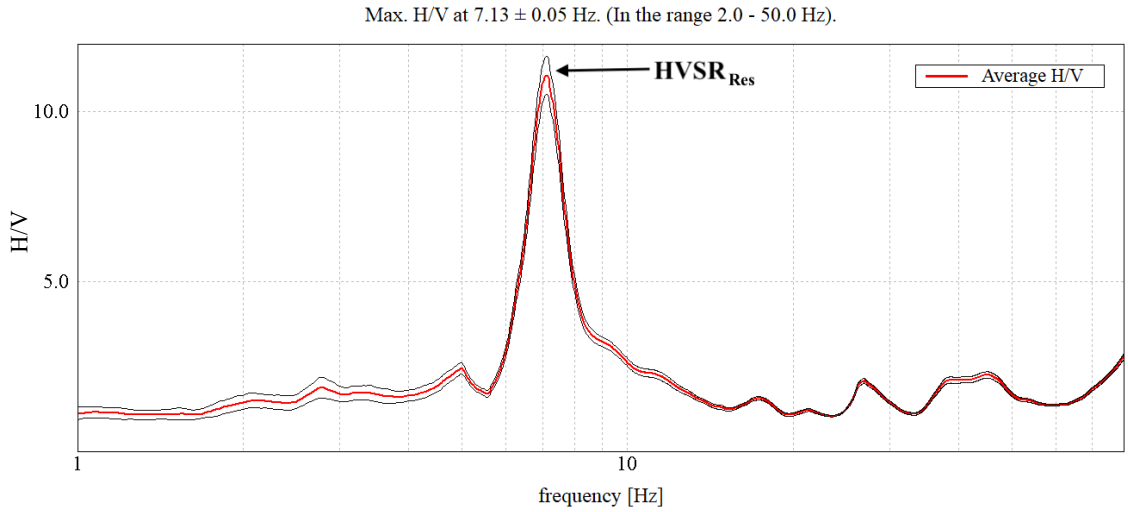

Figure 4: Average HVSR plot (red) produced by averaging the two directional HVSR plots with the peak frequency value called out as HVSRRes. (MIZ MiddleQuad Test 4 on Grass site).

The HVSR curve provides insights into site resonance characteristics. Nakamura's approach (1989) assumes that by dividing the horizontal spectrum (H) by the vertical spectrum (V), the influence of source effect is largely canceled out, allowing for the site's resonant frequency ($HVSR_{Res}$) to be identified (Figure 4). For sites with a consistent

sediment layer over bedrock (Lermo and Chavez-Garcia, 1993), the $HVSR_{Res}$ is related to the shear wave velocity of the soil layer (V_s) as:

$$HVSR_{Res} = \frac{V_s}{4H} \tag{2.1}$$

where $HVSR_{Res}$ is the resonant frequency of the vertically propagating shear wave, V_s is the velocity of the sedimentary layer, and H is the thickness of the layer.

There are two explanations for the origin of the $HVSR_{Res}$. The $HVSR_{Res}$ can be generated by the influence of surface waves or from vertically propagating shear waves. Surface waves consist of horizontal and vertical components. These components produce an elliptical wave (Rayleigh wave), that propagates near the ground's surface. Rayleigh waves are strongest at the surface and degrade with depth. When an impedance contrast is encountered (e.g., soil over bedrock), the vertical wave component diminishes near the shear wave resonance frequency, resulting in a peak on the HVSR plot (e.g., Goetz and Rosenblad, 2010).

The second explanation for the $HVSR_{Res}$ are body waves (comprised of compression and shear waves). When these waves reach HVSR instrumentation, the horizontal component primarily reflects shear waves (SH), while the vertical component mainly reflects compression waves (P), resulting in a $HVSR_{Res}$ computed directly from the measured shear wave resonance (e.g., Goetz and Rosenblad, 2010). In shallow-depth analyses, the HVSR measurements typically contain both surface and body wave energy, stemming from surface-level human activities, however the origin of the peak is mostly due to the surface wave ellipticity, as described above.

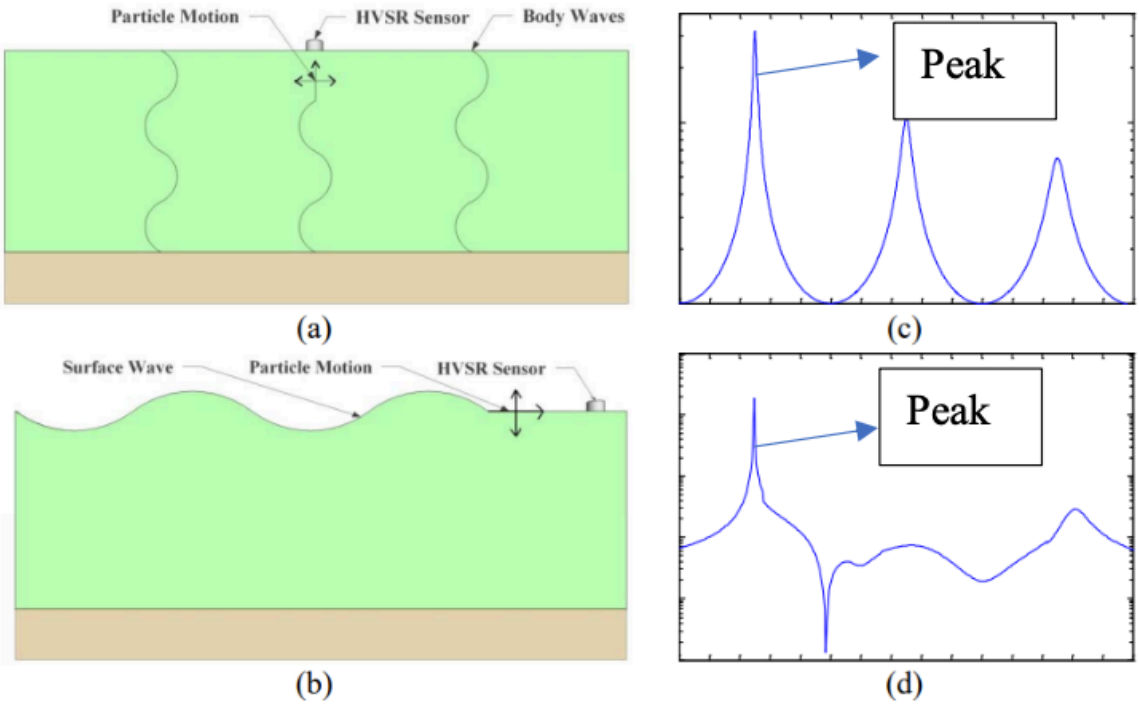

Figure 5: Two interpretations of the HVSR method in terms of body waves (a) and surface waves (b) showing the transfer function for 1D SH wave propagation (c) and the HVSR ratio for Rayleigh wave propagation (d) (Goetz and Rosenblad, 2010)

2.3 Application Studies of the HVSR Method

Many applications of the HVSR method are presented in both geotechnical and geological literature. One common application is for earthquake microzonation (e.g., Fäh et al., 1997; Zara et al., 1999; Lee et al., 2001; Gallipoli et al., 2011; Stanko et al., 2019; Ji et al., 2017; Harinaravan and Kumar, 2017; Putti and Satyam, 2020). Earthquake microzonation involves the assessment of sites' seismic hazard responses based on local site effects and site characterization. Determining $HVSR_{Res}$ provide insight into how variability in subsurface conditions affects ground motions.

Studies have also shown that the $HVSR_{Res}$ observed from an HVSR plot has a direct relationship to the thickness of the sedimentary layer and depth to bedrock as indicated in Section 2.2 (e.g., Ibs-von Seht and Wohlenberg, 1999; Delgado et al., 2000; Parolai et al.,

2002; Motamed et al., 2007; D'Amico et al., 2008; Lane et al., 2008; Gosar and Lenart, 2010; Paudyal et al., 2013; Bignardi, 2017; Liang et al., 2018; Bottelin et al., 2019; Dronefield et al., 2019; Chi, 2022). In addition to determining the sedimentary layer thickness, similar methods have been studied to identify landslide failure surfaces (Gallipoli et al., 2000; Méric et al., 2007; Pazzi et al., 2017).

Studies have shown that the HVSR method is not only valuable in determining site frequencies but also in determining average shear wave velocities (e.g., Chen et al., 1996; Bodin et al. 2001; Goetz and Rosenblad, 2010). Additional studies have shown the use of the HVSR method in fault detection (e.g., Khalili and Mirzakurdeh, 2019), oil seepage exploration (e.g., Fatma et al., 2019), coal basin exploration (e.g., Dronfields et al., 2019) , and mapping of archaeological sites (e.g., Abu Zeid et al. 2017). Based on the diverse and widespread approach of HVSR, it is important to better understand sources of variability in the HVSR method.

2.4 Variability Studies of the HVSR Method

Several studies have investigated the HVSR method to better understand the causes behind HVSR variability. In some cases, instrumentation effects (e.g., Guillier et al., 2008) were shown to be the source of the variability. Azimuthal effects (i.e., waves coming from different directions) have also been identified as a source of variability in HVSR measurements. The azimuthal studies have shown that nearby faults (e.g., Matsushima et al., 2014), lateral bedrock variability (Vantasseel et al., 2018), and acquisition on the edge of a basin (Uebayashi et al., 2012; Theodoulidis et al., 2018) are just some of the ways azimuthal variability arises. Seasonal variations in the environment have also been studied as a cause of HVSR variability (Bahavar and North, 2002; Panou et al., 2005). Panou et al.

(2005) observed seasonal changes of very low frequencies, typically < 0.4 Hz. In the assessment of the study presented here, seasonal variability is not an issue due to the much higher frequencies. However, variability caused by anthropical effects will be explored in more detail.

Chatelain et al. (2008) studied the variability that was observed when HVSR data were collected on concrete (versus soil). The study consisted of eleven tests that were all performed on concrete. Interpretation of the data concluded that recording on concrete does not dramatically change the HVSR results. Occasionally, marginal influences were observed for frequencies higher than 10 Hz. The study also concluded that concrete acted as a filter, filtering the amplitude of the HVSR curve and not the frequency. This outcome was also observed by Mucciarelli (1998) and Koller et al. (2004).

The work of Castellaro and Mulargia (2009) contradicted the findings of Chatelain et al. (2008). Castellaro and Mulargia (2009) studied six tests analyzed by the HVSR method. Results from all cases show the HVSR < 1. These findings indicate that the V component is larger than the H components resulting in inaccurate data. These findings lead to Castellaro and Mulargia's (2009) recommendation that HVSR measurements on concrete should always be avoided, which was confirmed by Molar (2022). Importantly, the study states that if HVSR measurements on concrete cannot be avoided, the HVSR curves should be analyzed in conjunction with the single spectral components. Natural (i.e., correct) and artificial (i.e., erroneous) HVSR peaks can often be distinguished by a clear 'eye-shape' when the H and V plots are overlaid. A natural HVSR peak is a peak that is strata based and an artificial HVSR peak is a peak that is related to vibrations and other occurrences not related to subsurface conditions. A natural $HVSR_{Res}$ is produced when the

V component diverges from the H components, forming the 'eye-shape,' as indicated by the solid circle in Figure 6. Figure 6 also shows an example of when artificial peaks occur, indicated by the dashed circles. Artificial peaks are created when the H and V components increase together creating peaks of different amplitudes.

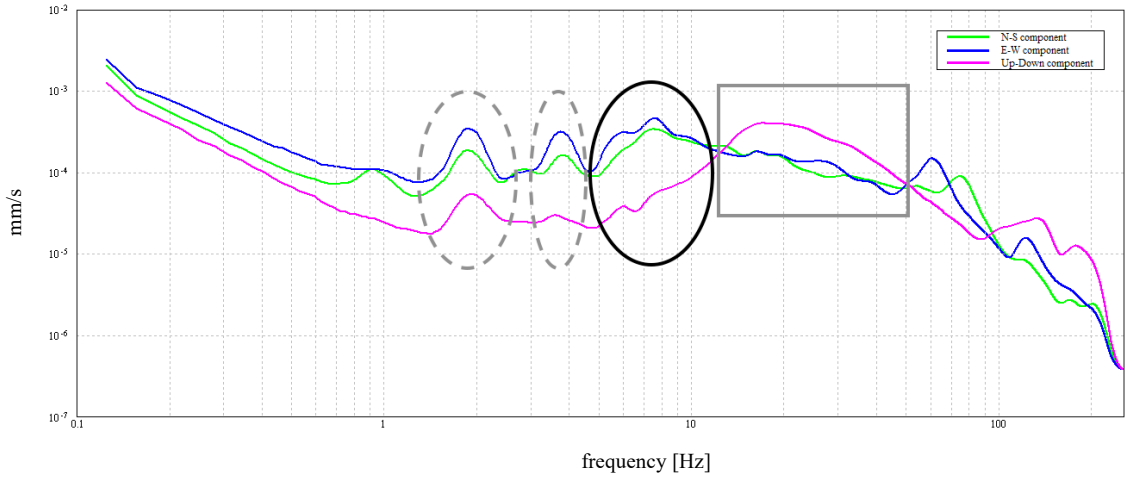

Figure 6: Spectral Component Plots (MIZ Quad Site 1 Test 1 on Grass site). The blue and green component lines indicate the H components, and the pink component line indicates the V component. The dashed circles indicate where artificial peaks are observed due to the H and V components increasing to a peak with different amplitudes. The dark solid circle indicates a natural peak due to the 'eye-shape.' The light square indicates where HVSR < 1.

Strong noise sources can also cause HVSR measurement variability. It is suggested throughout the literature to avoid performing HVSR measurements in the presence of strong noise sources. Koller et al., (2004) suggest avoiding acquiring HVSR measurements around operating machinery and vehicles that are ideal but stationary. Chatelain et al., (2008) and Mihaylov et al., (2016) agree with this recommendation. However, Chatelain et al., (2008) also suggests that if the duration of the strong noise sources is small compared to the total time record, the strong noise influences can be filtered out during data interpretation, resulting in no influence in the results.

The effect of proximity to buildings was also investigated by Chatelain et al. (2008). The study interpreted 13 measurements taken at different distances from a building. Strong changes in the measurements were reported for locations close to the building in the 5-10 Hz range. A range of testing location distances was not provided in the study, and due to the small amount of data, no concluding statement was provided.

Gallipoli et al. (2004) observed that tall buildings, defined as those with 20 or more stories, can affect ground measurements up to a horizontal distance equal to twice the building's height. In contrast, Mucciarelli et al. (1997) found that the influence of structures diminishes significantly at a distance equal to the height of the building. Guéguen et al. (2002) further suggested that the impact of such structures becomes negligible at a horizontal distance of ten times the length of the building's foundation.

Aside from the influence of nearby buildings, anthropic sources can cause variability in the HVSR results. For example, studies have shown that anthropic sources cause variability (Bahavar and North, 2002; Guillier et al., 2007; Panou et al., 2005). These studies found that measurements taken during the day generally led to an increase in the amplitude of the HVSR curves by several points, and in certain cases, this shift contributed to a change in the $HVSR_{Res}$.

2.5 . HVSR Data Collection Recommendations

SESAME (2005) provides standard guidelines for the HVSR method, which are often followed and referenced by many studies. The manufacturer (MoHo S.R.L) produces a widely used device (Tromino) for HVSR acquisition. The Tromino was the device used for HVSR data acquisition in this study. MoHo S.R.L (2020) provides guidelines that differ from some of the recommendations outlined in SESAME (2005). Both SESAME (2005)

and MoHo S.R.L (2020) offer guidelines for applying the HVSR method, covering aspects such as data collection (e.g., recording duration), data processing (e.g., window size, smoothing), and interpretation. The current study adhered to these guidelines for data collection, processing, and interpretation, which were consistent across both sources. Additionally, SESAME (2005) and MoHo S.R.L (2020) provide further recommendations for data collection, including advice on in-situ soil-sensor coupling, avoidance of noise disturbances, and presence of nearby structures, which is the primary focus of the study presented.

SESAME (2005) and TROMINO BLU User's Manual (MoHo S.R.L, 2020) are in agreement with each other for guidelines that involve noise disturbances. SESAME (2005) recommends avoiding measurements near construction machines, industrial machines, pumps, generators, etc. These can produce artificial HVSR peaks because of their natural operation frequencies. MoHo S.R.L recommendations do not go into detail, but it is recommended that data acquisition be performed in a quiet environment.

In-situ sensor coupling recommendations show a conflict between the SESAME (2005) and the MoHo S.R.L (2020) recommendations. SEASME (2005) reports that HVSR data acquisition on concrete will not affect the HVSR results in the frequency range typically of interest. It is noted that some perturbances may occur in the 7 – 8 Hz range, but do not affect the HVSR curve. Contradictory to SESAME (2005), MoHo S.R.L (2020) recommends that measurements should not take place on pavements (e.g., asphalt, concrete, masonry, etc.) as these couplings may affect the HVSR curves.

Additionally, SESAME (2005) advised that recording near structures be avoided due to the strong influence the structures pose at lower frequencies. These influences could

result in artificial peaks in HVSR curves because of the natural frequency of the building. MoHo S.R.L (2020) does not provide any recommendation for data regarding building proximity.

Finally, the study presented in this paper will investigate how the time-of-day when the measurement was performed along with proximity to buildings affects the HVSR method. Neither SESAME (2005) or MoHo S.R.L (2020) provide recommendations as to how time-of-day and building proximity can affect the HVSR method.

2.6 Summary

This chapter provided an overview of the HVSR method, its applications, and the existing contradictions in its guidelines. The limited literature addressing these contradictions highlights a critical gap, as inconsistent guidelines increase the likelihood of errors in data acquisition and interpretation.

3. METHODS

3.1 Introduction

The procedures and equipment used for HVSR data acquisition, the processing of the collected data, and details of the interpretation of the processed results are outlined in this chapter.

3.2 HVSR Ambient Noise Acquisition

HVSR measurements were recorded using a Tromino device produced by MoHo S.R.L. The Tromino is a compact device measuring 10 x 14 x 8 cm and weighing 1.1 kg (Figure 7), with an internal memory storage system. The internal system allows the Tromino to collect and store ambient noise data wirelessly, eliminating the need for external power or storage. These features make the Tromino highly portable, allowing a single operator to gather a substantial amount of data in a relatively short time.

Figure 7: Tromino device used in data acquisition. Image of Tromino devices aquiring data on concrete and grass simultaneously at MIZ Quad Site 4.

The instrument is equipped with three orthogonal electrodynamic velocimeters and three orthogonal digital accelerometers, enabling it to record both ambient and induced vibrations. To acquire ambient noise data for this study, the Tromino was positioned on the

ground using appropriate spikes (Figure 8). Ambient noise was collected from measurements on concrete walkways and grass throughout the project. Short spikes, as seen in Figure 8 (a), were used on concrete pavement, while longer spikes, as shown in Figure 8 (b), were utilized on grass. For each measurement, the Tromino was oriented with its north arrow aligned to true north as measured with a compass.

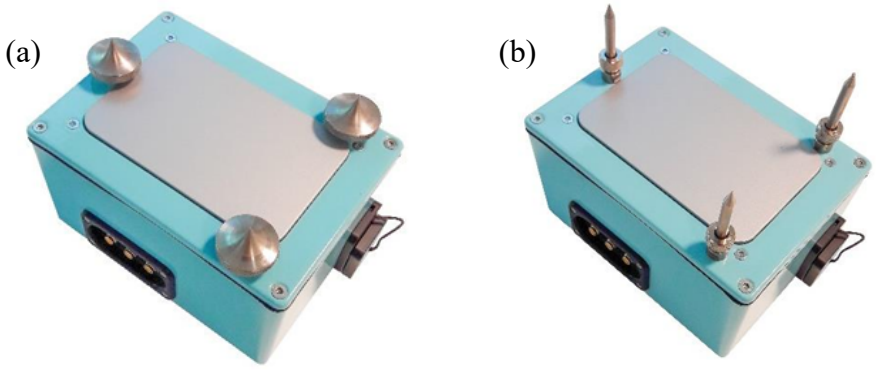

Figure 8: (a) Mounted Tromino short spikes (3 cm in length) used for acquisition on concrete, (b) Mounted Tromino long spikes (6 cm total length) used for acquisition on grass (MoHo S.R.L, 2020)

Ambient noise data were collected over a 16-minute period using the Tromino's internal memory system. *Program 2*, one of the Tromino's built-in acquisition programs was used during acquisition. *Program 2* was selected based on the MoHo S.R.L (2020), and was chosen due to its suitability for the following conditions:

1. GPS data is required, and the sky is visible for automatic acquisition to start.
2. Synchronization with other recordings is not needed.
3. The recording length is short (minutes) to intermediate (up to several hours).

All criteria were met during ambient noise data acquisition in the field. *Program 2* also enabled the acquisition and saving of ground motion data in the horizontal and vertical planes. The horizontal planes are labeled as North-South (N-S) and East-West (E-W), while

the vertical planes are labeled as Up-Down. GPS data were captured, and acquisition began automatically after a set delay time of 10 seconds.

With the program selected and delay set, the gain channels and frequency range were configured. Both HIGH and LOW gain channels were selected for data acquisition. MoHo S.R.L (2020) recommends using LOW gain channels for strong vibrations that may be induced by structures or machinery. It is also suggested to collect both HIGH and LOW gain channels together, as HIGH gain channels offer higher sensitivity during acquisition. For this reason, Channel 6 was selected to allow both HIGH and LOW gain channels to be acquired. For processing, a sampling frequency of 128 Hz or 512 Hz was used with most data collected at a sampling frequency of 512 Hz. A summary of the acquisition settings is provided in Table 1**.**

Table 1: Tromino Acquisition Parameters

Chosen Acquisition Parameters	
Program	2
Delay (sec)	10
GAIN Channels	HIGH and LOW (Channel 6)
Acquisition Length	16 min (960 sec)
Sampling Frequency (Hz)	128/512*

*NOTE: (*) indicates the sampling frequency for HVSR data acquisitions herein

3.2.1 Data Acquisition to Study the Influence of In-situ Concrete versus Grass Coupling on HVSR

To study the variability observed when HVSR measurements were conducted on concrete versus grass, 45 separate noise exposures were obtained. The ambient noise exposures were measured at 11 different sites. Data acquisition for each of the 45 ambient noise exposures was conducted using two Tromino devices. The devices were placed a few feet apart (one on grass and one on concrete), leveled, and the acquisition process was started simultaneously to ensure that the Tromino sensors were exposed to the same noise

waves. This placement ensured that the waves would travel through the same subsurface stratum before the waves reached the acquisition instrumentation.

3.2.2 Data Acquisition to Study the Influence of Strong, Nearby Noise on HVSR

The variably of the HVSR method was also investigated when data acquisition was subject to strong construction noise. A total of 23 noise exposures over 5 sites were used in this portion of the study. Data acquisition was conducted on concrete and grass for 4 of the 5 sites, while at 1 of the 5 sites data acquisition only occurred on grass. At the sites where concrete and grass acquisition occurred, two Tromino sensors were utilized. The sensors were placed a few feet apart (one on grass and one on concrete), as seen in Figure 7, leveled, and then the acquisition process was started simultaneously to ensure that the Tromino sensors were exposed to the same wavefield. This placement also ensured that the waves would travel through the same subsurface stratum before reaching the acquisition instrumentation.

3.2.3 Data Acquisition to Study Influence of Buildings Proximity on HVSR

To investigate the variability associated with proximity of the data acquisition location to buildings, 32 different ambient noise measurements at six different sites were performed. One criterion for test site selection required that the data acquisition occurred while no construction noise was present if the site was closer than 450 ft to a construction noise source (this was done to eliminate the effect of construction noise on variability). If the site was further than 450 ft from a construction site, data acquisitions was performed regardless of the presence of construction noise. This criterion was used to minimize the effect of nearby construction noise on the variability. Additionally, grass acquisitions were

exclusively used for this investigation to eliminate the effect of concrete coupling on variability.

3.2.4 Data Acquisition to Study Influence of Time of Day with Buildings Proximity on HVSR

To investigate variability associated with proximity of acquisition to buildings, 23 different ambient noise measurements at four different sites were performed. These sites were selected from the building proximity study where variability was observed. The sites selected were approximately 50 ft from the nearest building. Grass acquisitions were exclusively used for this investigation.

3.3 HVSR Ambient Noise Processing

The HVSR data collected by the Tromino sensors were processed using the *Grilla* software, produced by MoHo S.R.L. The processing of ambient noise data followed the data processing guidelines presented in SESAME (2005). The Tromino's data acquisition system collected and saved the ambient noise measurement in the time domain. The time domain data were imported from the Tromino into the *Grilla* software. The *Grilla* software interface can be seen in Figure 9

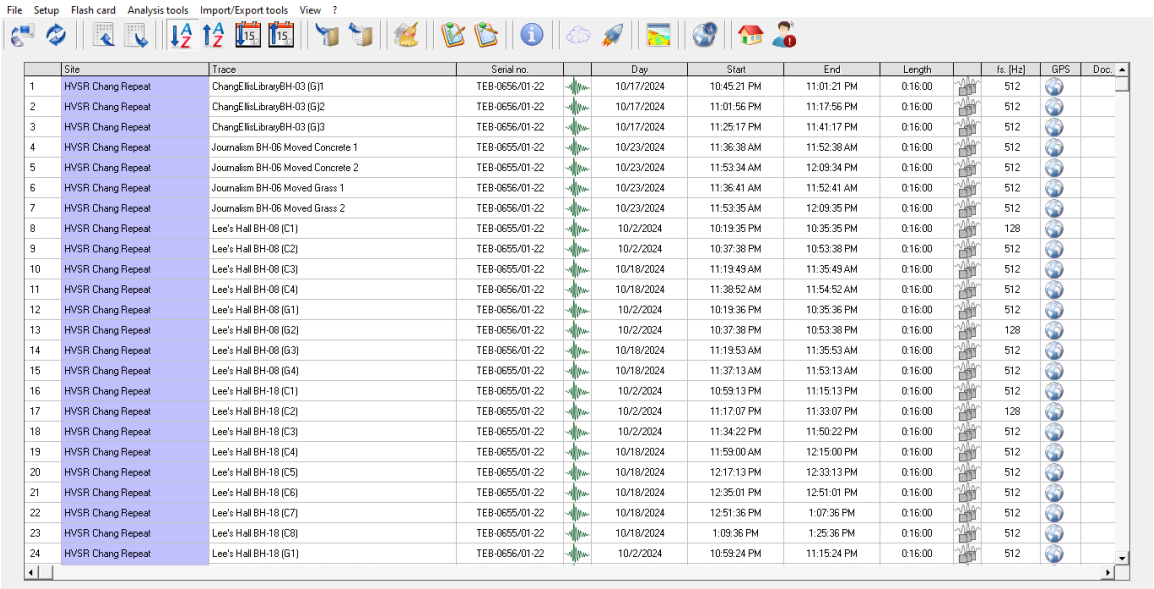

	Site	Trace	Serial no.		Day	Start	End	Length		fs. [Hz]	GPS	Doc.
1	HVSR Chang Repeat	ChangEllisLibraryBH-03 (G)1	TEB-0656/01-22		10/17/2024	10:45:21 PM	11:01:21 PM	0:16:00		512		
2	HVSR Chang Repeat	ChangEllisLibraryBH-03 (G)2	TEB-0656/01-22		10/17/2024	11:01:56 PM	11:17:56 PM	0:16:00		512		
3	HVSR Chang Repeat	ChangEllisLibraryBH-03 (G)3	TEB-0656/01-22		10/17/2024	11:25:17 PM	11:41:17 PM	0:16:00		512		
4	HVSR Chang Repeat	Journalism BH-06 Moved Concrete 1	TEB-0655/01-22		10/23/2024	11:36:38 AM	11:52:38 AM	0:16:00		512		
5	HVSR Chang Repeat	Journalism BH-06 Moved Concrete 2	TEB-0655/01-22		10/23/2024	11:53:34 AM	12:09:34 PM	0:16:00		512		
6	HVSR Chang Repeat	Journalism BH-06 Moved Grass 1	TEB-0656/01-22		10/23/2024	11:36:41 AM	11:52:41 AM	0:16:00		512		
7	HVSR Chang Repeat	Journalism BH-06 Moved Grass 2	TEB-0656/01-22		10/23/2024	11:53:35 AM	12:09:35 PM	0:16:00		512		
8	HVSR Chang Repeat	Lee's Hall BH-08 (C1)	TEB-0655/01-22		10/2/2024	10:19:35 PM	10:35:35 PM	0:16:00		128		
9	HVSR Chang Repeat	Lee's Hall BH-08 (C2)	TEB-0655/01-22		10/2/2024	10:37:38 PM	10:53:38 PM	0:16:00		512		
10	HVSR Chang Repeat	Lee's Hall BH-08 (C3)	TEB-0655/01-22		10/18/2024	11:19:49 AM	11:35:49 AM	0:16:00		512		
11	HVSR Chang Repeat	Lee's Hall BH-08 (C4)	TEB-0656/01-22		10/18/2024	11:38:52 AM	11:54:52 AM	0:16:00		512		
12	HVSR Chang Repeat	Lee's Hall BH-08 (G1)	TEB-0656/01-22		10/2/2024	10:19:36 PM	10:35:36 PM	0:16:00		512		
13	HVSR Chang Repeat	Lee's Hall BH-08 (G2)	TEB-0656/01-22		10/2/2024	10:37:38 PM	10:53:38 PM	0:16:00		128		
14	HVSR Chang Repeat	Lee's Hall BH-08 (G3)	TEB-0656/01-22		10/18/2024	11:19:53 AM	11:35:53 AM	0:16:00		512		
15	HVSR Chang Repeat	Lee's Hall BH-08 (G4)	TEB-0655/01-22		10/18/2024	11:37:13 AM	11:53:13 AM	0:16:00		512		
16	HVSR Chang Repeat	Lee's Hall BH-18 (C1)	TEB-0655/01-22		10/2/2024	10:59:13 PM	11:15:13 PM	0:16:00		512		
17	HVSR Chang Repeat	Lee's Hall BH-18 (C2)	TEB-0655/01-22		10/2/2024	11:17:07 PM	11:33:07 PM	0:16:00		128		
18	HVSR Chang Repeat	Lee's Hall BH-18 (C3)	TEB-0655/01-22		10/2/2024	11:34:22 PM	11:50:22 PM	0:16:00		512		
19	HVSR Chang Repeat	Lee's Hall BH-18 (C4)	TEB-0655/01-22		10/18/2024	11:59:00 AM	12:15:00 PM	0:16:00		512		
20	HVSR Chang Repeat	Lee's Hall BH-18 (C5)	TEB-0655/01-22		10/18/2024	12:17:13 PM	12:33:13 PM	0:16:00		512		
21	HVSR Chang Repeat	Lee's Hall BH-18 (C6)	TEB-0655/01-22		10/18/2024	12:35:01 PM	12:51:01 PM	0:16:00		512		
22	HVSR Chang Repeat	Lee's Hall BH-18 (C7)	TEB-0655/01-22		10/18/2024	12:51:36 PM	1:07:36 PM	0:16:00		512		
23	HVSR Chang Repeat	Lee's Hall BH-18 (C8)	TEB-0655/01-22		10/18/2024	1:09:36 PM	1:25:36 PM	0:16:00		512		
24	HVSR Chang Repeat	Lee's Hall BH-18 (G1)	TEB-0656/01-22		10/2/2024	10:59:24 PM	11:15:24 PM	0:16:00		512		

Figure 9: Grilla Software Interface

The standard analysis parameters of the *Grilla* software were utilized for the computation of HVSR for this study. Of the four analysis options provided by *Grilla*, the automatically selected windows parameter option was chosen. The parameter option disregarded windows when moving standard deviation divided by the total standard deviation was less than 2. A window size of 20 seconds and smoothing set to 10% was used during analysis. The analyses were conducted in a frequency range of 2 to 50 Hz for each test. The 2 to 50 Hz range was selected to encompass expected HVSR frequencies for this region, as observed by Chi (2022) at similar locations around the University of Missouri-Columbia campus. The analysis parameters are summarized in Table 2. HVSR analysis in the *Grilla* software was conducted as follows:

1. The time trace was subdivided into non-overlapping 20 second windows, meeting the analysis criteria. The windows that did not meet the analysis criteria are shown as white in Figure 10.

2. Each window meeting the analysis criteria was detrended, for each recorded channel, and narrowed with a Bartlett window,
3. The Fast Fourier Transform (FFT) amplitude spectra were computed for each window of each channel,
4. Each window of the amplitude spectrum for each channel were smoothed according to the selected smoothing parameters (Triangular - 10%) (Figure 11 shows the smoothed amplitude spectrums).
5. The HVSR was then computed for each window of each spectrum as a function of the frequency using the geometric average of the two horizonal components, as shown in Equation (3.1):

$$HVSR = \frac{\sqrt{H_1 + H_2}}{V} \tag{3.1}$$

where H_1 and H_2 are the smoothed amplitude spectra components and V is the smoothed vertical spectra components.

6. The average HVSR (the red line seen in Figure 12) was produced by taking the average of the HVSR for each window in Step 5. The thinner black line is the 95% confidence interval relative to the HVSR amplitudes. Included in Figure 12 are the directional HVSR plots (N-S and E-W).

Table 2: Grilla Analysis Parameters

***Grilla* Analysis Parameters**	
HVSR Averaging Function	Geometric Average
Analysis Criteria	Automatically Selected Windows $\frac{Moving\ std.dev}{total\ std.dev} < 2$
Window Size (sec)	20
Smoothing	Triangular – 10%
Analysis Between (Hz)	2 - 50
Directional HVSR Analysis - Angular Step	10°

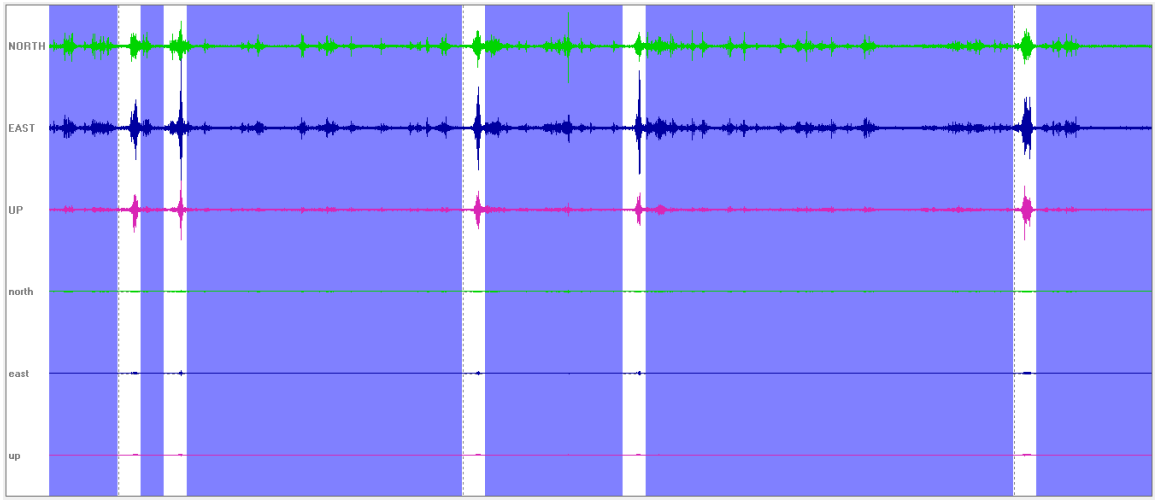

Figure 10: Time trace of Lee's Hall BH-08 Test 2 on Grass site, auto-selected windows by the *Grilla* software for windows that meet the analysis criteria. The white section did not meet the selection criteria and are disregarded during analysis.

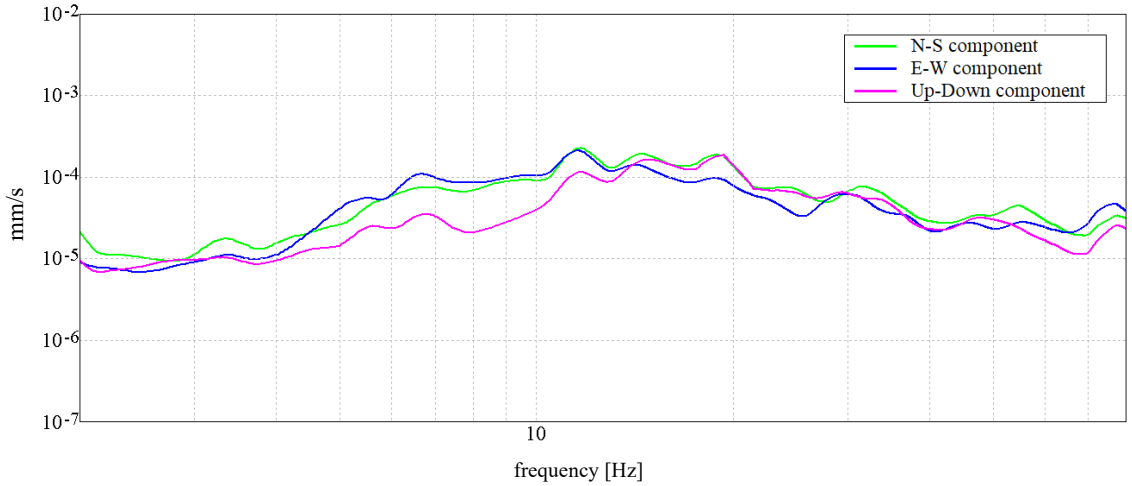

Figure 11:V and H spectrum plots for Journalism B-06 B Test 1 on Grass site. Green line indicates the N-S component, blue line indicates the E-W component, and pink line indicates the Up-Down component.

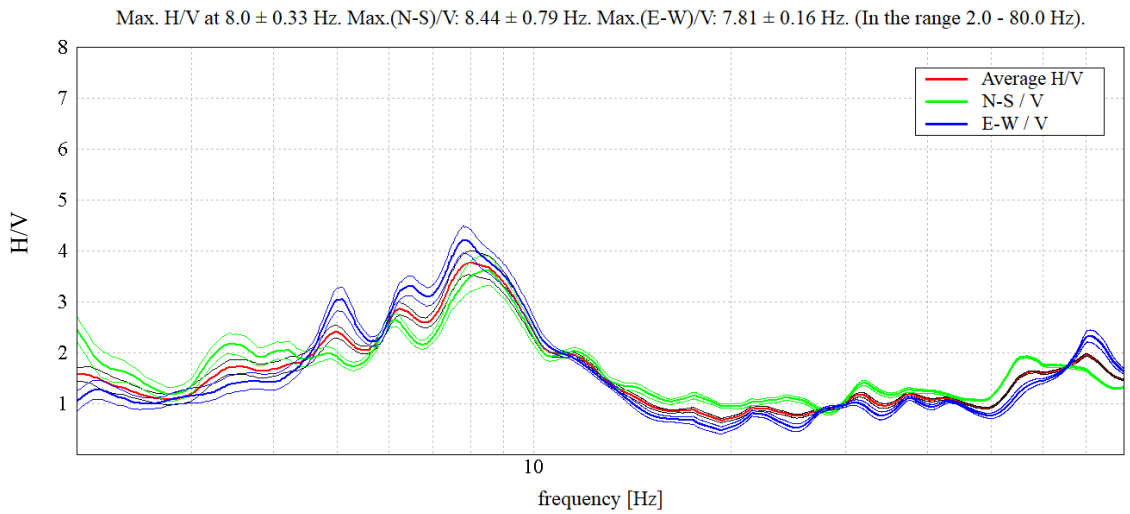

Figure 12: HVSR plots for Journalism B-06 B Test 1 on Grass site. HVSR versus Frequency (Hz): Red line indicates the average HVSR, green line indicates the N-S/V, and blue line indicates the E-W/V.

3.4 HVSR Data Interpretation

Following the processing of the ambient noise data, a critical part of HVSR analysis is the identification and interpretation of $HVSR_{Res}$. SESAME offers specific guidelines for identifying meaningful peaks which include:

1. The $HVSR_{Res}$ should have a clear amplitude contrast from frequencies surrounding the peak. SESAME (2005) suggests a minimum amplitude contrast of 2 (i.e., the peak amplitude should be at least twice that of the adjacent lower and higher frequencies).
2. The $HVSR_{Res}$ should be well-defined and stable across multiple windows and measurements. Peaks that appear inconsistently or shift significantly between windows may indicate the presence of noise or site heterogeneity.

The second SESAME guideline above was a driving force behind this investigation. While the $HVSR_{Res}$ should be well-defined and stable across the windows, the $HVSR_{Res}$ often showed variability from test to test at a selected site.

In some cases, the natural $HVSR_{Res}$ can be clearly observed, as shown in Figure 13**.** The peak was chosen at the maximum value observed in the HVSR plot that is within the range of analysis (2 - 50 Hz). When the HVSR produced a clear $HVSR_{Res}$, the HVSR peak indicates that a change occurred in the subsurface stratum. In most cases, the $HVSR_{Res}$ indicates that a "hard" layer, such as rock, was encountered. The single peak in the HVSR plot can be correlated with the “eye-shape” seen in the amplitude spectra plot (Figure 14**)** which typically indicates that the peak was produced by stratigraphic origin (Castellaro and Mulargia, 2009). The “eye-shape” in the amplitude spectra plot occurs when the vertical amplitude spectra drop off while the horizontal spectra remain constant or increases.

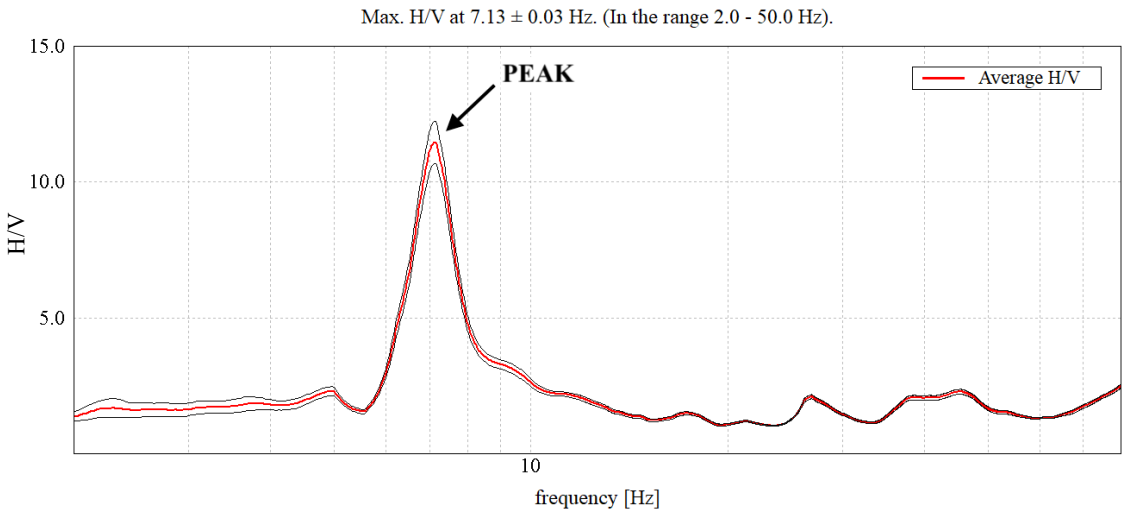

Figure 13: $HVSR_{Res}$ example from MIZ MiddleQuad Test 5 on Grass

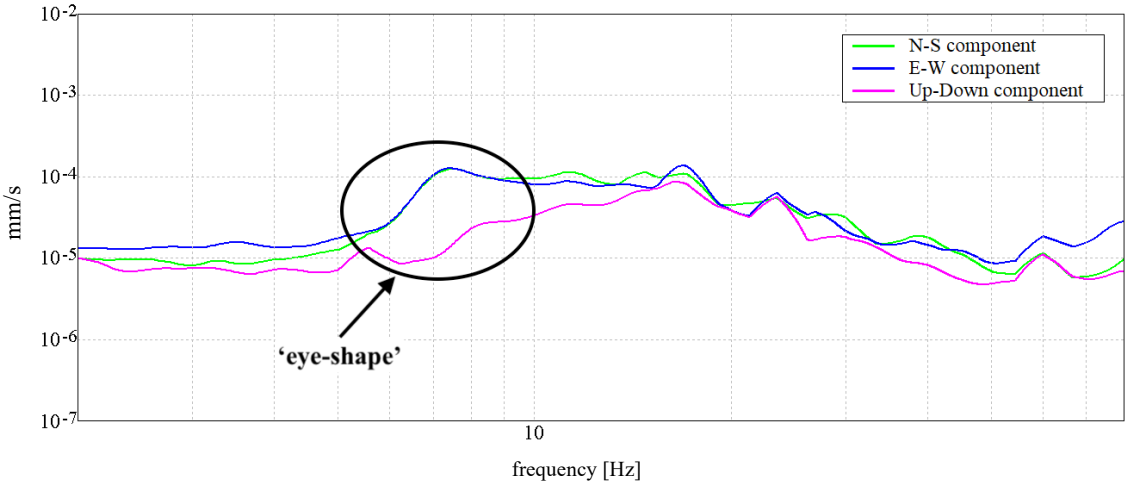

Figure 14: Amplitude spectra 'eye-shape' example from MIZ middlequad Test 5 on Grass site.

For other cases, the natural $HVSR_{Res}$ can be more difficult to determine (Figure 15). Plots such as Figure 15 show multiple peak frequencies throughout the HVSR plot. These multiple frequencies can be produced by several factors, including natural or artificial occurrences. The peaks can signal multiple subsurface stratum layers at the selected site or be a result of a human-made occurrence. To distinguish between natural and artificial occurrences, a closer interpretation of the amplitude spectra plot (Figure 16) was necessary to identify the natural $HVSR_{Res}$. A natural $HVSR_{Res}$ can be predicted when the amplitude spectrum plot shows a drop-off of the vertical spectra while the horizontal spectra remain constant or increase. Artificial peaks can be observed at frequencies in the HVSR plot that correspond to narrow peaks with varying amplitudes of all spectral components in the amplitude spectrum plot (Castellaro and Mulargia, 2009). Natural and artificial peaks are shown in Figure 15. Figure 16 indicates the "eye-shape" (natural) and narrow peaks (artificial) that correspond to the peaks in Figure 15.

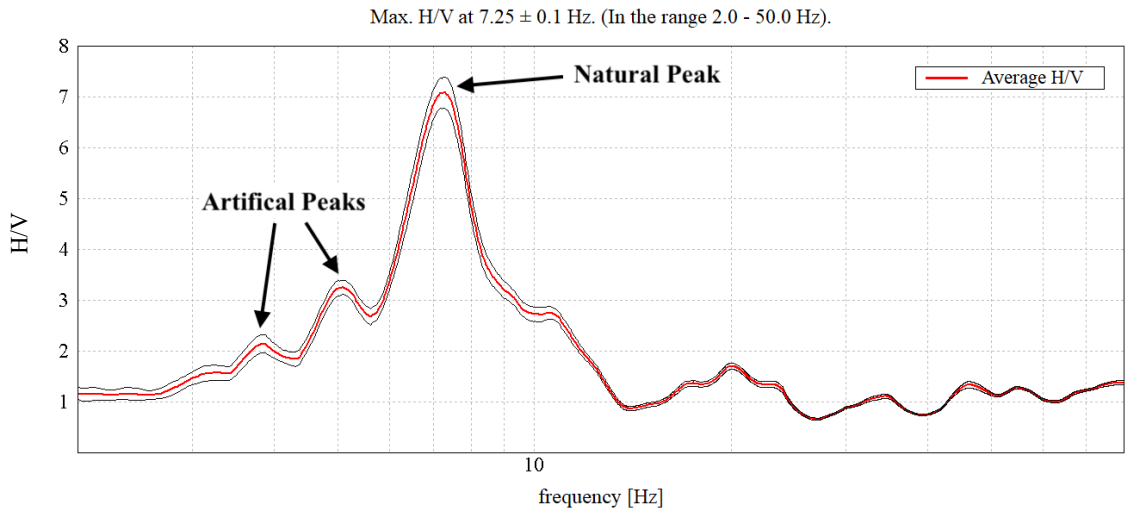

Figure 15: HVSR curve artificial and natural peaks from MIZ Quad Site 4 Test 6 on Grass site.

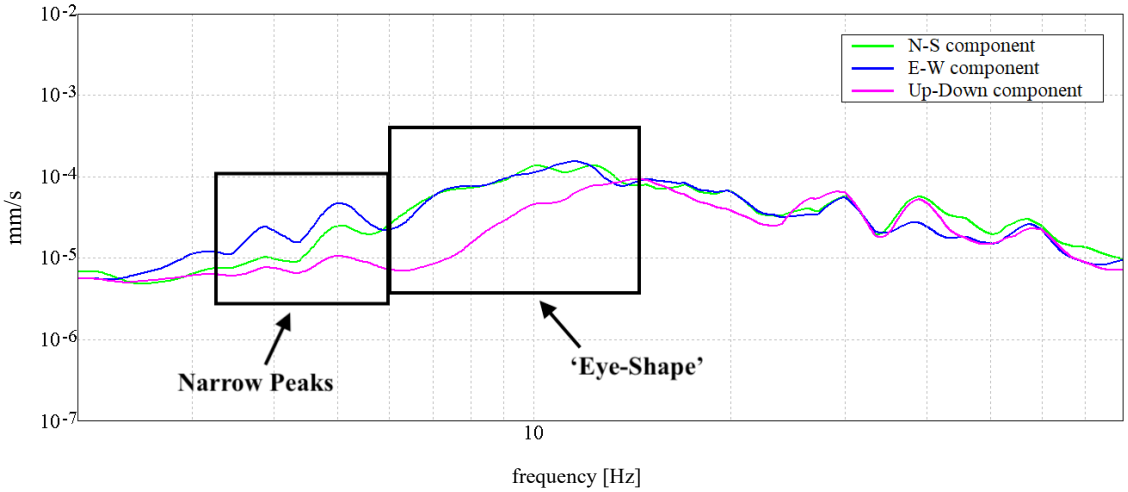

Figure 16: Amplitude spectra showing narrow peaks (Artificial) and 'eye-shape' (Natural) example from MIZ Quad Site 4 Test 6 on Grass site.

Automatic selection was used for the majority of the data interpretation for this thesis. Section 5.6 of this thesis utilized both automatic selection of the largest peak ($HVSR_{Grilla}$) and the manual approach ($HVSR_{Man}$) in some cases.

3.5 Summary

The equipment and procedures used to perform HVSR data acquisition, the HVSR data processing, and the interpretation of the HVSR results were covered in this chapter. A

summary of the HVSR equipment was first presented. The procedure utilized to select sites and acquiring the HVSR was discussed before a discussion about processing the HVSR data. Finally, the interpretation of the HVSR data was detailed.

4. HVSR DATA COLLECTION SITES

4.1 Introduction

Descriptions for each of the HVSR measurement locations around the University of Missouri-Columbia campus are presented in this chapter. Five areas of the campus were utilized for investigating the variability of HVSR measurements (Figure 17). Across the five areas, 16 locations were selected where 126 HVSR measurements were conducted to examine HVSR variability. Site locations were selected so that HVSR variability could be studied for the following conditions:

1) In-situ coupling through concrete versus grass
2) In-situ coupling through concrete versus grass with strong, nearby noise influence, such as construction
3) Influence of building proximity to acquisition site
4) Influences of time of day with building proximity

In addition, some sites were selected based on results from the study by Chi (2022). These sites were chosen to further explore the variability observed by Chi (2022) when repeated measurements were collected and analyzed using the HVSR method. Ellis Library BH-03 B, Lee's Hall BH-08, and Journalism BH-6 were chosen to investigate the variability observed by Chi (2022) in measurement interpretations. Additionally, Lee's Hall BH-18 was chosen due to the low variability in measurements, with an attempt to replicate the data observed by Chi (2022).

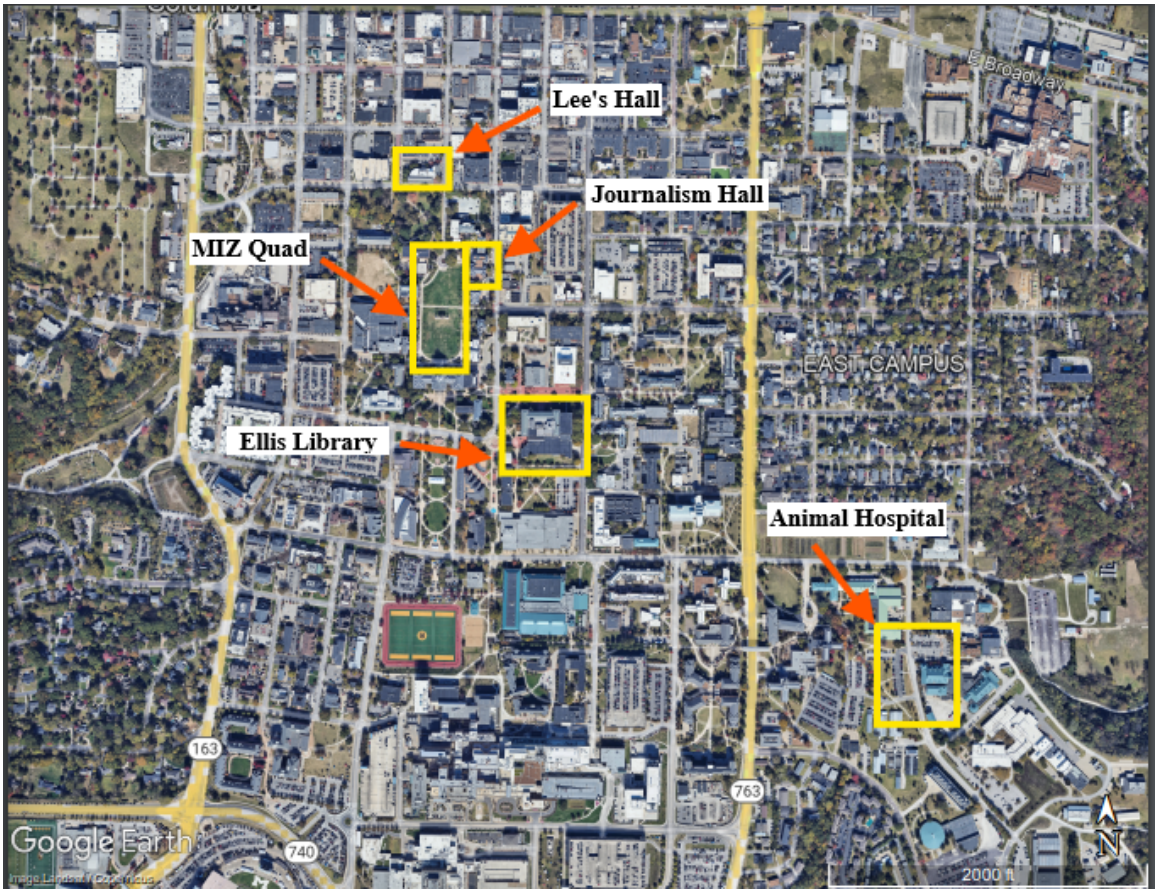

Figure 17: Locations of the 5 data acquisition areas on the University of Missouri-Columbia campus.

4.2 Data Acquisition Locations and Descriptions

Table 3 is a summary of all the sites. The summary includes the approximate coordinates of each site, along with which assessment sites were used in. Detailed descriptions of each site follow Table 3. Additional site photos can be found in APPENDIX E.

Table 3: Summary of test site locations and conditions

Location Name	Approximate Coordinates		Assessment Studies				
	Latitude	Longitude	Concrete vs. Grass	Influence of Strong, Nearby Noise [ft]	Proximity to Buildings [ft]	Time of Day Buildings	Chi (2022) Repeat
Animal Hospital 1	38°56'24.8" N	092°19'07.1" W	*	65*	90		
Animal Hospital 2	38°56'26.4" N	092°19'07.3" W	*	190*	45		
Ellis Library BH-01	38°56’37.8” N	092°19'35.4" W			25*	*	
Ellis Library BH-03 A	Concrete: 38°56'38.2" N Grass: 38°56'38.0" N	Concrete: 092°19'33.3" W Grass: 092°19'33.4" W			2*	*	
Ellis Library BH-03 B	38°56'37.8" N	092°19'33.3" W			25		*
Journalism B-06 A	38°56'48.8" N	092°19'41.6" W	*		15*	*	*
Journalism B-06 B	38°56'48.8" N	092°19'41.3" W	*		8		
Lee’s Hall BH-08	38°56'55.6" N	092°19'46.9" W	*		45		*
Lee’s Hall BH-18	38°56'55.9" N	092°19'46.7" W	*		50		*
Lee’s Hall Selected	38°56'55.5" N	092°19'46.2" W			3*	*	
MIZ Quad Site 1	38°56'49.5" N	092°19'43.7" W	*		95*		
MIZ Quad Site 2	38°56'49.0" N	092°19'42.0" W	*		30		
MIZ Quad Site 3	38°56'48.5" N	092°19'45.2" W	*		23		
MIZ Quad Site 4	38°56'44.8" N	092°19'45.1" W	*	25*	26		
MIZ Quad Site 5	38°56’46.5” N	092°19'42.2" W	*	225*	100		
MIZ Quad MiddleQuad	38°56’44.9” N	092°19'43.8" W		15*	105*		

*Note: (*) indicates location site was used in the corresponding Assessment Study

4.2.1 Animal Hospital 1

Eight data acquisitions conducted at Animal Hospital 1 were used to examine HVSR variability due to different instrumentation coupling conditions (concrete versus grass) and proximity to strong construction noise (near versus far). The Animal Hospital 1

site was approximately 65 ft (18.8 m) from an active construction site. The construction site included an excavation, heavy machinery (e.g., excavator, forklift), and generators. This site was also chosen because the Tromino sensors could be used on both concrete and grass simultaneously, ensuring that the same wavefield was recorded during data acquisition. The coordinates of Animal Hospital 1 are found in Table 3 and can be observed in Figure 18, along with an image of test set up. Boring logs were not available for this selected site.

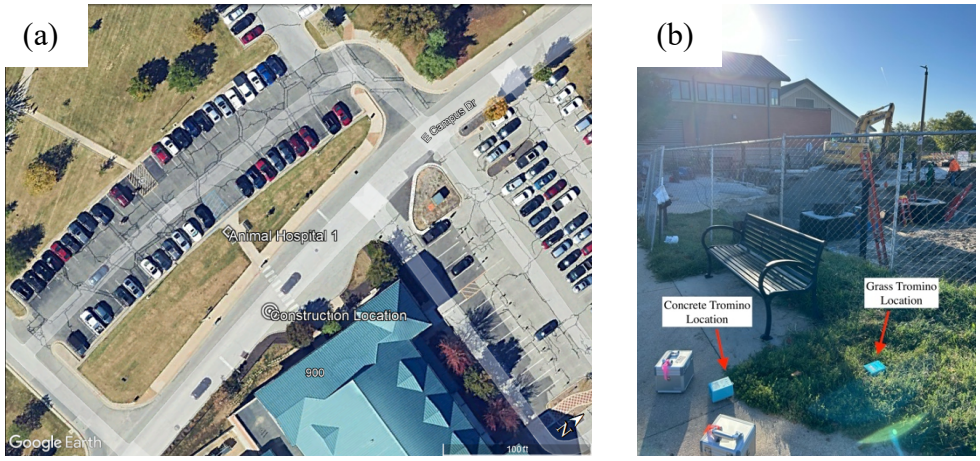

Figure 18: (a) An aerial photo of Animal Hospital 1 site location, and (b) is a photo of the Tromino set up before data acquisition.

4.2.2 Animal Hospital 2

Six data acquisitions conducted at Animal Hospital 2 were used to examine HVSR variability due to different instrumentation coupling conditions (concrete versus grass) and proximity to strong construction noise (near versus far). The Animal Hospital 2 site was approximately 190 ft (57.9 m) from an active construction site. The construction site included an excavation, heavy machinery (e.g., excavator, forklift), and generators. This site was also chosen because the Tromino sensors could be used on concrete and grass simultaneously, ensuring that the same wavefield was recorded during data acquisition.

The coordinates of Animal Hospital 2 are found in Table 3 and can be observed in Figure 19, along with an image of test set up. Boring logs were not available for this selected site.

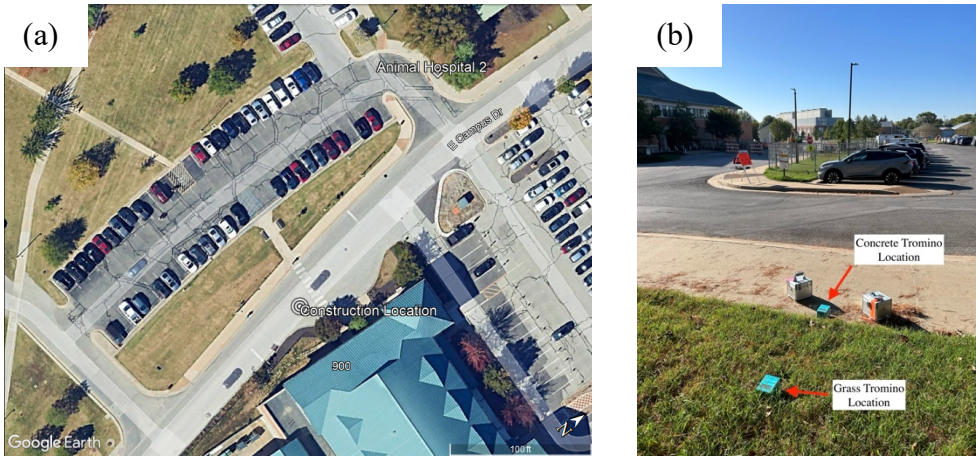

Figure 19: (a) An aerial photo of Animal Hospital 2 site location, and (b) is a photo of the Tromino set up before data acquisition.

4.2.3 Ellis Library BH-01

Six data acquisitions conducted at Ellis Library BH-01 were used to examine HVSR variability due to the proximity to a building (near to far) and time of day building influence (occupancy status). The Ellis Library BH-01 site was approximately 25 ft (7.6 m) south of the Ellis Library structure. Data acquisition at Ellis Library BH-01 was conducted exclusively on grass, due to the absence of concrete. The coordinates of Ellis Library BH-01 are in Table 3 and can be observed in Figure 20 along with an image of test set up. Boring logs from this site indicate a 22.5 ft (6.9 m) layer of clay underlain by a 19 ft (5.8) layer of sand. Limestone was first encountered at a depth of 41.5 ft (12.6 m) below the ground surface.

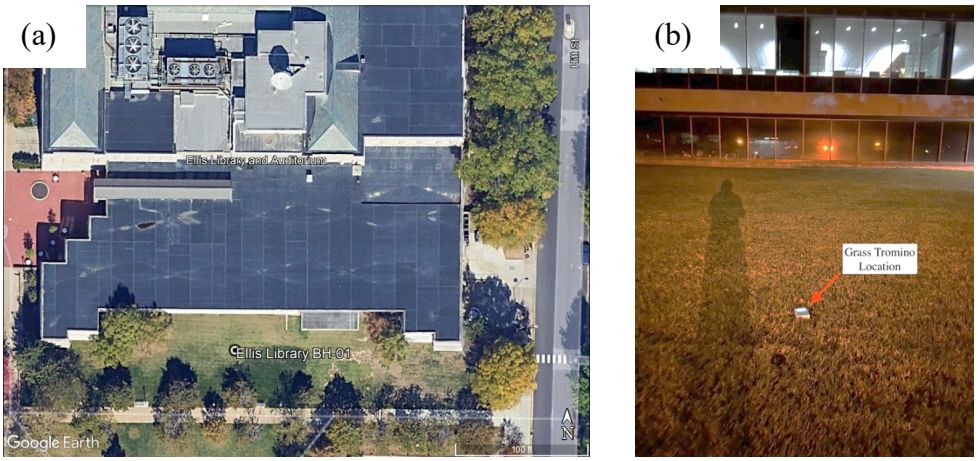

Figure 20: (a) An aerial photo of Ellis Library BH-01 site location, and (b) is a photo of the Tromino set up before data acquisition.

4.2.4 Ellis Library BH-03 A

Ten data acquisitions conducted at Ellis Library BH-03 A were used to examine HVSR variability due to different instrumentation coupling conditions (concrete versus grass), proximity to a building (near to far), and time of day building influence (occupancy status). The Ellis Library BH-03 A site was approximately 2 ft (0.6 m) from the southeast corner of the Ellis Library structure. Data acquisition at Ellis Library BH-03 A was conducted on concrete and grass simultaneously, ensuring that the same wavefield was recorded during data acquisition. The concrete acquisition at Ellis Library BH-03 A was approximately 15 ft (4.6 m) north of the grass acquisition site. The coordinates of Ellis Library BH-03 A are found in Table 3 and can be observed in Figure 21 along with an image of test set up. Boring logs from this site indicate a 27.5 ft (8.4 m) layer of clay underlain by a 9 ft (2.7 m) layer of clayey sand and sandy clay. Limestone was first encountered at a depth of 36.5 ft (11.1 m) below the ground surface.

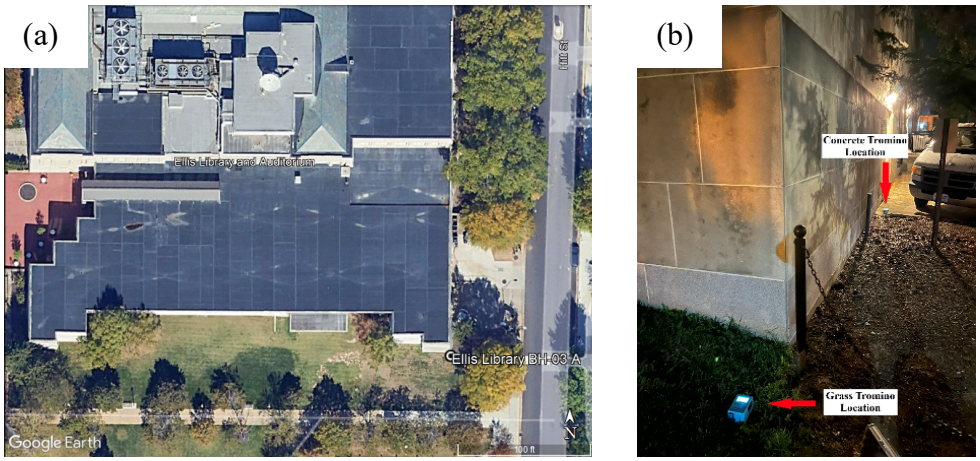

Figure 21: (a) An aerial photo of Ellis Library BH-03 A site location, and (b) is a photo of the Tromino set up before data acquisition.

4.2.5 Ellis Library BH-03 B

Three data acquisitions conducted at Ellis Library BH-03 B were used in an attempt to replicate variability presented by Chi (2022). Chi (2022) observed variability of the $HVSR_{Res}$ of approximately 15%. The Ellis Library BH-03 B site was approximately 25 ft (7.6 m) away from the southeast corner of the Ellis Library structure. Data acquisition at Ellis Library BH-03 B was conducted exclusively on grass. The coordinates of Ellis Library BH-03 B are found in Table 3 and can be observed in Figure 22 along with an image of test set up. Boring logs from this site indicate a 27.5 ft (8.4 m) layer of clay underlain by a 9 ft (2.7 m) layer of clayey sand and sandy clay. Limestone was first encountered at a depth of 36.5 ft (11.1 m) below the ground surface.

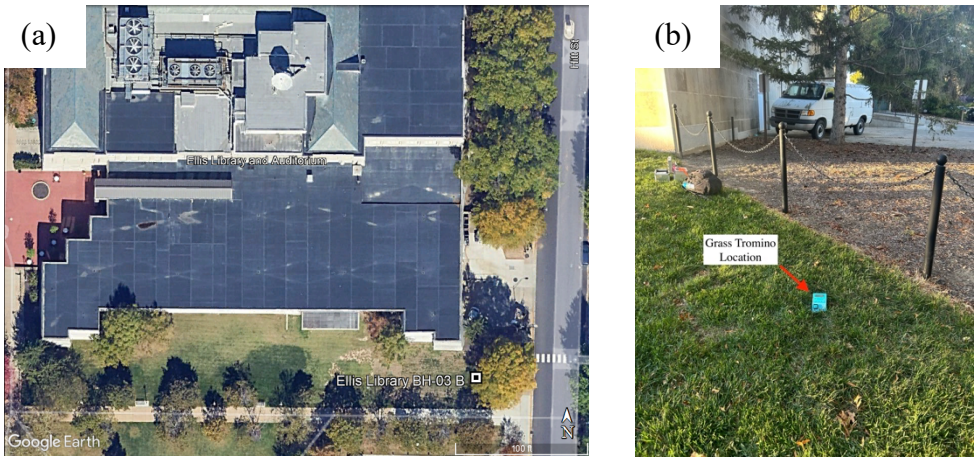

Figure 22: (a) An aerial photo of Ellis Library BH-03 B site location, and (b) is a photo of the Tromino set up before data acquisition.

4.2.6 Journalism B-06 A

Twelve data acquisitions conducted at Journalism B-06 A were used to examine HVSR variability due to different instrumentation coupling conditions (concrete versus grass), proximity to a building (near versus far), time of day building influence (occupancy status), proximity to strong construction noise (near versus far). It was also used in an attempt to replicate variability presented by Chi (2022). This site was chosen because the Tromino sensors could be used on concrete and grass simultaneously, ensuring that the same wavefield was recorded during data acquisition. The Journalism B-06 A site was located 15 ft (4.6 m) from the nearest building, Pickard Hall, and approximately 432 ft (132 m) from an active construction site. The construction site included an excavation, heavy machinery (e.g., excavator, forklift), and generators. Chi (2022) observed variability of the maximum peak frequency of approximately 18%. The coordinates of Journalism B-06 A are found in Table 3 and can be observed in Figure 23, along with an image of test set up. Boring logs from this site indicate 15 ft (4.6 m) layer of clay underlain by a 4 ft (1.2 m) layer of sand and an 8 ft (2.4 m) layer of clay. Shale was first encountered at a depth of 27 ft (8.2 m) and limestone was encountered at 43 ft (13.1 m) below the ground surface.

Figure 23: (a) An aerial photo of Journalism BH-06 A site location, and (b) is a photo of the Tromino set up before data acquisition.

4.2.7 Journalism BH-06 B

Four data acquisitions conducted at Journalism B-06 B were used to examine HVSR variability due to different instrumentation coupling conditions (concrete versus grass). The site was also chosen because the Tromino sensors could be used on concrete and grass simultaneously, ensuring that the same wavefield was recorded during data acquisition. Journalism B-06 B was located approximately 8 ft (2.4 m) from Pickard Hall. Journalism B-06 B was located 27 ft (8.2 m) from the Journalism B-06 A site, thus it was used to identify potential reasons for the variability observed at Journalism B-06 A. The coordinates of Journalism B-06 B are found in Table 3 and can be observed in Figure 24 along with an image of test set up. Boring logs from this site indicate 15 ft (4.6 m) layer of clay underlain by a 4 ft (1.2 m) layer of sand and an 8 ft (2.4 m) layer of clay. Shale was first encountered at a depth of 27 ft (8.2 m) and limestone was encountered at 43 ft (13.1 m) below the ground surface.

Figure 24: (a) An aerial photo of Journalism BH-06 B site location, and (b) is a photo of the Tromino set up before data acquisition.

4.2.8 Lee's Hall BH-08

Eight data acquisitions conducted at Lee's Hall BH-08 were used to examine HVSR variability due to different instrumentation coupling conditions (concrete versus grass) and used in an attempt to replicate variability presented by Chi (2022. This site was chosen because the Tromino sensors could be used on concrete and grass simultaneously, ensuring that the same wavefield was recorded during data acquisition. Chi (2022) observed variability of the maximum peak frequency of approximately 17%. The Lee's Hall BH-08 site was located approximately 45 ft (13.7 m) from the Lee's Hall structure, 4 ft (1.2 m) from a sidewalk, and 10 ft (3 m) from a roadway. Wavefields were variable at this location due to fluctuating vehicle and foot traffic which was related to the time of day. The coordinates of Lee's Hall BH-08 are found in Table 3 and can be observed in Figure 25 along with an image of test set up. Boring logs from this site indicate an 8 ft (2.4 m) layer of clay, with weathered shale first encountered at a depth of 8 ft (2.4 m). This was followed by thin layers of weathered shale and weathered limestone, with auger refusal in limestone at a depth of 16.7 feet (5.1 m) below the ground surface.

Figure 25: (a) An aerial photo of Lee's Hall BH-08 site location, and (b) is a photo of the Tromino set up before data acquisition.

4.2.9 Lee's Hall BH-18

Eleven data acquisitions conducted at Lee's Hall BH-18 were used to examine HVSR variability due to different instrumentation coupling conditions (concrete versus grass) and in an attempt to replicate variability presented by Chi (2022). This site was chosen because the Tromino sensors could be used on concrete and grass simultaneously, ensuring that the same wavefield was recorded during data acquisition. Lee's Hall BH-18 was the least variable site reported by Chi (2022) with variability around 4%. The Lee's Hall BH-18 site was located approximately 50 ft (15.2 m) from the Lee's Hall structure, 14.5 ft (4.4 m) from a sidewalk, and 30 ft (7.6 m) from a roadway. Wavefields were changing at this location due to levels of vehicle and foot traffic, based on the time of day. The coordinates of Lee's Hall BH-18 are found in Table 3 and can be observed in Figure 26 along with an image of test set up. Boring logs from this site indicate an 8.5 ft (2.6 m) layer of clay. Weathered shale was first encountered at a depth of 8.5 feet (2.6 m) and auger refusal on limestone was encountered at 15 ft (4.6 m) below the ground surface.

Figure 26: (a) An aerial photo of Lee's Hall BH-18 site location, and (b) is a photo of the Tromino set up before data acquisition.

4.2.10 Lee's Hall Selected

Five data acquisitions conducted at Lee's Hall Selected were used to examine HVSR variability due to the proximity to a building (near to far) and time of day building influence (occupancy status). The Lee's Hall Selected site was approximately 3 ft (0.9 m) away from the southwest corner of the Lee's Hall structure. Data acquisition at Lee's Hall Selected was conducted exclusively on grass, due to the absence of concrete. The coordinates of Lee's Hall Selected are found in Table 3 and can be observed in Figure 27, along with an image of test set up. Boring logs were not available for this selected site.

Figure 27: (a) An aerial photo of Lee's Hall Selected site location, and (b) is a photo of the Tromino set up before data acquisition.

4.2.11 MIZ Quad Site 1

Twelve data acquisitions conducted at MIZ Quad Site 1 were used to examine HVSR variability due to different instrumentation coupling conditions (concrete versus grass) and proximity to a building (near to far). This site was chosen because the Tromino sensors could be used on concrete and grass simultaneously, ensuring that the same wavefield was recorded during data acquisition. The MIZ Quad Site 1 was located 95 ft (29 m) from the nearest building, MIZ Geology. The coordinates of MIZ Quad Site 1 are found in Table 3 and can be observed in Figure 28, along with an image of test set up. Boring logs were not available for this selected site.

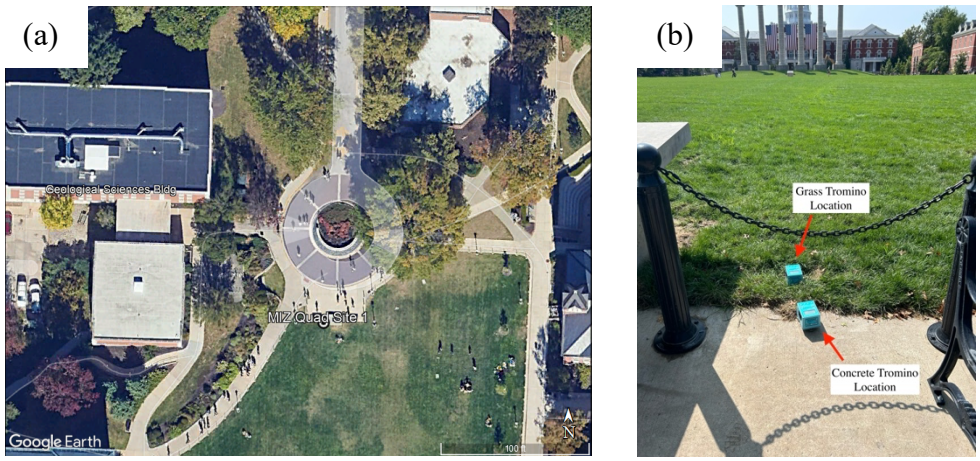

Figure 28: (a) An aerial photo of MIZ Quad Site 1 site location, and (b) is a photo of the Tromino set up before data acquisition.

4.2.12 MIZ Quad Site 2

Four data acquisitions conducted at MIZ Quad Site 2 were used to examine HVSR variability due to different instrumentation coupling conditions (concrete versus grass). This site was chosen because the Tromino sensors could be used on concrete and grass simultaneously, ensuring that the same wavefield was recorded during data acquisition. The MIZ Quad Site 2 was located 30 ft (9.1 m) from the Reynolds Journalism structure. The coordinates of MIZ Quad Site 2 are found in Table 3 and can be observed in Figure 29, along with an image of test set up. Boring logs were not available for this selected site.

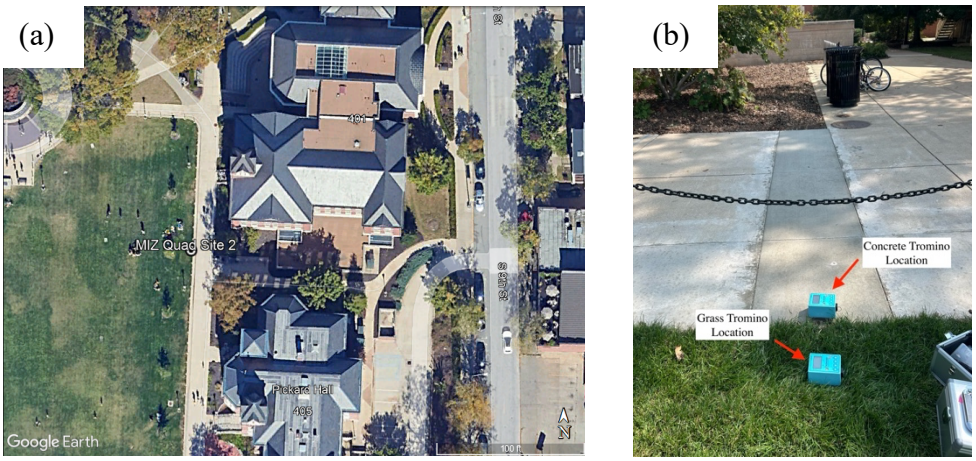

Figure 29: (a) An aerial photo of MIZ Quad Site 2 site location, and (b) is a photo of the Tromino set up before data acquisition.

4.2.13 MIZ Quad Site 3

Twelve data acquisitions conducted at MIZ Quad Site 3 were used to examine HVSR variability due to different instrumentation coupling conditions (concrete versus grass). This site was chosen because the Tromino sensors could be used on concrete and grass simultaneously, ensuring that the same wavefield was recorded during data acquisition. The MIZ Quad Site 3 was located 23 ft (7 m) from the Reynolds Journalism structure. The coordinates of MIZ Quad Site 3 are found in Table 3 and can be observed in Figure 30, along with an image of test set up. Boring logs were not available for this selected site.

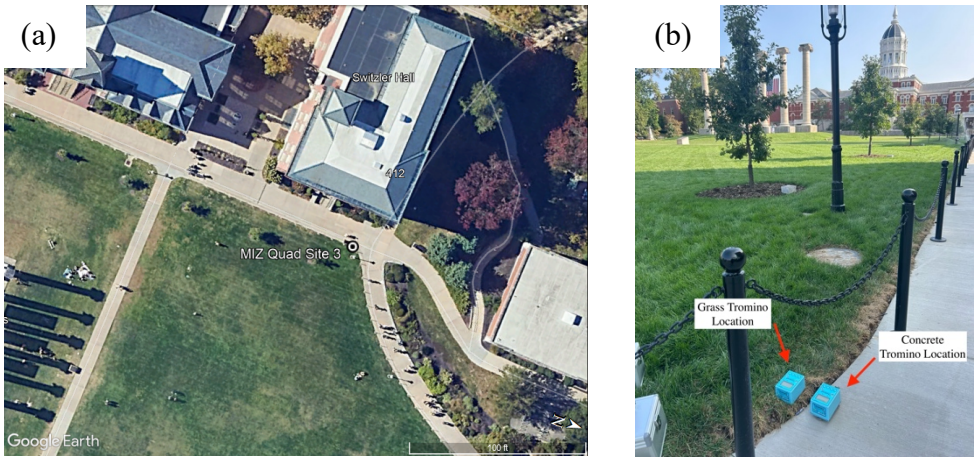

Figure 30: (a) An aerial photo of MIZ Quad Site 3 site location, and (b) is a photo of the Tromino set up before data acquisition.

4.2.14 MIZ Quad Site 4

Twelve data acquisitions conducted at MIZ Quad Site 4 were used to examine HVSR variability due to different instrumentation coupling conditions (concrete versus grass) and proximity to strong construction noise (near versus far). This site was chosen because the Tromino sensors could be used on concrete and grass simultaneously, ensuring that the same wavefield was recorded during data acquisition. The MIZ Quad Site 4 was located 26 ft (7.9 m) from the Lafferre Hall structure, and approximately 25 ft (7.6 m) from an active construction site. The construction site included an excavation, heavy machinery (e.g., excavator, forklift), and generators. The coordinates of MIZ Quad Site 4 are found in Table 3 and can be observed in Figure 31, along with an image of test set up. Boring logs were not available for this selected site.

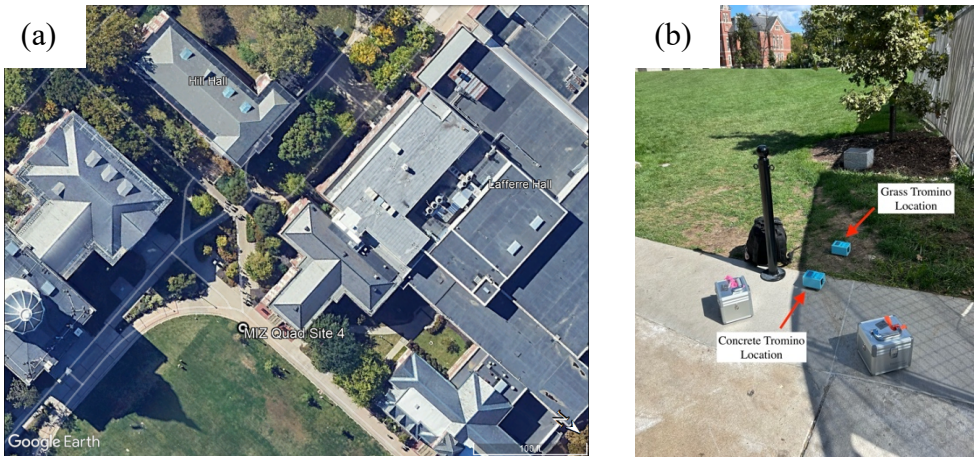

Figure 31: (a) An aerial photo of MIZ Quad Site 4 site location, and (b) is a photo of the Tromino set up before data acquisition.

4.2.15 MIZ Quad Site 5

Six data acquisitions conducted at MIZ Quad Site 5 were used to examine HVSR variability due to different instrumentation coupling conditions (concrete versus grass) and proximity to strong construction noise (near versus far). This site was chosen because the Tromino sensors could be used on concrete and grass simultaneously, ensuring that the same wavefield was recorded during data acquisition. The MIZ Quad Site 5 was located 100 ft (30.5 m) from the Residence on Francis Quadrangle, and approximately 225 ft (68.6 m) from an active construction site. The construction site included an excavation, heavy machinery (e.g., excavator, forklift), and generators. The coordinates of MIZ Quad Site 5 are found in Table 3 and can be observed in Figure 32, along with an image of test set up. Boring logs were not available for this selected site.

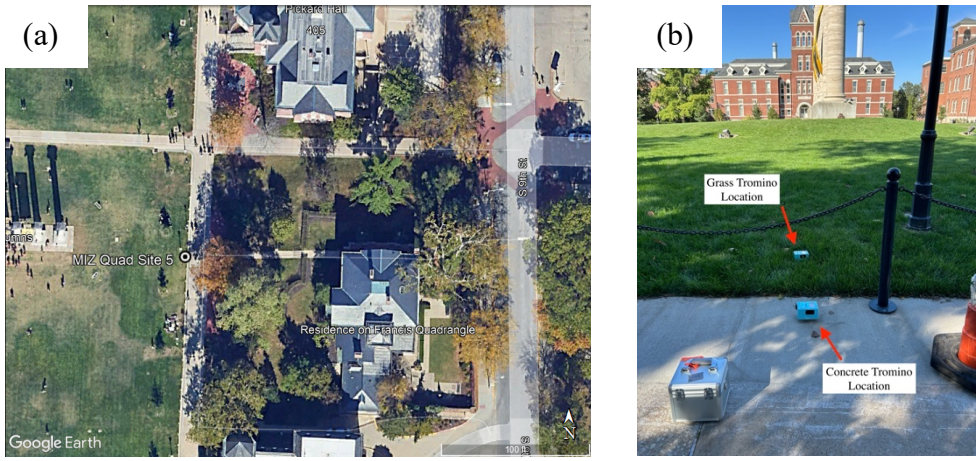

Figure 32: (a) An aerial photo of MIZ Quad Site 5 site location, and (b) is a photo of the Tromino set up before data acquisition.

4.2.16 MIZ MiddleQuad

Seven data acquisitions conducted at MIZ MiddleQuad were used to examine HVSR variability due to the proximity to a building (near to far) and proximity to strong construction noise (near versus far). The MIZ MiddleQuad site was located 105 ft (32 m) from the nearest building, Jesse Hall, and approximately 15 ft (4.6 m) from an active construction site. The construction site included an excavation, heavy machinery (e.g., excavator, forklift), and generators. Chi (2022) observed a variability of the maximum peak frequency of approximately 18%. The coordinates of MIZ MiddleQuad are found in Table 3 and can be observed in Figure 33, along with an image of test set up. Boring logs were not available for this selected site.

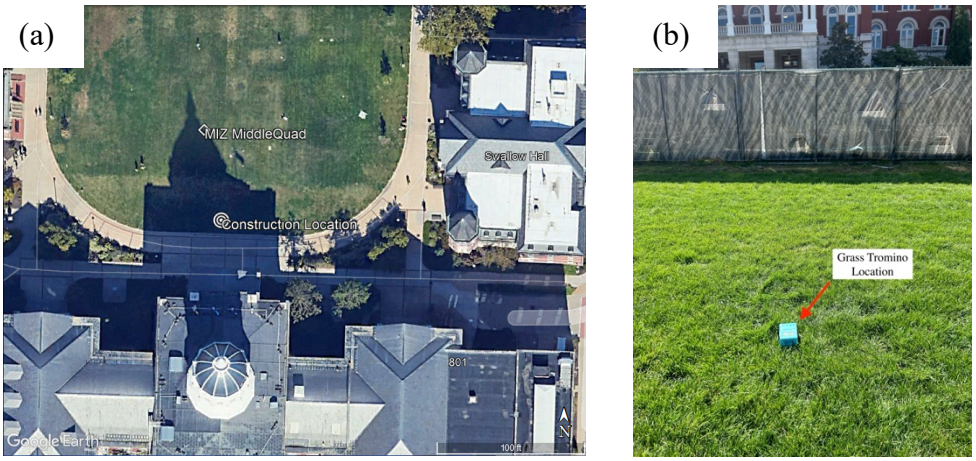

Figure 33: (a) An aerial photo of MIZ MiddleQuad site location, and (b) is a photo of the Tromino set up before data acquisition.

4.3 Summary

Described in this chapter, are the HVSR measurement locations around the University of Missouri-Columbia campus, where five distinct areas were utilized for investigating the variability of HVSR measurements. Effects on ambient noise collection were studied at 16 locations with variability including data collection instrumentation couplings (concrete versus grass), proximity to a construction site, and proximity to buildings which were recorded at different time-of-days consistent with the building being occupied or unoccupied.

Several sites were also chosen based on a study by Chi (2022) to explore variability observed in repeated measurements. These include Ellis Library BH-03, Lee's Hall BH-08, Lee's Hall BH-18, and Journalism BH-06. Data were collected at each site to assess the potential causes of variability in the HVSR results. Additionally, MIZ Quad Sites and MiddleQuad were selected to study the effects of strong nearby construction noise on HVSR measurements. These sites were subjected to varying levels of pedestrian activity and noise from nearby construction, with data collected during both high and low traffic periods.

5. RESULTS

5.1 Introduction

This chapter presents the results of an assessment of the variability observed in HVSR measurements under different scenarios. Each acquisition was categorized based on an assessment and ranking of the quality of the HVSR curves. Following the categorization of the curves, the results of variability in the $HVSR_{Res}$ values were studied. The first results section presents the variability of $HVSR_{Res}$ for in-situ coupling conditions (concrete versus grass), followed by the $HVSR_{Res}$ variability of in-situ coupling when strong, nearby noise sources are present. An assessment of the $HVSR_{Res}$ variability due to the proximity of the acquisition site to buildings was completed. Finally, the effect of the time-of-day of the measurement for measurements near buildings was investigated (termed occupied versus unoccupied in this chapter).

5.2 Data Quality Categorization

At different sites in this study, HVSR measurements from 76 different noise exposures (i.e., tests) were collected using 126 individual acquisitions. Each of the 126 HVSR curves were inspected and put into one of four categories based on a qualitative assessment of the interpreted ambiguity.

Category 1 - High Quality: assigned to HVSR curves that had one clear, single peak with few (or no) secondary peaks that were far from the frequency of interest. Figure 34 shows an example of a Category 1 site.

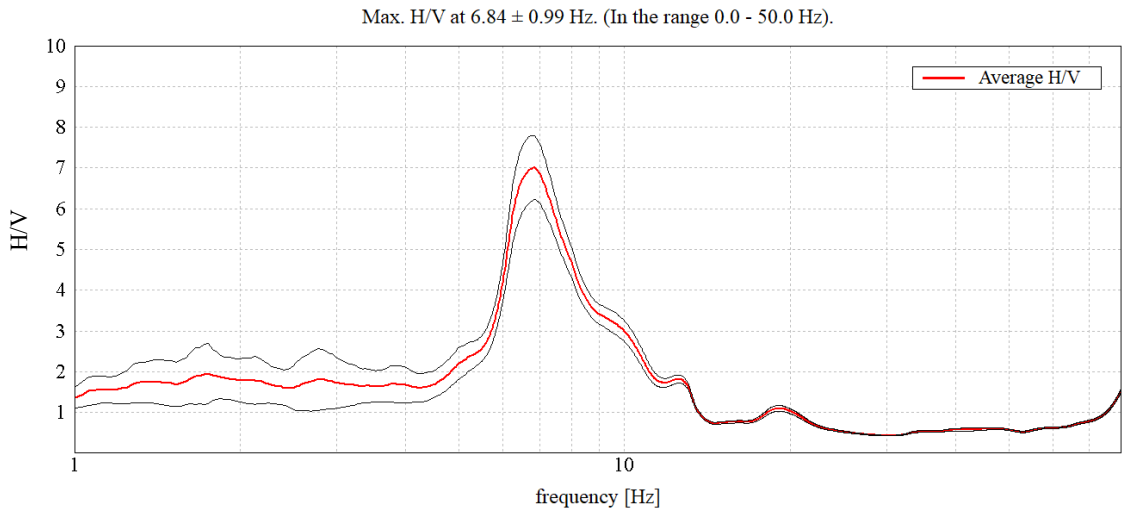

Figure 34: Example of HVSR data categorized as Category 1 (MIZ Quad Site 1, Test 6 on Concrete site).

Category 2 - Medium Quality: assigned to HVSR curves when the frequency of interest (maximum peak) was accompanied by secondary peaks that were not likely to be mistaken for the correct peak. The secondary peaks observed in these HVSR curves were of a much lower amplitude or far from the main peak, allowing for clear identification of $HVSR_{Res}$. Figure 35 is an example of a Category 2 HVSR categorization.

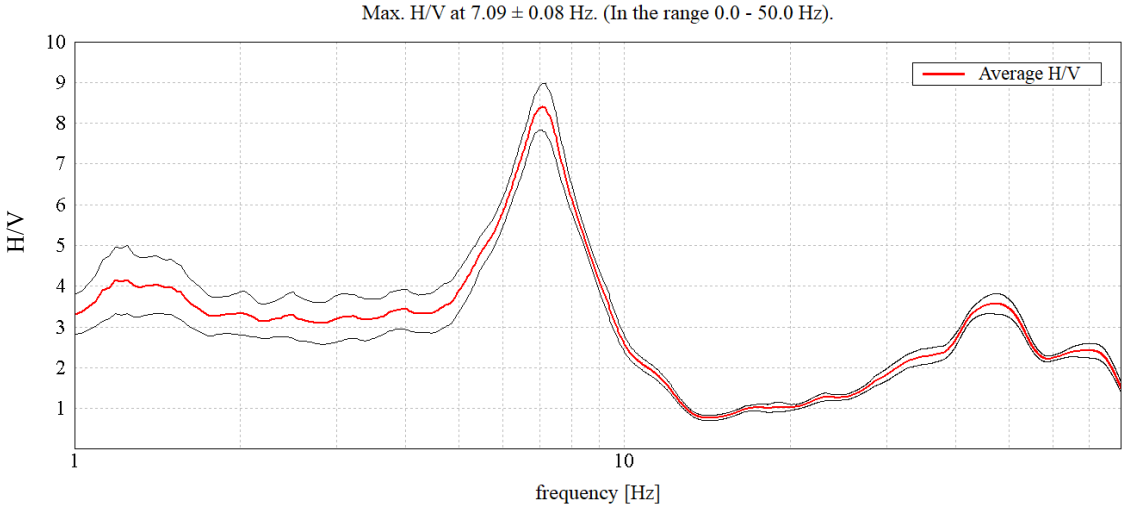

Figure 35: Example of HVSR data categorized as Category 2 (Animal Hospital 2, Test 2 on Grass site).

Category 3 - Low Quality: assigned to HVSR curves with several peaks of similar amplitudes observed in the frequency range of interest, or a single low-amplitude, wide

peak with no clear frequency value. Figure 36 is an example of an HVSR curve that was categorized as a Category 3 curve.

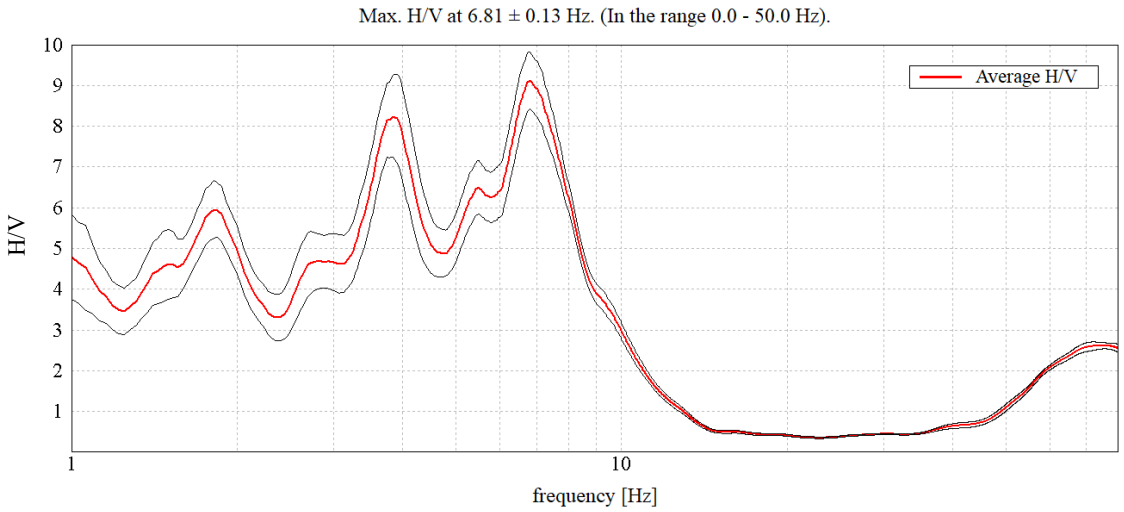

Figure 36: Example HVSR data categorized as Category 3 (MIZ Quad Site 1, Test 1 on Grass site).

Category 4 -Uninterpretable: was designated to be assigned to HVSR curves where no identifiable peak was produced, as was the case for several examples from the literature. However, this category was not encountered in any of the 126 curves from this study, so there is no example to show.

Categories 1 and 2 are acquisitions where $HVSR_{Res}$ are clear, and the data should be easy to interpret. Categories 3 and 4 are assigned to acquisitions where the ability to select the $HVSR_{Res}$, indicative of the subsurface strata, is difficult to select or nonexistent and the results may be erroneous. Each of the 126 HVSR curves were inspected and placed into 1 of the 4 categories based on a qualitative assessment of the HVSR plot. A summary of the categorization of each HVSR curve is presented in Table 4. All HVSR plots can be found in APPENDIX A.

Table 4: Category Assignment for acquisition conducted at each investigation site.

Location Name	Repeat Test No.	Acquisition Quality Category	
		Grass	Concrete
Animal Hospital 1	Test 1	2	1
	Test 2	1	1
	Test 3	2	2
	Test 4	1	2
Animal Hospital 2	Test 1	2	2
	Test 2	2	2
	Test 3	2	2
Ellis Library BH-01	Test 1	3	-
	Test 2	3	-
	Test 3	3	-
	Test 4	3	-
	Test 5	1	-
	Test 6	1	-
Ellis Library BH-03 A	Test 1	3	3
	Test 2	3	2
	Test 3	3	-
	Test 4	3	-
	Test 5	2	2
	Test 6	2	2
Ellis Library BH-03 B	Test 1	1	-
	Test 2	1	-
	Test 3	3	-
Journalism B-06 A	Test 1	3	3
	Test 2	3	3
	Test 3	3	3
	Test 4	2	3
	Test 5	3	3
	Test 6	3	3
Journalism B-06 B	Test 1	3	3
	Test 2	2	3
Lee's Hall BH-08	Test 1	3	3
	Test 2	3	3
	Test 3	3	3
	Test 4	3	3
Lee's Hall BH-18	Test 1	1	1
	Test 2	1	1
	Test 3	2	1
	Test 4	-	1
	Test 5	-	2
	Test 6	-	1
	Test 7	-	1
	Test 8	-	1

Table 4 continued

Location Name	Repeat Test No.	Acquisition Quality Category	
		Grass	Concrete
Lee's Hall Selected	Test 1	3	-
	Test 2	3	-
	Test 3	3	-
	Test 4	3	-
	Test 5	3	-
MIZ MiddleQuad	Test 1	1	-
	Test 2	1	-
	Test 3	1	-
	Test 4	1	-
	Test 5	1	-
	Test 6	1	-
	Test 7	1	-
MIZ Quad Site 1	Test 1	3	3
	Test 2	3	3
	Test 3	3	3
	Test 4	1	1
	Test 5	2	3
	Test 6	1	1
MIZ Quad Site 2	Test 1	2	2
	Test 2	2	2
MIZ Quad Site 3	Test 1	2	2
	Test 2	2	2
	Test 3	2	2
	Test 4	2	2
	Test 5	1	1
	Test 6	2	2
MIZ Quad Site 4	Test 1	3	3
	Test 2	3	3
	Test 3	3	3
	Test 4	3	3
	Test 5	1	1
	Test 6	2	3
MIZ Quad Site 5	Test 1	2	2
	Test 2	2	2
	Test 3	3	3

*NOTE: (-) indicates the test was not performed for this condition

5.3 Influence of In-situ Instrumentation Coupling Conditions on HVSR Measurements

The $HVSR_{Res}$ values used in this section to compare the influence of in-situ coupling conditions on the HVSR measurements were automatically selected by the *Grilla* software ($HVSR_{Grilla}$) based on being the highest peaks in the HVSR curve.

5.3.1 Qualitative Assessment of HVSR on Concrete versus Grass

A single test comprised two data acquisitions performed simultaneously on concrete and grass to record the same wavefield. In total, 90 acquisitions (45 on concrete and 45 on grass) were conducted to evaluate the influence of performing HVSR measurements on concrete as compared to grass. HVSR measurements on grass ($HVSR_{Grass}$) were considered the reference value, as the Tromino User's Manual (MoHo S.R.L, 2020) and the findings of Castellaro and Mulargia (2009), indicate it should provide more reliable results.

To assess the reliability of HVSR measurements on concrete ($HVSR_{Concrete}$), the categorization number (CAT) assigned to the concrete acquisition ($CAT_{Concrete}$) were compared with the CAT assigned to the grass acquisition (CAT_{Grass}) for the same locations and tests. This comparison was quantified using Equation (5.1):

$$\Delta CAT = CAT_{Concrete} - CAT_{Grass} \quad (5.1)$$

If there was no change in the quality of the data, the category difference (ΔCAT) was zero, while a positive value for ΔCAT indicated a reduction in the quality of HVSR results on concrete and a negative result indicated improved quality on concrete. Results indicated that 38 of the 45 tests (84.4%) produced $\Delta CAT = 0$, meaning the quality of the data was similar for both $HVSR_{Concrete}$ and $HVSR_{Grass}$. Two tests (4.4%) resulted in $\Delta CAT = -1$, where the quality of $HVSR_{Grass}$ was worse than that of $HVSR_{Concrete}$. Conversely, five

tests (11.1%) produced ΔCAT = 1, indicating poorer quality results from $HVSR_{Concrete}$ than $HVSR_{Grass}$. These findings are presented in Figure 37.

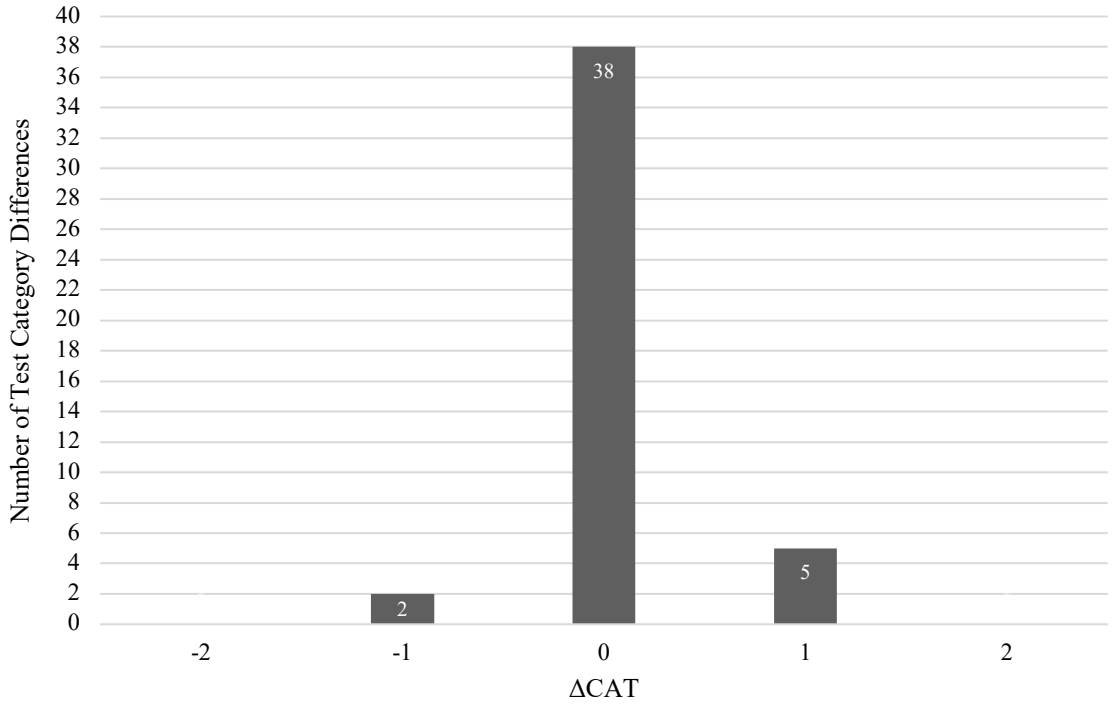

Figure 37: Quantitative Assessment of HVSR Test categorization based on difference in category numbers.

A further breakdown of the test results is presented in Table 5 (the average percent difference shown in Table 5 will be discussed later in this section). Interestingly, of the tests that produced a ΔCAT = 0, 47% (18 out of 38) were of the lowest quality (Category 3). These findings showed that the quality of HVSR measurements for in-situ coupling of concrete and grass often tended to be low quality for both $HVSR_{Concrete}$ and $HVSR_{Grass}$, indicating that other factors were affecting the quality of the measurements.

Table 5: Number of tests for different Categorization combinations and average of the percent difference for each Categorization combination

	Quality Categorization Combinations																	
CAT No.	C	G	C	G	C	G	C	G	C	G	C	G	C	G	C	G	C	G
	1	1	1	2	1	3	2	2	2	1	2	3	3	3	3	1	3	2
No. of Test	7		2		0		13		1		0		18		0		4	
Average % Difference between $HVSRs_{Concrete}$ and $HVSR_{Grass}$ for each Categorization Combination	-1.9%		-0.3%		-		0.3%		-0.3%		-		-12.4%		-		-7.1%	

Overall, 51% of the tests were of high to medium quality (Category 1 or 2) HVSR curves while 40% showed low quality HVSR curves (Category 3 for both surfaces). Only 9% of tests showed transition from low quality $HVSR_{Concrete}$ ($CAT_{Concrete}$ = 3) to a medium quality $HVSR_{Grass.}$ (CAT_{Grass} = 2). Based on these results, it appears that the coupling surface had little impact on the quality (i.e., interpretability) of the HVSR plots.

5.3.2 Quantitative Assessment of HVSR on Concrete versus Grass

Figure 38 plots 45 points indicating each of the 45 tests performed for this investigation. The points are comprised of $HVSR_{Concrete}$ (y-coordinate) and the $HVSR_{Grass}$ (x-coordinate). Plotted points should ideally align along a 45-degree line, indicating little or no variability due to the in-situ coupling on concrete versus grass. Of the 45 points plotted, 68.8% (31 out of 45) of the $HVSR_{Concrete}$ were within 5% of the $HVSR_{Grass.}$, while 31.2% showed differences that were greater than 5% and considered significant. The tests where $HVSR_{Concrete}$ were outside of ±5% of the $HVSR_{Grass}$ are circled in Figure 38.

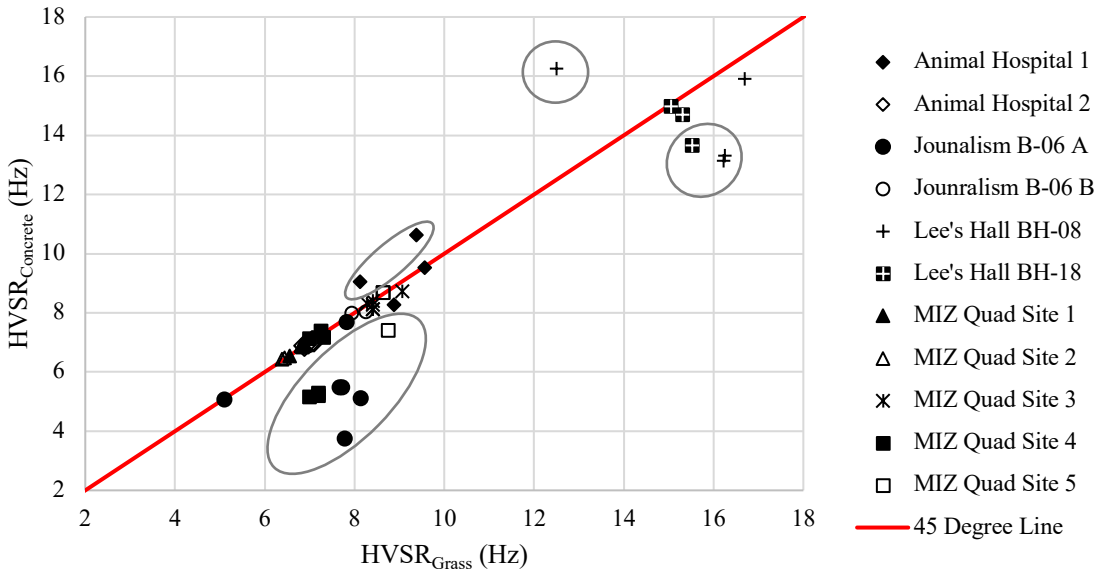

Figure 38: HVSRs$_{Concrete}$ versus HVSRs$_{Grass}$ from 45 tests at same location measuring the same wavefield. The circled points indicate the tests showing a ±5% difference in the HVSRs$_{Concrete}$ compared to HVSRs$_{Grass}$

To further analyze variability between HVSR$_{Concrete}$ and HVSR$_{Grass}$, the percent difference between the maximum peak frequencies was calculated for each test. The percent difference was computed under the assumption that the HVSR$_{Grass}$ peak was the true value. These calculations, along with the HVSR$_{Res}$, are detailed in Table 6. The average percent difference by quality category was also calculated and presented in Table 5. Calculating an average percent difference assisted in the quantitative assessment and allowed for the following observations: (1) When both HVSR$_{Concrete}$ and HVSR$_{Grass}$ of a test have been categorized as high quality (Category 1 or 2), the average percent difference ranged from 0% to 2%. (2) When low quality measurements for HVSR$_{Concrete}$ and HVSR$_{Grass}$ (Category 3) are observed, the average percent difference increased to 12.4%.

The findings from the quantitative assessment support the observation from the qualitative assessment of the influence of in-situ instrumentation coupling. The in-situ coupling on the instrumentation is not likely the cause of the HVSR measurement

variability because both the $HVSR_{Concrete}$ and $HVSR_{Grass}$ are of low quality, indicating that other factors are attributing to the variability observed in the $HVSR_{Res}$. The $HVSR_{Grass}$ versus the percent differences are presented in Figure 39.

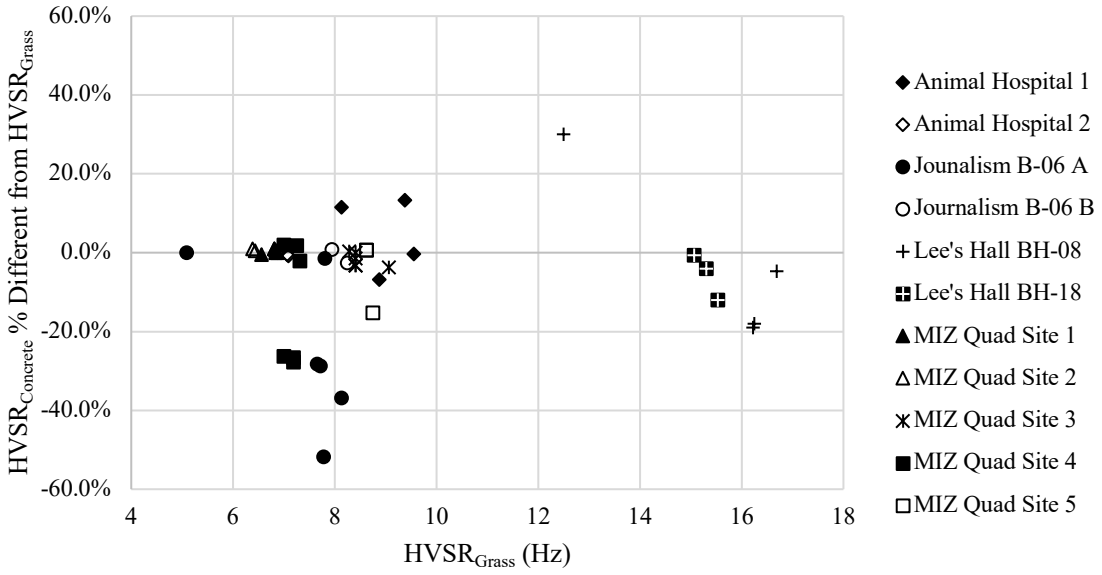

Figure 39: HVSRGrass versus precent difference of HVSRConcrete to HVSRGrass.

Table 6: Results from repeat measurements with simultaneous acquisition of concrete and grass, and the percent difference of the $HVSR_{Concrete}$ to $HVSR_{Grass}$.

Location Name	Repeat Test No.	Acquisition CAT No.		$HVSR_{Grilla}$ (Hz)		% Diff. $HVSR_{Concrete}$ from $HVSR_{Grass}$
		Grass	Concrete	$HVSR_{Grass}$	$HVSR_{Concrete}$	
Animal Hospital 1	Test 1	2	1	8.13	9.06	11.4%
	Test 2	1	1	8.88	8.28	-6.8%
	Test 3	2	2	9.38	10.63	13.3%
	Test 4	1	2	9.56	9.53	-0.3%
Animal Hospital 2	Test 1	2	2	6.88	6.88	0.0%
	Test 2	2	2	7.09	7.03	-0.8%
	Test 3	2	2	7.06	7.03	-0.4%
Journalism B-06 A	Test 1	3	3	7.72	5.5	-28.8%
	Test 2	3	3	7.81	7.69	-1.5%
	Test 3	3	3	7.78	3.75	-51.8%
	Test 4	2	3	7.66	5.5	-28.2%
	Test 5	3	3	5.09	5.09	0.0%
	Test 6	3	3	8.13	5.13	-36.9%
Journalism B-06 B	Test 1	3	3	7.94	8	0.8%
	Test 2	2	3	8.25	8.03	-2.7%

Table 6 continued

Location Name	Repeat Test No.	Acquisition CAT No.		$HVSR_{Grilla}$ (Hz)		% Diff. $HVSR_{Concrete}$ from $HVSR_{Grass}$
		Grass	Concrete	$HVSR_{Grass}$	$HVSR_{Concrete}$	
Lee's Hall BH-08	Test 1	3	3	16.22	13.13	-19.1%
	Test 2	3	3	16.25	13.31	-18.1%
	Test 3	3	3	16.69	15.91	-4.7%
	Test 4	3	3	12.5	16.25	30.0%
Lee's Hall BH-18	Test 1	1	1	15.31	14.69	-4.0%
	Test 2	1	1	15.06	14.97	-0.6%
	Test 3	2	1	15.53	13.66	-12.0%
MIZ Quad Site 1	Test 1	3	3	6.81	6.88	1.0%
	Test 2	3	3	6.56	6.53	-0.5%
	Test 3	3	3	6.81	6.88	1.0%
	Test 4	1	1	6.88	6.88	0.0%
	Test 5	2	3	6.84	6.88	0.6%
	Test 6	1	1	6.84	6.84	0.0%
MIZ Quad Site 2	Test 1	2	2	6.38	6.44	0.9%
	Test 2	2	2	6.44	6.47	0.5%
MIZ Quad Site 3	Test 1	2	2	8.41	8.28	-1.5%
	Test 2	2	2	8.41	8.13	-3.3%
	Test 3	2	2	8.28	8.31	0.4%
	Test 4	2	2	8.41	8.13	-3.3%
	Test 5	1	1	8.41	8.41	0.0%
	Test 6	2	2	9.06	8.72	-3.8%
MIZ Quad Site 4	Test 1	3	3	7	5.16	-26.3%
	Test 2	3	3	7.19	5.19	-27.8%
	Test 3	3	3	7.19	5.28	-26.6%
	Test 4	3	3	7	7.13	1.9%
	Test 5	1	1	7.31	7.16	-2.1%
	Test 6	2	3	7.25	7.38	1.8%
MIZ Quad Site 5	Test 1	2	2	8.63	8.69	0.7%
	Test 2	2	2	8.63	8.69	0.7%
	Test 3	3	3	8.75	7.41	-15.3%

5.4 Influence of In-situ Instrumentation Coupling in the Presence of a Strong, Nearby Noise Source

All the $HVSR_{Res}$ used in this section to compare the influence of in-situ coupling condition under strong, nearby noise sources on the HVSR measurements were $HVSR_{Grilla}$ (i.e., automatically selected by the *Grilla* software based on the highest peak)

5.4.1 Qualitative Assessments of HVSR Due to Construction Noise

The variability of the HVSR results was investigated under conditions of strong construction noise. A total of 23 noise measurements across five sites were analyzed for this portion of the study. Four scenarios were considered: (1) Acquisition close to a construction site with strong construction noise (CN). (2) Acquisition close to a construction site without strong construction noise (QN). (3) Acquisition at a distance from a construction site with strong construction noise (CD). (4) Acquisition at a distance from a construction site without strong construction noise (QD).

Sites were classified as "close" if a site was located within 65 feet of the construction site, and as "at a distance" if it was farther than 65 feet. The 65-foot threshold was chosen based on a distinct break in the site location distances used in the study. Assessments of HVSR data quality categories are presented in Figure 40. When data acquisition occurred “near” and “on grass”, acquisition categorization showed that 75% of the HVSR curves were easy to interpret (Categories 1 and 2). On the contrary, acquisitions that took place “near” the active construction site and “on concrete” showed that only 50% of the HVSR fell into Categories 1 or 2. Test sites that were at a distance from the construction noise produced HVSR values that typically fell in the medium quality (Category 2) to low quality (Category 3) HVSR curves. The lower quality tests are most likely attributed to factors other than the construction noise, such as proximity to buildings, which will be discussed in Section 5.5.

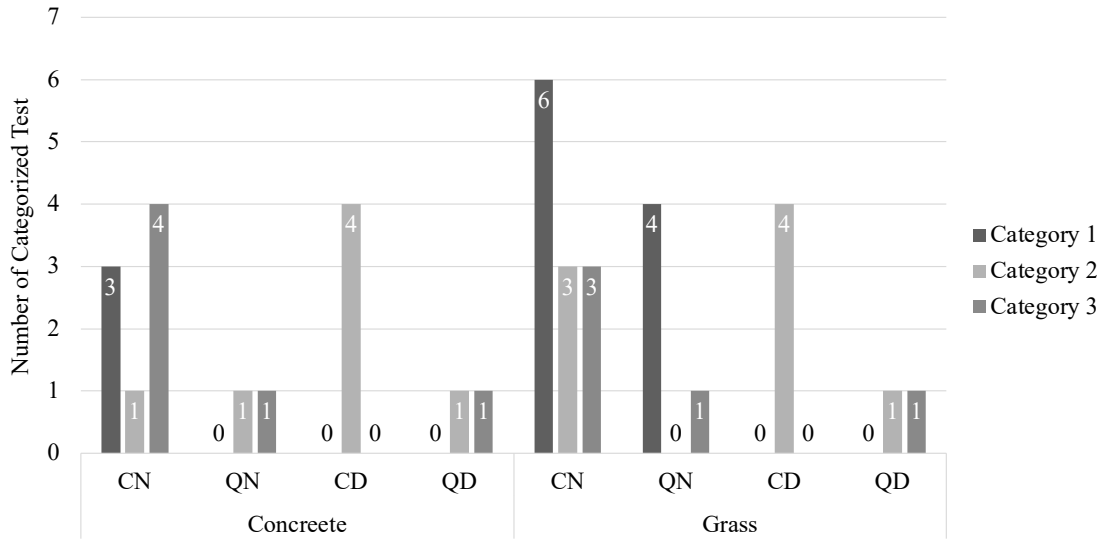

Figure 40: Quantitative assessment of test categorization based on presence of construction noise and distance from construction site

5.4.2 Quantitative Assessments of HVSR Due to Construction Noise

To further assess variability due to construction noise, a reference frequency was established for each site. Reference frequencies are the expected frequency value for the site. These values were determined using available boring logs and the depth-to-bedrock relationships presented by Chi (2022). When boring logs were unavailable, reference frequencies were selected based on reasonable fits with the Chi (2022) relationship. These reference frequencies were used to compute the percent difference between the $HVSR_{Grilla}$ HVSR peak and the reference frequency, for each test. The data are summarized in Table 7. Additionally, each test was plotted against the reference frequency to illustrate variability due to strong construction noise. These plots are shown in Figure 41 and Figure 42.

Figure 41 and Figure 42 demonstrate the reliability of repeat test results under different scenarios of proximity and noise levels. As observed in Figure 41, most of the repeat measurements where variability beyond 5% (7 out of 8) was observed were from measurement on concrete ($HVSR_{Concrete}$) in the presence of construction noise. $HVSR_{Grass}$

represents only 17% of the HVSR repeat measurements that were beyond 5% variability from the reference value when construction noise was present. Table 7 further categorizes the sites and lists the computed percent differences in frequency.

Table 7: Classifications and Categorization of Site with Selected Baseline and Percent Different Calculation

Location Name	Repeat Test No.	Prox.to Construction	Construction Noise Class	CAT		$HVSR_{Grilla}$ [Hz]		Ref. Freq [Hz]	% Diff. Grass to Ref.	% Diff. Conc to Ref.
				Grass	Concrete	Grass	Concrete			
Animal Hospital 1	Test 1	Close	CN	2	1	8.13	9.06	9.56	-14.96 %	-5.23 %
	Test 2		CN	1	1	8.88	8.28		-7.11%	-13.39 %
	Test 3		CN	2	2	9.38	10.63		-1.88%	11.19 %
	Test 4*		QN	1	2	9.56	9.53		0.00%	-0.31 %
MIZ Quad Site 4	Test 1	Close	CN	3	3	7	5.16	7	0.00%	-26.29 %
	Test 2		CN	3	3	7.19	5.19		2.71%	-25.86 %
	Test 3		CN	3	3	7.19	5.28		2.71%	-24.57 %
	Test 4*		QN	3	3	7	7.13		0.00%	1.86 %
	Test 5		CN	1	1	7.31	7.16		4.43%	2.29 %
	Test 6		CN	2	3	7.25	7.38		3.57%	5.43 %
MIZ MiddleQuad	Test 1	Close	CN	1	-	7.09	-	7.13	-0.56%	-
	Test 2		CN	1	-	7.16	-		0.42%	-
	Test 3		CN	1	-	7.06	-		-0.98%	-
	Test 4*		QN	1	-	7.13	-		0.00%	-
	Test 5		QN	1	-	7.13	-		0.00%	-
	Test 6		QN	1	-	7.13	-		0.00%	-
	Test 7		CN	1	-	7	-		-1.82%	-
Animal Hospital 2	Test 1	Distance	CD	2	2	6.88	6.88	7.06	-2.55%	-2.55 %
	Test 2		CD	2	2	7.09	7.03		0.42%	-0.42 %
	Test 3*		QD	2	2	7.06	7.03		0.00%	-0.42 %
MIZ Quad Site 5	Test 1	Distance	CD	2	2	8.63	8.69	8.75	-1.37%	-0.69 %
	Test 2		CD	2	2	8.63	8.69		-1.37%	-0.69 %
	Test 3*		QD	3	3	8.75	7.41		0.00%	-15.31 %

The results indicate that construction noise can significantly impact the variability of HVSR measurements, particularly on concrete surfaces. When exposed to strong construction noise, data collected on concrete exhibited greater variability compared to data collected on grass. This trend, illustrated in Figure 41, shows the percent difference from the reference frequency for "close" sites. Figure 42 indicates that construction noise is usually not an issue for "at a distance" sites, where the construction noise may be a good source of ambient noise. Ultimately, these findings suggest that proximity to strong construction noise introduces variability to HVSR measurements performed on concrete, but did not have much influence on $HVSR_{Grass}$. This is an important caveat to the prior findings that concrete coupling did not affect the quality of the HVSR measurements. A more detailed discussion on the influence of construction noise is provided in Chapter 6.

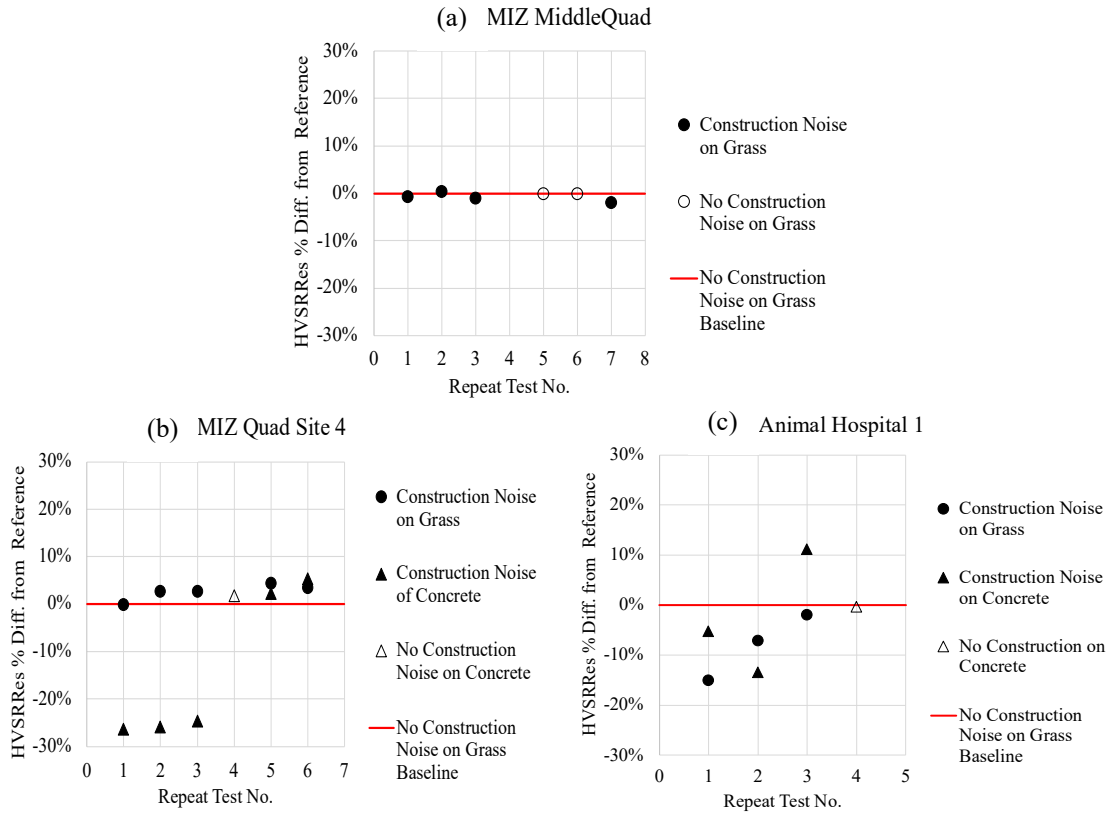

Figure 41: Percent Difference of $HVSR_{Res}$ to Selected Baseline $HVSR_{Res}$ for Sites Classified as "Close": (a) MIZ MiddleQuad (b) MIZ Quad Site 4 (c) Animal Hospital 1.

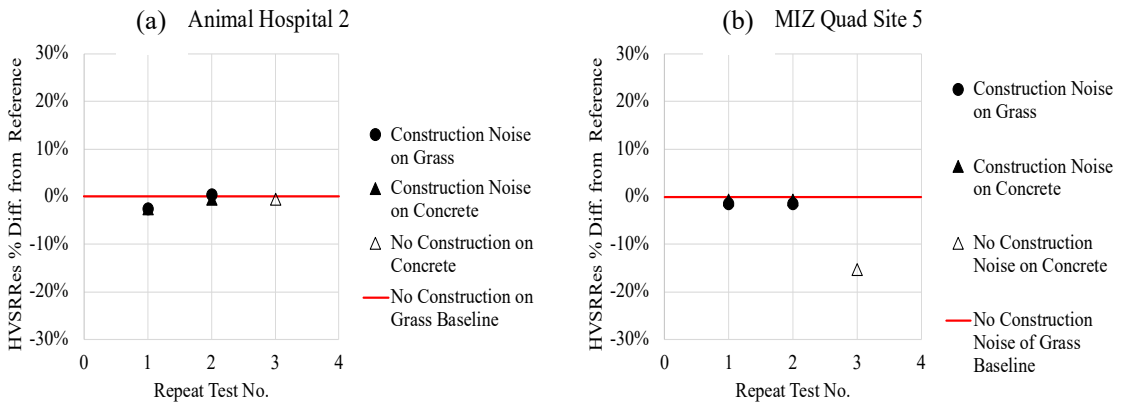

Figure 42: Percent Difference of $HVSR_{Res}$ to Selected Baseline $HVSR_{Res}$ for Sites Classified as "Distance": (a) Animal Hospital 2 (b) MIZ Quad Site 5.

5.5 Influence of Proximity to Buildings on HVSR Measurements

All the $HVSR_{Res}$ used in this section to assess the proximity of buildings on the HVSR measurements were $HVSR_{Grilla}$ values.

5.5.1 Qualitative Assessments of HVSR due to Proximity to Buildings

Guidelines provided by SESAME (2005) recommend conducting measurements at locations sufficiently distant from buildings to minimize their influence on data acquisition. To investigate the impact of proximity to buildings, 32 tests were analyzed across six different sites. Each site was categorized based on its distance from the nearest building. No explicit distance recommendations are provided by SESAME (2005), while some studies presented findings that correlated the building height to an influence distance (e.g., Mucciarelli et al., 1997; Gallipoli et al., 2004; Chatelain et al., 2008). The data were classified into three proximity groups (Near, Intermediate, and Far) as shown in Table 8.

HVSR measurements were conducted around buildings that were three to four stories in height, typically ranging from 30 to 50 ft (approximately 9 to 15 m). According to Mucciarelli et al. (1997), the influence of buildings diminishes at a horizontal distance

equal to the building height. As a result, sites located farther than 50 ft (15 m) from the buildings were classified into the “Far” group. Sites within 50 ft of a building were categorized as "Near" or "Intermediate" based on a distinct break in the site location distances used in the study.

Table 8: Proximity to Building Grouping Criteria

Near	Intermediate	Far
$d \leq 8$ ft	8 ft $< d \leq 50$ ft	$d > 50$ ft

After assigning each test to a proximity group, the HVSR curves were evaluated and categorized as described in Section 5.2. The occurrence rate of tests assigned to each category was analyzed within each proximity group to assess the reliability of HVSR measurements relative to building proximity. The results are shown in Figure 43 and summarized in Table 9.

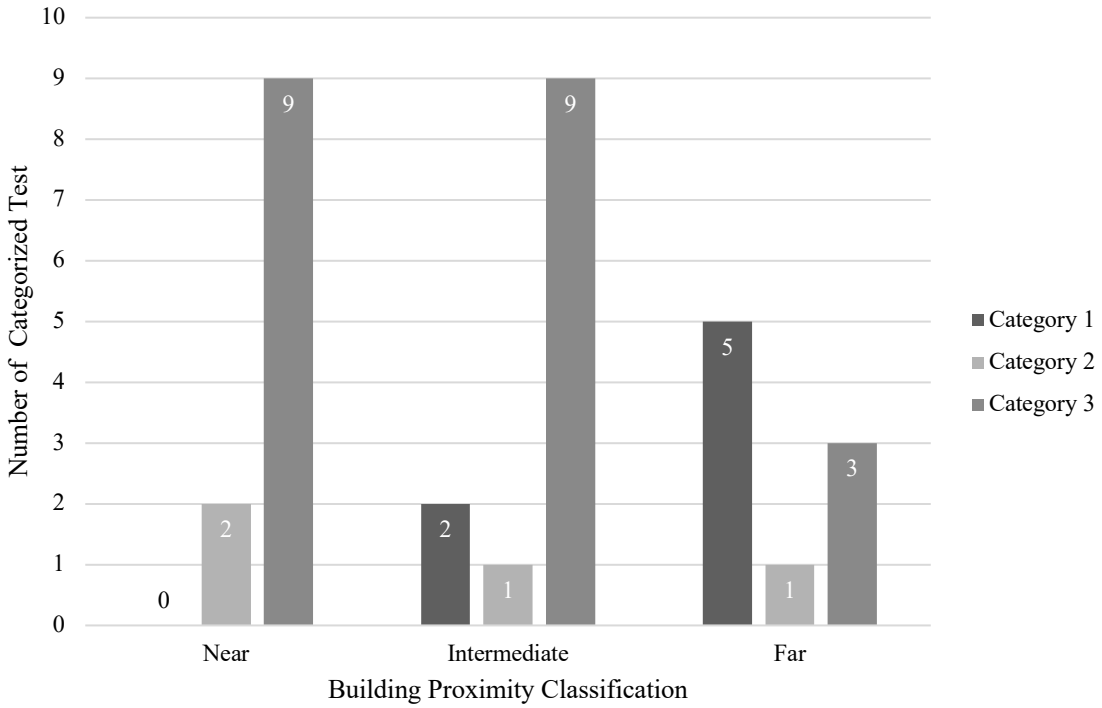

Figure 43: Data quality Category as a function of the building proximity.

Table 9: Data quality Category separated into building proximity groupings

CAT No.	Near	Intermediate	Far
1	0	2	5
2	2	1	1
3	9	9	3

The results indicate that as the proximity to buildings decreases, the quality of the HVSR curve tends to degrade. For example, the "Near" group exhibited the highest number of Category 3 (low quality) curves, while the "Far" group had the highest number of Category 1 (high quality) curves. Additionally, the average categorization values for each proximity group (Table 10) reveals a trend of decreasing quality with decreasing distance to buildings. The "Far" group had the lowest average category number (1.78), indicating higher quality HVSR curves, whereas the "Near" group had the highest average category number (2.82).

Table 10: Average Acquisition Category Number for Each Proximity Grouping

	Near	Intermediate	Far
CAT No. Average	2.82	2.58	1.78

5.5.2 Quantitative Assessments of HVSR due to Proximity to Buildings

To evaluate variability, a reference frequency was selected using the same method as in previous analyses. The percent differences of the measured frequencies relative to reference values were calculated. The percent differences are summarized in Table 11 and shown in Figure 44. The results demonstrate that repeat measurements variability is small for measurements in the "Far" group. In contrast, sites in the "Near" and "Intermediate" groups show higher variability, as evidenced by larger deviations from the reference frequencies. The large differences are likely due to frequencies emanating from the

building dominating the HVSR results and producing large differences from the expected stratigraphy based frequencies.

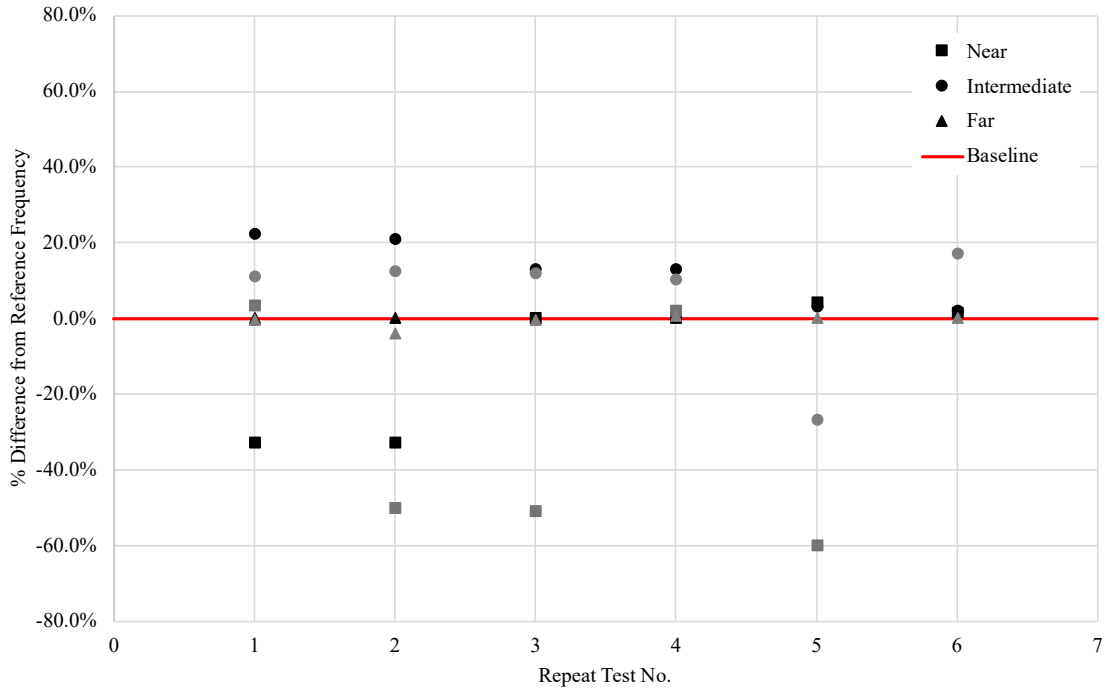

Figure 44: Percent difference of select sites from the reference value for repeated test

Table 11: Results from repeat measurements with different proximity to buildings

Location Name	Proximity to Building	Repeat Test No	CAT No.	$HVSR_{Grilla}$ (Hz)	Reference Frequency (Hz)	% Diff from Baseline
			Grass	Grass		
Ellis Library BH-03 A	Near	Test 1	3	4.75	7.09	-33.0%
		Test 2	3	4.75		-33.0%
		Test 3	3	7.09		0.0%
		Test 4	3	7.09		0.0%
		Test 5	2	7.38		4.1%
		Test 6	2	7.19		1.4%
Lee's Hall Selected	Near	Test 1	3	14.88	14.40	3.3%
		Test 2	3	7.19		-50.1%
		Test 3	3	7.06		-51.0%
		Test 4	3	14.69		2.0%
		Test 5	3	5.75		-60.1%
Ellis Library BH-01	Intermediate	Test 1	3	6.22	5.09	22.2%
		Test 2	3	6.16		21.0%
		Test 3	3	5.75		13.0%
		Test 4	3	5.75		13.0%
		Test 5	1	5.25		3.1%
		Test 6	1	5.19		2.0%
Journalism B-06 A	Intermediate	Test 1	3	7.72	6.95	11.1%
		Test 2	3	7.81		12.4%
		Test 3	3	7.78		11.9%
		Test 4	2	7.66		10.2%
		Test 5	3	5.09		-26.8%
		Test 6	3	8.13		17.0%
MIZ MiddleQuad*	Far	Test 4	1	7.13	7.13	0.0%
		Test 5	1	7.13		0.0%
		Test 6	1	7.13		0.0%
MIZ Quad Site 1	Far	Test 1	3	6.81	6.84	-0.4%
		Test 2	3	6.56		-4.1%
		Test 3	3	6.81		-0.4%
		Test 4	1	6.88		0.6%
		Test 5	2	6.84		0.0%
		Test 6	1	6.84		0.0%

*Note : (*) indicates site was into 450 ft of construction site so selected test were when no construction was present

5.6 Influence of Time of Day with Building Proximity

Although no specific guidelines address the influence of building occupancy on HVSR measurements, recommendations from SESAME (2005) and the Tromino User's Manual (MoHo S.R.L, 2020) suggest conducting measurements in a quiet environment. To

evaluate the effect of building occupancy on HVSR data variability, 23 tests were analyzed. These data were collected from two sites from the "Near" grouping and two sites in the "Intermediate" grouping. Measurements were performed both during operating hours and non-operating hours. Tests were classified as “Occupied” measurements (Occ.) which occurred during the building normal operating hours. This time corresponded to high ambient noise levels and presumably high building noise levels. “Unoccupied” measurements (NOcc.) were typically performed very early in the morning (4 A.M. – 7 A.M.) when the building was likely unoccupied and ambient noise levels were also low due to lack of traffic noise and other activity (the exact times of each acquisition are provided in APPENDIX F). The $HVSR_{Res}$ used in this section to assess the influence of building occupancy status on the HVSR measurements were both the software selected values ($HVSR_{Grilla}$) as well as manually selected HVSR values ($HVSR_{Man}$) determined from examining the direction spectra separately.

5.6.1 Qualitative Assessments of HVSR Due to Occupancy Status

Of the 23 tests, 10 were conducted during occupancy, while 13 occurred during non-occupancy. The results were also separated by proximity groupings, as shown in Figure 45 and Table 12.

The data suggest that the most challenging scenario for obtaining reliable results occurs during non-business hours (i.e., non-occupied buildings). Measurements collected during business hours (i.e., occupied buildings) yielded four easily interpreted results, compared to only one in non-occupied buildings. This highlights a weak but consistent trend suggesting that measurements during occupancy may produce more reliable data.

Possible reasons for this observation are presented in Influence of Proximity to Buildings in Section 6.1.3.

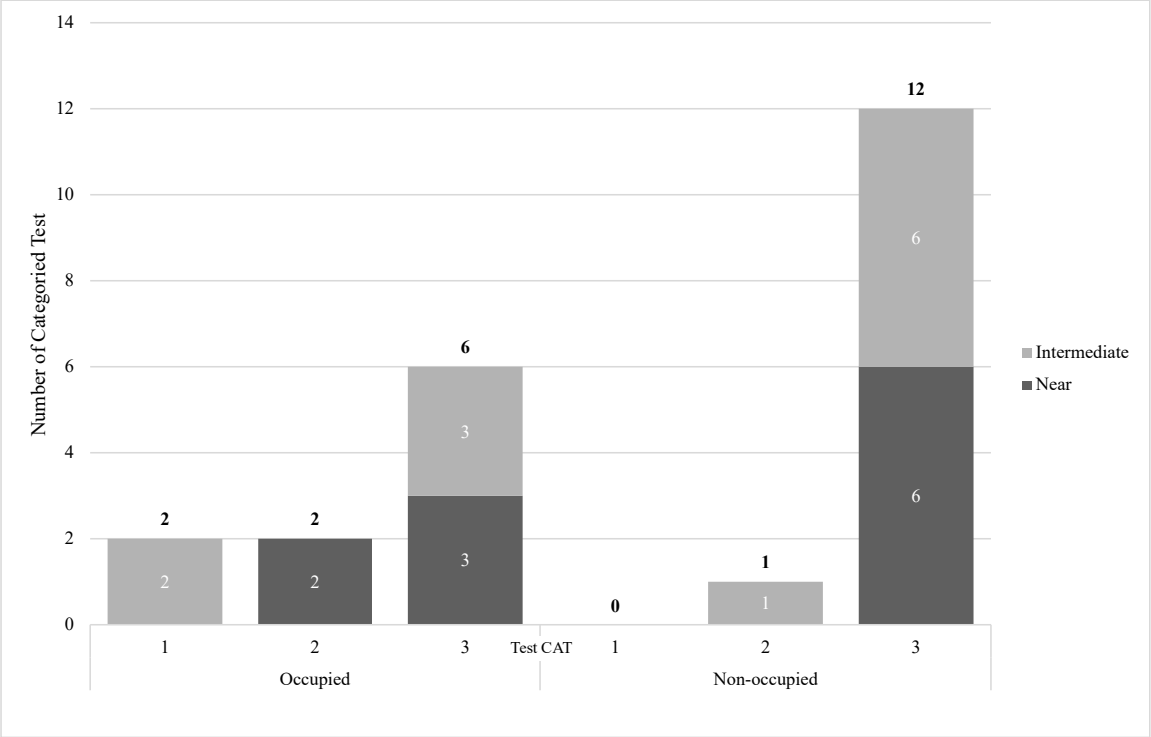

Figure 45: Data quality Category as a function of building occupancy and proximity

Table 12: Amount of Categorized test depending on building occupancy and proximity grouping

Occupancy	CAT No.	Near	Intermediate	Total
Occ.	1	-	2	2
	2	2	-	2
	3	3	3	6
NOcc.	1	-	-	-
	2	-	1	1
	3	6	6	12

5.6.2 Quantitative Assessments of HVSR Due to Occupancy Status

A percentage difference calculation was used to assess the influence of occupancy status of a building on HVSR measurements. The percent difference was computed between the $HVSR_{Grilla}$ and $HVSR_{Man}$ to the corresponding reference frequency (i.e., expected values). Results of the calculations can be found in Table 13. Some HVSR curves

exhibited multiple peaks (Category 3), so the manual method was used to see if the natural peak could be identified versus artificial peaks (as detailed in Section 3.4).

Manual inspection of the HVSR curves was often required to identify the true natural peak, as in some cases a large artificial peak was selected by the *Grilla* software because it was the highest peak. For example, Figure 46 shows a case where the $HVSR_{Grilla}$ peak was selected at 4.75 Hz, while the $HVSR_{Man}$ identified the a peak at 7.09 Hz using the procedure described in Section 3.4. Conversely, Figure 47 demonstrates a situation where *Grilla* successfully selected the natural peak at 7.09 Hz only because it was slightly higher. Figure 48 and Figure 49 show cases where time-of-day (i.e., building occupancy) influenced the $HVSR_{Grilla}$ selection and where use of $HVSR_{Man}$ would provide an improved interpretation.

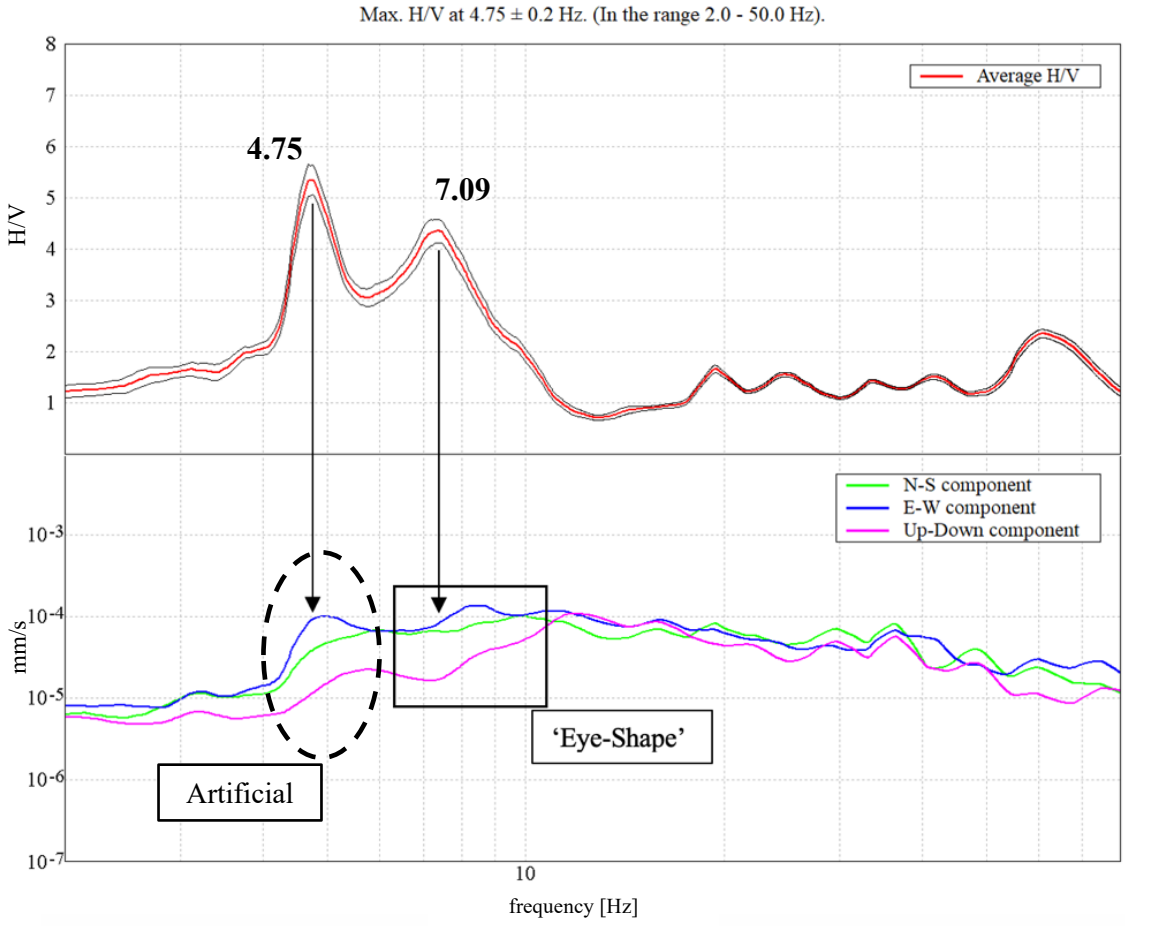

Figure 46: HVSR curve (top) and amplitude spectra (bottom) plots (Ellis Library BH-03 A, Test 2 on Grass site) is an example of when the *Grilla* software selected an $HVSR_{Res}$ (4.75 Hz) that was produced by artificial peaks in the amplitude spectra plots. Manual interpretation would indicate that 4.75 Hz is the incorrect $HVSR_{Res}$ because it is not associated with an 'eye-shape' in the amplitude spectra plots. The $HVSR_{Res}$ determined by manual interpretation would be selected as 7.09 Hz due to the 'eye-shape' that was also selected by determining the 'eye-shape' due to manual interpretation.

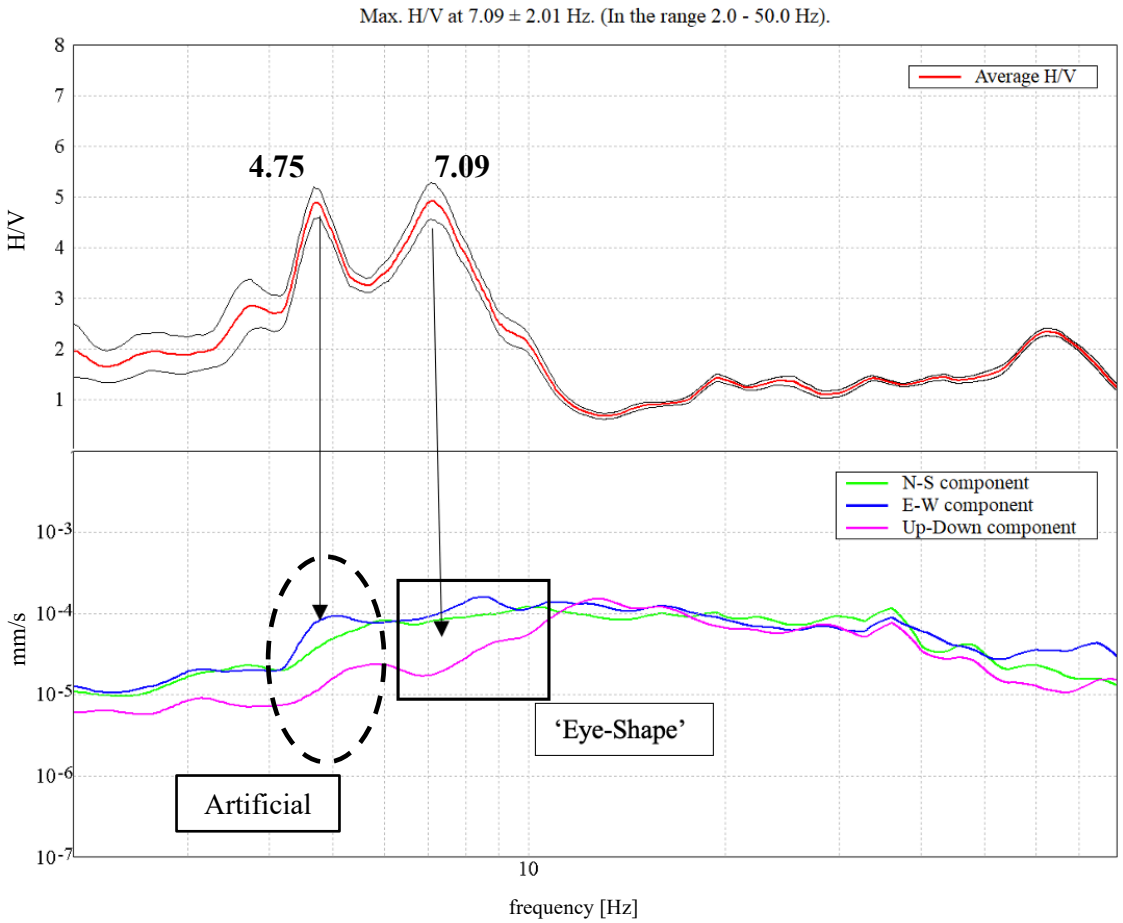

Figure 47: HVSR curve (top) and amplitude spectra (bottom) plots (Ellis Library BH-03 A, Test 4 on Grass site) is an example of when the *Grilla* software selected an $HVSR_{Res}$ (7.09 Hz) that was also selected by determining the 'eye-shape' due to manual interpretation. *Grilla* software did not select 4.75 Hz due to the amplitude being less than the 7.09 $HVSR_{Res}$.

Table 13: Percent Difference of Grilla Selected Frequency and Manual Inspection Frequency to Reference Frequency for Sites Assigned to Building Proximity Groupings "Near" and "Intermediate"

Location Name	Proximity Group	Repeat Test No.	CAT No.	Occupancy Status	$HVSR_{Grilla}$ (Hz)	$HVSR_{Man}$ (Hz)	Ref.* Frequency (Hz)	$HVSR_{Grilla}$ % Diff from Reference Frequency	$HVSR_{Man}$ % Diff from Reference Frequency
					Grass	Grass	Grass		
Ellis Library BH-03 A	Near	Test 1	3	NOcc.	4.75	7.31	7.09	-33.0%	3.1%
		Test 2	3	NOcc.	4.75	7.42		-33.0%	4.7%
		Test 3	3	NOcc.	7.09	7.09		0.0%	0.0%
		Test 4	3	NOcc.	7.09	7.09		0.0%	0.0%
		Test 5	2	Occ.	7.38	7.37		4.1%	3.9%
		Test 6	2	Occ.	7.19	7.25		1.4%	2.3%
Lee's Hall Selected	Near	Test 1	3	Occ.	14.88	14.47	14.40	3.3%	0.5%
		Test 2*	3	Occ.	7.19	14.53		-50.1%	0.9%
		Test 3	3	NOcc.	7.06	14.07		-51.0%	-2.3%
		Test 4*	3	NOcc.	14.69	14.69		2.0%	2.0%
		Test 5 *	3	Occ.	5.75	Inconclusive		-60.1%	-
Ellis Library BH-01	Intermediate	Test 1	3	NOcc.	6.22	6.2	5.09	22.2%	21.8%
		Test 2	3	NOcc.	6.16	6.15		21.0%	20.8%
		Test 3*	3	NOcc.	5.75	6.55		13.0%	28.7%
		Test 4*	3	NOcc.	5.75	6.24		13.0%	22.6%
		Test 5	1	Occ.	5.25	5.25		3.1%	3.1%
		Test 6	1	Occ.	5.19	5.19		2.0%	2.0%
Journalism B-06 A	Intermediate	Test 1	3	Occ.	7.72	7.74	6.95	11.1%	11.4%
		Test 2	3	Occ.	7.81	7.84		12.4%	12.8%
		Test 3	3	Occ.	7.78	7.78		11.9%	11.9%
		Test 4	2	NOcc.	7.66	7.67		10.2%	10.4%
		Test 5	3	NOcc.	5.09	5.11		-26.8%	-26.5%
		Test 6	3	NOcc.	8.13	8		17.0%	15.1%

*Note: reference frequencies are the expected value based on site conditions

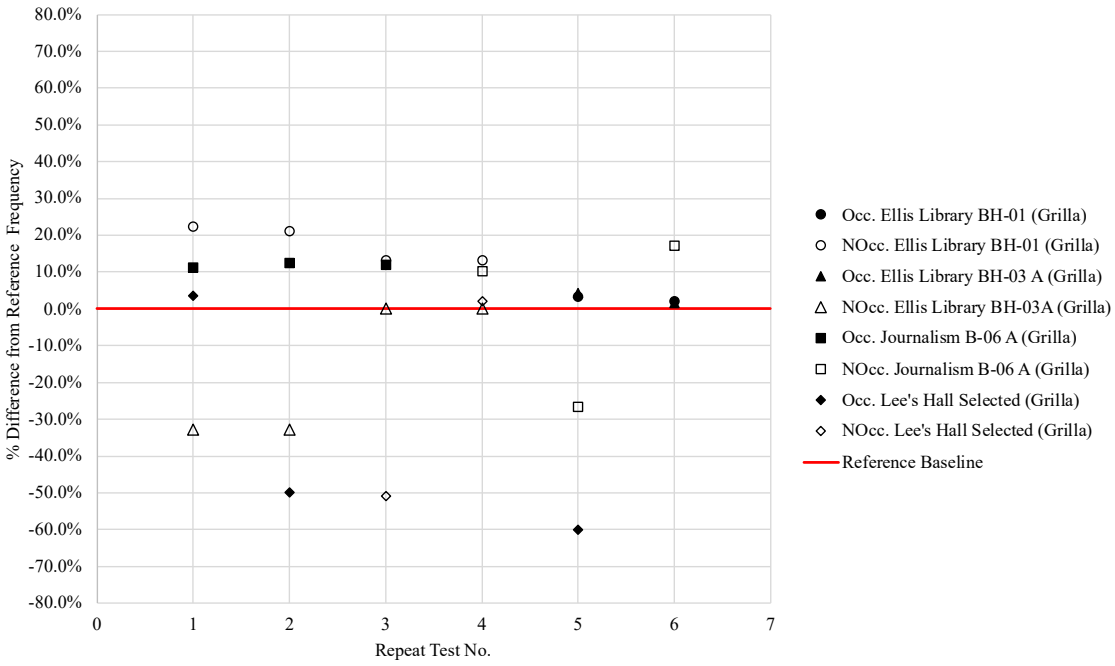

Figure 48: $HVSR_{Grilla}$ percent difference from reference frequency for selected sites (Open symbols: non-occupied. Closed symbols: occupied)

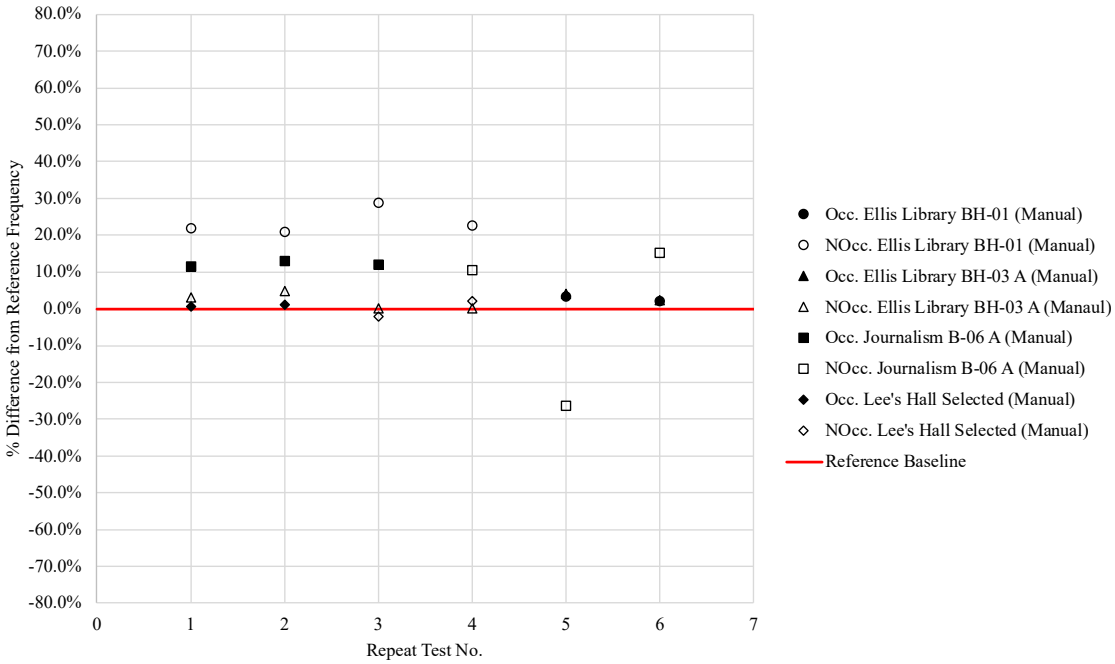

Figure 49: $HVSR_{Man}$ percent difference from reference frequency for selected sites (Open symbols: non-occupied. Closed symbols: occupied)

The results, presented in Figure 48 and Figure 49, indicate that building occupancy significantly influences the reliability of HVSR data. Analysis using automated peak selection ($HVSR_{Grilla}$) revealed that, for measurements during off-hours (unoccupied buildings) 77% (10 out of 13) of repeated measurements exhibited a variability greater than 5% from the reference frequency. In contrast, measurements during normal business hours (occupied buildings), only 50% (5 out of 10) of the acquisitions showed variability exceeding 5%. These findings suggest that measurements collected during hours of building occupancy generally yielded more consistent results. Reason for this observation are discussed in Chapter 6.

Figure 49 demonstrates that $HVSR_{Man}$ has the capability to reduce variability in certain scenarios. Under unoccupied building conditions, $HVSR_{Man}$ decreased the proportion of repeated tests showing variability greater than 5% from 77% to 53%. A similar reduction was observed for measurements performed during building occupancy hours, where the percentage of repeated measurements with variability exceeding 5% dropped from 50% to 40%.

These findings highlight the potential of manual HVSR analysis to improve data consistency and will be discussed in greater depth in Chapter 6.

5.7 Summary

In this chapter, variability findings of HVSR maximum peak frequencies based on 76 noise exposures across 16 sites and a total of 126 acquisitions were presented. The investigation focused on four primary factors: in-situ instrumentation surface coupling (concrete vs. grass), influence of a strong, nearby noise source, proximity to buildings, and

measurement time-of-day (i.e., building occupancy) during acquisition. These findings are summarized below.

1. In-situ Instrumentation Surface Coupling (Concrete vs. Grass):
    - The variability in HVSR measurements between concrete and grass was generally minor (0% - 2%) when $HVSR_{Concrete}$ and $HVSR_{Grass}$ were both of high quality (51% of the tests).
    - Notable variability was observed when both $HVSR_{Concrete}$ and $HVSR_{Grass}$ were classified as Category 3, suggesting that other factors are likely the primary source of the variability.
2. Influence of Strong Construction Noise:
    - Strong construction noise had a minimal impact on HVSR measurements taken on grass, with only 2 test showing variability in $HVSR_{Res}$, from the referncee value, that was greater than 5%.
    - A more important observation taken from this study was that larger variability was observed for $HVSR_{Concrete}$ measurements under similar noise conditions (88%).
3. Proximity to Buildings:
    - Results indicated increased variability in HVSR data at sites located closer to buildings.
    - The influence of building was more pronounced at “near” and “intermediate” sites (0 – 50ft). Multiple peaks were observed in the HVSR curves, one likely from the building vibrations and one from ambient noise. The various peaks

result in low quality acquisitions with potential large errors in the interpreted frequency (especially if automated methods are used).

4. Building Occupancy:
    - Repeat measurements conducted near occupied buildings were less variable (50% variability) compared to those taken near unoccupied buildings (77% variability).
    - Manual interpretation of HVSR curves showed a decrease in the variability from the reference frequency (i.e., expected value) for all measurements, both occupied and unoccupied.

The findings underscore the importance of considering environmental and site-specific factors when conducting HVSR measurements. While some variability is unavoidable, the results highlight the need for careful interpretation of data, particularly in urban settings. These findings will be discussed in the next chapter.

6. DISCUSSION

6.1 Introduction

The main objective of this thesis was to perform qualitative and quantitative assessments of four potential influences on HVSR variability in urban environments as follows: (1) The influence of in-situ instrumentation surface coupling (concrete versus grass), (2) the influence of in-situ coupling with strong, nearby noise sources, (3) the effect of building proximity, and (4) the influence of time of day in combination with building proximity (i.e., building occupancy). In this chapter, results presented in Chapter 5 are discussed and the findings are compared to past studies before suggestions for future studies are discussed.

6.1.1 Influence of In-situ Instrumentation Coupling (Concrete vs. Grass)

The results demonstrated minimal variability in $HVSR_{Res}$ between measurements conducted on concrete and grass surfaces, except in cases where both surfaces produced low quality (Category 3) HVSR curves. These findings suggest that surface type does not significantly influence HVSR results under normal conditions. This finding is in agreement with the SESAME (2005) guidelines and supporting literature (Koller et al., 2004 and Chatelain et al., 2008) but contradicts recommendations from equipment manufacturer MoHo S.R.L.

For instances of increased variability, the likely cause is subsurface complexity or other factors rather than the surface material itself. This result emphasizes the need to carefully analyze Category 3 curves, as these are likely influenced by more complex factors (i.e., subsurface complexity, buildings, environmental conditions, etc.).

6.1.2 Influence of In-situ Instrumentation Coupling in the Presence of a Strong, Nearby Noise Source

Contrary to expectations, the influence of in-situ instrumentation coupling in the presence of a strong, nearby noise source (strong construction noise) had a minimal impact on repeated measurements performed on grass ($HVSR_{Grass}$). However, repeated measurements performed on concrete ($HVSR_{Concrete}$) near construction noise showed greater variability, likely due to coupling of the propagation of vibrations through the concrete with low amounts of attenuation. These observations partially support the recommendations produced by SESAME (2005), MoHo S.R.L (2020), and supporting literature (e.g., Koller et al., 2004; Chatelain et al., 2008; Mihaylov et al., 2016) but provide some additional nuance. The findings suggest that in-situ conditions are a factor of influence in the HVSR variability in the presence of strong noise sources. If data acquisition occurs near a strong noise source, an instrumentation-grass coupling typically produces HVSR measurements with low variability, likely to do the excess noise attenuating before reaching the instruments. On the other hand, instrumentation-concrete coupling showed that attention may not be occurring in the concrete resulting in HVSR measurement variability.

6.1.3 Influence of Proximity to Buildings

Proximity to buildings was found to be a significant source of variability in HVSR measurements. The closer a measurement site was to a building, the more likely it was for building-induced frequencies to influence the HVSR data. Additionally, transient and ambient noise from the building environment contributed to the observed variability. These findings highlight the need for users to consider building proximity when conducting

HVSR measurements in urban environments. Measurements taken near buildings should be supplemented by careful manual inspection to differentiate between the natural HVSR subsurface peak and other artificial building-induced peaks. The results indicated that minimal variability in measurements was observed when the distance from the building was approximately the same as the building height which agrees with Mucciarelli et al. (1997). The overall observation aligns with SESAME (2005) and MoHo S.R.L (2020), reinforcing the importance of maintaining sufficient distance from buildings to obtain reliable HVSR measurements.

6.1.4 Influence of Time of Day with Building Proximity

The investigation of building occupancy revealed slight but notable differences in the reliability of HVSR measurements based on whether data acquisition occurred during a building's operating or non-operating hours. Tests were classified as "Occupied" measurements (Occ.) which occurred during the building's normal operating hours which was also a time when ambient noise levels were high. "Unoccupied" measurements (NOcc.) were typically early in the morning (4 A.M. – 7 A.M.) when the building was likely unoccupied and ambient noise levels were low. Measurements taken during operating hours generally produced higher quality HVSR results.

Additionally, it was observed that manual inspection of the HVSR curves reduced the amount of variability in both the occupied and unoccupied cases. The decrease in variability through manual inspection is a result of $HVSR_{Grilla}$ selecting the absolute maximum peak in the HVSR curve which is not always consistent with the $HVSR_{Res}$. In some cases, typically unoccupied building HVSR tests, building frequencies dominated the time record, often resulting in large artificial peaks in the HSVR plot. Manual inspection

often allowed for the artificial peaks to be identified and disregarded during interpretation. This highlights the importance of human inspection of the directional spectra when analyzing HVSR data near structures.

A general observation was that some of the most accurate data, when compared to the expected results, was observed when ambient noise conditions were increased (i.e., pedestrian and roadway traffic), even though data was being acquired before the normal operating hours of the building.

Neither SESAME (2005) nor MoHo S.R.L (2020) provides recommendations on this specific influence; however, they do recommend that data acquisition take place a distance from the building and when noise levels are low. The findings from this study would suggest that, if HVSR measurement must be acquired within 50 ft of a building, high ambient noise levels are recommended regardless of the occupancy status of the building.

6.2 Future Studies

This research examined four sources of variability in the HVSR method, providing a foundation for future investigations aimed at improving HVSR guidelines and applications. The following areas of research are recommended to address key challenges identified in this study.

6.2.1 Influence of Building Proximity and Height

This study observed that proximity to buildings significantly affected HVSR measurements. Future research should investigate how building height influences these effects, enabling the development of distance guidelines that account for building height. Previous studies have suggested a correlation between building height and the distance at

which its influence on HVSR data is observed. However, current HVSR guidelines do not provide recommendations for incorporating building height into data acquisition or for identifying conditions under which measurements may become unreliable. For instance, acceptable HVSR results might be obtained at a certain distance from a tall building during calm weather, but the presence of wind could result in a magnification of the building frequency and introduce significant variability. A study combining distance and environmental criteria would improve the robustness of HVSR guidelines.

6.2.2 Software Processing Parameters

The study presented in this thesis used the default parameters for data processing. A study was not conducted to investigate how data processing parameters could affect the variability of the HVSR results. A future study could involve varying window size, smoothing, acquisition length, and acquisition frequency to determine if data variability can be reduced through better processing procedures.

6.2.3 Subsurface Complexity and Variability

This study found that sites classified as Category 3 exhibited significant variability, which could possibly be attributed to complex subsurface conditions. The study herein did not look directly at the variability caused by the subsurface complexity, rather, the borings were used to help determine a reference value for qualitative analysis. To address possible variability as a result of subsurface complexity and variability, future investigations should incorporate detailed geotechnical analyses, such as borehole logging or seismic refraction studies, to establish clearer correlations between subsurface heterogeneities and HVSR variability. Such studies could provide new insights into how layered or irregular geology

influences HVSR measurements, ultimately improving data interpretation in complex urban environments.

6.2.4 Azimuthal Variability Analysis

The data in this study used the North-South and East-West HVSR measurements, but the data can be resolved into any direction. Resolving the measures in different azimuthal directions has been shown to produce HVSR peaks that are direction dependent. A future study should investigate this issue, especially around buildings where noise directions relative to the building and receiver locations could be especially important.

6.3 Summary

Discussions of observation of four influences on the HVSR method in urban environments were presented in this chapter as follows: (1) The influence of in-situ instrumentation surface coupling, particularly comparing concrete and grass surfaces, revealed that coupling was not a significant issue. Instead, the variability in HVSR measurements was likely caused by other factors. (2) The influence of in-situ coupling with strong, nearby noise sources demonstrated that measurements taken on concrete surfaces exhibited greater variability. This was possibly attributed to the lower attenuation of construction vibration through the concrete medium. (3) The effect of building proximity was analyzed, with results indicating that the further the measurement was taken from buildings, the higher the quality of the HVSR results and the lower the variability. (4) The influence of time of day in combination with building proximity (i.e., building occupancy) was examined. It was concluded that building occupancy itself may not significantly affect measurements. Instead, ambient noise levels played a more substantial role in contributing to variability. This section also highlighted the importance of manual inspection of HVSR

curves, as artificial peaks could be identified and disregarded from the analysis, thereby reducing variability. Finally, the chapter concluded with suggestions for future studies based on observations from this research that could not be further investigated within the scope of the current work.

7. CONCLUSION

7.1 Summary

Geotechnical site investigation is a critical step of an engineering project (e.g., depth to bedrock for support of structures). A wide range of geotechnical investigation techniques are used for investigation, some intrusive (e.g., SPT, CPT) while others are non-intrusive (e.g., seismic refraction, electrical resistivity, GPR). One such geophysical method has recently gained popularity for subsurface investigative purposes, the Horizontal-to-Vertical Spectral Ratio (HVSR) method. This single-station geophysical technique usage has increased due to the relatively low cost and the ease of deployment. The HVSR method does not require an active source, rather it uses ambient noise to obtain subsurface information. With no requirement for an active noise source (i.e., Earthquake-Simulating Truck, hammer impact, etc.), the HVSR method can be set up and complete data acquisition in a matter of minutes.

The primary object of this paper is to provide qualitative and quantitative assessments of four potential influences on HVSR variability in urban environments by assessing the influence of in-situ coupling conditions (concrete versus grass), the influence of in-situ coupling conditions in the presence of strong nearby noise (construction), the proximity to buildings, and the time of day with building proximity. Each of these factors was analyzed to provide practical insights into the applicability and limitations of the HVSR method for urban geotechnical and seismic assessments.

A total of 126 data acquisitions were performed around the University of Missouri-Columbia campus to study the influence of the HVSR method. A Tromino device (MoHo S.R.L) was used for data acquisition for this study. The acquired data was processed,

analyzed, and interpreted in *Grilla* software which was developed by the Tromino manufacturer. The findings for each of the four research questions are summarized below.

Research Question 1 – In-situ instrumentation coupling through concrete versus grass

Results showed that variability of HVSR measurements of concrete to grass was generally minor ranging from 0% - 2% when both, $HVSR_{Concrete}$ and $HVSR_{Grass}$, were of high quality. The data from this study demonstrated that when $HVSR_{Concrete}$ quality was low, $HVSR_{Grass}$ quality was typically low as well. Out of the 45 tests conducted for this investigation, 22 included at least one acquisition categorized as Category 3. Among these 22 tests, 18 showed that both $HVSR_{Concrete}$ and $HVSR_{Grass}$ were classified as Category 3, representing low quality. The remaining four tests revealed a discrepancy were $HVSR_{Concrete}$ was classified as Category 3, while $HVSR_{Grass}$ was categorized as Category 2. Overall, 38 out of the 45 tests showed a $\Delta CAT = 0$, indicating that the quality of the concrete and grass acquisitions were the same. These findings suggest that in-situ acquisition coupling did not significantly influence the HVSR measurements.

Research Question 2 – In-situ instrumentation coupling through concrete versus grass with strong, nearby noise influence (i.e., construction activity)

Results showed that strong construction noise had a minimal impact on HVSR measurements performed on grass, with variability in $HVSR_{Res}$ confined to a few tests. Of the tests performed with construction noise, two tests showed variability that was greater than 5% from the reference value. A more important observation taken from this study was that larger variability was observed for $HVSR_{Concrete}$ measurements under similar ambient noise conditions (88%). In some cases, the $HVSR_{Concrete}$ measurements showed a percent

difference from the reference value of more than 26%, whereas the percent difference for simultaneous acquired $HVSR_{Grass}$ measurement was effectively 0%.

Research Question 3 – Influence of proximity of HVSR measurements to buildings

Results indicated an increase in variability of HVSR curves at sites located closer to buildings. The quality of the HVSR curves shows the same trend. The "Near" group ($d \leq 8$ ft from buildings) had an average Category number of 2.82 indicating that the HVSR curves were trending toward low quality results. The "Far" group ($d > 50$ ft from buildings) had an average Category number of 1.78 which indicated that the HVSR curves for the grouping tended to be of high quality. The average Category number for the "Intermediate" group (8 ft $< d \leq 50$ ft from buildings) was 2.58, which is between the average Category values for the "Near" and "Far" grouping, indicating that as the distance from the building increases, the quality of the HVSR curve also increases.

Research Question 4 – Influence of time-of-day with building proximity

Results from repeat measurements show that 50% of the acquisitions conducted near occupied buildings had a variability greater than 5% from the reference value while 77% of the acquisitions taken near unoccupied buildings had a variability greater than 5% from the reference value. Manual inspection of HVSR curves to determine the HVSR peak produced a decrease in the variability from the reference frequency for cases when buildings were occupied and unoccupied. When manual inspection of the HVSR curves was implemented, for occupied buildings, the percentage or acquisition that showed variability greater than 5% dropped from 50% to 40%. The same trend was observed for unoccupied buildings showing a drop from 77% to 53%.

7.2 Conclusions

Research Question 1 – In-situ instrumentation coupling through concrete versus grass

Results indicate that the HVSR measurements taken on concrete surfaces generally exhibit comparable peak frequency values to those taken on grass, aligning with SESAME (2005) guidelines. Minimal variability was observed in maximum peak frequencies, except in cases where low quality HVSR curves were produced, often due to external noise or improper coupling. The findings challenge some existing guidelines (e.g., MoHo S.R.L, 2020), which discourage measurements on concrete. This research supports the conclusion that HVSR acquisition on concrete does not affect HVSR measurements, except when performed near construction noise, as noted below.

Research Question 2 – In-situ instrumentation coupling through concrete versus grass with strong, nearby noise influence (i.e., construction activity)

The presence of strong nearby noise sources, such as construction activities, showed limited overall impact on HVSR measurements. Measurements conducted on grass, near construction sites displayed minor inconsistencies, while those on concrete surfaces demonstrated greater variability, likely due to the rigid surface better coupling construction vibrations. These findings suggest that while strong noise sources can affect measurements, the impact can be minimized through careful site selection and data analysis. Additionally, the findings elaborate on the recommendations produced by SESAME (2005), MoHo S.R.L (2020), and supporting literature (e.g., Koller et al., 2004; Chatelain et al., 2008; Mihaylov et al., 2016). The finding from this thesis would suggest that site conditions have a larger influence on HVSR variability than the strong nearby noise source itself.

Research Question 3 – Influence of proximity of HVSR measurements to buildings

Proximity to buildings was identified as a significant source of variability in HVSR measurements. Measurement sites located closer to buildings were more likely to experience building-induced frequencies influencing the HVSR data. These findings emphasize the importance of accounting for building proximity when performing HVSR measurements in urban settings. To ensure accurate results, measurements taken near buildings should be accompanied by thorough manual inspection to distinguish the natural subsurface HVSR peak from artificial, building-induced peaks. This observation is consistent with the recommendations of SESAME (2005) and MoHo S.R.L (2020), which stress the necessity of maintaining adequate distance from buildings to achieve reliable HVSR measurements. This study did not investigate the distance from which building have influence on the HVSR method, some previous studies have correlated the height to distance of disturbance (e.g., Mucciarelli et al., 1997; Gallipoli et al., 2004).

Research Question 4 – Influence of time-of-day with building proximity

The time of day relative to building occupancy status had a noticeable effect on HVSR measurements near buildings. Measurements taken during operating hours generally produced higher quality HVSR results. During periods of low occupancy or nighttime, artificial peaks associated with building vibrations were more pronounced. To combat the more pronounced building vibrations, manual inspection allows for the artificial peaks to be disregarded during interpretation. In contrast, increased anthropogenic noise during the day often masked these peaks, resulting in reduced variability in HVSR measurements. A general observation was results that were closest to the expected values were observed when ambient noise conditions were increased (i.e., pedestrian and roadway

traffic), but data was acquired before the normal operating hours of the building. While neither SESAME (2005) nor MoHo S.R.L provides recommendations on this specific influence, they do recommend that data acquisition take place a distance from buildings and when noise levels are quiet. The finding from this study would suggest that, if HVSR measurement must be acquired within 50 ft of a building, high ambient noise levels are recommended regardless of the occupancy status of the building.

7.3 Recommendations

The study highlights the robustness of the HVSR method for urban geotechnical investigations. Based on the findings of this investigation the following recommendations are presented for data acquisitions. (1) In-situ instrumentation coupling on concrete or grass will produce HVSR measurements that are generally in accordance with one another (i.e., within a few %), except as noted below. (2) If data acquisition is required to be conducted in close proximity to a strong noise source (construction), it is recommended that the user acquire data on grass, as a concrete acquisition may produce inaccurate HVSR measurements as a result of construction noise coupling. (3) Data acquisition should be taken at a distance from three or four story buildings (> 50 ft), if possible. (4) If HVSR measurements must be acquired within 50 ft of a building, conditions of high ambient noise levels are recommended regardless of the occupancy (i.e., building noise levels) status of the building. (5) Due to possible variability in HVSR measurements, regardless of in-situ coupling or building proximity, it is recommended that the HVSR results be examined manually using the individual direction spectra to ensure the correct values are being chosen by the processing software.

Based on the observations made during this study, several recommendations for future research are proposed. One recommendation is to conduct HVSR measurements at varying distances from a building to determine the minimum distance required to eliminate building-induced influences on the HVSR data. Additionally, there is a need to investigate how different software parameter configurations—such as window size and smoothing—might enhance the quality and reliability of HVSR data interpretation. Furthermore, studies should explore the effects of complex and irregular geological conditions on the HVSR method. Lastly, future research should focus on the impact of azimuthal variability on HVSR measurements to better understand its influence on the method.

REFERENCES

Abu Zeid, N., Corradini, E., Bignardi, S., Nizzo, V., and Santarato, G. (2017). "The Passive Seismic Technique 'HVSR' as a Reconnaissance Tool for Mapping Paleo-soils: The Case of the Pilastri Archaeological Site, Northern Italy." Archaeol. Prospect., 24, 245–258. doi:10.1002/arp.1568.

Bahavar, M. and North, R. (2002). "Estimation of Background Noise for International Monitoring System Seismic Stations." Pure Appl. Geophys., 159, 911–944. doi:https://doi.org/10.1007/s00024-002-8666-2

Bignardi, S. (2017). "The Uncertainty of Estimating the Thickness of Soft Sediments with the HVSR Method: A Computational Point of View on Weak Lateral Variations." Journal of Applied Geophysics, 145, 28-38.

Bodin, P., Smith, K., Horton, S., and Hwang H. (2001). "Microtremor Observations of Deep Sediment Resonance in Metropolitan Memphis, Tennessee." Engineering Geology, 62(1–3), 159–168.

Bottelin, P., Dufréchou, G., Seoane, L., Llubes, M., and Monod, B. (2019). "Geophysical Methods for Mapping Quaternary Sediment Thickness: Application to the Saint-Lary Basin (French Pyrenees)." Comptes Rendus Geoscience, 351(6), 407-419. doi:https://doi.org/10.1016/j.crte.2019.07.001

Castellaro, S. and Mulargia, F. (2009). "The Effect of Velocity Inversions on H/V." Pure appl. geophys., 166, 567–592. doi:https://doi.org/10.1007/s00024-009-0474-5

Chatelain, J.L., Guillier, B., Cara, F., Duval, A.M., Atakan, K., Bard, P.Y., and The WP02 SESAME team. (2008). "Evaluation of the Influence of Experimental Conditions

on H/V Results from Ambient Noise Recordings." Bulletin of Earthquake Engineering, 6, 33–74. doi:https://doi.org/10.1007/s10518-007-9040-7

Chen, K.C., Chiu, J.M., and Yang, Y.T. (1996). "Shear-Wave Velocity of the Sedimentary Basin in the Upper Mississippi Embayment Using S-to-P Converted Waves." Bulletin of the Seismological Society of America, 86(3), 848–856. doi:https://doi.org/10.1785/BSSA0860030848

Chi, C. (2022). "Experimental Investigation of the Horizontal-to-Vertical Spectral Ratio (HVSR) Method for Estimating Depth of Bedrock in Central Missouri." University of Missouri-Columbia. doi:https://doi.org/10.32469/10355/91706

D'Amico, V., Picozzi, M., Baliva, F., and Albarello, D. (2008). "Ambient Noise Measurements for Preliminary Site-Effects Characterization in the Urban Area of Florence, Italy." Bulletin of the Seismological Society of America, 98(3), 1373–1388.

Delgado, J., Casado, C.L., Estevez, A., Giner, J., Cuenca, A., and Molina, S. (2000) "Mapping Soft Soils in the Segura River Valley (SESpain): A Case Study of Microtremors as an Exploration Tool." J. Appl. Geo-phys., 45(1), 19–32.

Dronfields, T., Stannard, D., and Meyers, J. (2019). "Passive Seismic Horizontal to Vertical Spectral Ratio (HVSR) Surveying to Help Define Bedrock Depth, Structure and Layering in Shallow Coal Basins." ASEG Extended Abstracts, 1, 1-5. doi:10.1080/22020586.2019.12073175

Fäh, D., Rüttener, E., Noack, T. and Kruspan, P. (1997). "Microzonation of the City of Basel." Journal of Seismology, 1(1), 87-102.

Fatma, Yuliyanto, G., and Harmoko, U. (2019). “Identify the Oil Seepage in Plantungan Geothermal Manifestation, Kendal Using HVSR Method.” E3S Web of Conference, 125. doi:https://doi.org/10.1051/e3sconf/201912515004

Gallipoli M.R., Lapenna V., Lorenzo P., Mucciarelli M., Perrone A., Piscitellis S., and Sdao, F. (2000). “Comparison of Geological and Geophysical Prospecting Techniques in the Study of a Landslide in Southern Italy.” European J. Env. Eng. Geophys., 4, 117-128.

Gallipoli M.R., Mucciarelli M, Castro RR, Monachesi G, Contri P. (2004). “Structure, soil-structure response and effects of damage based on observations of horizontal-to-vertical spectral ratios of microtremors.” Soil Dyn Earth Eng., 24, 487–495

Gallipoli, M.R., Albarello, D., Mucciarelli, M. and Bianca, M. (2011). “Ambient Noise Measurements to Support Emergency Seismic Microzonation: the Abruzzo 2009 Earthquake Experience.” Boll. Geof. Teor. Appl., 52, 539-559.

Goetz, R. & Rosenblad, B (2010). “Study of the H/V spectral ratio method for determining average shear wave velocities in the Mississippi embayment. Engineering Geology - ENG GEOL. 112. 13-20. 10.1016/j.enggeo.2010.01.006.

Gosar, A. and Lenart, A. (2010). “Mapping the Thickness of Sediments in the Ljubljana Moor Basin (Slovenia) Using Microtremors.” Bulletin of Earthquake Engineering, 8(3), 501–518.

Guillier, B., Atakan, K., Chatelain, J.L., Havskov, J., Ohrnberger, M., Cara, F., Duval, A.M., and Zacharopoulos, S. (2008). “Influence of Instruments on the H/V Spectral Ratios of Ambient Vibrations.” Bulletin of Earthquake Engineering, 6, 3–31. doi:https://doi.org/10.1007/s10518-007-9039-0

Guillier, B., Chatelain, J.L., Bonnefoy-Claudet, S., and Haghshenas, E. (2007). “Use of Ambient Noise: From Spectral Amplitude Variability to H/V Stability.” Journal of Earthquake Engineering, 11(6), 925–942. doi:https://doi.org/10.1080/13632460701457249

Guéguen, P., Bard, P-Y., Chávez-García, F.J. (2002) “Site-City Seismic Interaction in Mexico City-Like Environments: An Analytical Study.” Bulletin of the Seismological Society of America, 92(2), 794–811.

Harinarayan, N.H. and Kumar, A. (2017). “Site Classification of Strong Motion Stations of Uttarakhand, India, Based on Standard Spectral Ratio, and Horizontal-to-Vertical Spectral Ratio Methods.” Geohazards, 281, 141–149.

Ibs-von Seht, M. and Wohlenberg, J. (1999). “Microtremor Measurements Used to Map Thickness of Soft Sediments.” Bulletin of the Seismological Society of America, 89(1), 250–259.

Ji, K., Ren, Y., and Wen, R. (2017). “Site Classification for National Strong Motion Observation Network System (NSMONS) Stations in China Using an Empirical H/V Spectral Ratio Method.” Journal of Asian Earth Sciences, 147, 79–94.

Khalili, M. and Mirzakurdeh, A.V. (2019). “Fault Detection Using Microtremor Data (HVSR-Based Approach) and Electrical Resistivity Survey.” Journal of Rock Mechanics and Geotechnical Engineering, 11(2), 400–408.

Koller, M.G., Chatelain, JL., Guillier, B., Duval, AM., Atakan, K., Lacave, C., Bard, PY, and the SESAME participants. (2004). “Pradtical User Guildines and Software for the Implentation of the H/V Ratio Technique: Measuring Conditiosn, Processing

Method and Results Interpretation." *13th World Conference on Earthquake Engineering*, Vancouver, B.C., Canada, Paper No. 3132

Lane, J.W., Jr., White, E.A., Steele, G.V., and Cannia, J.C. (2008). "Estimation of Bedrock Depth Using the Horizontal-to-Vertical (H/V) Ambient-Noise Seismic Method." Symposium on the Application of Geophysics to Engineering and Environmental Problems

Lee, C.T., Cheng, C.T., Liao, C.W., Tsai, Y.B. (2001). "Site Classification of Taiwan Free-Field Strong-Motion Stations." Bulletin of the Seismological Society of America, 91(5), 1283–1297.

Lermo, J. and Chavez-Garcia F.J. (1993). "Site Effect Evaluation Using Spectral Ratios with Only One Station." Bulletin of the Seismological Society of America, 83, 1574-1794.

Liang, D., Gan, F., Zhang, W., and Jia, L. (2018). "The Application of HVSR Method in Detecting Sediment Thickness in Karst Collapse Area of Pearl River Delta, China." Environ Earth Sci., 77, 259. doi:https://doi.org/10.1007/s12665-018-7439-x

Matsushima, S., Hirokawa, T., De Martin, F., Kawase, H., and Sánchez-Sesma, F.J. (2014). "The Effect of Lateral Heterogeneity on Horizontal-to-Vertical Spectral Ratio of Microtremors Inferred from Observation and Synthetics." Bulletin of the Seismological Society of America, 104(1), 381–393.

Méric, O., Garambois, S., Malet, J.P., Cadet, H., Guéguen P., and Jongmans, D. (2007). "16 Seismic Noise-Based Methods for Soft-Rock Landslide Characterization." Bulletin de la Societe Geologique de France, 2, 137-148.

Mihaylov, D., El Naggar M.H., Dineva, S., (2016). “Separation of High- and Low-Level Ambient Noise for HVSR: Application in City Conditions for Greater Toronto Area.” Bulletin of the Seismological Society of America, 106(5), 2177–2184. doi:https://doi.org/10.1785/0120150389

MOHO Science and Technology. (2020). “TROMINO Blu User's Manual: Guidelines for Ambient Noise Measurement and Analysis Using the HVSR Method”. MOHO Science and Technology.

Molnar, S., Sirohey, A., Assaf, J. Bard, P-Y., Casterallero, C., Cox, B-C., Guillier, B., Hassani, B., Kawase, H., Mastsushima, S., Sáchez-Sesma, F.J., Yong, A. (2022). “A review of the microtremor horizontal-to-vertical spectral ratio (MHVSR) method.” Jounral of Seismology, 26, 653–685. doi:https://doi.org/10.1007/s10950-021-10062-9

Motamed, R., Ghalandarzadeh, A., Tawhata, I., and Tabatabaei, S.H., (2007). “Seis-mic Microzonation and Damage Assessment of Bam City, South- Eastern Iran.” J. Earth Eng. 11(1), 110–132.

Mucciarelli, M., Bettinali, F., Zaninetti, A., Mendez, A., Vanini, M., and Galli, P. (1997). “Refining Nakamura's technique: processing techniques and innovative instrumentation.” Proceedings of the XXV E.S.C. General Assembly, Reykjavik, 411-416

Mucciarelli, M. (1998). “Reliability and Applicability of Nakamura’s Technique Using Microtremors: an Experimental Approach.” J. Earthq. Eng., 2(4), 625–638.

Nakamura, Y. (1989). “A Method for Dynamic Characteristics Estimation of Subsurface using Microtremor on the Ground Surface.” Quarterly Report of Railway Technical Research Institute (RTRI), 30(1)

Nogoshi, M. and Igarashi, T. (1971). “On the Amplitude Characteristics of Microtremor (Part 2) (in Japanese with English abstract).” Jour. Seism. Soc. Japan, 24, 26-40.

Panou, A., Theodulidis, N., Hatzidimitriou, P., Savvaidis, A.S., and Papazachos, C.B. (2005). “Reliability of Ambient Noise Horizontal-to-Vertical Spectral Ratio in Urban Environments: The Case of Thessaloniki City (Northern Greece). Pure appl. geophys., 162, 891–912. doi:https://doi.org/10.1007/s00024-004-2647-6

Parolai, S., Bormann, P., and Milkereit, C. (2002). “New Relationships Between vs, Thickness of Sediments, and Resonance Frequency Calculated by the H/V Ratio of Seismic Noise for the Cologne Area (Germany).” Bulletin of the Seismological Society of America, 92(6), 2521–2527.

Paudyal, Y.R., Yatabe, R., Bhandary, N.P., and Dahal, R.K. (2013). “Basement Topography of the Kathmandu Basin Using Microtremor Observation.” J. Asian Earth Sci., 62, 627–637.

Pazzi, V., Tanteri, L., Bicocchi, G., D’Ambrosio, M., Caselli, A., and Fanti, R. (2017). “H/V Measurements as an Effective Tool for the Reliable Detection of Landslide Slip Surfaces: Case Studies of Castagnola (La Spezia, Italy) and Roccalbegna (Grosseto, Italy).” Physics and Chemistry of the Earth, 98, 136–153

Putti, S.P. and Satyam, N. (2020). “Evaluation of Site Effects Using HVSR Microtremor Measurements in Vishakhapatnam.” Earth Systems and Environment, 4(2), 439–454.

SESAME European Research Project. (2005). Guidelines for the implementation of the H/V spectral ratio technique on ambient vibrations: Measurements, processing, and interpretation. SESAME Deliverable D23.12. European Commission – Research General Directorate.

Stanko, D., Markušić, S., Gazdek, M., Sanković, V., Slukan, I. and Ivančić, I. (2019). "Assessment of the Seismic Site Amplification in the City of Ivanec (NW Part of Croatia) Using the Microtremor HVSR Method and Equivalent-Linear Site Response Analysis." Geosciences, 9(7), 312.

Theodoulidis, N., Cultrera, G., Cornou, C., Bard, P.Y., Boxberger, T., DiGiulio, G., Imtiaz, A., Kementzetzidou, D., Makra, K., and The Argostoli NERA Team (2018). "Basin Effects on Ground Motion: the Case of a High-Resolution Experiment in Cephalonia (Greece)." Bulletin of Earthquake Engineering, 16(2), 529–560.

Uebayashi, H., Kawabe, H., and Kamae, K. (2012). "Reproduction of Microseism H/V Spectral Features Using a Three-Dimensional Complex Topographical Model of the Sediment-Bedrock Interface in the Osaka Sedimentary Basin." Geophys. J. Int., 189(2), 1060–1074.

Vantassel, J., Cox, B., Wotherspoon, L., and Stolte, A., (2018). "Mapping Depth to Bedrock, Shear Stiffness, and Fundamental Site Period at Centreport, Wellington, Using Surface-Wave Methods: Implications for Local Seismic Site Amplification." Bulletin of the Seismological Society of America, 108(3B), 1709–1721.

Zara, M., Bard, P., and Ghaforyashtiany, M. (1999). “Site Characterizations from the Iranian Strong Motion Network.” Cancer Research, 71(89), 74–94.

Zeid, N.A., Corradini, E., Bignaedi, S., and Nizzo V. (2017). “The Passive Seismic Technique ‘HVSR’ as a Reconnaissance Tool for Mapping Paleo-Soils: the Case of the Pilastri Archaeological Site, Northern Italy.” Archaeological Prospection, 24(3), 245–258.

APPENDIX A

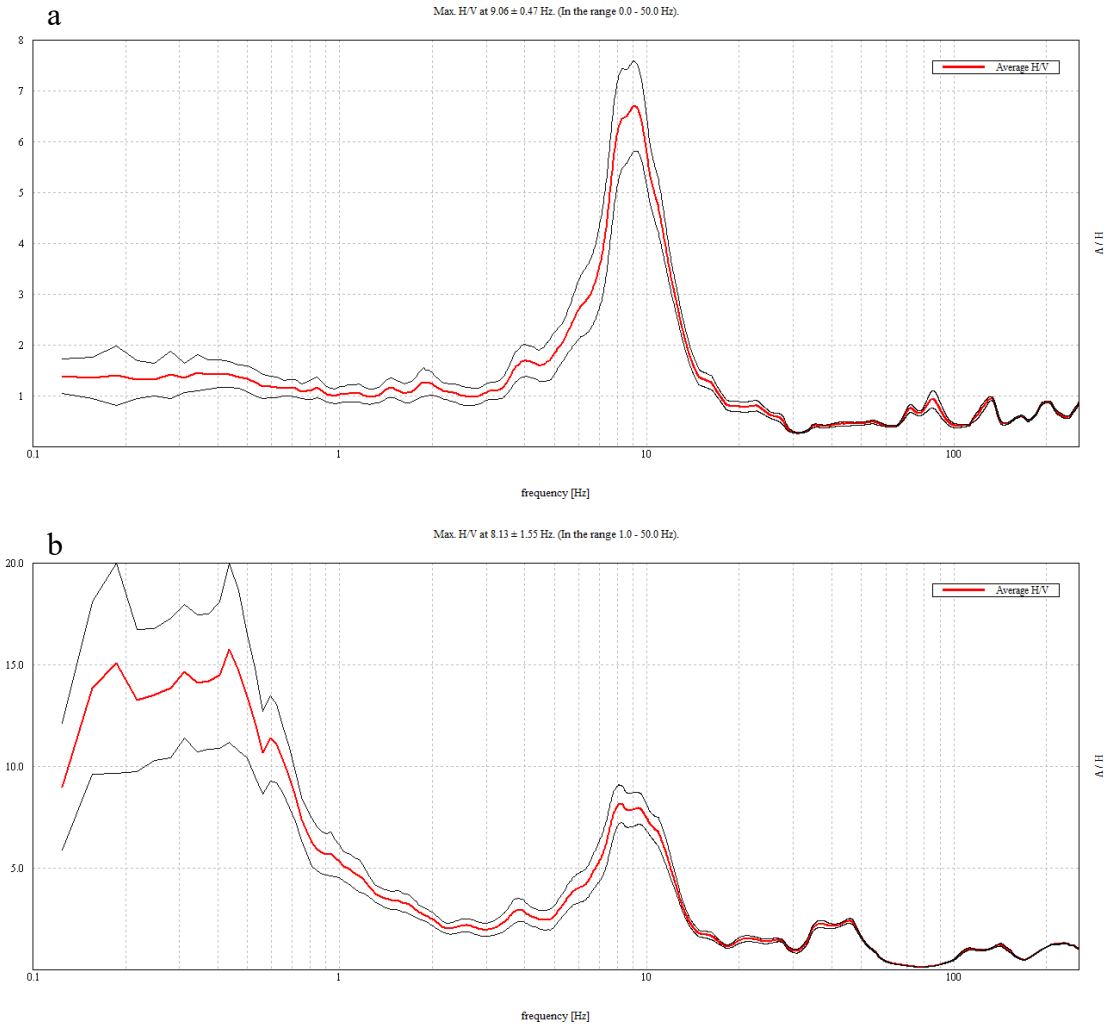

Figure A-1 Animal Hospital 1 site, Test 1, concrete (a), grass (b)

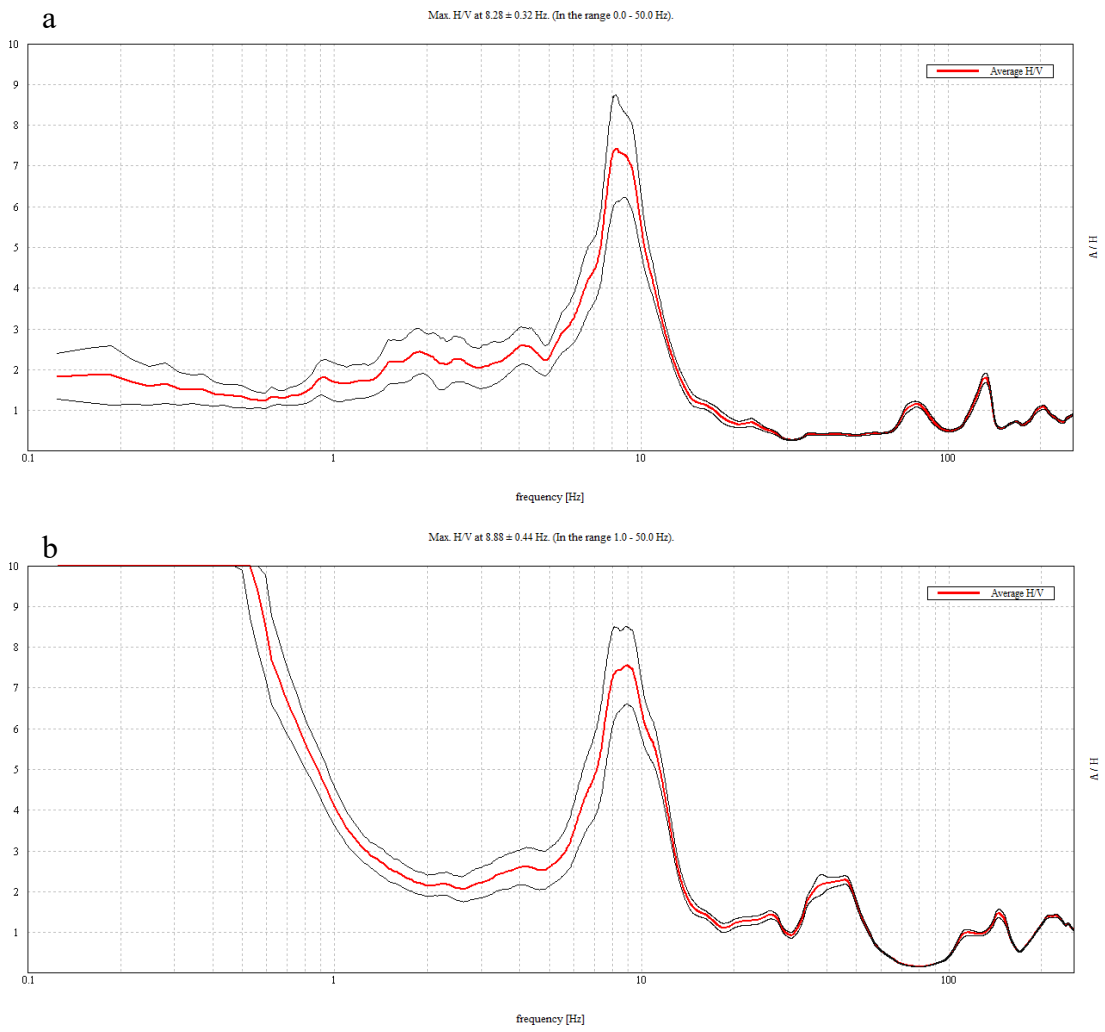

Figure A-2 Animal Hospital 1 site, Test 2, concrete (a), grass (b)

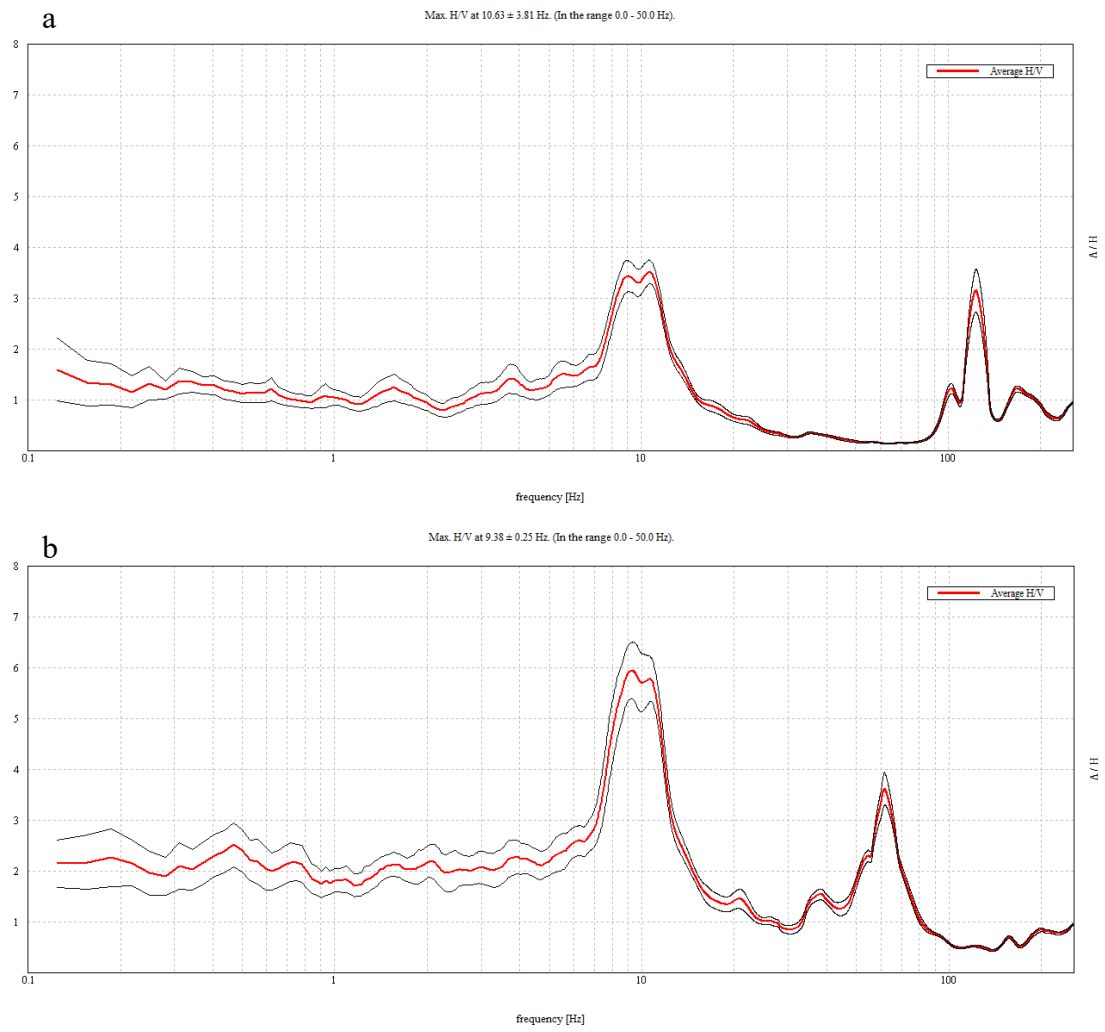

Figure A-3 Animal Hospital 1 site, Test 3, concrete (a), grass (b)

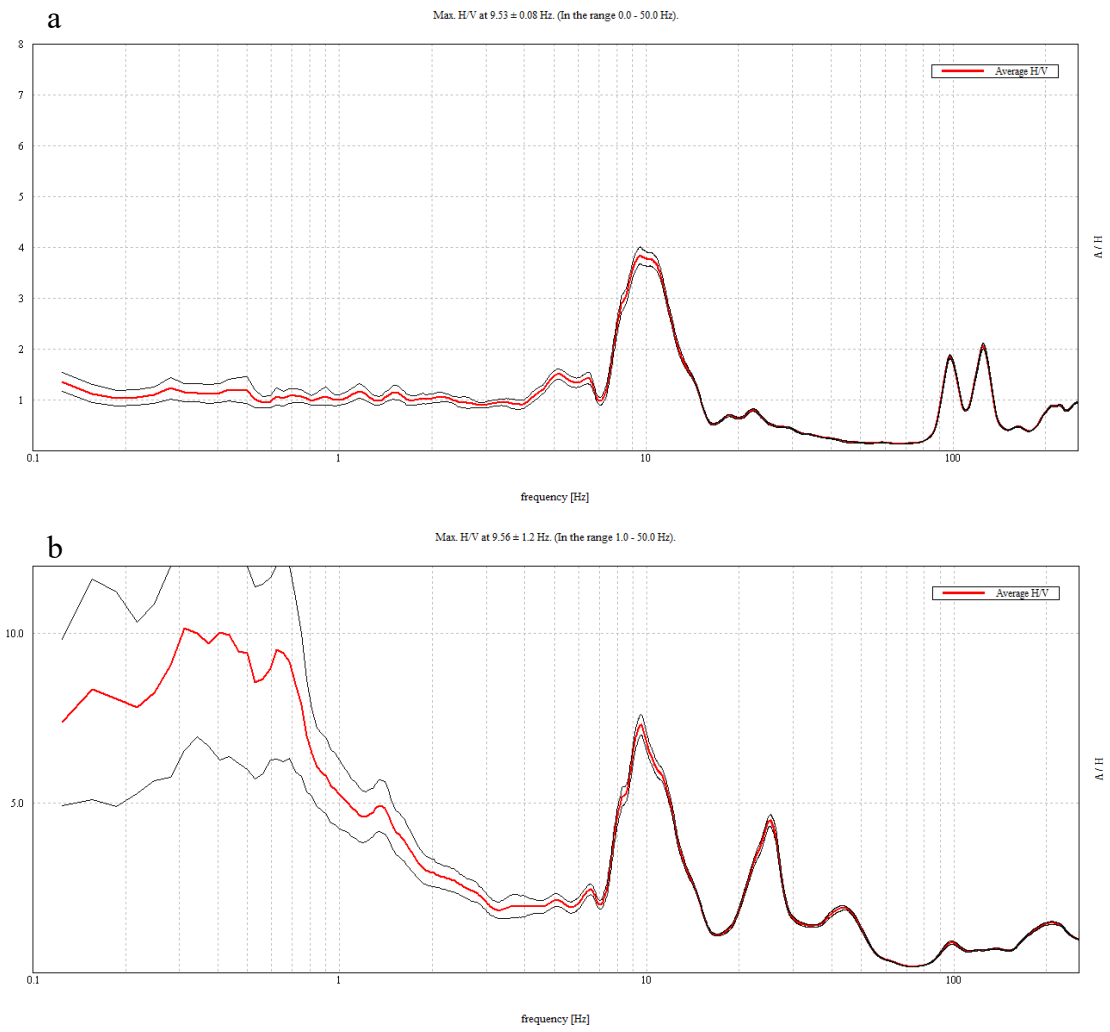

Figure A-4 Animal Hospital 1 site, Test 4, concrete (a), grass (b)

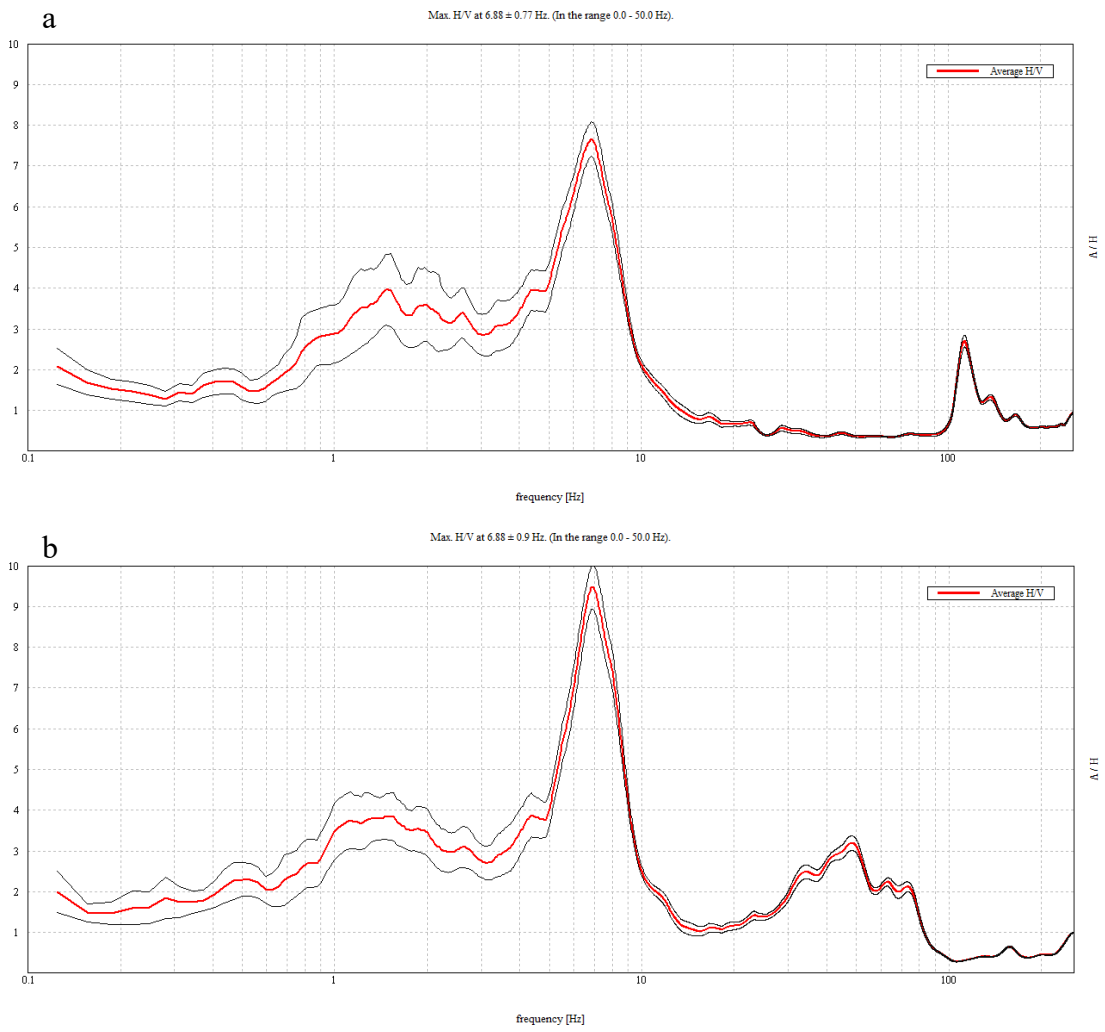

Figure A-5 Animal Hospital 2 site, Test 1, concrete (a), grass (b)

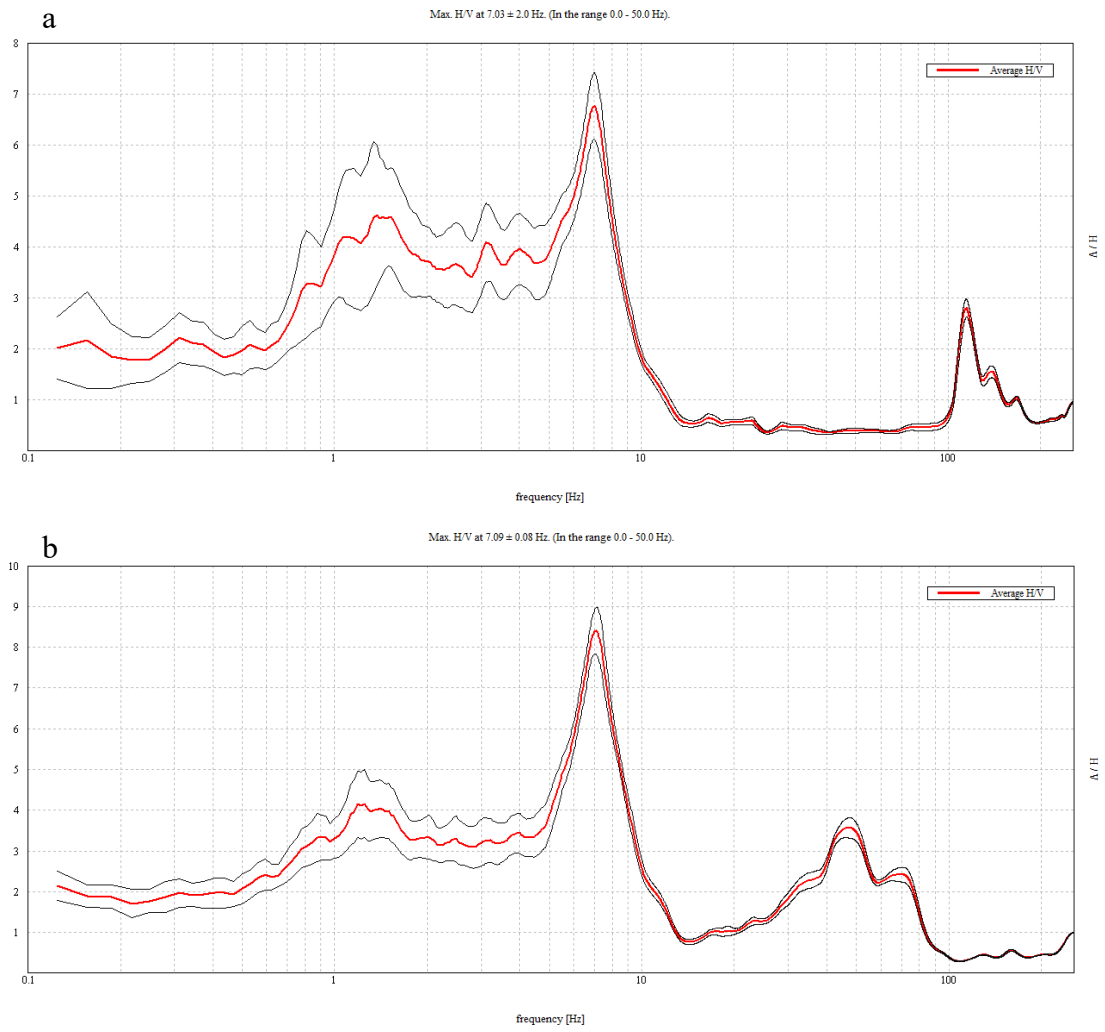

Figure A-6 Animal Hospital 2 site, Test 2, concrete (a), grass (b)

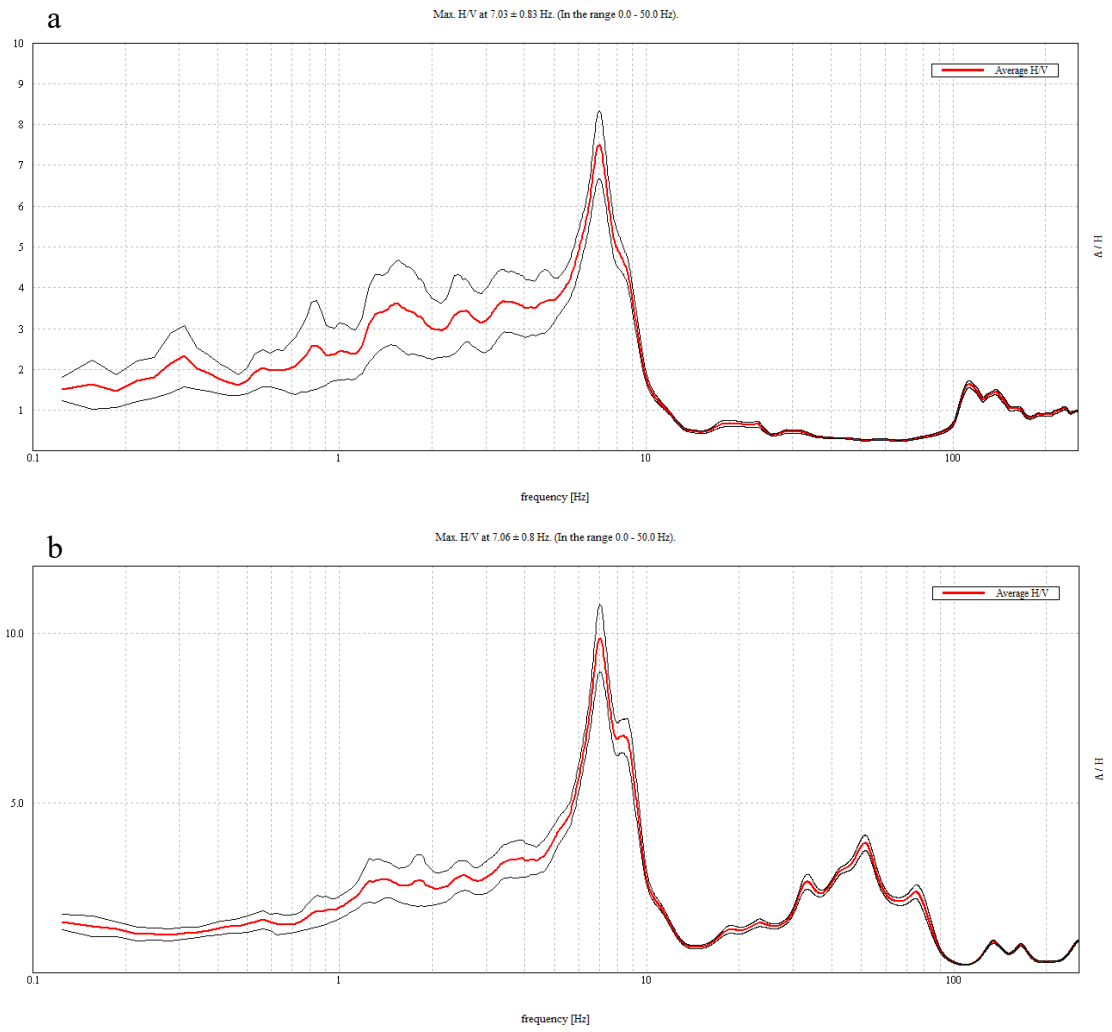

Figure A-7 Animal Hospital 2 site, Test 3, concrete (a), grass (b)

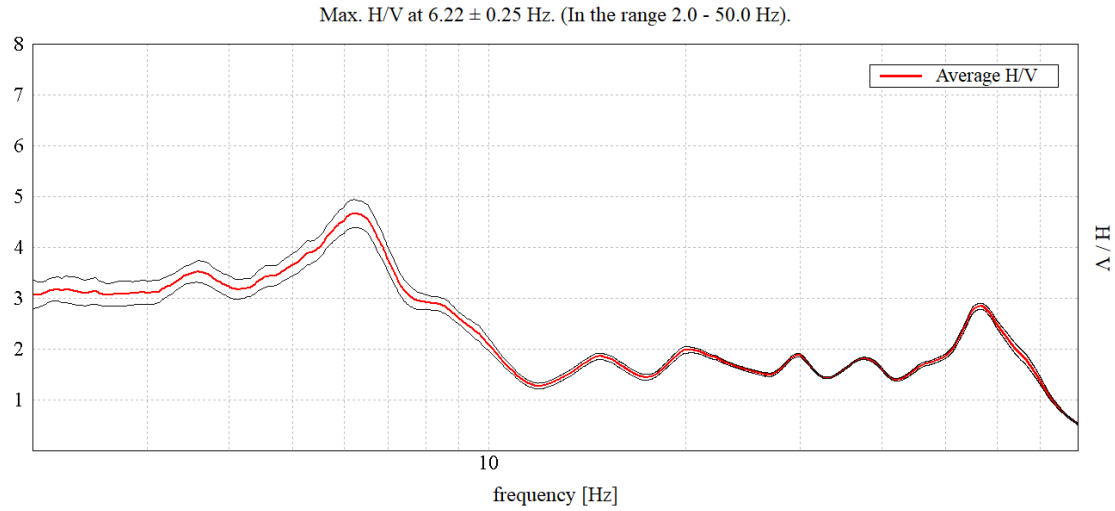

Figure A-8 Ellis Library BH-01 site, Test 1, grass

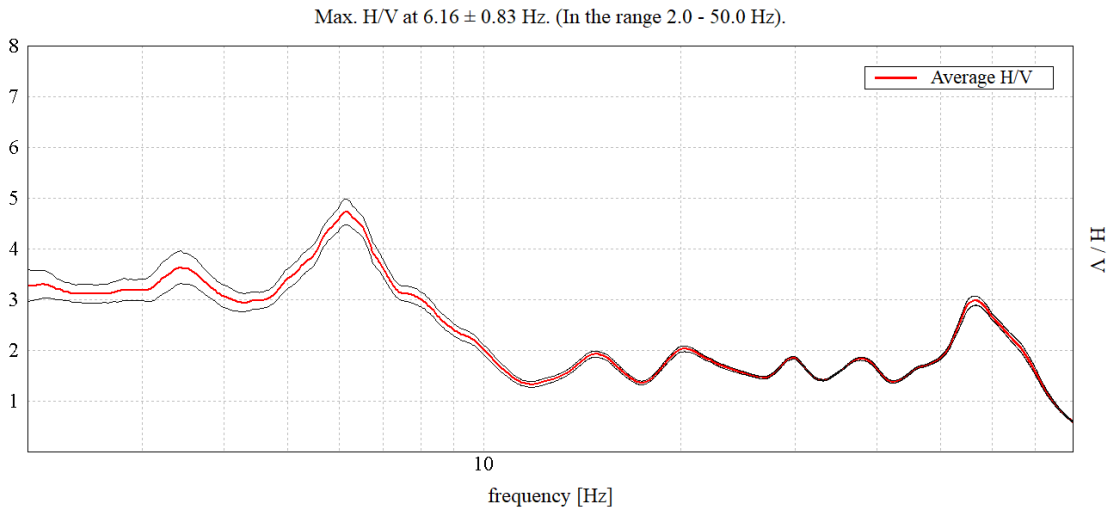

Figure A-9 Ellis Library BH-01 site, Test 2, grass

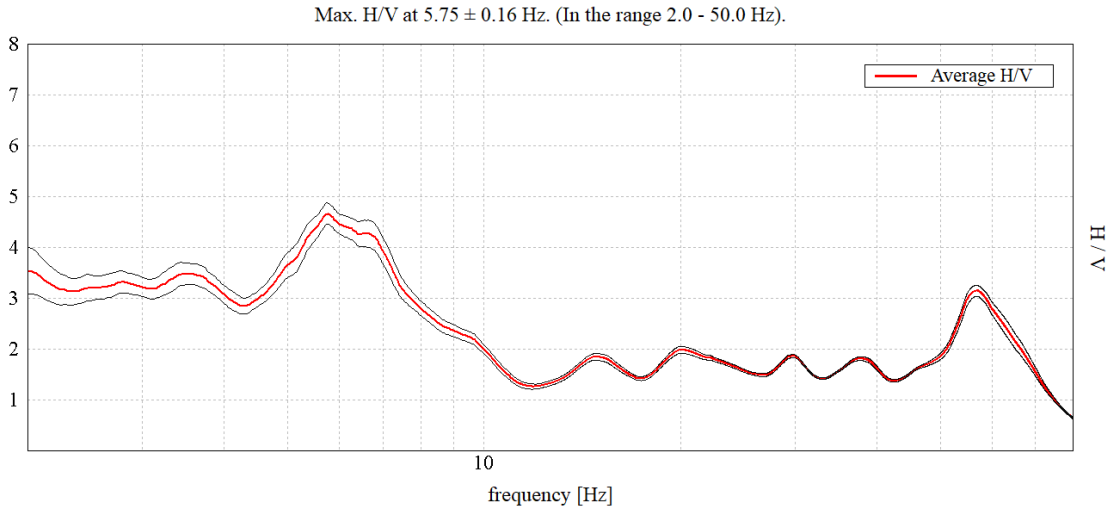

Figure A-10 Ellis Library BH-01 site, Test 3, grass

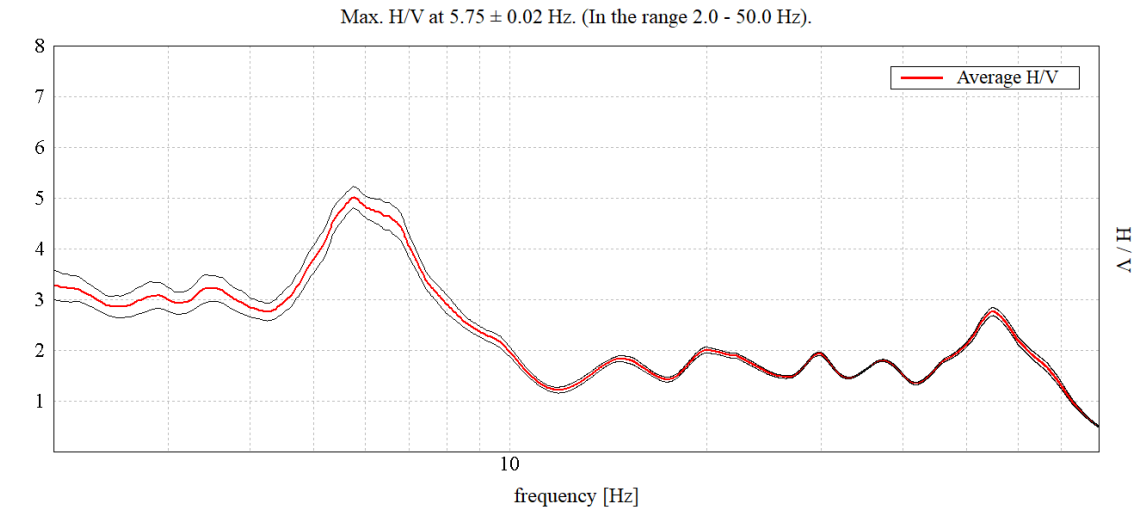

Figure A-11 Ellis Library BH-01 site, Test 4, grass

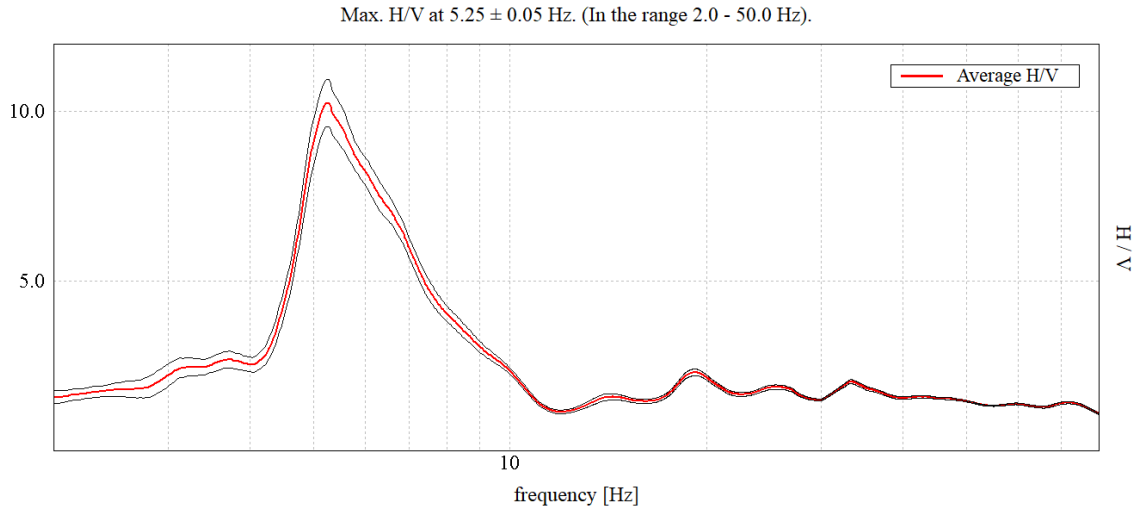

Figure A-12 Ellis Library BH-01 site, Test 5, grass

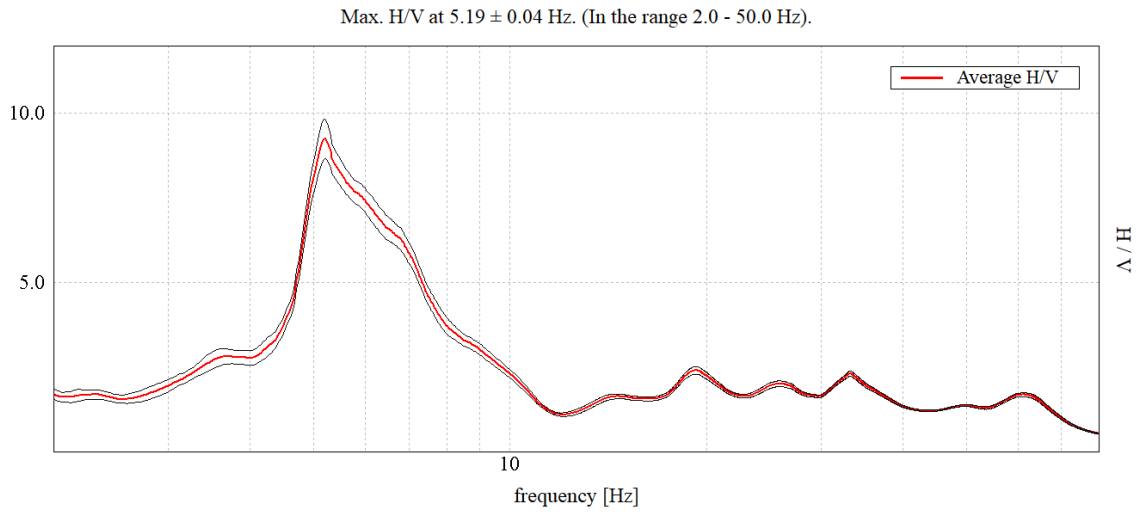

Figure A-13 Ellis Library BH-01 site, Test 6, grass

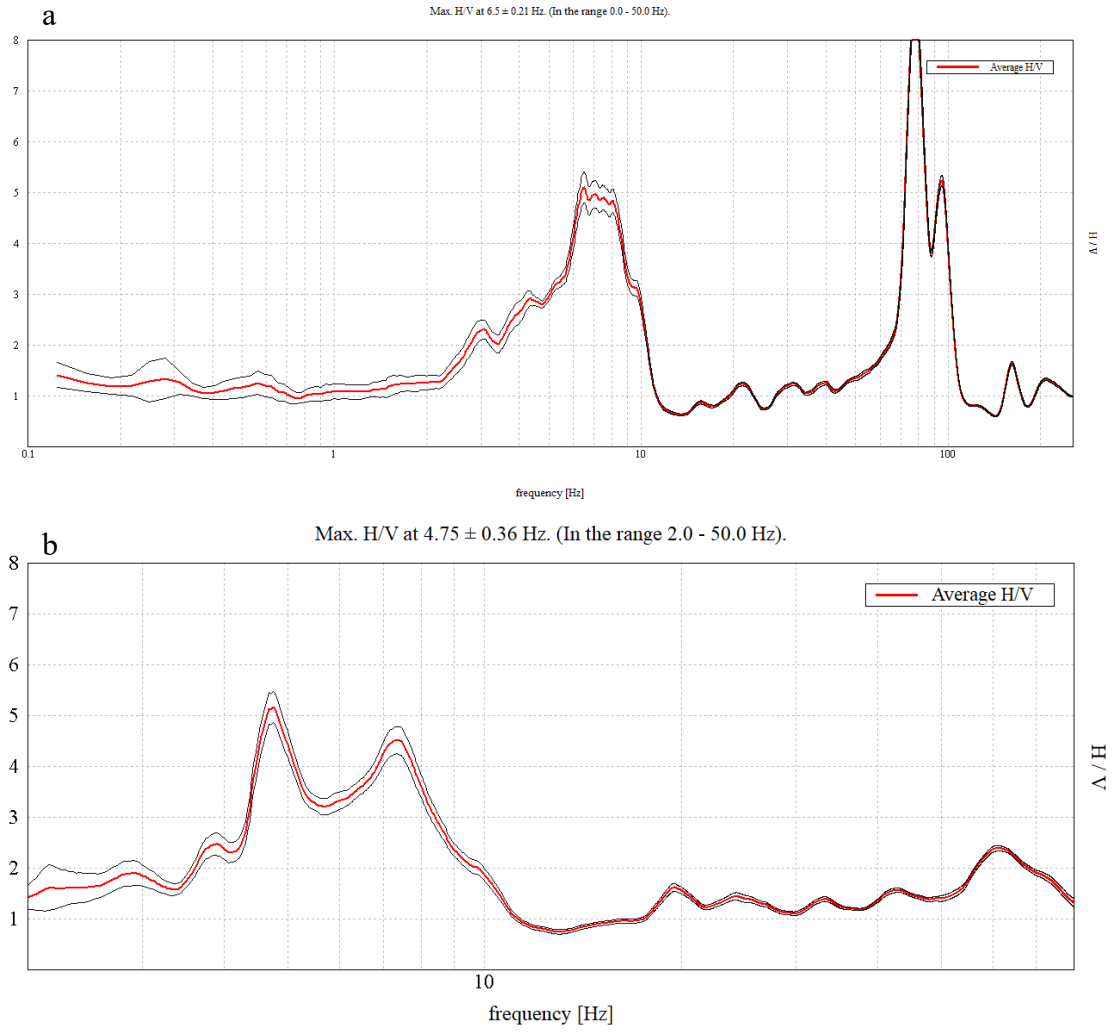

Figure A-14 Ellis Library BH-03 A site, Test 1, concrete (a), grass (b)

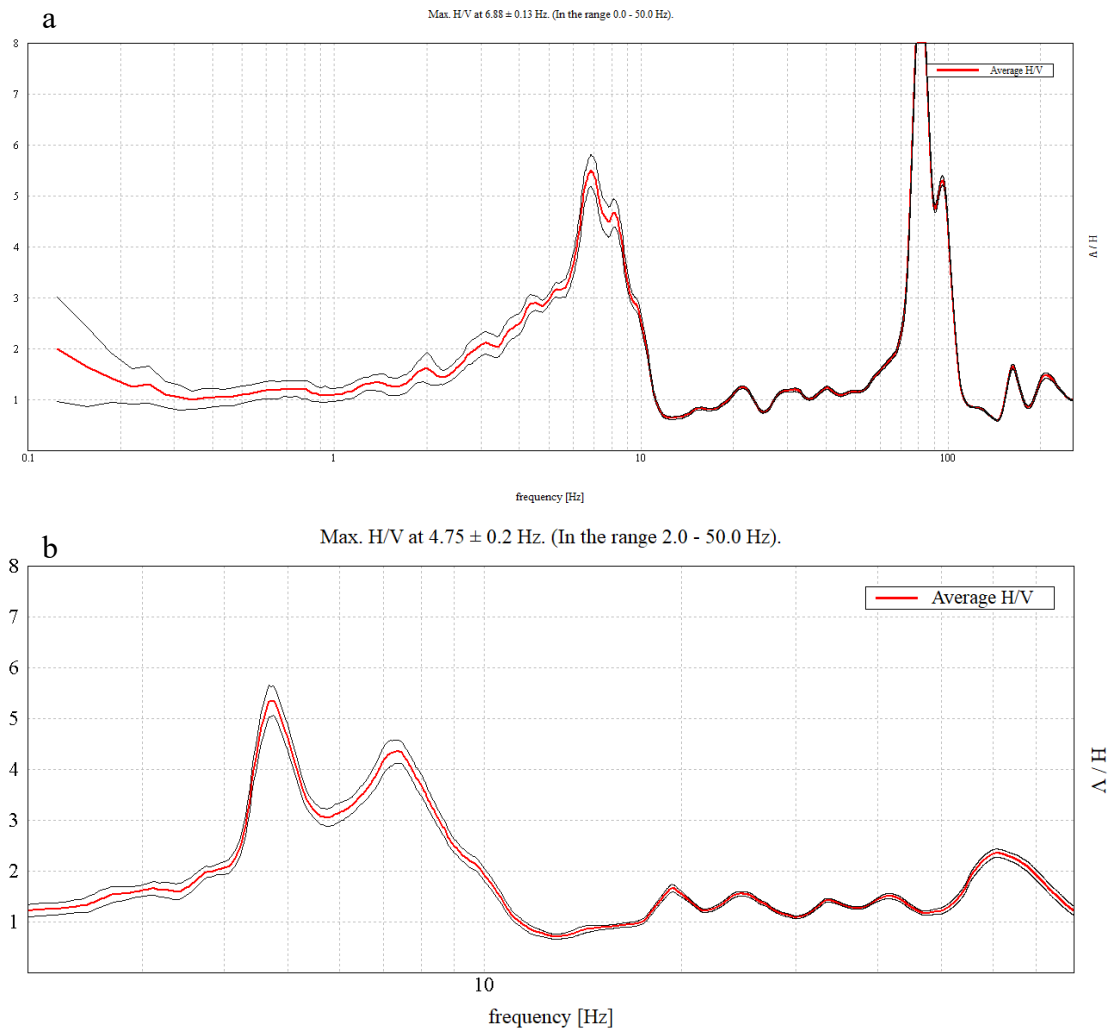

Figure A-15 Ellis Library BH-03 A site, Test 2, concrete (a), grass (b)

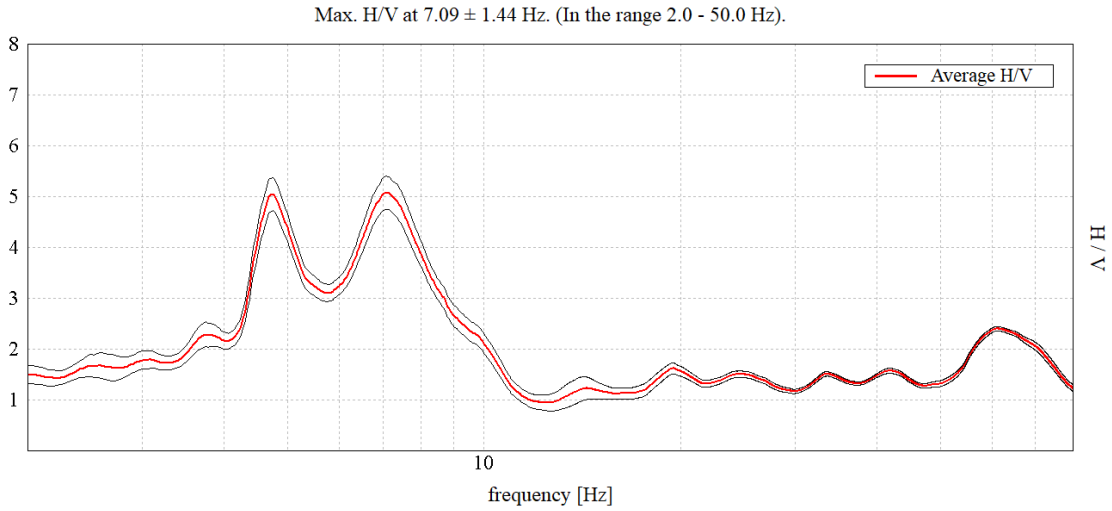

Figure A-16 Ellis Library BH-03 A site, Test 3, grass

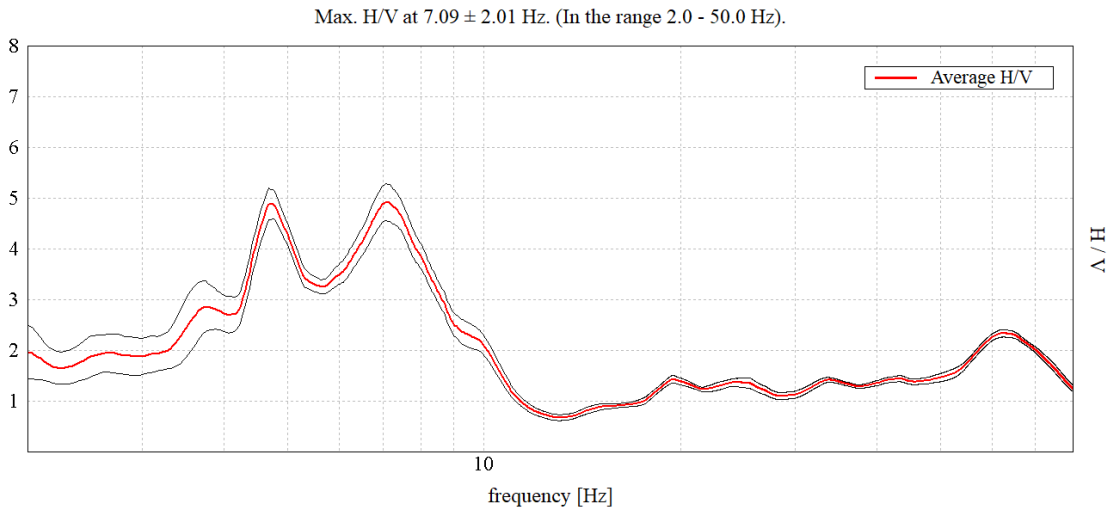

Figure A-17 Ellis Library BH-03 A site, Test 4, grass

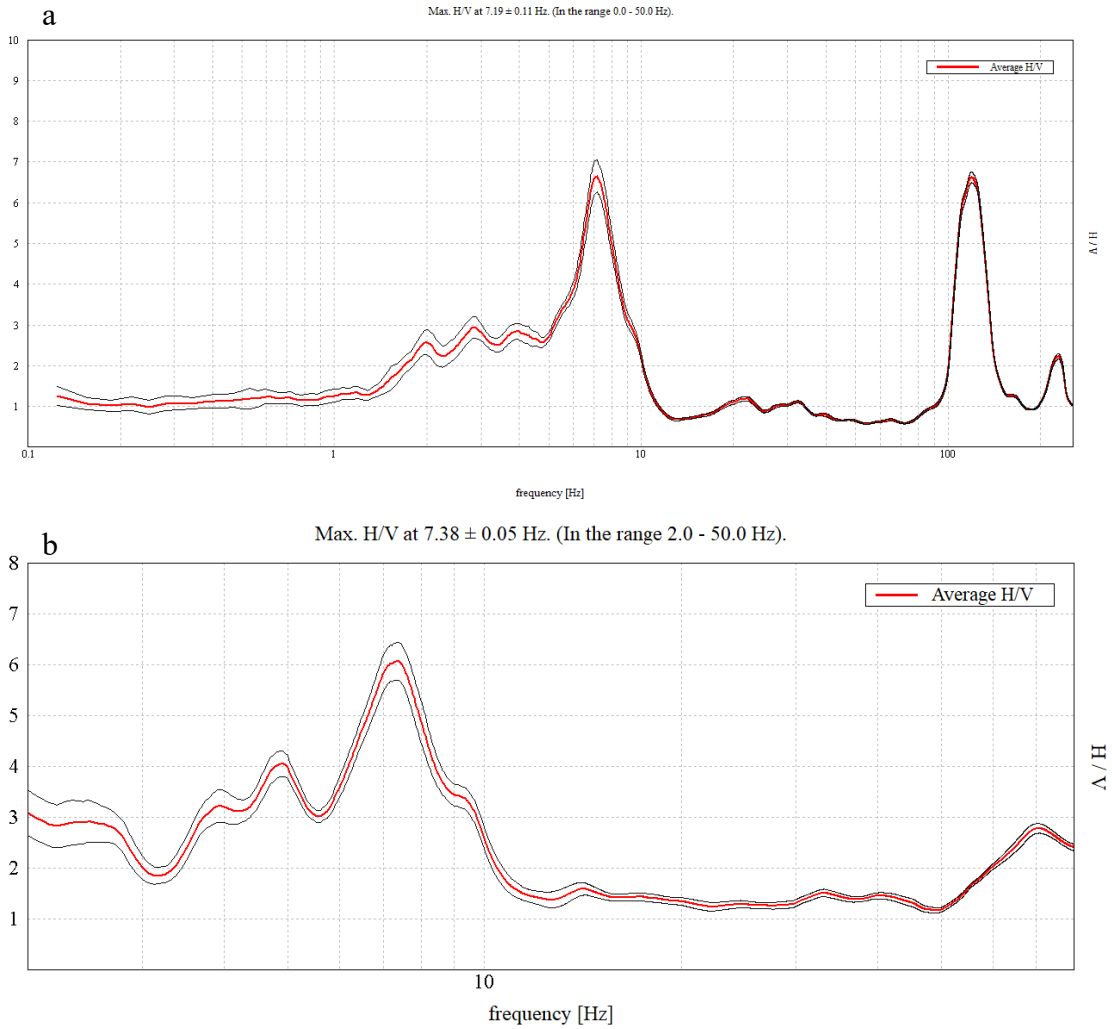

Figure A-18 Ellis Library BH-03 A site, Test 5, concrete (a), grass (b)

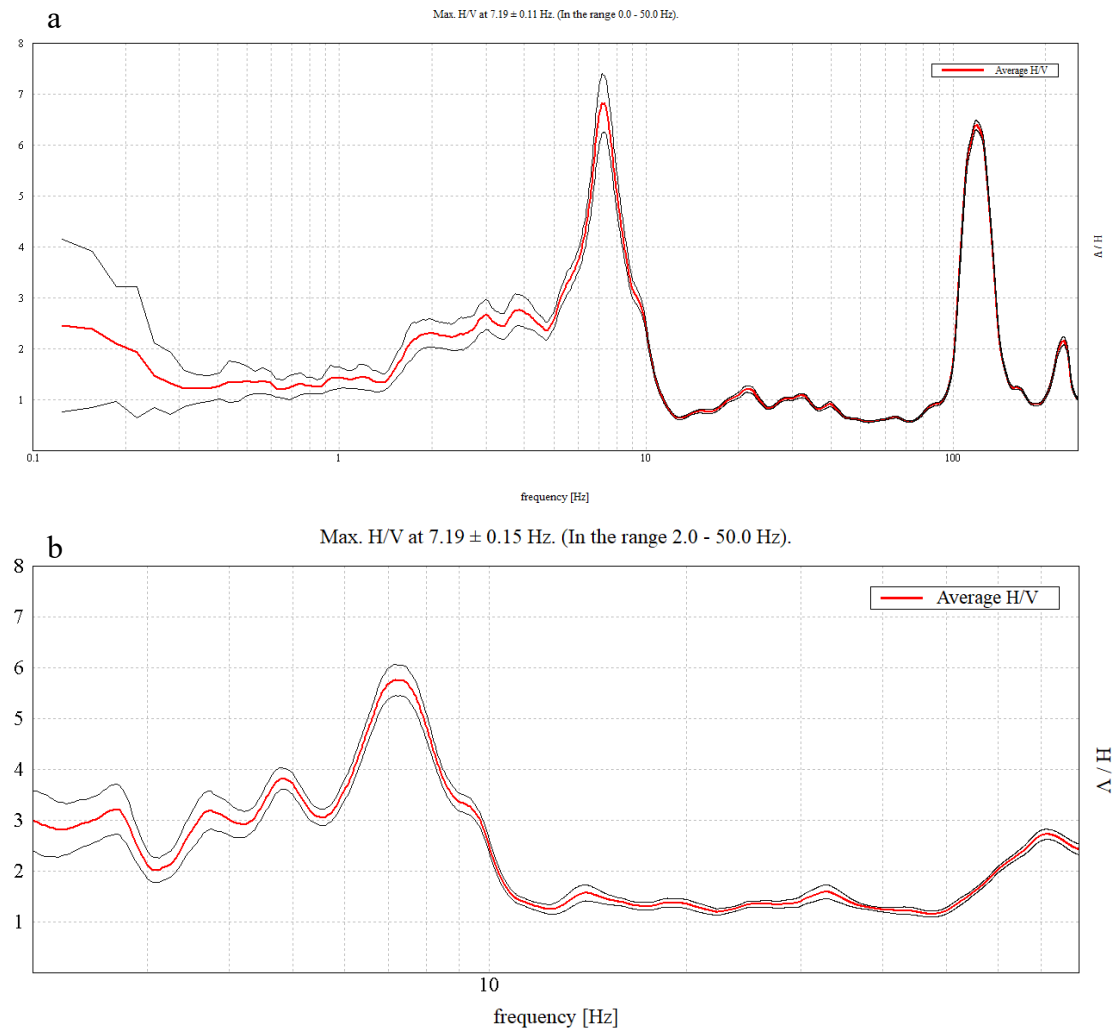

Figure A-19 Ellis Library BH-03 A site, Test 6, concrete (a), grass (b)

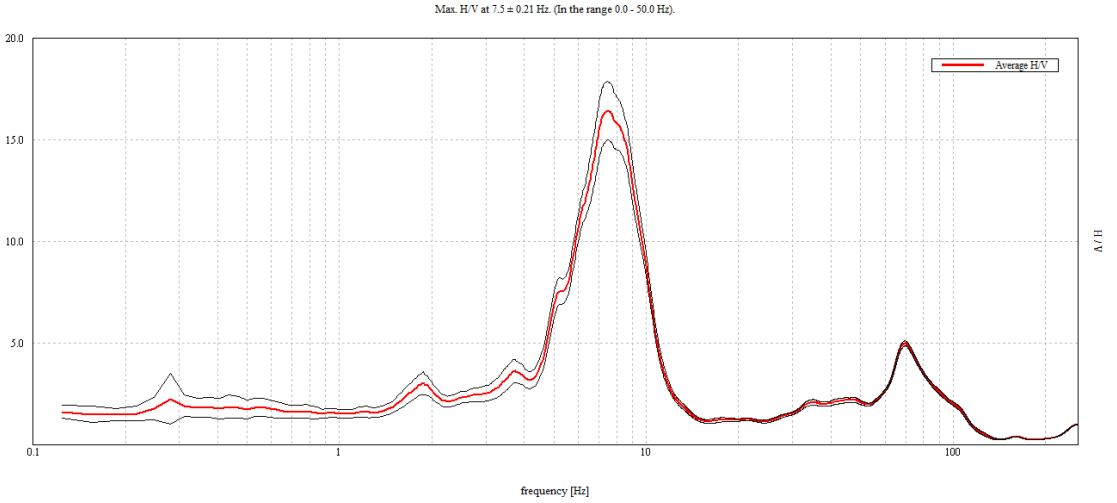

Figure A-20 Ellis Library BH-03 B site, Test 1, grass

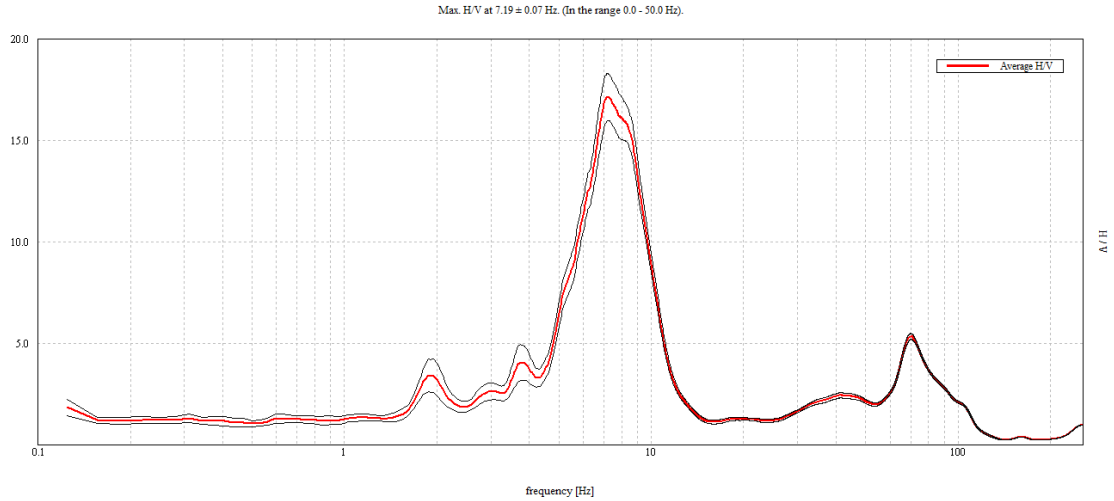

Figure A-21 Ellis Library BH-03 B site, Test 2, grass

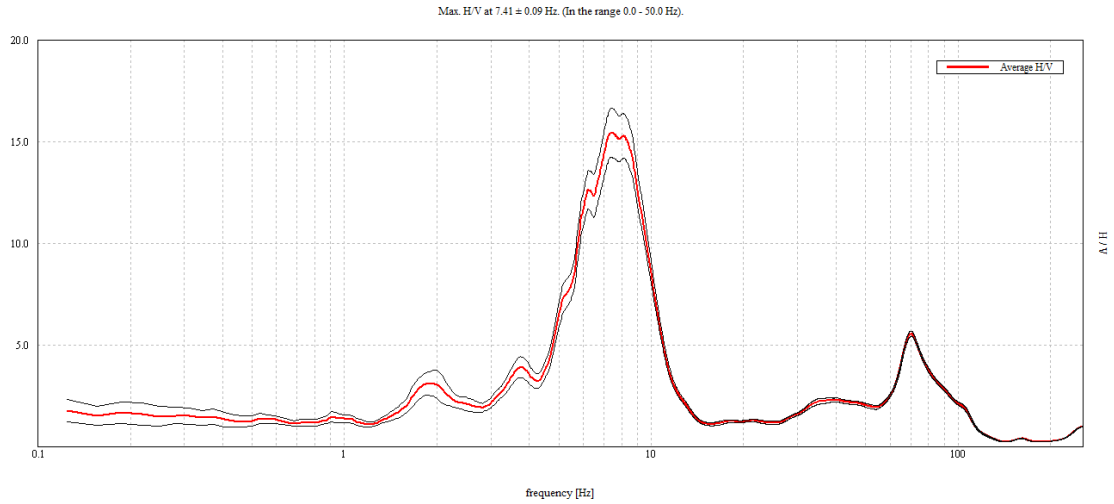

Figure A-22 Ellis Library BH-03 B site, Test 3, grass

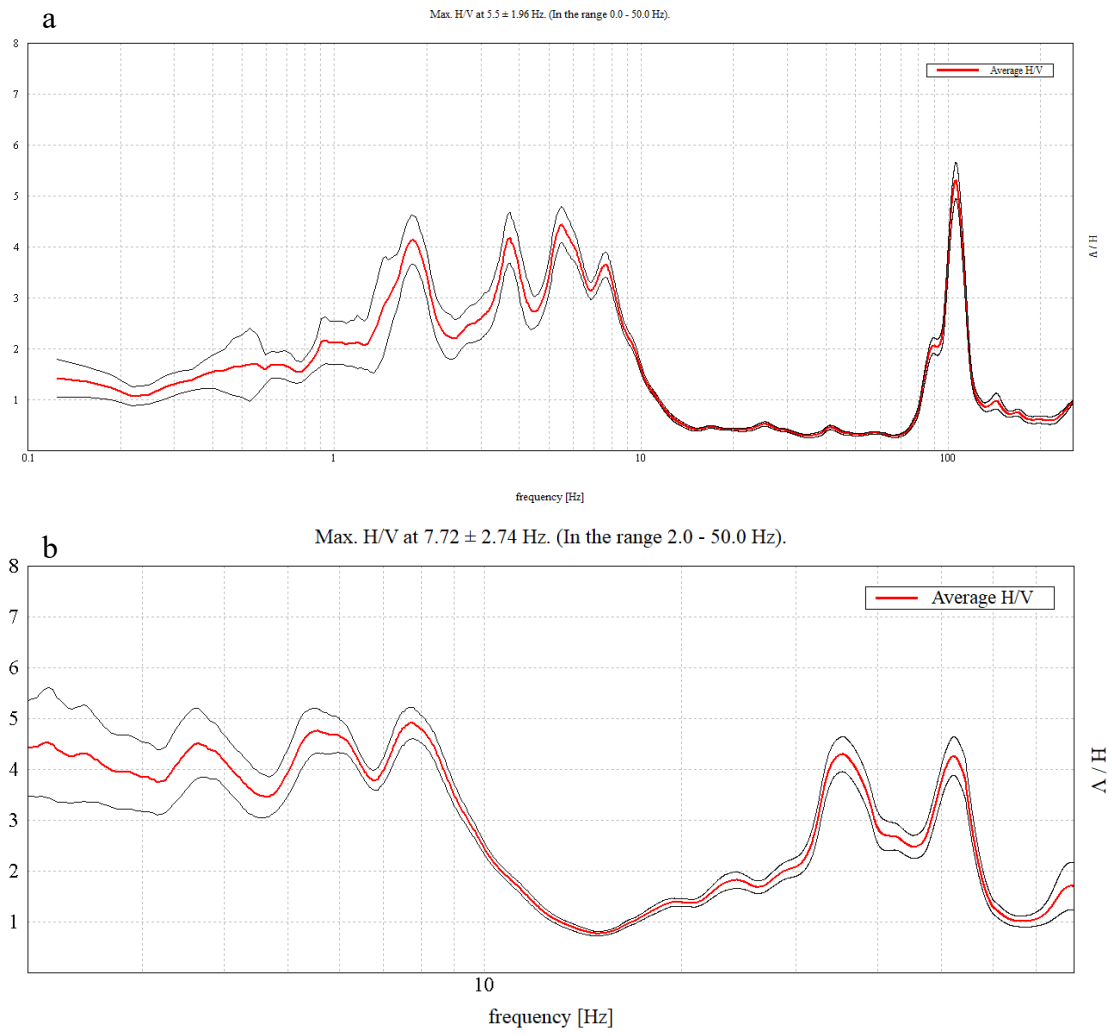

Figure A-23 Journalism B-06 A site, Test 1, concrete (a), grass (b)

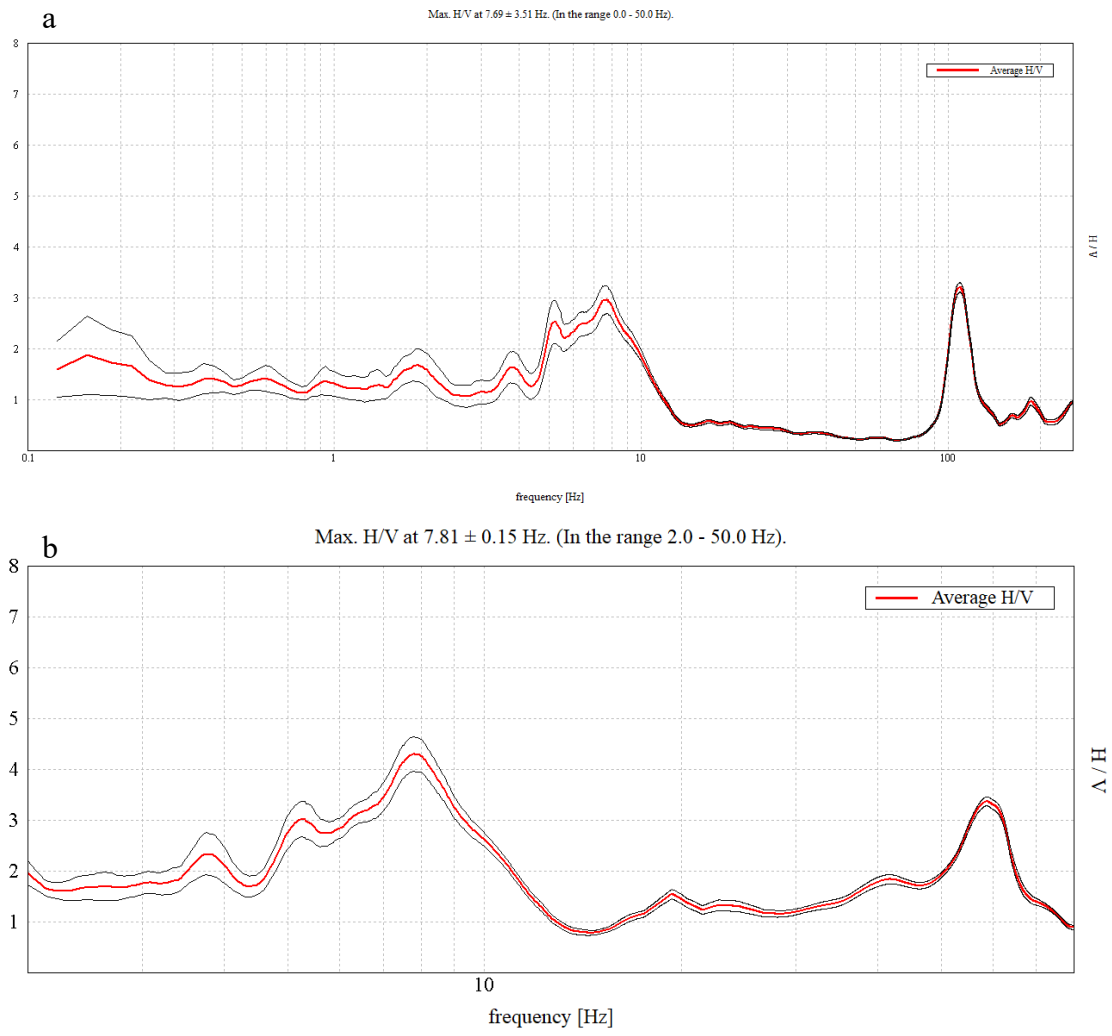

Figure A-24 Journalism B-06 A site, Test 2, concrete (a), grass (b)

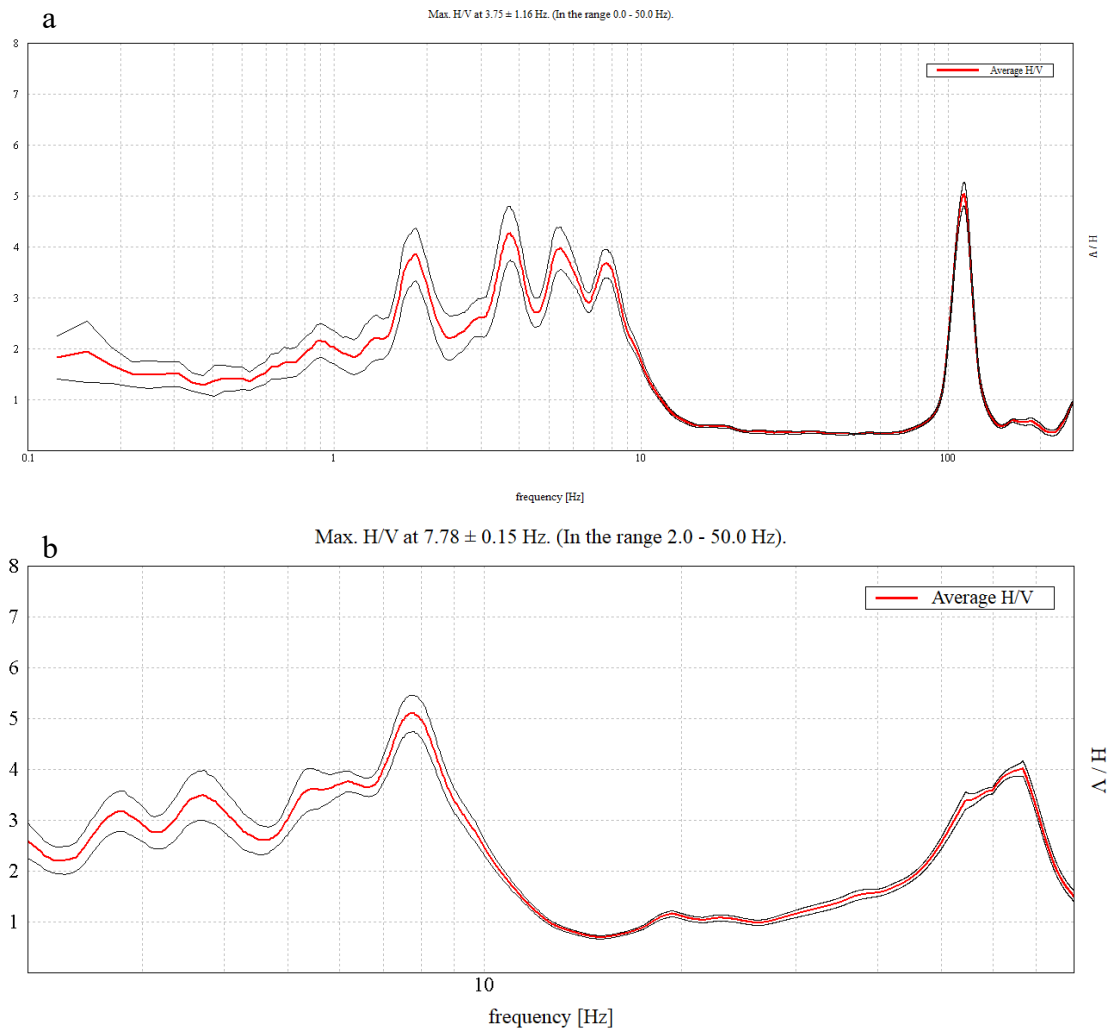

Figure A-25 Journalism B-06 A site, Test 3, concrete (a), grass (b)

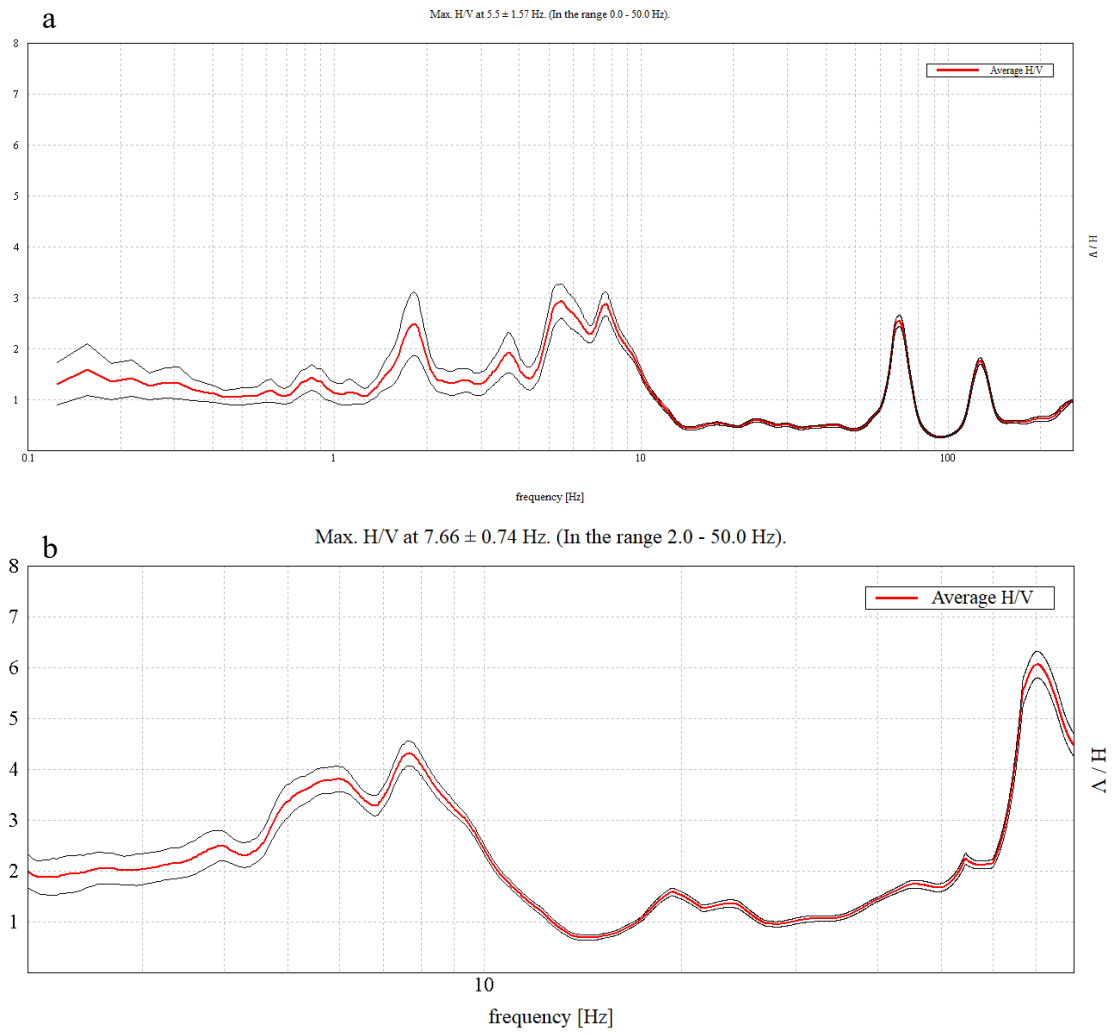

Figure A-26 Journalism B-06 A site, Test 4, concrete (a), grass (b)

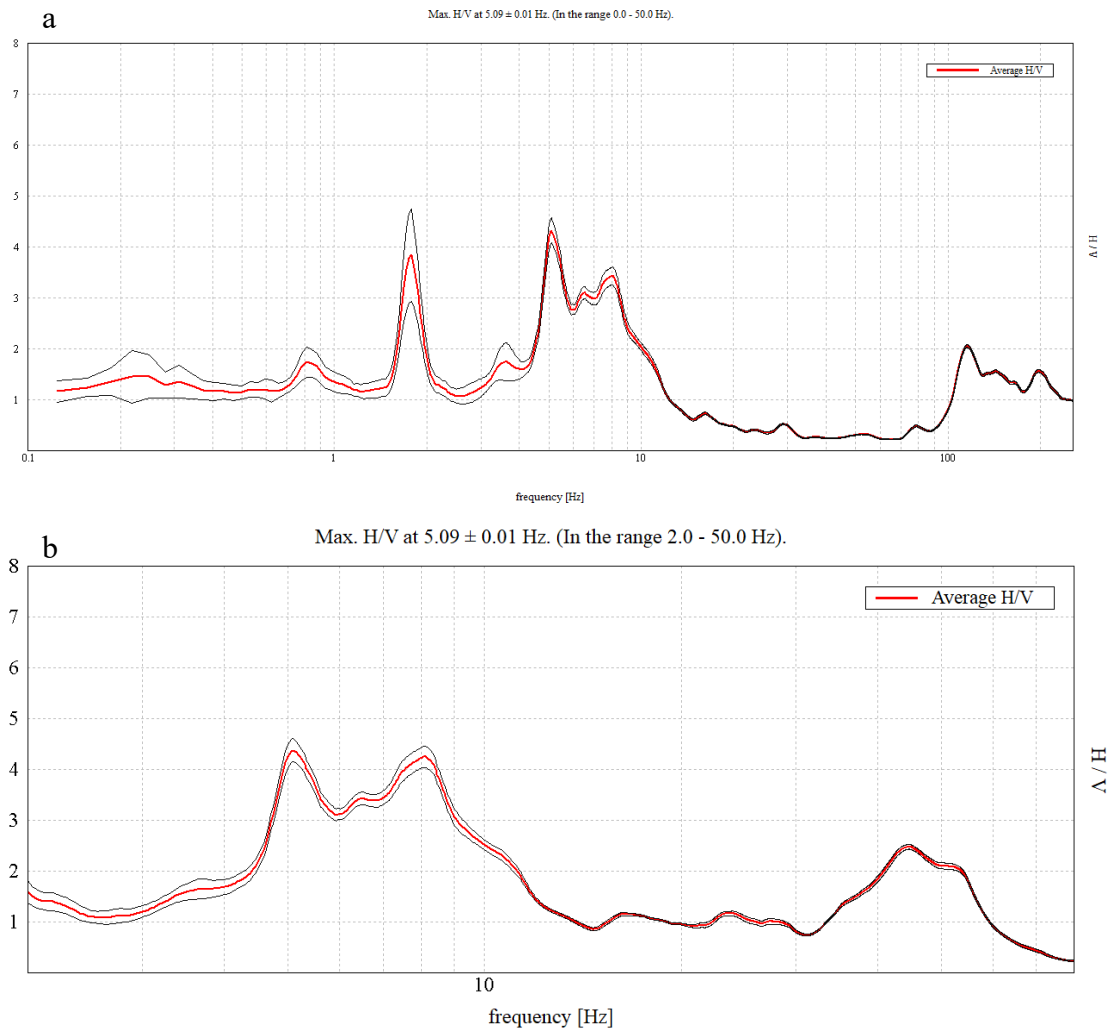

Figure A-27 Journalism B-06 A site, Test 5, concrete (a), grass (b)

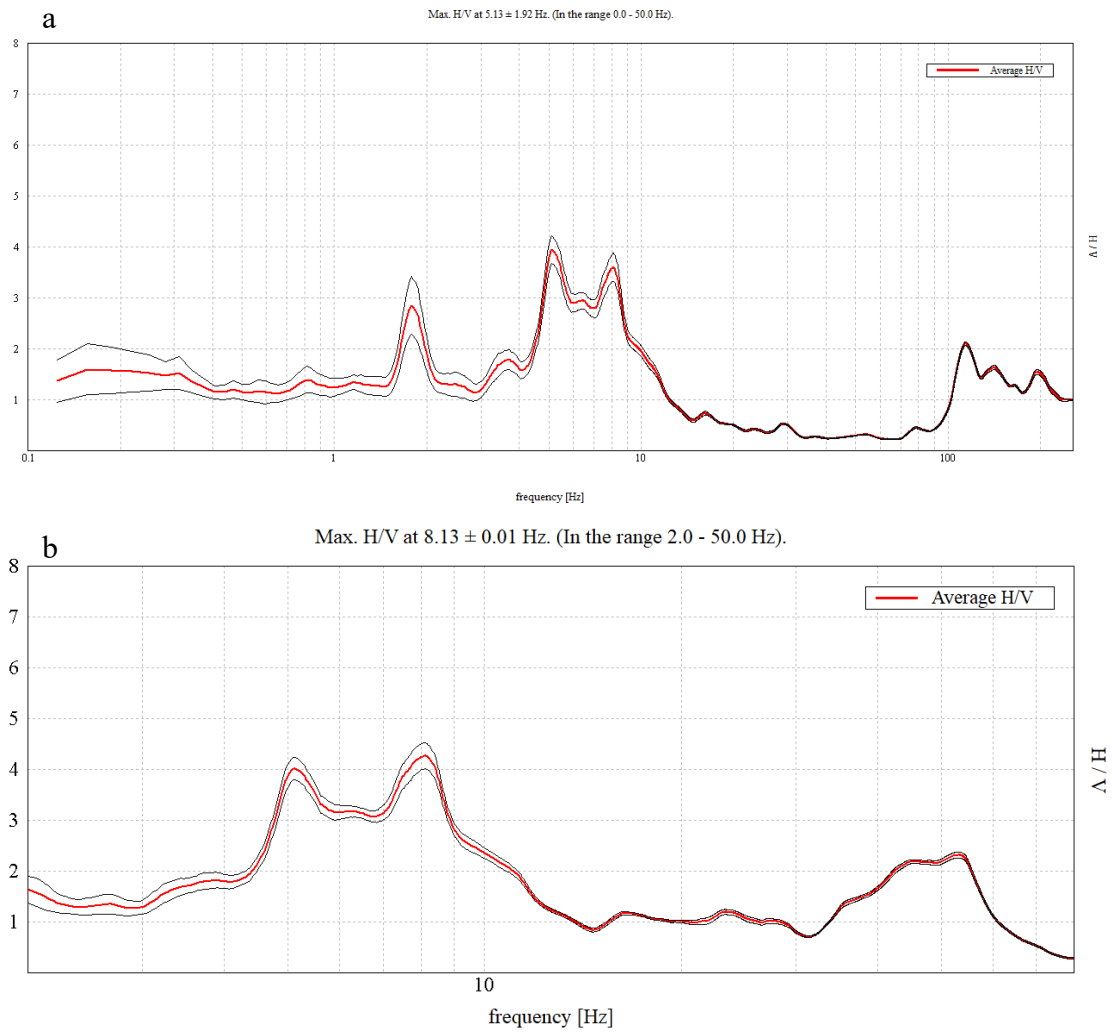

Figure A-28 Journalism B-06 A site, Test 6, concrete (a), grass (b)

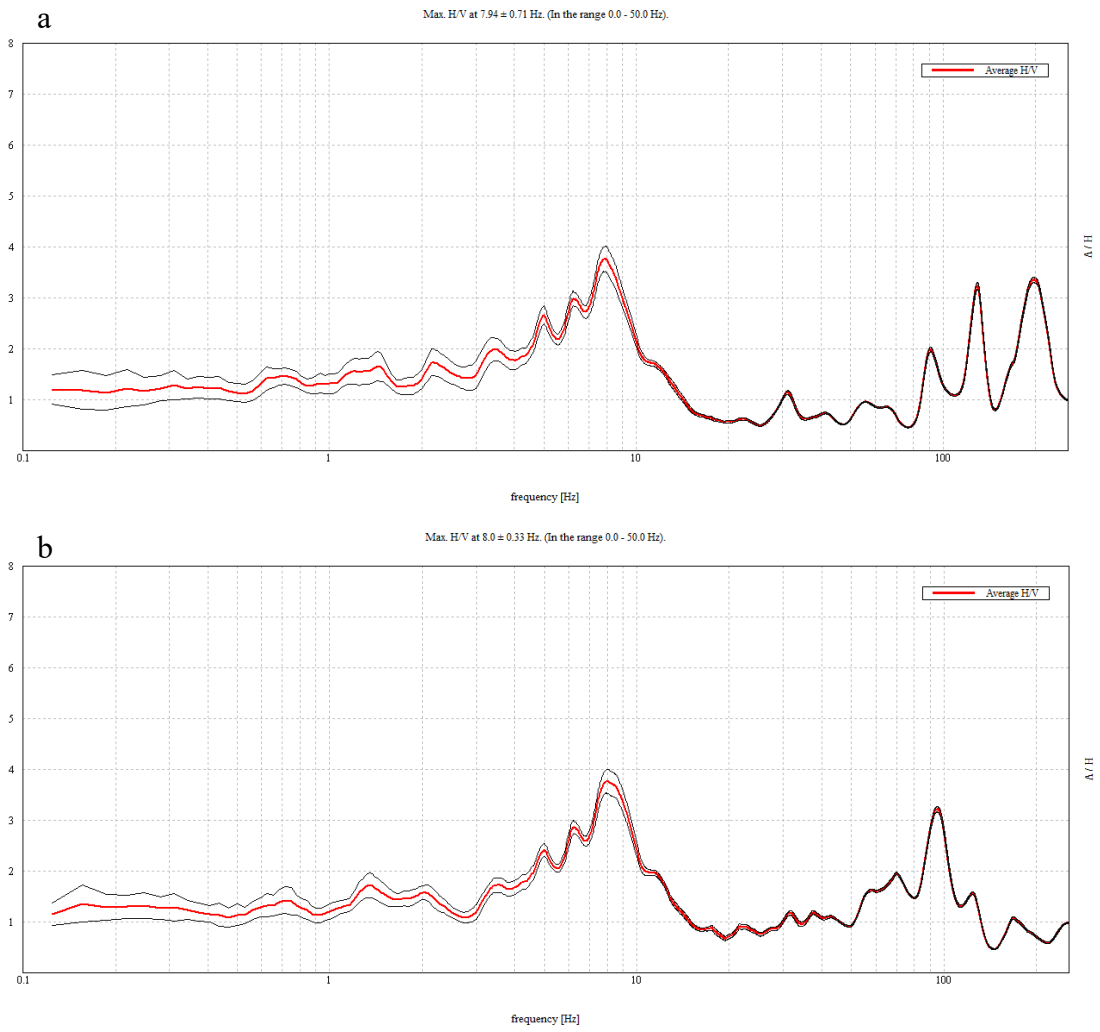

Figure A-29 Journalism B-06 B site, Test 1, concrete (a), grass (b)

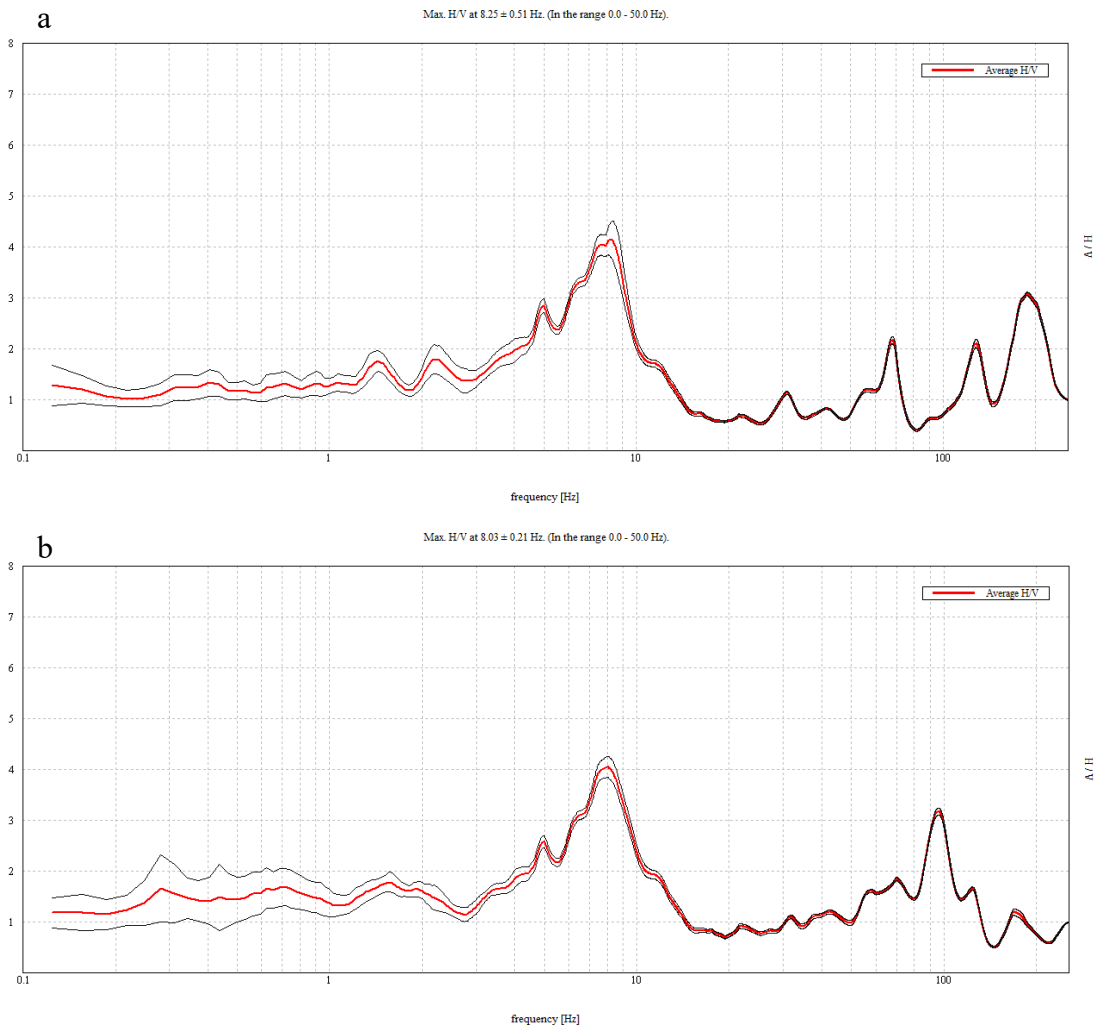

Figure A-30 Journalism B-06 B site, Test 2, concrete (a), grass (b)

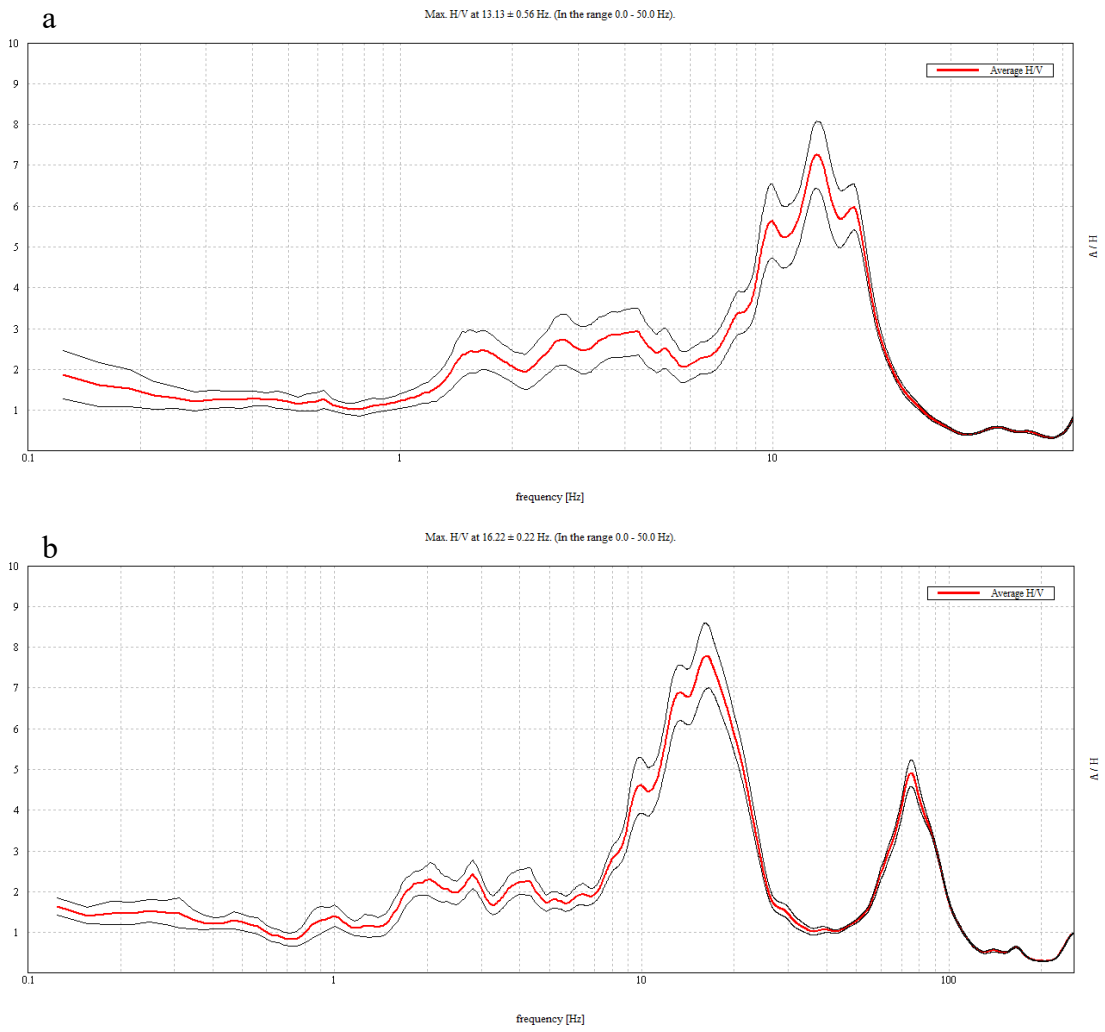

Figure A-31 Lee's Hall BH-08 site, Test 1, concrete (a), grass (b)

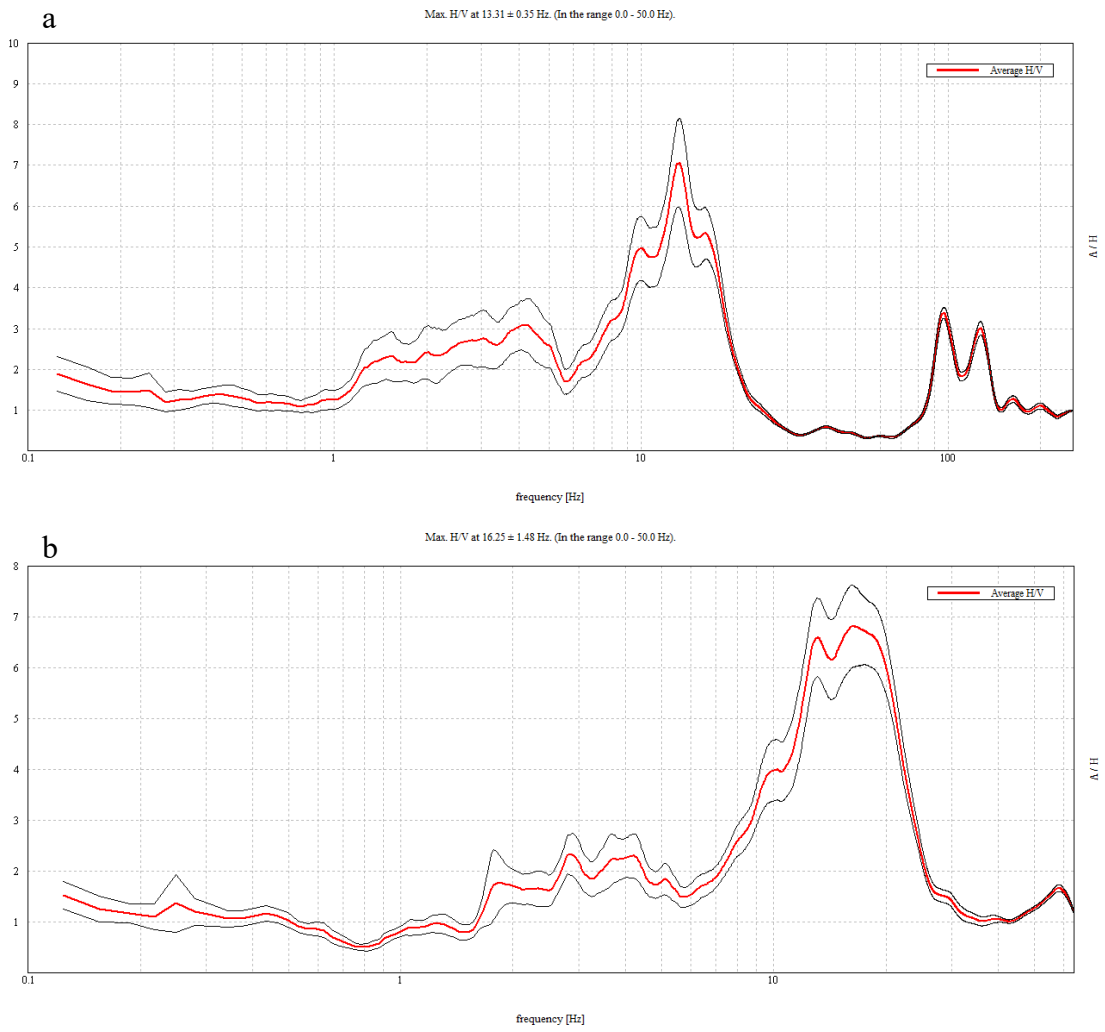

Figure A-32 Lee's Hall BH-08 site, Test 2, concrete (a), grass (b)

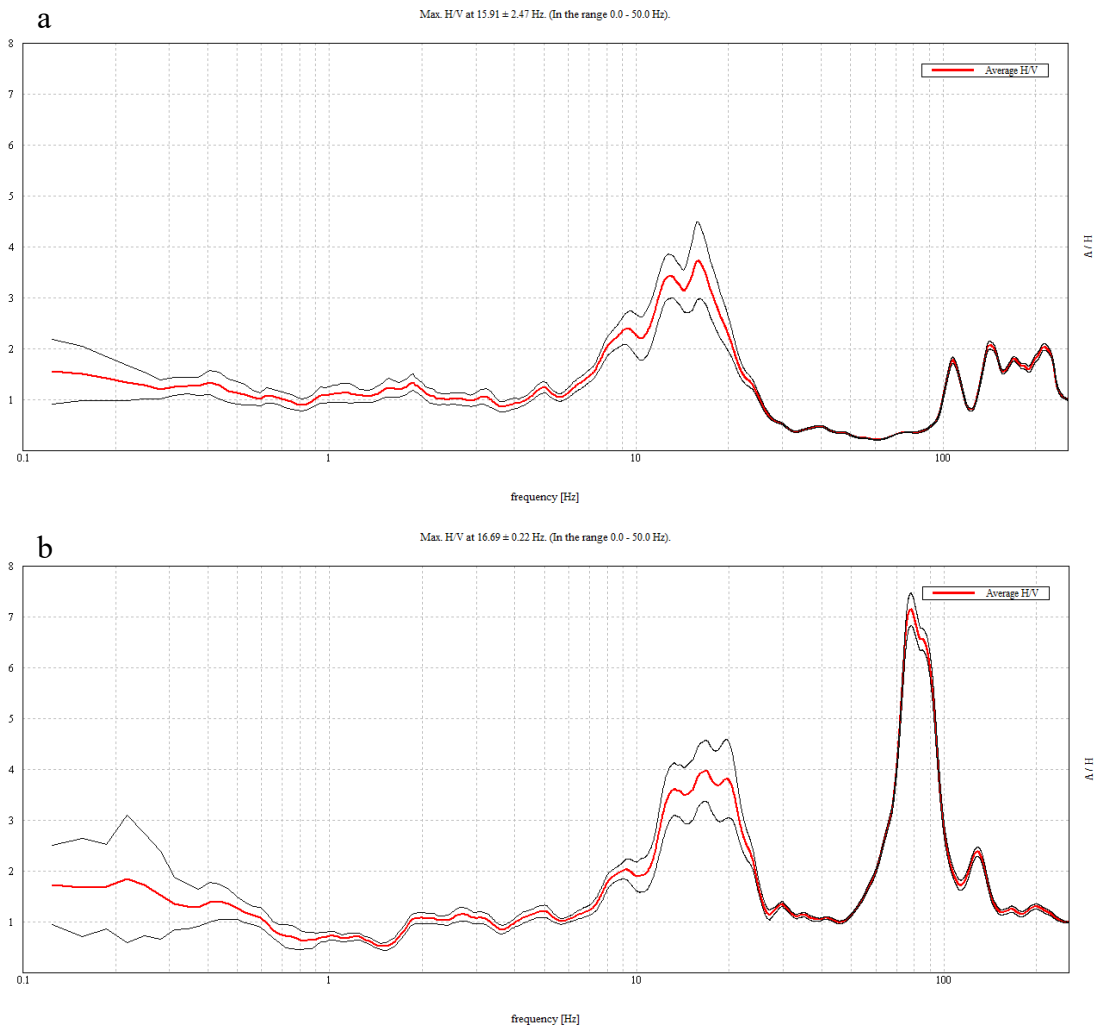

Figure A-33 Lee's Hall BH-08 site, Test 3, concrete (a), grass (b)

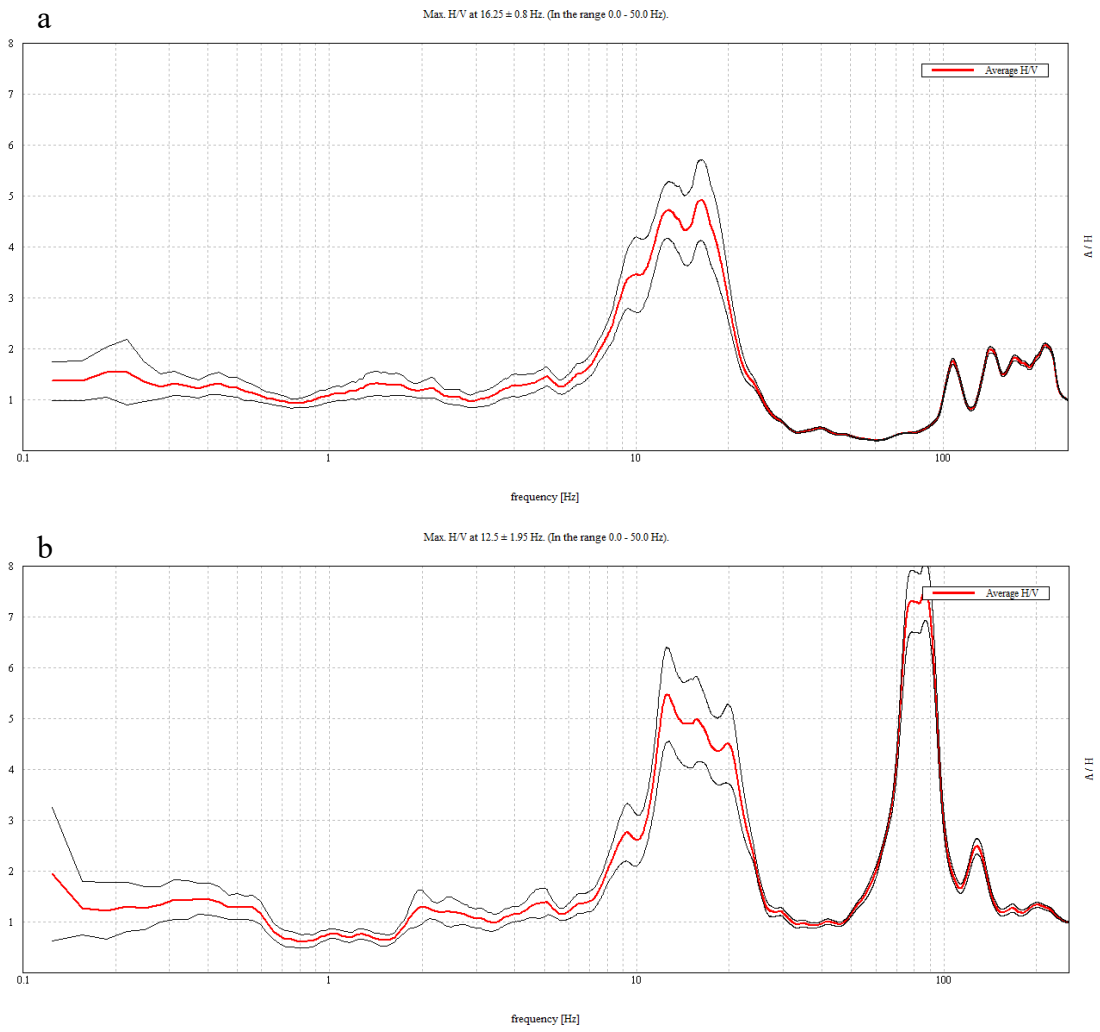

Figure A-34 Lee's Hall BH-08 site, Test 4, concrete (a), grass (b)

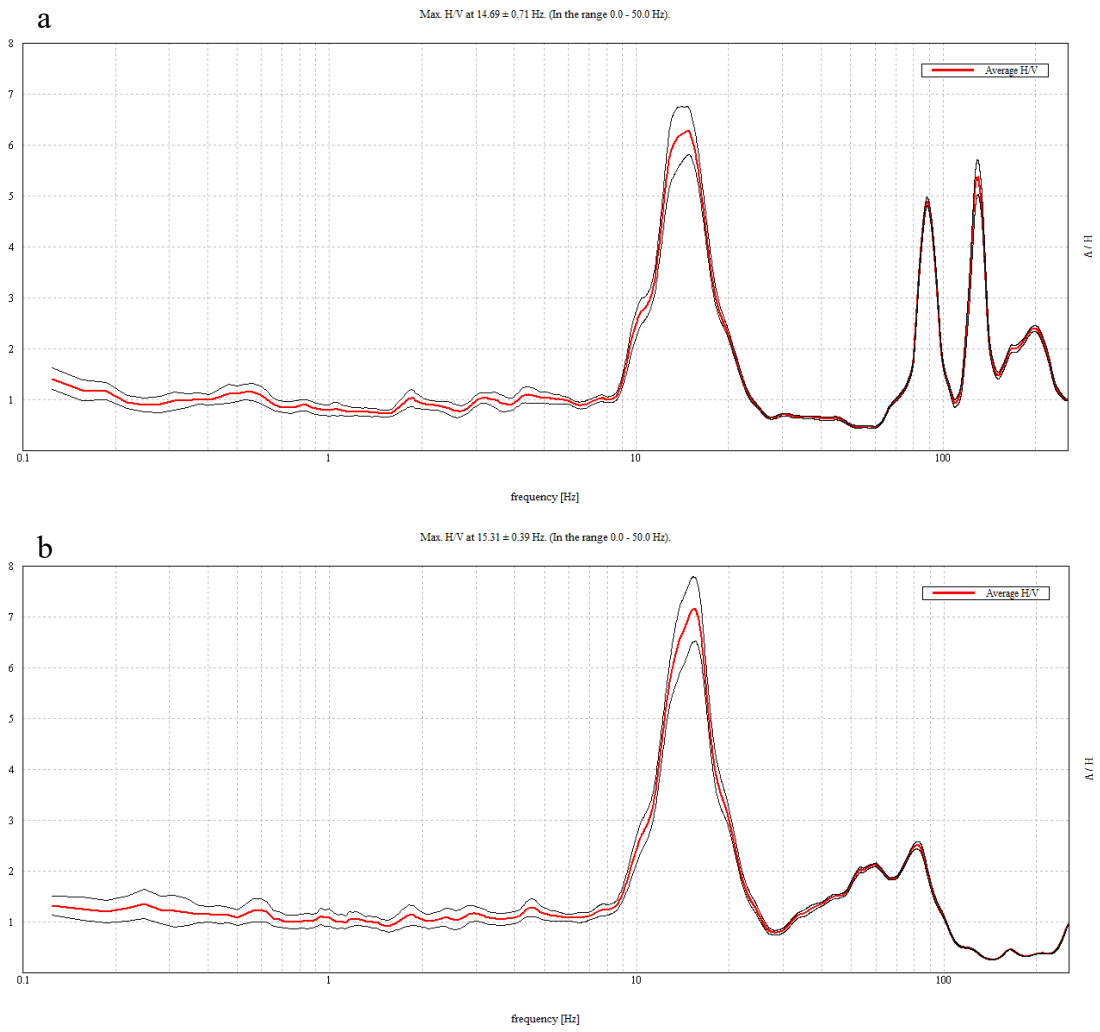

Figure A-35 Lee's Hall BH-18 site, Test 1, concrete (a), grass (b)

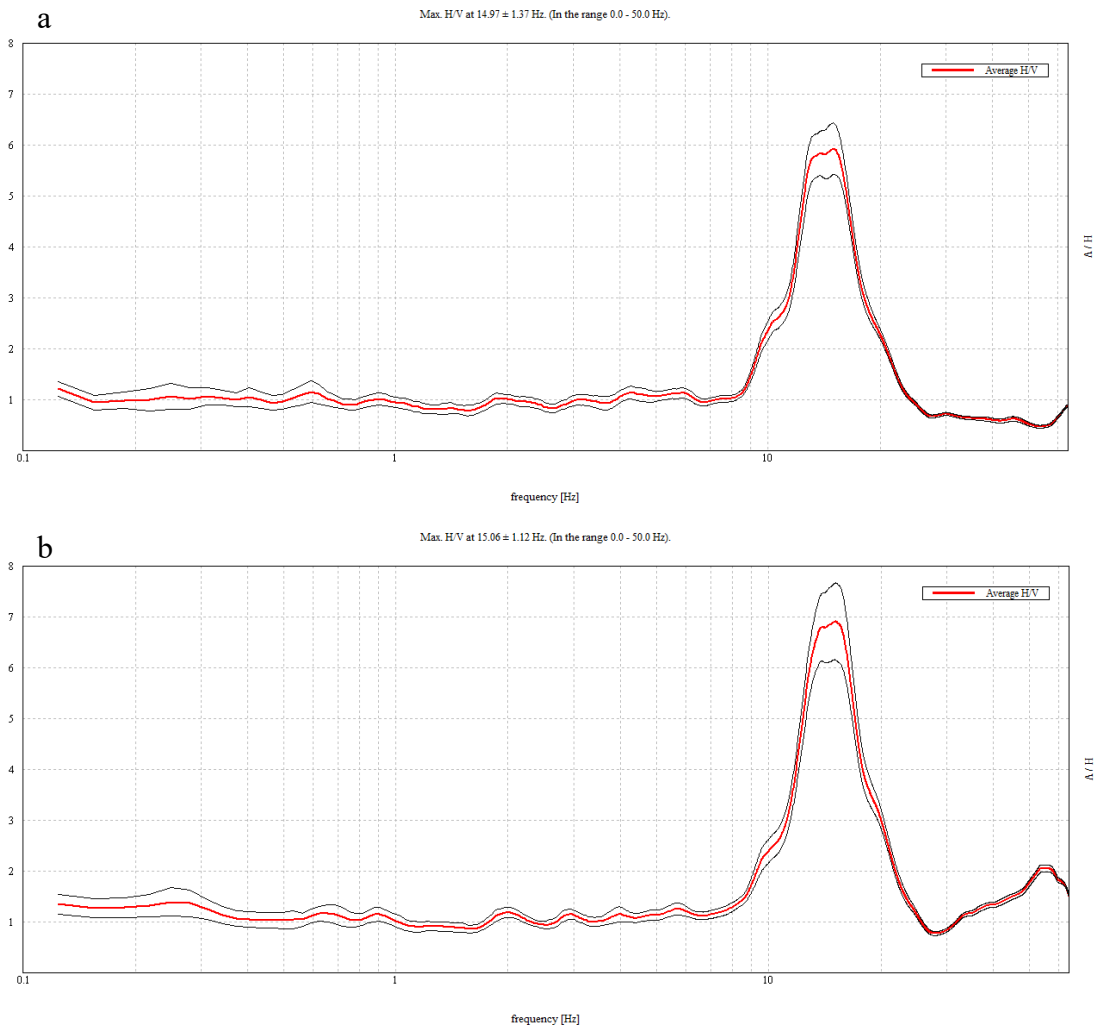

Figure A-36 Lee's Hall BH-18 site, Test 2, concrete (a), grass (b)

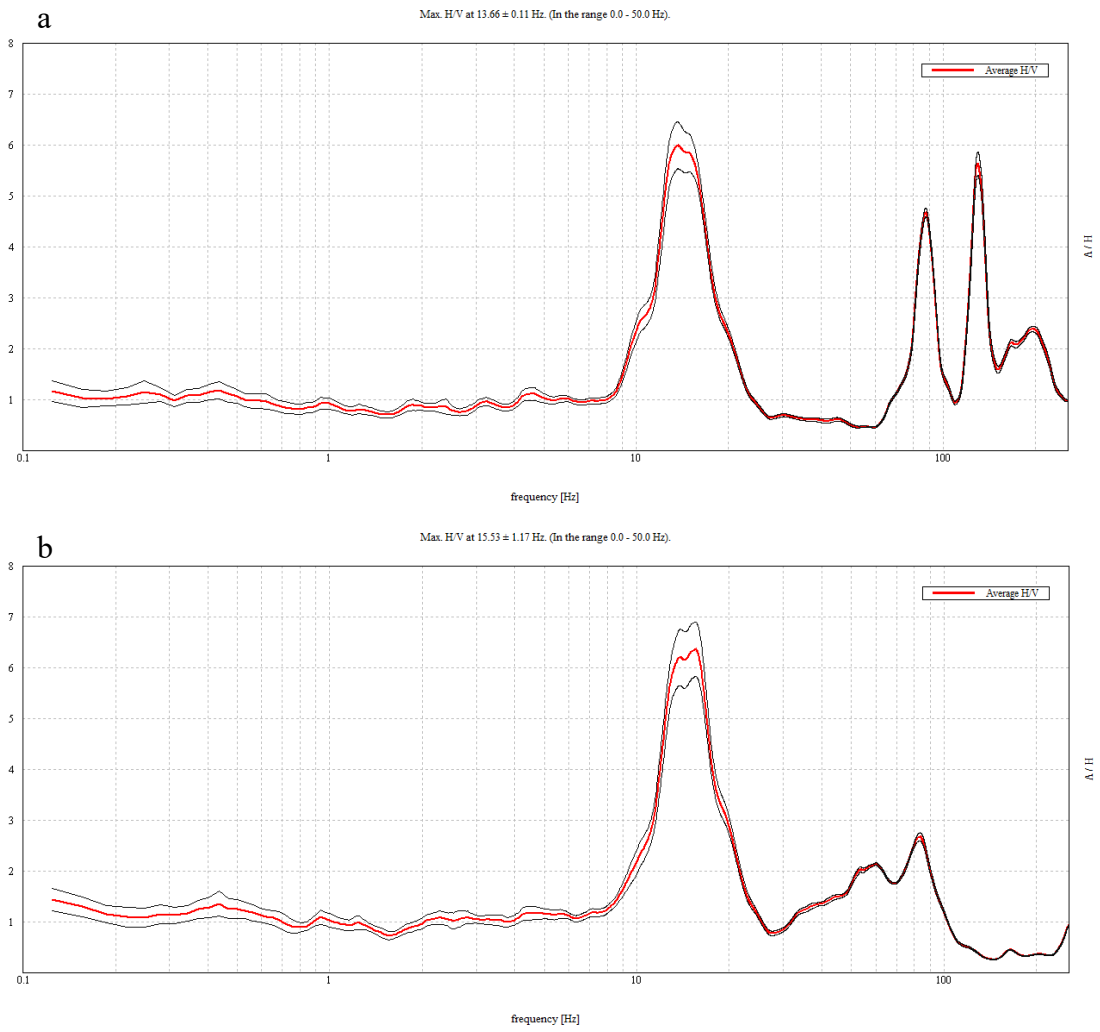

Figure A-37 Lee's Hall BH-18 site, Test 3, concrete (a), grass (b)

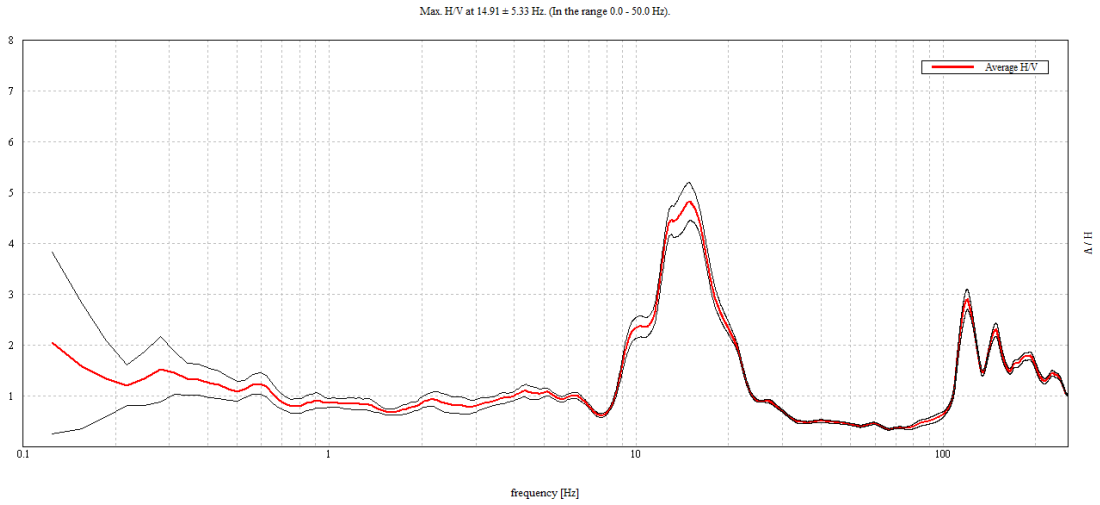

Figure A-38 Lee's Hall BH-18 site, Test 4, concrete

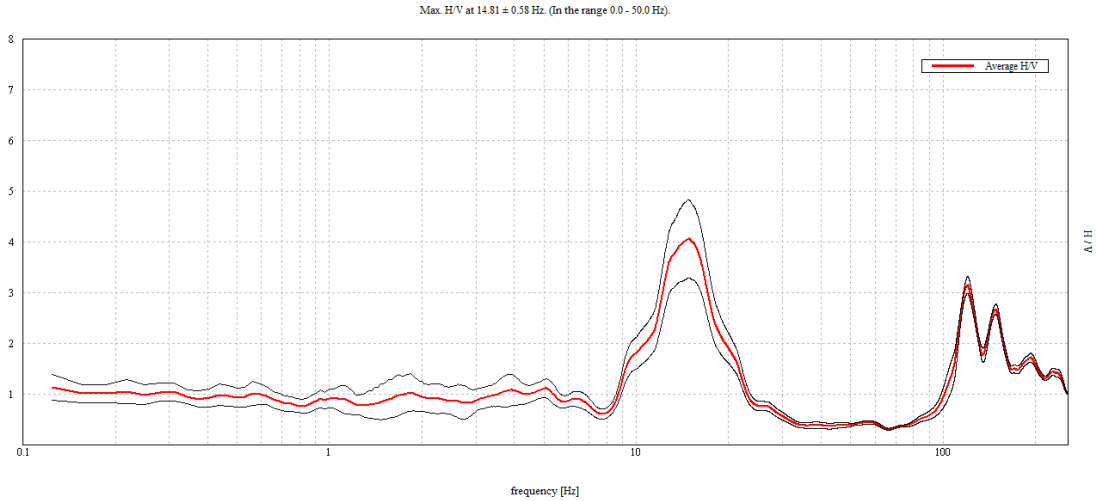

Figure A-39 Lee's Hall BH-18 site, Test 5, concrete

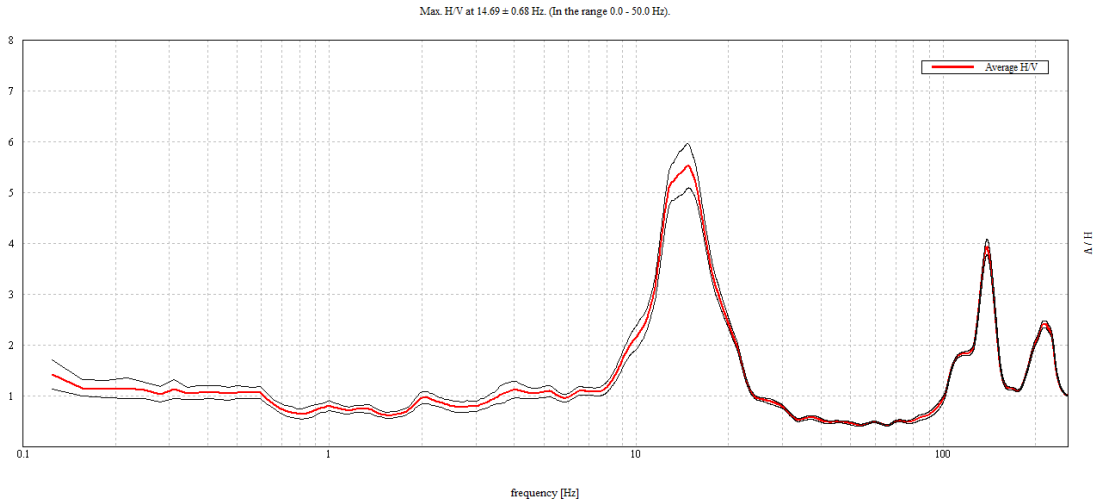

Figure A-40 Lee's Hall BH-18 site, Test 6, concrete

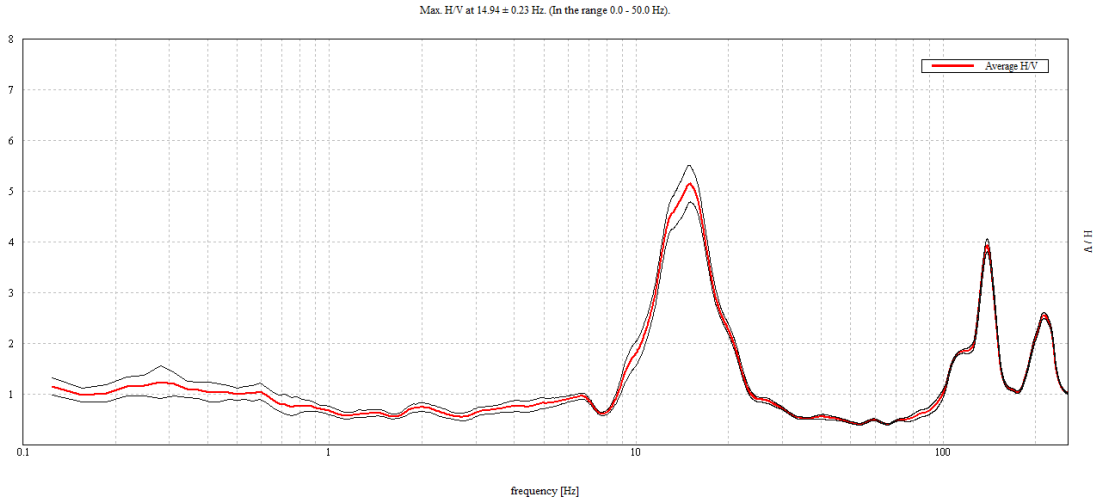

Figure A-41 Lee's Hall BH-18 site, Test 7, concrete

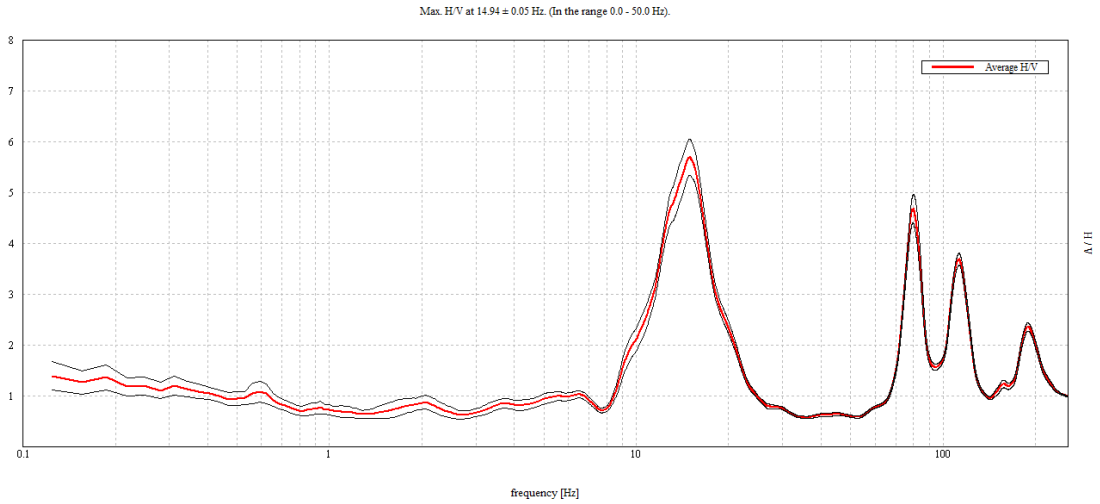

Figure A-42 Lee's Hall BH-18 site, Test 8, concrete

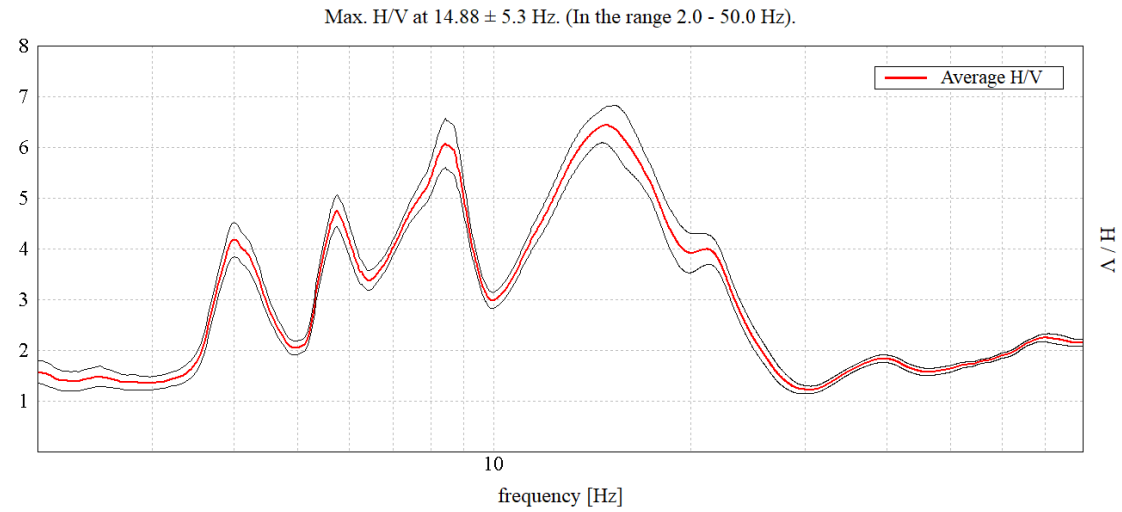

Figure A-43 Lee's Hall Selected site, Test 1, grass

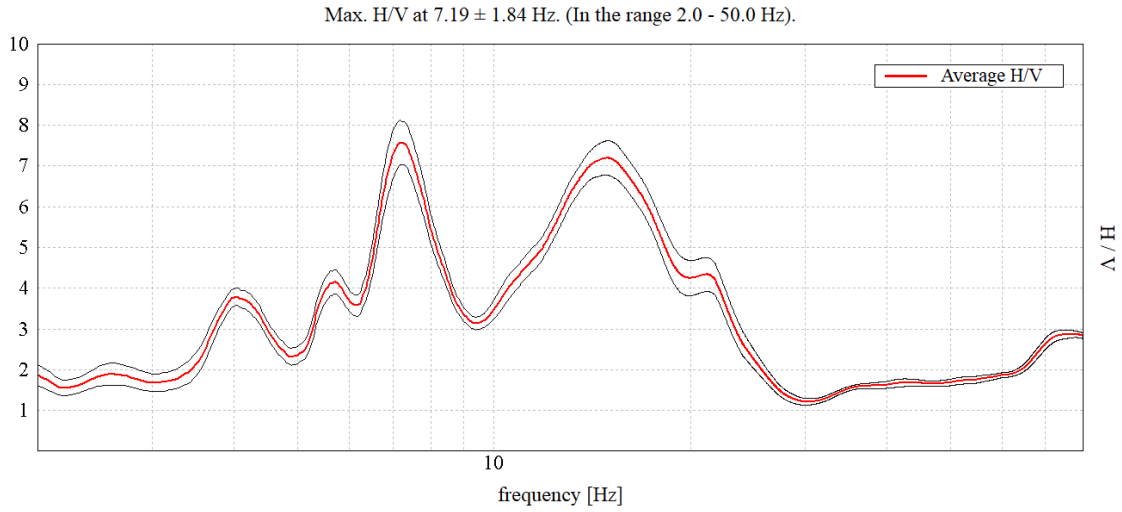

Figure A-44 Lee's Hall Selected site, Test 2, grass

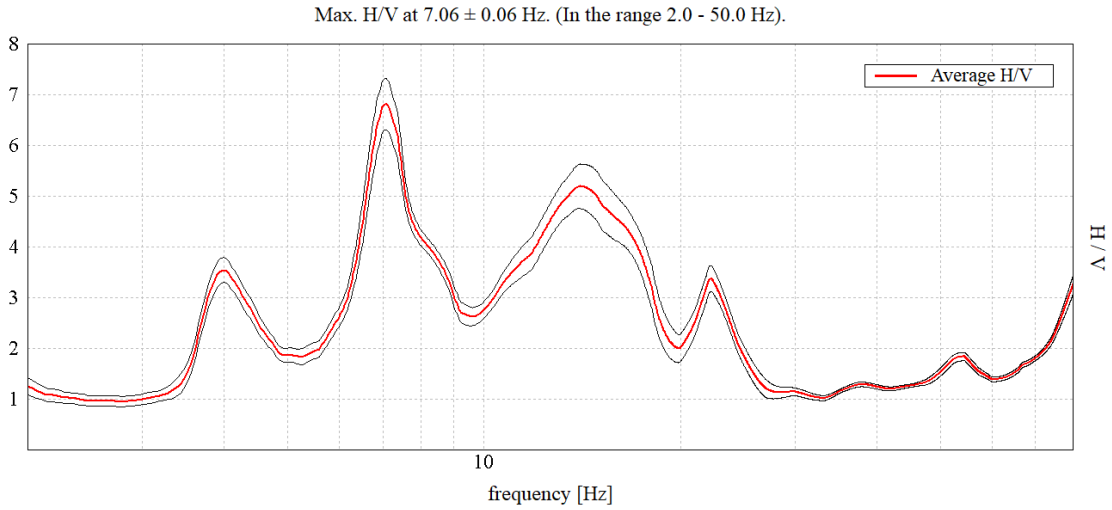

Figure A-45 Lee's Hall Selected site, Test 3, grass

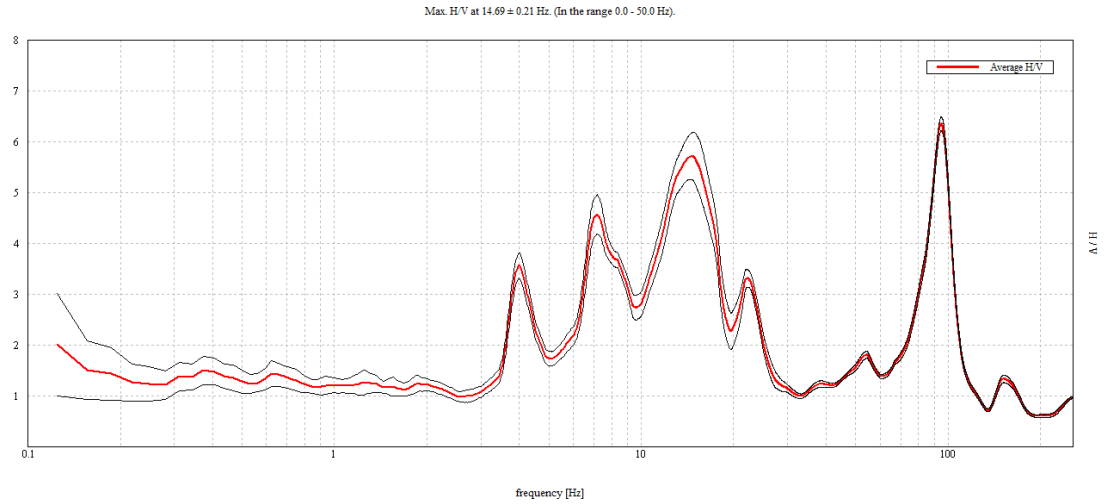

Figure A-46 Lee's Hall Selected site, Test 4, grass

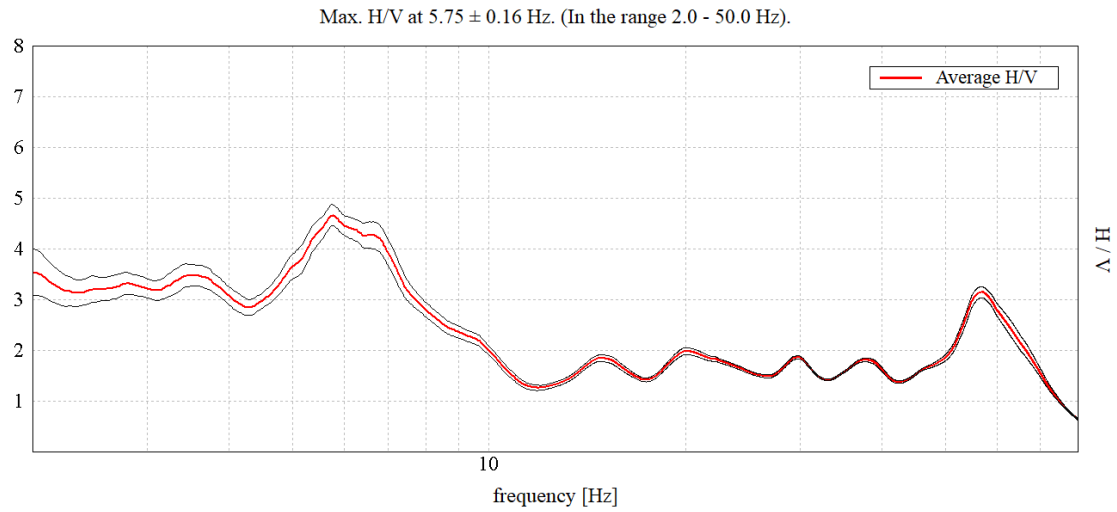

Figure A-47 Lee's Hall Selected site, Test 5, grass

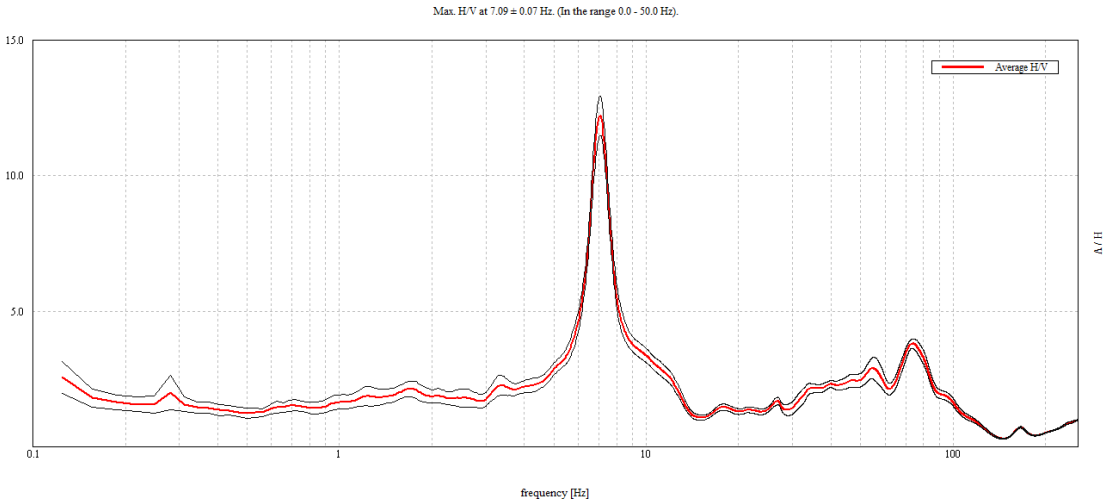

Figure A-48 MIZ Middle Quad site, Test 1, grass

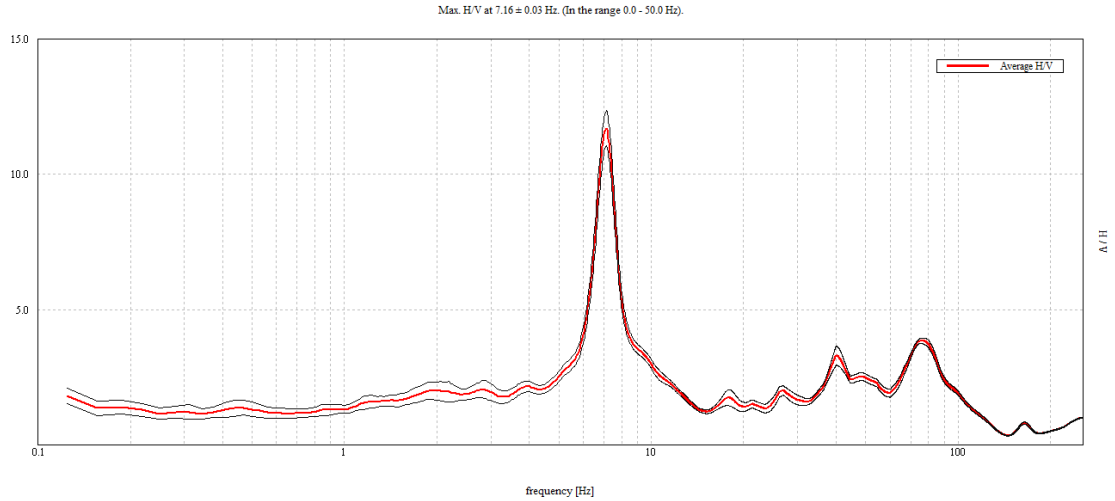

Figure A-49 MIZ Middle Quad site, Test 2, grass

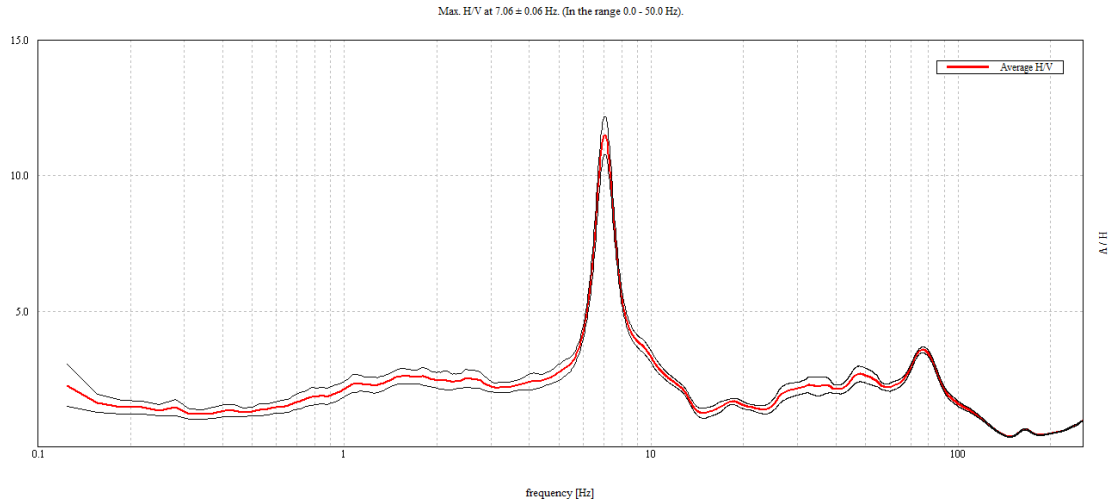

Figure A-50 MIZ Middle Quad site, Test 3, grass

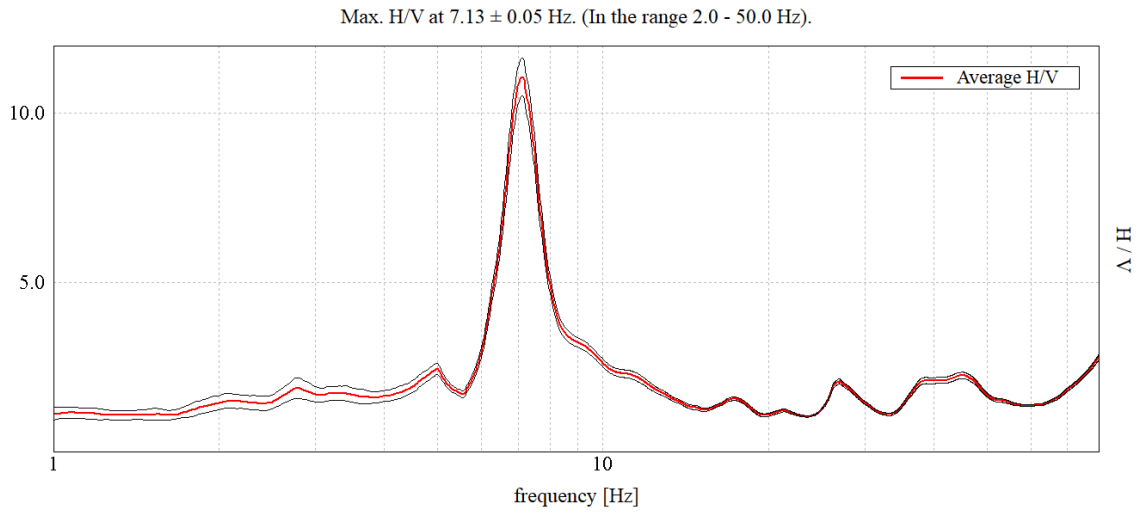

Figure A-51 MIZ Middle Quad site, Test 4, grass

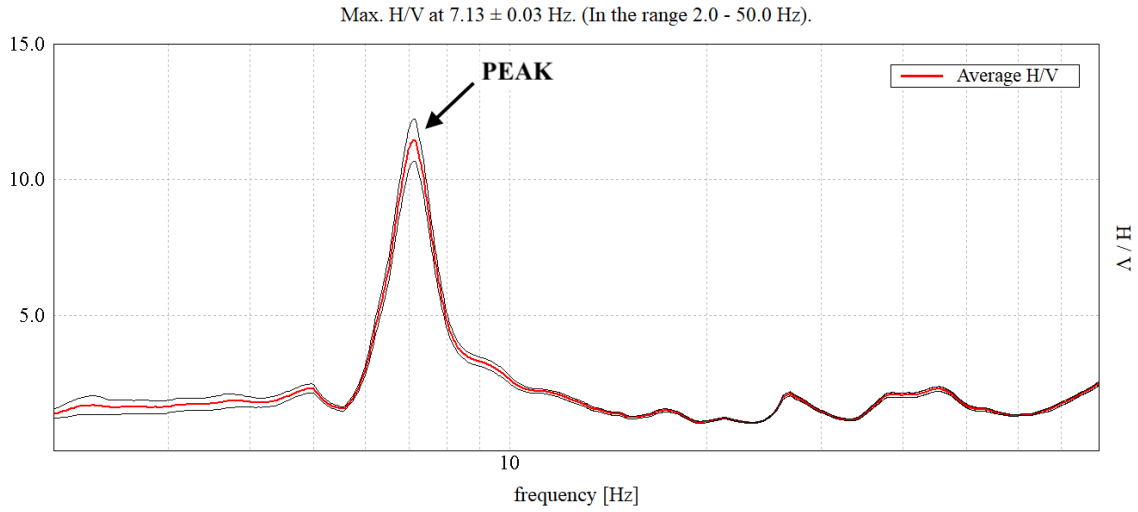

Figure A-52 MIZ Middle Quad site, Test 5, grass

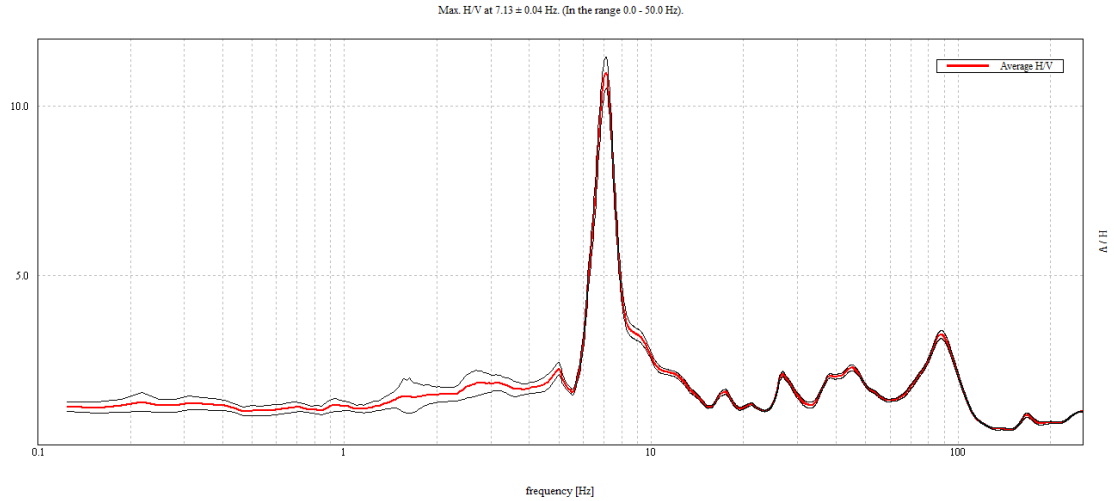

Figure A-53 MIZ Middle Quad site, Test 6, grass

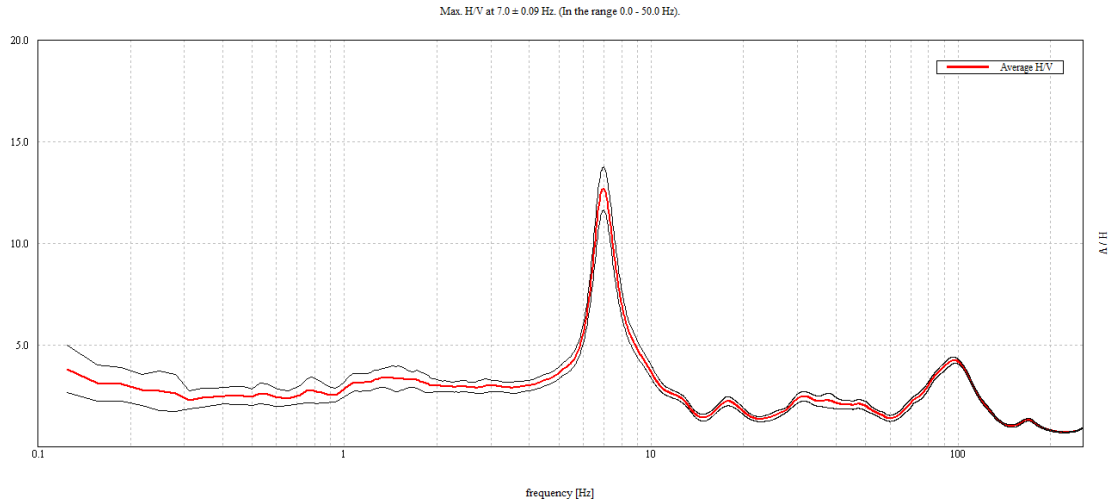

Figure A-54 MIZ Middle Quad site, Test 7, grass

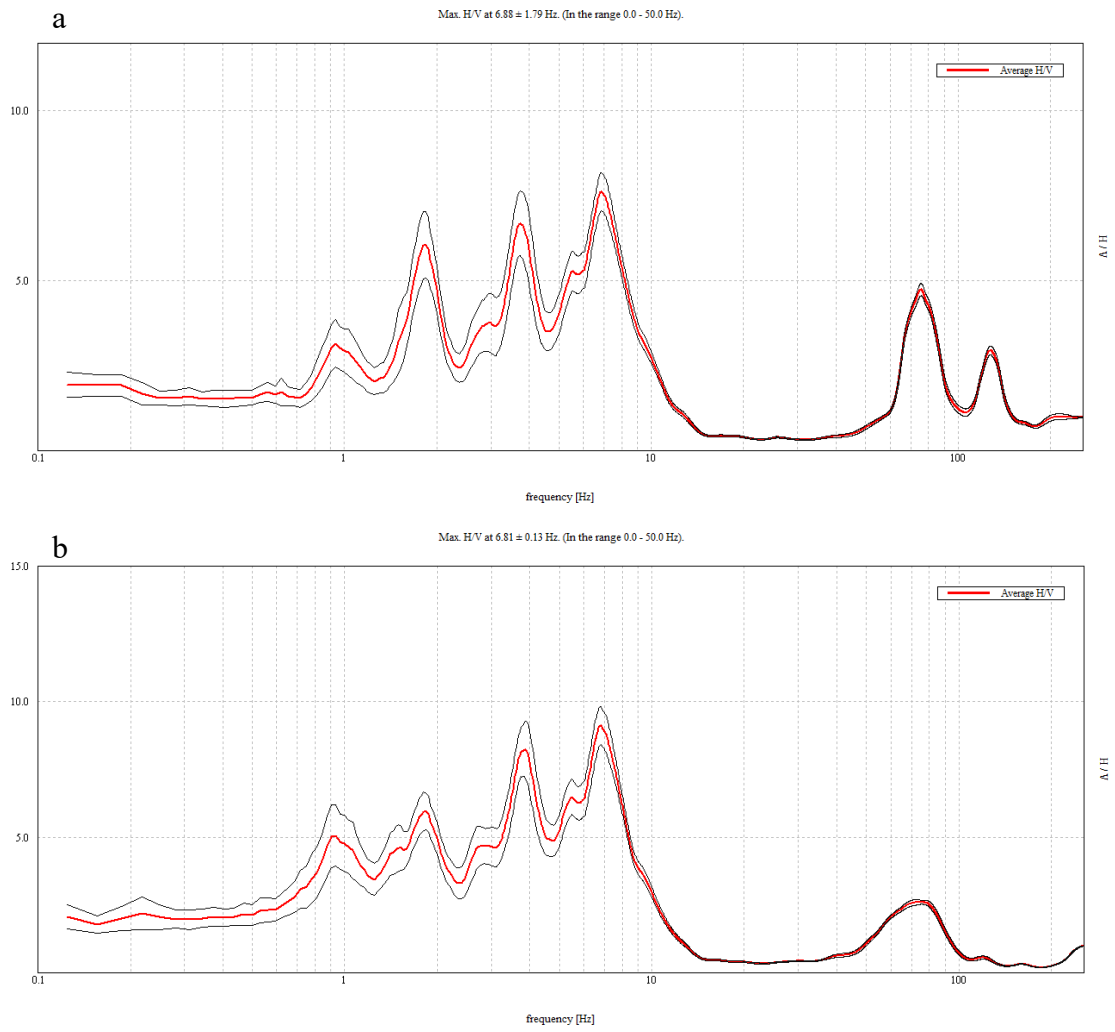

Figure A-55 MIZ Quad Site 1 site, Test 1, concrete (a), grass (b)

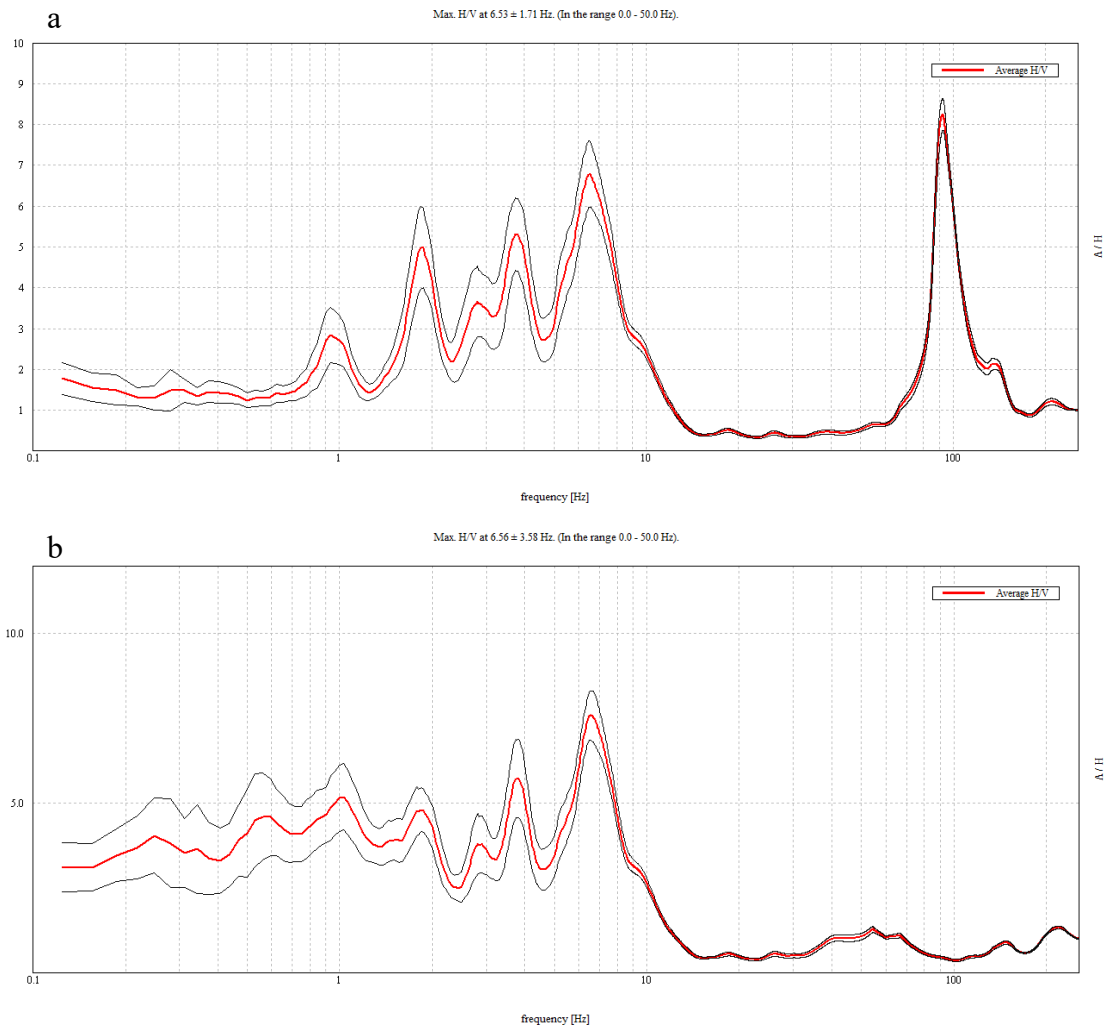

Figure A-56 MIZ Quad Site 1 site, Test 2, concrete (a), grass (b)

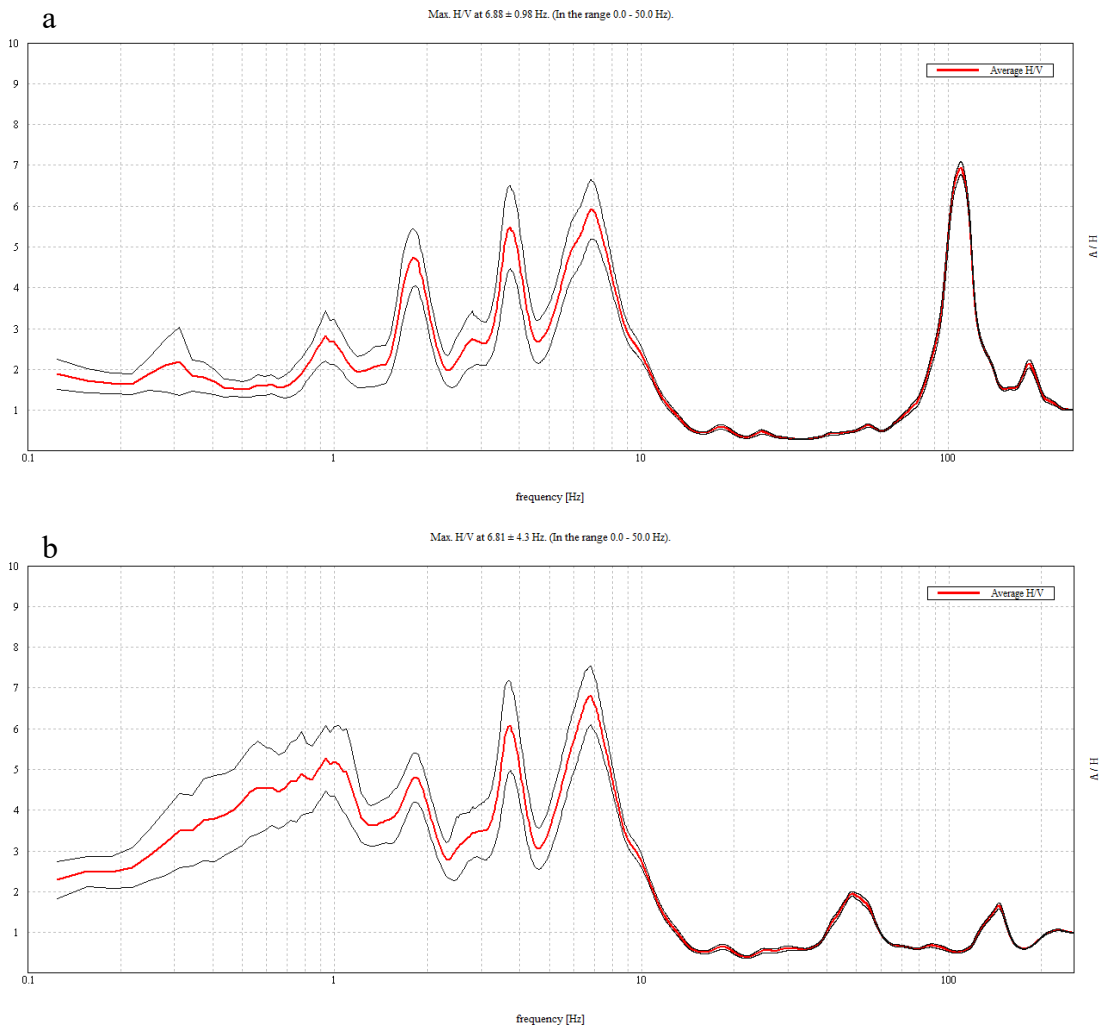

Figure A-57 MIZ Quad Site 1 site, Test 3, concrete (a), grass (b)

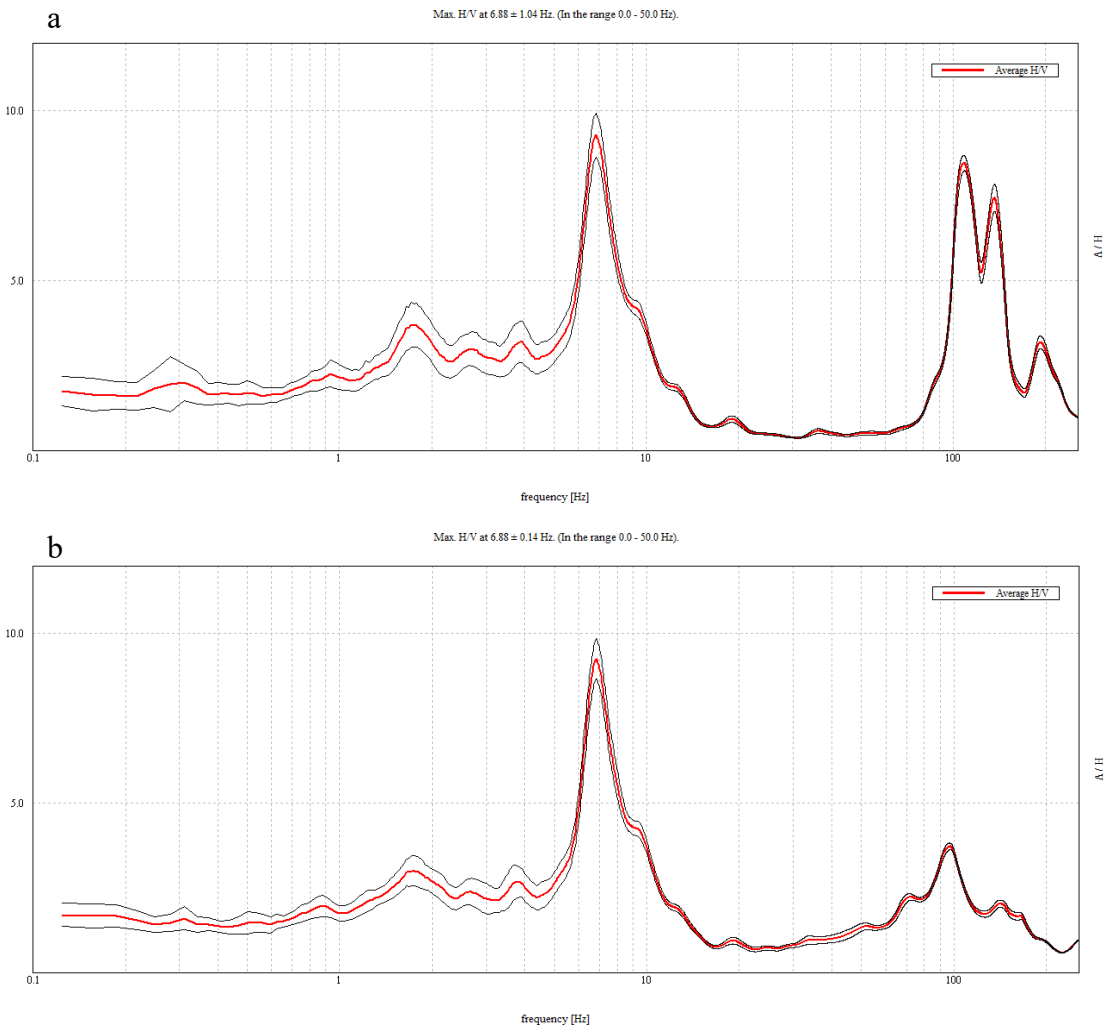

Figure A-58 MIZ Quad Site 1 site, Test 4, concrete (a), grass (b)

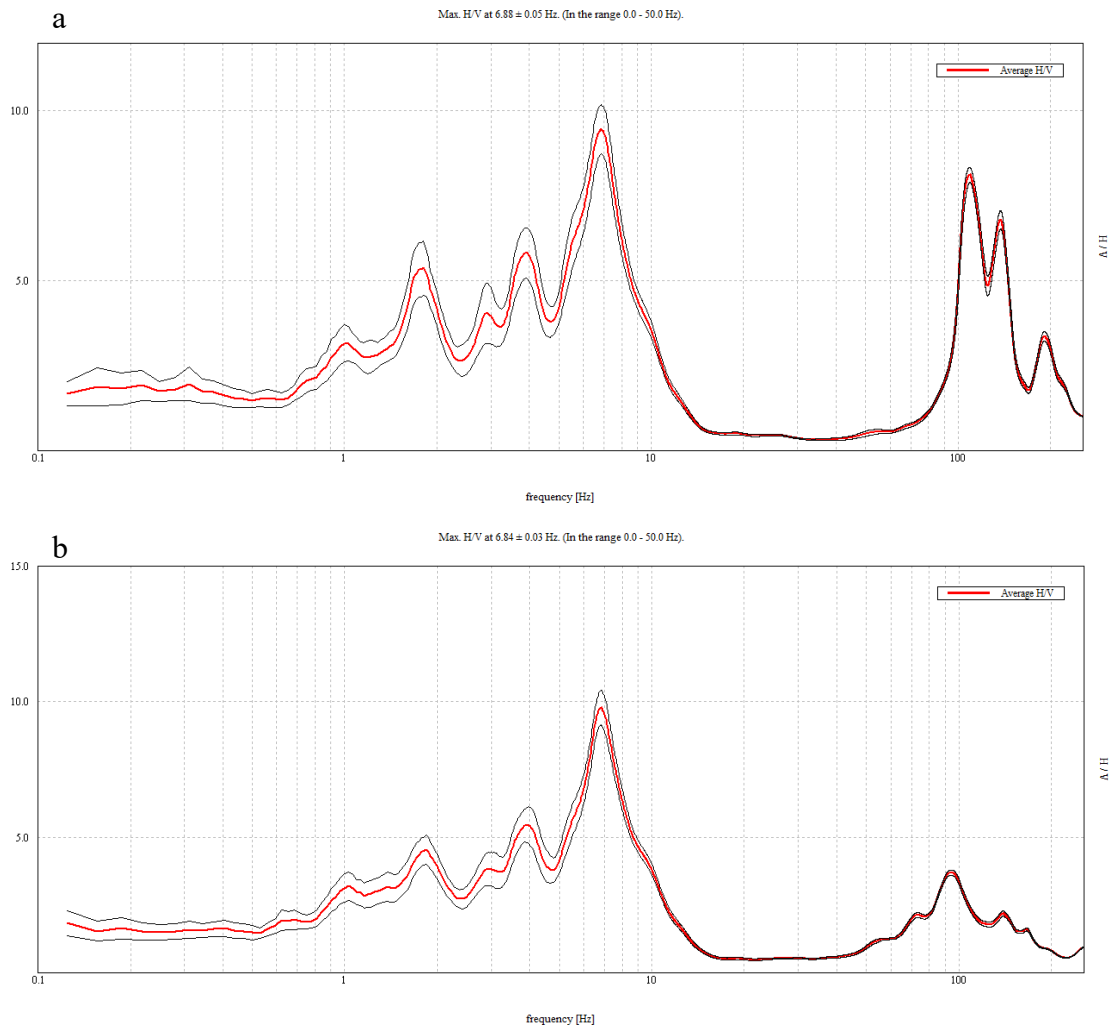

Figure A-59 MIZ Quad Site 1 site, Test 5, concrete (a), grass (b)

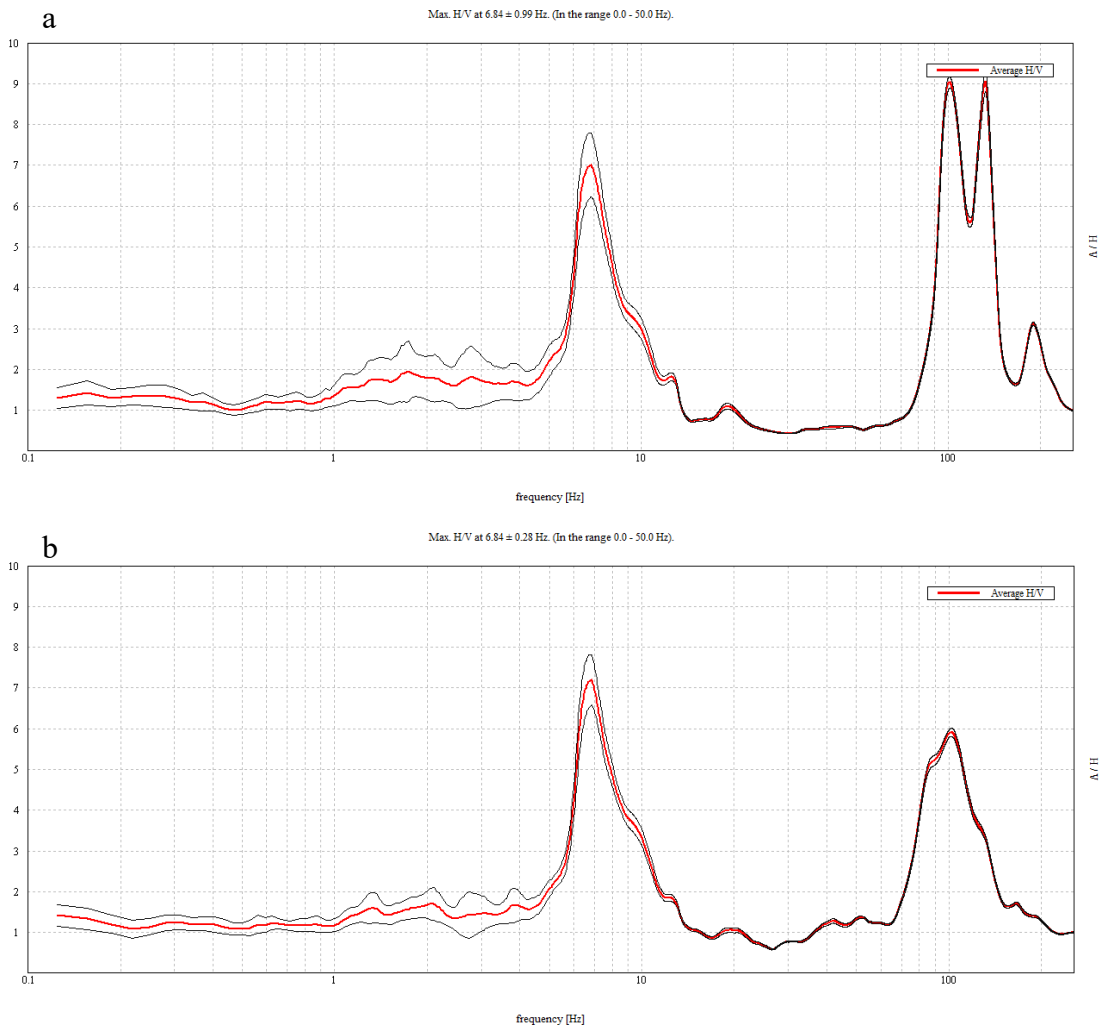

Figure A-60 MIZ Quad Site 1 site, Test 6, concrete (a), grass (b)

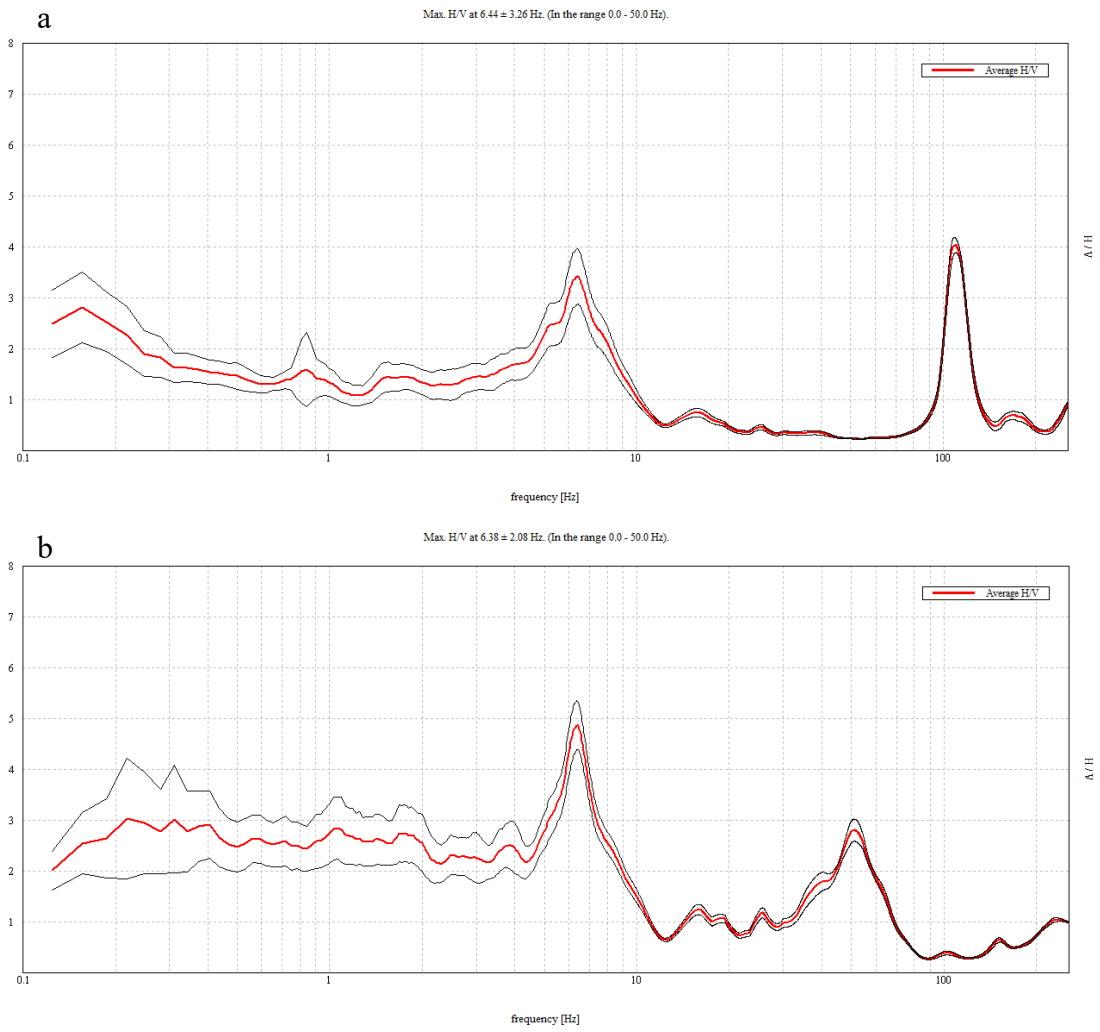

Figure A-61 MIZ Quad Site 2 site, Test 1, concrete (a), grass (b)

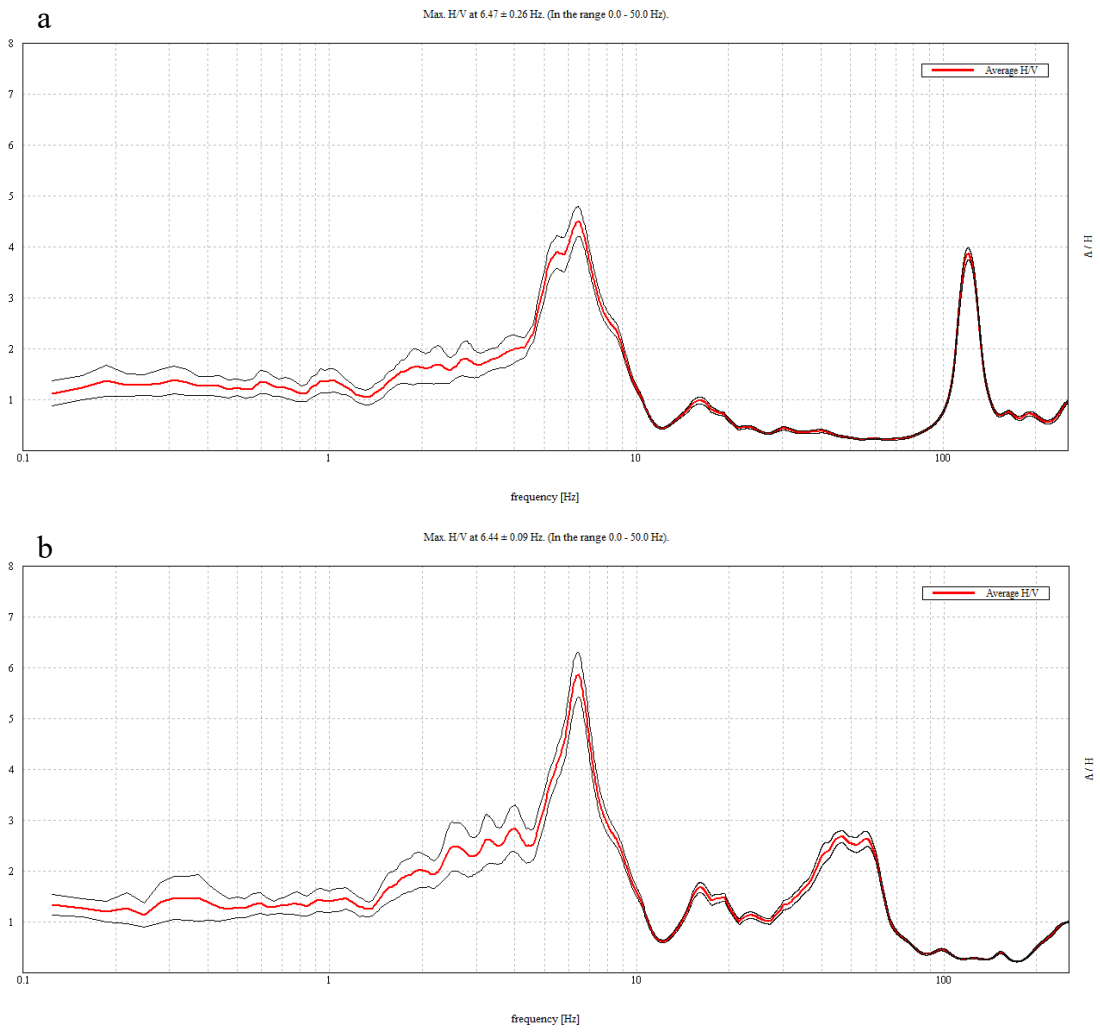

Figure A-62 MIZ Quad Site 2 site, Test 2, concrete (a), grass (b)

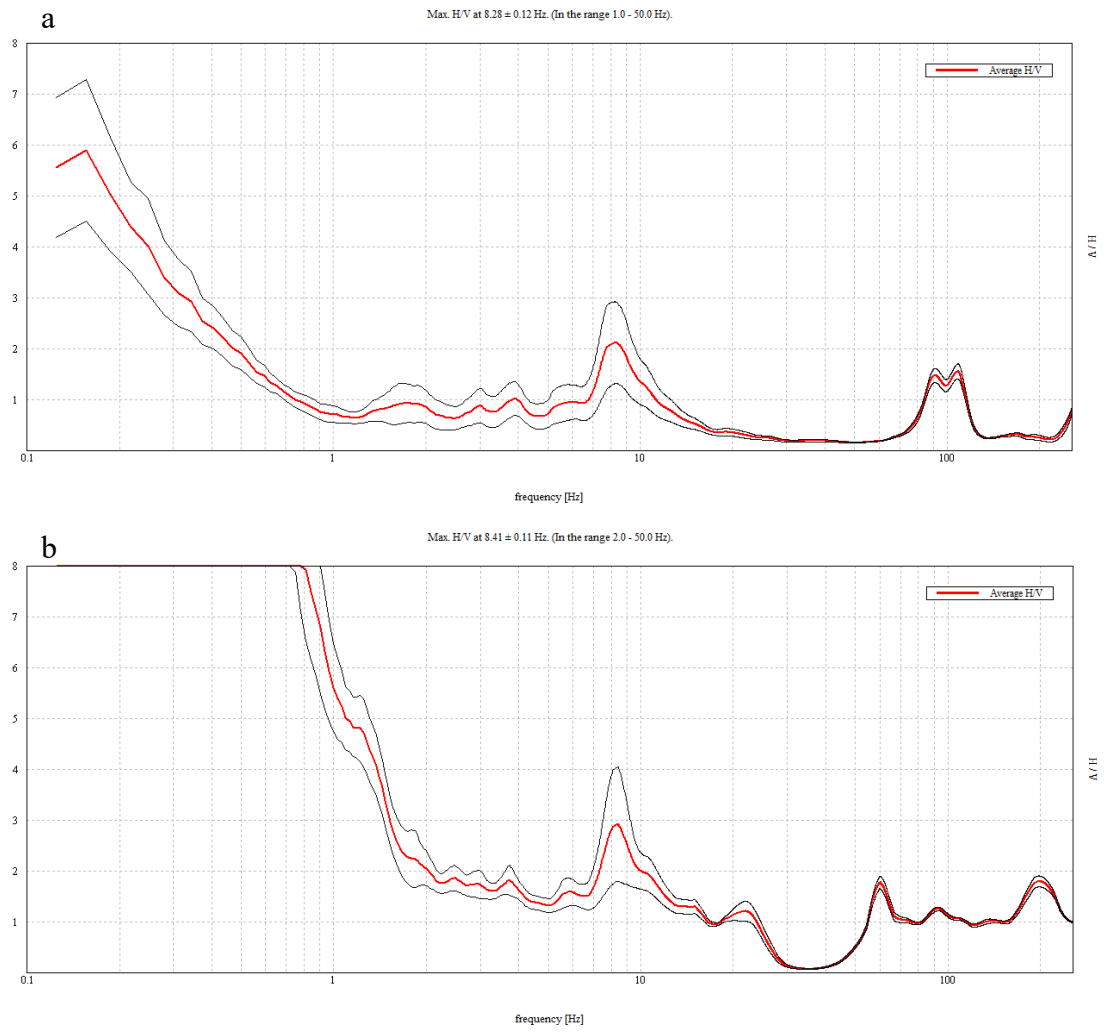

Figure A-63 MIZ Quad Site 3 site, Test 1, concrete (a), grass (b)

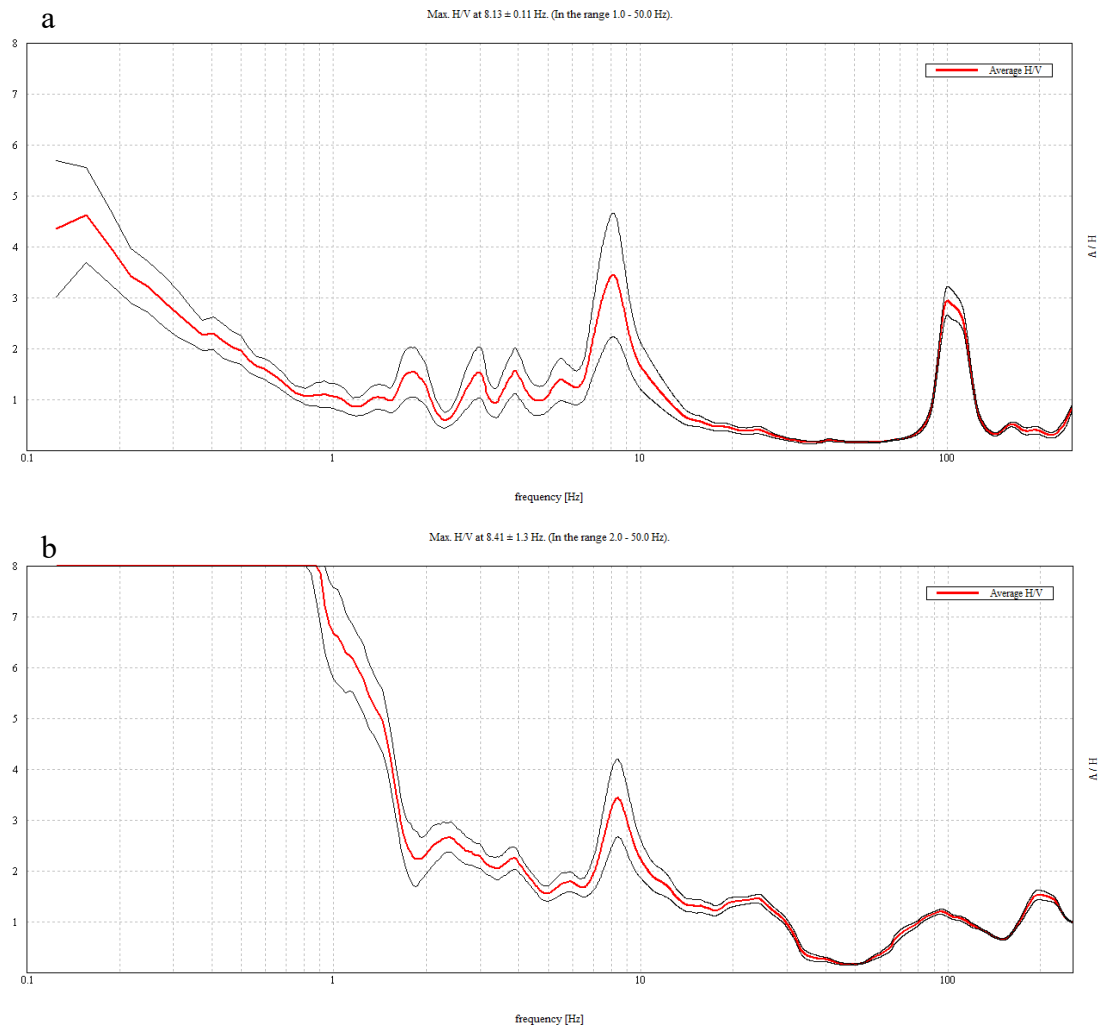

Figure A-64 MIZ Quad Site 3 site, Test 2, concrete (a), grass (b)

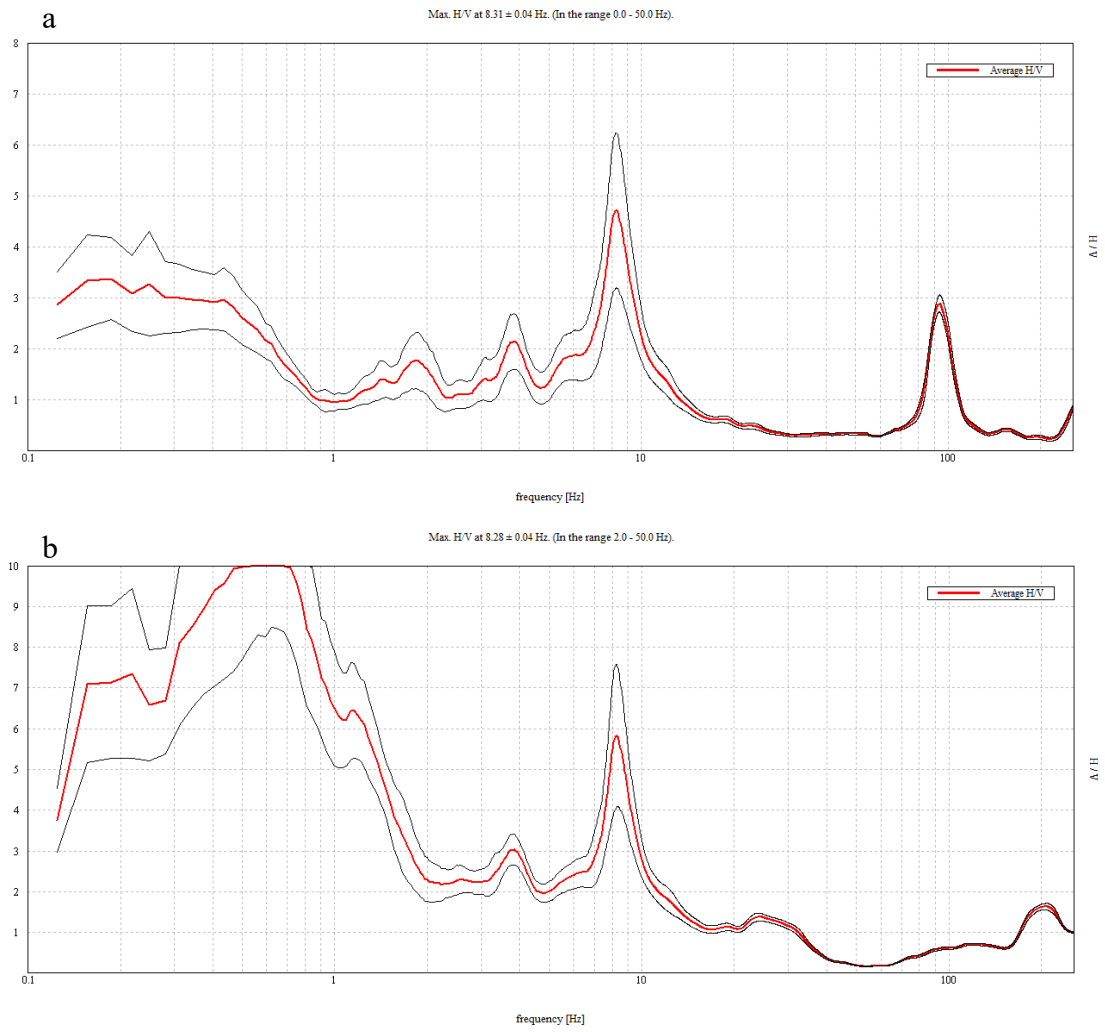

Figure A-65 MIZ Quad Site 3 site, Test 3, concrete (a), grass (b)

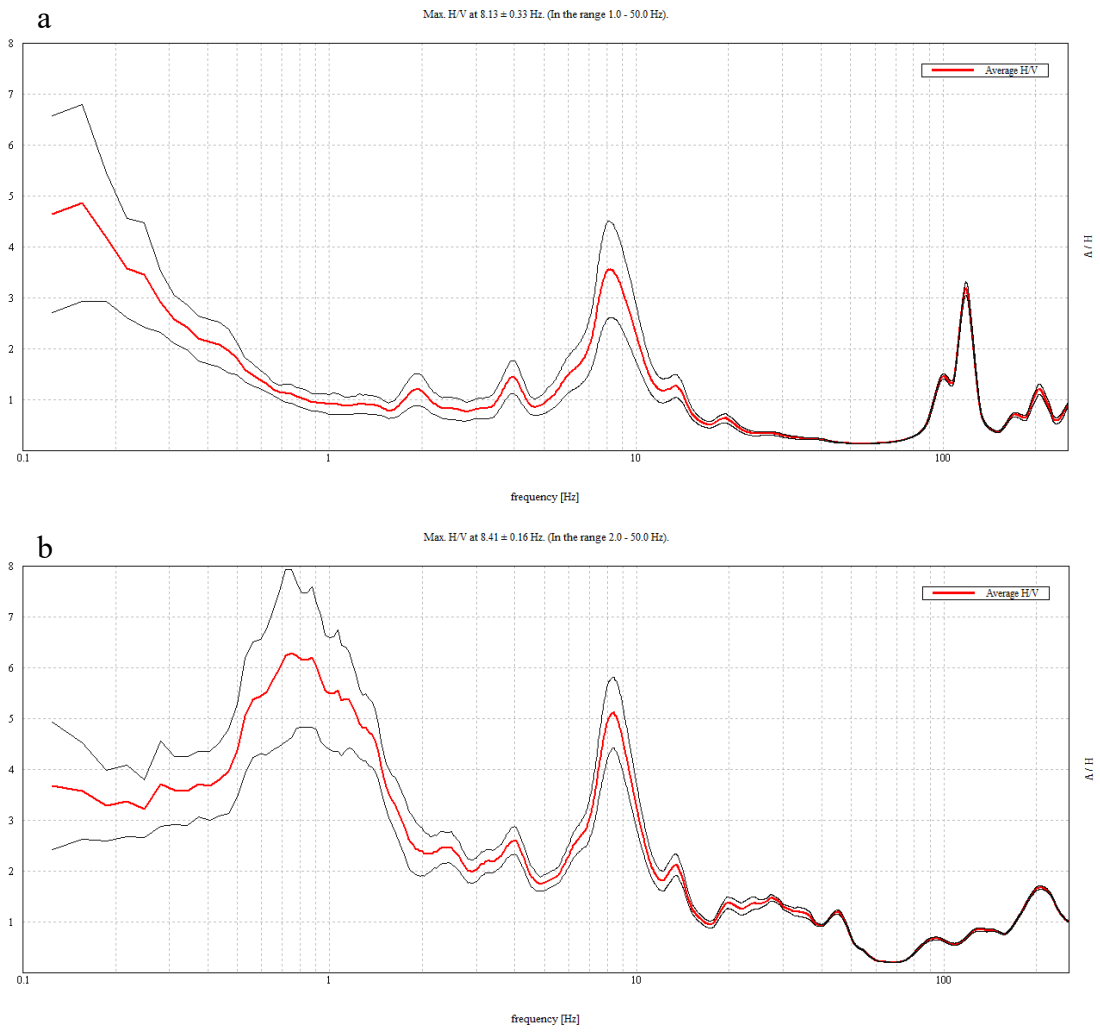

Figure A-66 MIZ Quad Site 3 site, Test 4, concrete (a), grass (b)

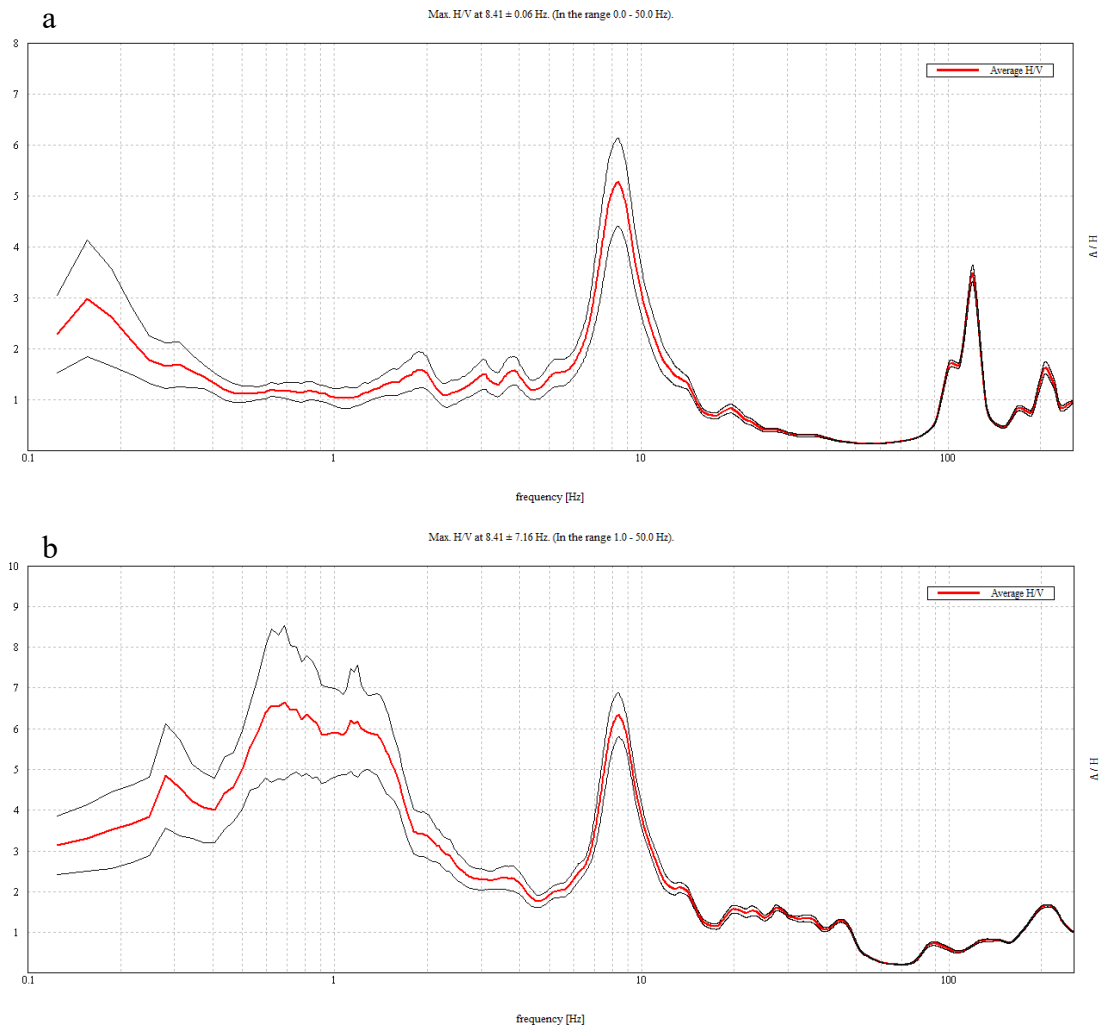

Figure A-67 MIZ Quad Site 3 site, Test 5, concrete (a), grass (b)

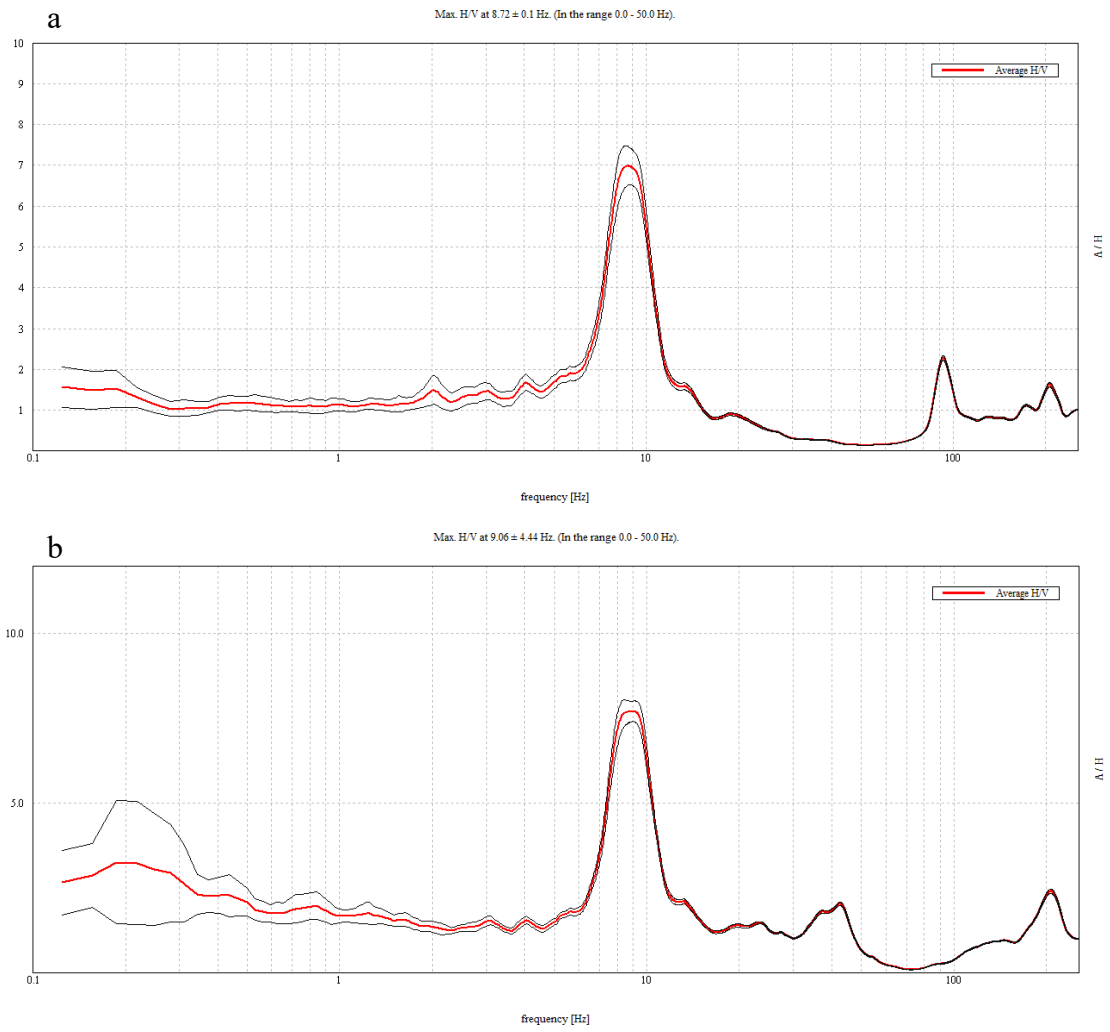

Figure A-68 MIZ Quad Site 3 site, Test 6, concrete (a), grass (b)

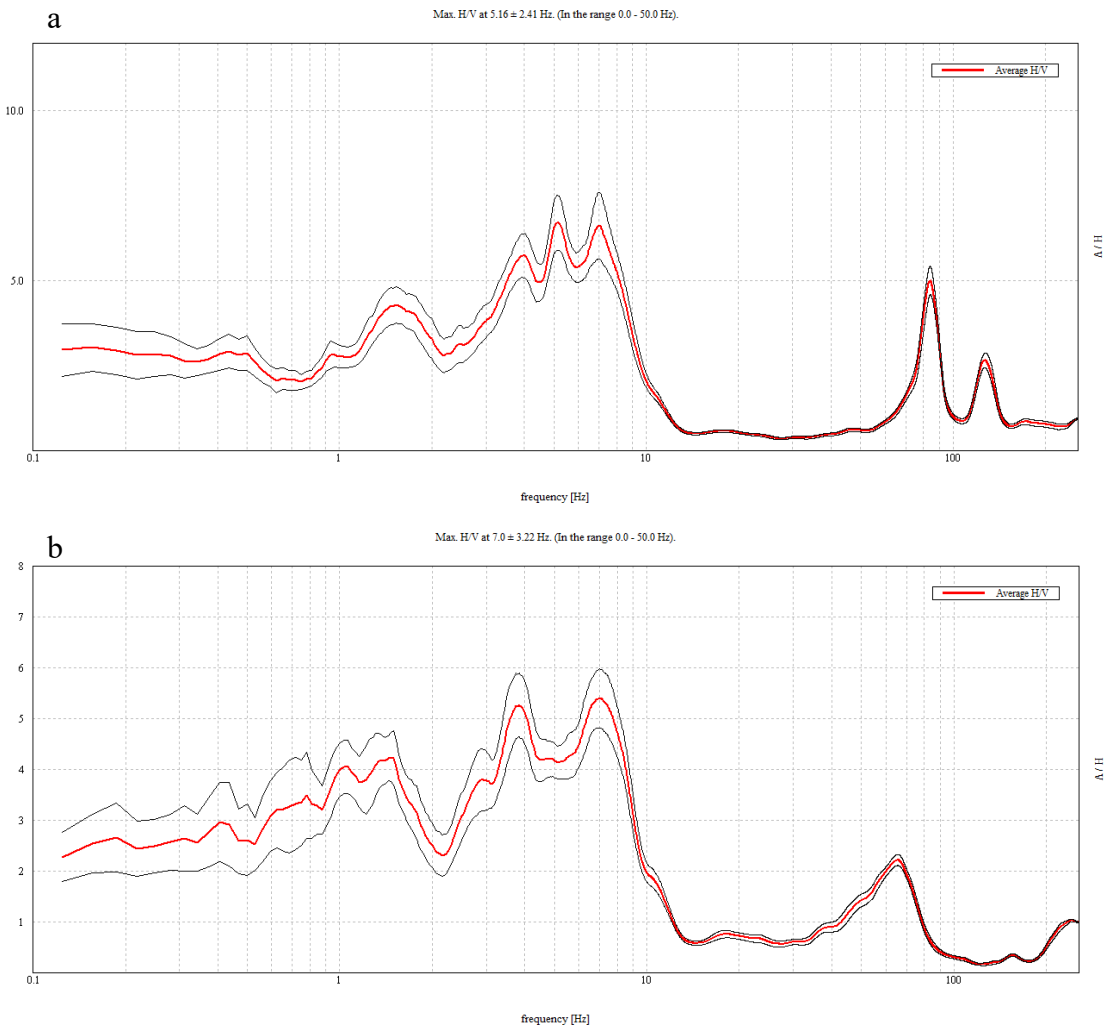

Figure A-69 MIZ Quad Site 4 site, Test 1, concrete (a), grass (b)

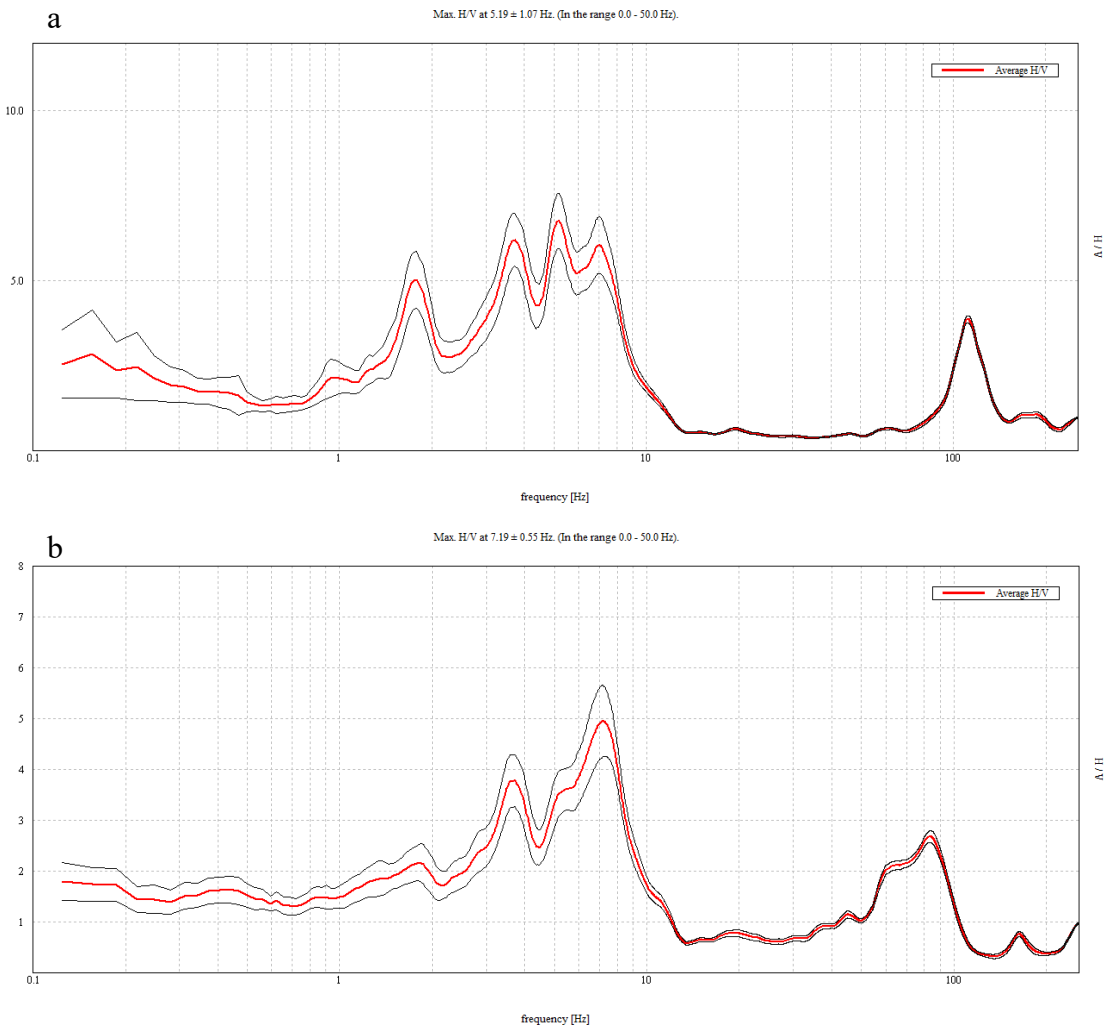

Figure A-70 MIZ Quad Site 4 site, Test 2, concrete (a), grass (b)

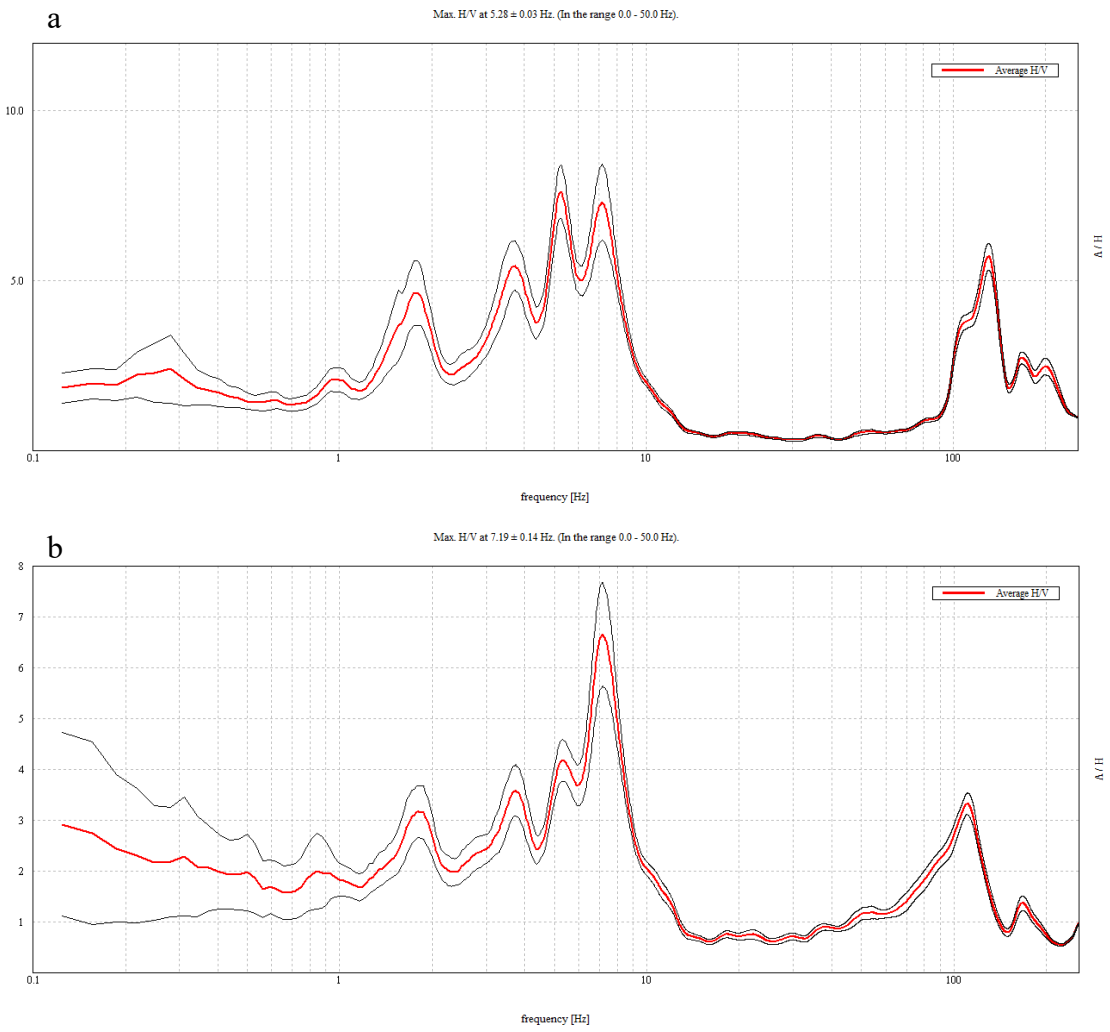

Figure A-71 MIZ Quad Site 4 site, Test 3, concrete (a), grass (b)

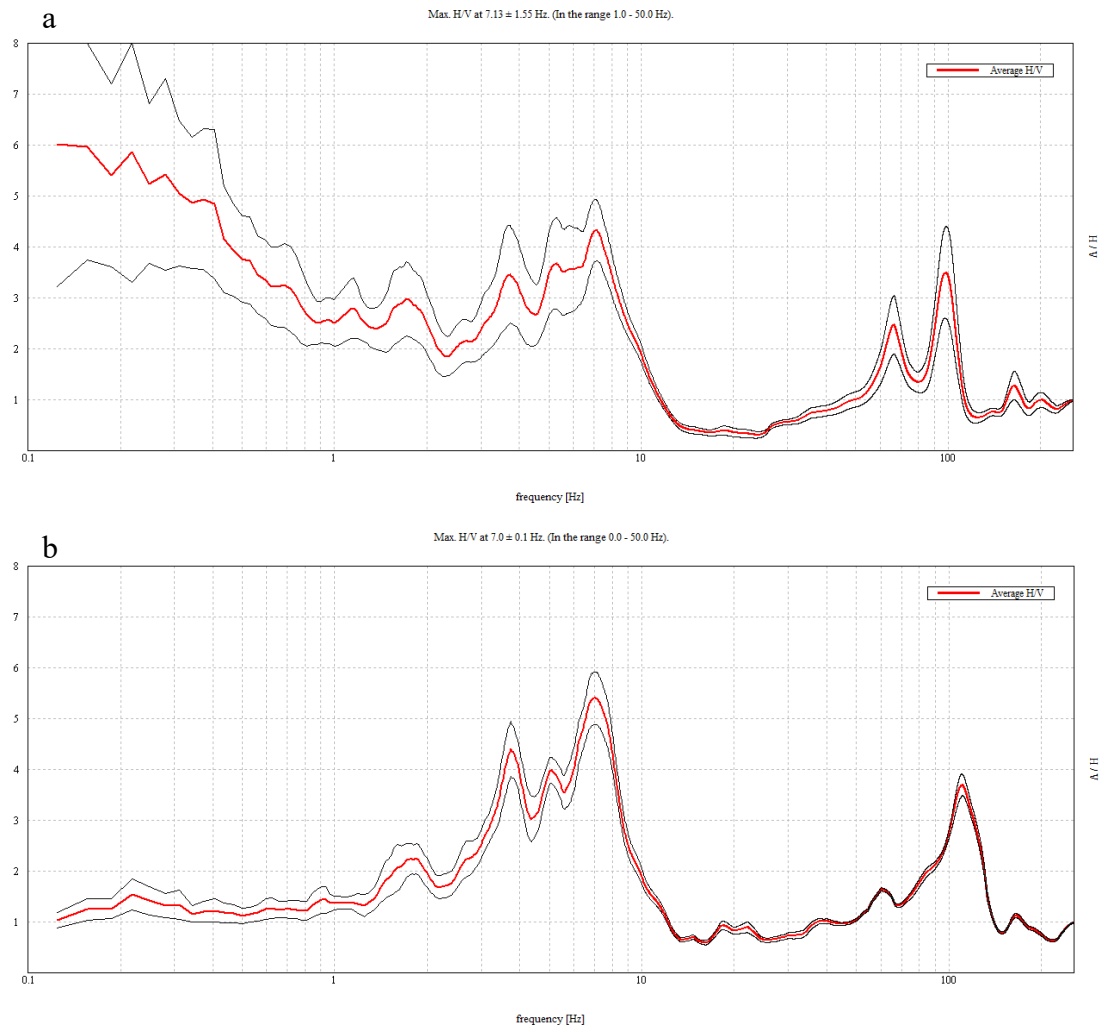

Figure A-72 MIZ Quad Site 4 site, Test 4, concrete (a), grass (b)

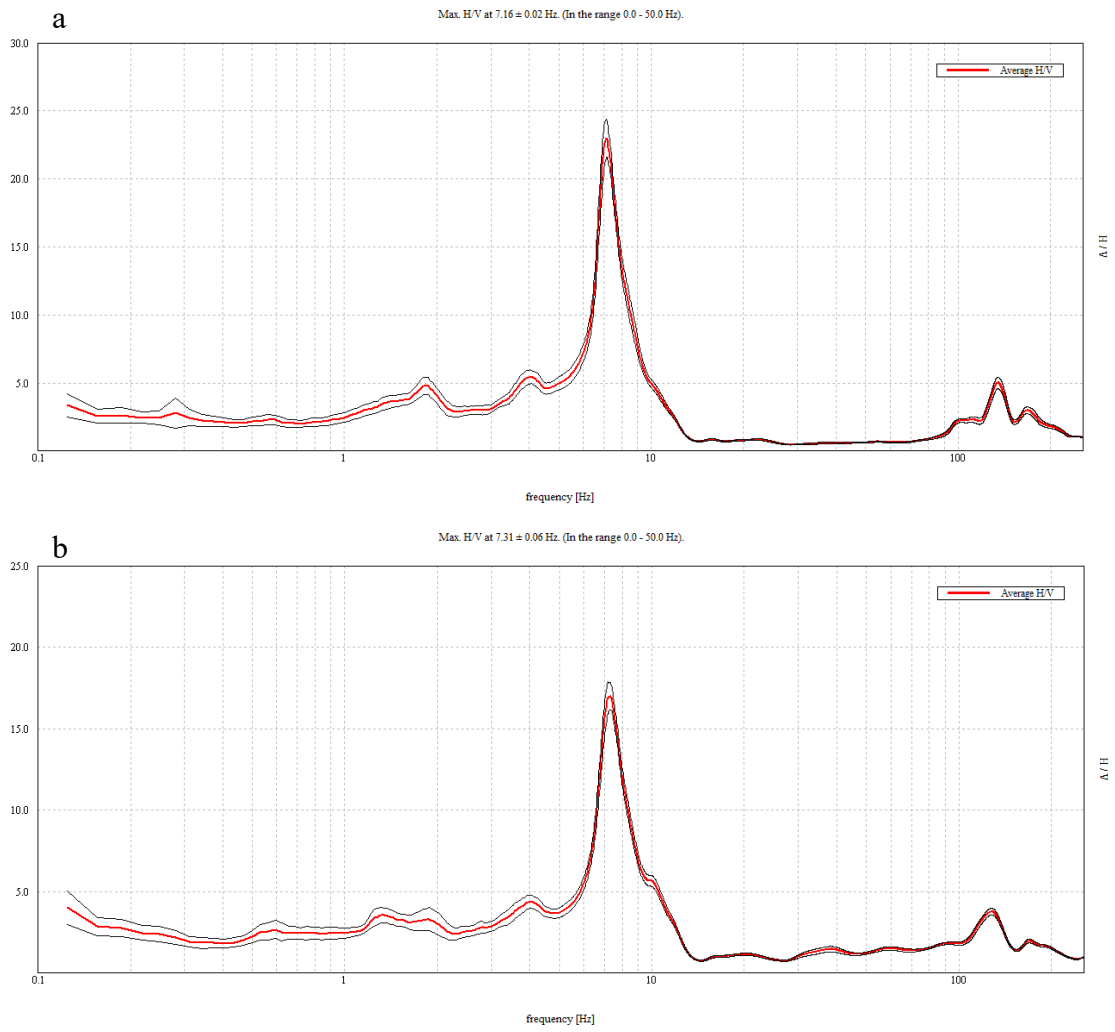

Figure A-73 MIZ Quad Site 4 site, Test 5, concrete (a), grass (b)

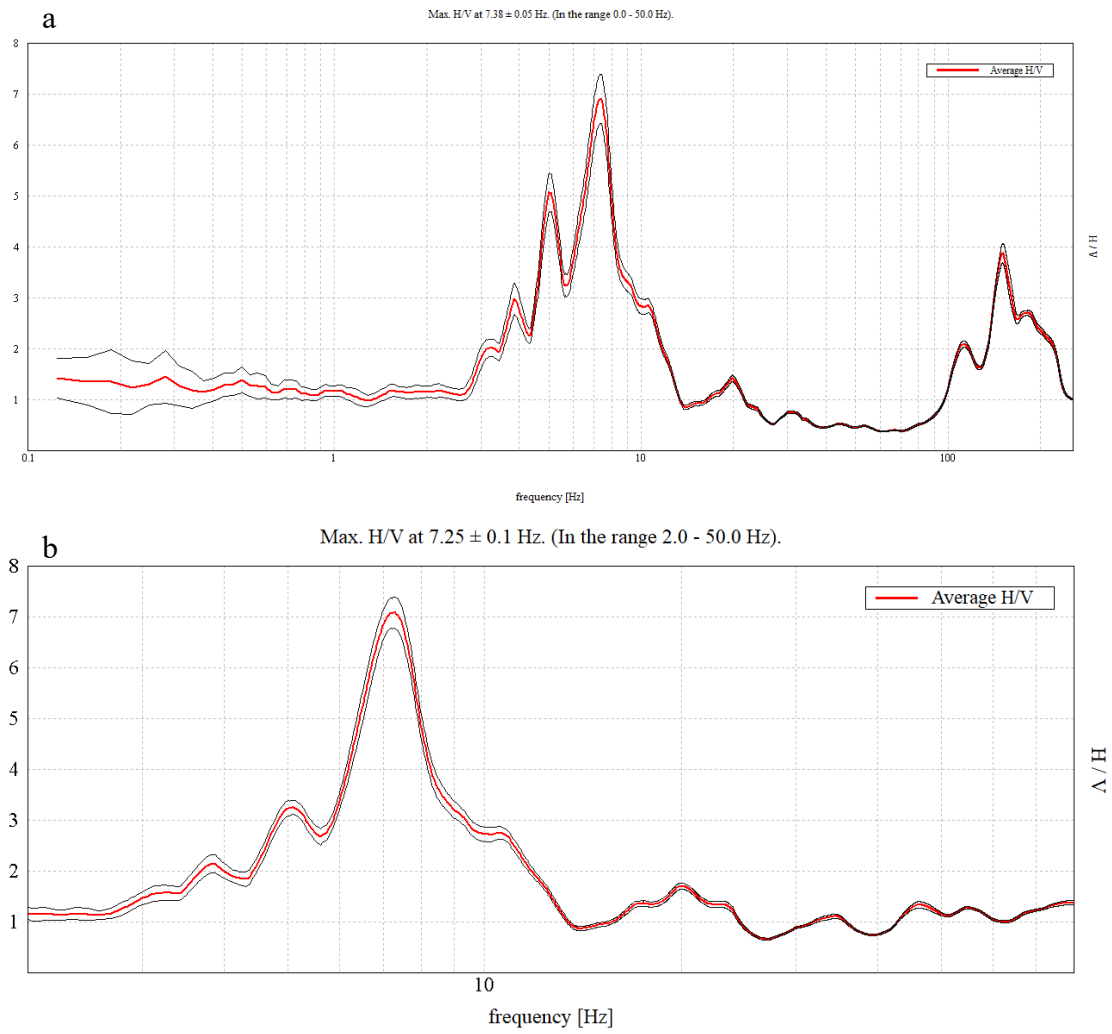

Figure A-74 MIZ Quad Site 4 site, Test 6, concrete (a), grass (b)

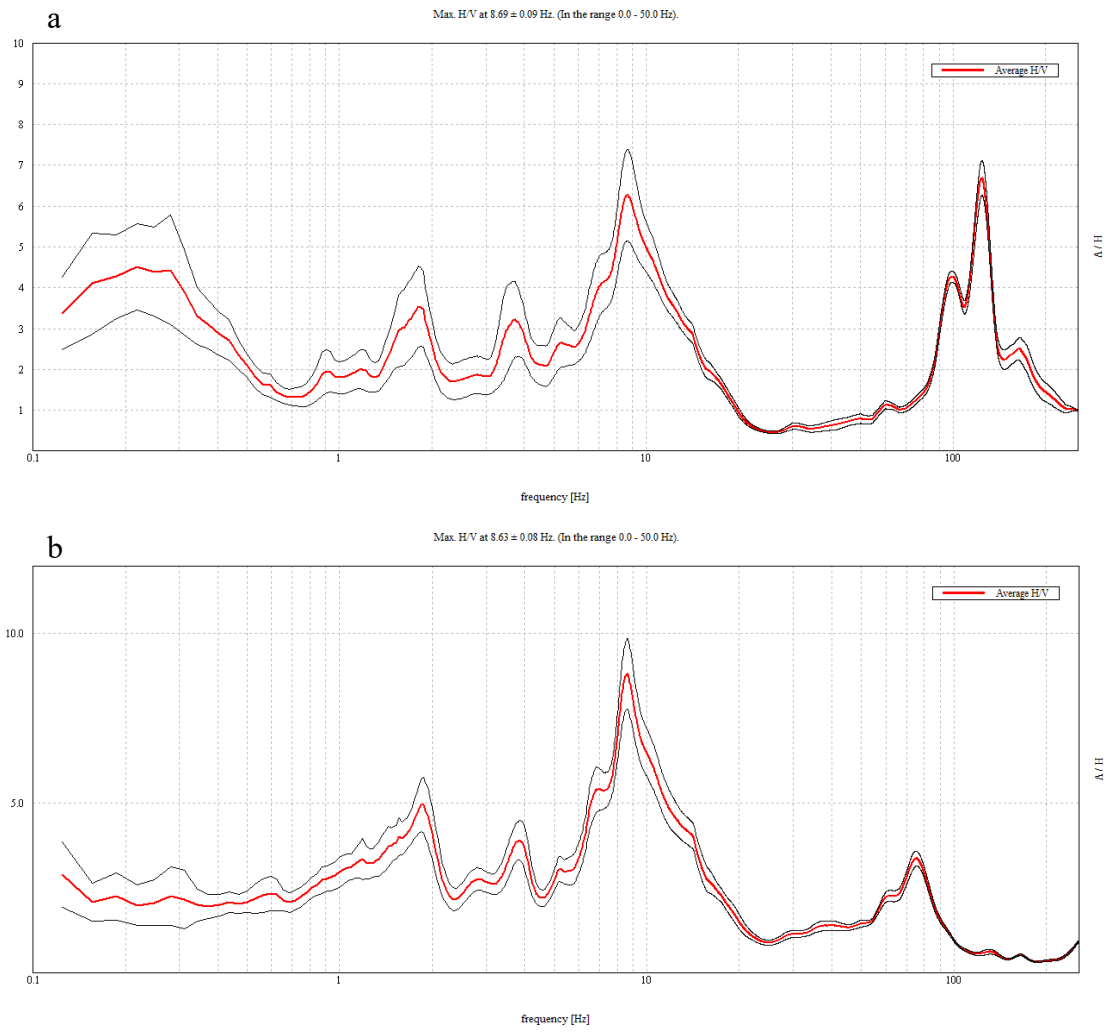

Figure A-75 MIZ Quad Site 5 site, Test 1, concrete (a), grass (b)

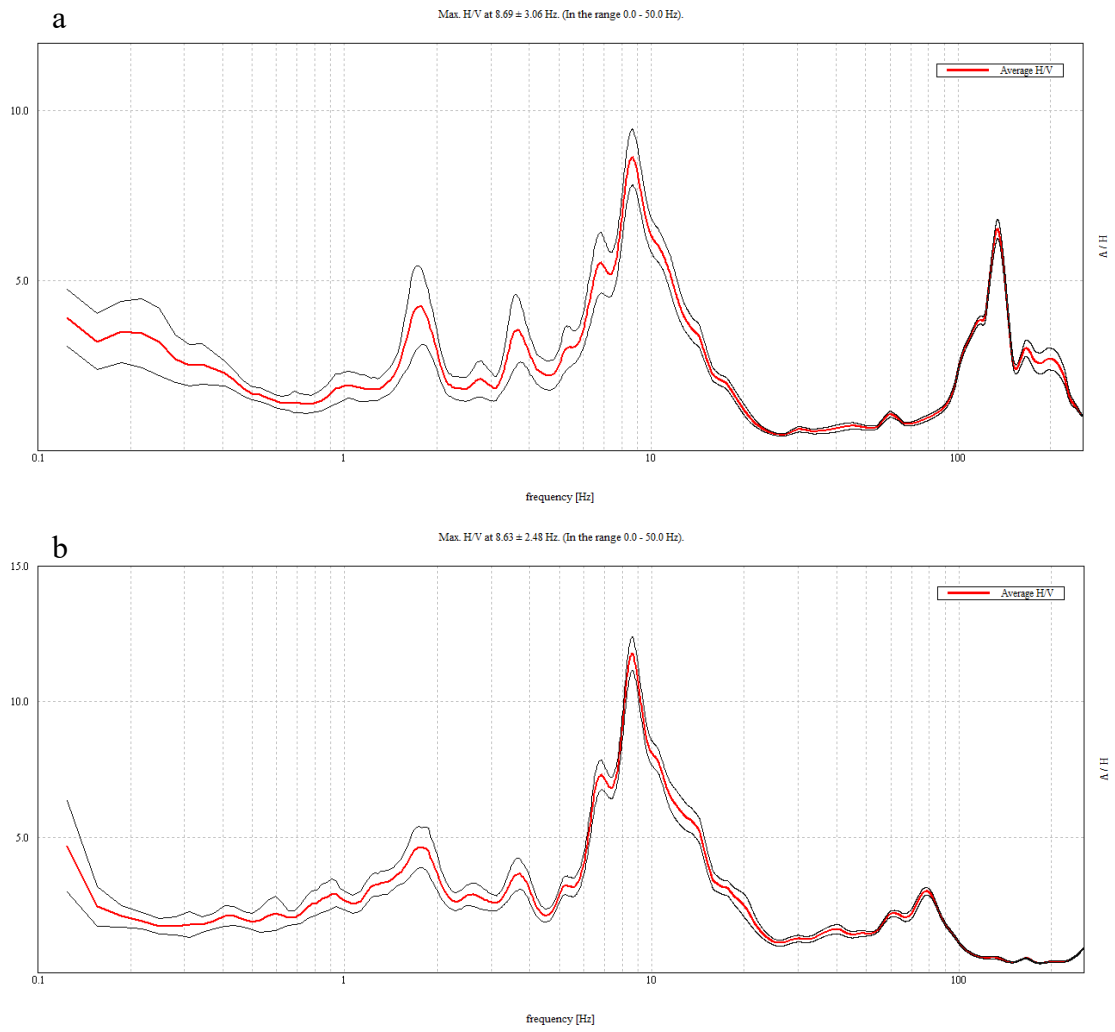

Figure A-76 MIZ Quad Site 5 site, Test 2, concrete (a), grass (b)

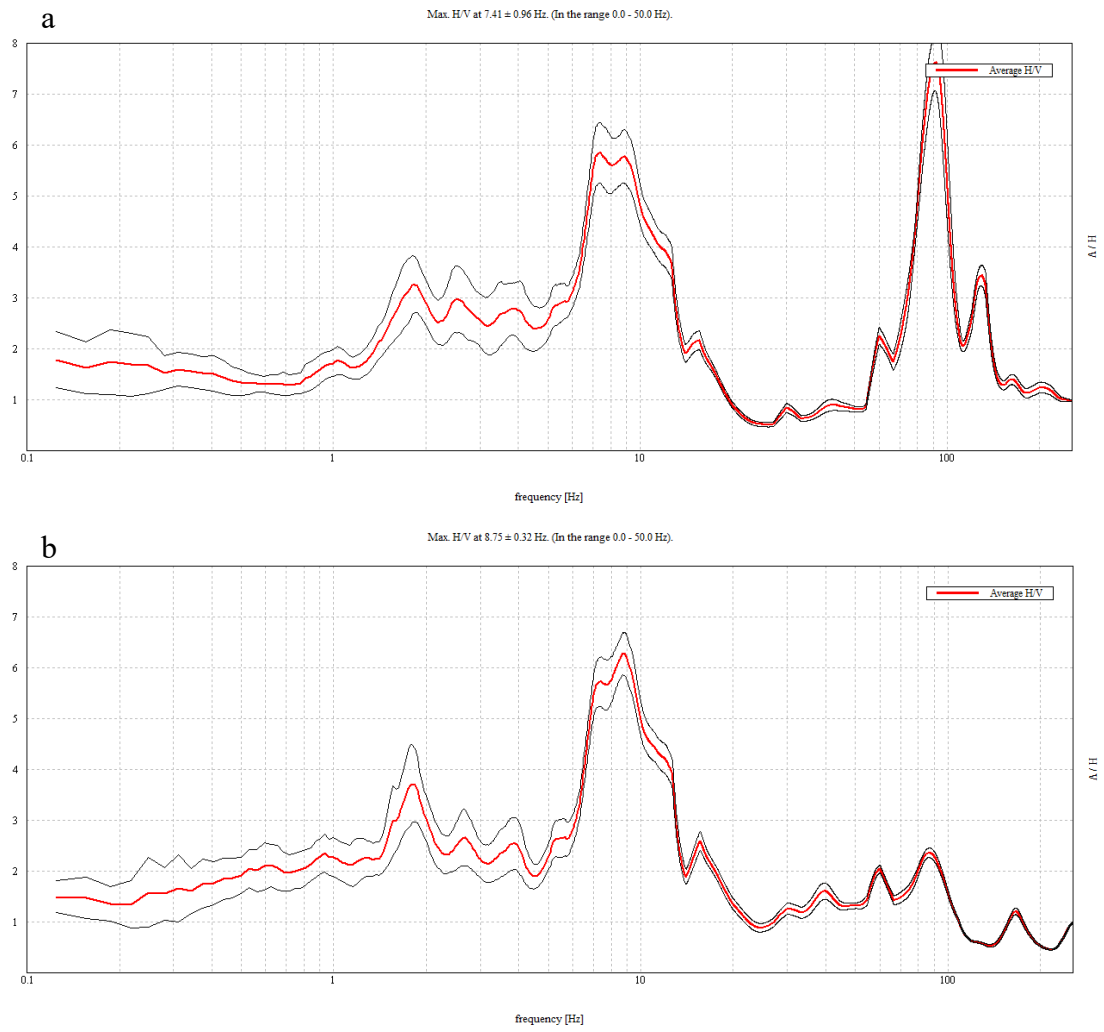

Figure A-77 MIZ Quad Site 5 site, Test 3, concrete (a), grass (b)

APPENDIX B

Importing Amplitude graph [H-V All]

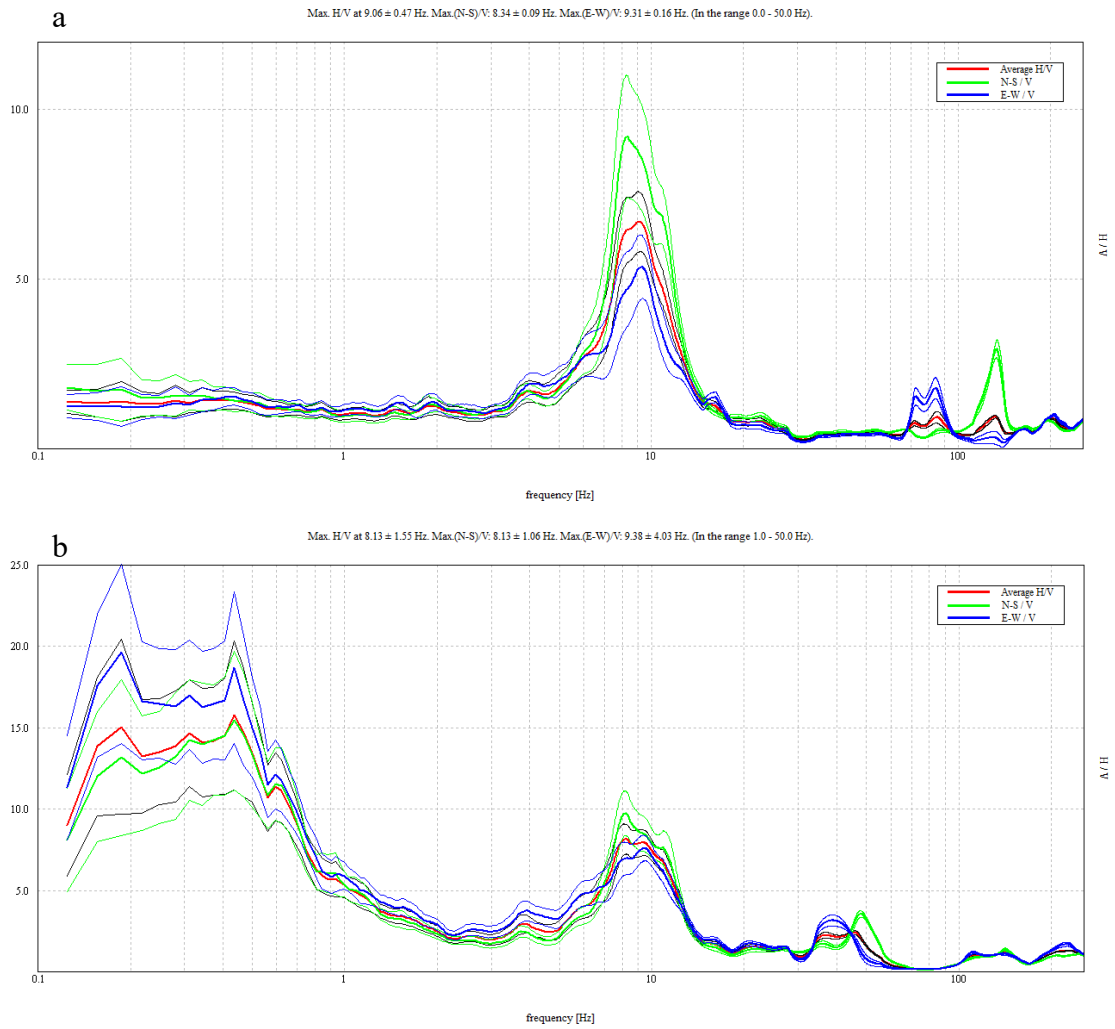

Figure B-1 Animal Hospital 1 site, Test 1, concrete (a), grass (b)

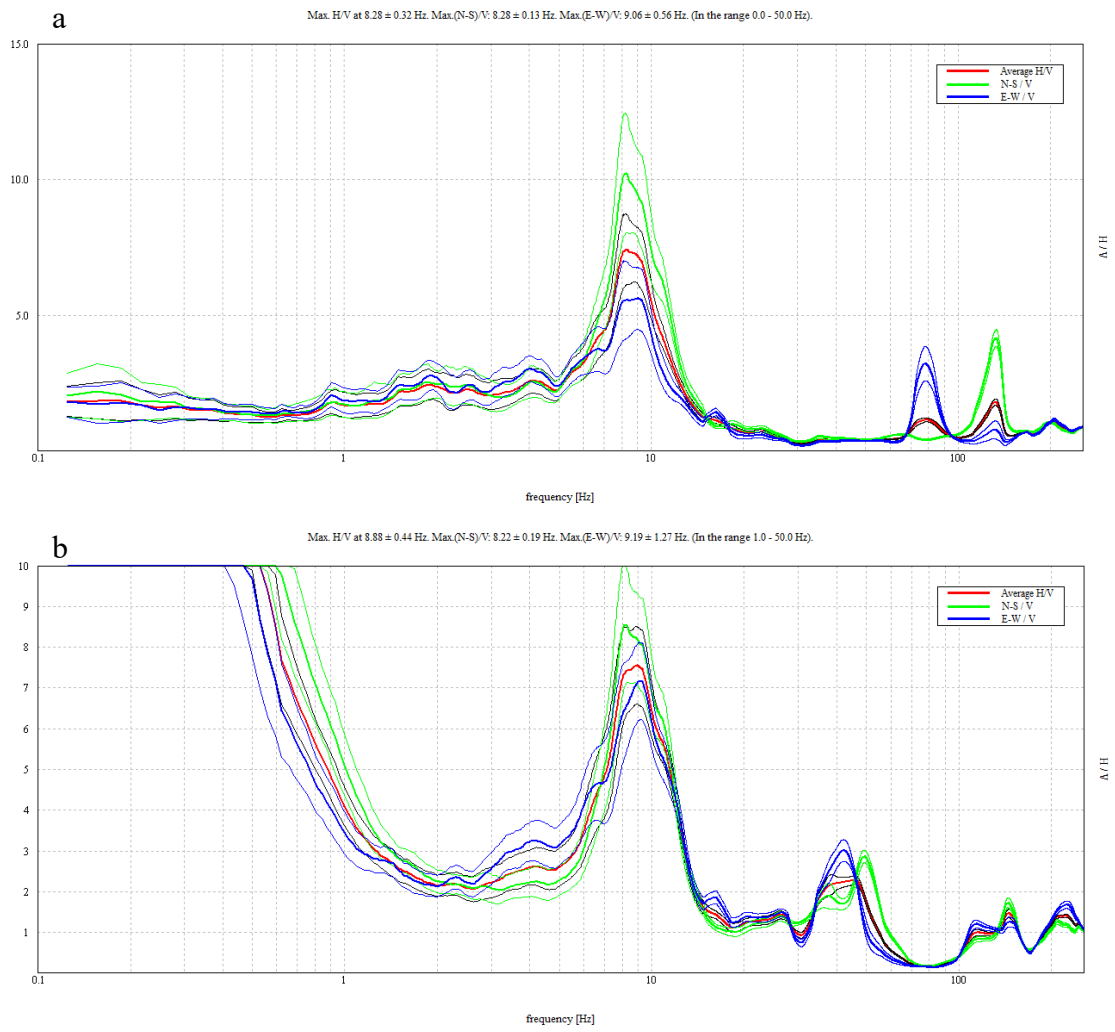

Figure B-2 Animal Hospital 1 site, Test 2, concrete (a), grass (b)

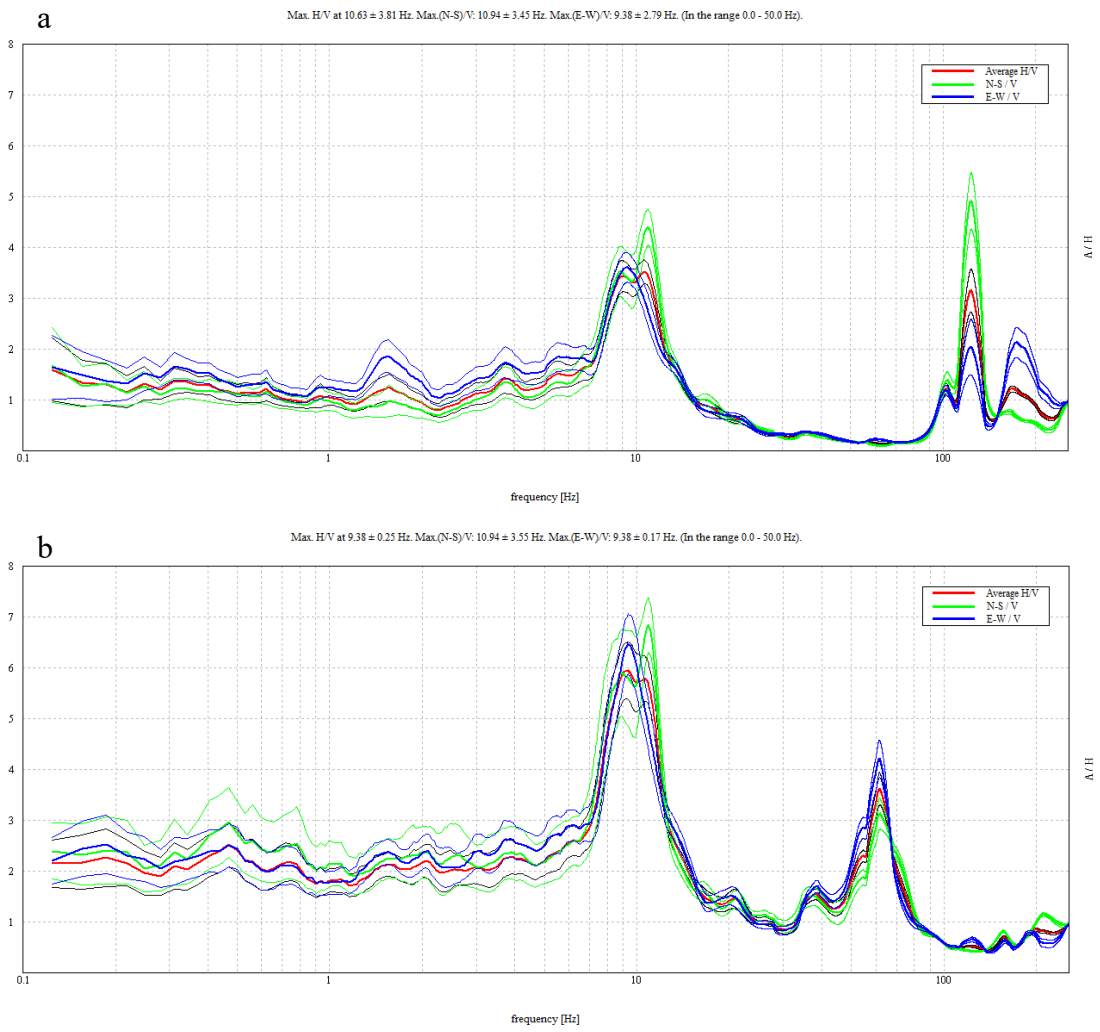

Figure B-3 Animal Hospital 1 site, Test 3, concrete (a), grass (b)

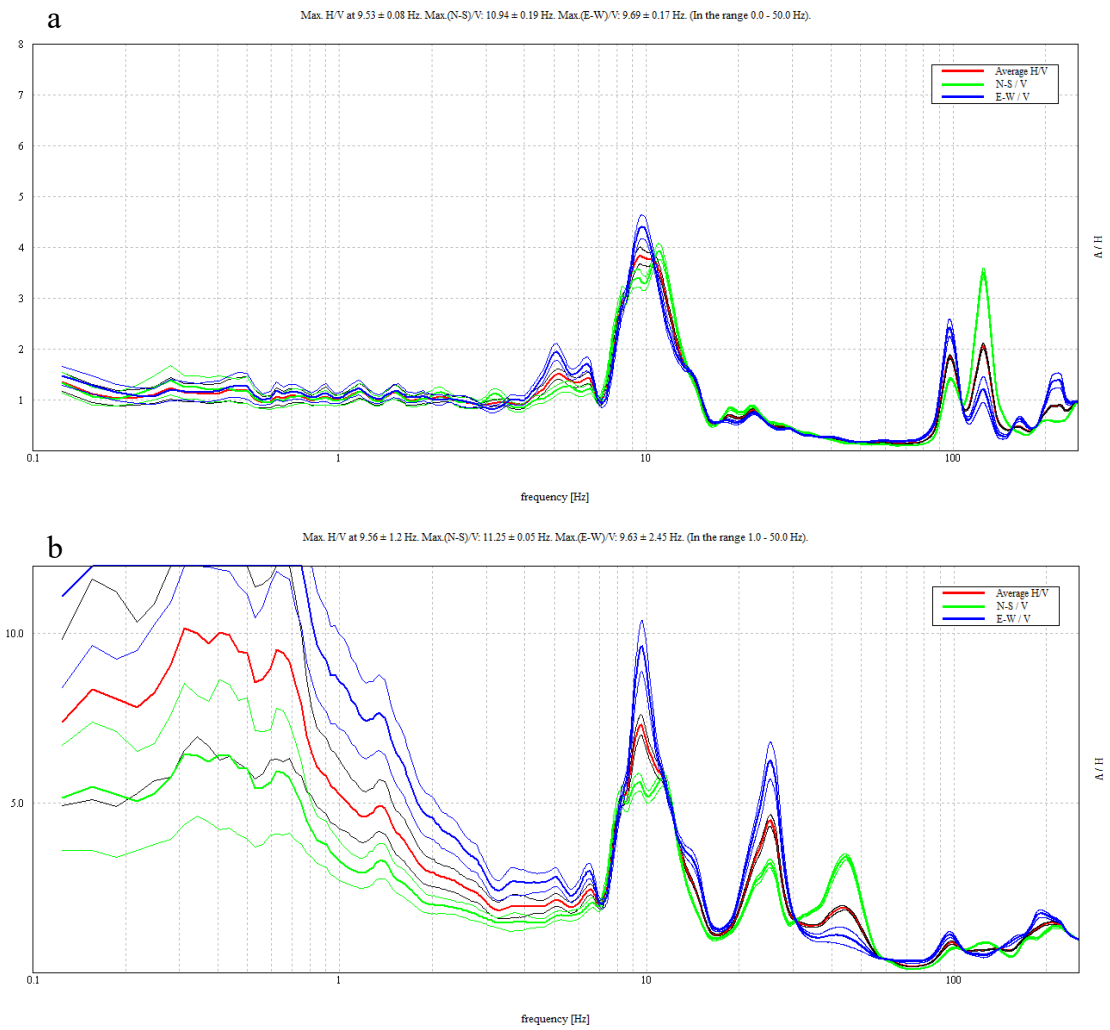

Figure B-4 Animal Hospital 1 site, Test 4, concrete (a), grass (b)

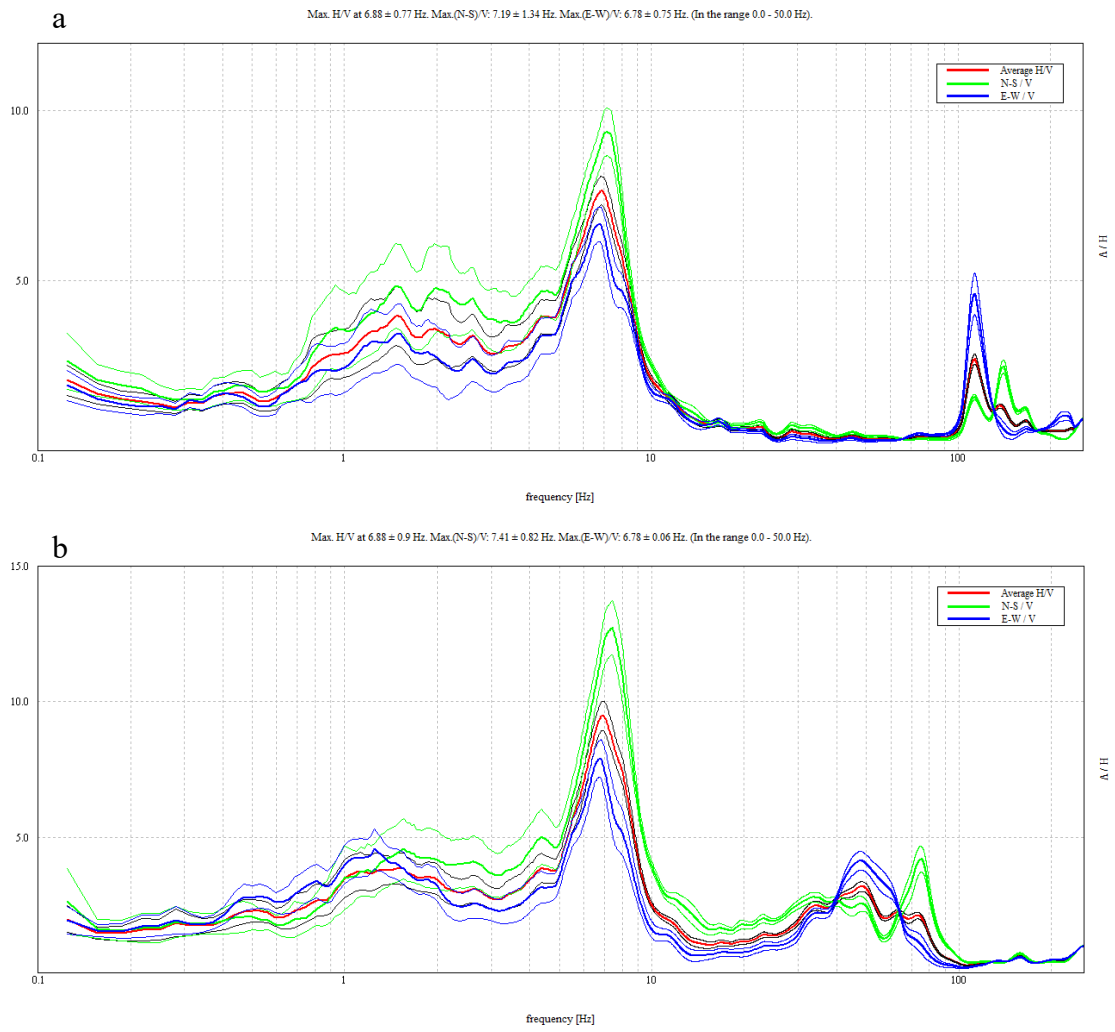

Figure B-5 Animal Hospital 2 site, Test 1, concrete (a), grass (b)

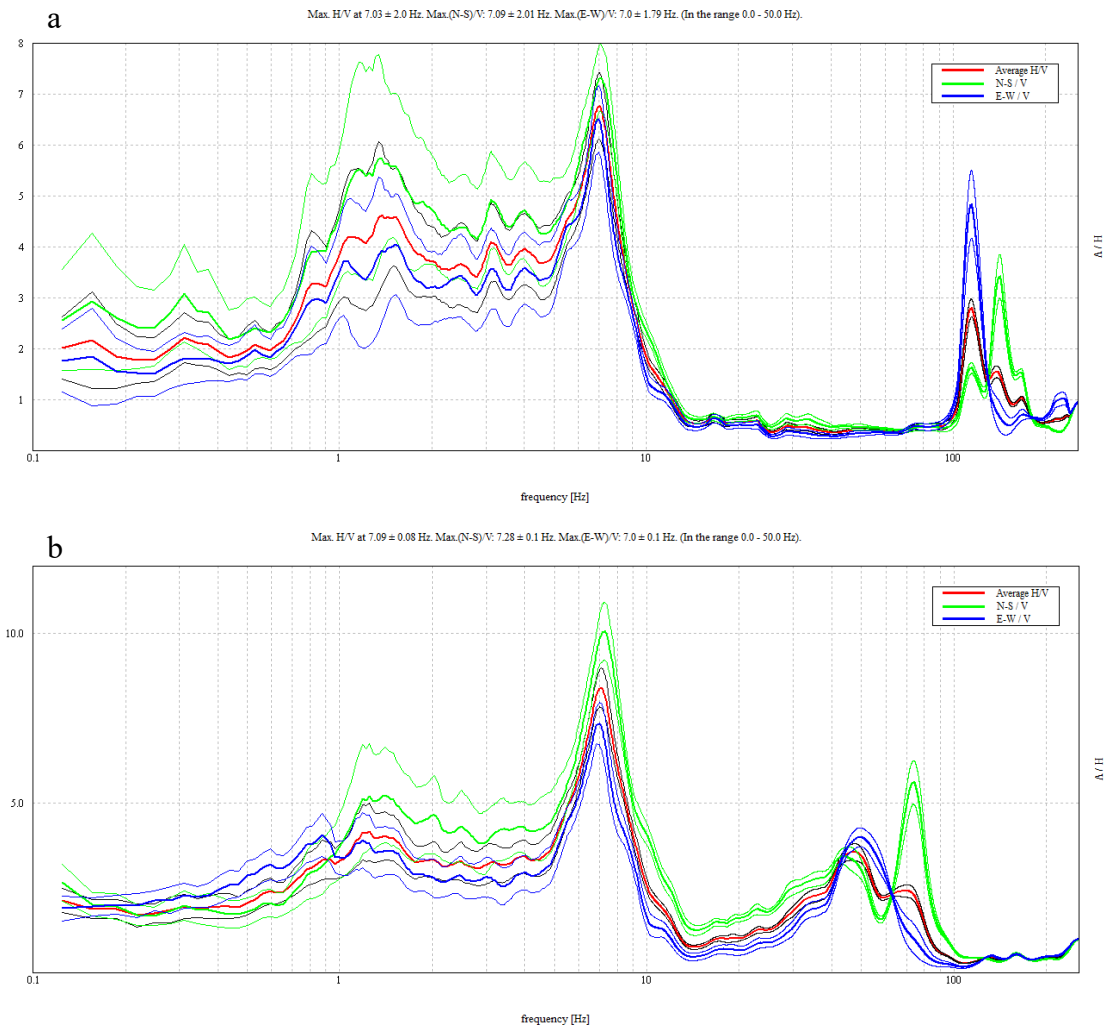

Figure B-6 Animal Hospital 2 site, Test 2, concrete (a), grass (b)

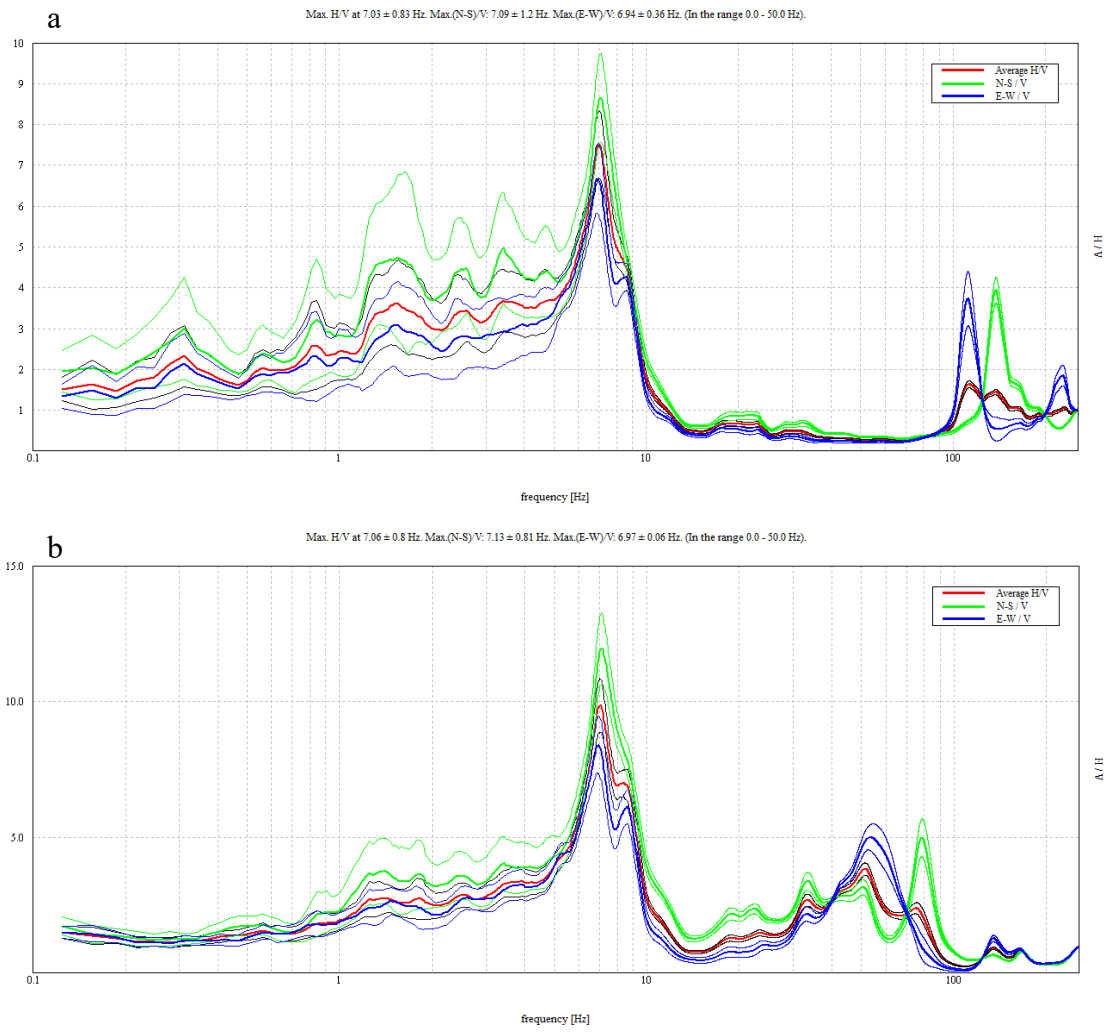

Figure B-7 Animal Hospital 2 site, Test 3, concrete (a), grass (b)

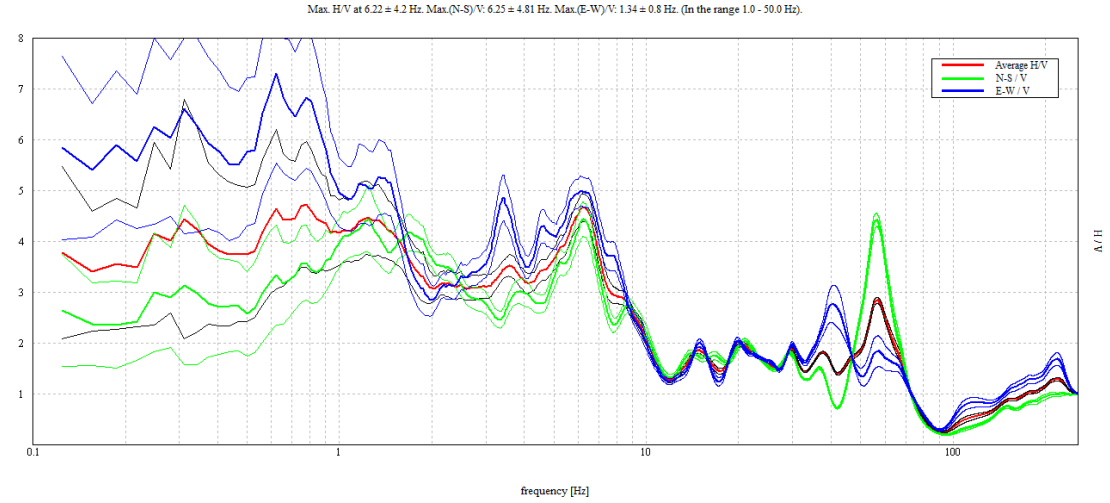

Figure B-8 Ellis Library BH-01 site, Test 1, grass

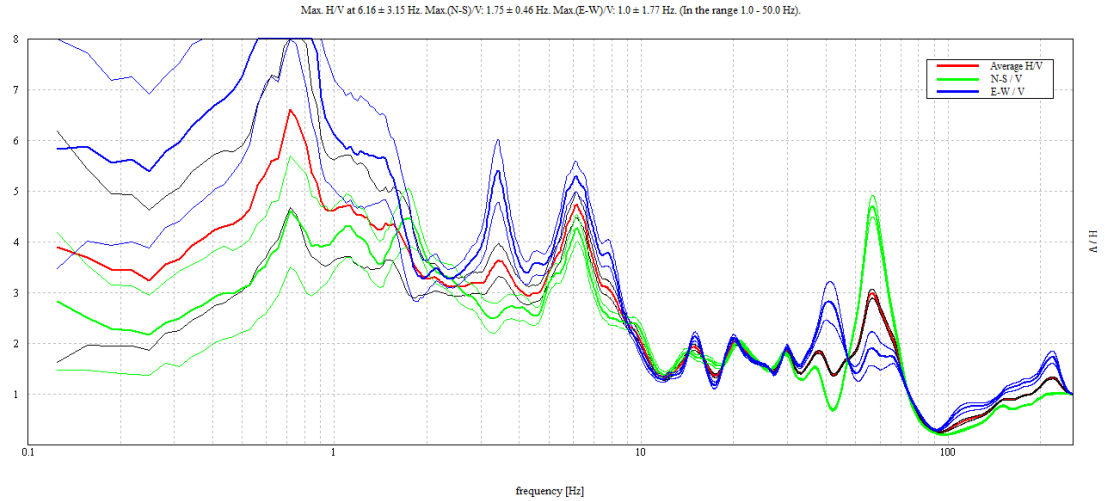

Figure B-9 Ellis Library BH-01 site, Test 2, grass

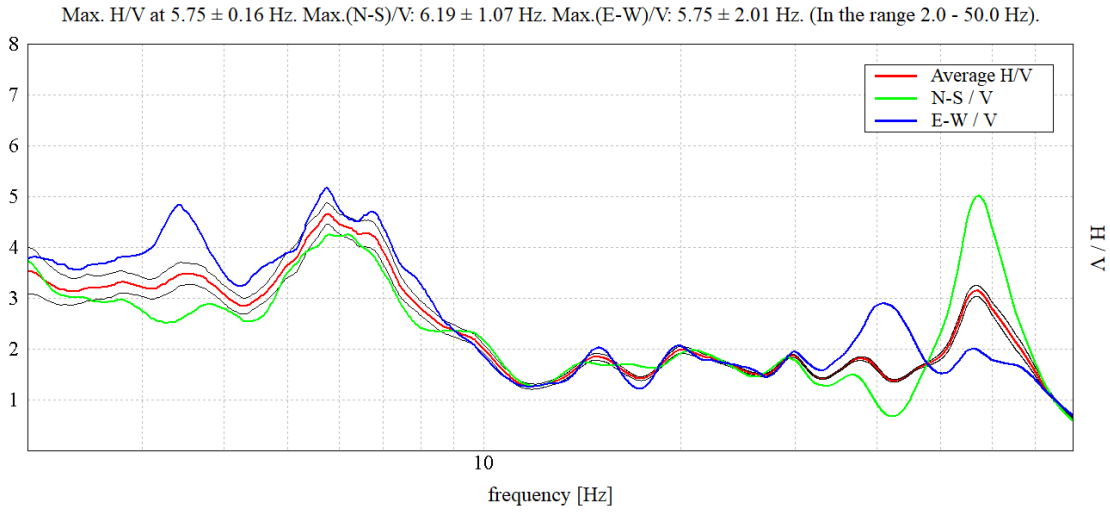

Figure B-10 Ellis Library BH-01 site, Test 3, grass

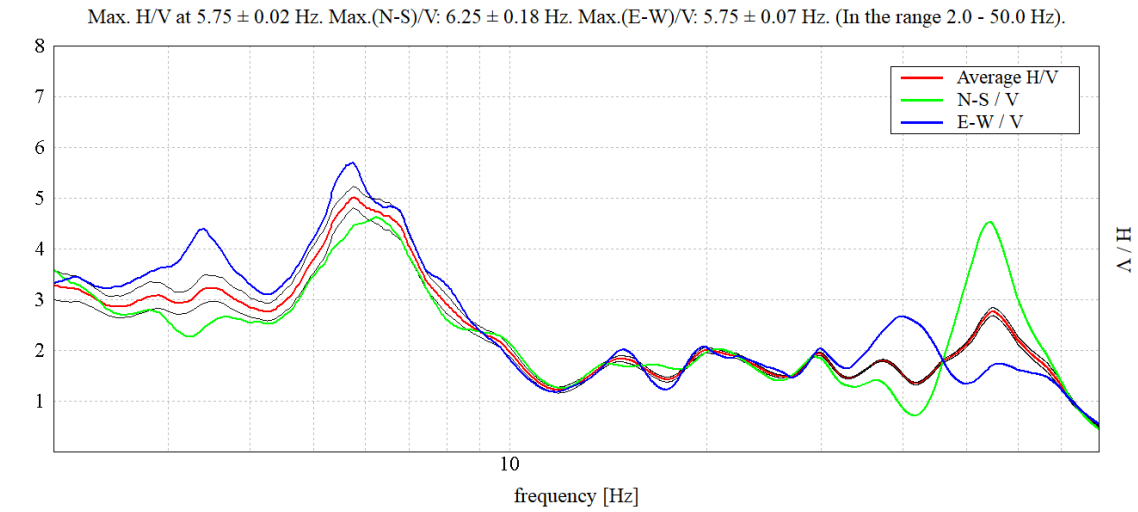

Figure B-11 Ellis Library BH-01 site, Test 4, grass

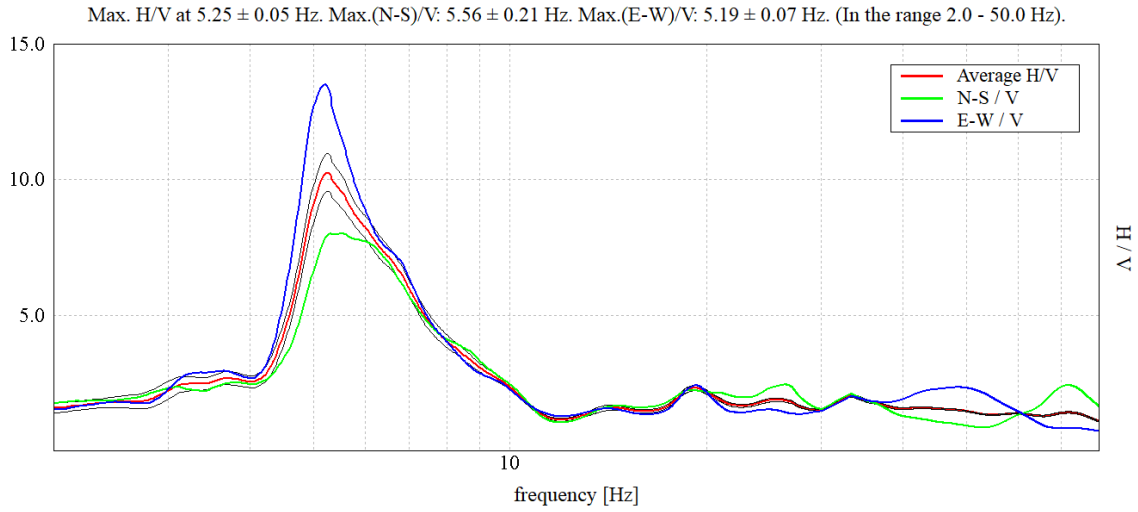

Figure B-12 Ellis Library BH-01 site, Test 5, grass

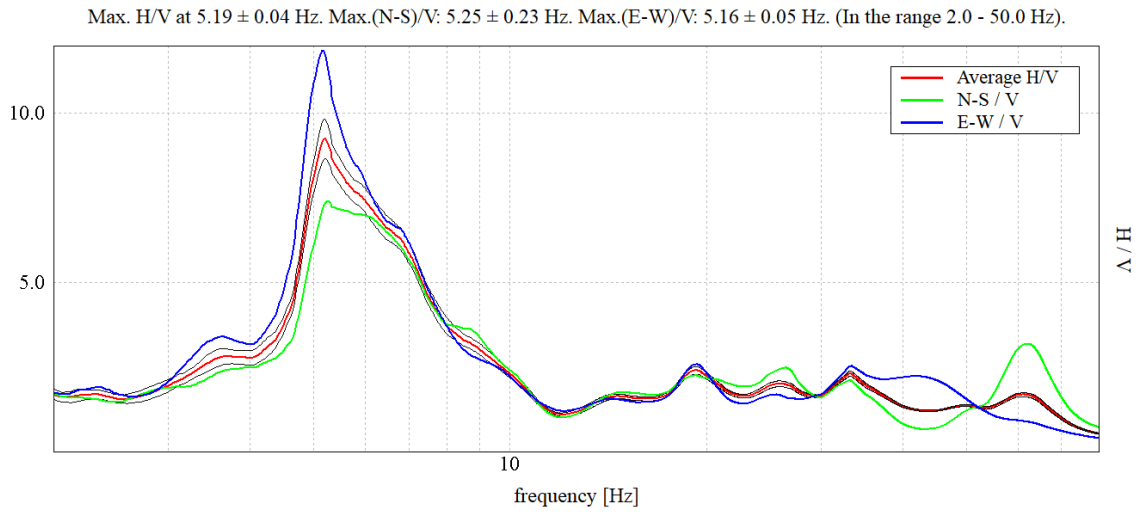

Figure B-13 Ellis Library BH-01 site, Test 6, grass

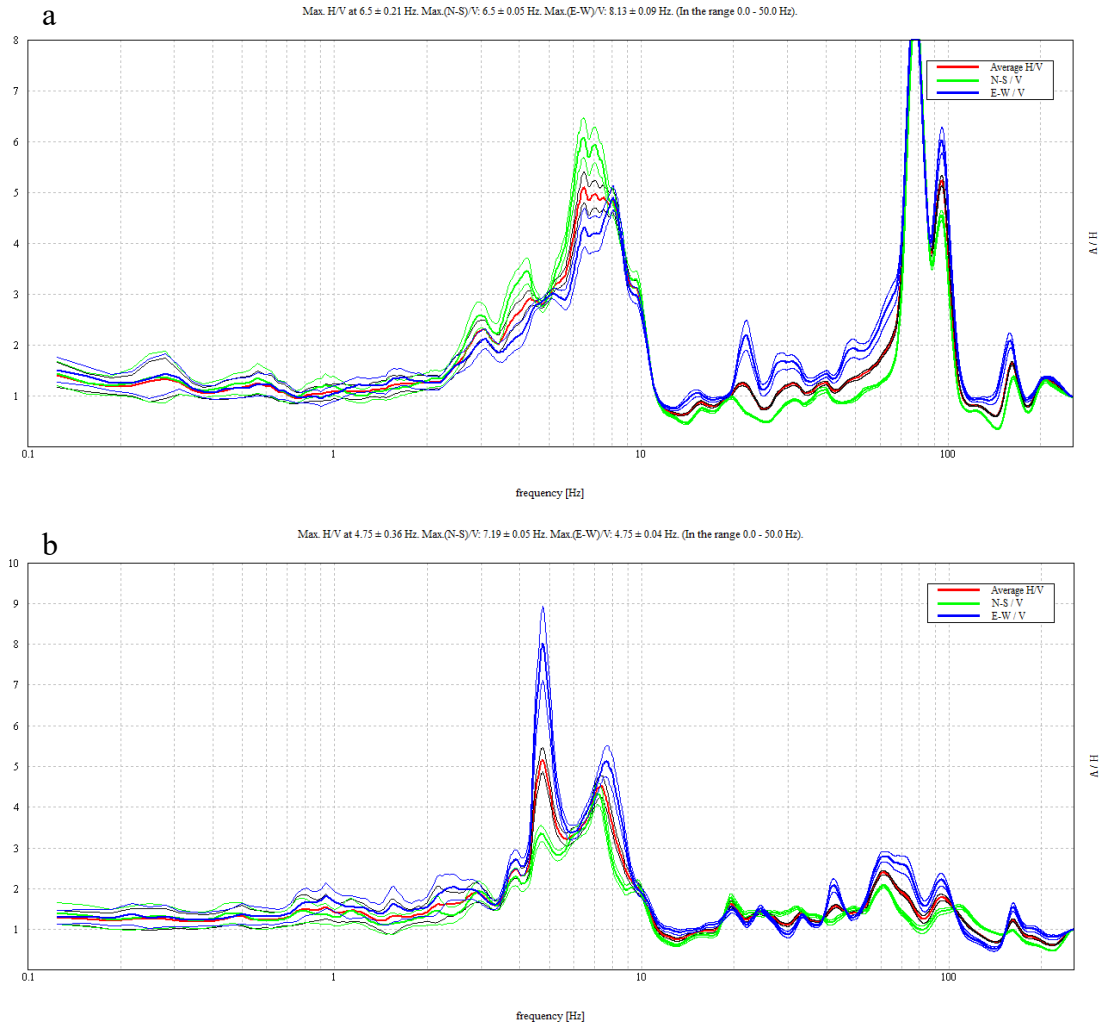

Figure B-14 Ellis Library BH-03 A site, Test 1, concrete (a), grass (b)

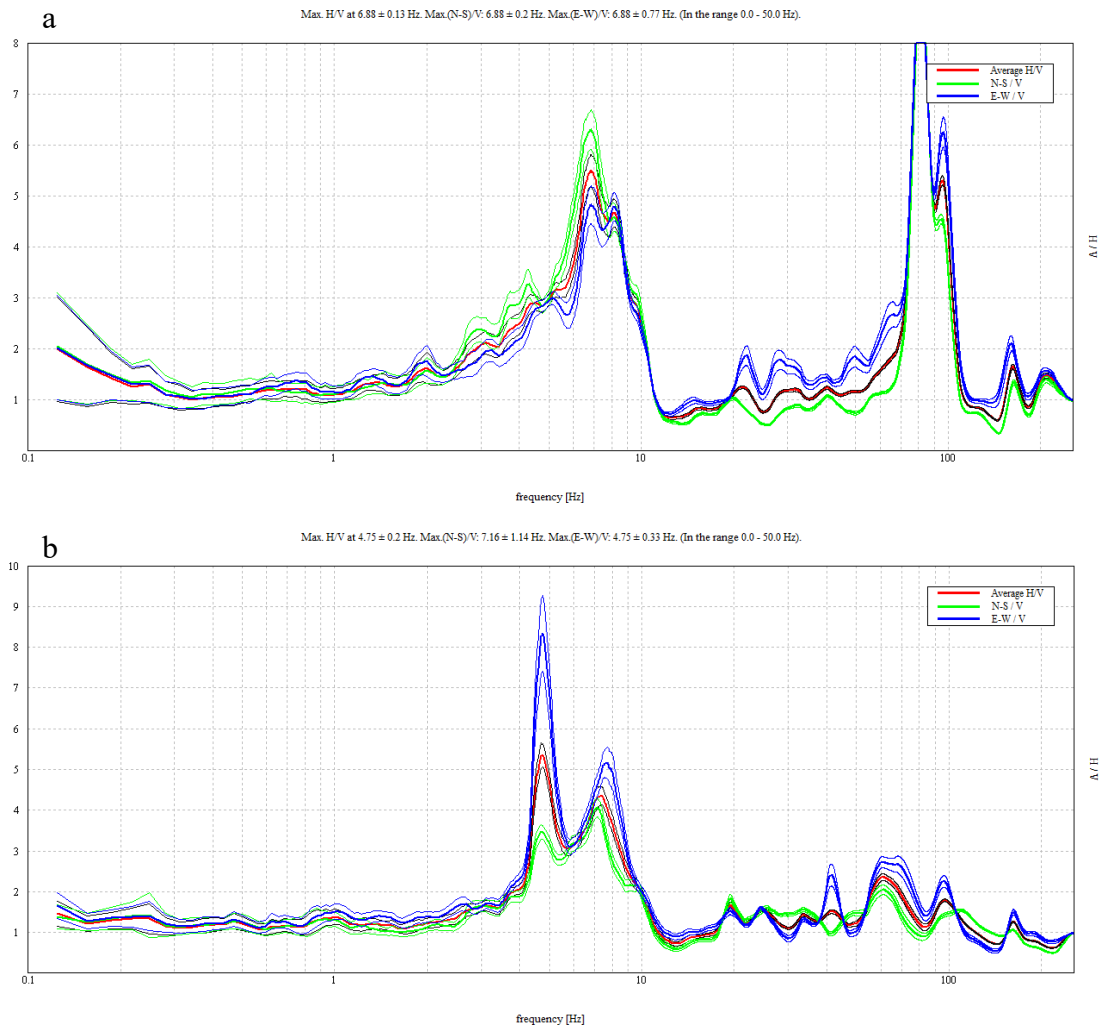

Figure B-15 Ellis Library BH-03 A site, Test 2, concrete (a), grass (b)

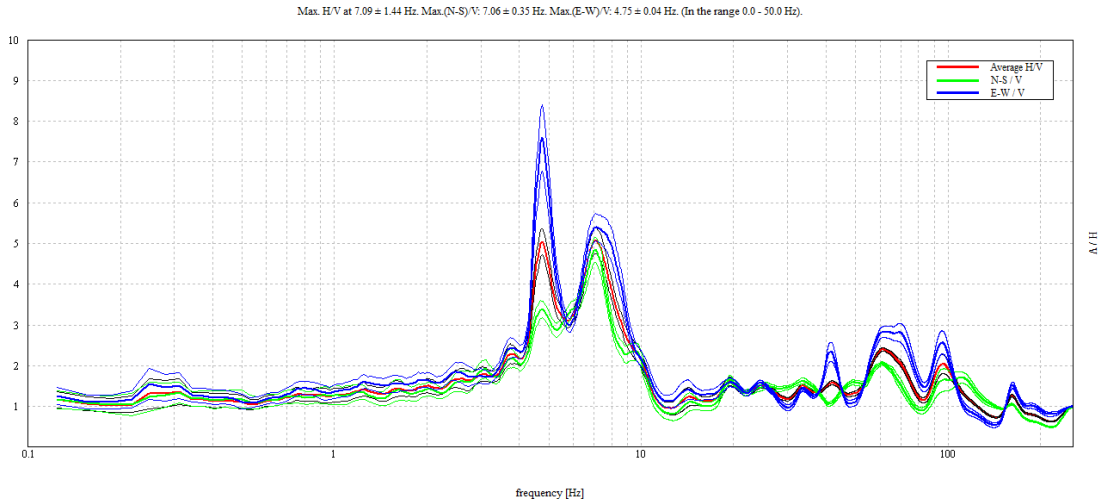

Figure B-16 Ellis Library BH-03 A site, Test 3, grass

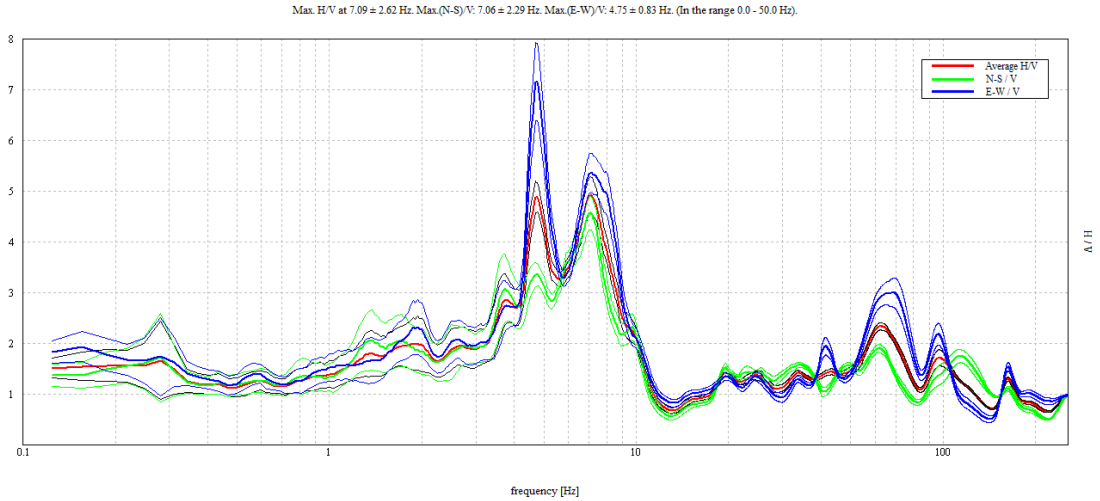

Figure B-17 Ellis Library BH-03 A site, Test 4, grass

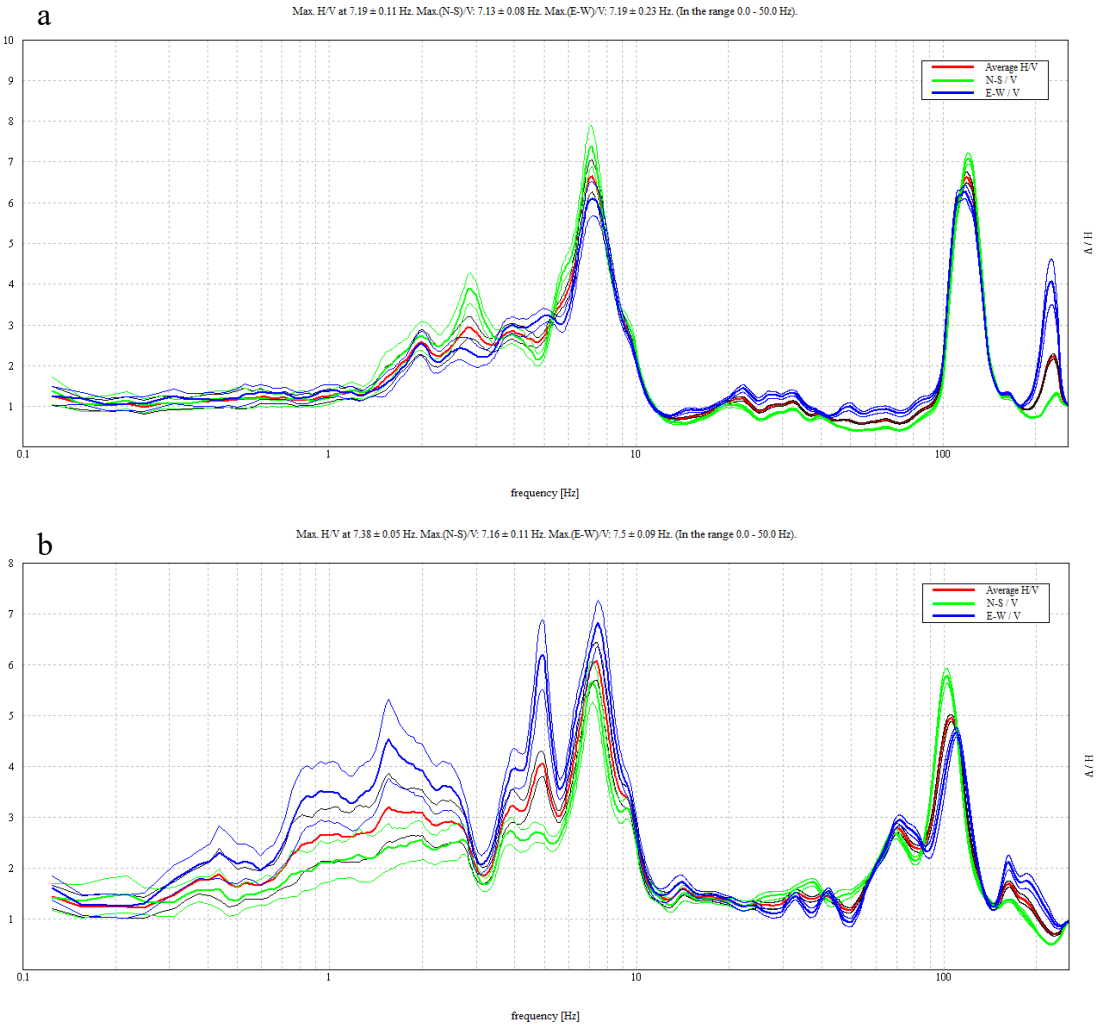

Figure B-18 Ellis Library BH-03 A site, Test 5, concrete (a), grass (b)

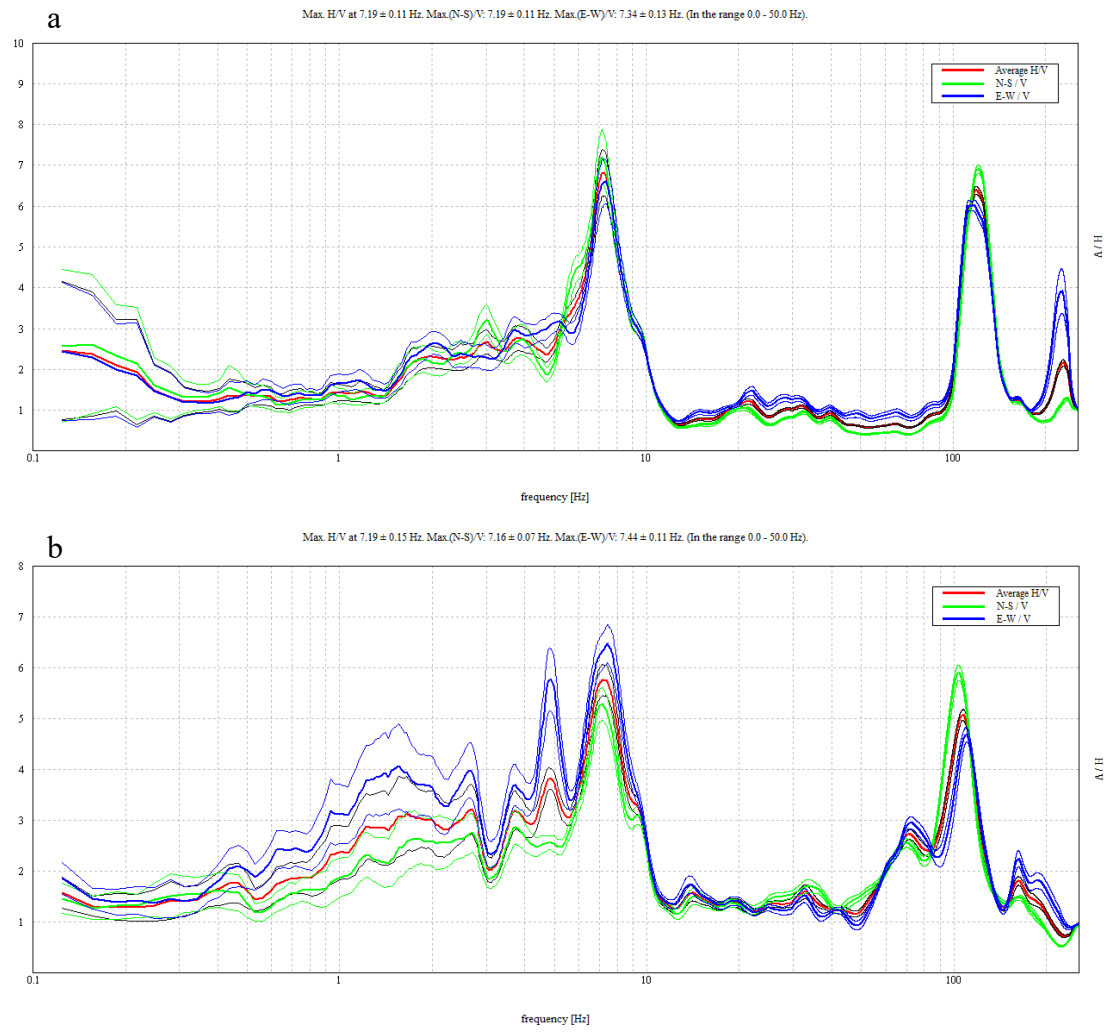

Figure B-19 Ellis Library BH-03 A site, Test 6, concrete (a), grass (b)

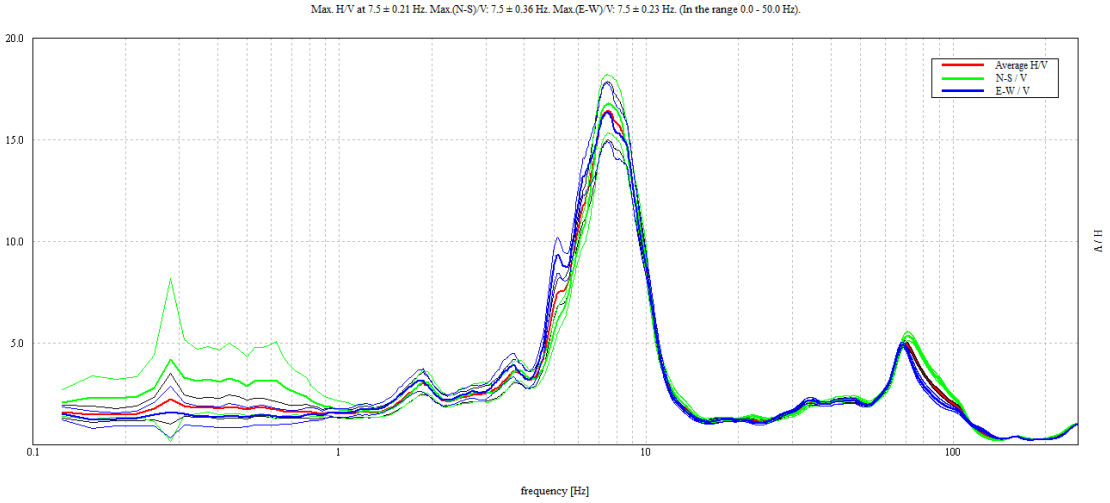

Figure B-20 Ellis Library BH-03 B site, Test 1, grass

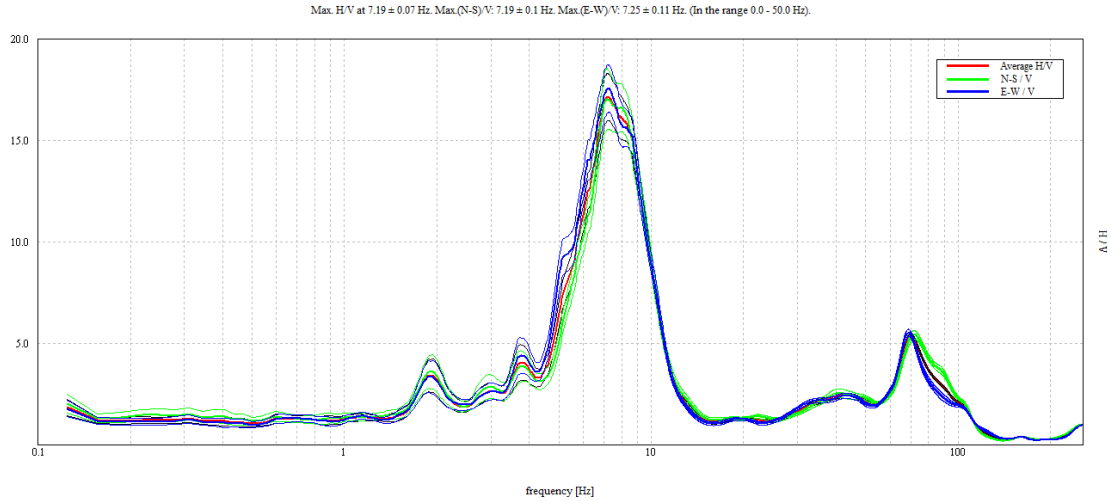

Figure B-21 Ellis Library BH-03 B site, Test 2, grass

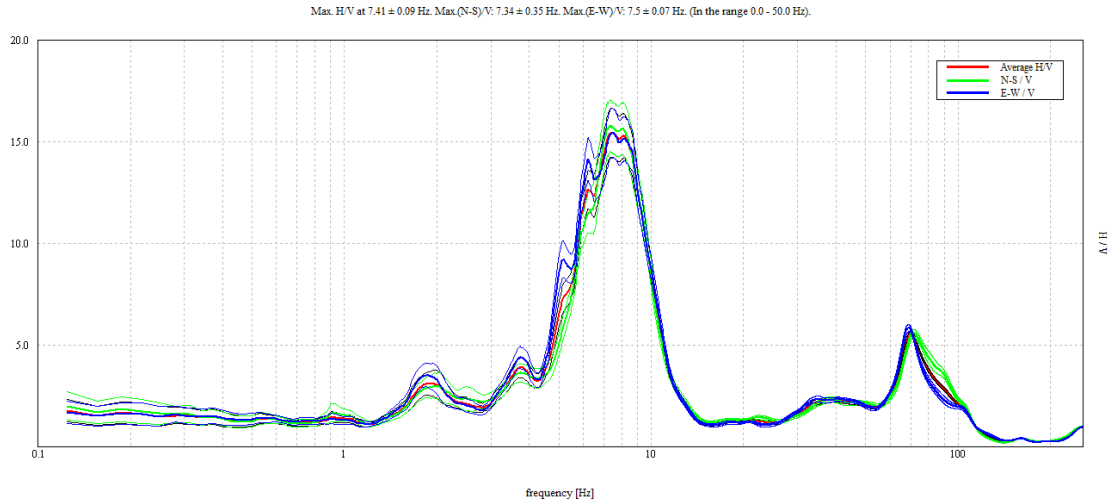

Figure B-22 Ellis Library BH-03 B site, Test 3, grass

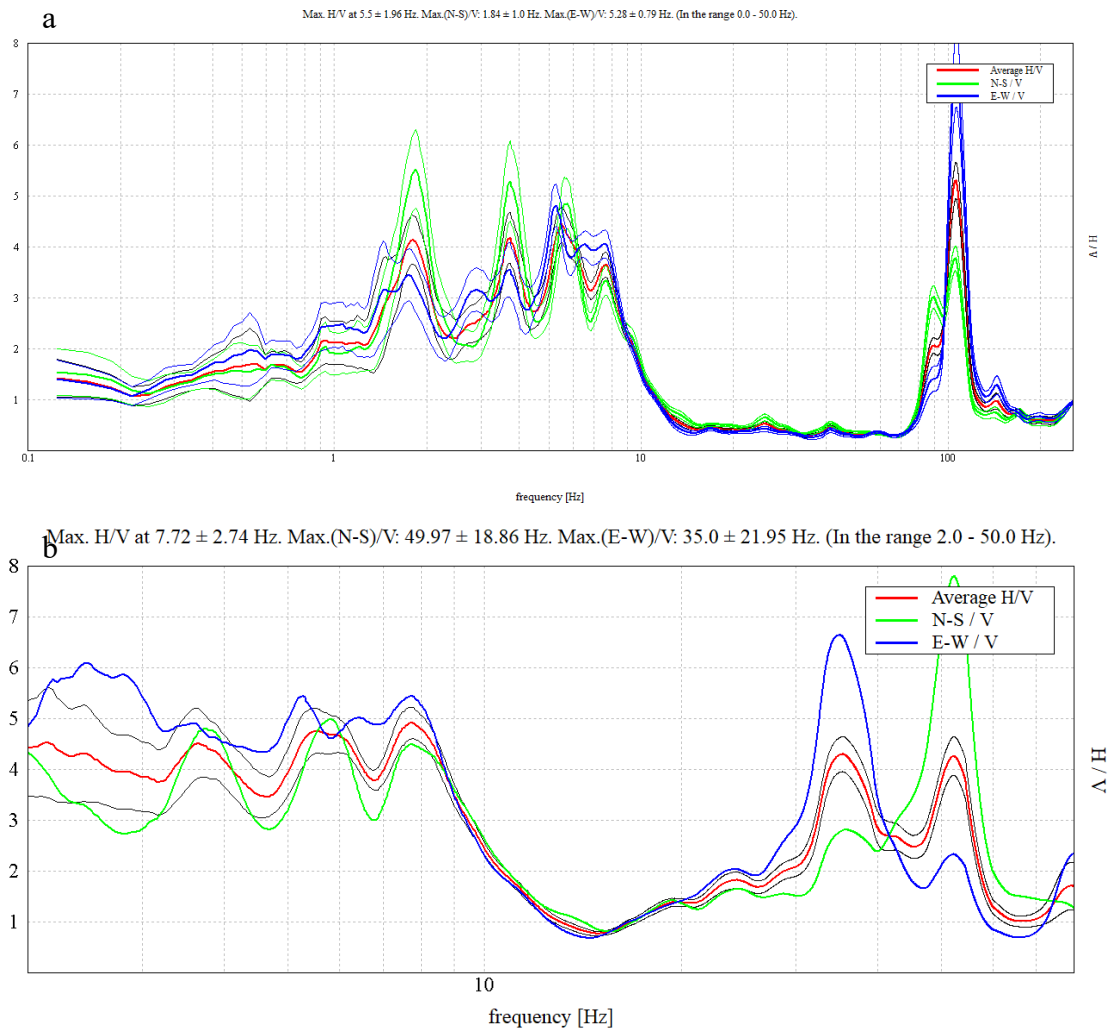

Figure B-23 Journalism B-06 A site, Test 1, concrete (a), grass (b)

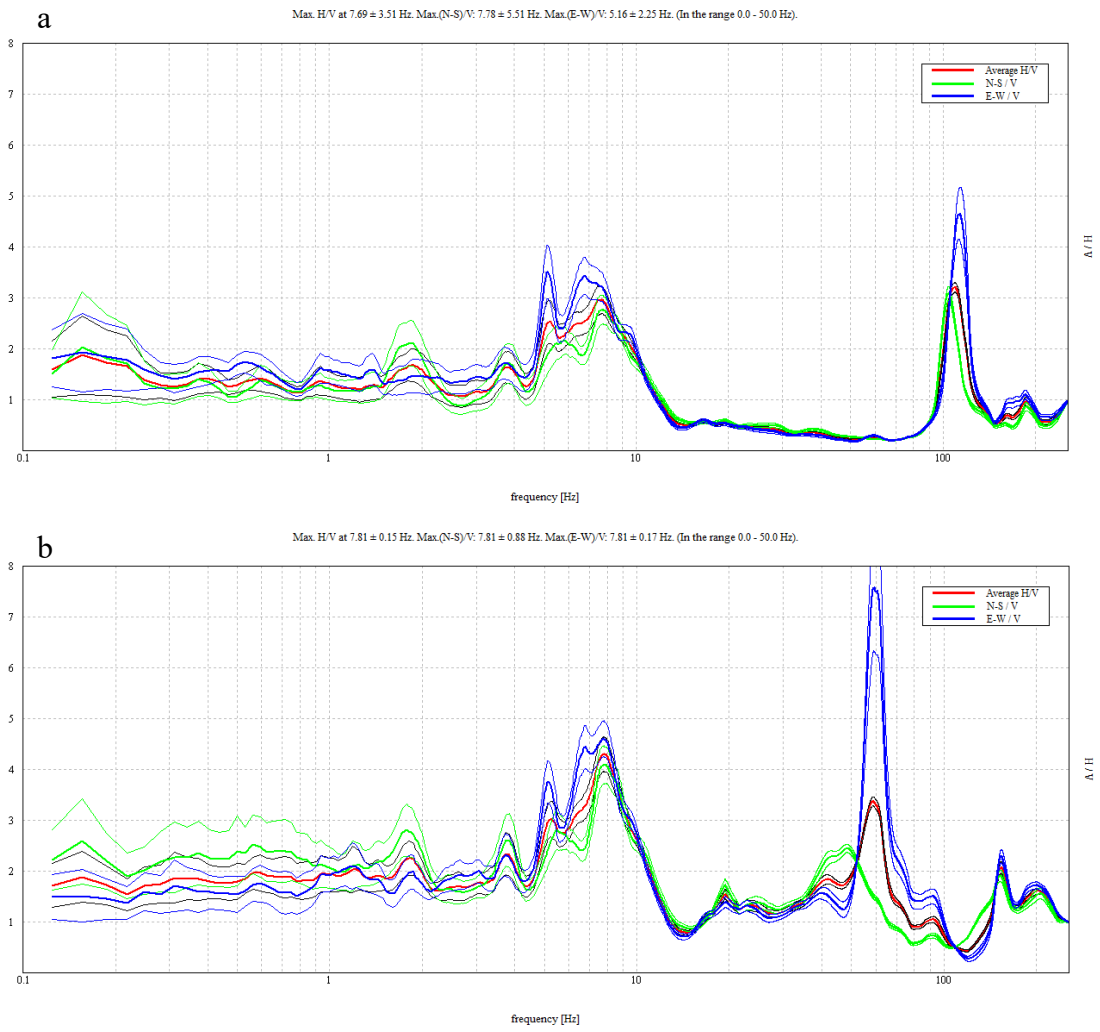

Figure B-24 Journalism B-06 A site, Test 2, concrete (a), grass (b)

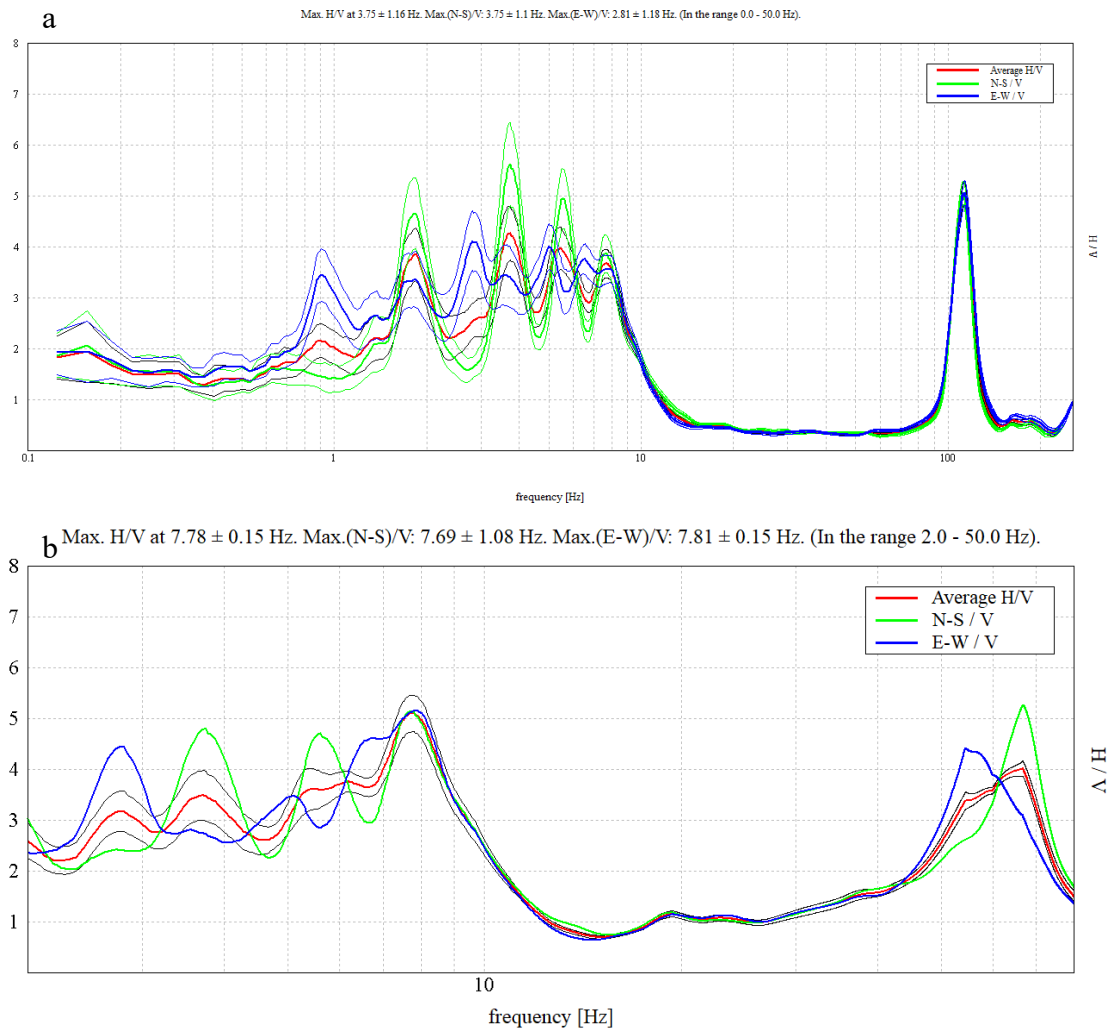

Figure B-25 Journalism B-06 A site, Test 3, concrete (a), grass (b)

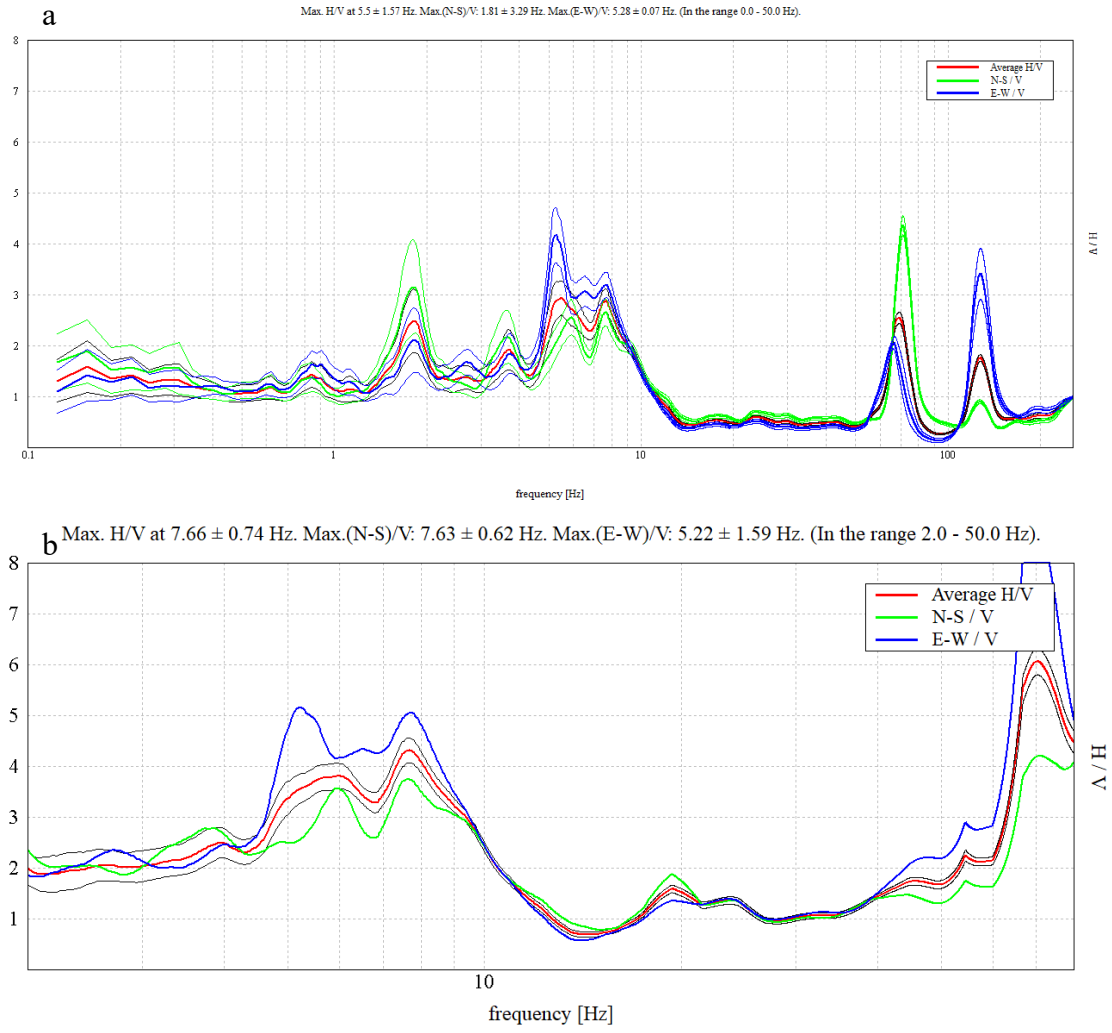

Figure B-26 Journalism B-06 A site, Test 4, concrete (a), grass (b)

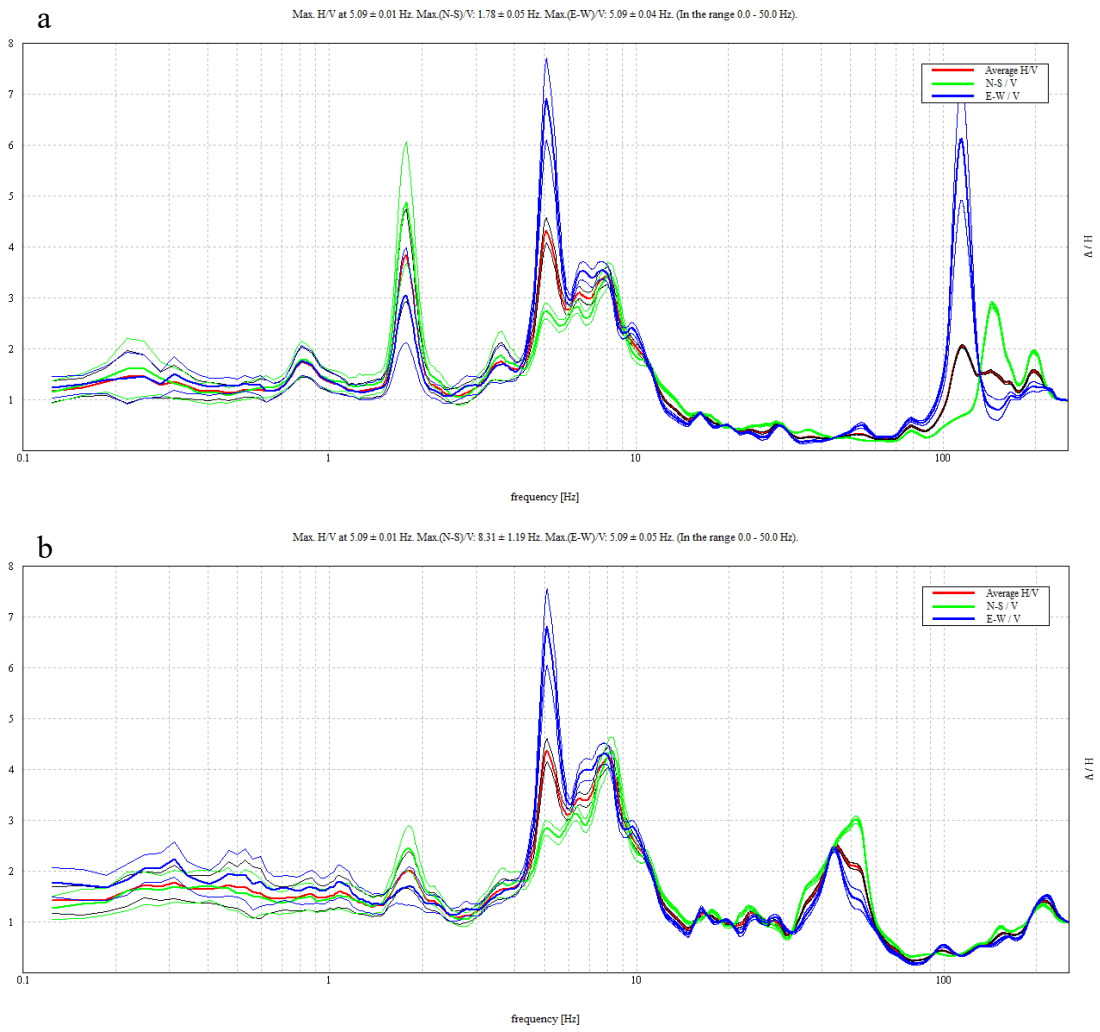

Figure B-27 Journalism B-06 A site, Test 5, concrete (a), grass (b)

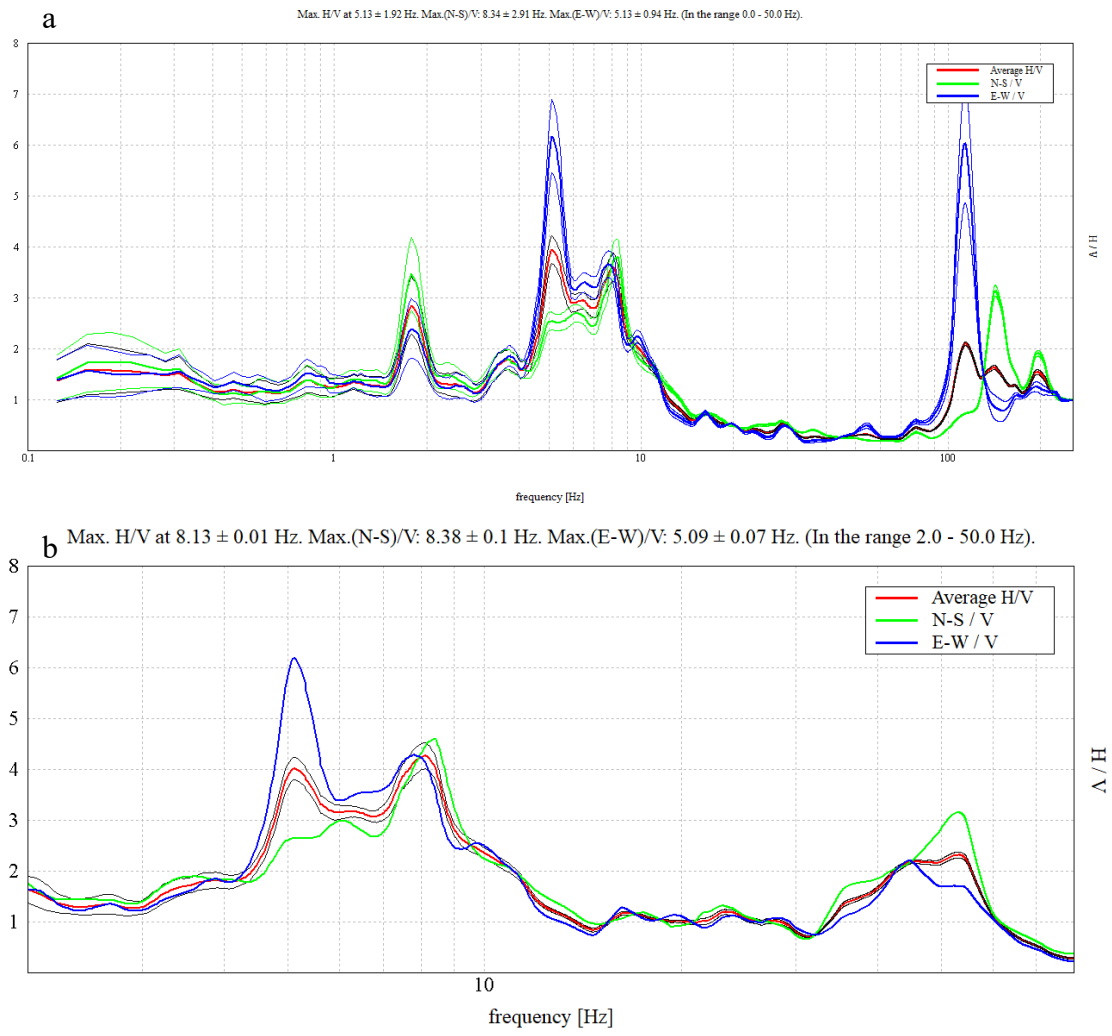

Figure B-28 Journalism B-06 A site, Test 6, concrete (a), grass (b)

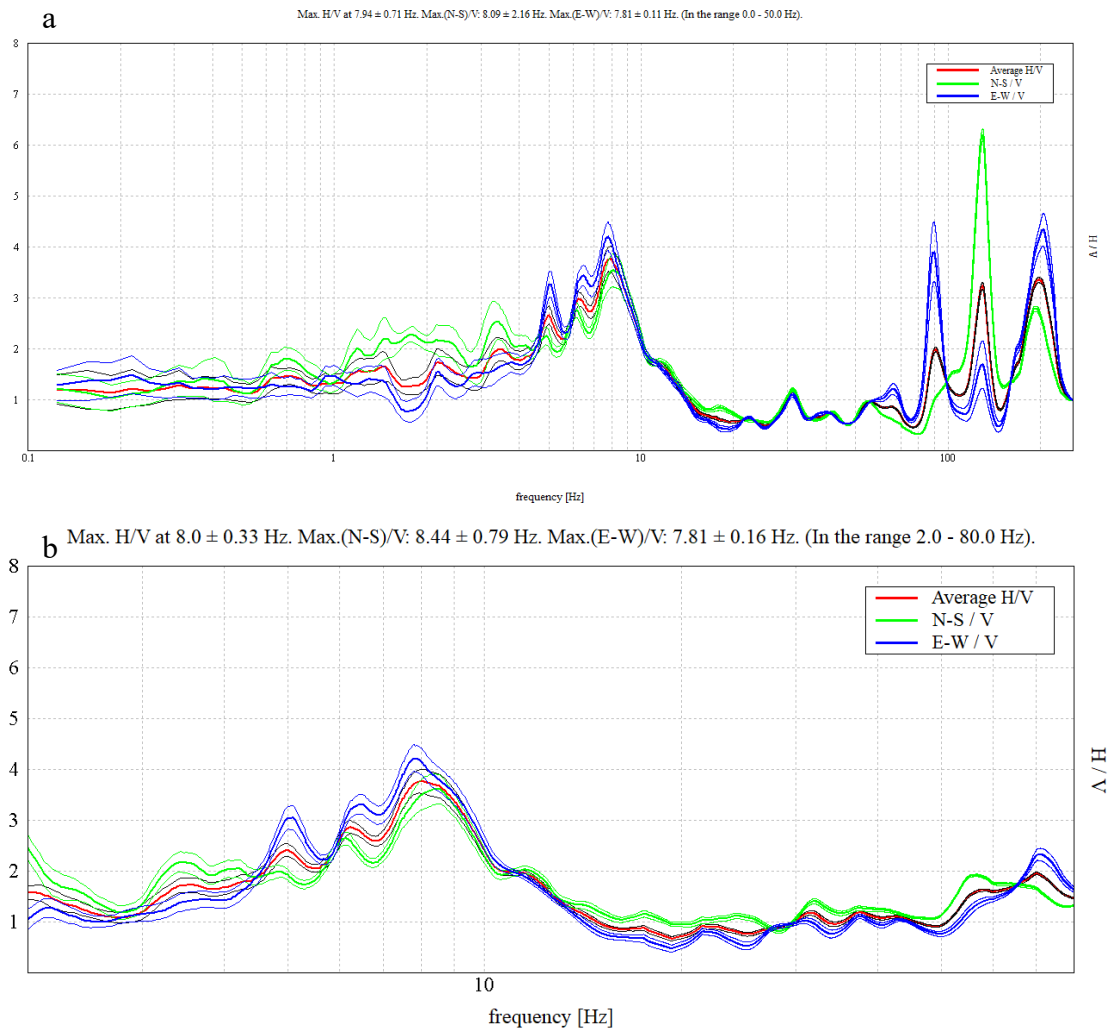

Figure B-29 Journalism B-06 B site, Test 1, concrete (a), grass (b)

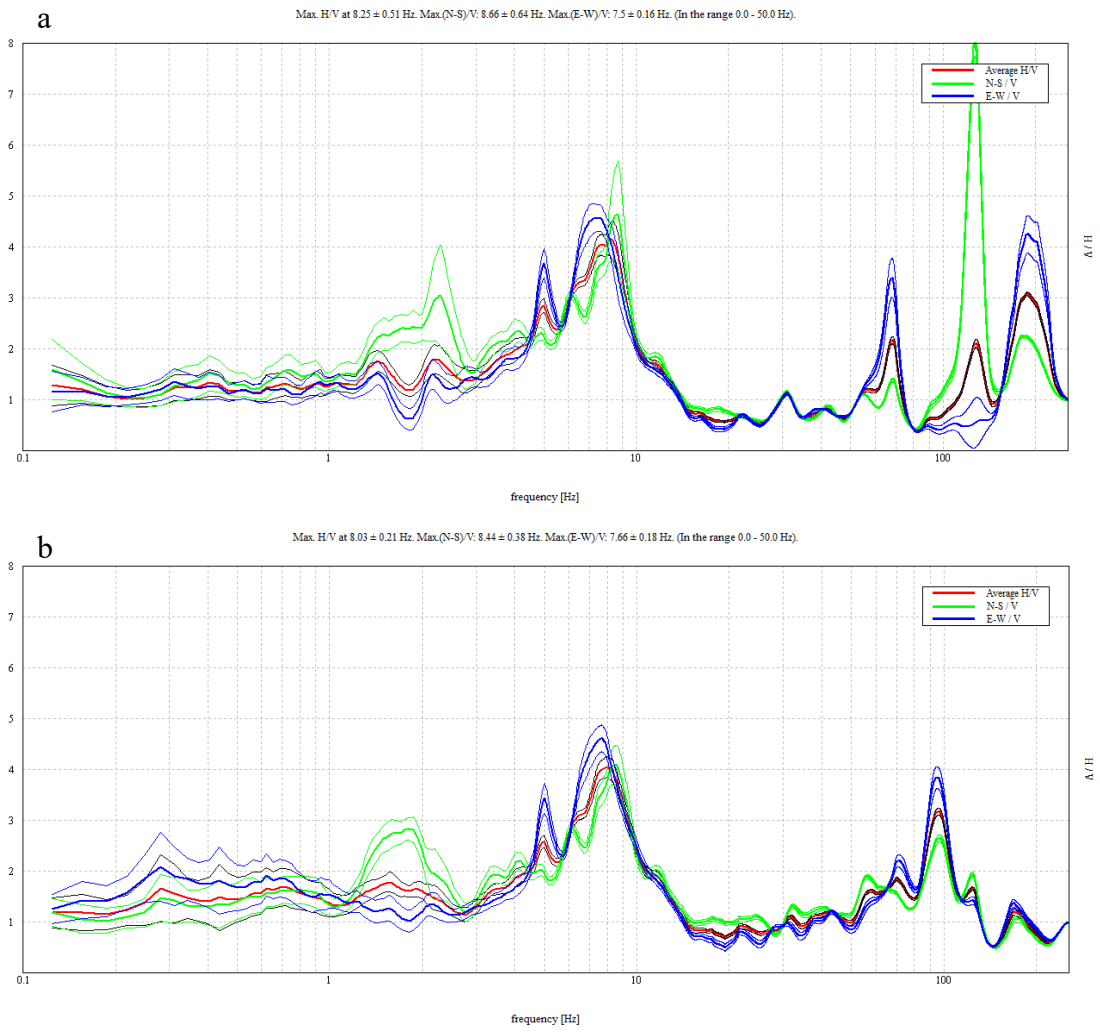

Figure B-30 Journalism B-06 B site, Test 2, concrete (a), grass (b)

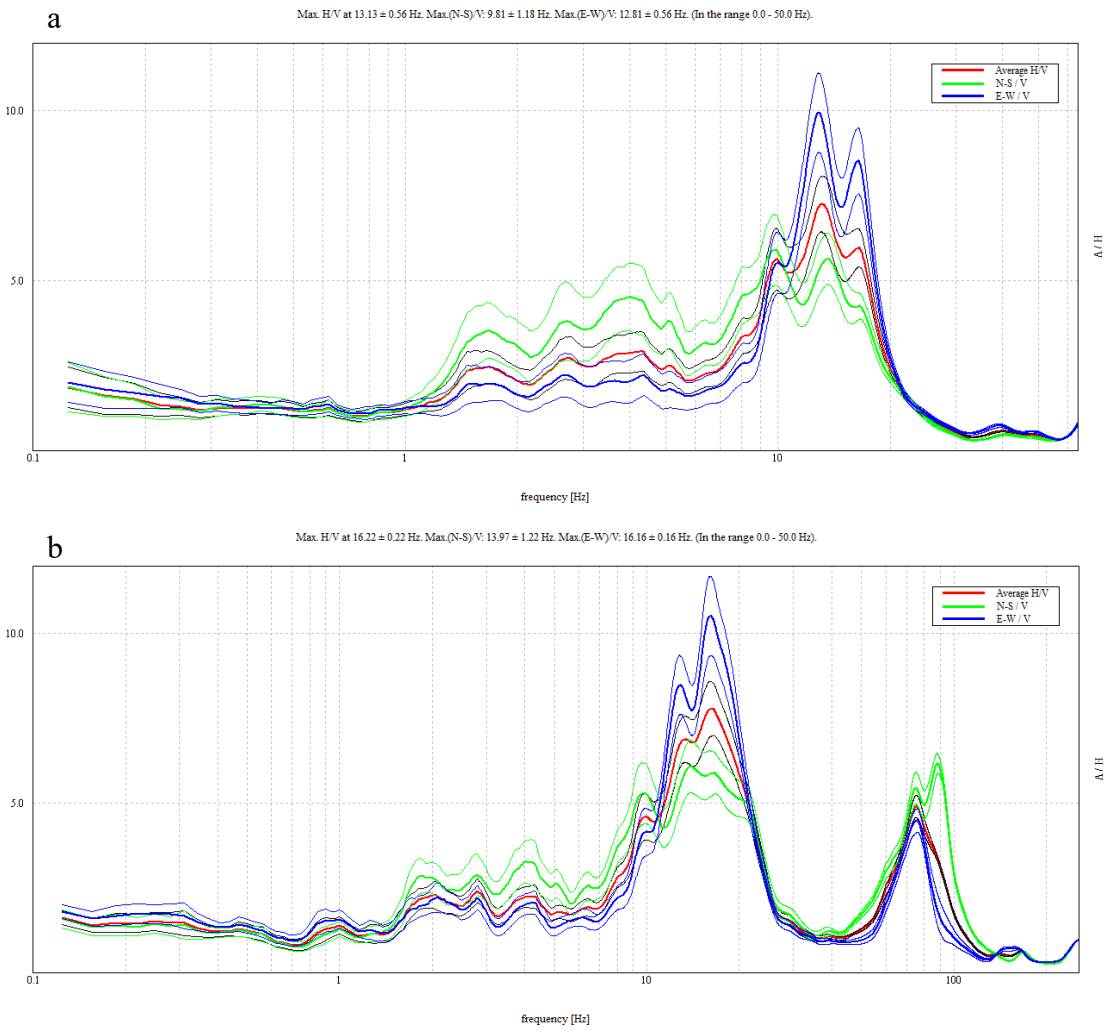

Figure B-31 Lee's Hall BH-08 site, Test 1, concrete (a), grass (b)

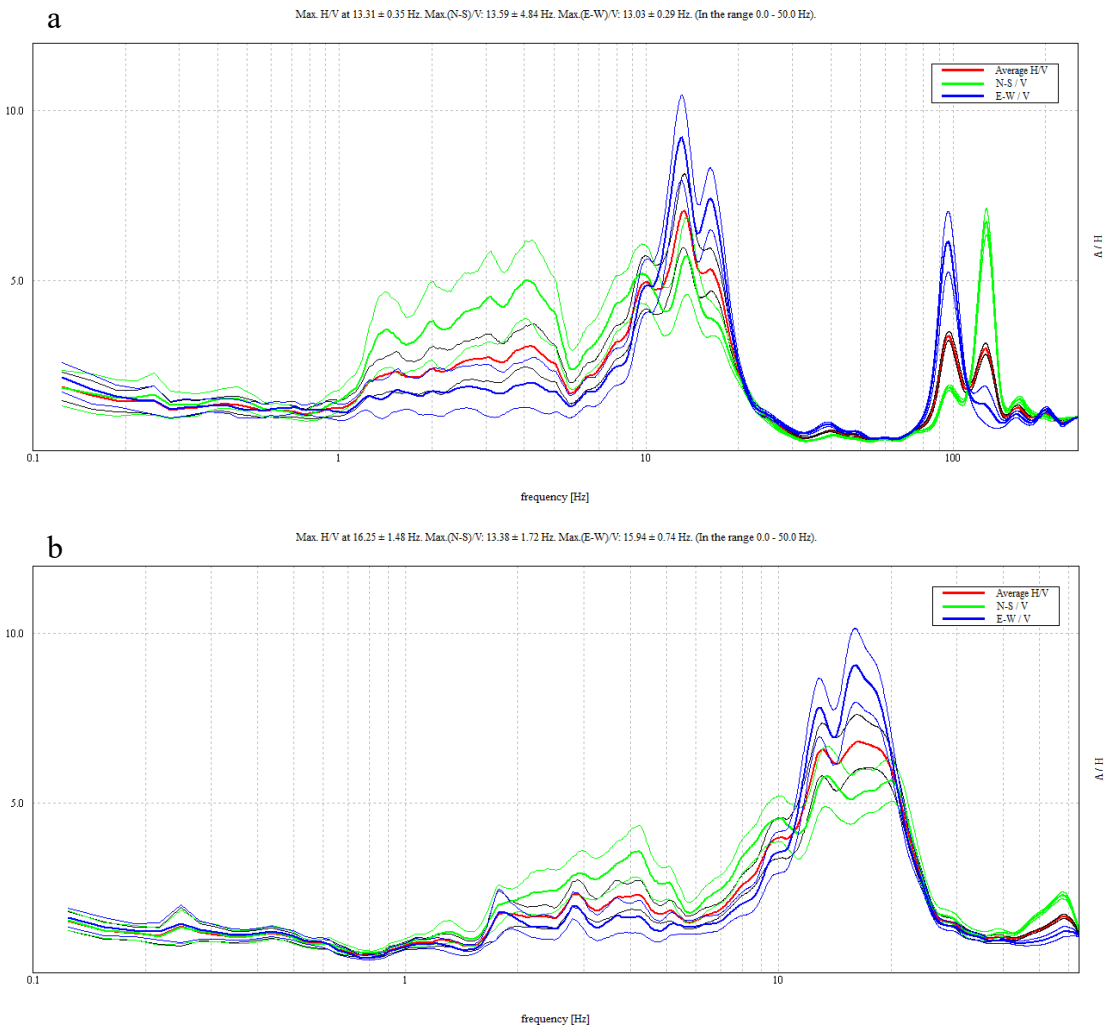

Figure B-32 Lee's Hall BH-08 site, Test 2, concrete (a), grass (b)

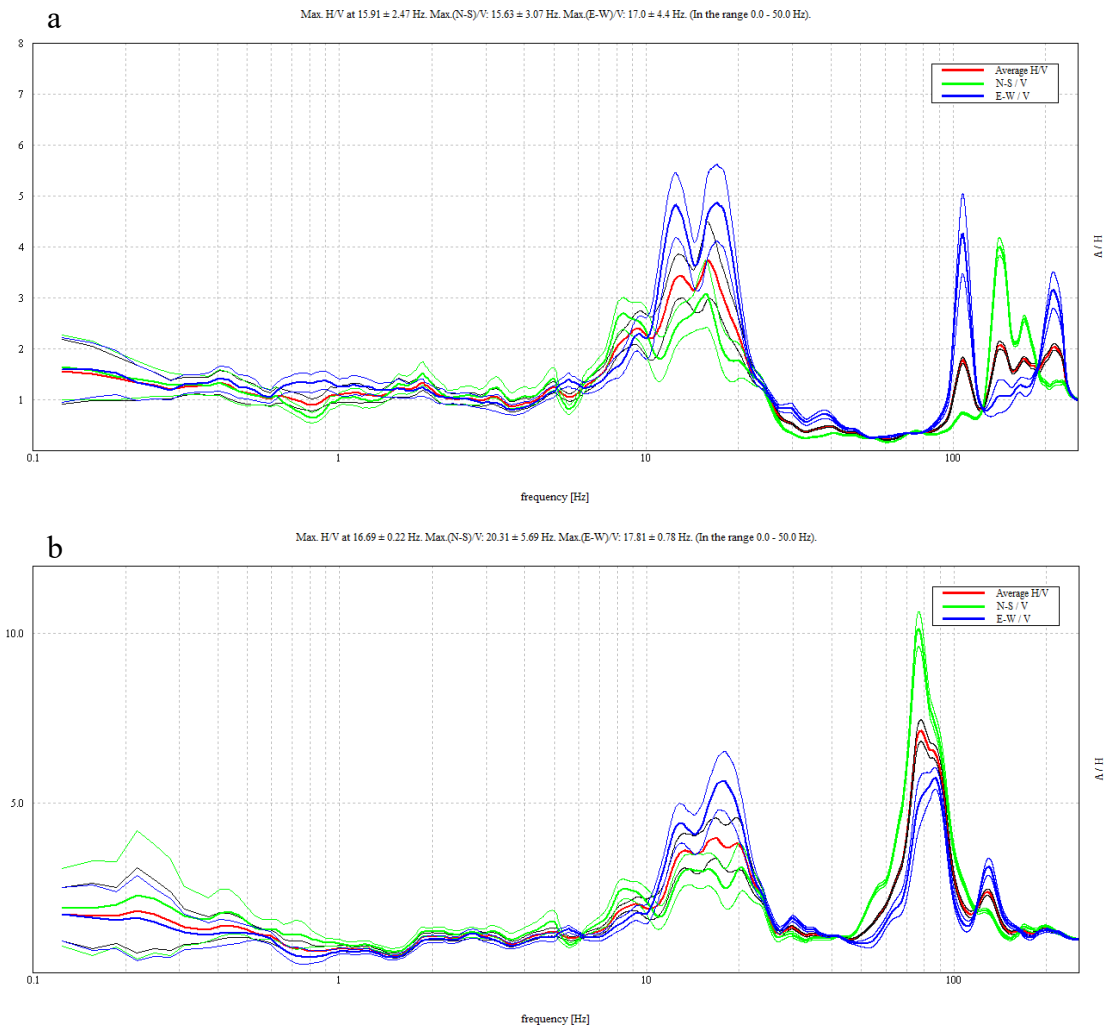

Figure B-33 Lee's Hall BH-08 site, Test 3, concrete (a), grass (b)

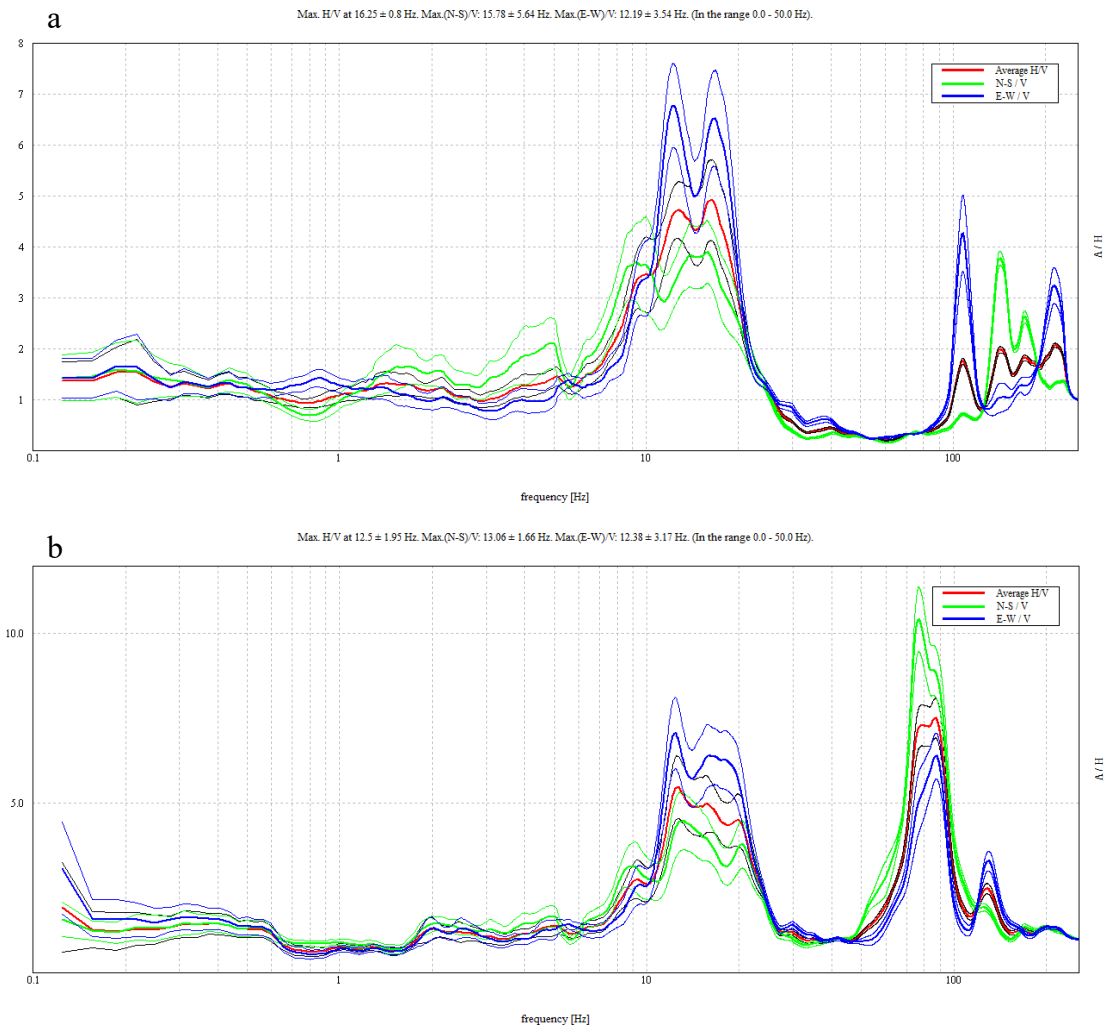

Figure B-34 Lee's Hall BH-08 site, Test 4, concrete (a), grass (b)

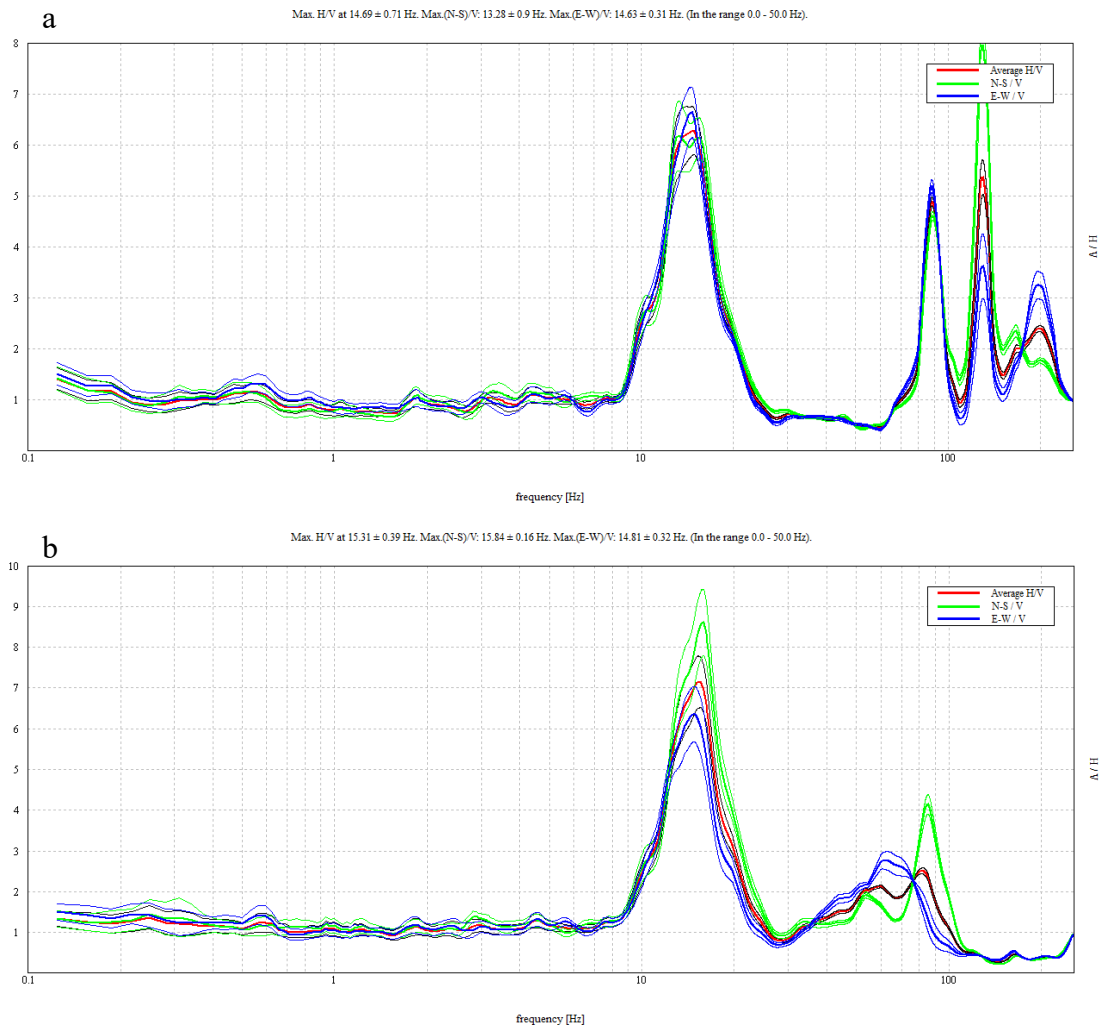

Figure B-35 Lee's Hall BH-18 site, Test 1, concrete (a), grass (b)

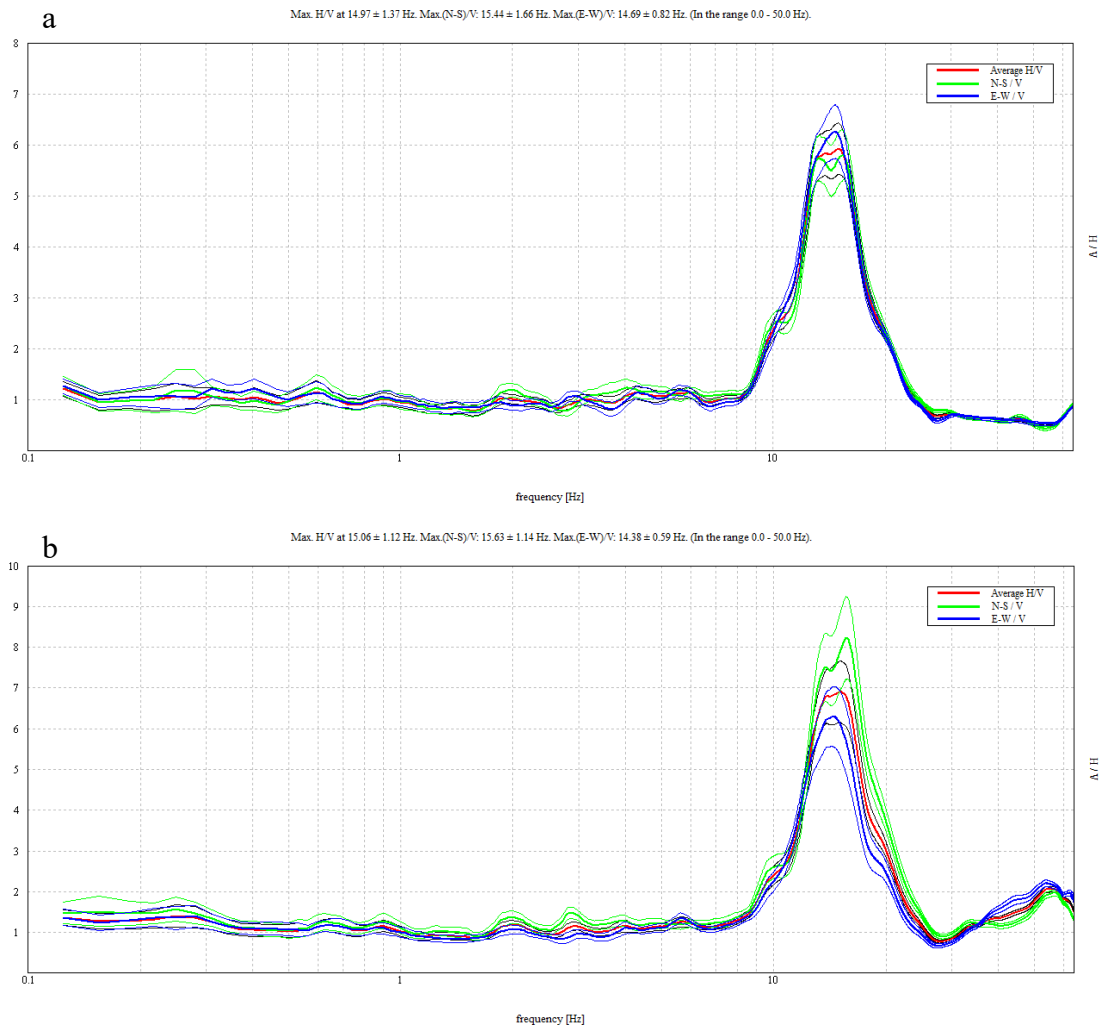

Figure B-36 Lee's Hall BH-18 site, Test 2, concrete (a), grass (b)

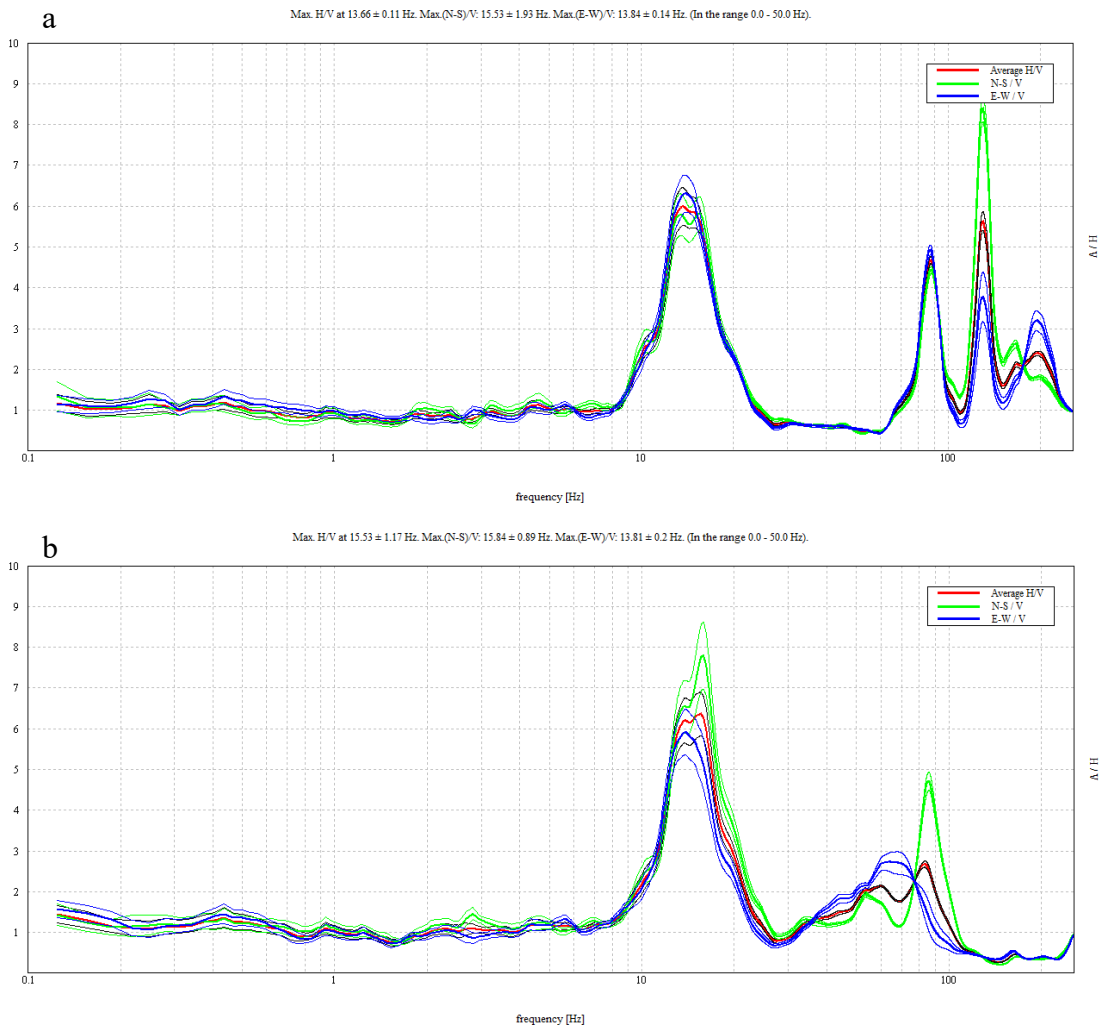

Figure B-37 Lee's Hall BH-18 site, Test 3, concrete (a), grass (b)

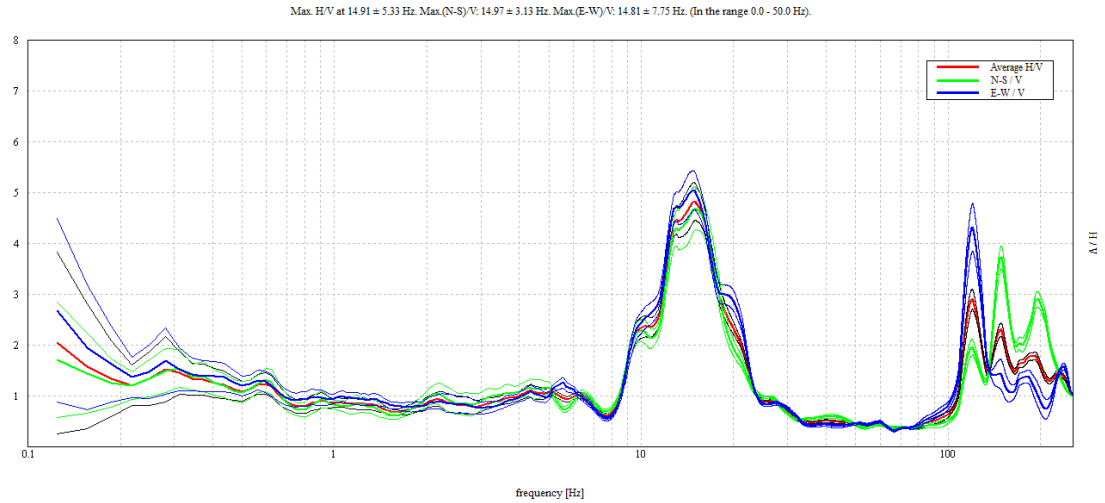

Figure B-38 Lee's Hall BH-18 site, Test 4, concrete

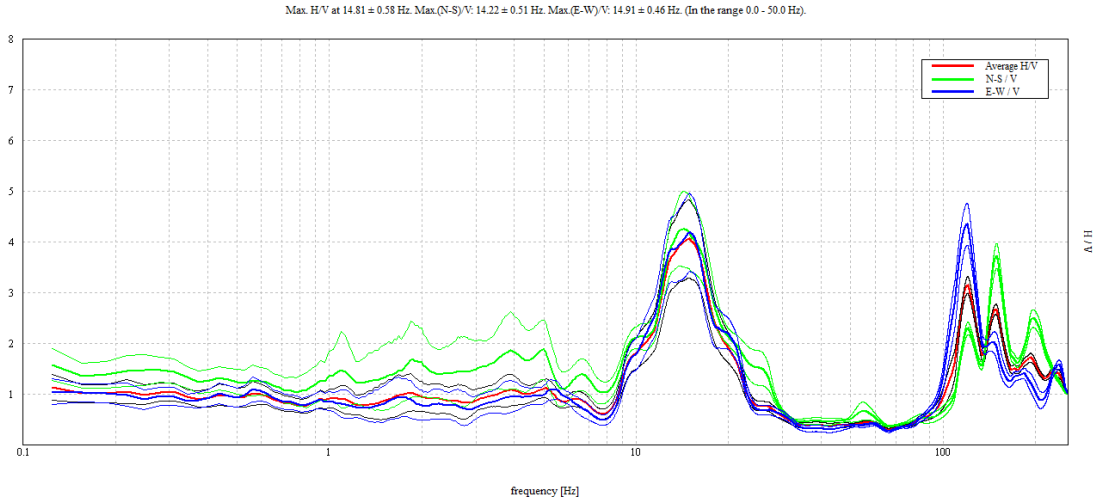

Figure B-39 Lee's Hall BH-18 site, Test 5, concrete

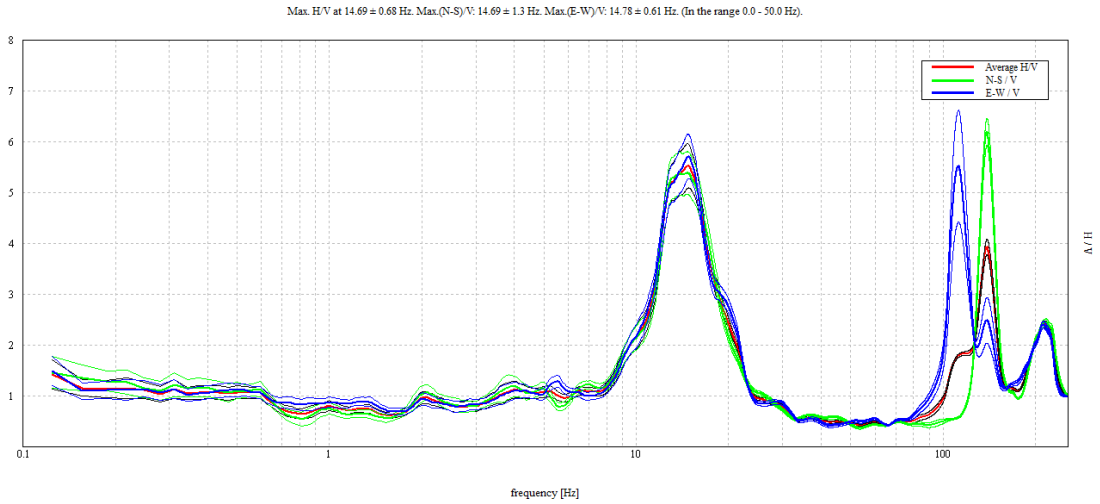

Figure B-40 Lee's Hall BH-18 site, Test 6, concrete

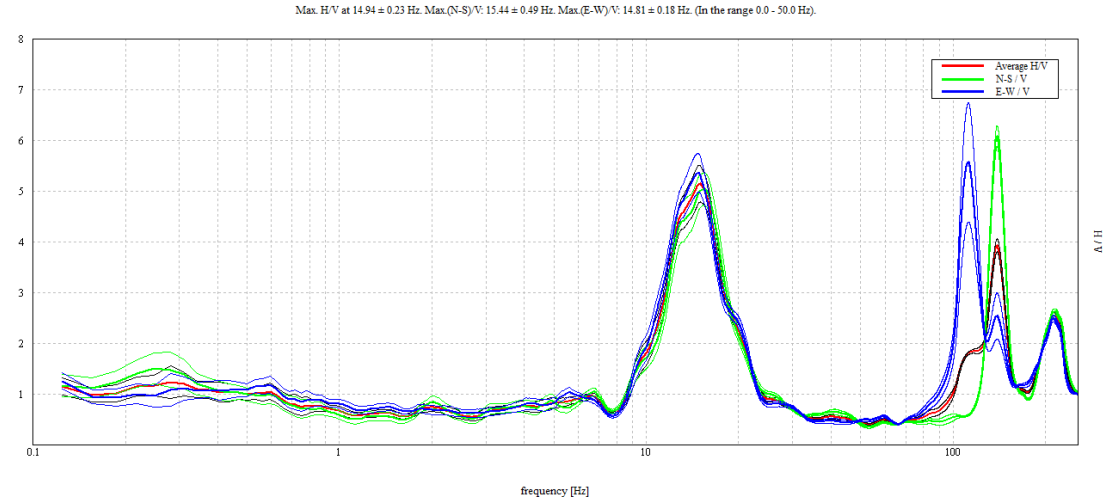

Figure B-41 Lee's Hall BH-18 site, Test 7, concrete

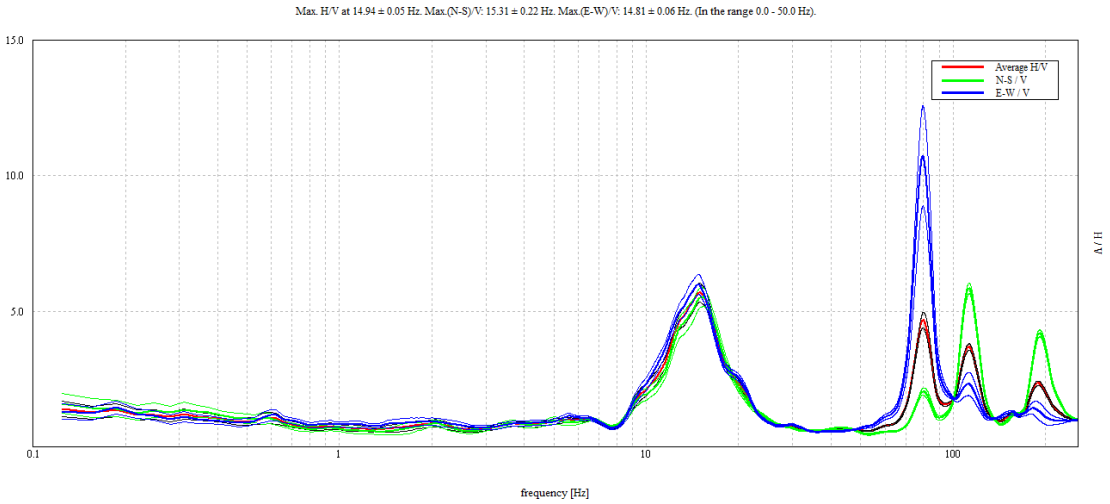

Figure B-42 Lee's Hall BH-18 site, Test 8, concrete

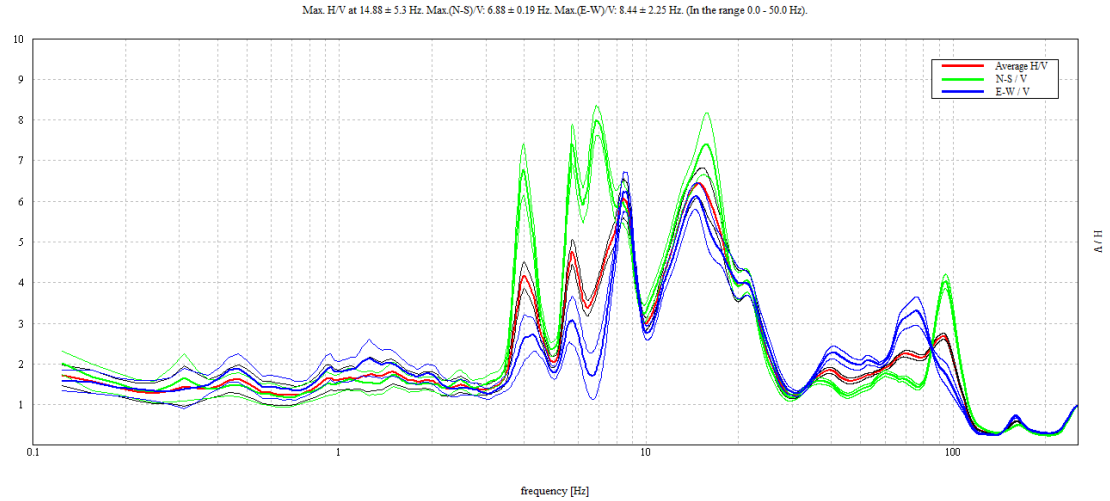

Figure B-43 Lee's Hall Selected site, Test 1, grass

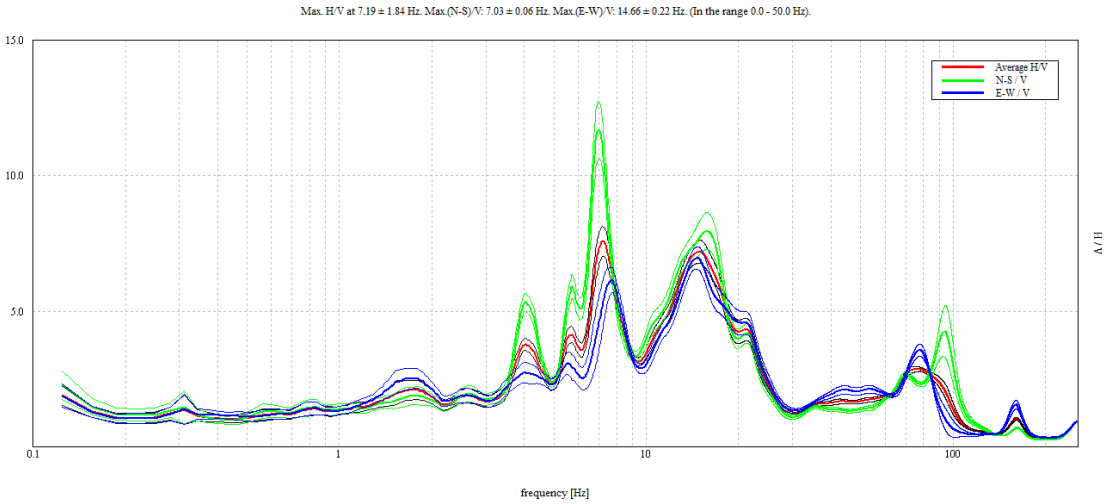

Figure B-44 Lee's Hall Selected site, Test 2, grass

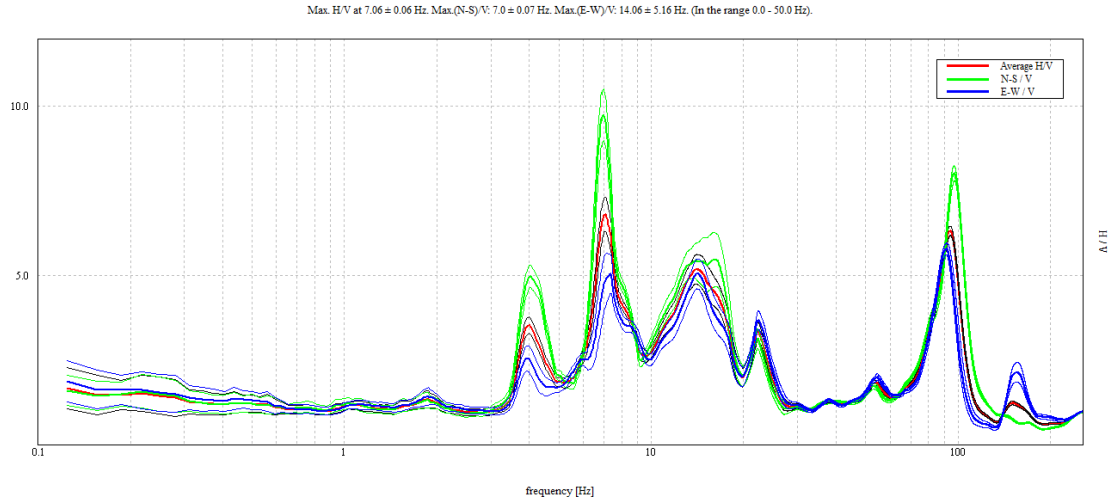

Figure B-45 Lee's Hall Selected site, Test 3, grass

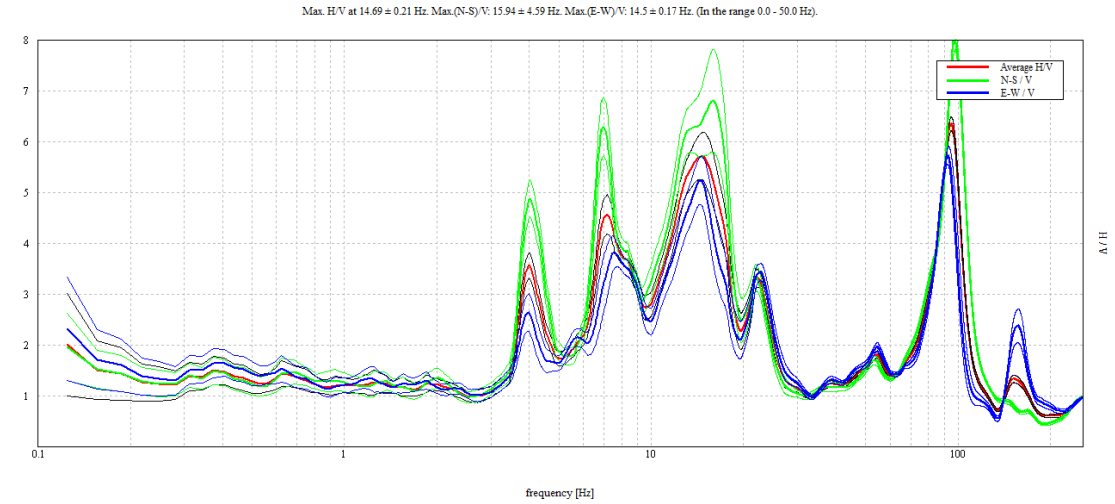

Figure B-46 Lee's Hall Selected site, Test 4, grass

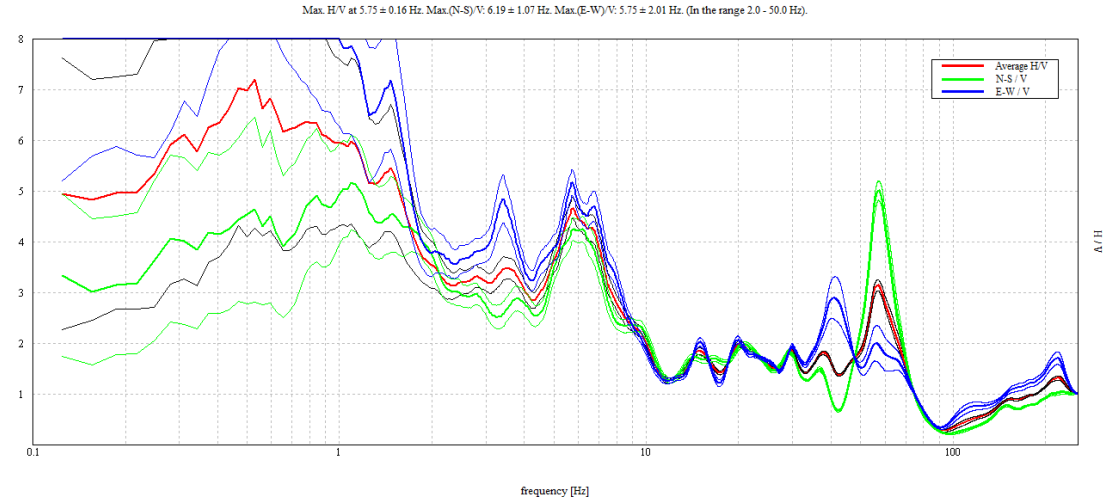

Figure B-47 Lee's Hall Selected site, Test 5, grass

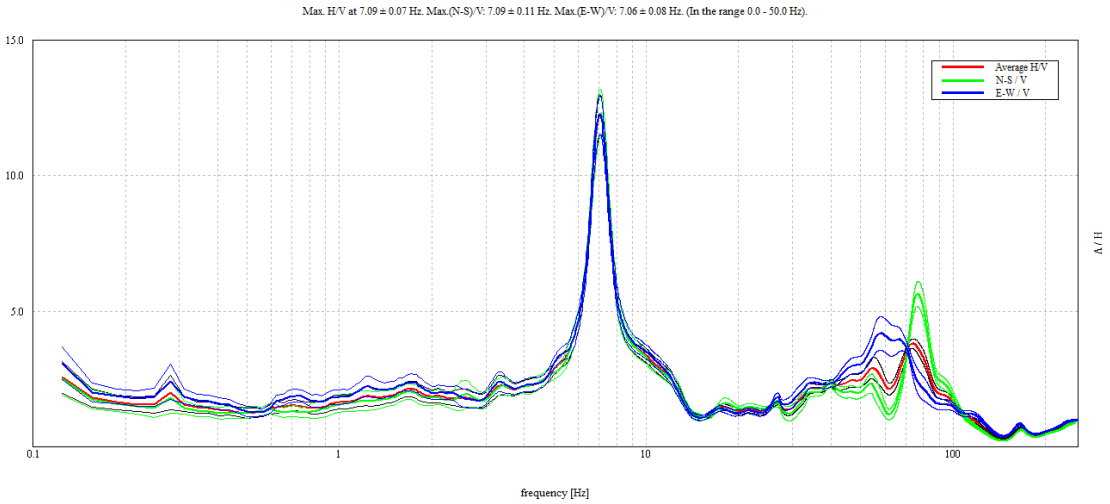

Figure B-48 MIZ Middle Quad site, Test 1, grass

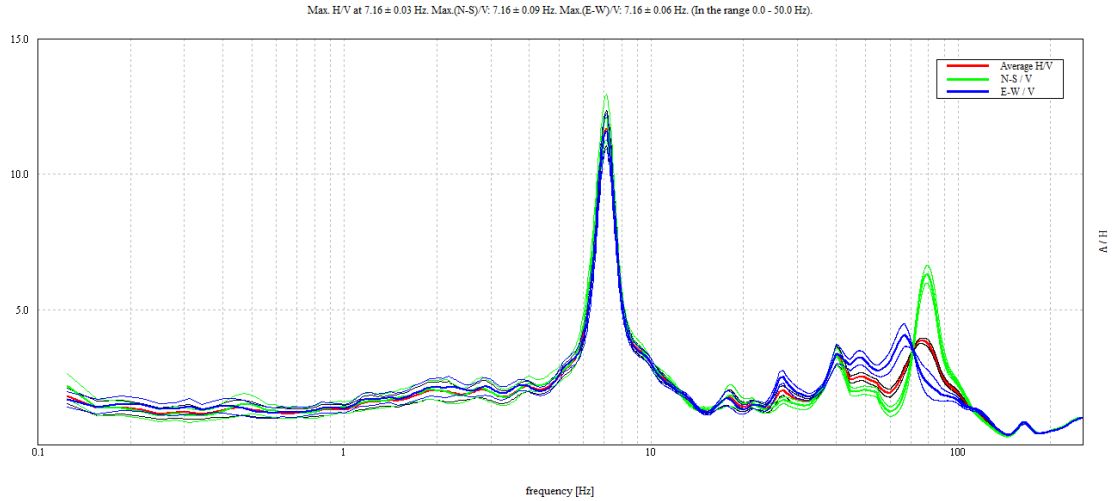

Figure B-49 MIZ Middle Quad site, Test 2, grass

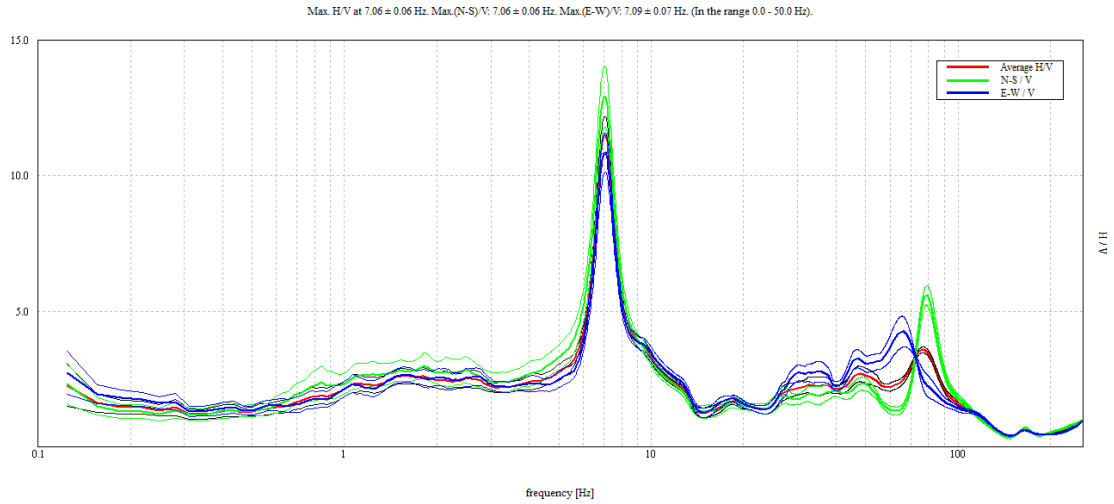

Figure B-50 MIZ Middle Quad site, Test 3, grass

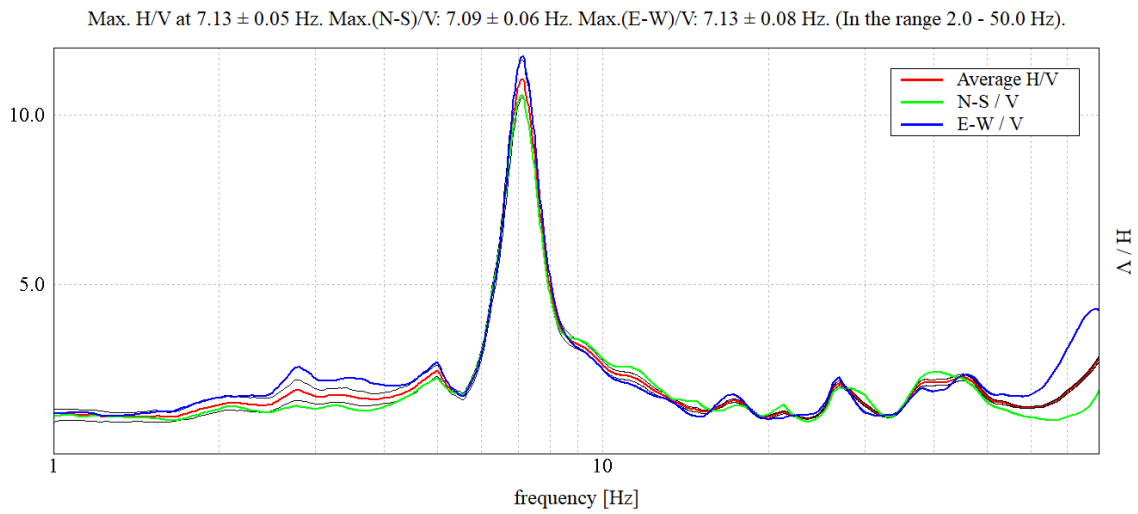

Figure B-51 MIZ Middle Quad site, Test 4, grass

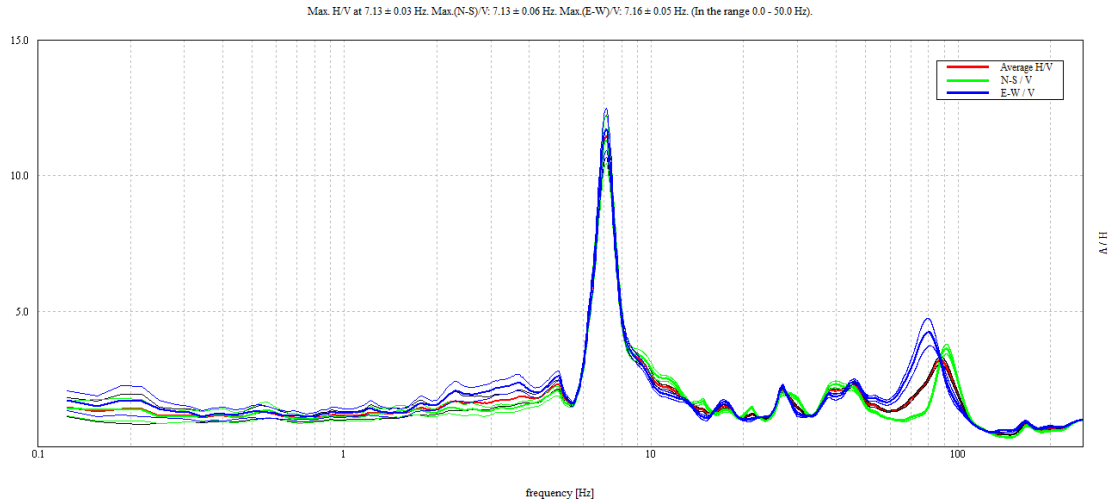

Figure B-52 MIZ Middle Quad site, Test 5, grass

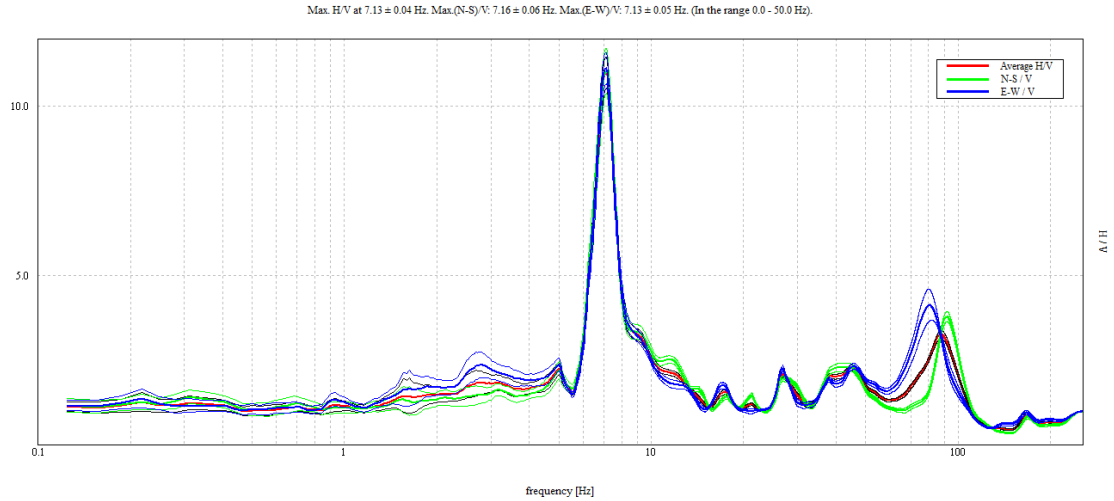

Figure B-53 MIZ Middle Quad site, Test 6, grass

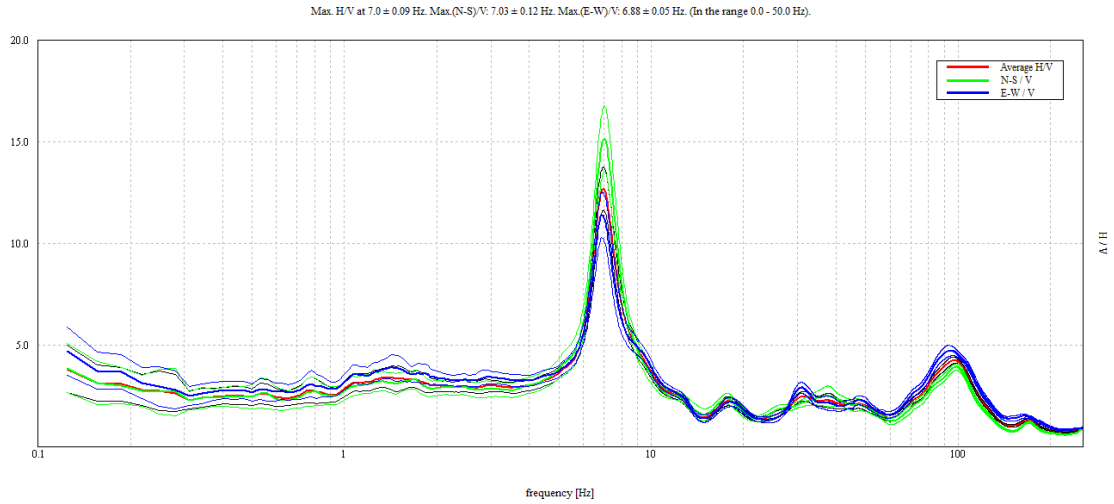

Figure B-54 MIZ Middle Quad site, Test 7, grass

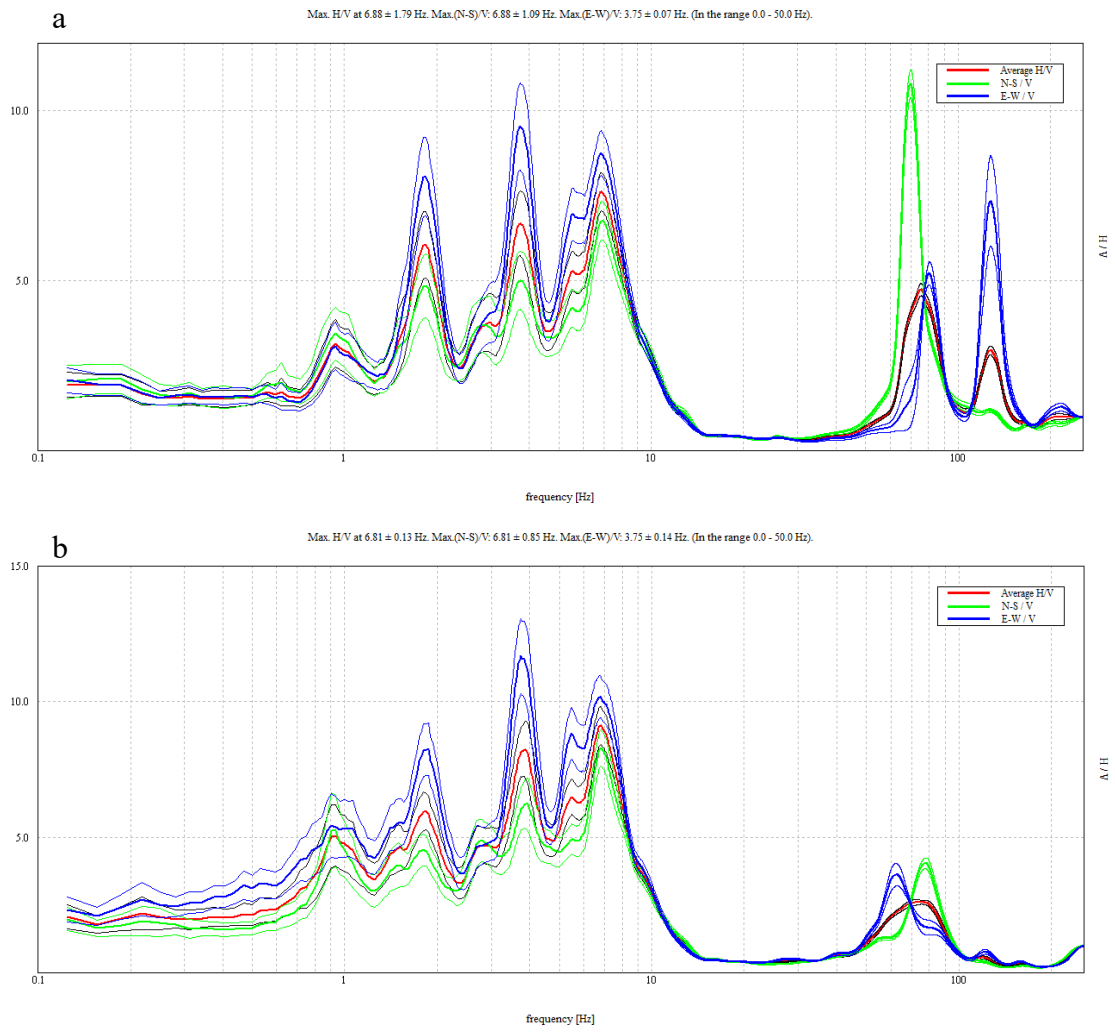

Figure B-55 MIZ Quad Site 1 site, Test 1, concrete (a), grass (b)

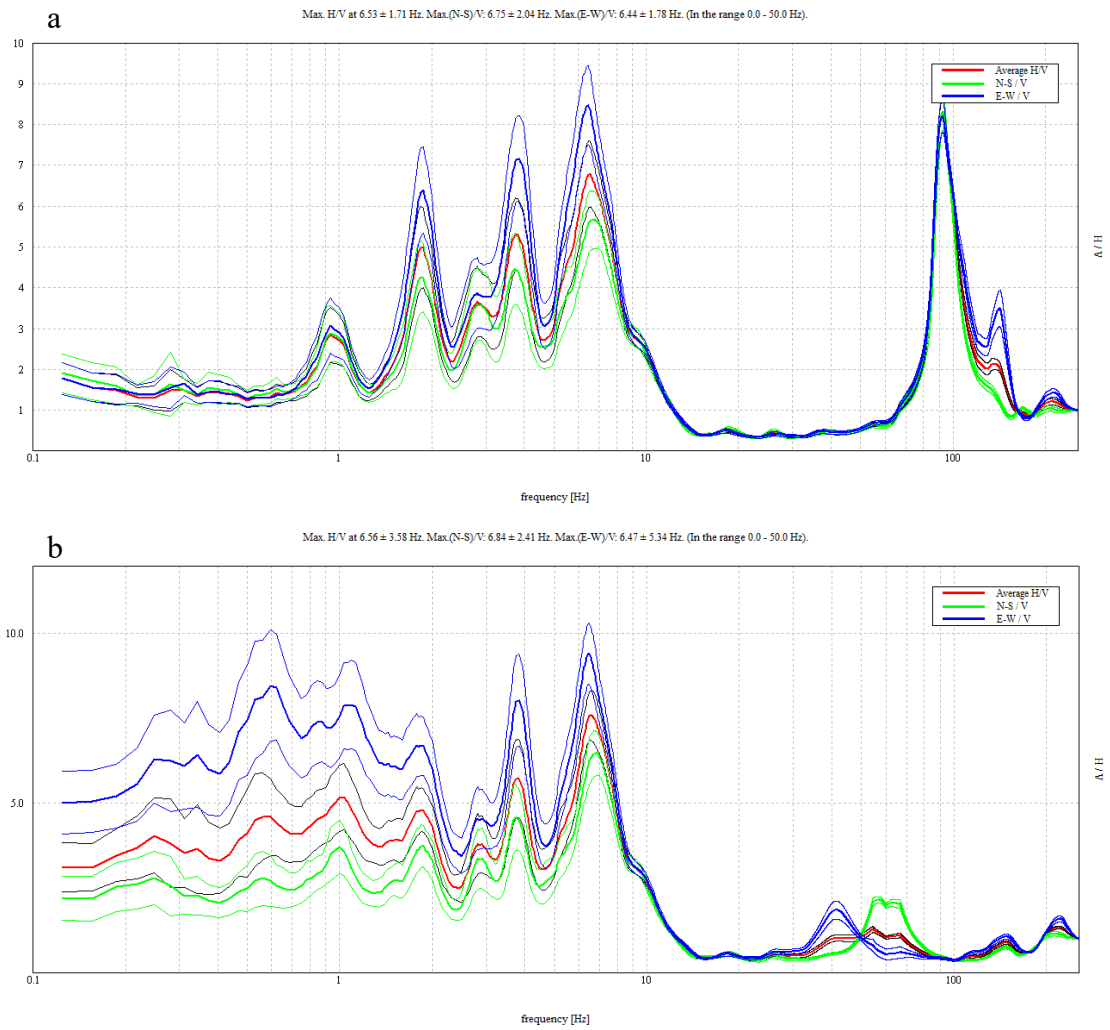

Figure B-56 MIZ Quad Site 1 site, Test 2, concrete (a), grass (b)

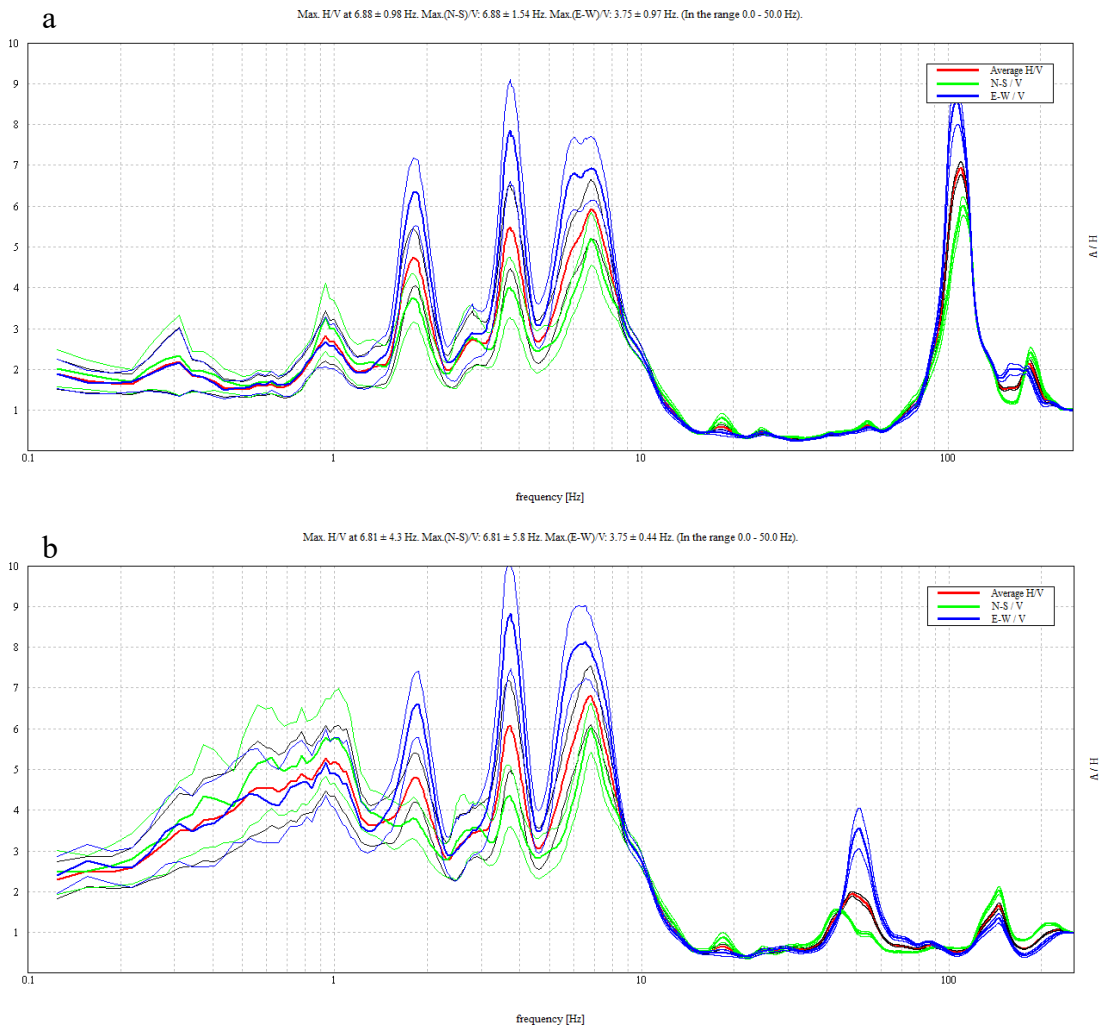

Figure B-57 MIZ Quad Site 1 site, Test 3, concrete (a), grass (b)

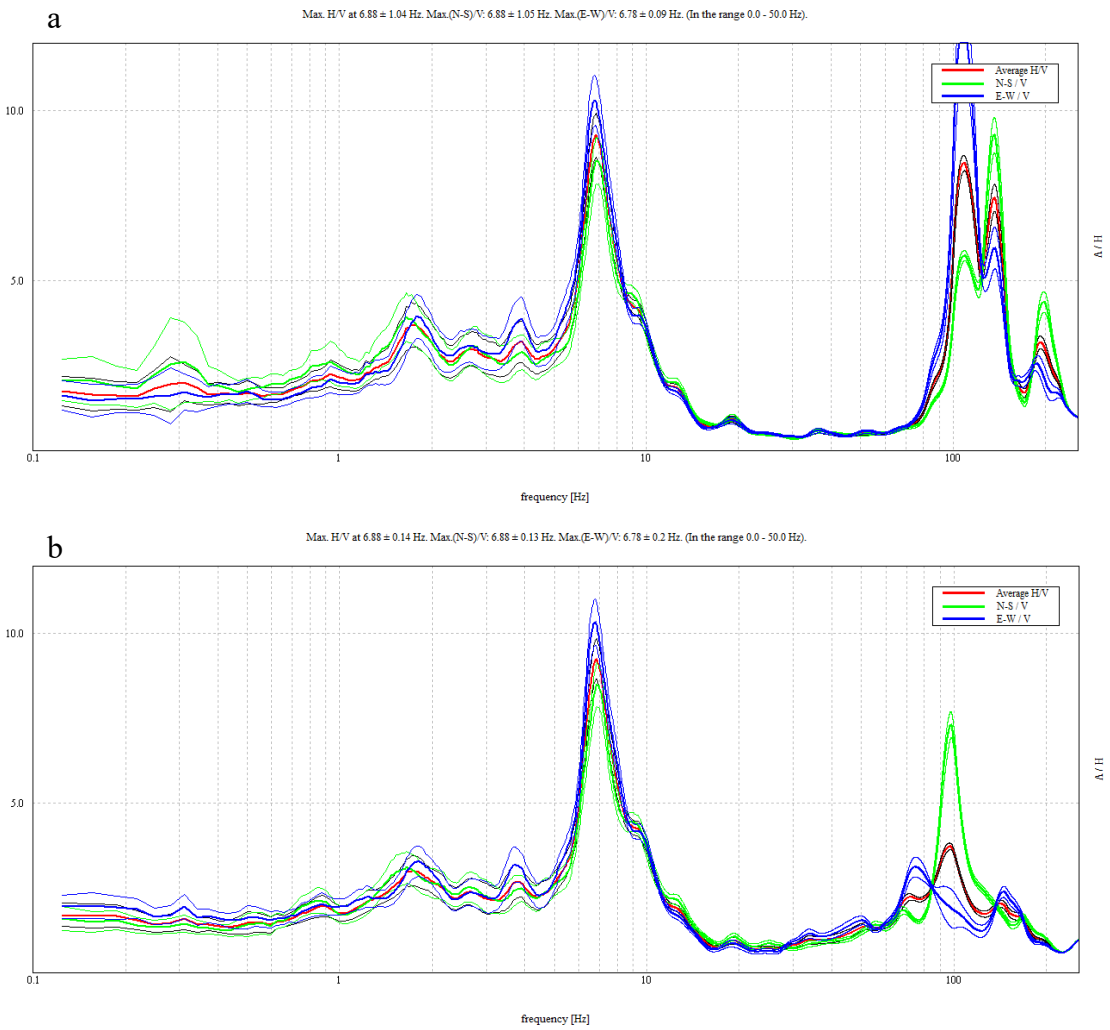

Figure B-58 MIZ Quad Site 1 site, Test 4, concrete (a), grass (b)

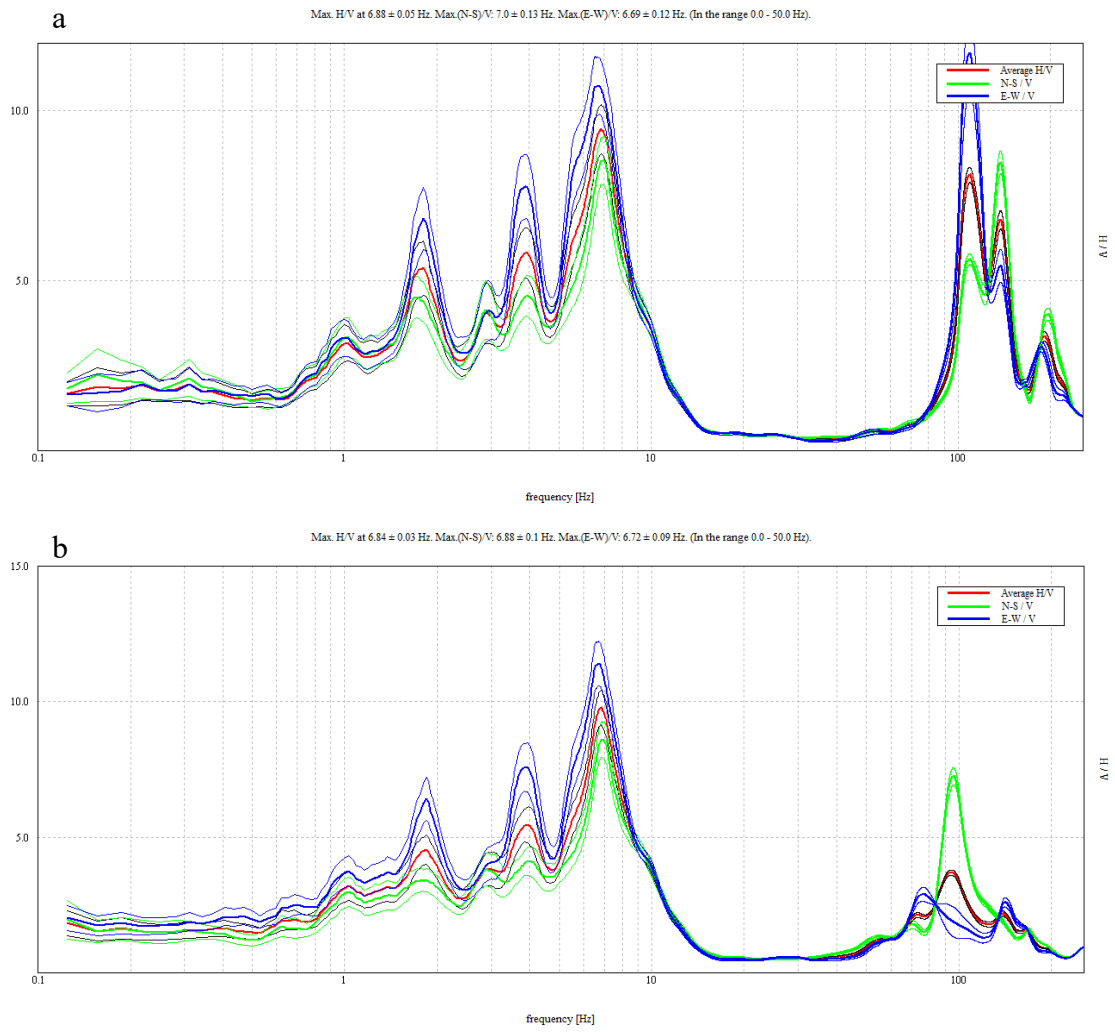

Figure B-59 MIZ Quad Site 1 site, Test 5, concrete (a), grass (b)

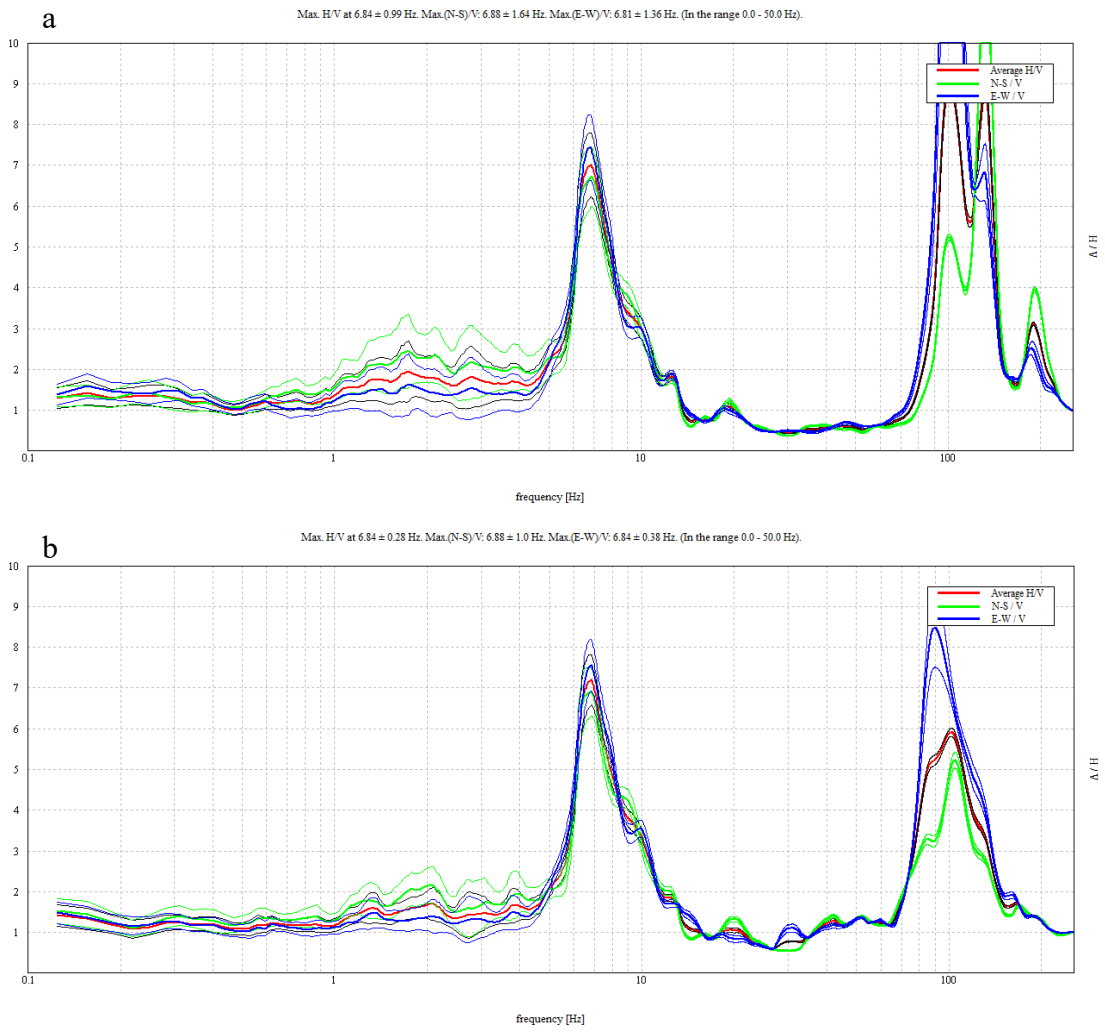

Figure B-60 MIZ Quad Site 1 site, Test 6, concrete (a), grass (b)

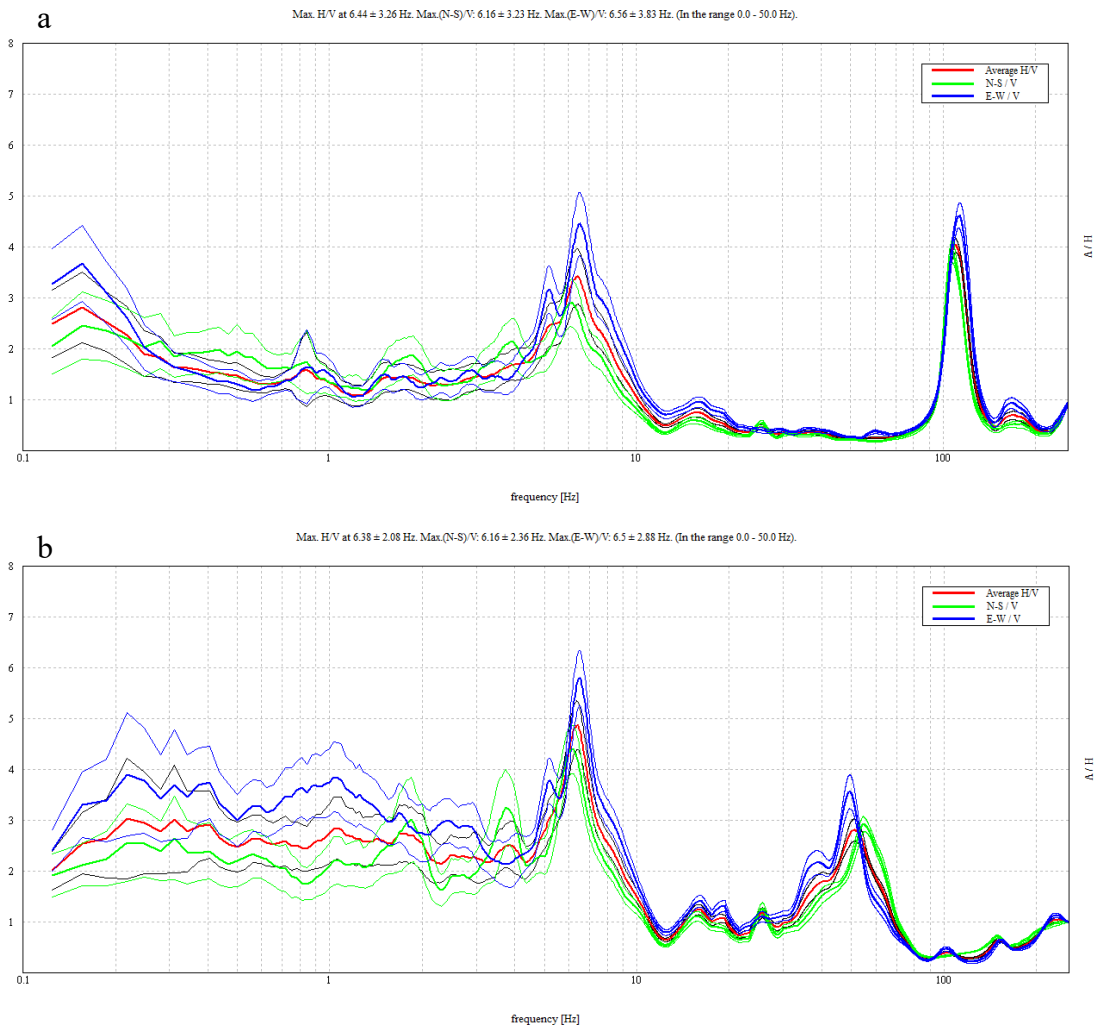

Figure B-61 MIZ Quad Site 2 site, Test 1, concrete (a), grass (b)

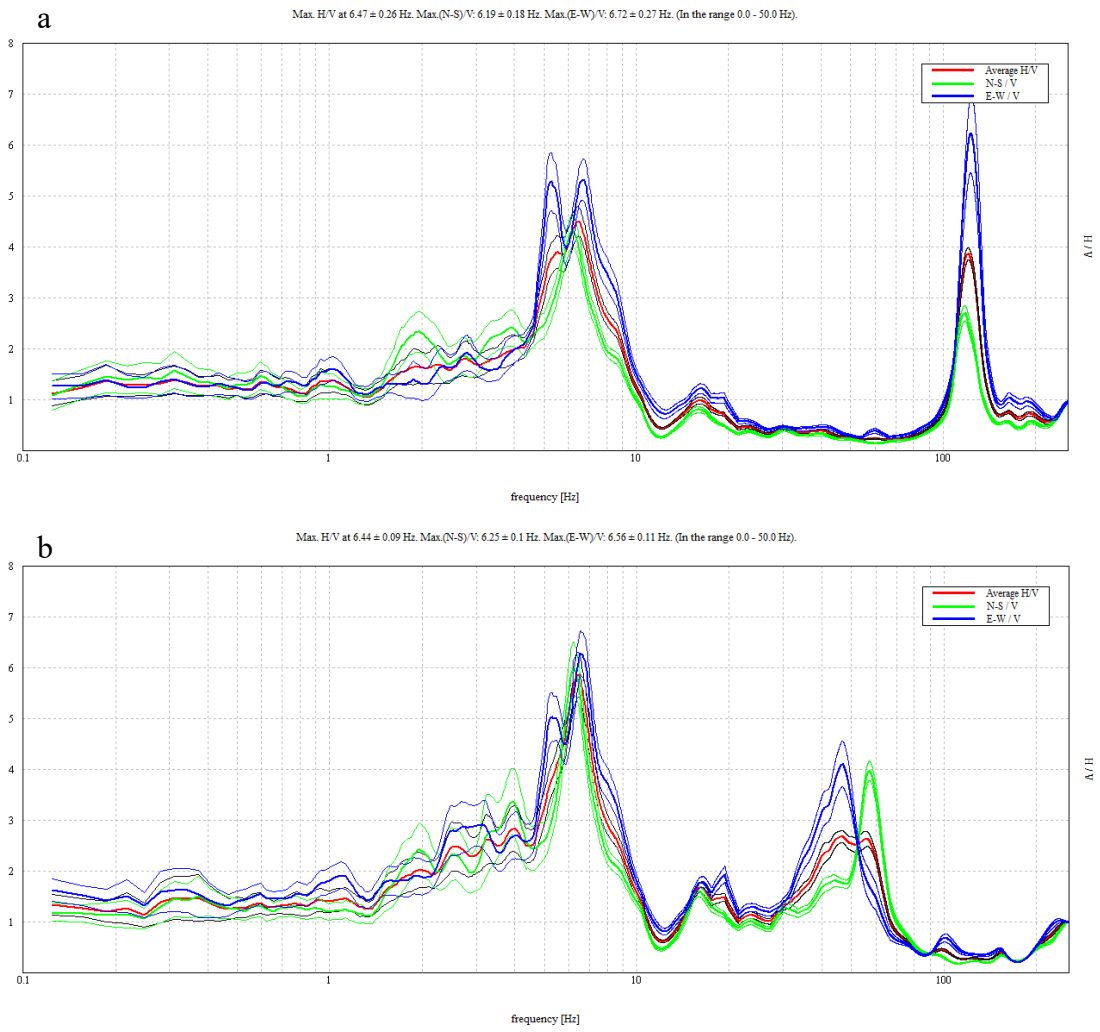

Figure B-62 MIZ Quad Site 2 site, Test 2, concrete (a), grass (b)

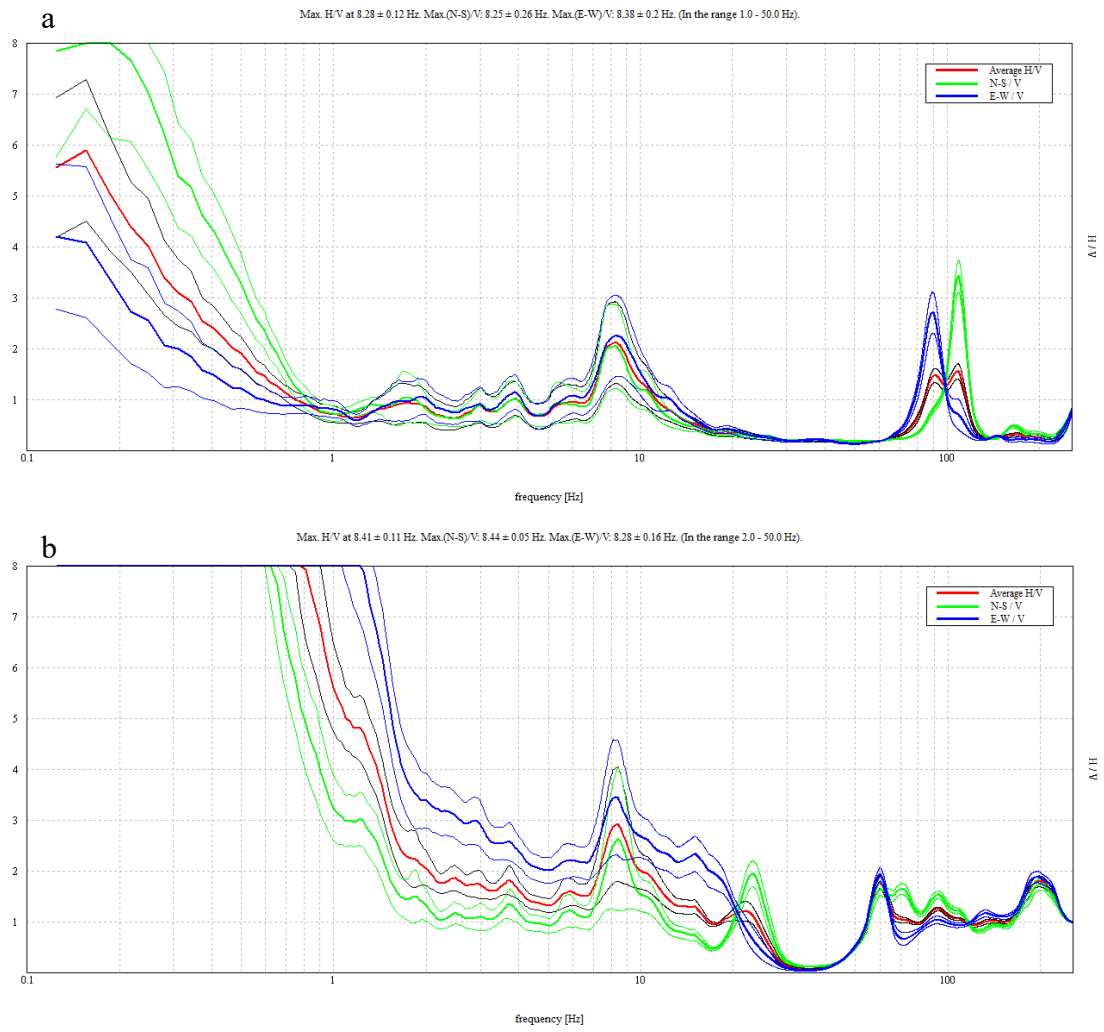

Figure B-63 MIZ Quad Site 3 site, Test 1, concrete (a), grass (b)

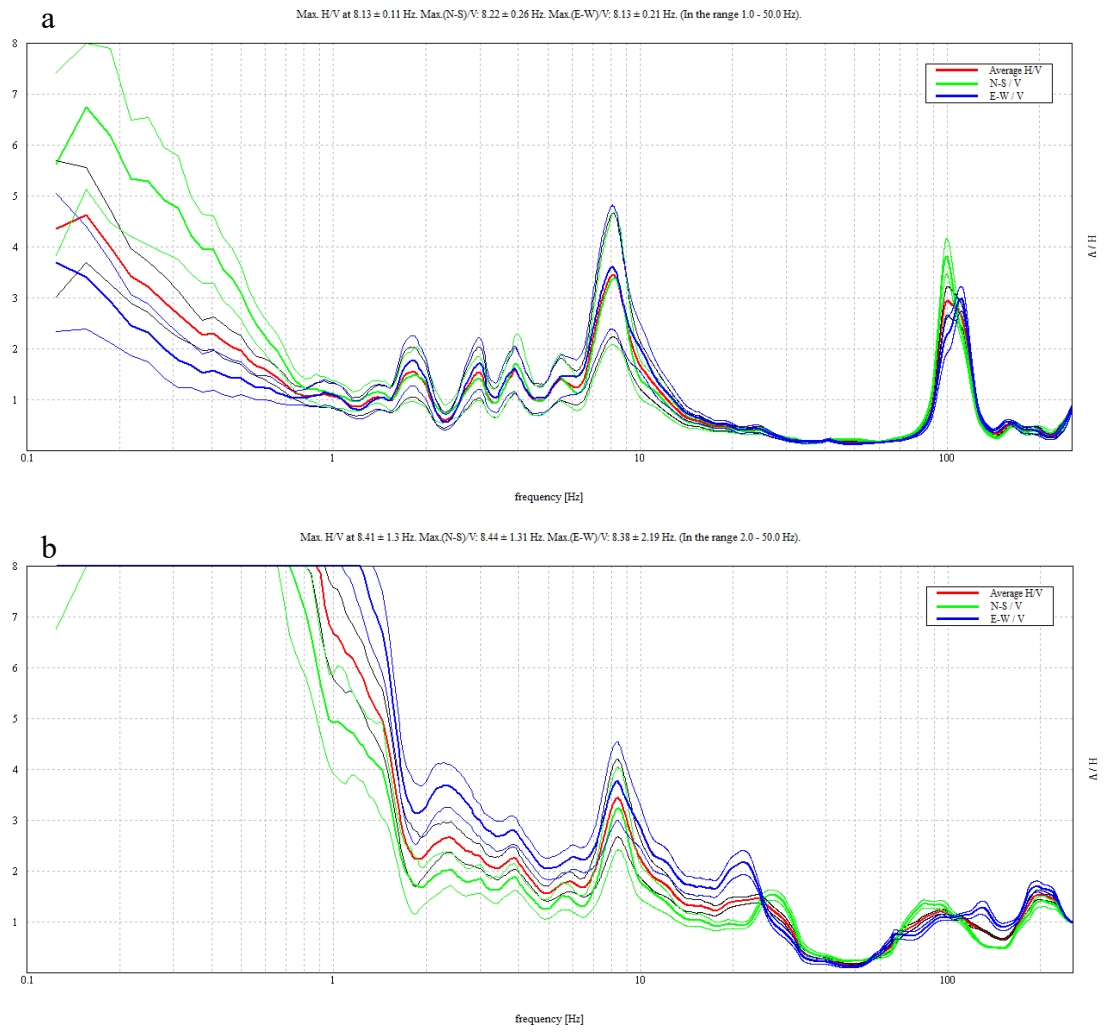

Figure B-64 MIZ Quad Site 3 site, Test 2, concrete (a), grass (b)

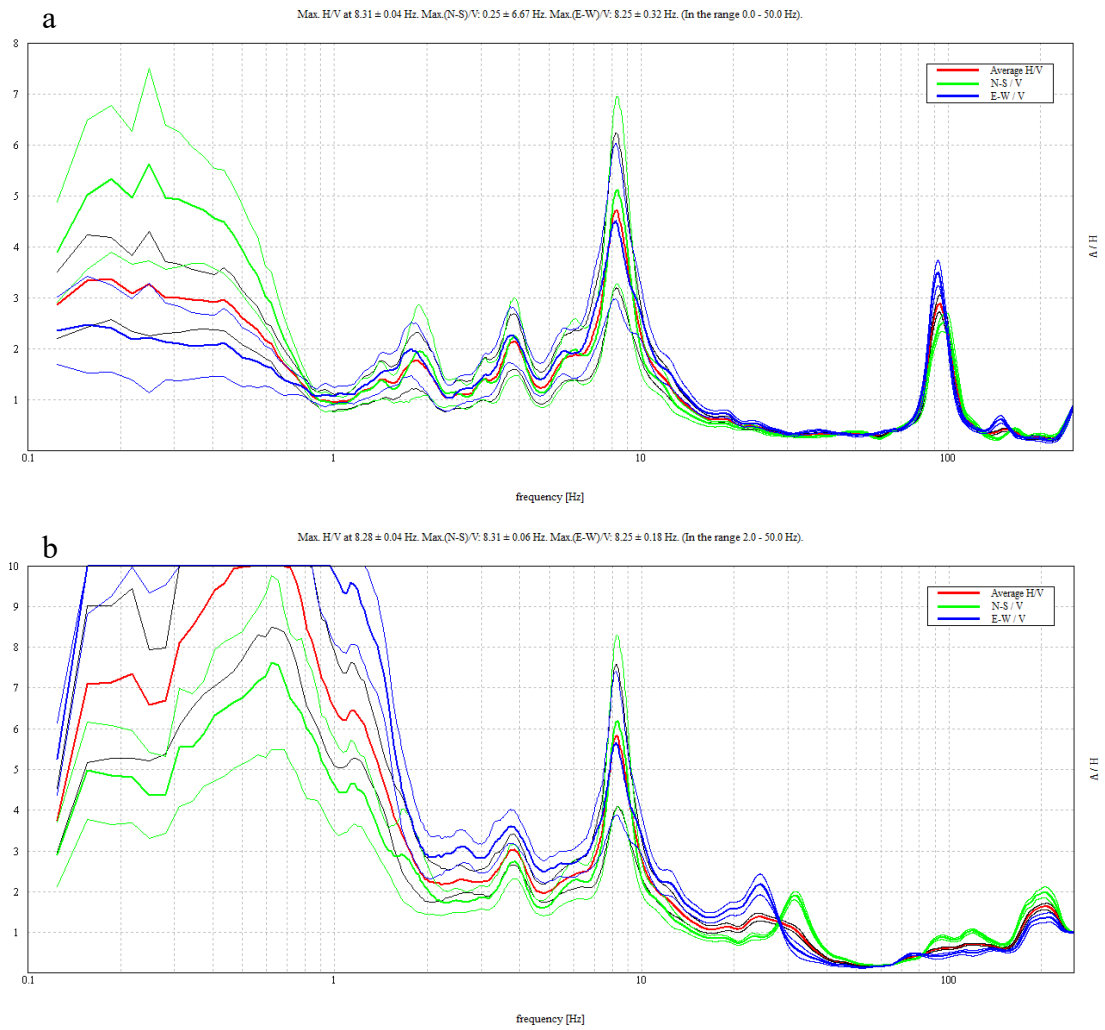

Figure B-65 MIZ Quad Site 3 site, Test 3, concrete (a), grass (b)

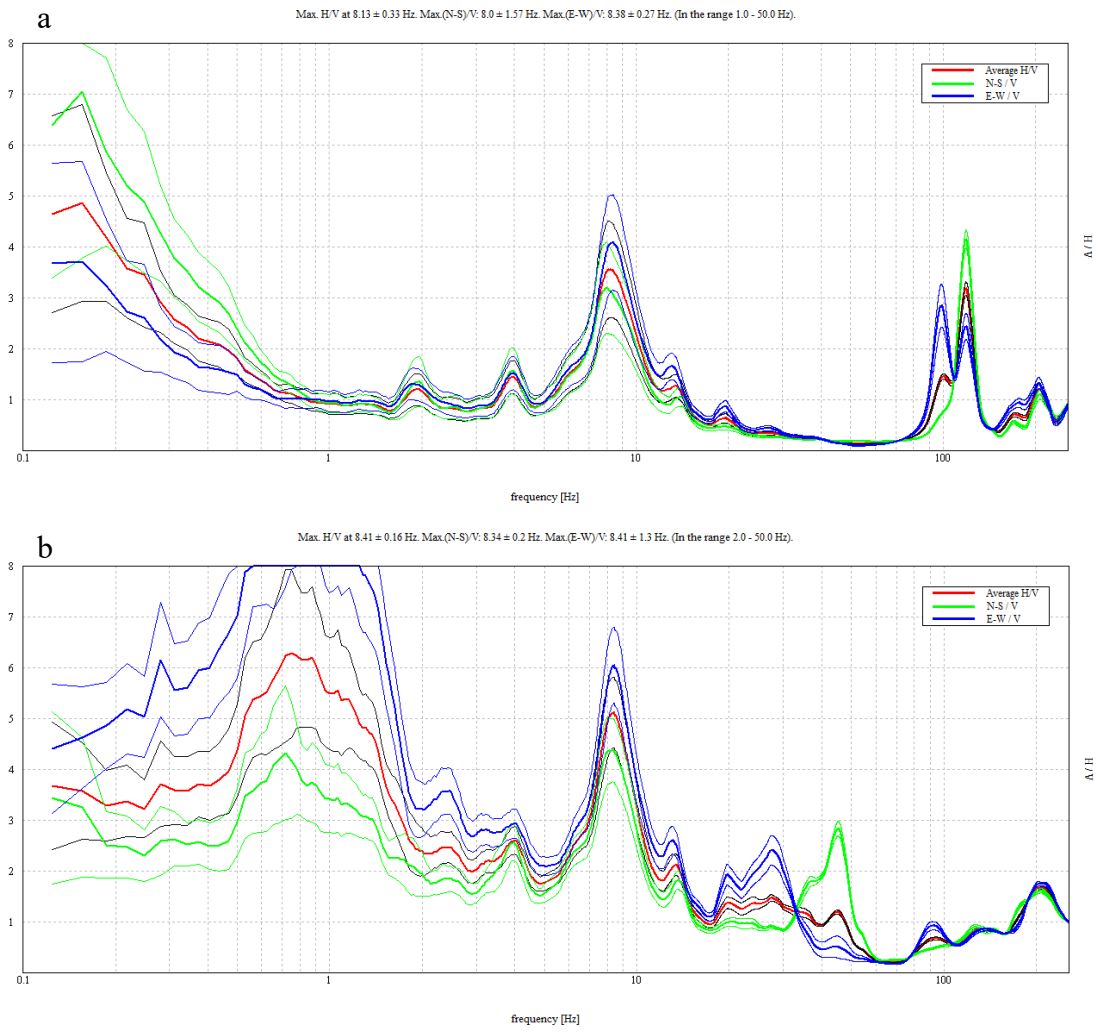

Figure B-66 MIZ Quad Site 3 site, Test 4, concrete (a), grass (b)

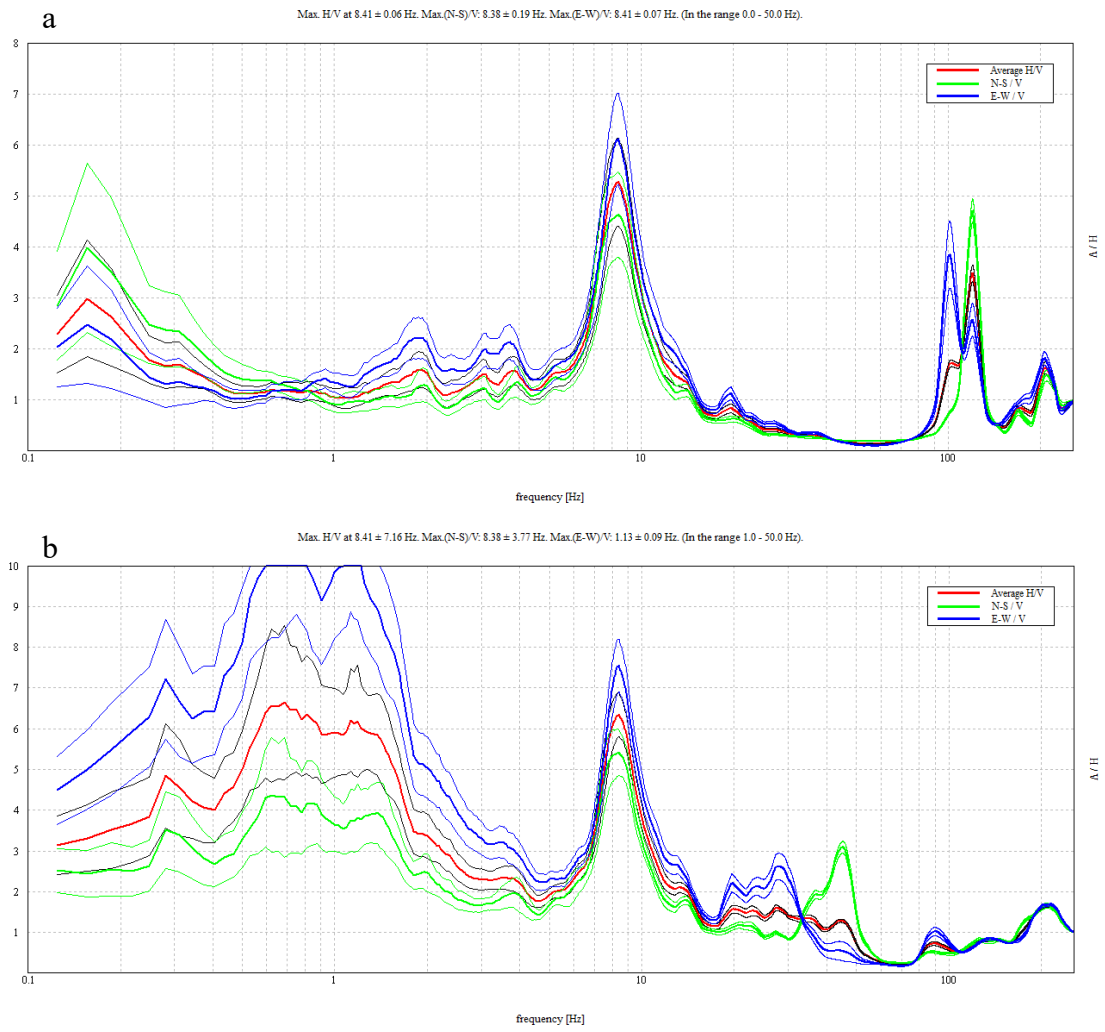

Figure B-67 MIZ Quad Site 3 site, Test 5, concrete (a), grass (b)

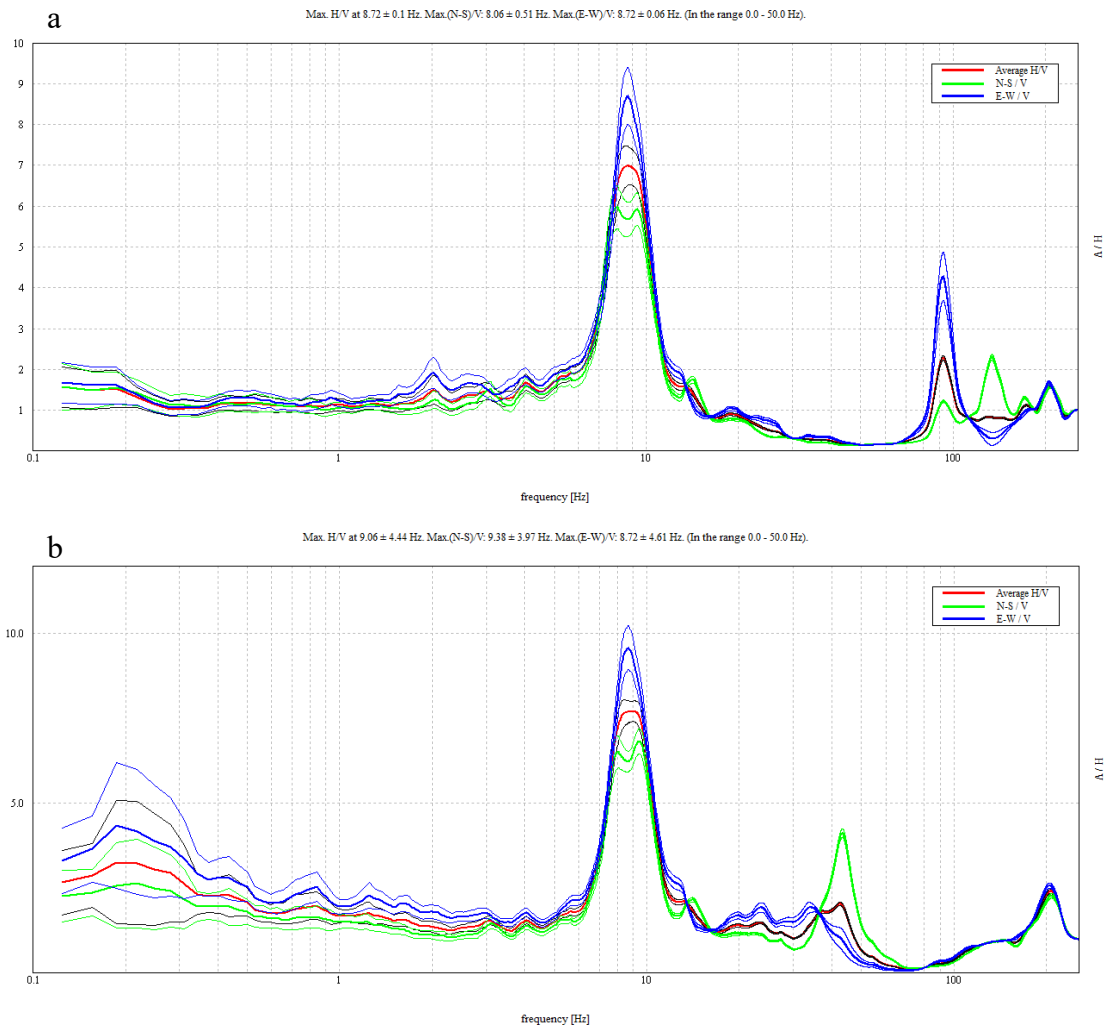

Figure B-68 MIZ Quad Site 3 site, Test 6, concrete (a), grass (b)

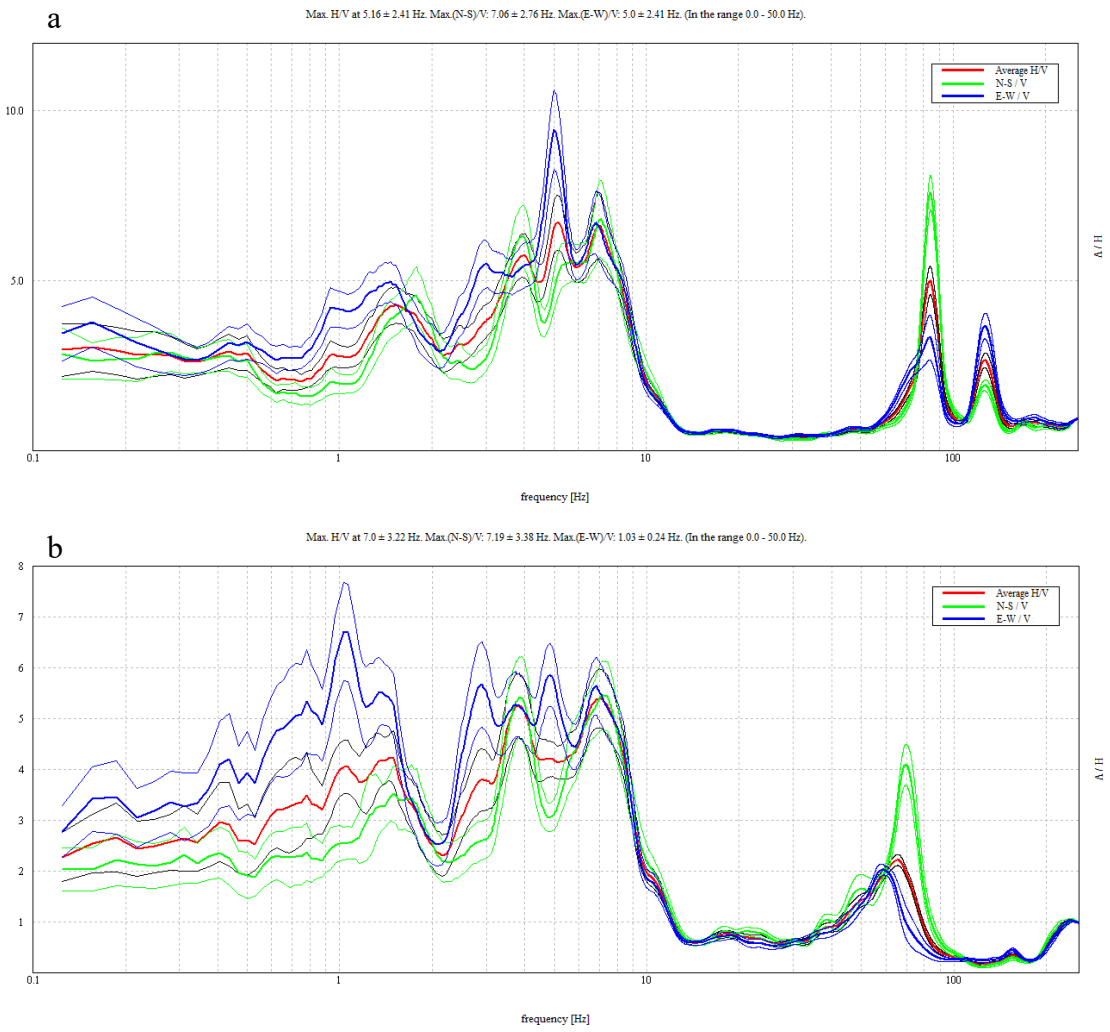

Figure B-69 MIZ Quad Site 4 site, Test 1, concrete (a), grass (b)

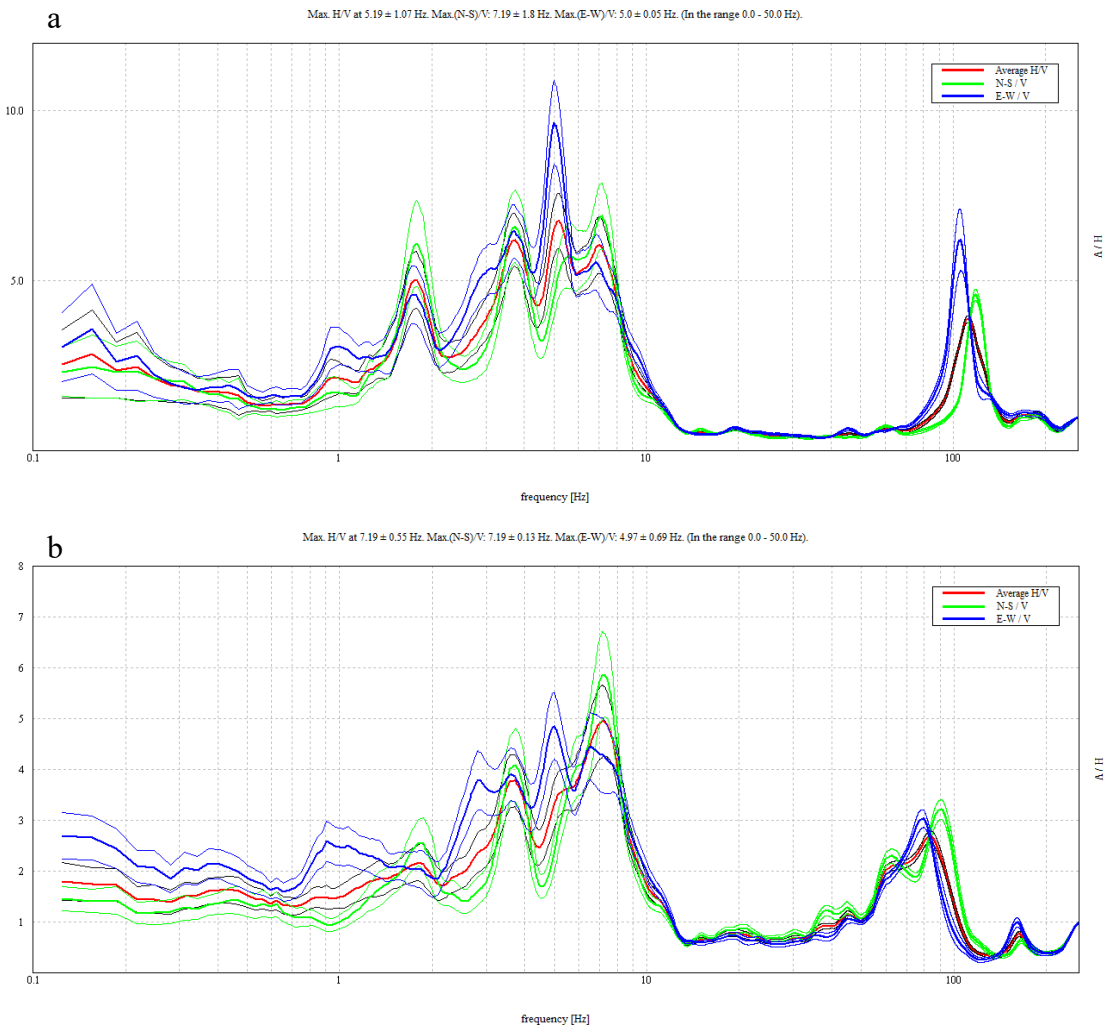

Figure B-70 MIZ Quad Site 4 site, Test 2, concrete (a), grass (b)

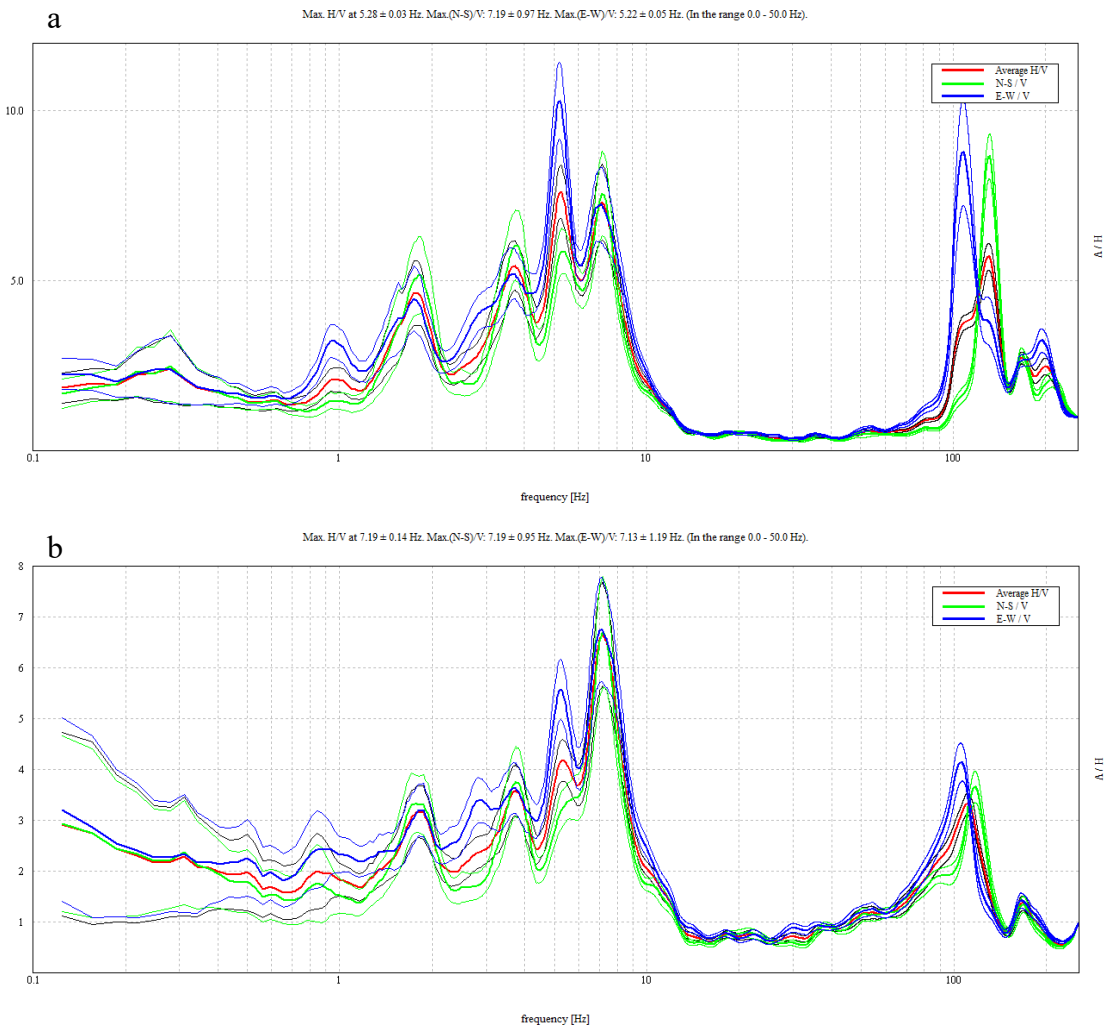

Figure B-71 MIZ Quad Site 4 site, Test 3, concrete (a), grass (b)

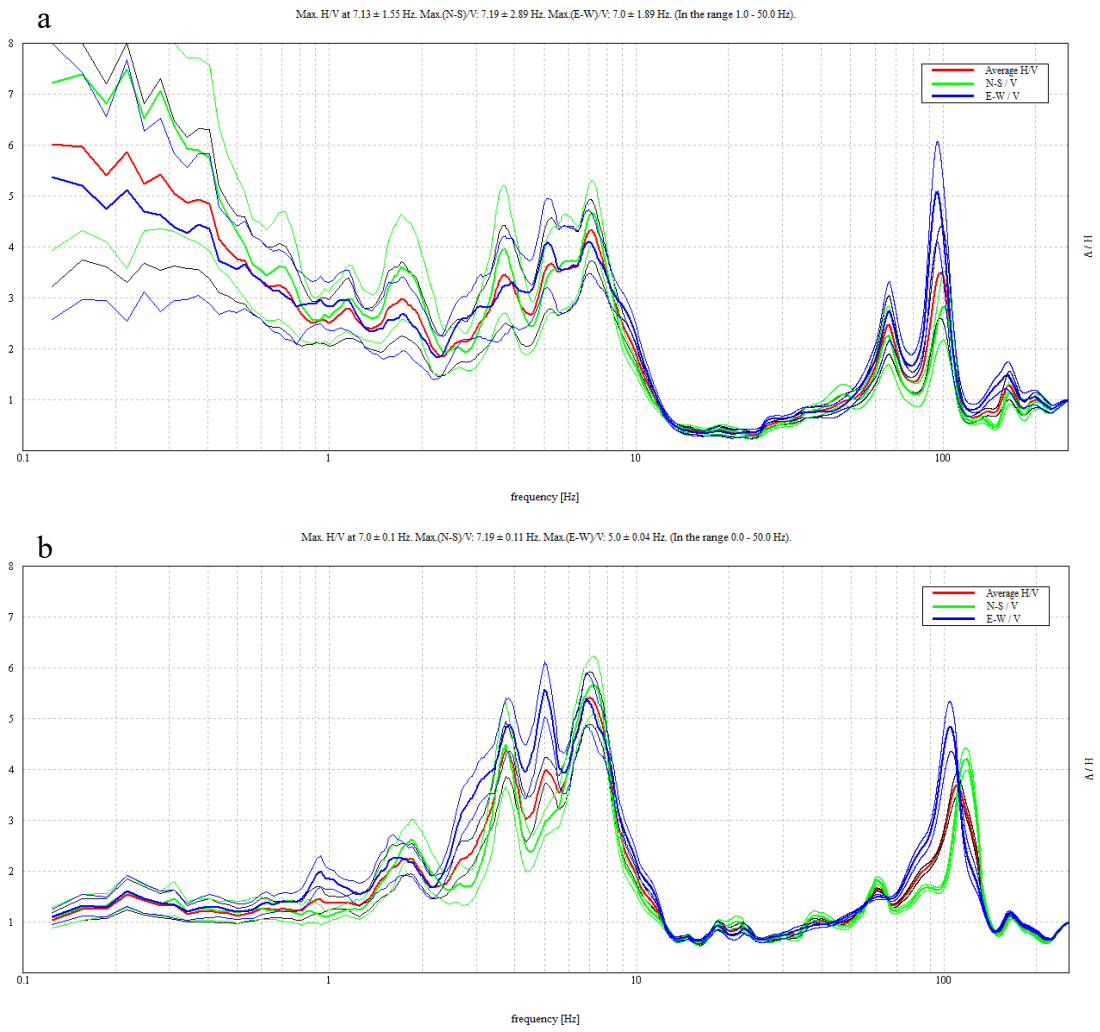

Figure B-72 MIZ Quad Site 4 site, Test 4, concrete (a), grass (b)

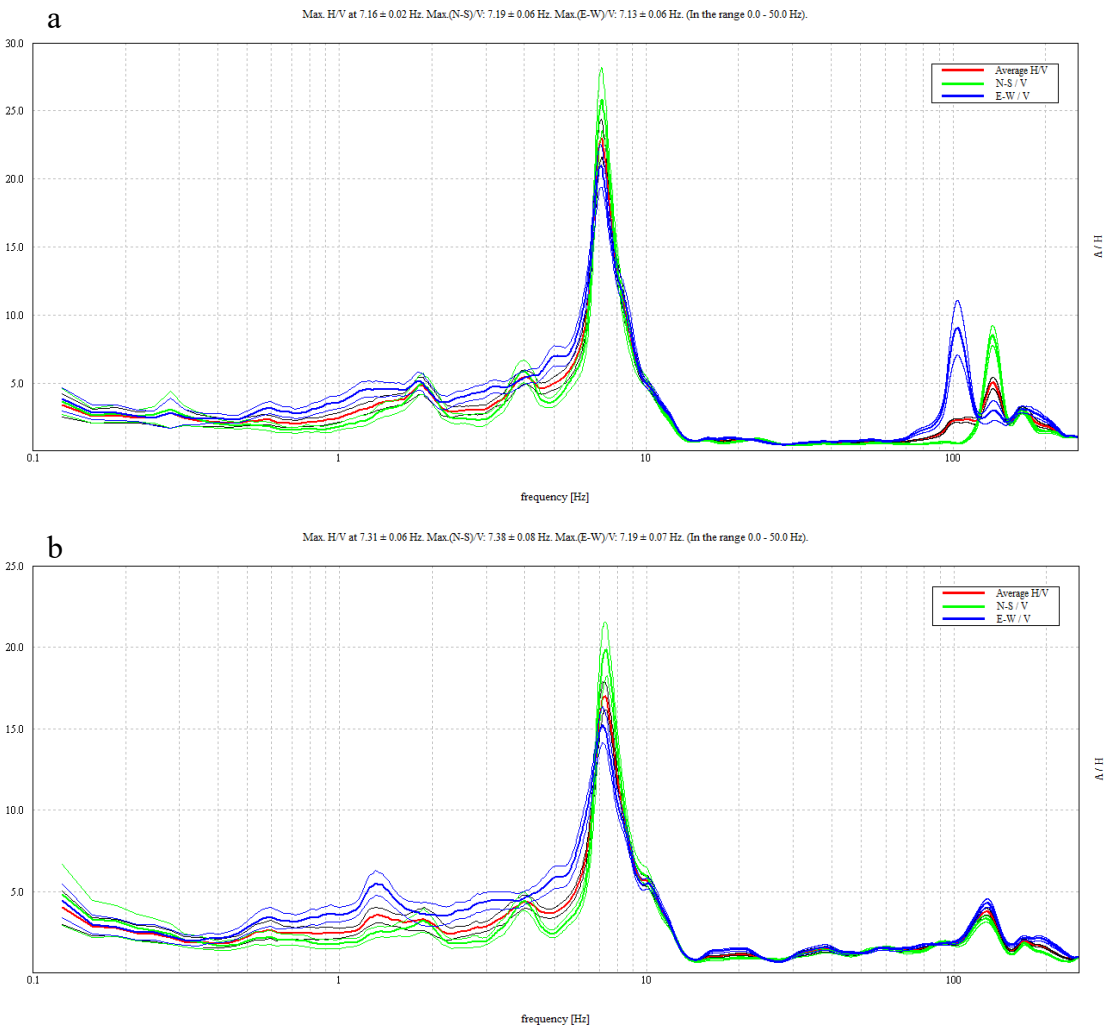

Figure B-73 MIZ Quad Site 4 site, Test 5, concrete (a), grass (b)

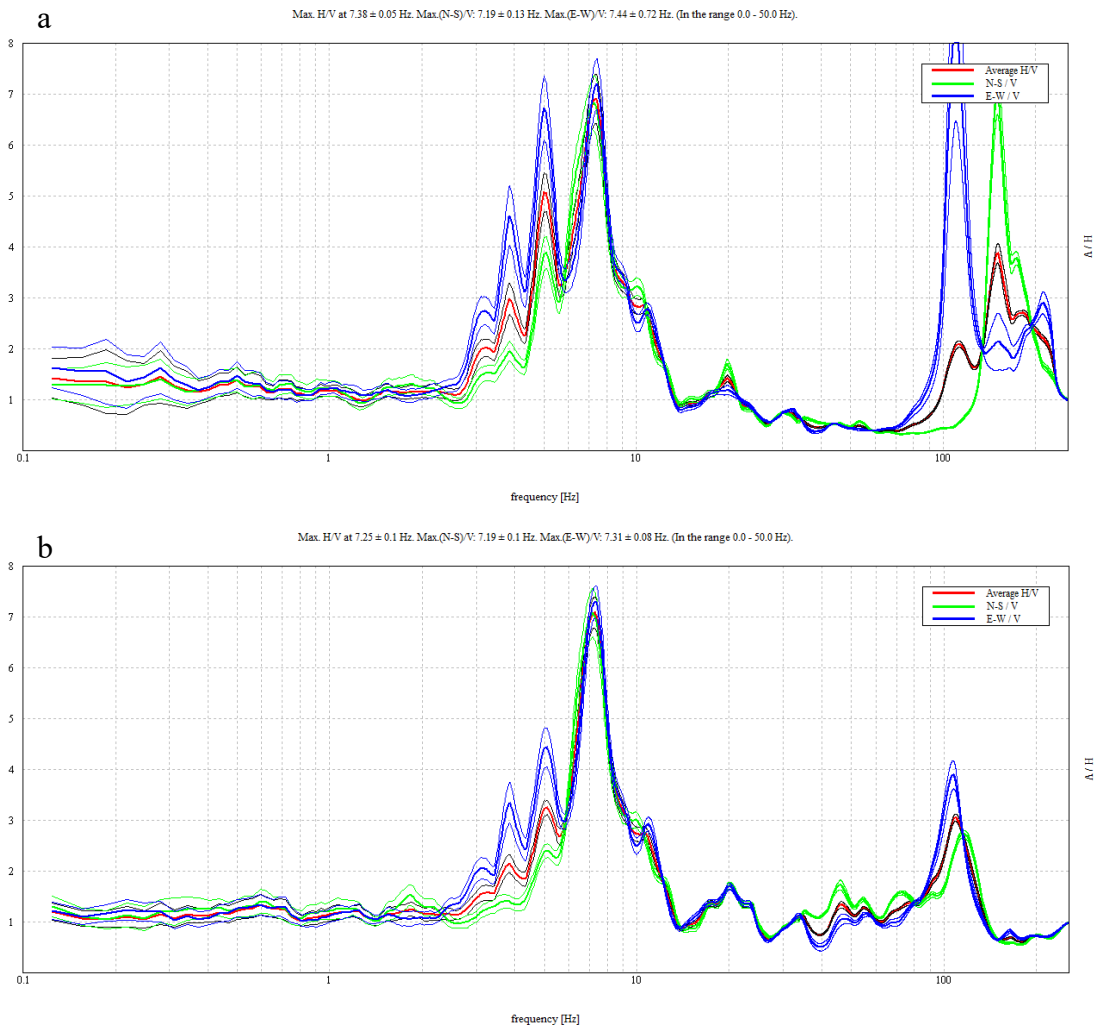

Figure B-74 MIZ Quad Site 4 site, Test 6, concrete (a), grass (b)

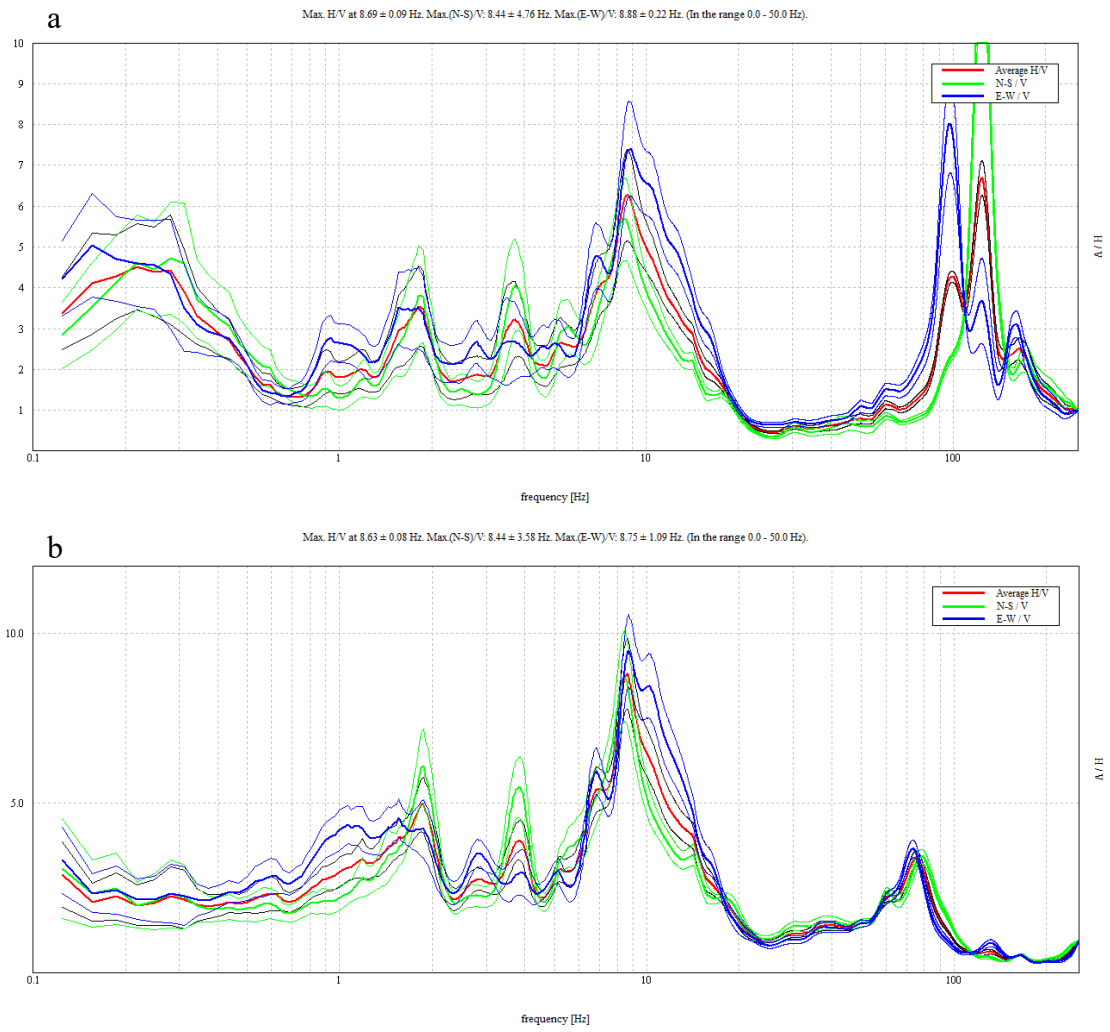

Figure B-75 MIZ Quad Site 5 site, Test 1, concrete (a), grass (b)

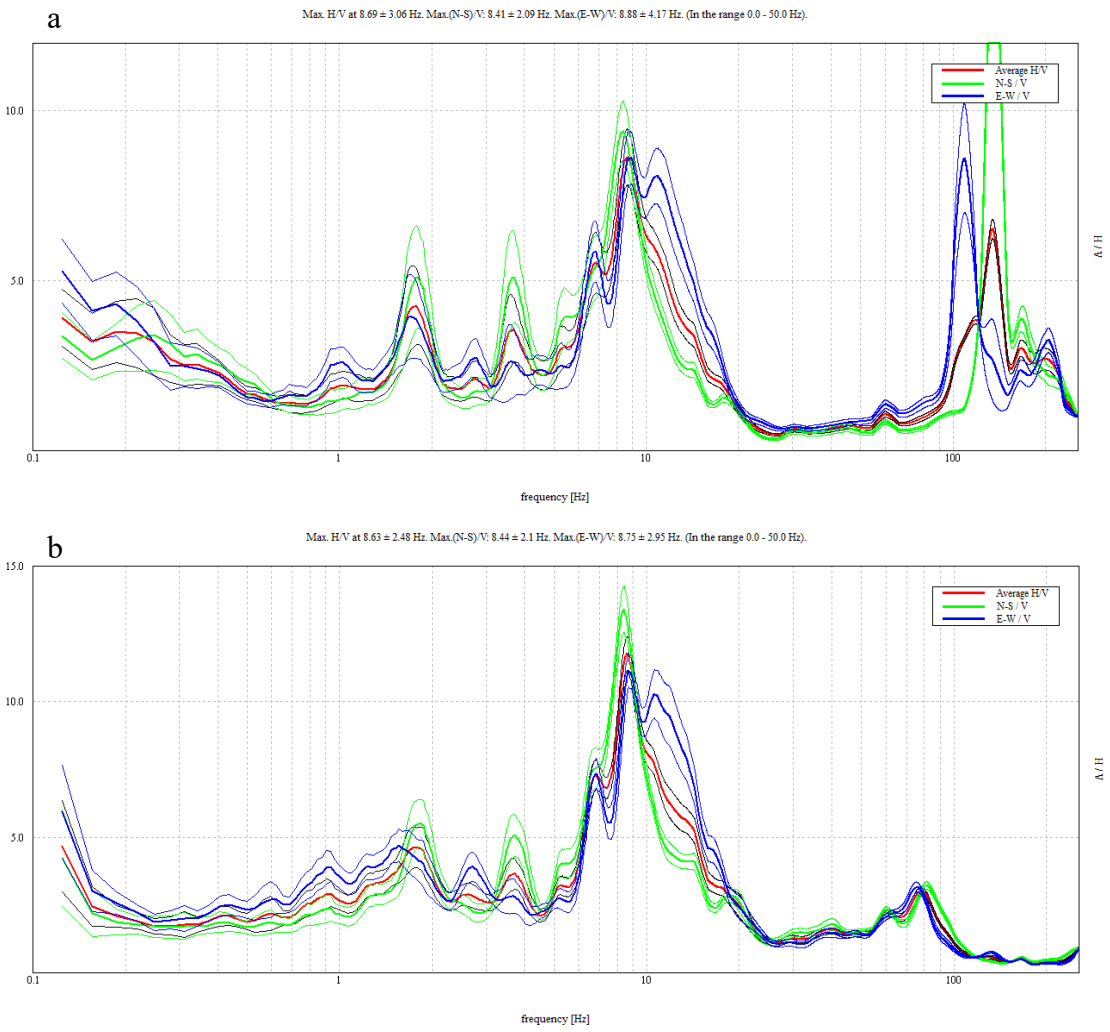

Figure B-76 MIZ Quad Site 5 site, Test 2, concrete (a), grass (b)

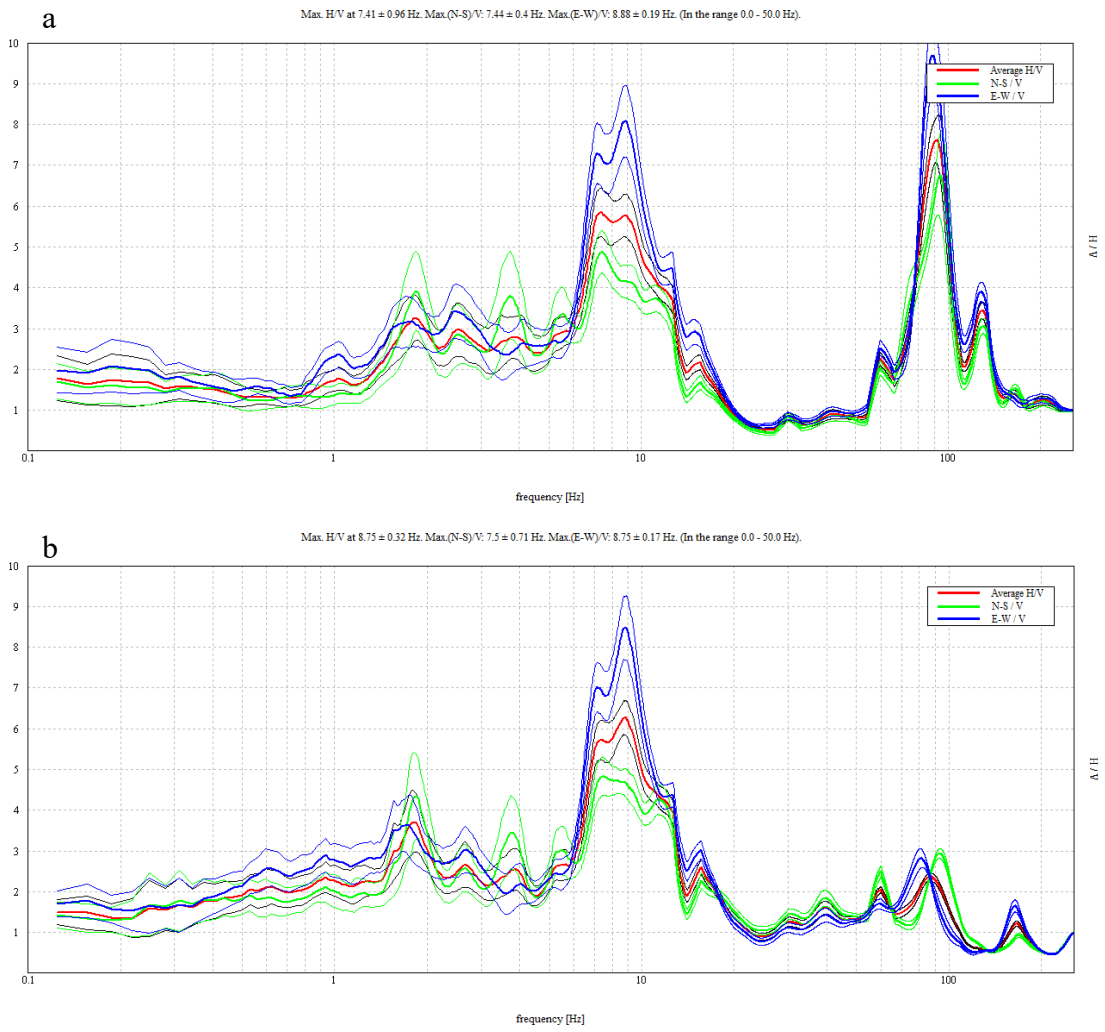

Figure B-77 MIZ Quad Site 5 site, Test 3, concrete (a), grass (b)

APPENDIX C

Importing Time record [Amp Spec]

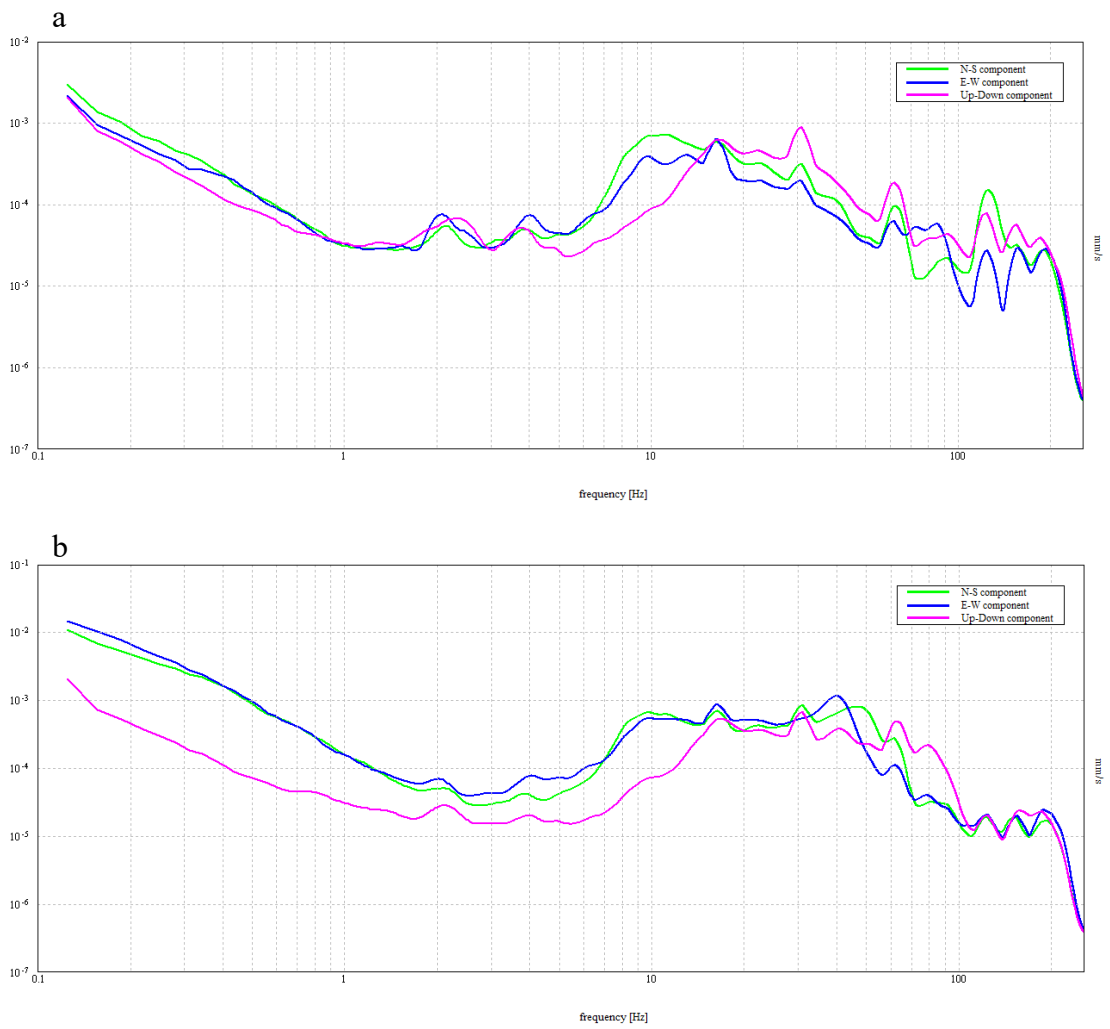

Figure C-1 Animal Hospital 1 site, Test 1, concrete (a), grass (b)

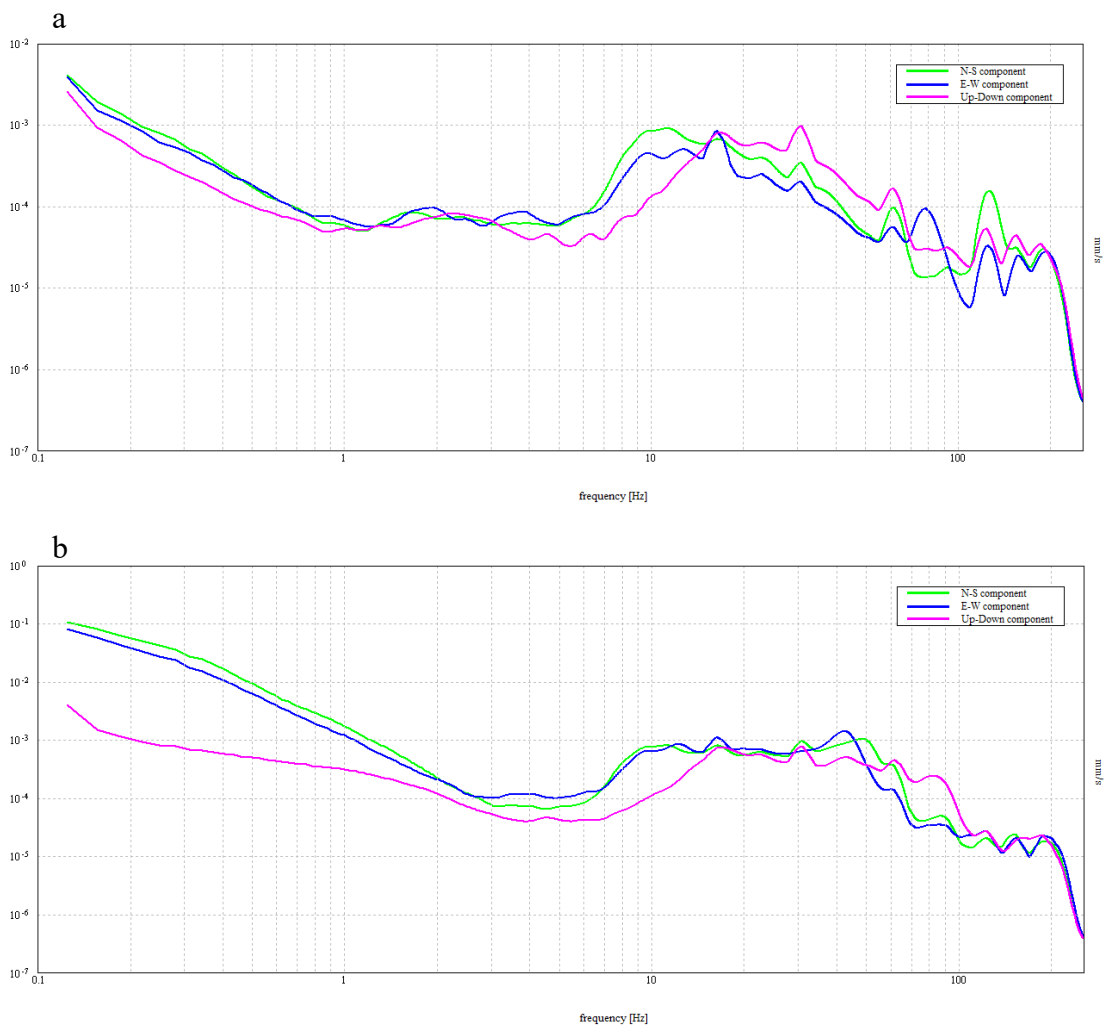

Figure C-2 Animal Hospital 1 site, Test 2, concrete (a), grass (b)

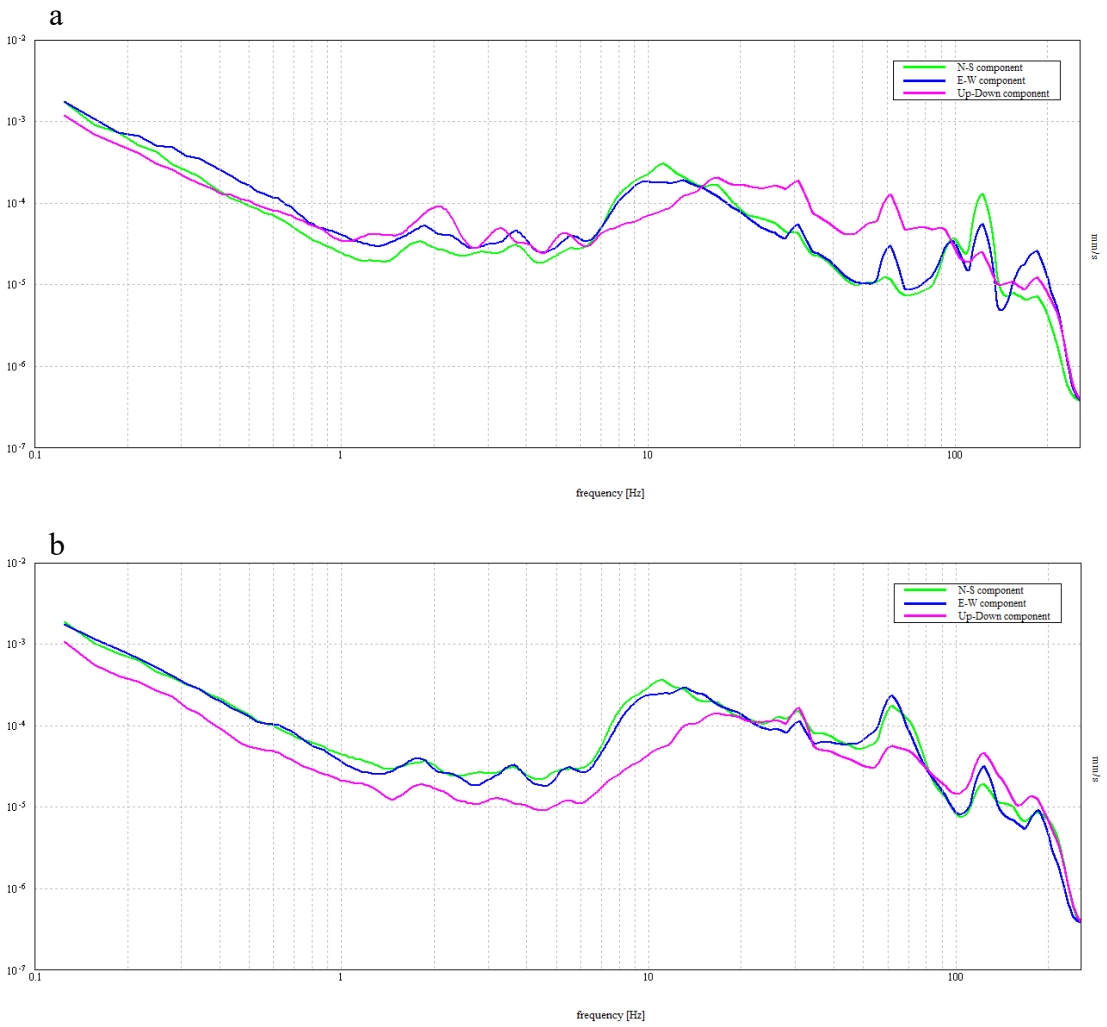

Figure C-3 Animal Hospital 1 site, Test 3, concrete (a), grass (b)

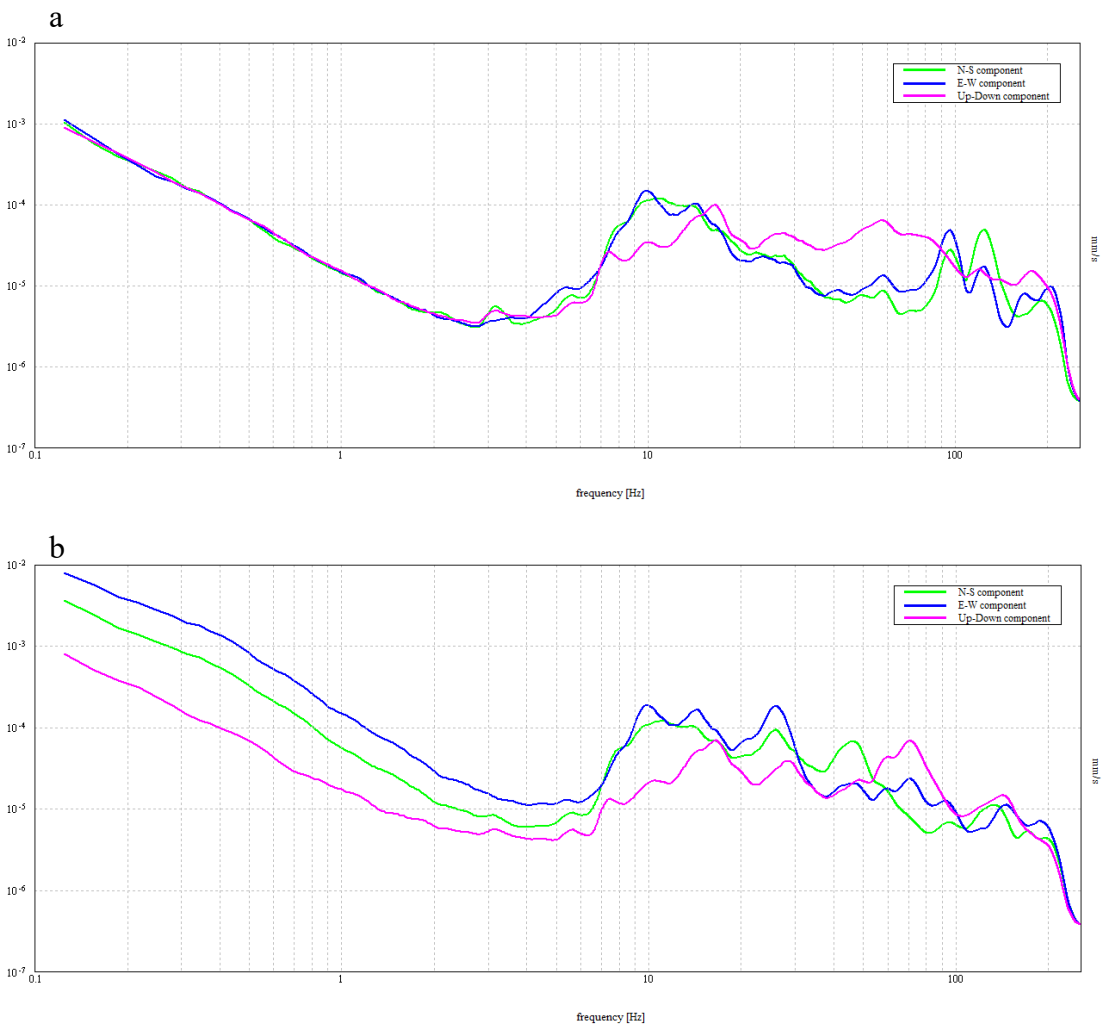

Figure C-4 Animal Hospital 1 site, Test 4, concrete (a), grass (b)

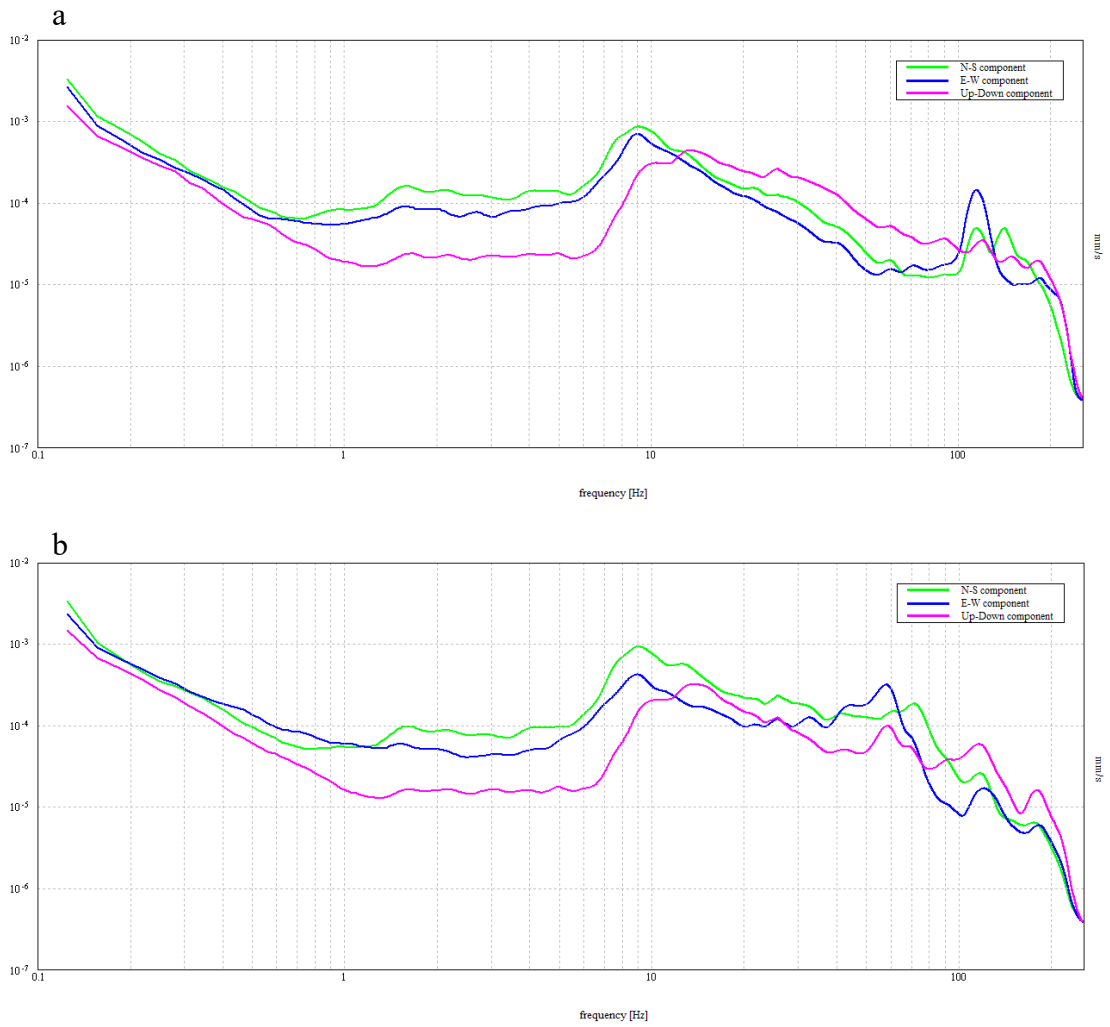

Figure C-5 Animal Hospital 2 site, Test 1, concrete (a), grass (b)

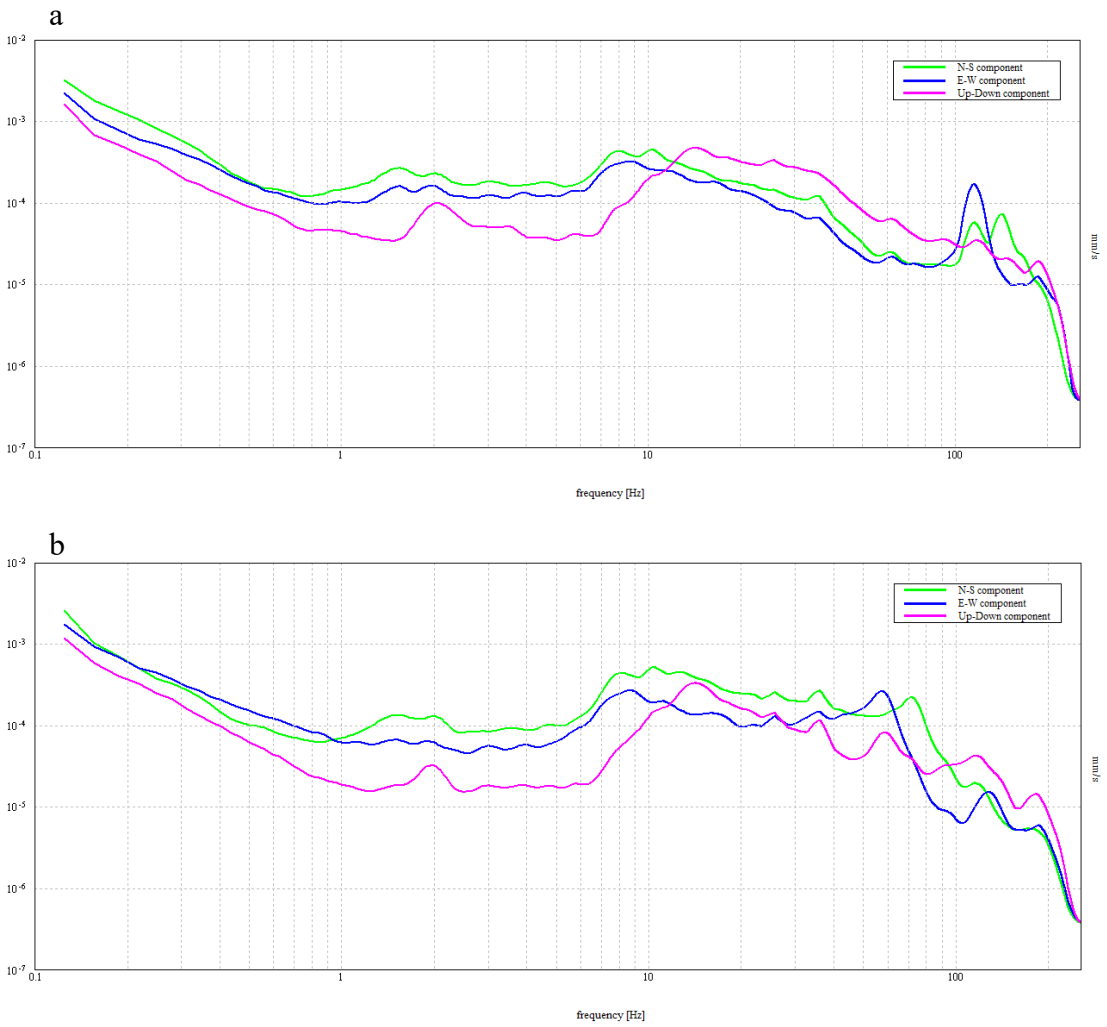

Figure C-6 Animal Hospital 2 site, Test 2, concrete (a), grass (b)

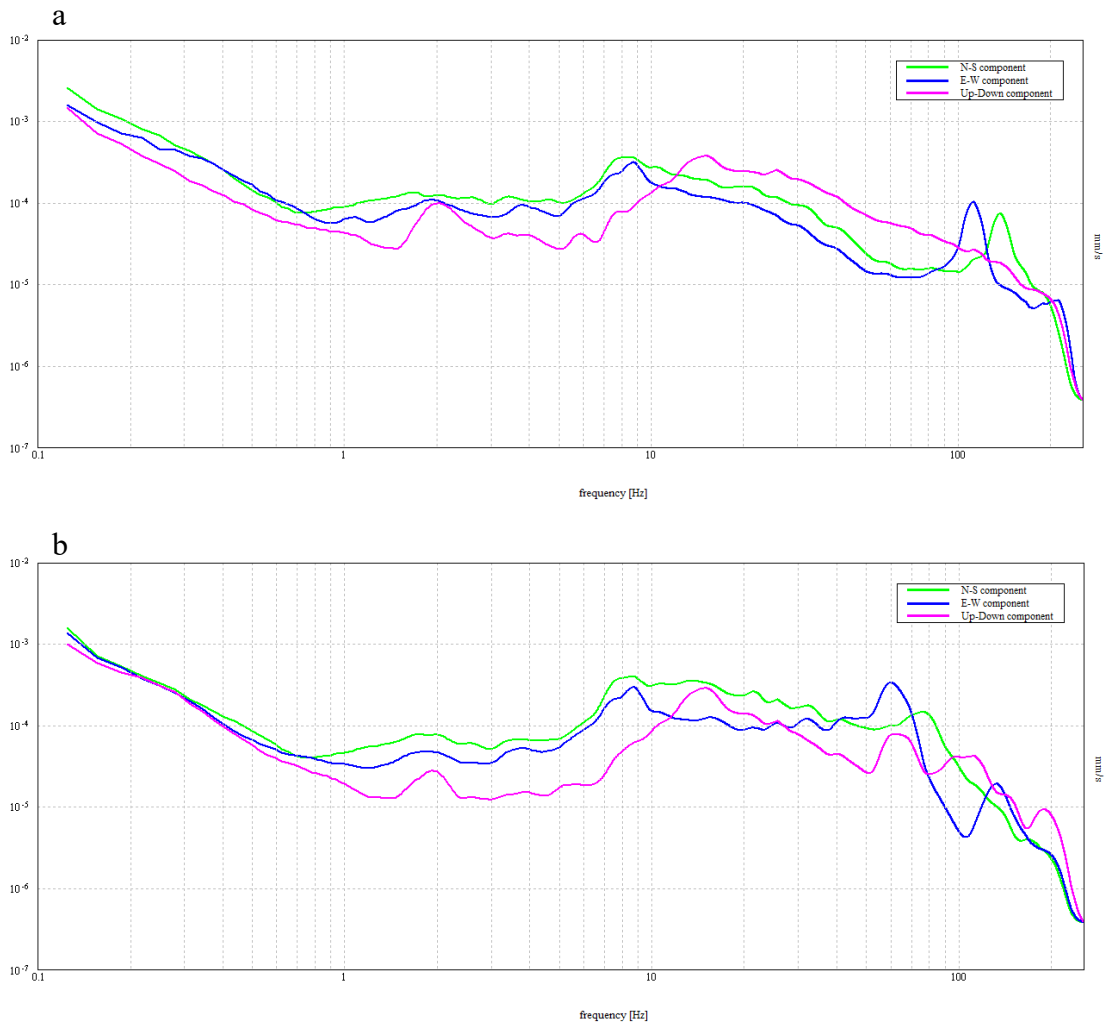

Figure C-7 Animal Hospital 2 site, Test 3, concrete (a), grass (b)

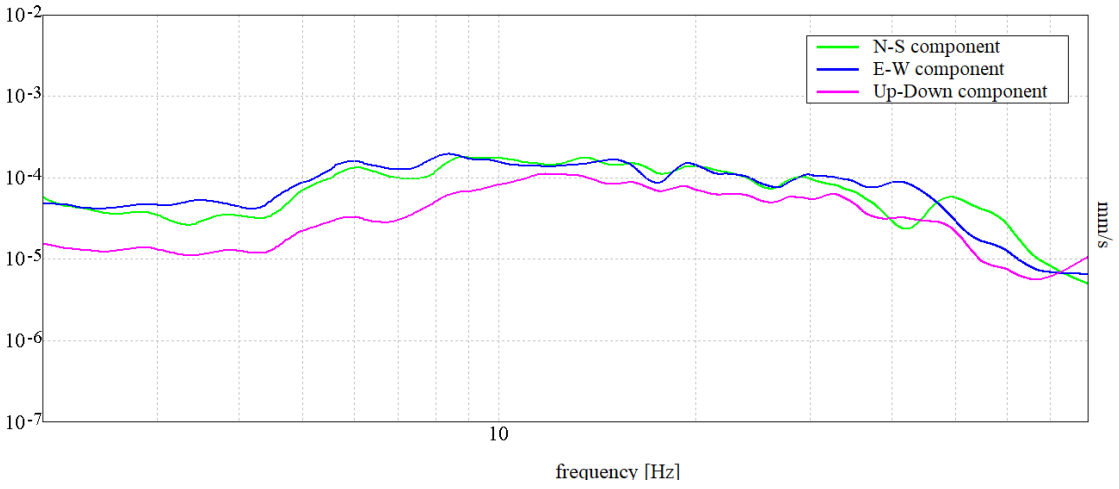

Figure C-8 Ellis Library BH-01 site, Test 1, grass

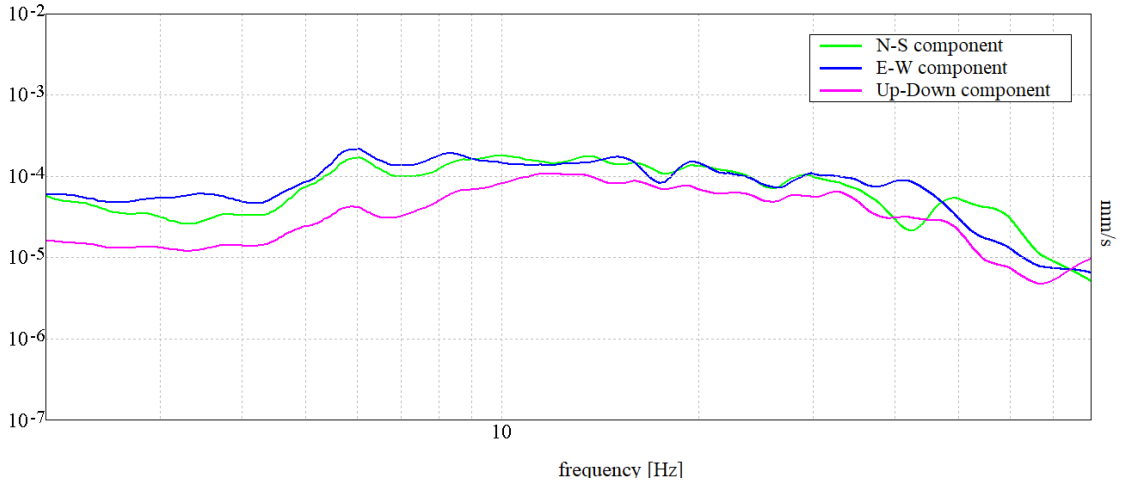

Figure C-9 Ellis Library BH-01 site, Test 2, grass

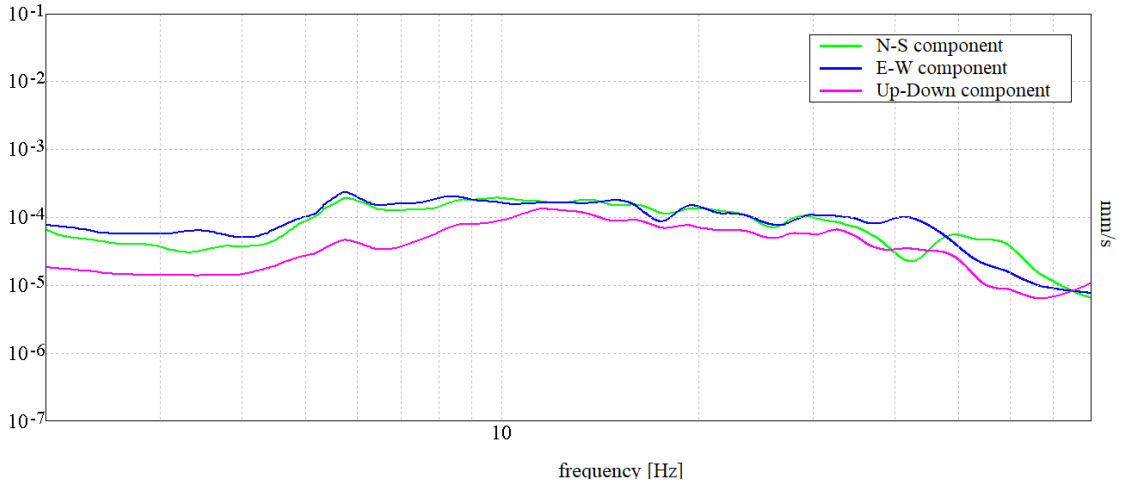

Figure C-10 Ellis Library BH-01 site, Test 3, grass

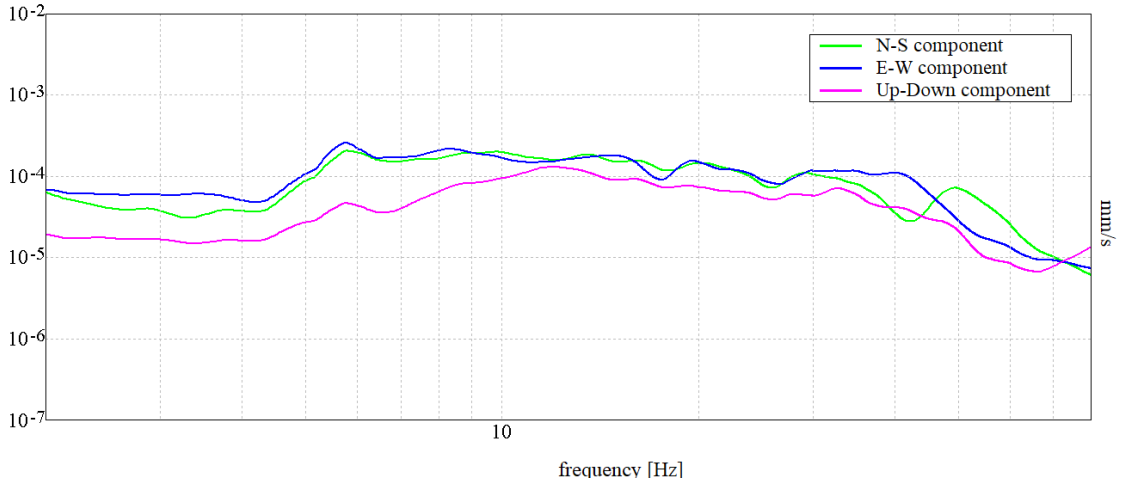

Figure C-11 Ellis Library BH-01 site, Test 4, grass

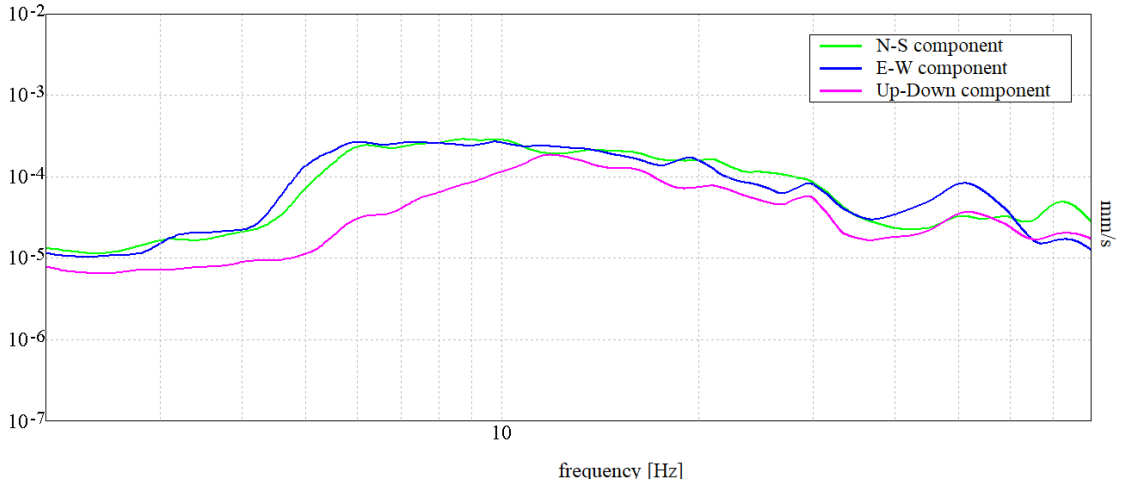

Figure C-12 Ellis Library BH-01 site, Test 5, grass

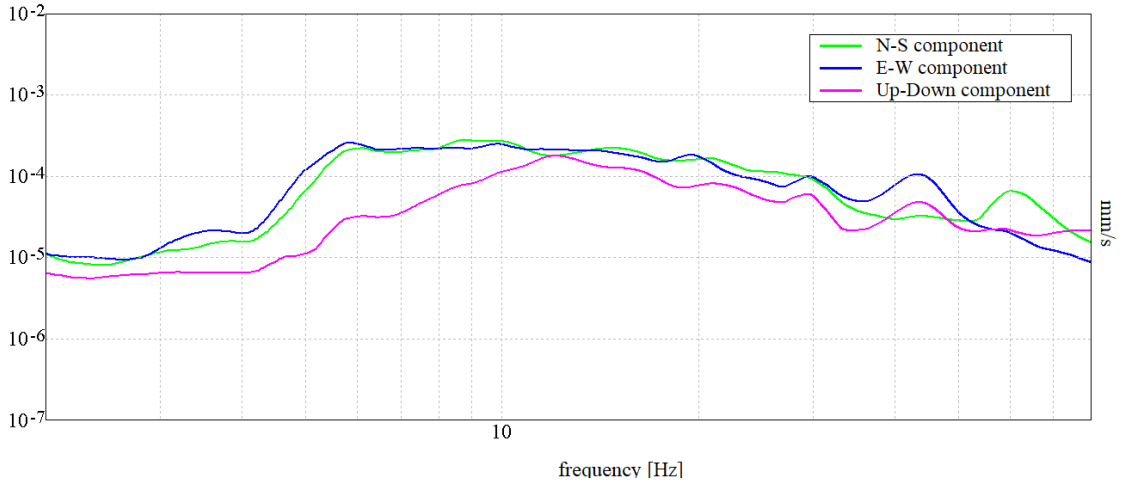

Figure C-13 Ellis Library BH-01 site, Test 6, grass

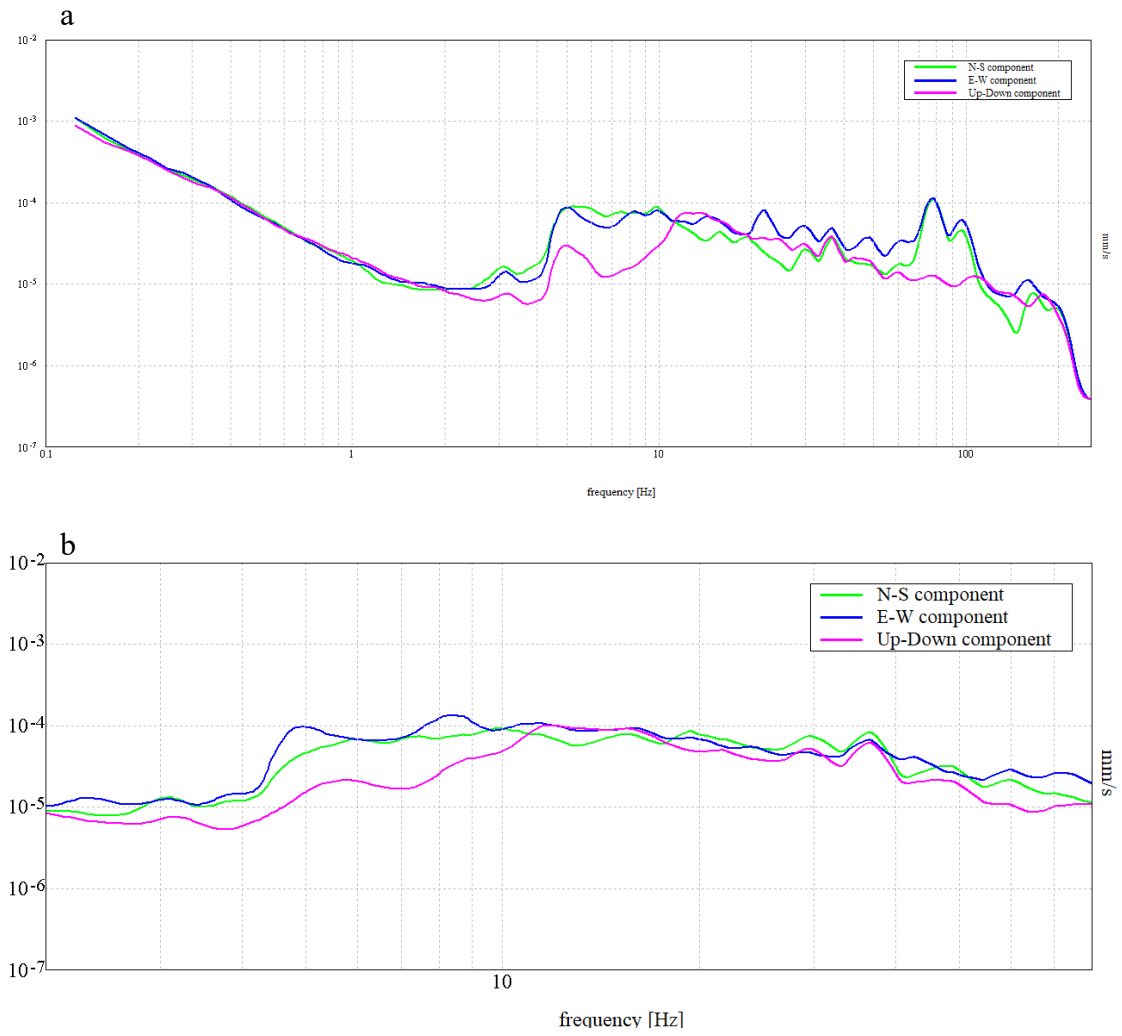

Figure C-14 Ellis Library BH-03 A site, Test 1, concrete (a), grass (b)

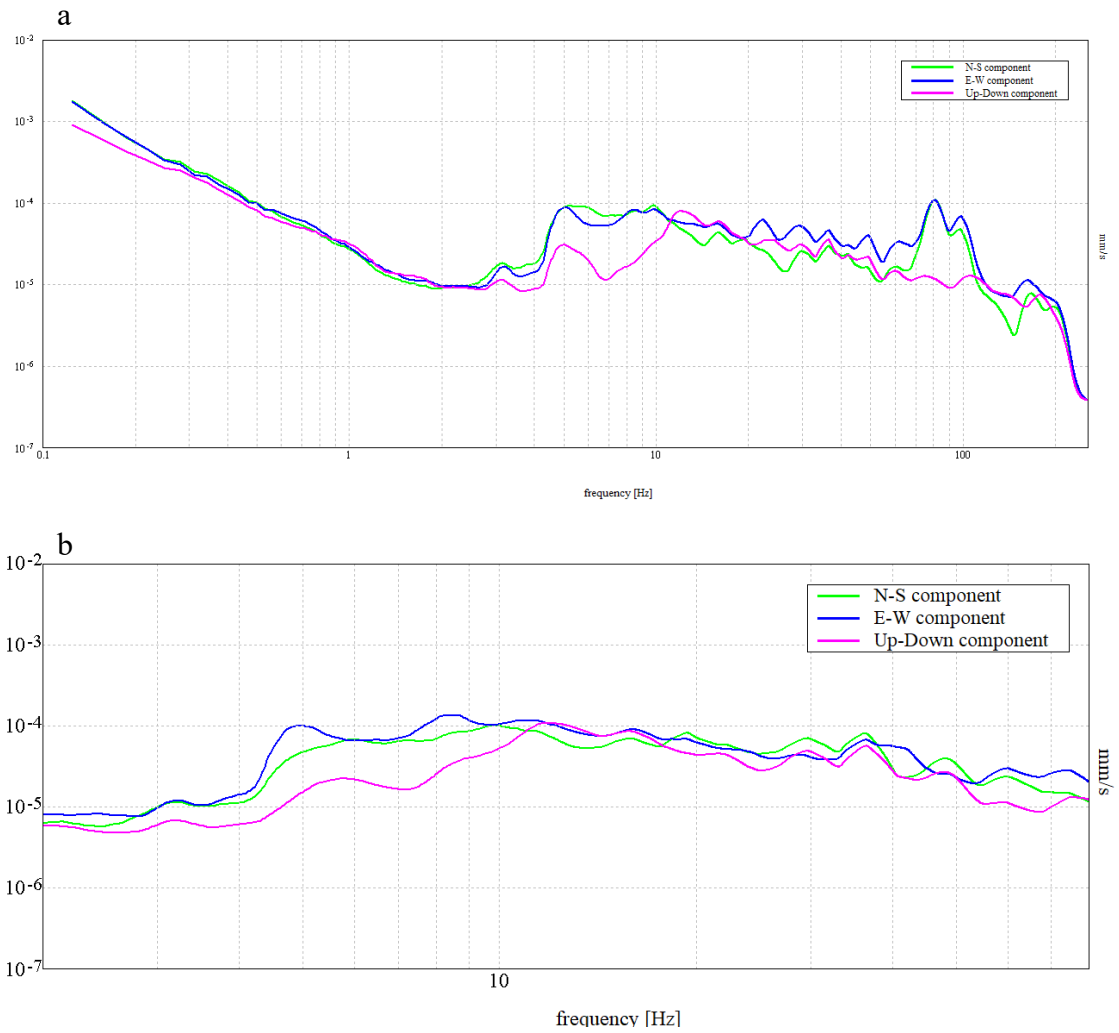

Figure C-15 Ellis Library BH-03 A site, Test 2, concrete (a), grass (b)

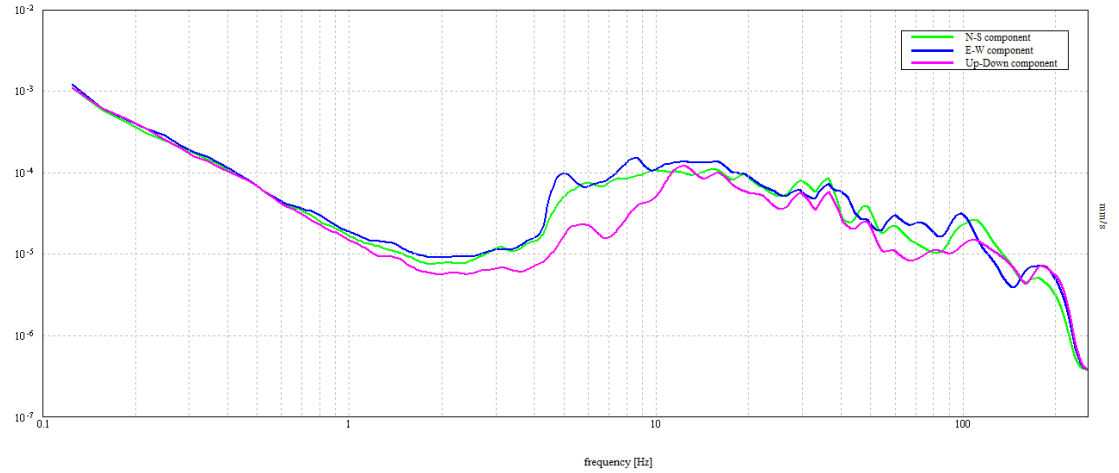

Figure C-16 Ellis Library BH-03 A site, Test 3, grass

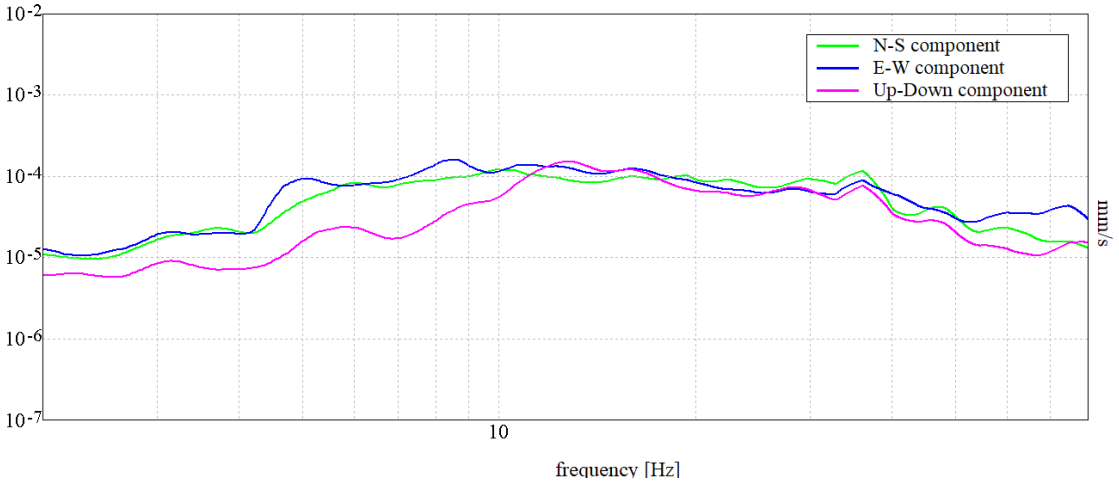

Figure C-17 Ellis Library BH-03 A site, Test 4, grass

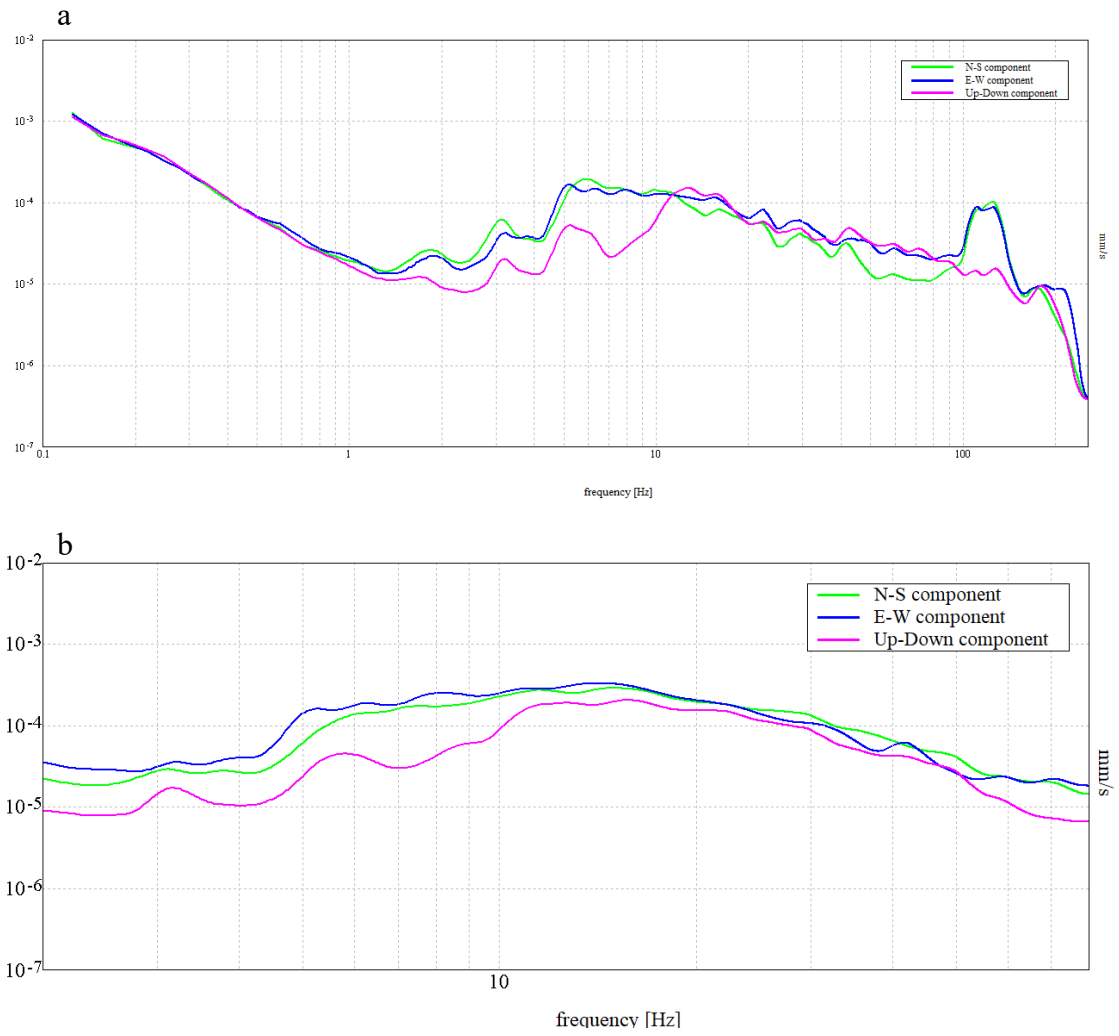

Figure C-18 Ellis Library BH-03 A site, Test 5, concrete (a), grass (b)

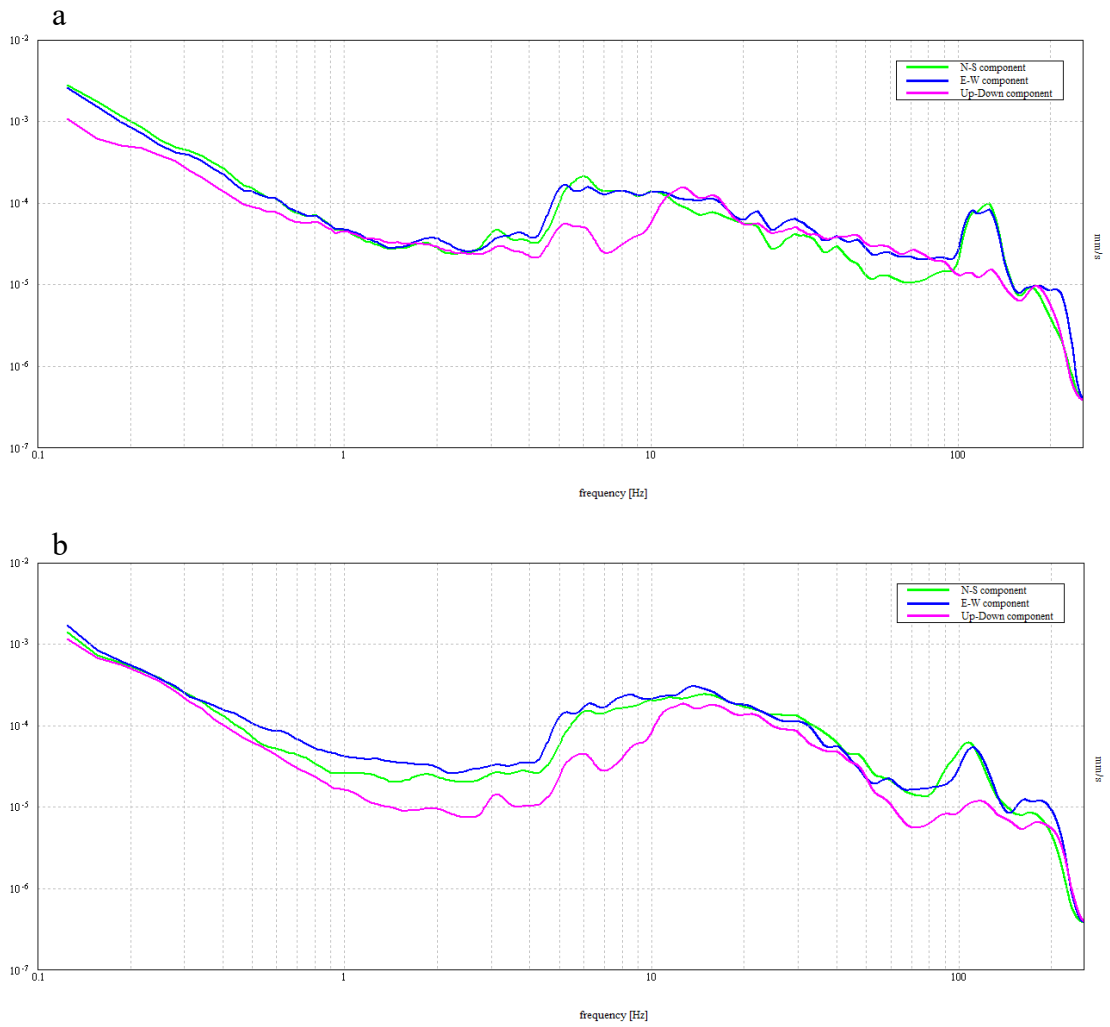

Figure C-19 Ellis Library BH-03 A site, Test 6, concrete (a), grass (b)

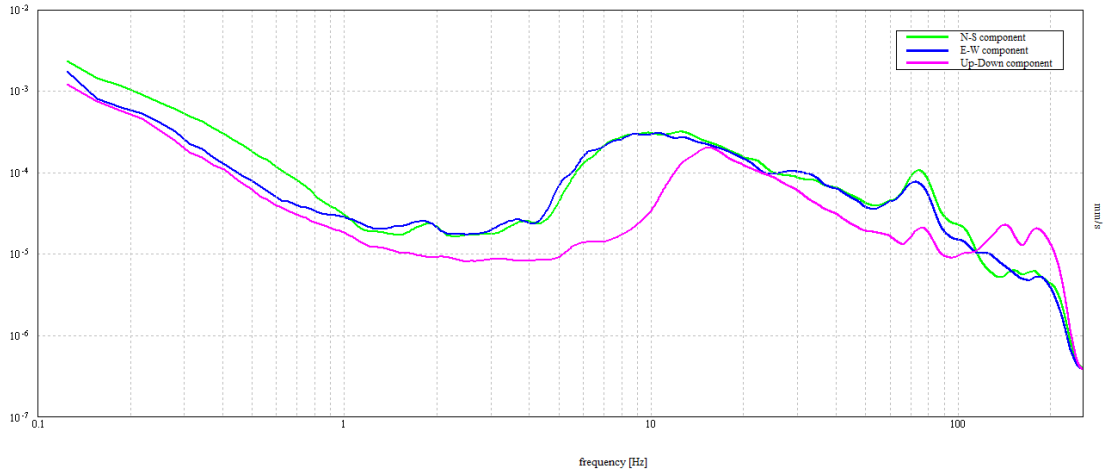

Figure C-20 Ellis Library BH-03 B site, Test 1, grass

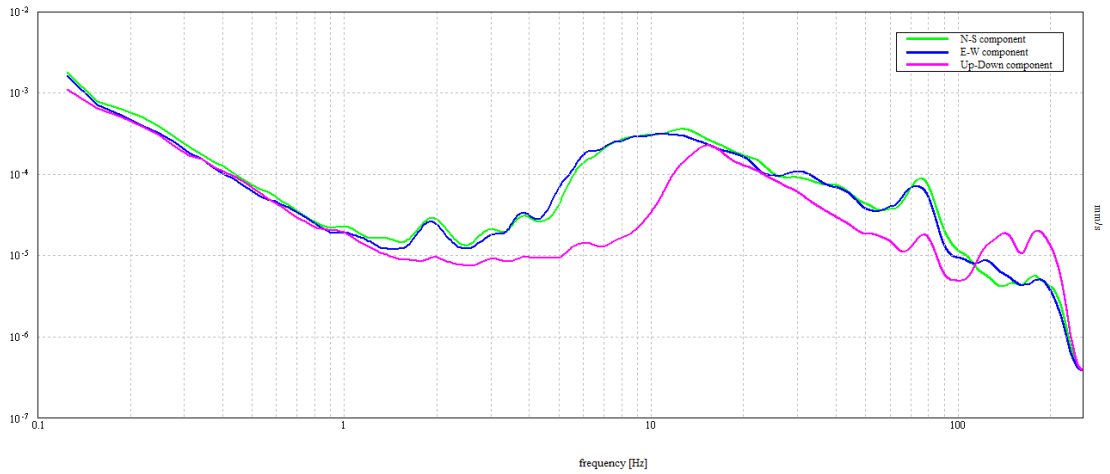

Figure C-21 Ellis Library BH-03 B site, Test 2, grass

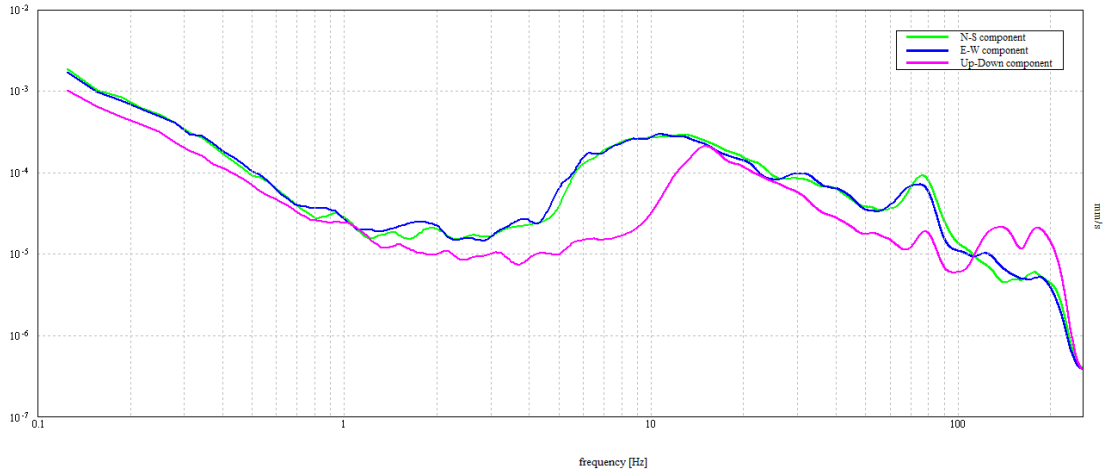

Figure C-22 Ellis Library BH-03 B site, Test 3, grass

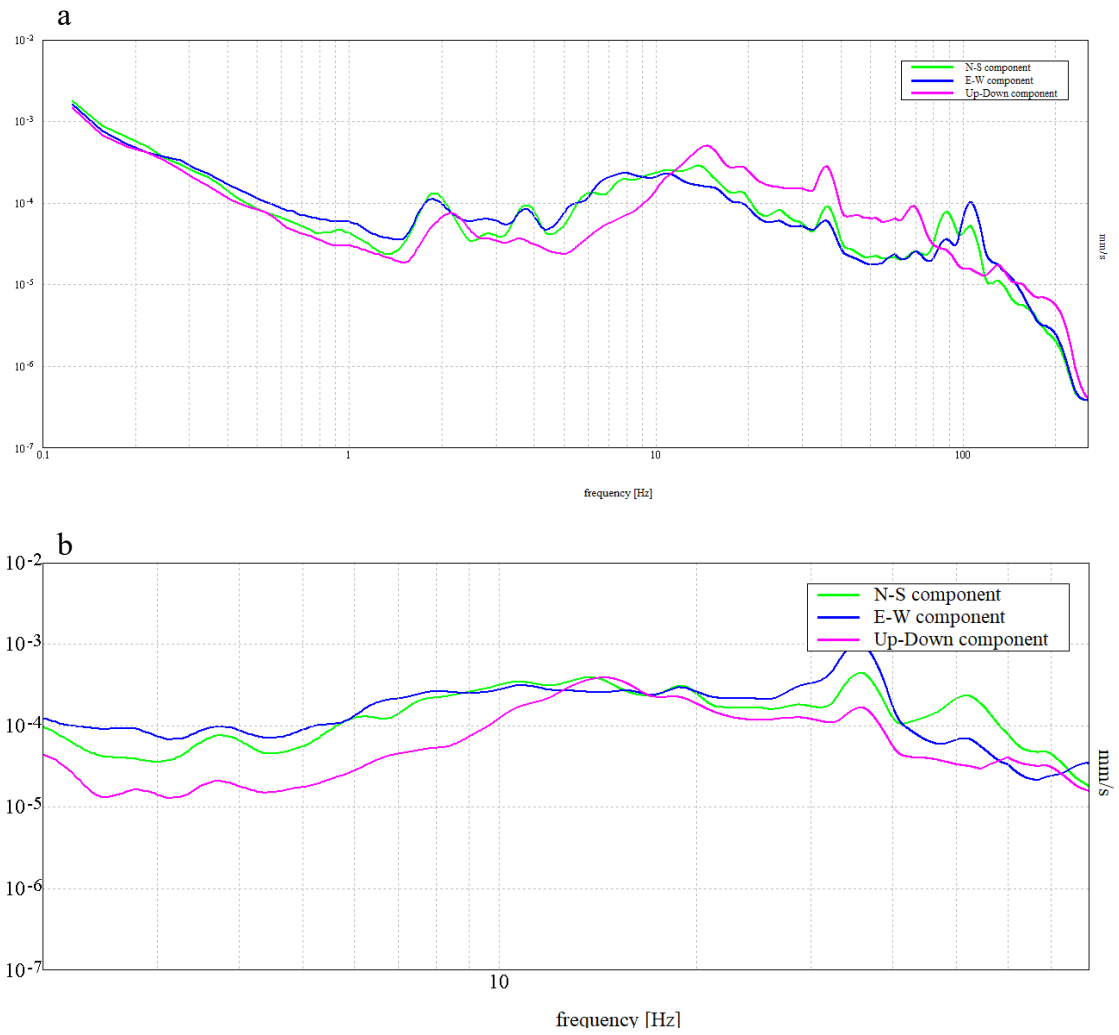

Figure C-23 Journalism B-06 A site, Test 1, concrete (a), grass (b)

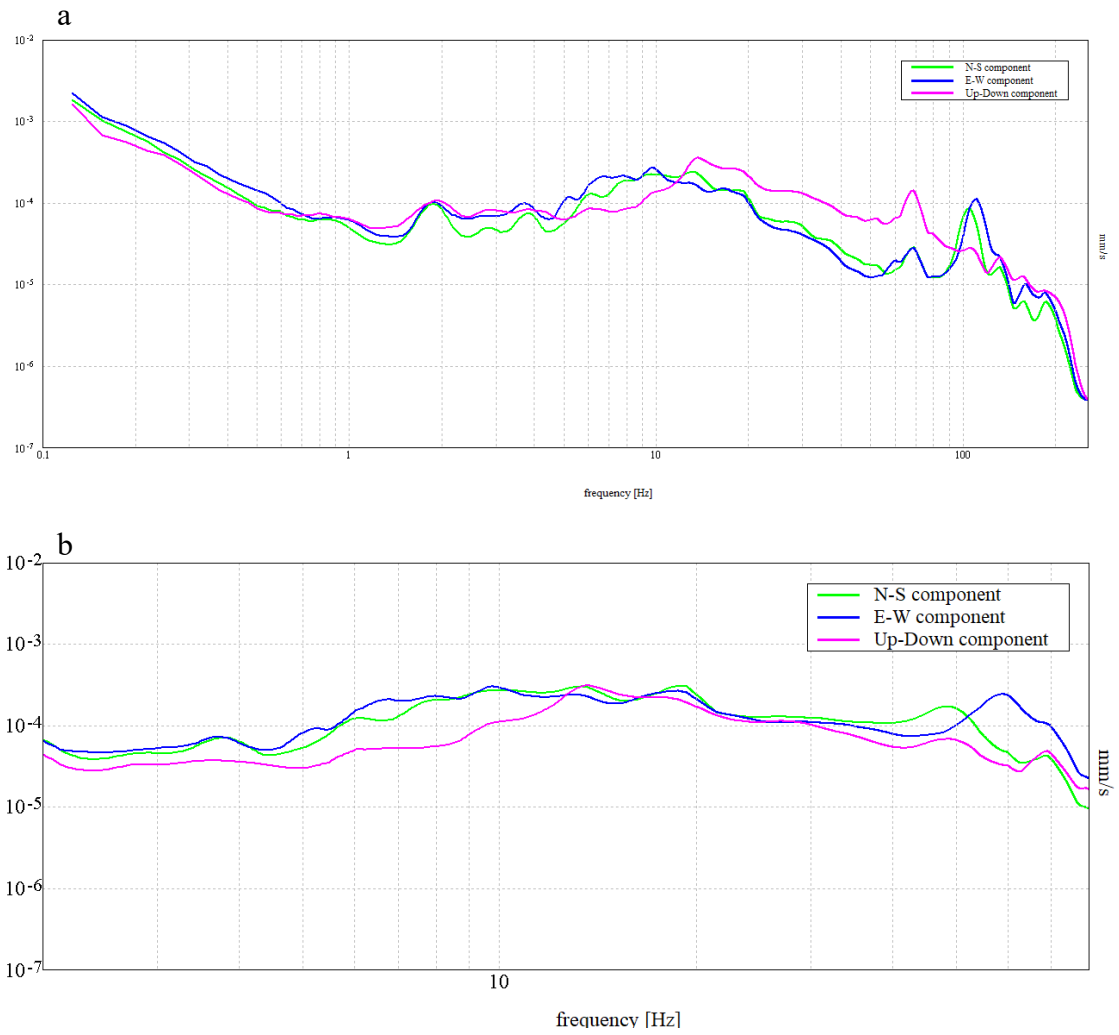

Figure C-24 Journalism B-06 A site, Test 2, concrete (a), grass (b)

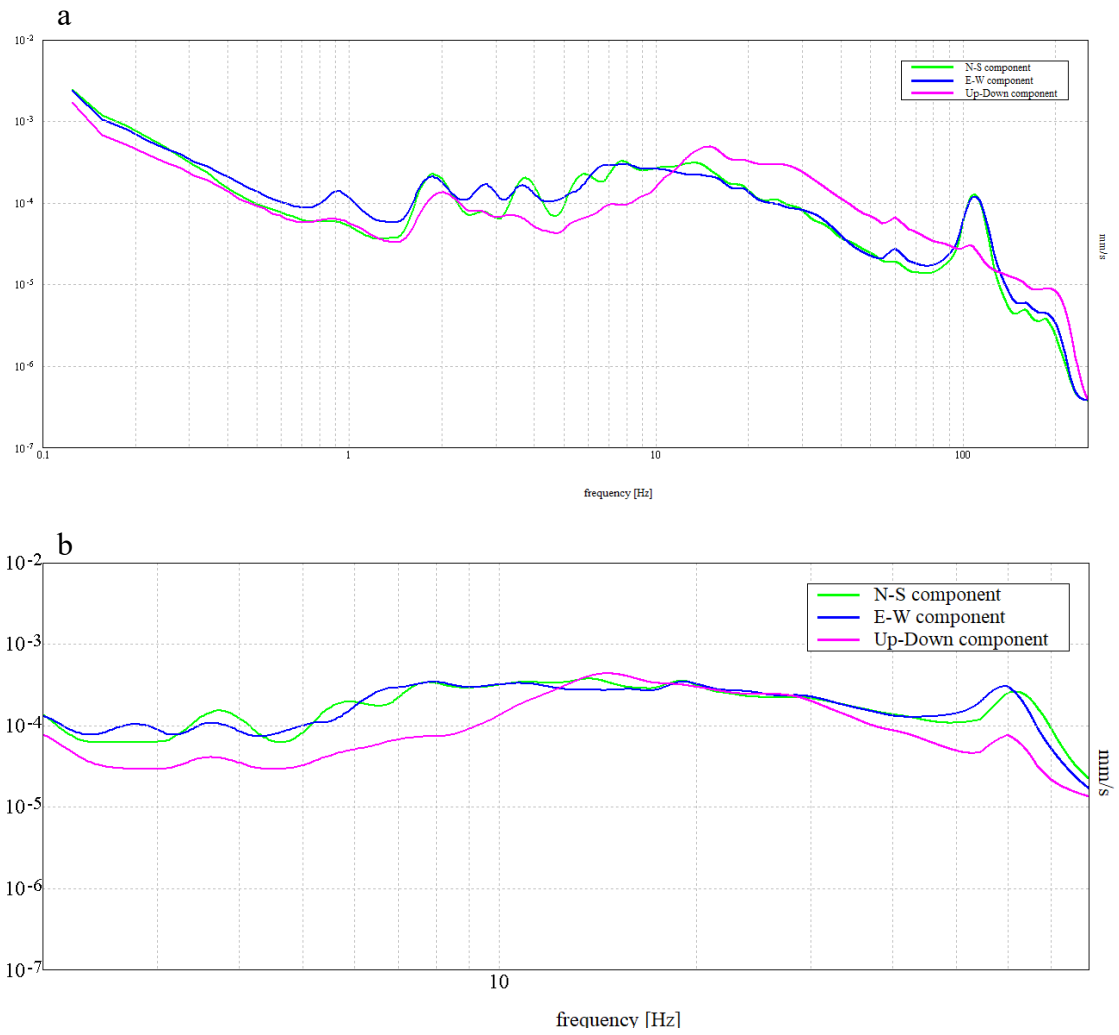

Figure C-25 Journalism B-06 A site, Test 3, concrete (a), grass (b)

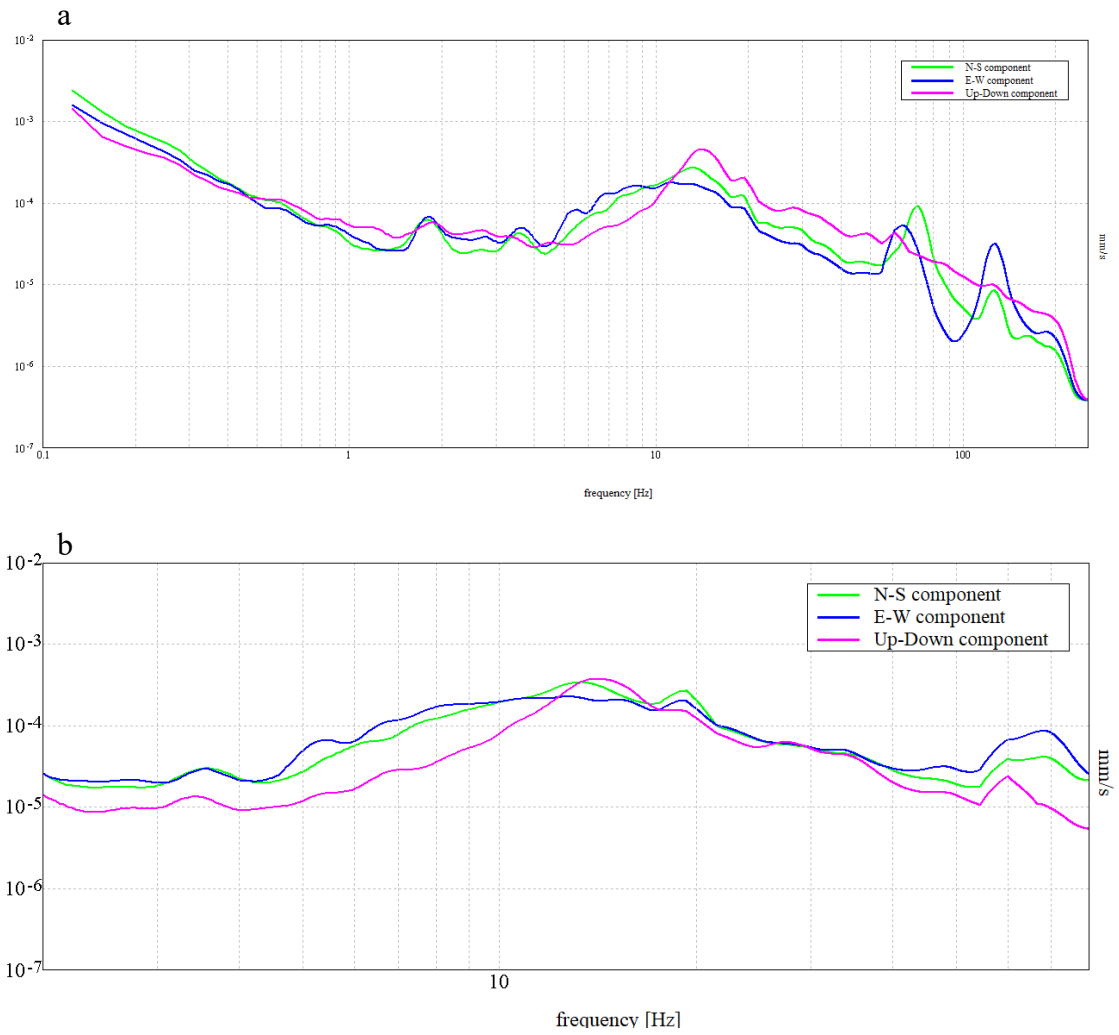

Figure C-26 Journalism B-06 A site, Test 4, concrete (a), grass (b)

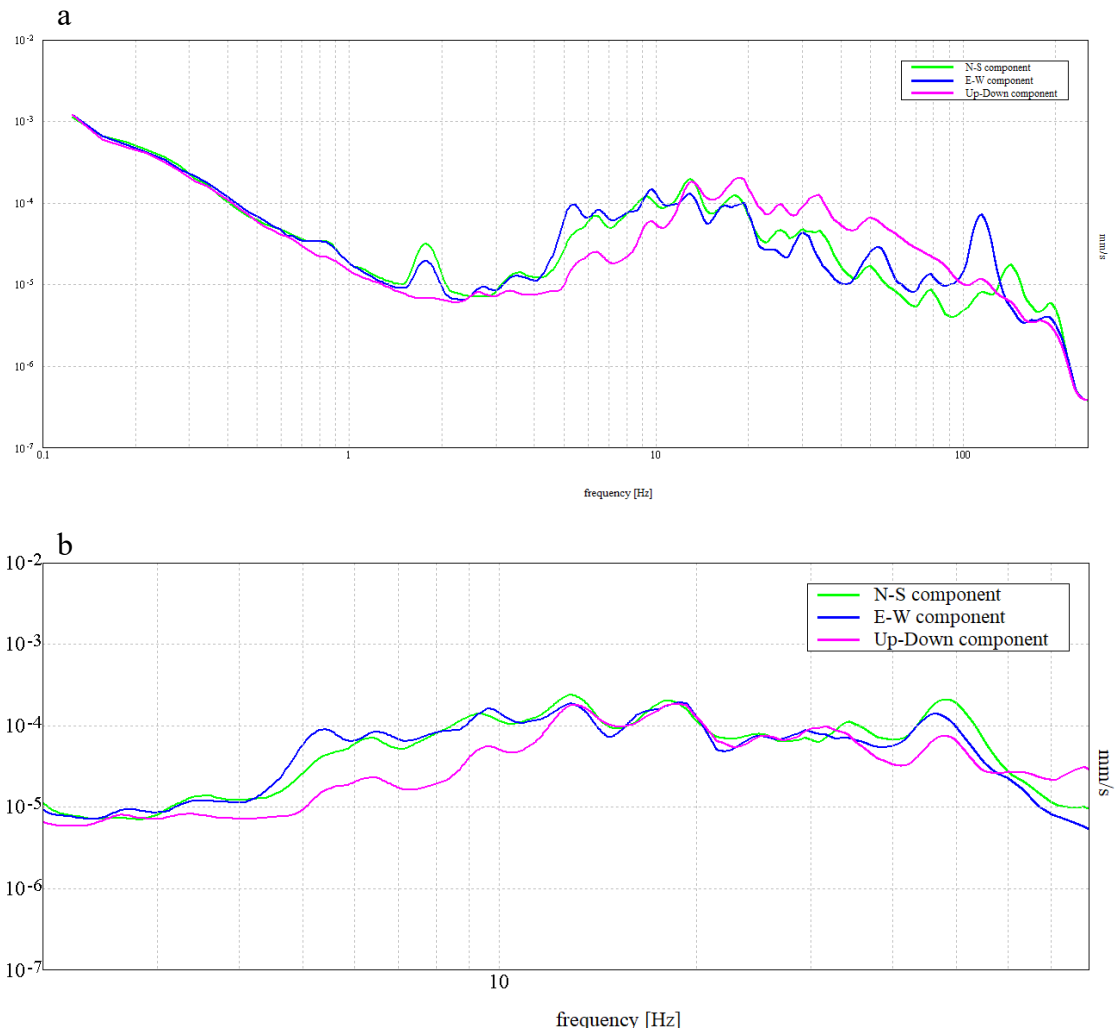

Figure C-27 Journalism B-06 A site, Test 5, concrete (a), grass (b)

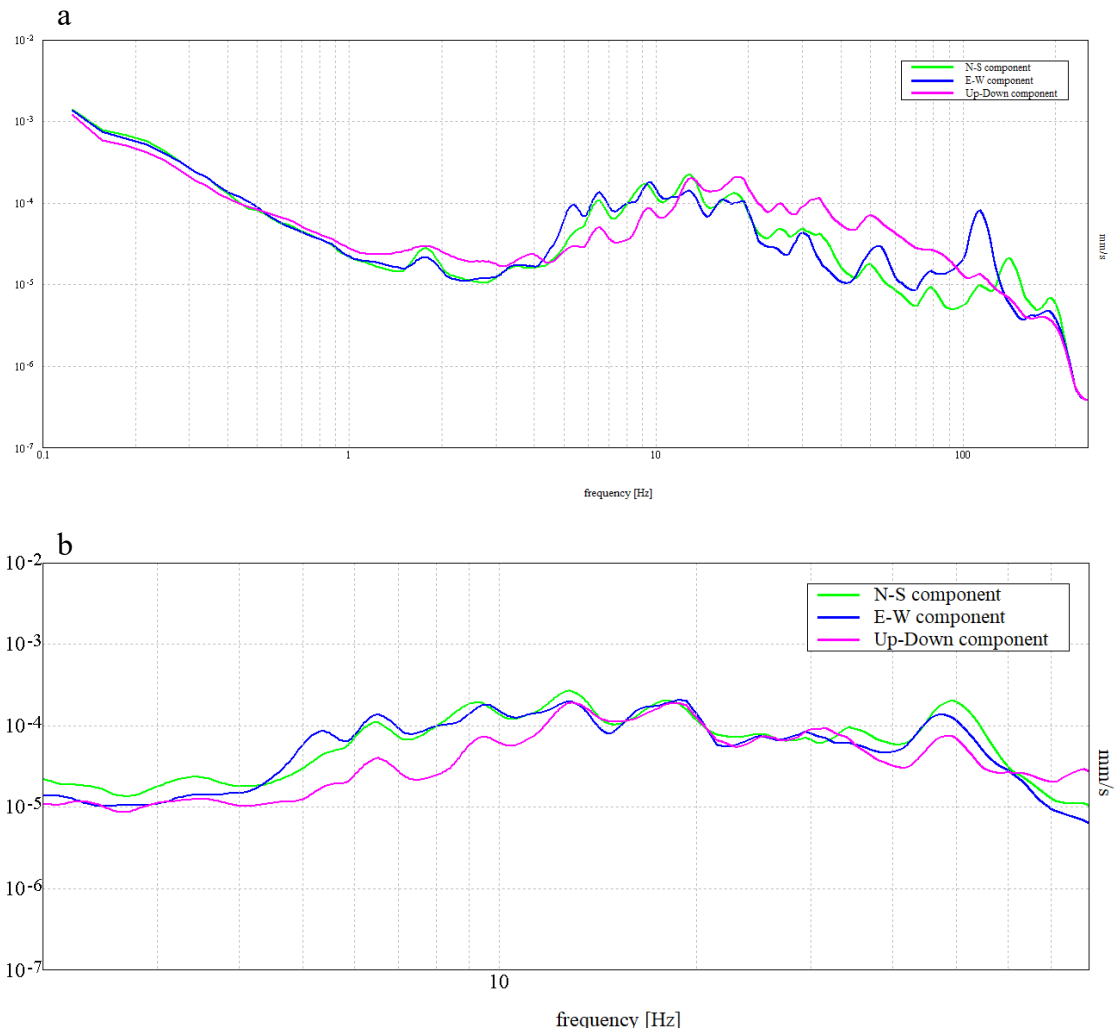

Figure C-28 Journalism B-06 A site, Test 6, concrete (a), grass (b)

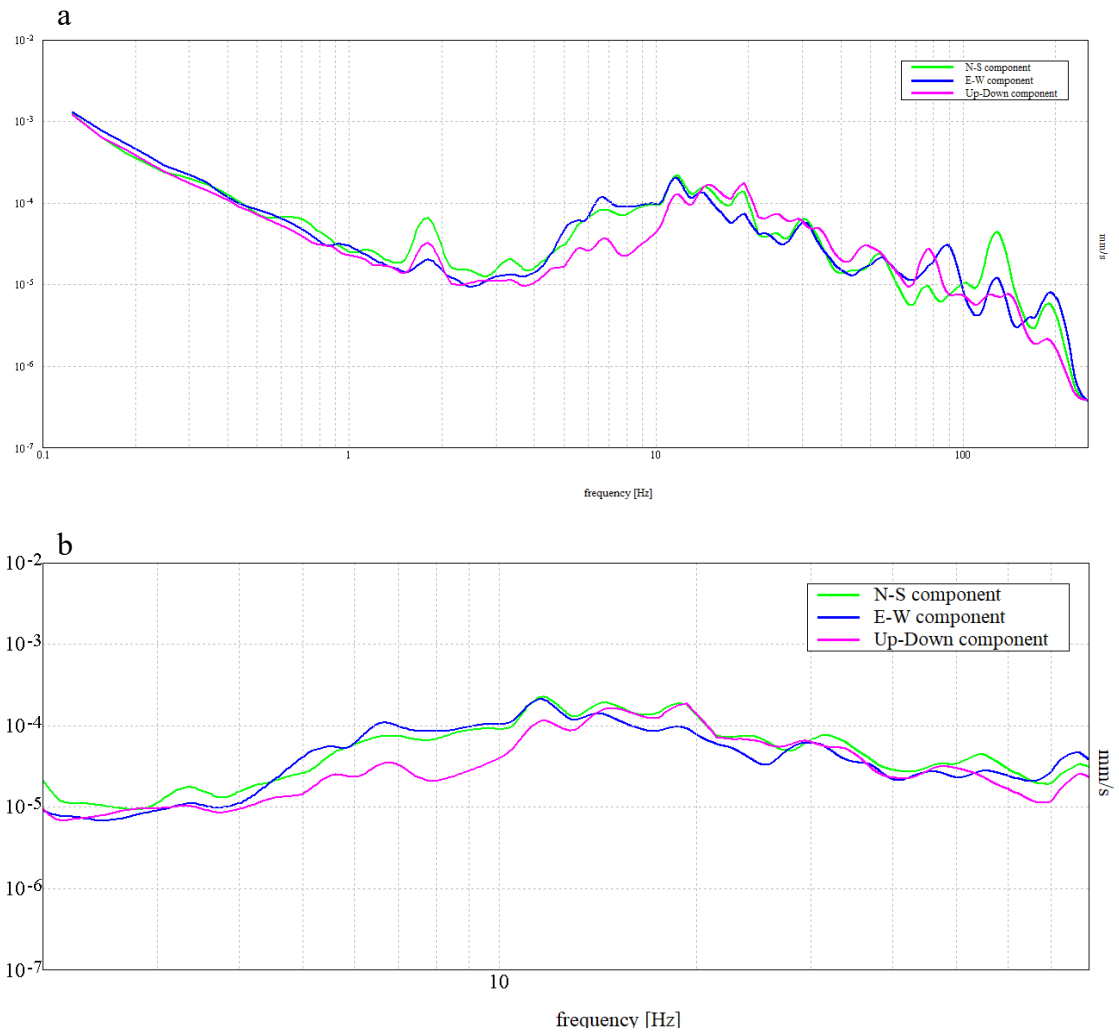

Figure C-29 Journalism B-06 B site, Test 1, concrete (a), grass (b)

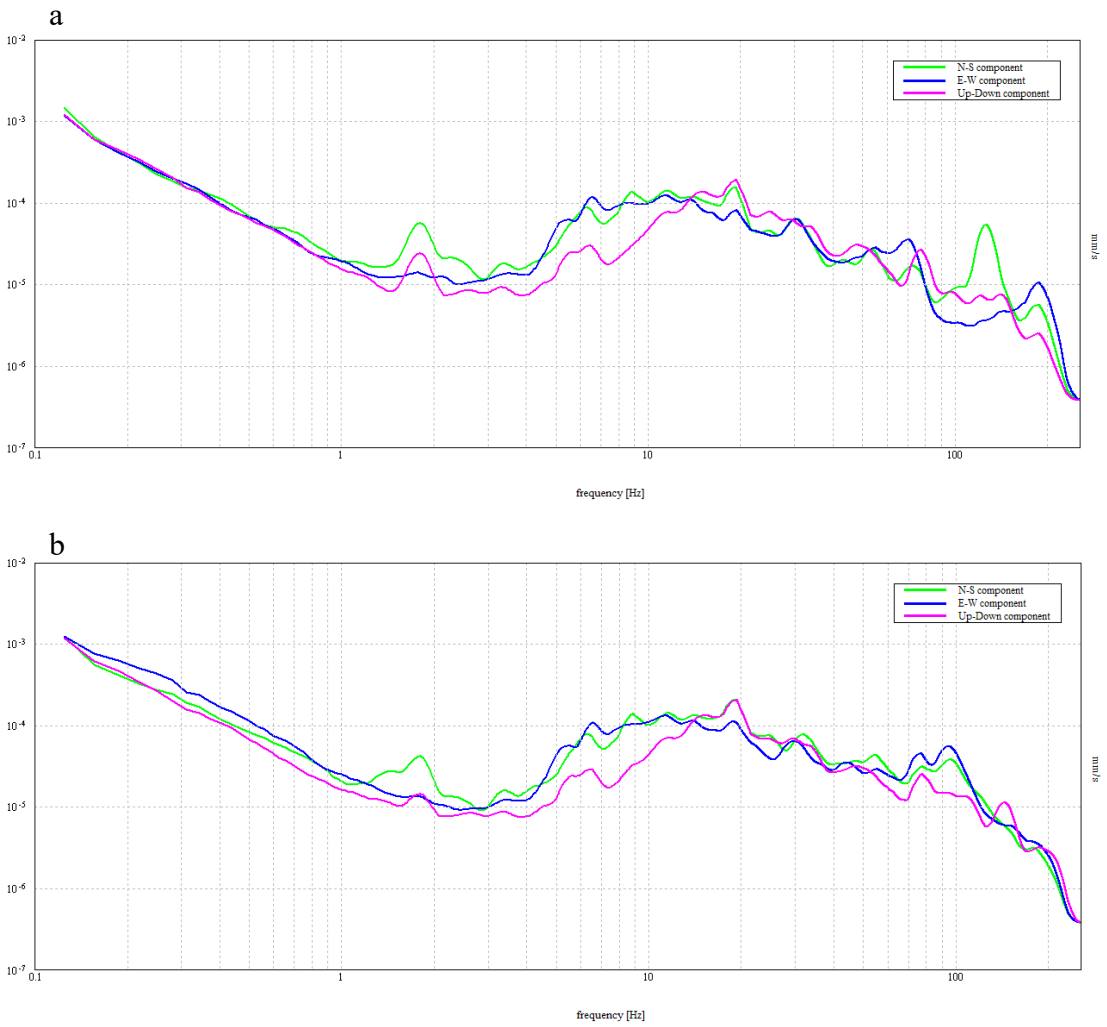

Figure C-30 Journalism B-06 B site, Test 2, concrete (a), grass (b)

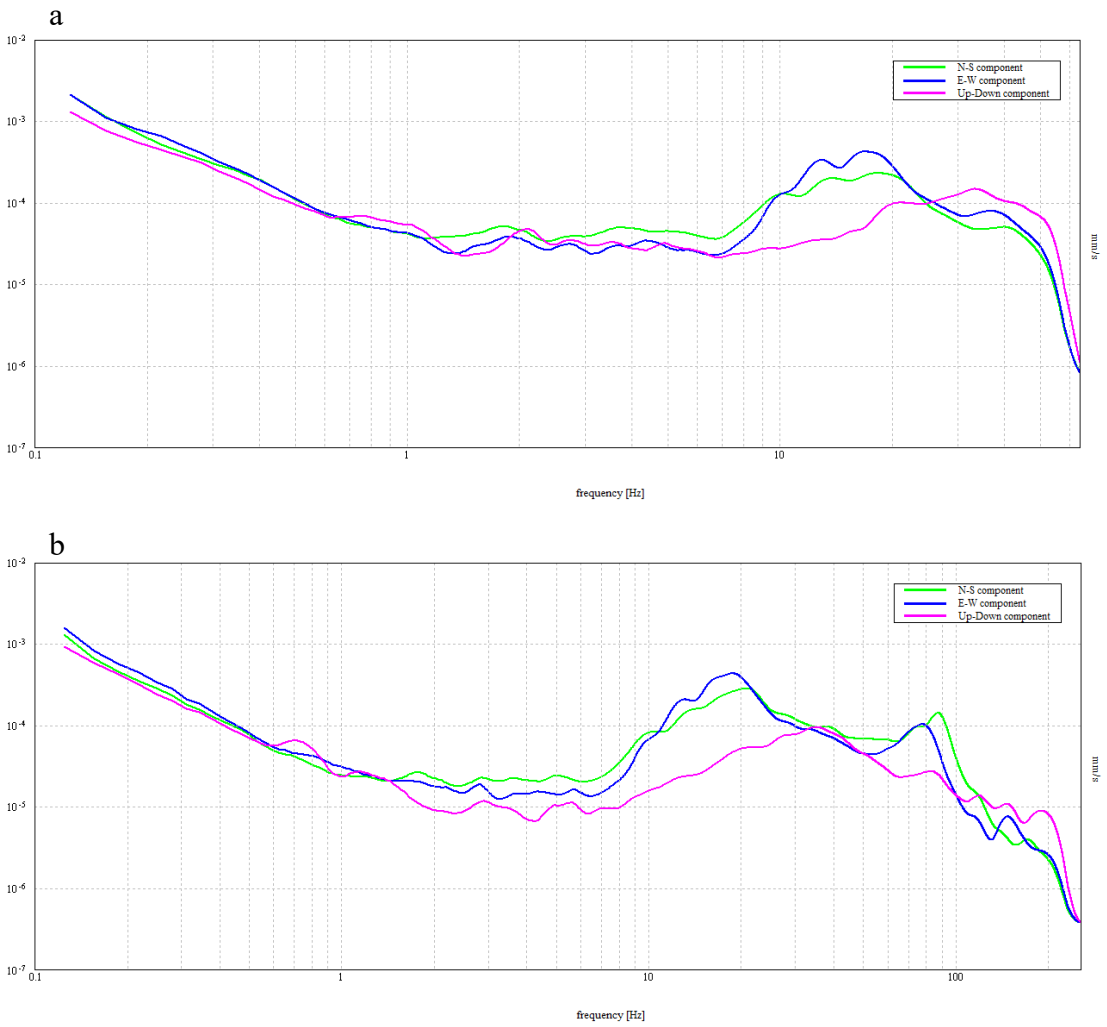

Figure C-31 Lee's Hall BH-08 site, Test 1, concrete (a), grass (b)

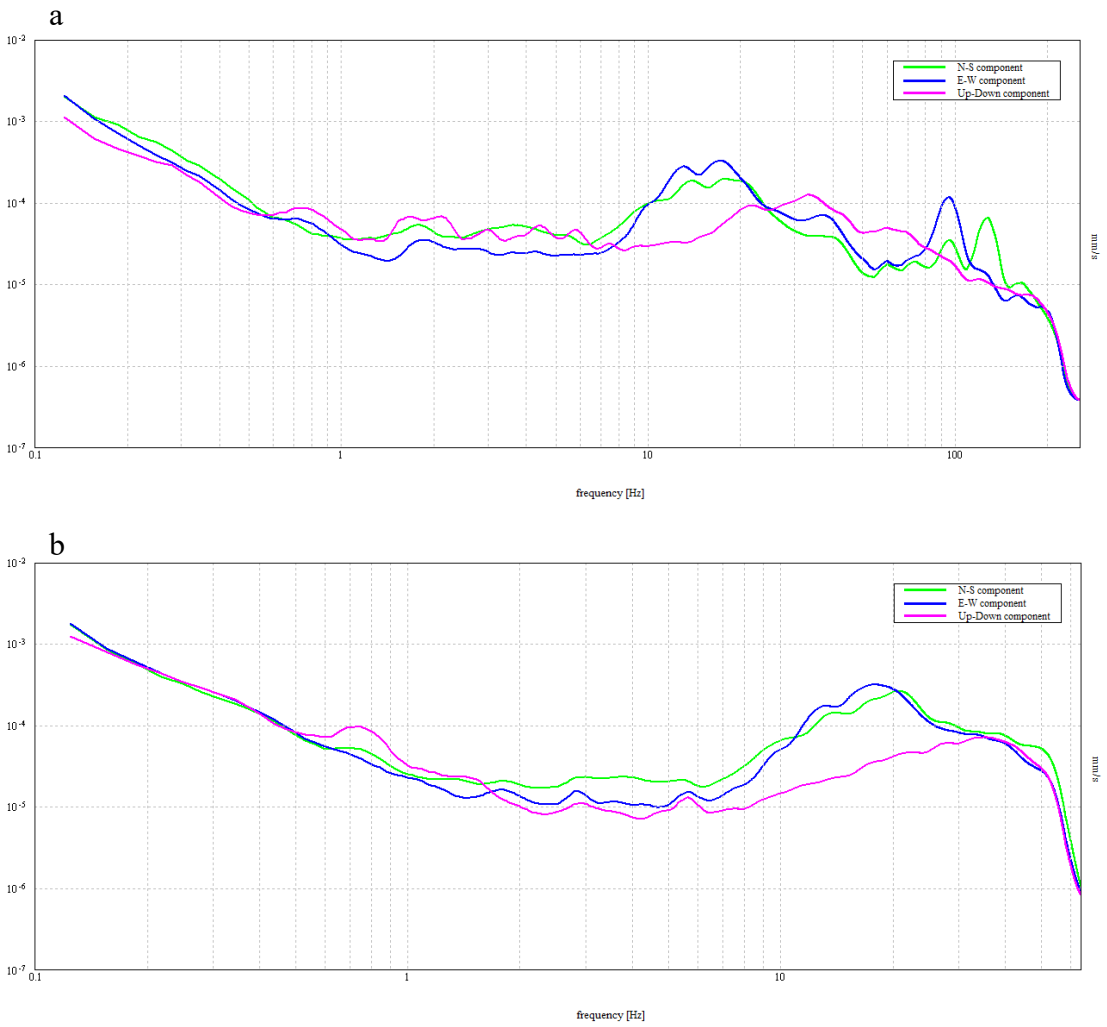

Figure C-32 Lee's Hall BH-08 site, Test 2, concrete (a), grass (b)

a

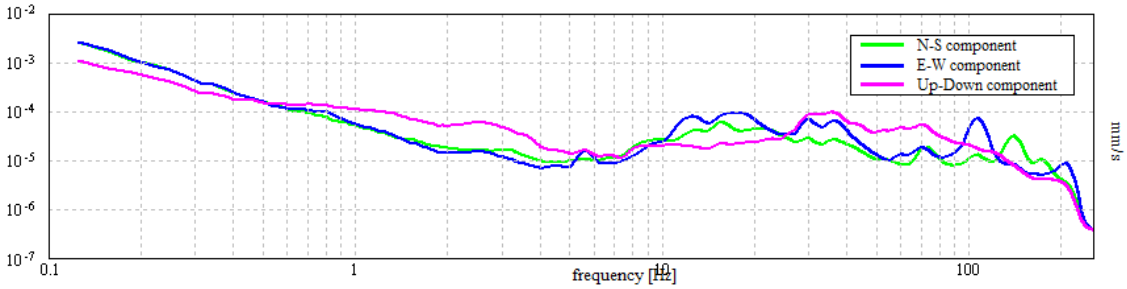

b

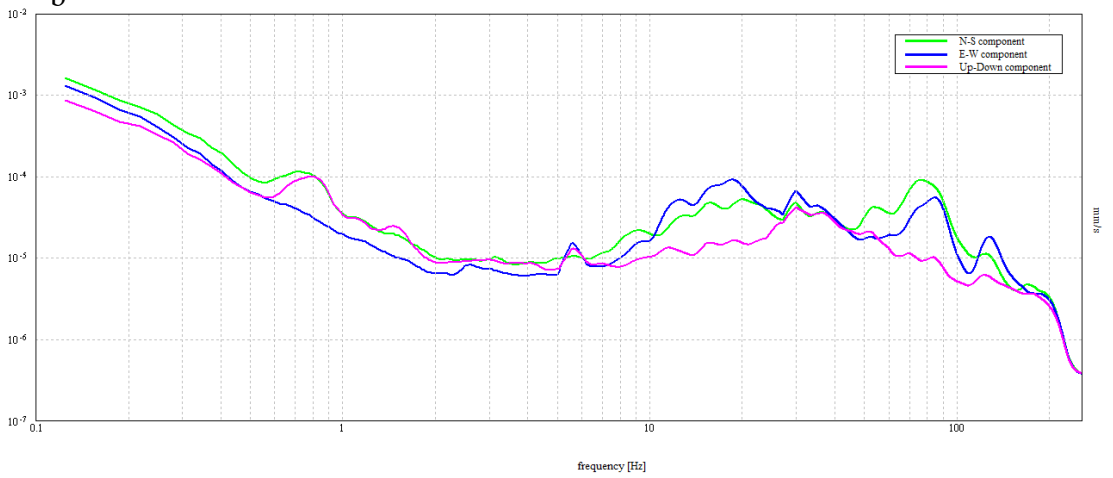

Figure C-33 Lee's Hall BH-08 site, Test 3, concrete (a), grass (b)

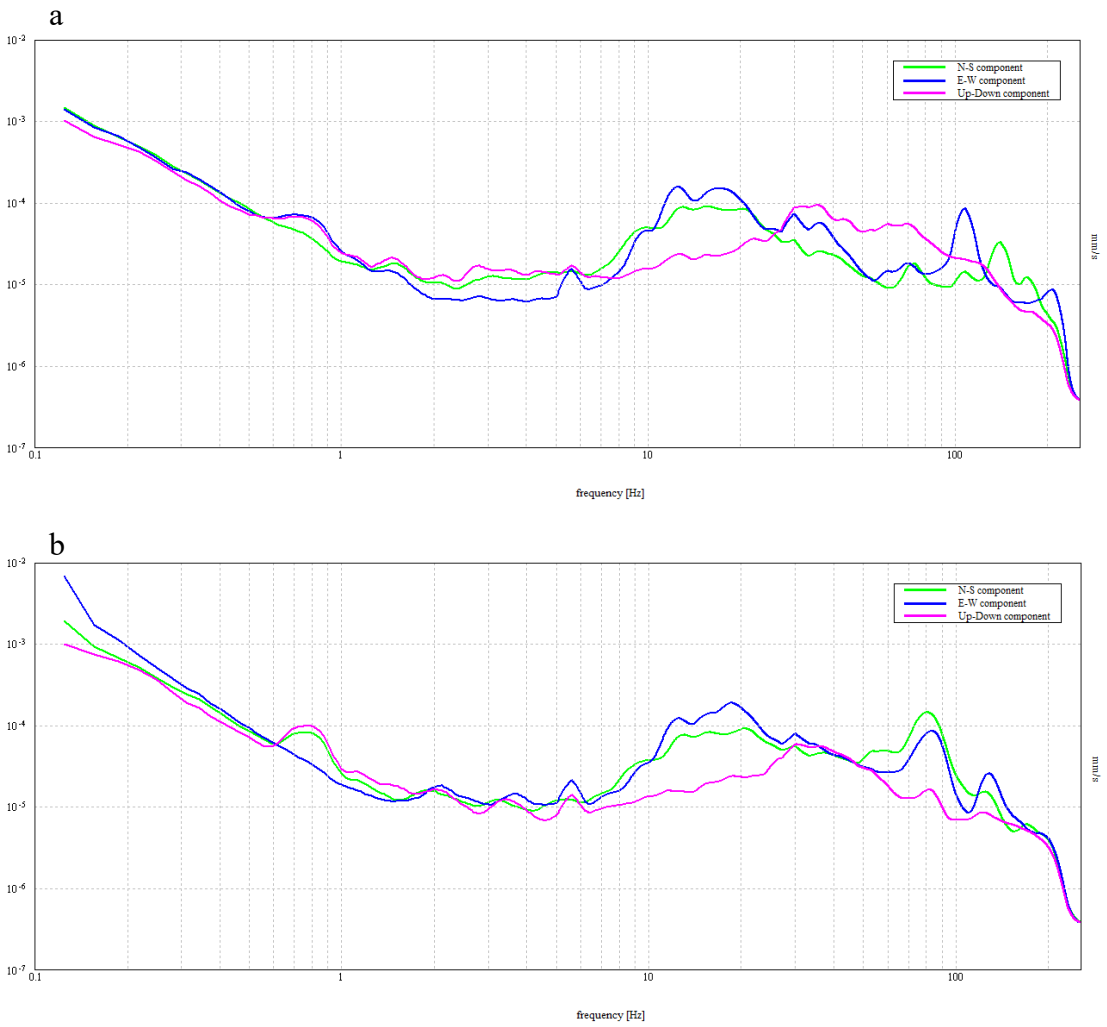

Figure C-34 Lee's Hall BH-08 site, Test 4, concrete (a), grass (b)

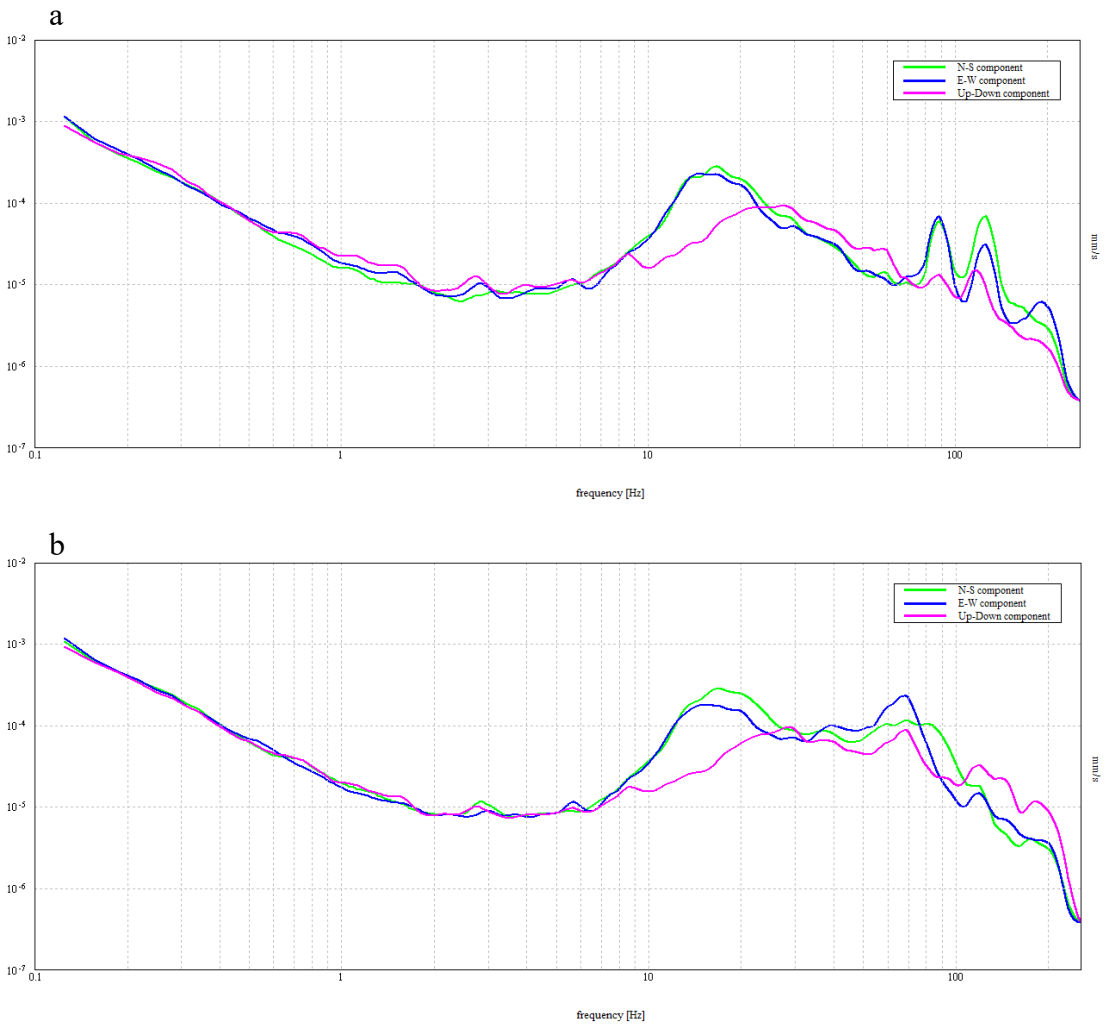

Figure C-35 Lee's Hall BH-18 site, Test 1, concrete (a), grass (b)

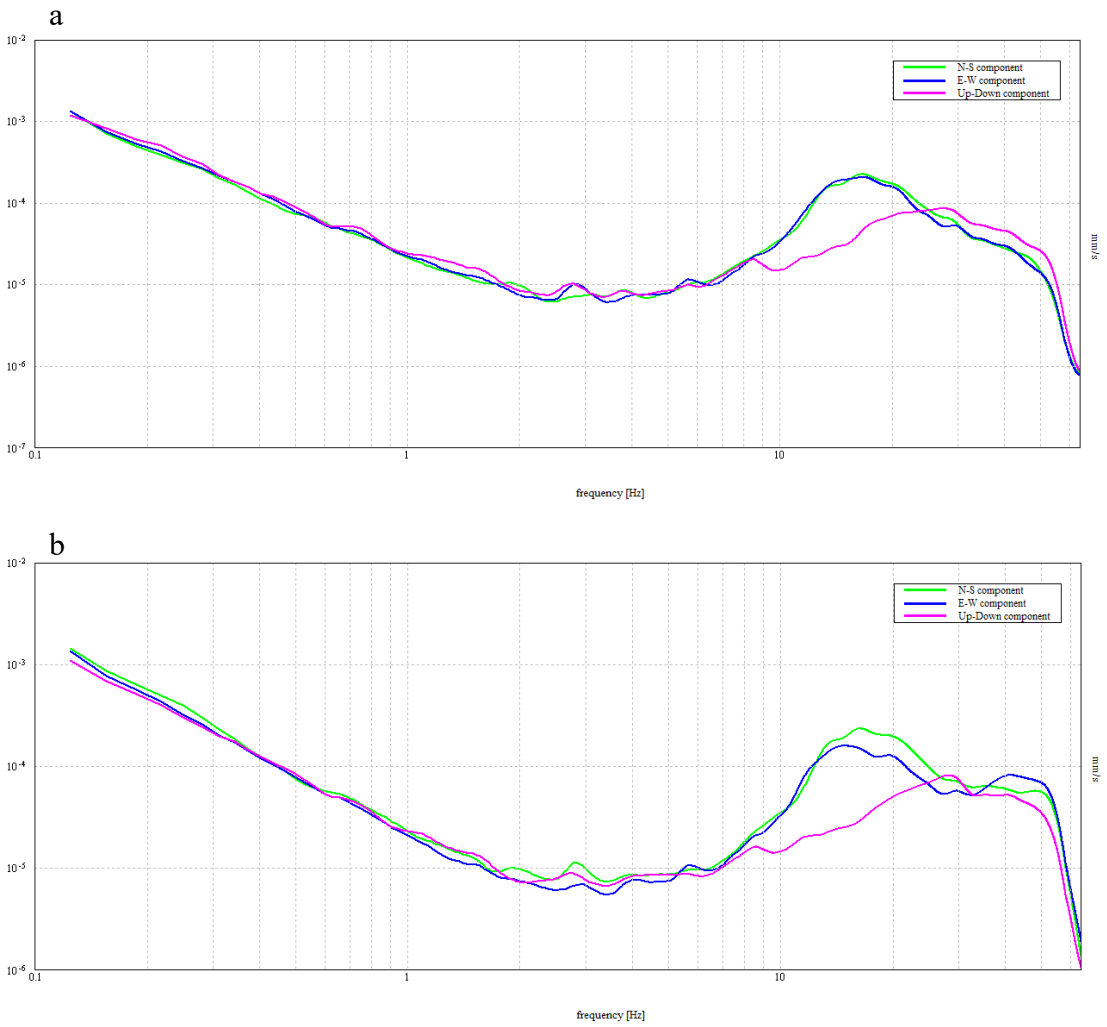

Figure C-36 Lee's Hall BH-18 site, Test 2, concrete (a), grass (b)

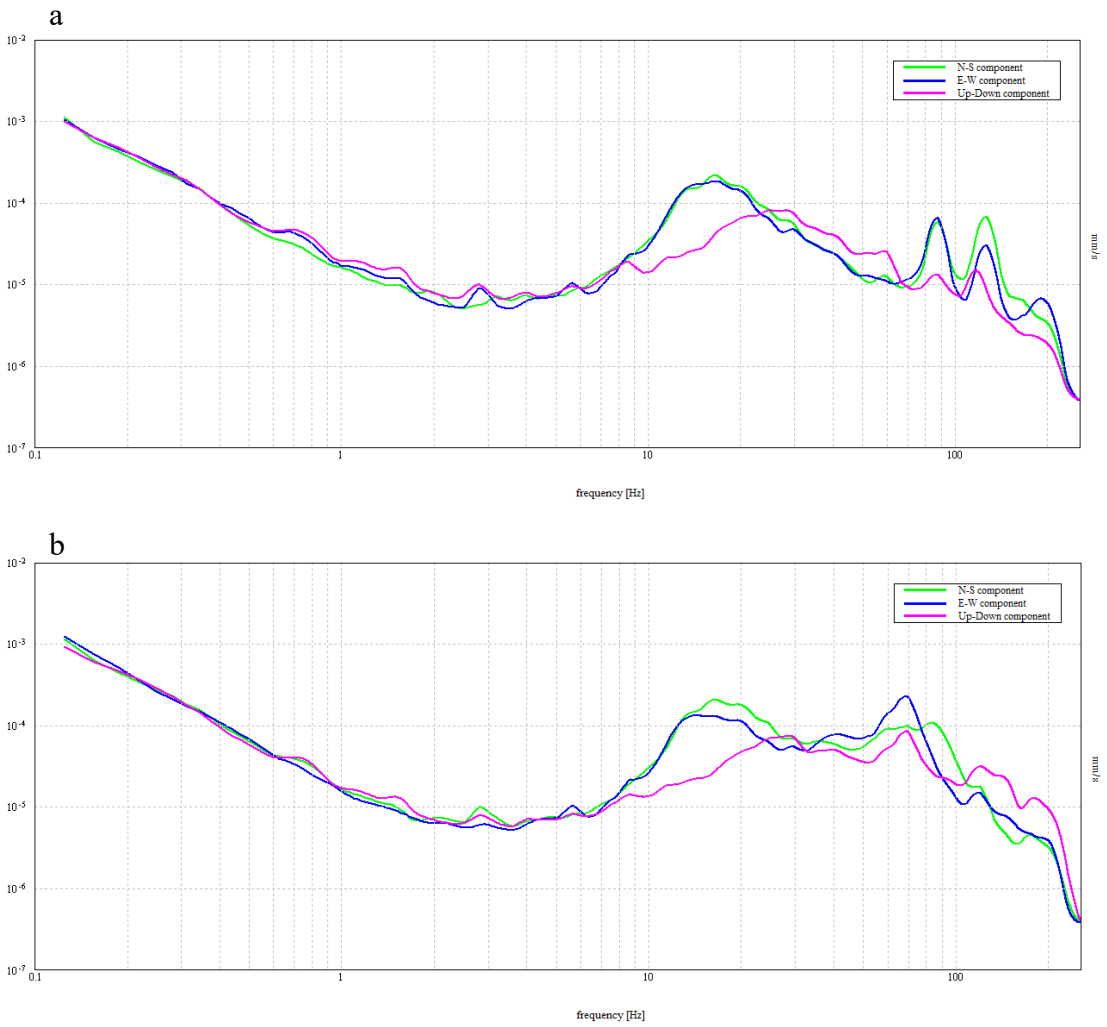

Figure C-37 Lee's Hall BH-18 site, Test 3, concrete (a), grass (b)

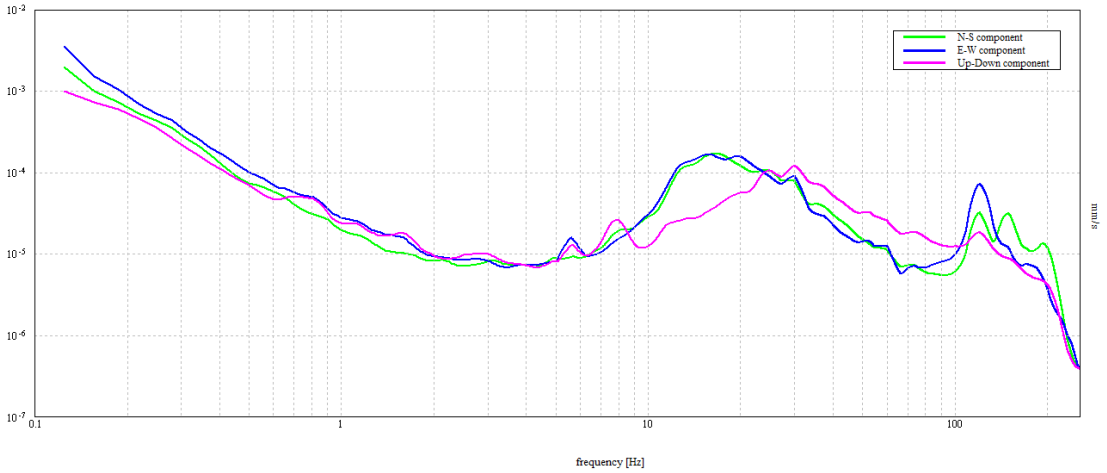

Figure C-38 Lee's Hall BH-18 site, Test 4, concrete

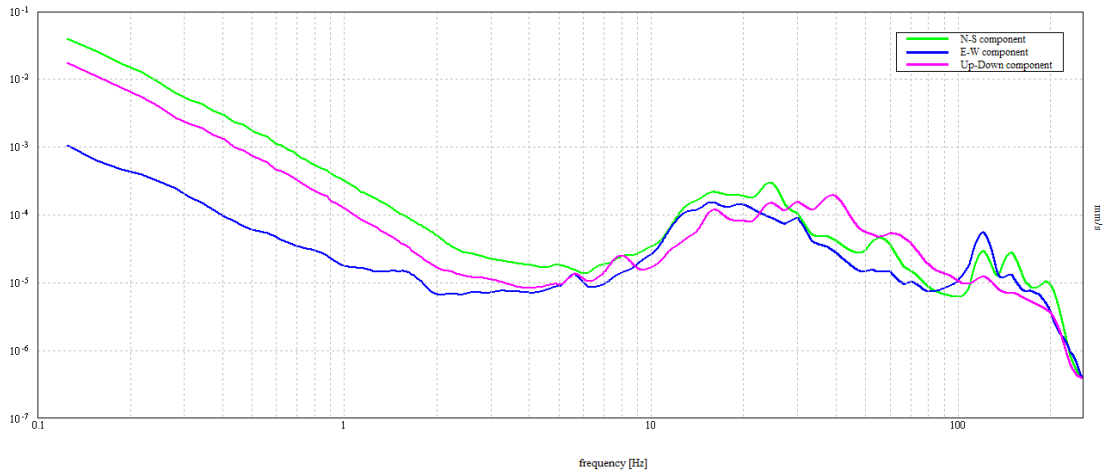

Figure C-39 Lee's Hall BH-18 site, Test 5, concrete

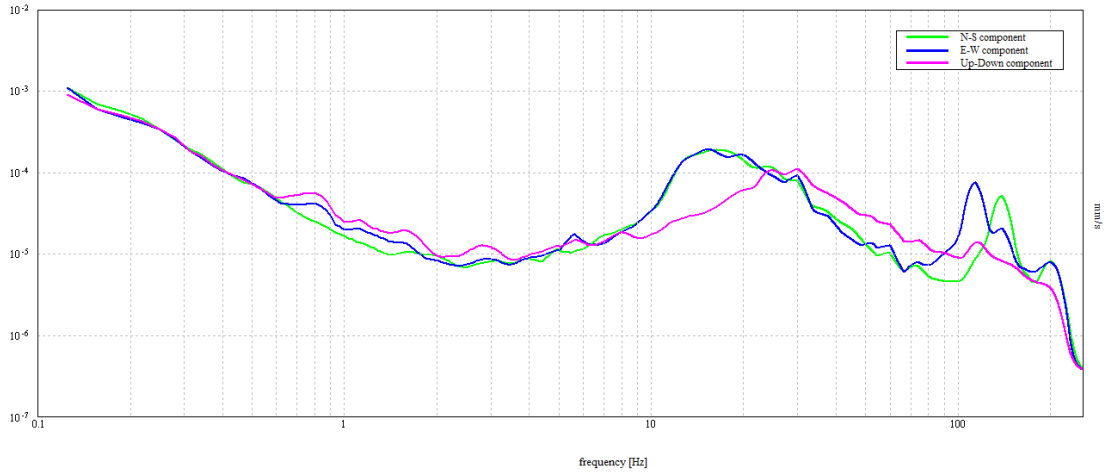

Figure C-40 Lee's Hall BH-18 site, Test 6, concrete

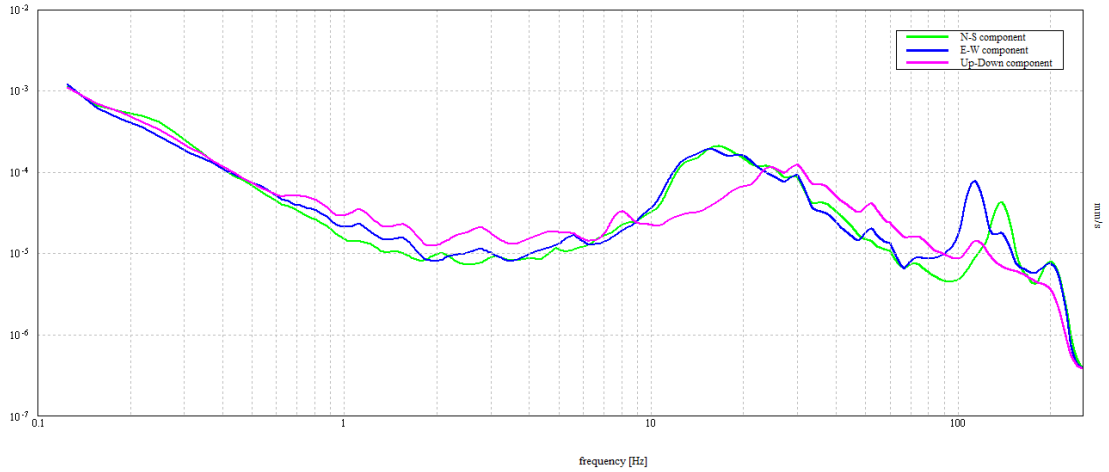

Figure C-41 Lee's Hall BH-18 site, Test 7, concrete (a)

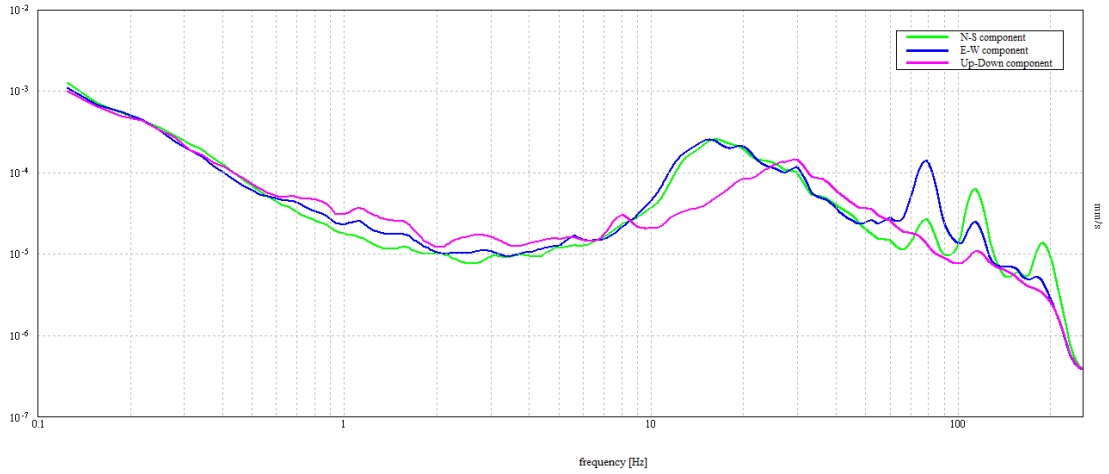

Figure C-42 Lee's Hall BH-18 site, Test 8, concrete

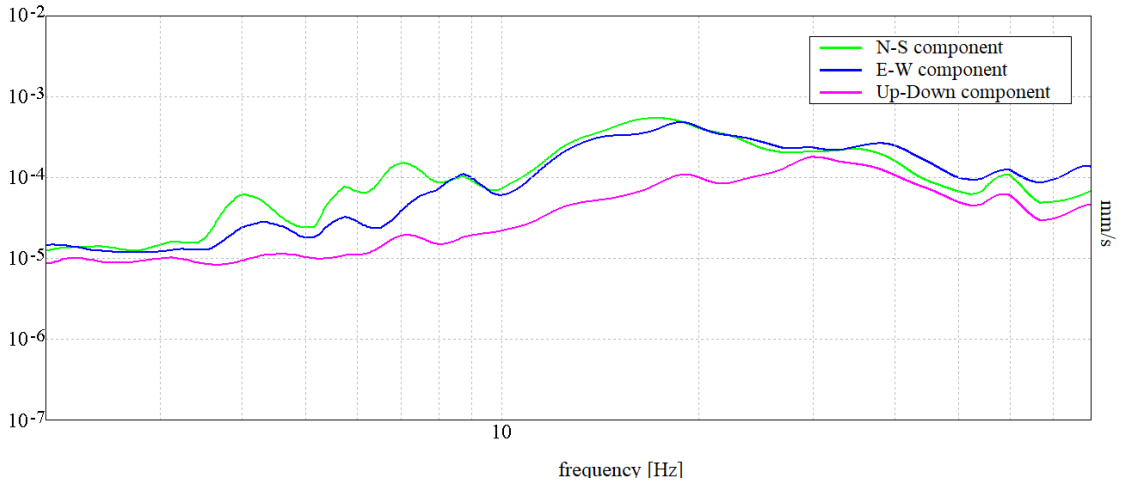

Figure C-43 Lee's Hall Selected site, Test 1, grass

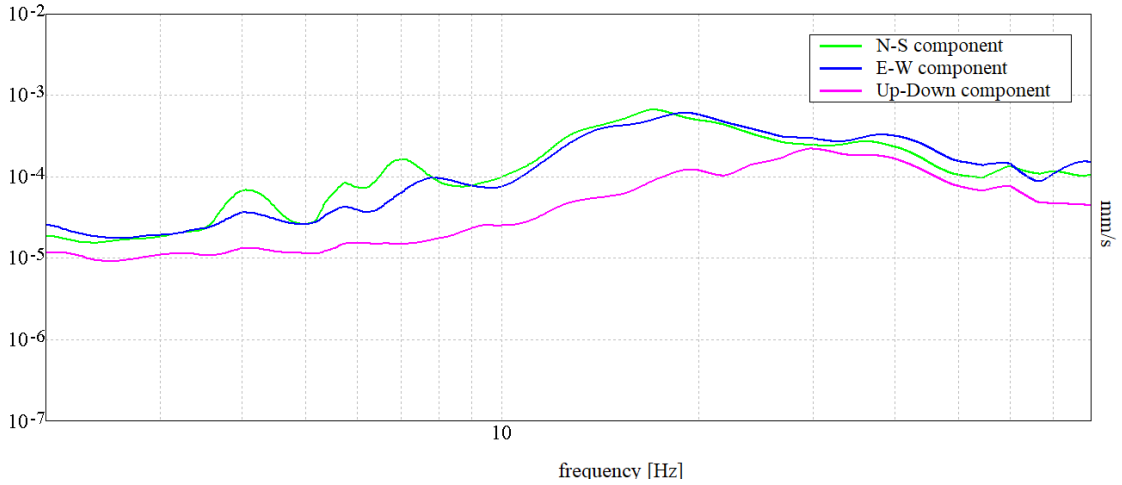

Figure C-44 Lee's Hall Selected site, Test 2, grass

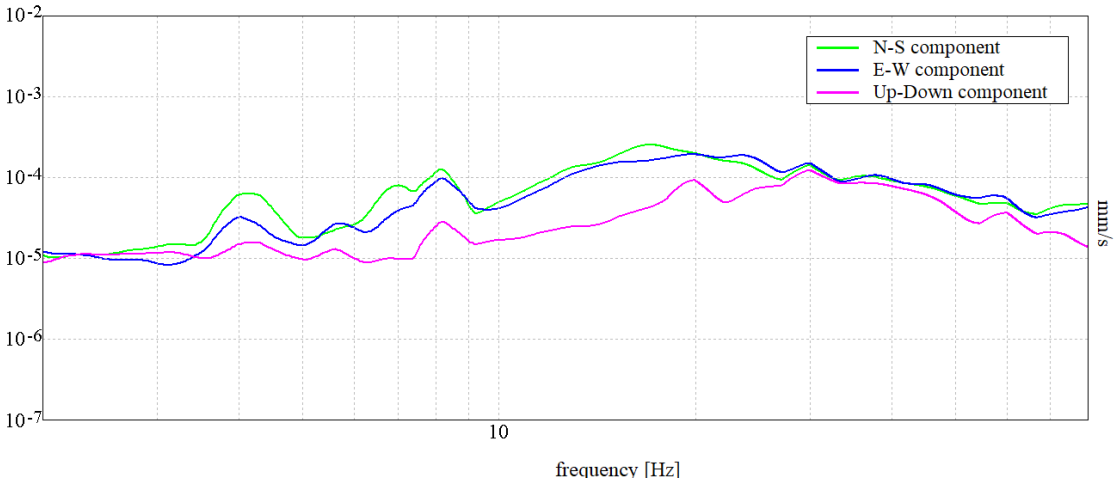

Figure C-45 Lee's Hall Selected site, Test 3, grass

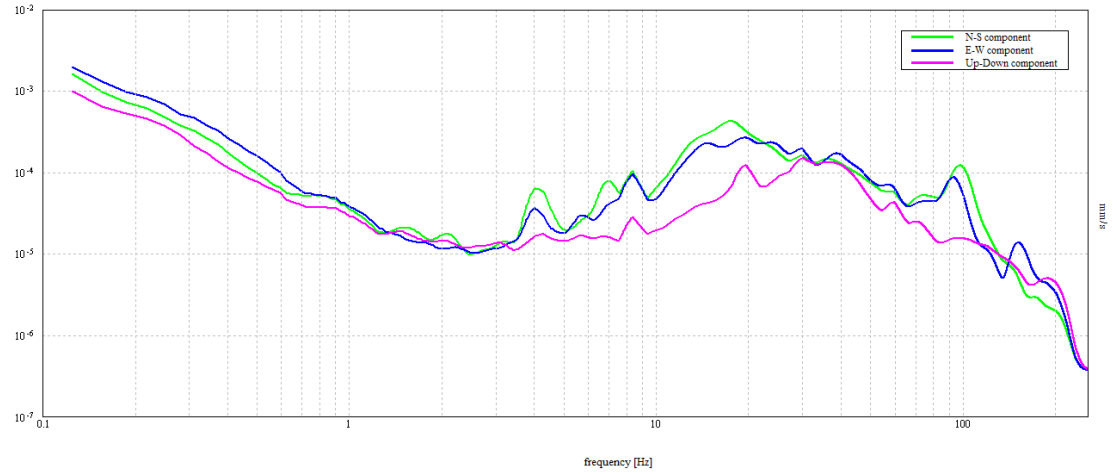

Figure C-46 Lee's Hall Selected site, Test 4, grass

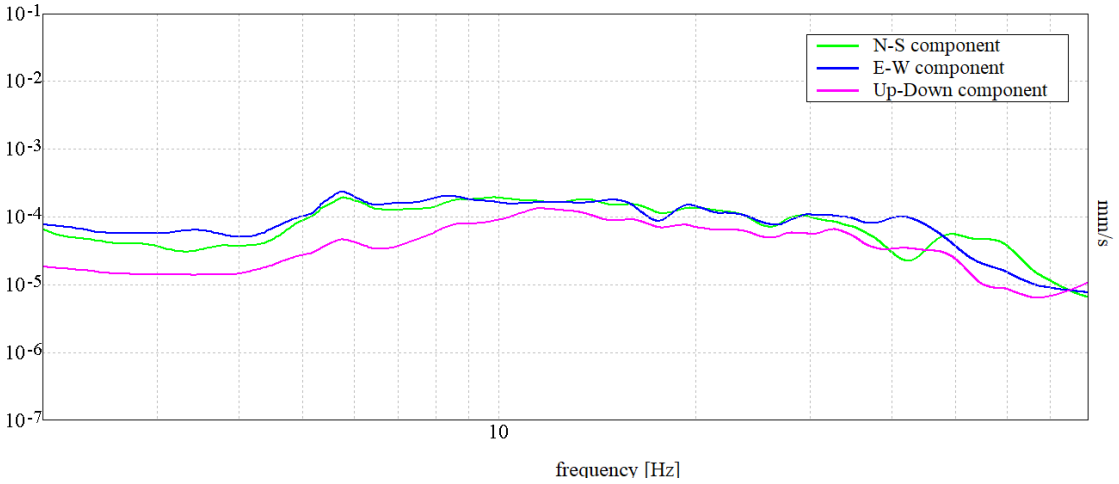

Figure C-47 Lee's Hall Selected site, Test 5, grass

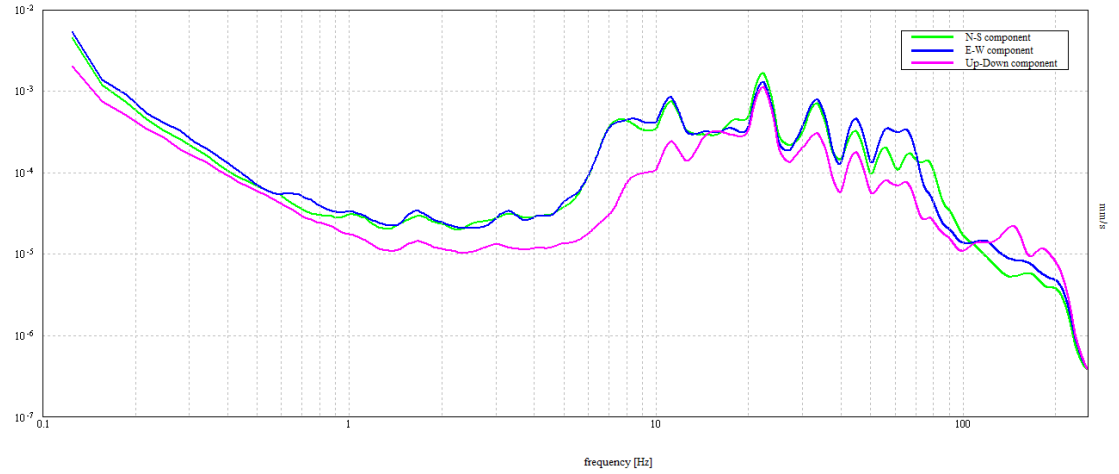

Figure C-48 MIZ Middle Quad site, Test 1, grass

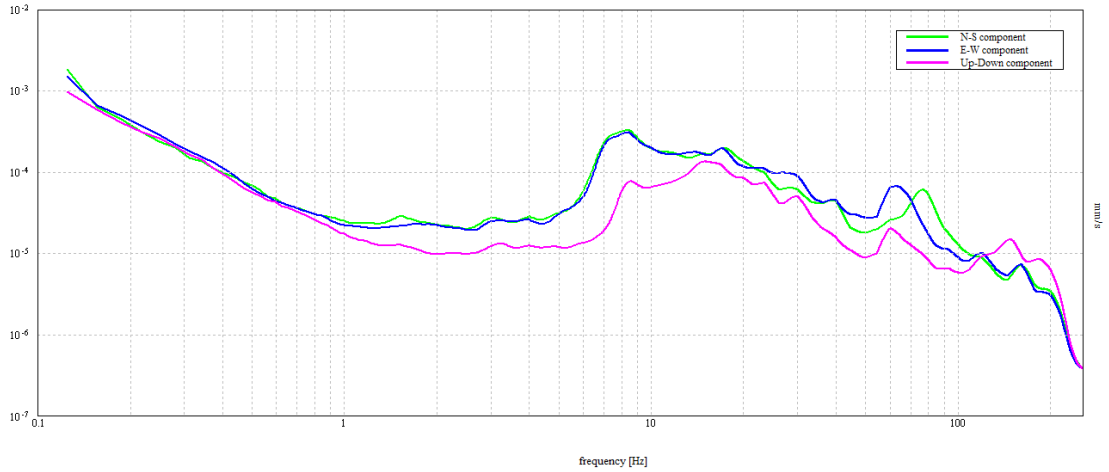

Figure C-49 MIZ Middle Quad site, Test 2, grass

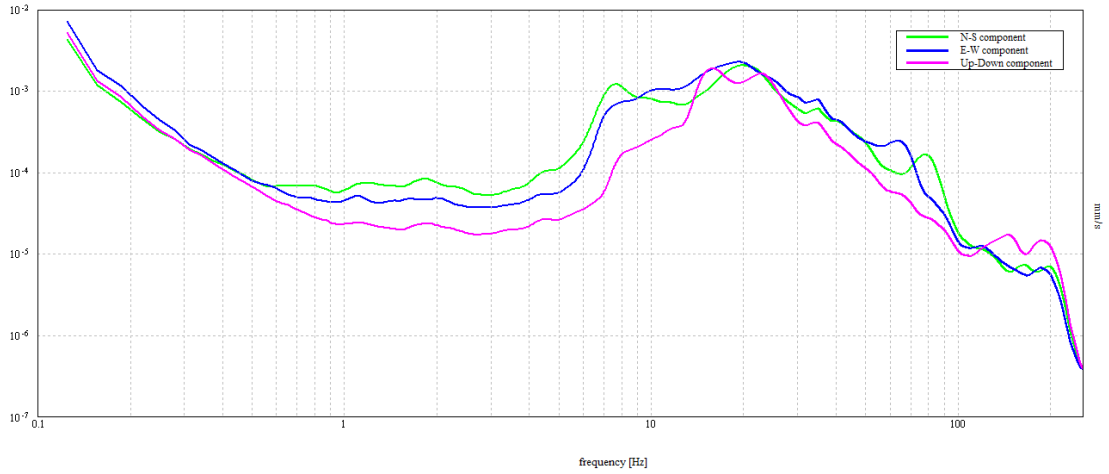

Figure C-50 MIZ Middle Quad site, Test 3, grass

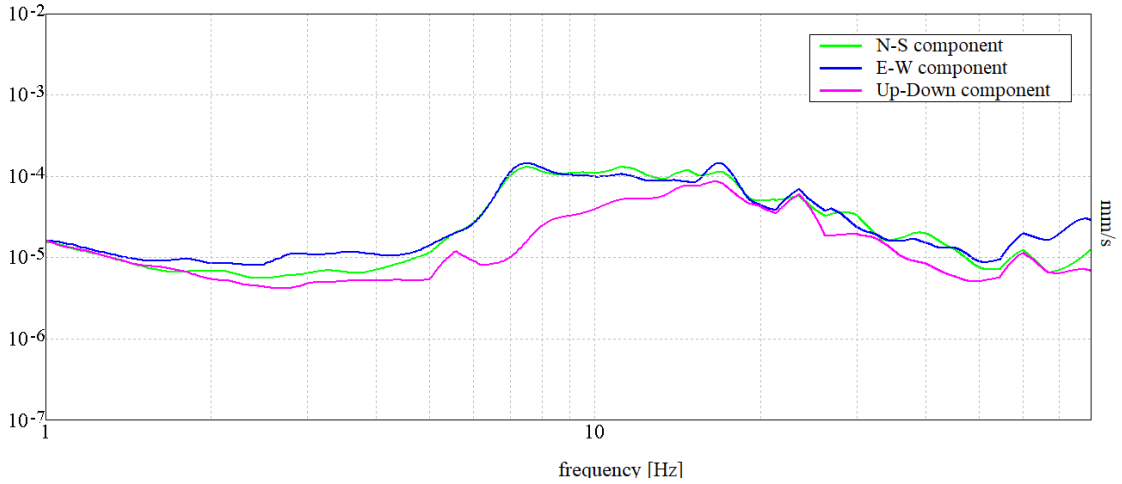

Figure C-51 MIZ Middle Quad site, Test 4, grass

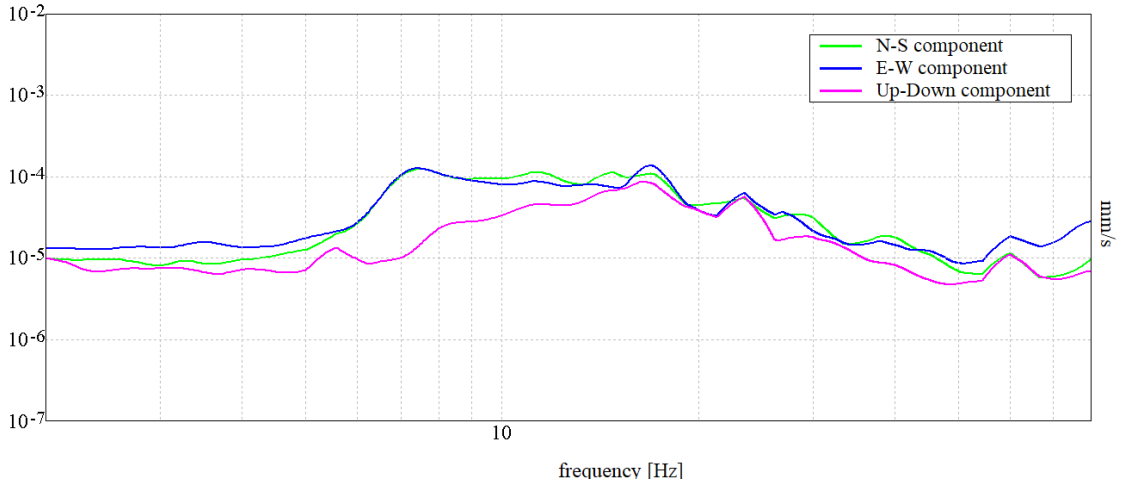

Figure C-52 MIZ Middle Quad site, Test 5, grass

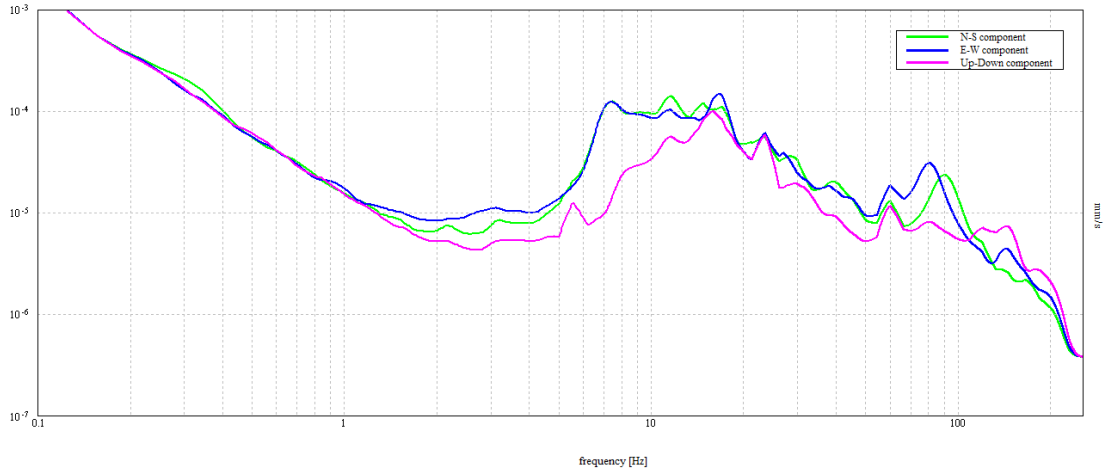

Figure C-53 MIZ Middle Quad site, Test 6, grass

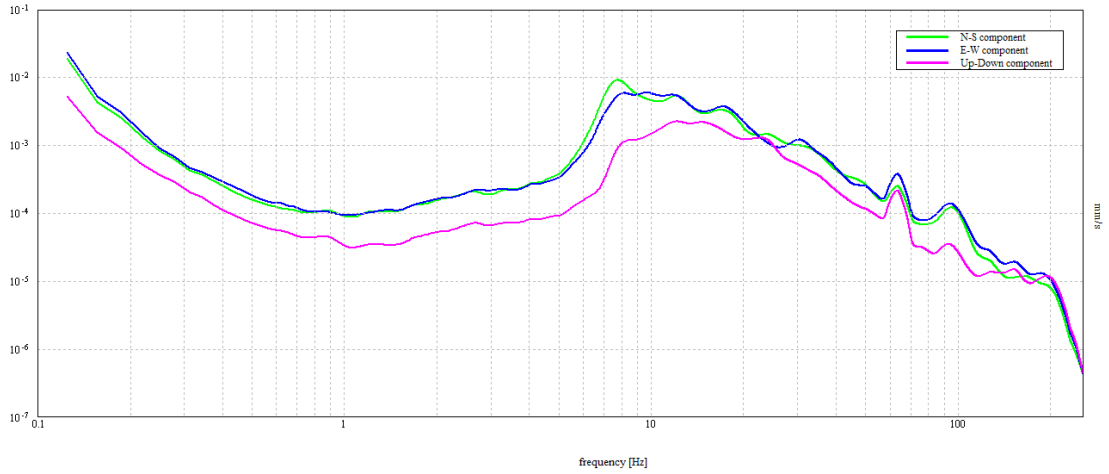

Figure C-54 MIZ Middle Quad site, Test 7, grass

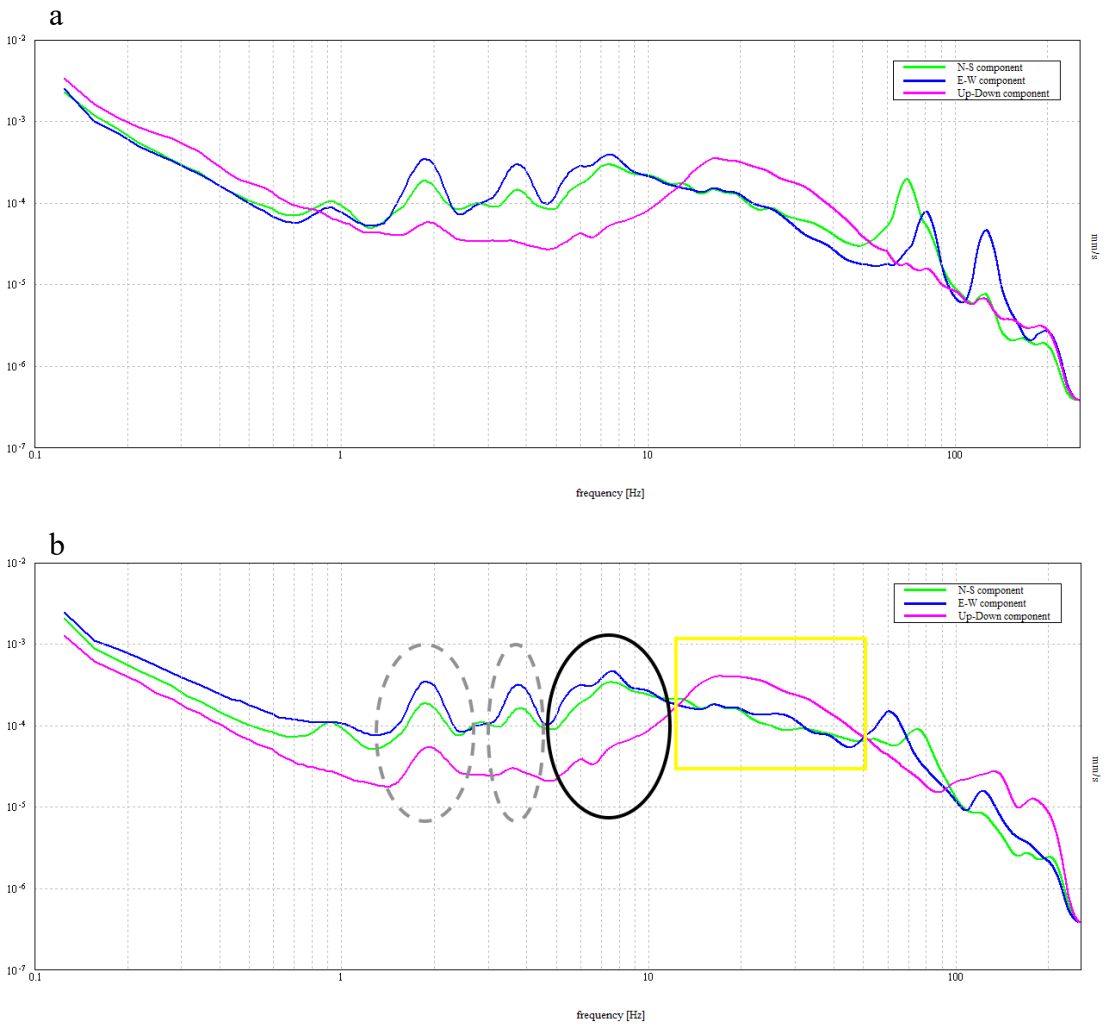

Figure C-55 MIZ Quad Site 1 site, Test 1, concrete (a), grass (b)

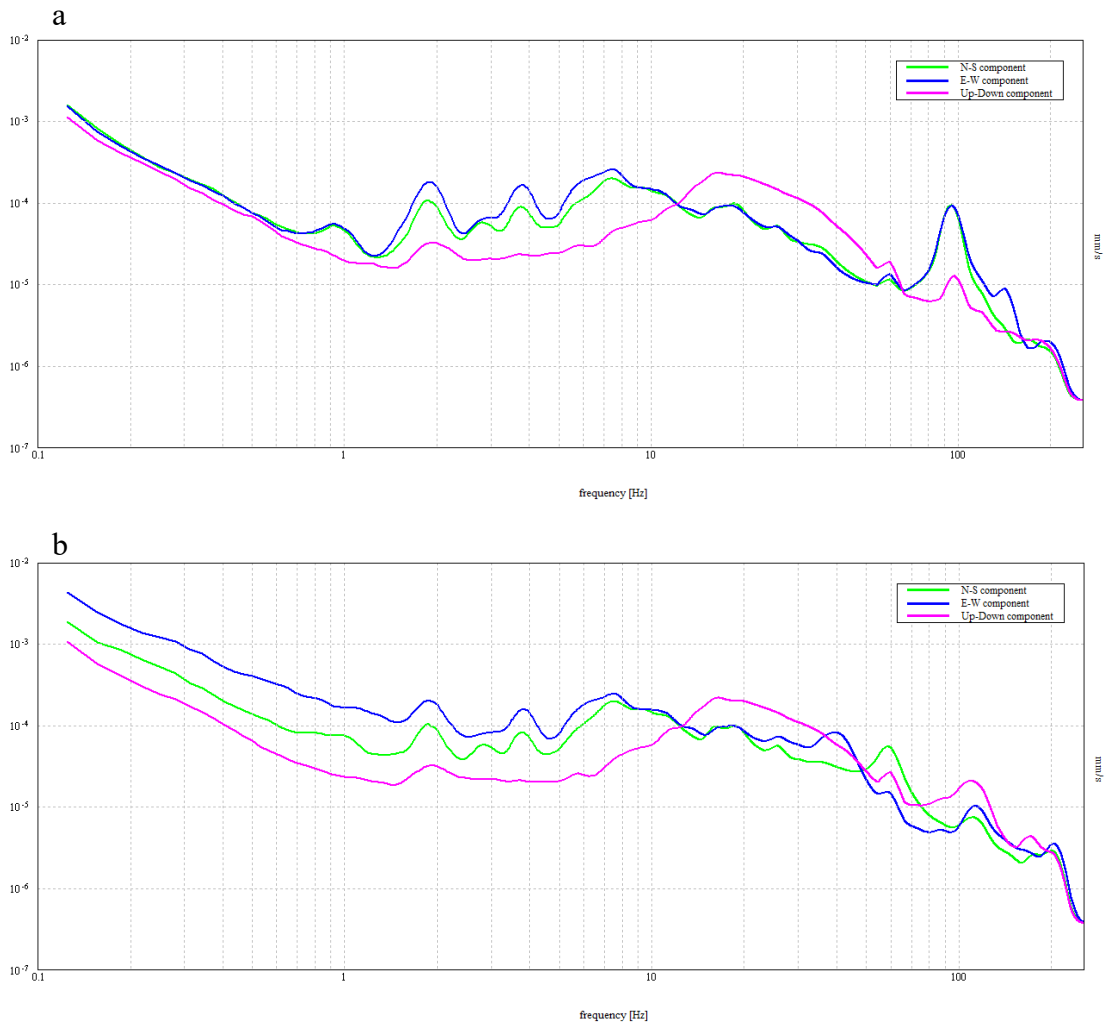

Figure C-56 MIZ Quad Site 1 site, Test 2, concrete (a), grass (b)

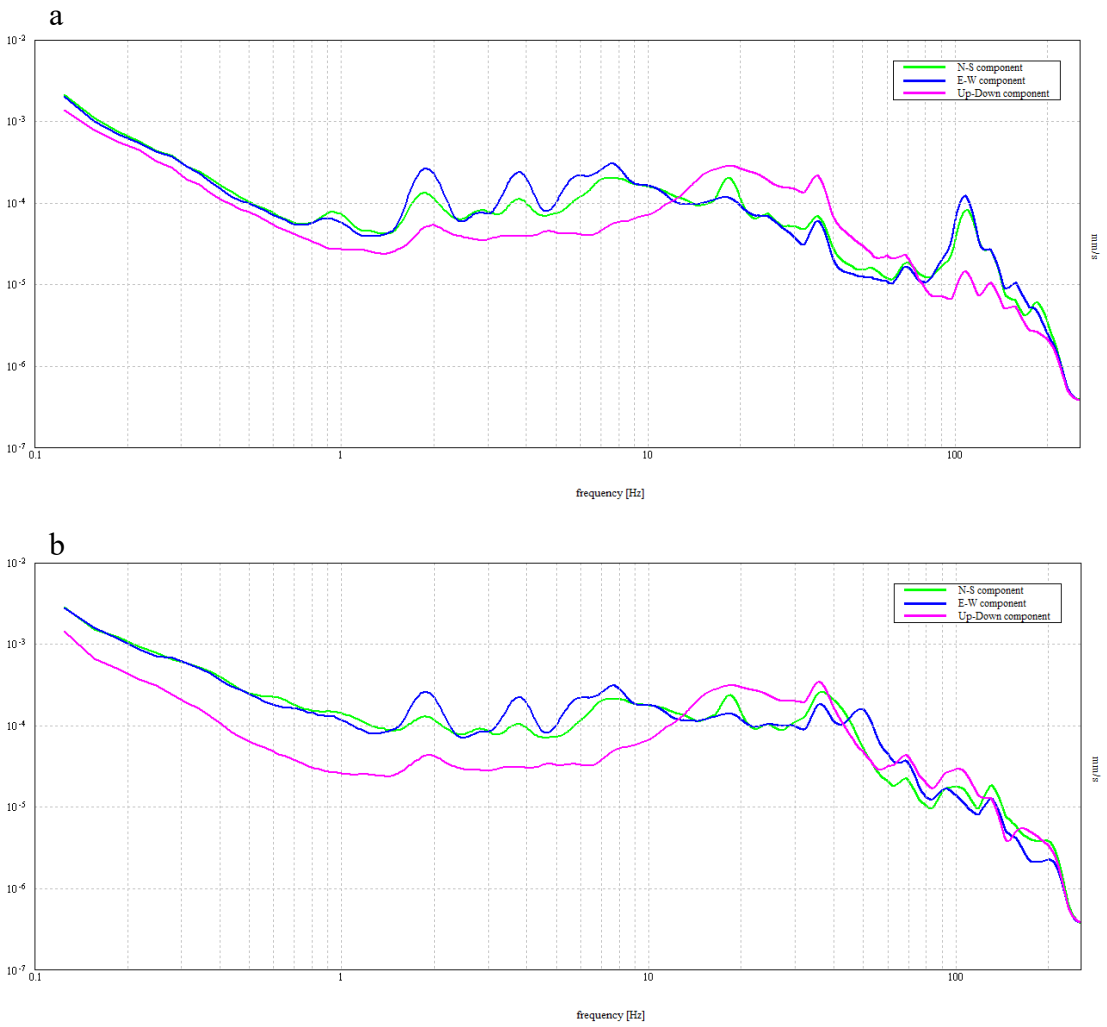

Figure C-57 MIZ Quad Site 1 site, Test 3, concrete (a), grass (b)

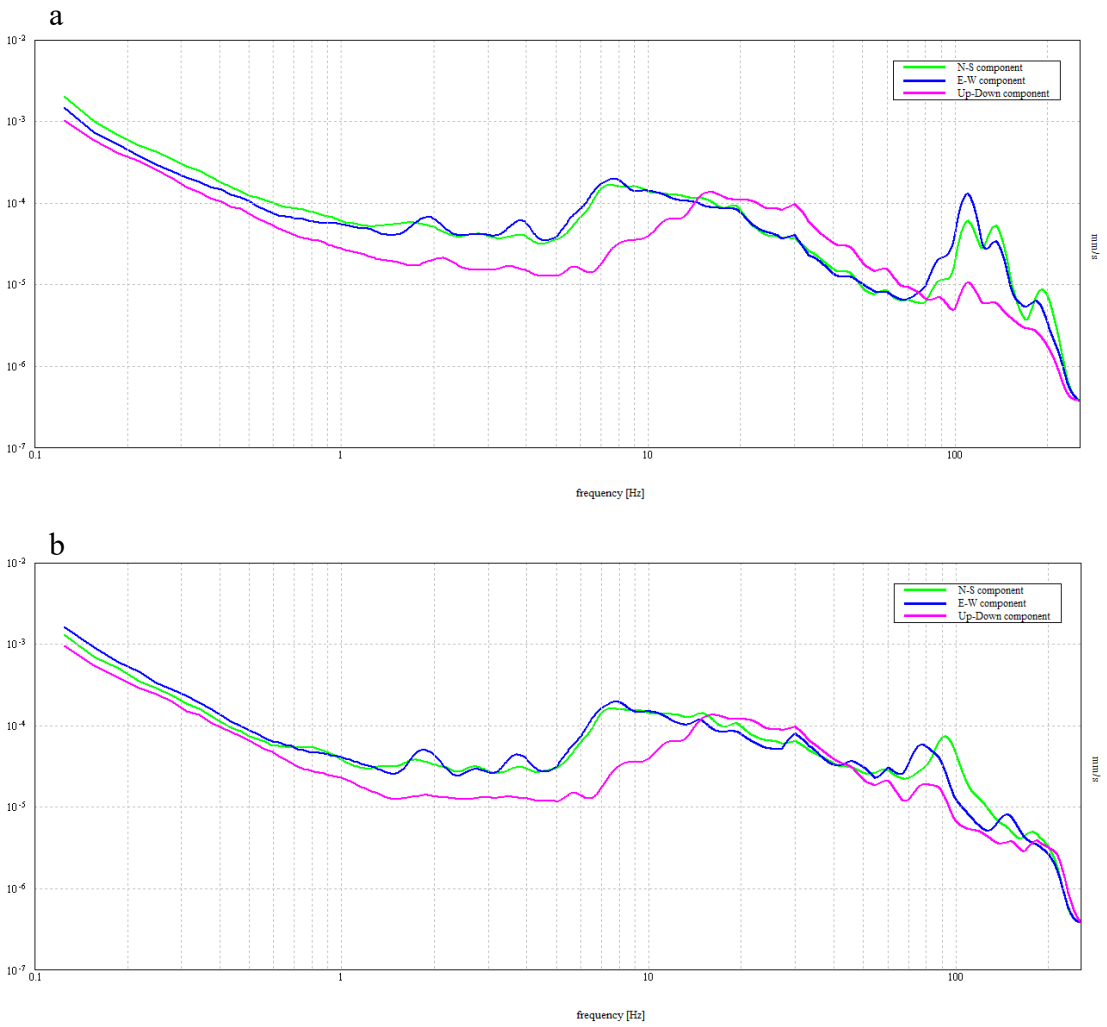

Figure C-58 MIZ Quad Site 1 site, Test 4, concrete (a), grass (b)

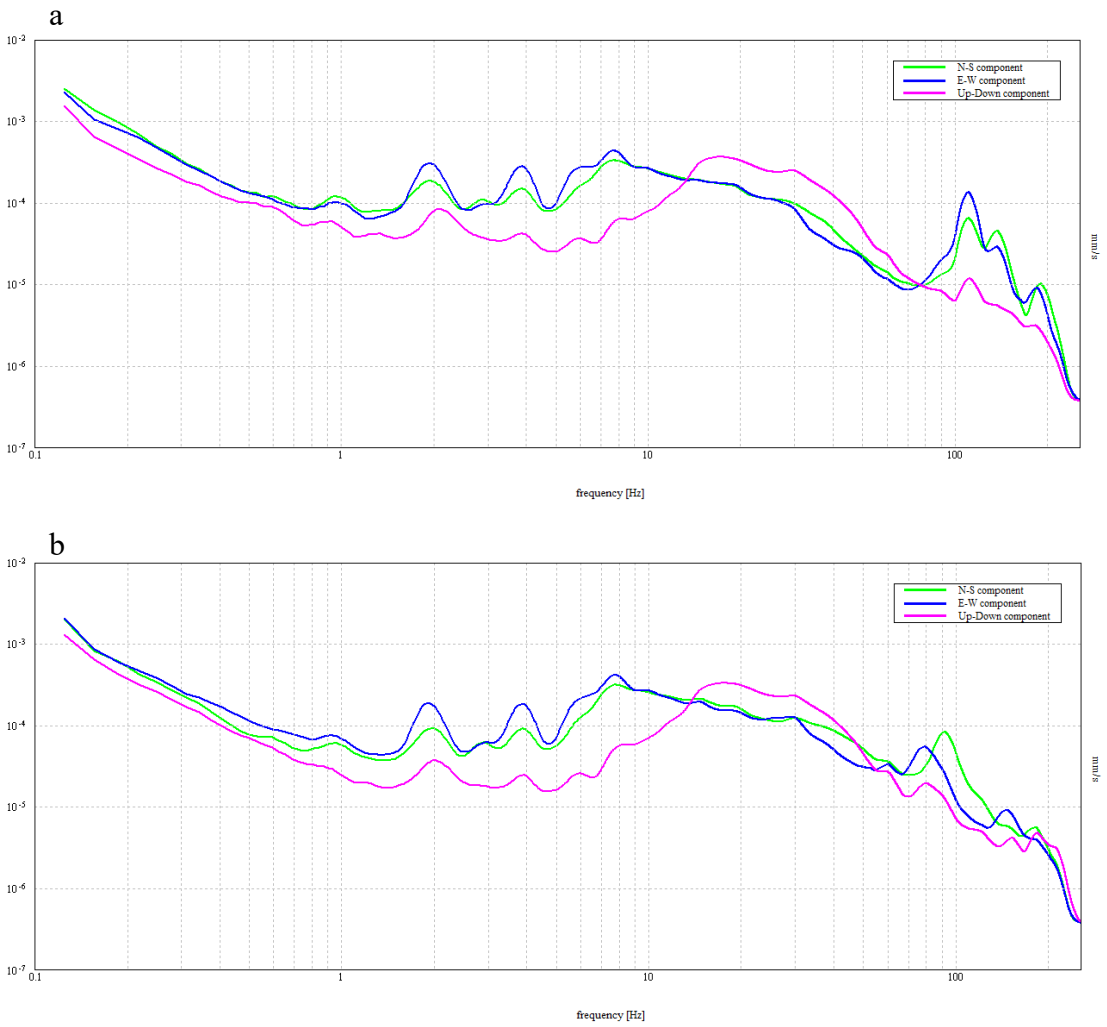

Figure C-59 MIZ Quad Site 1 site, Test 5, concrete (a), grass (b)

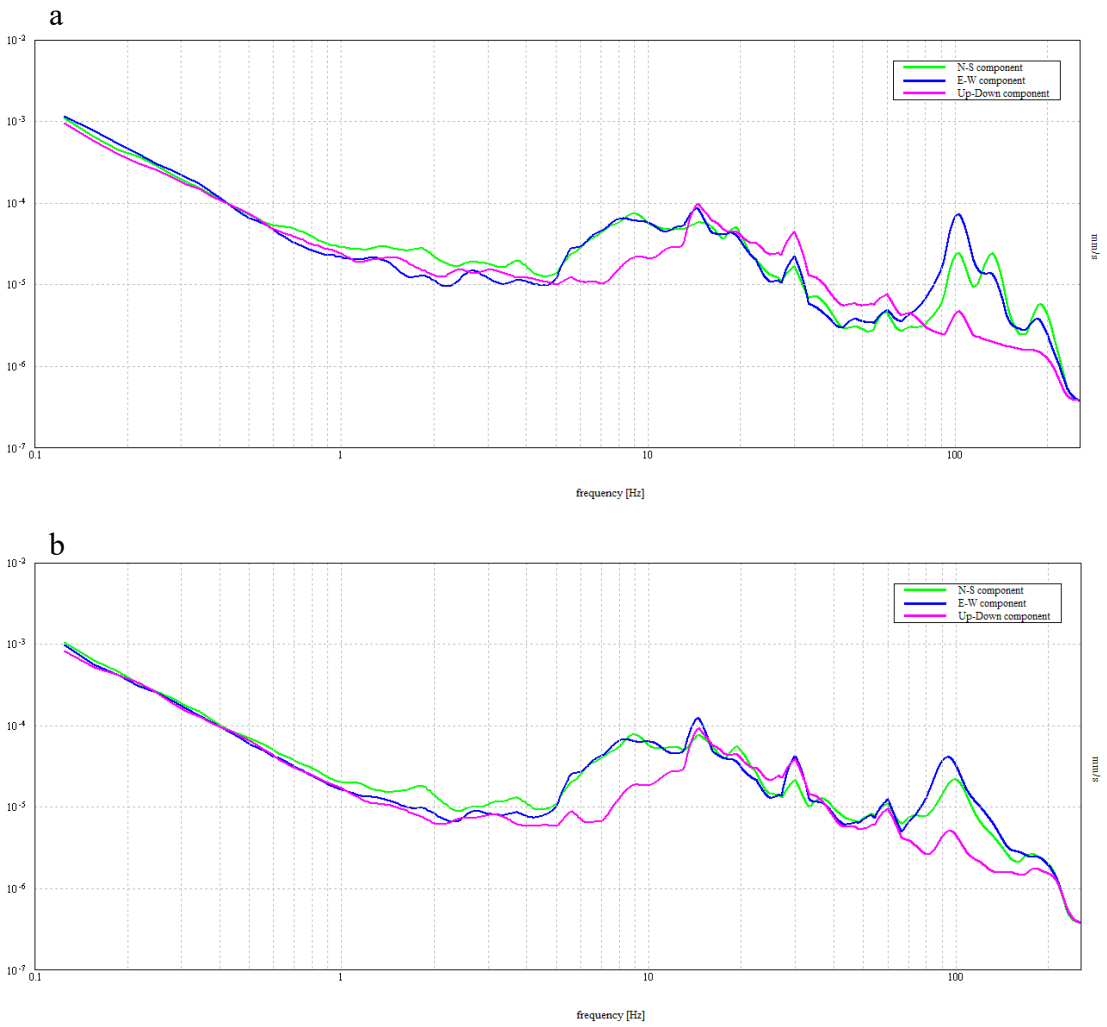

Figure C-60 MIZ Quad Site 1 site, Test 6, concrete (a), grass (b)

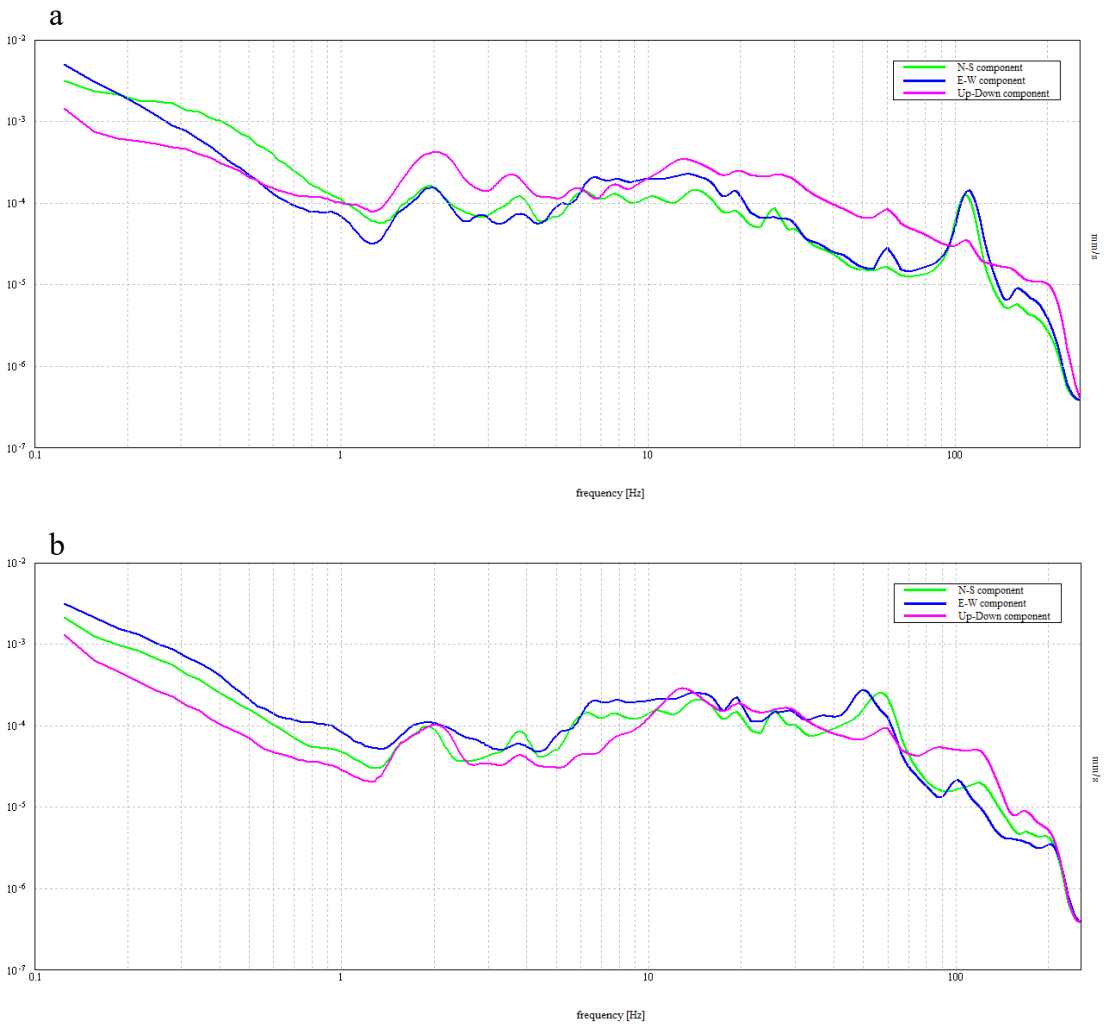

Figure C-61 MIZ Quad Site 2 site, Test 1, concrete (a), grass (b)

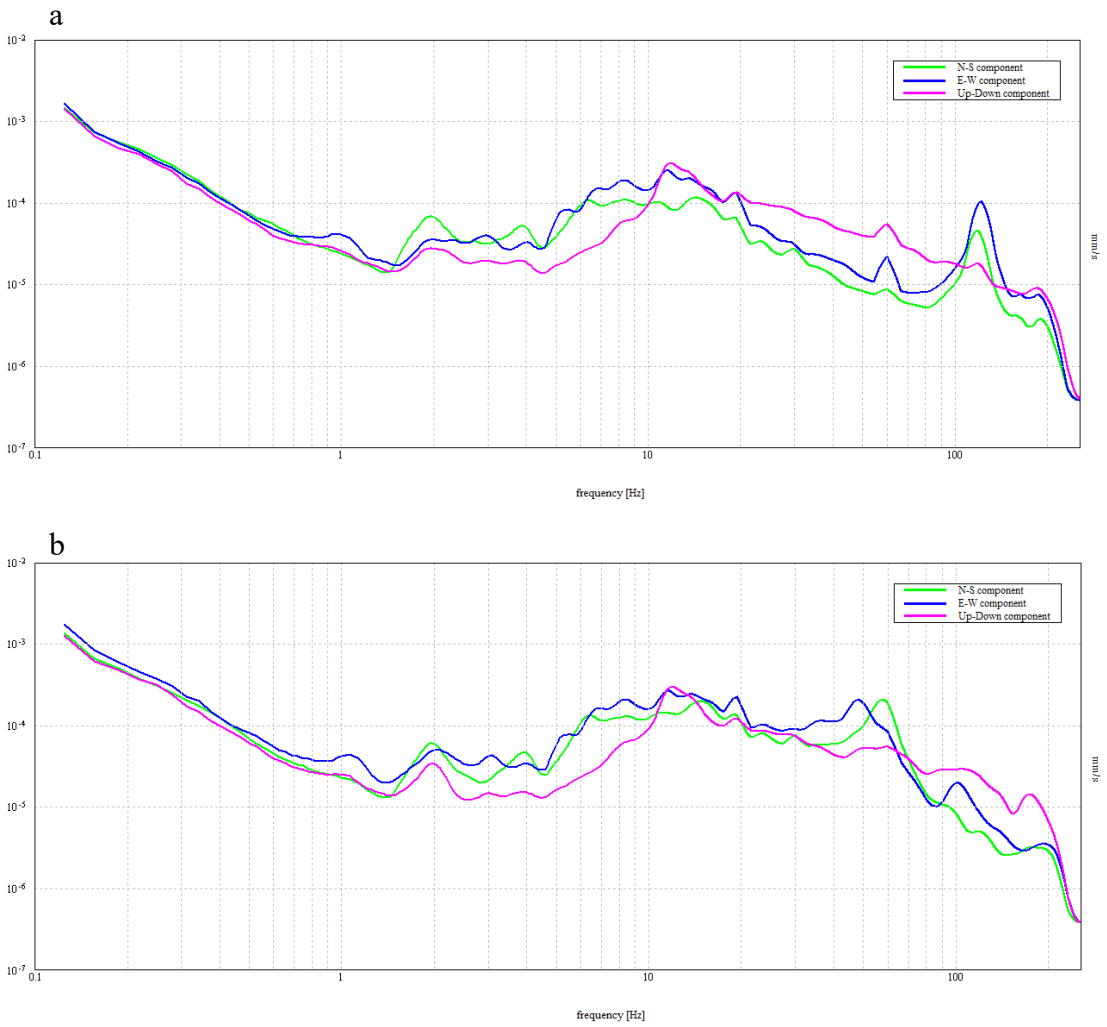

Figure C-62 MIZ Quad Site 2 site, Test 2, concrete (a), grass (b)

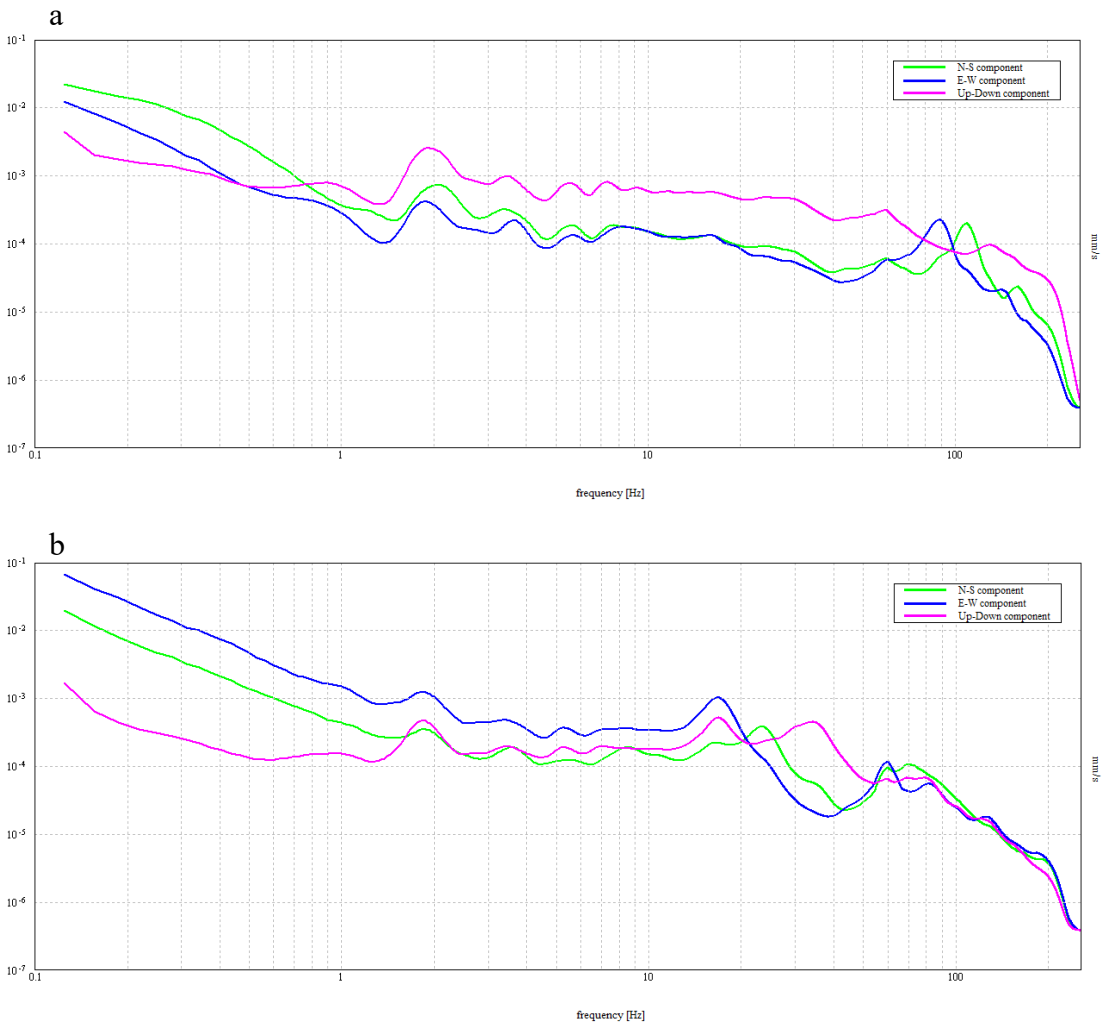

Figure C-63 MIZ Quad Site 3 site, Test 1, concrete (a), grass (b)

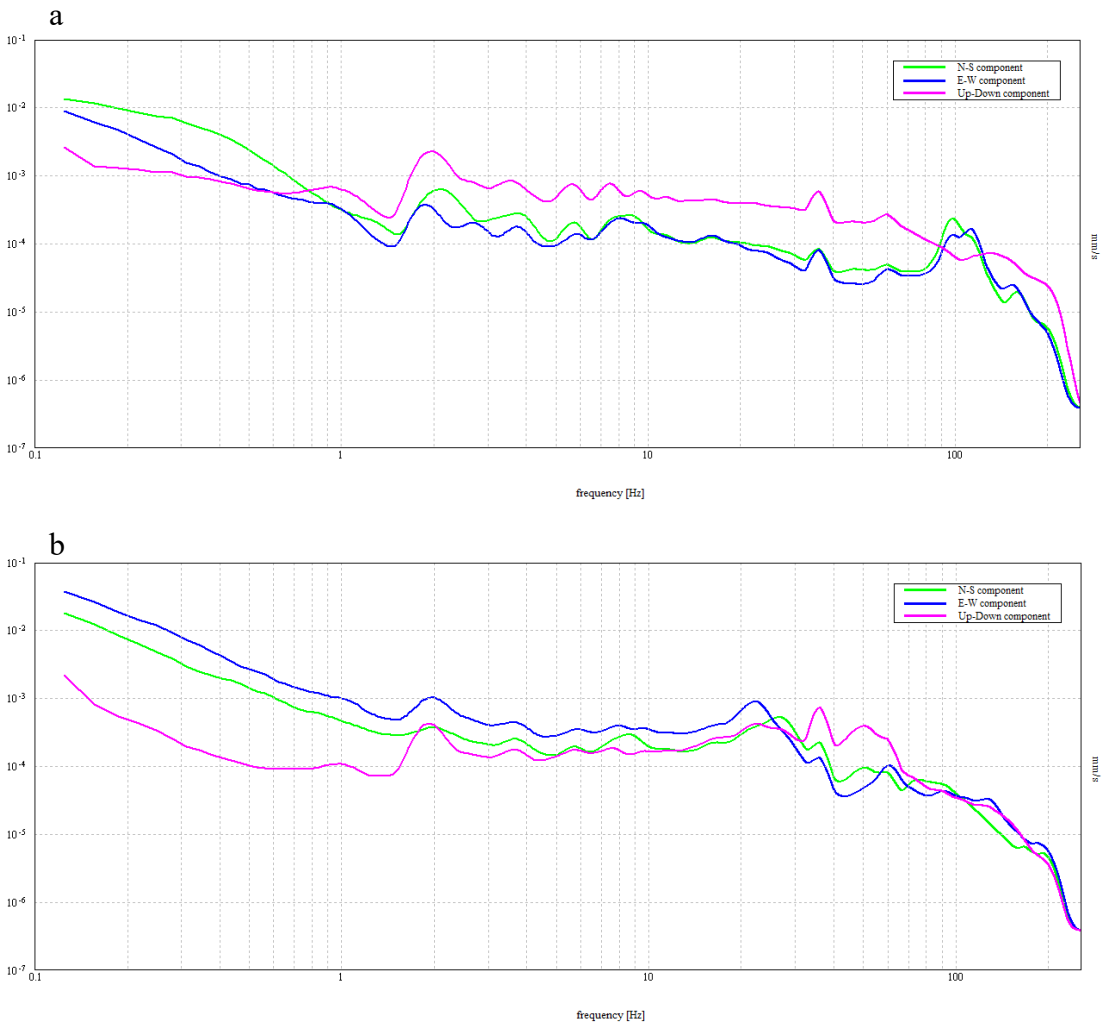

Figure C-64 MIZ Quad Site 3 site, Test 2, concrete (a), grass (b)

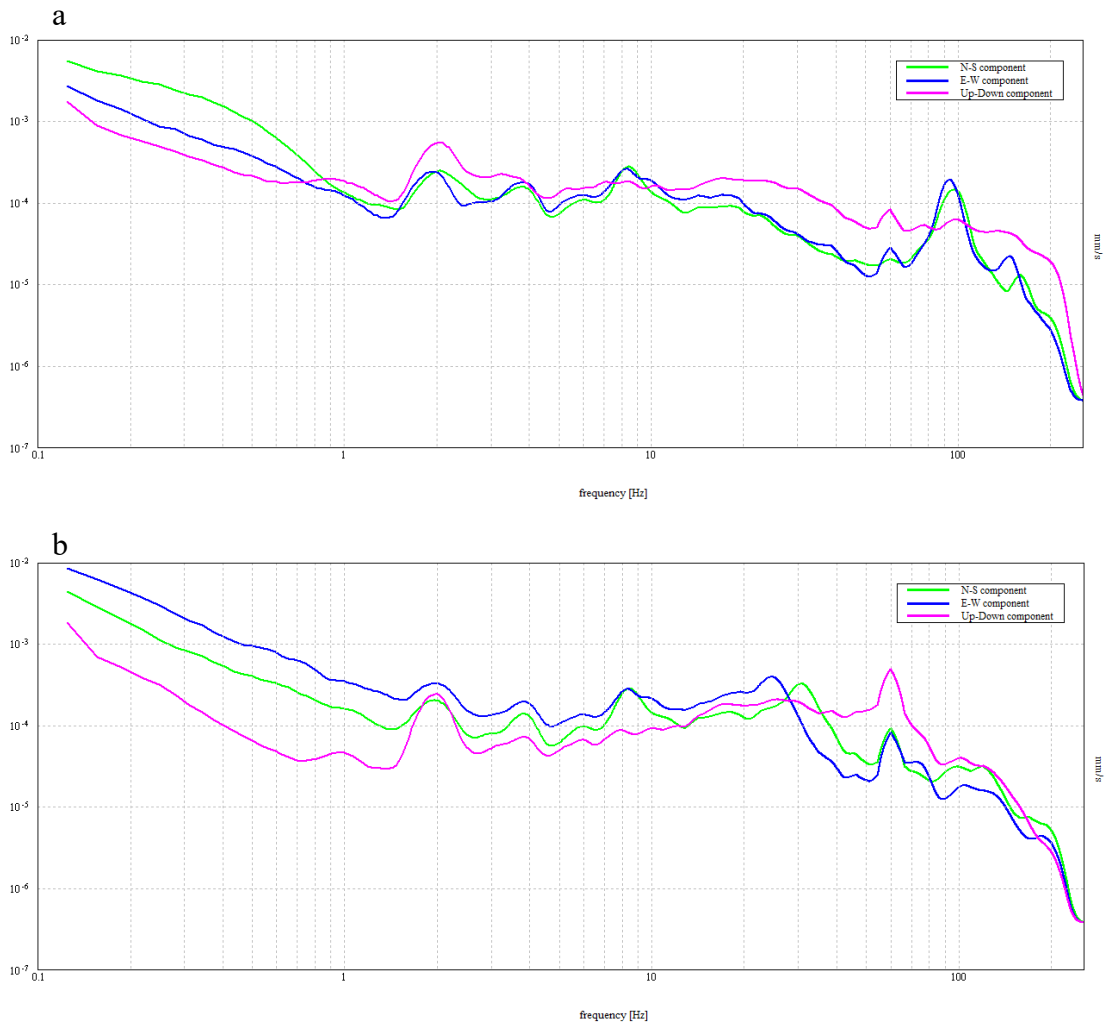

Figure C-65 MIZ Quad Site 3 site, Test 3, concrete (a), grass (b)

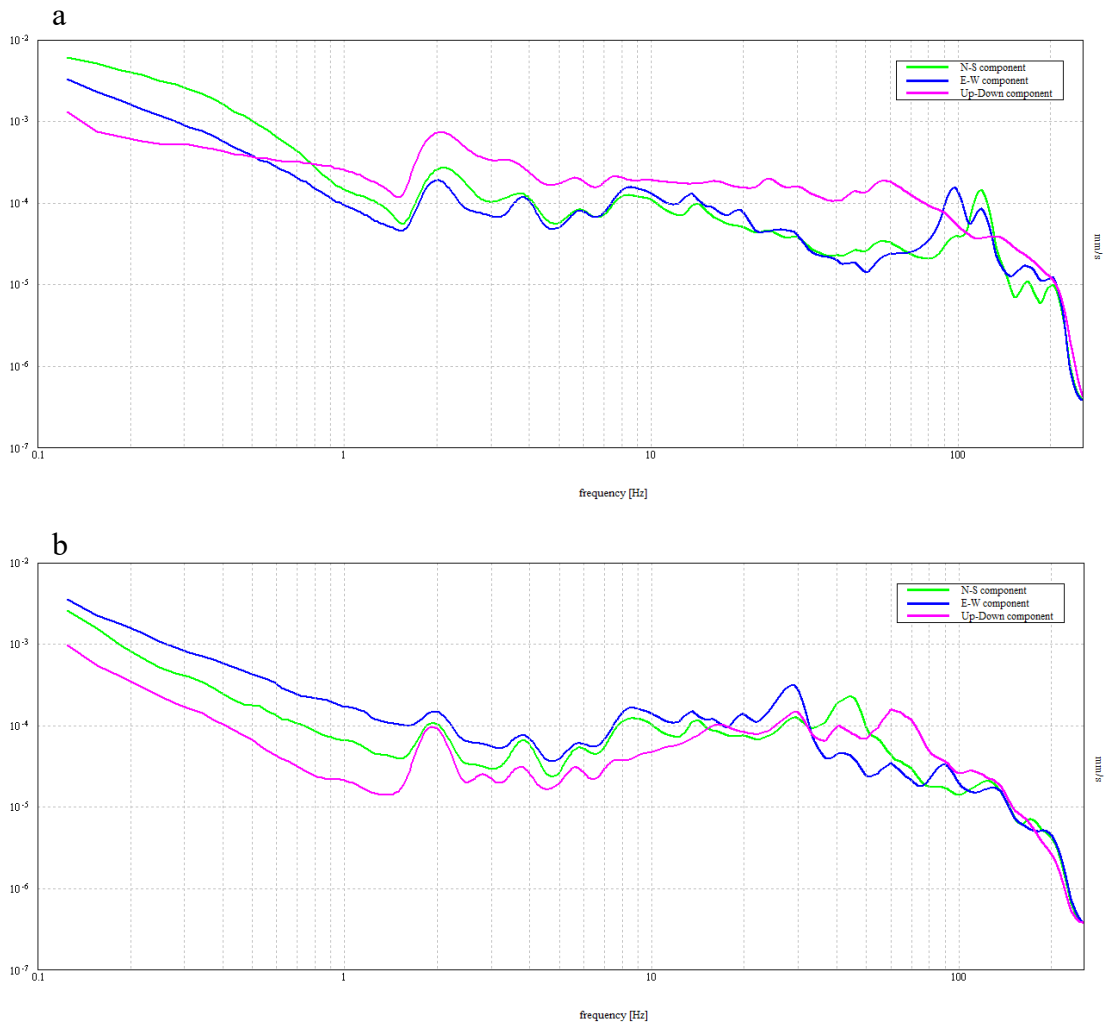

Figure C-66 MIZ Quad Site 3 site, Test 4, concrete (a), grass (b)

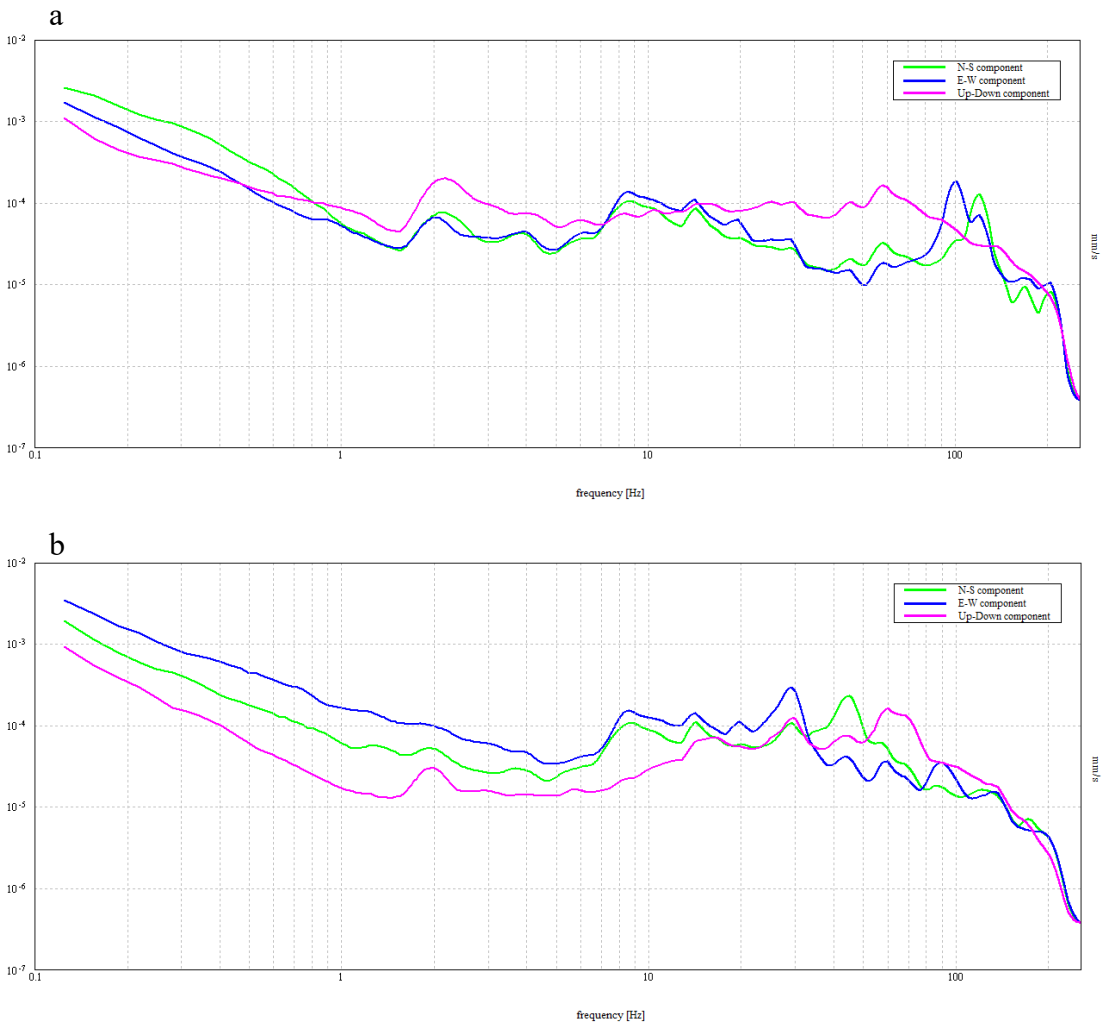

Figure C-67 MIZ Quad Site 3 site, Test 5, concrete (a), grass (b)

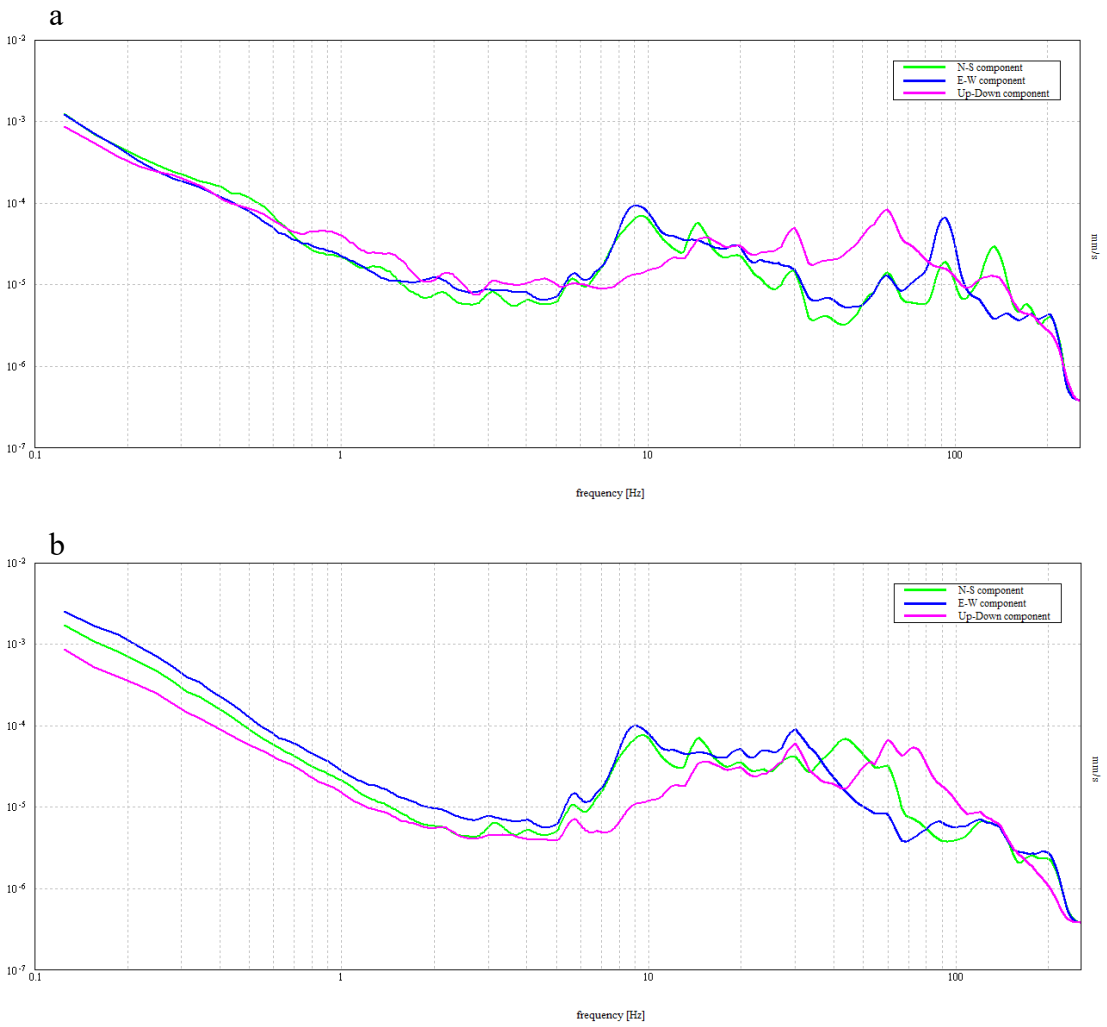

Figure C-68 MIZ Quad Site 3 site, Test 6, concrete (a), grass (b)

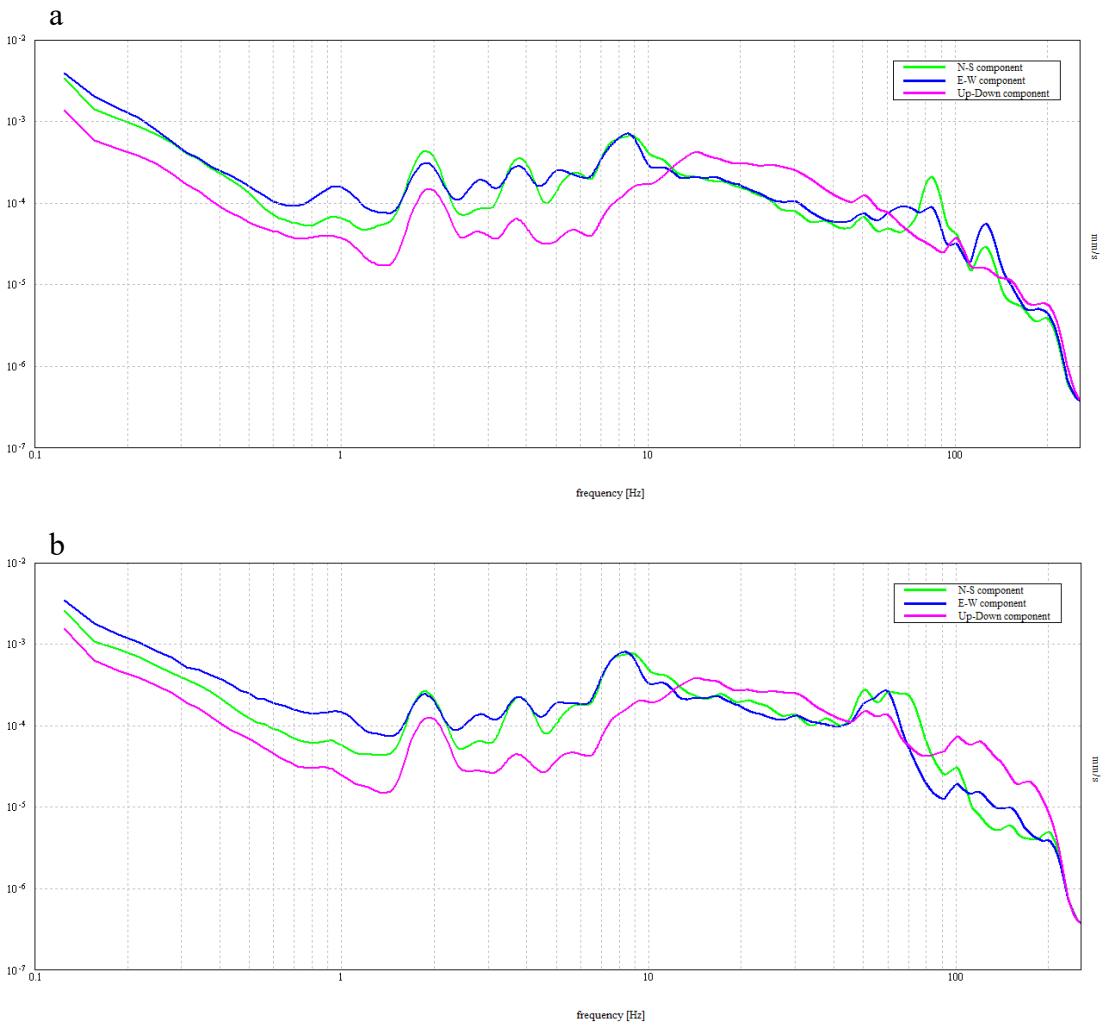

Figure C-69 MIZ Quad Site 4 site, Test 1, concrete (a), grass (b)

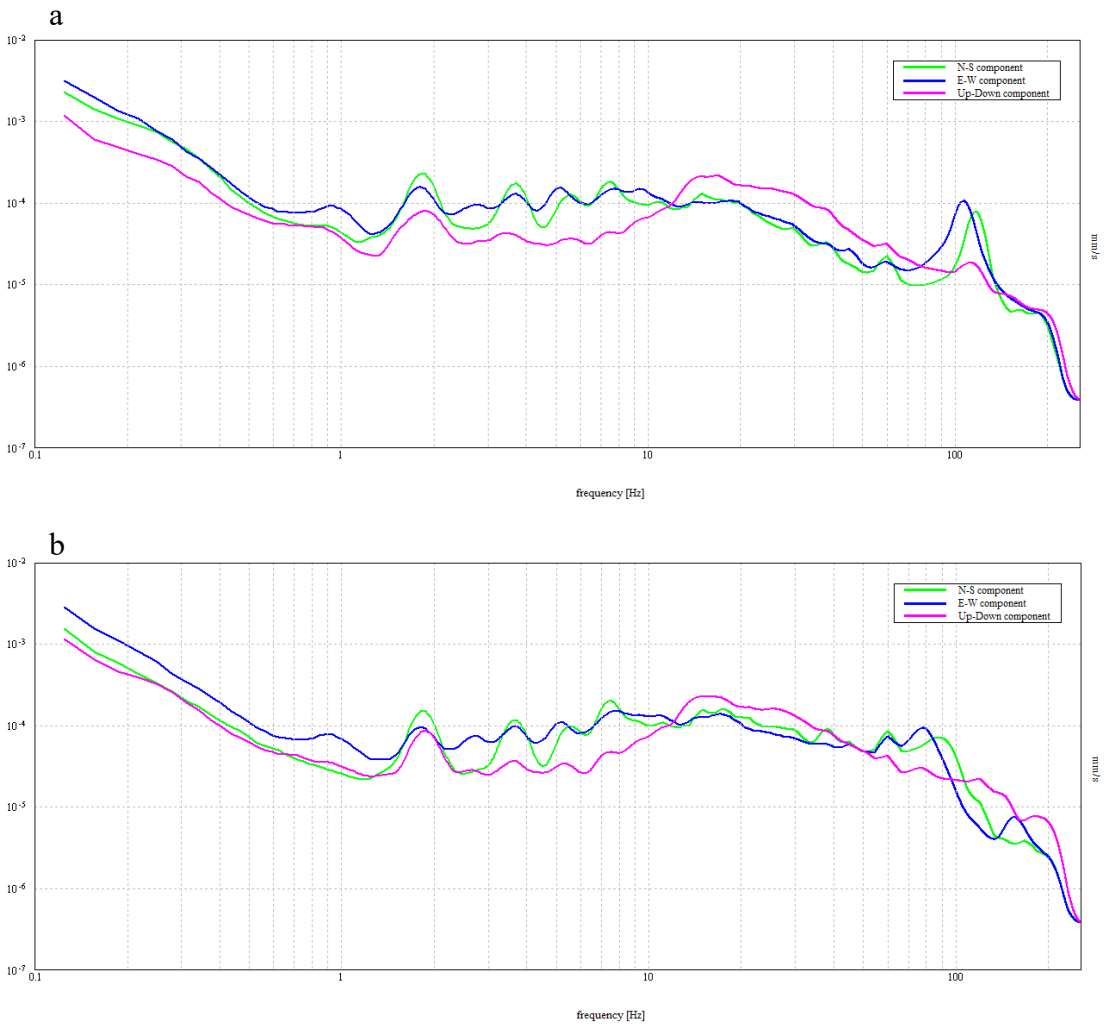

Figure C-70 MIZ Quad Site 4 site, Test 2, concrete (a), grass (b)

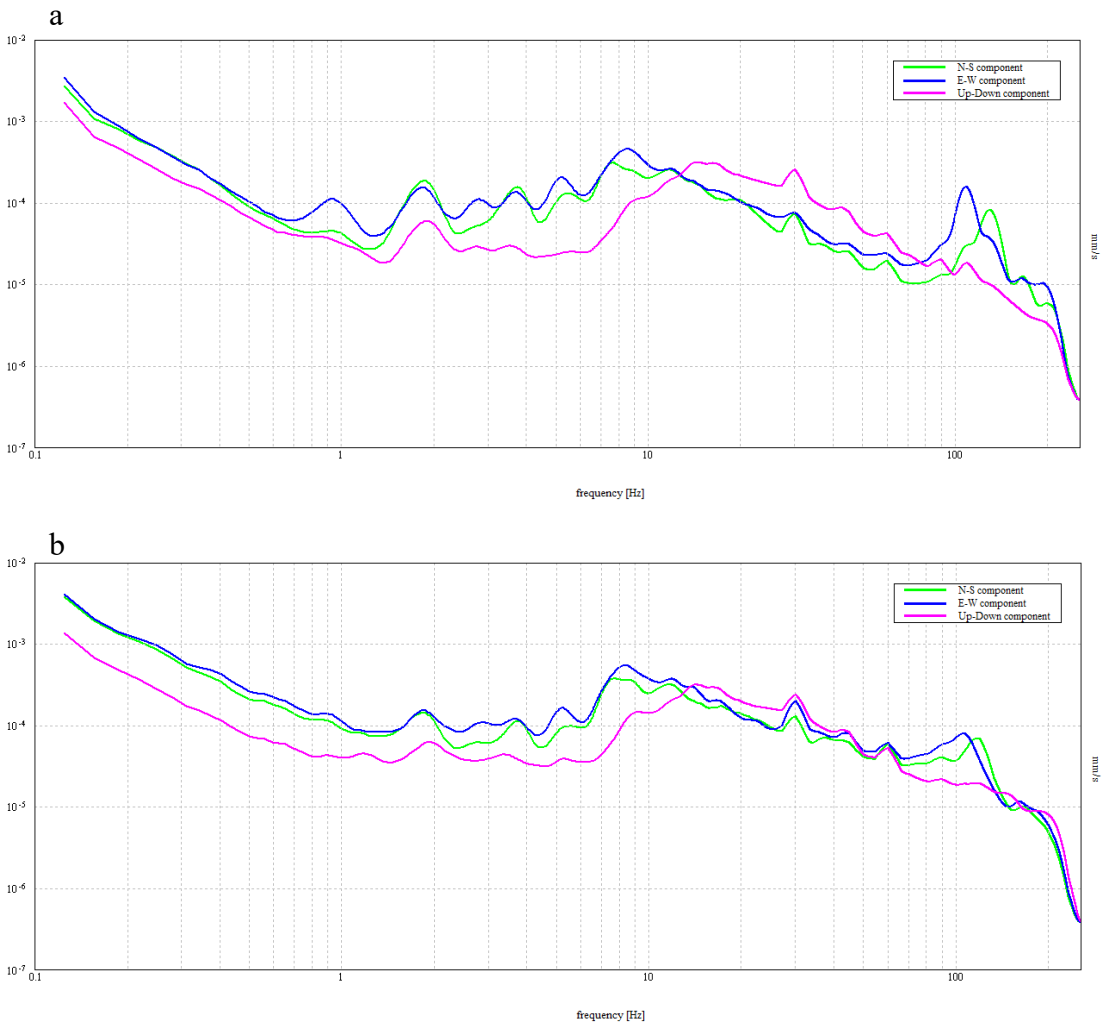

Figure C-71 MIZ Quad Site 4 site, Test 3, concrete (a), grass (b)

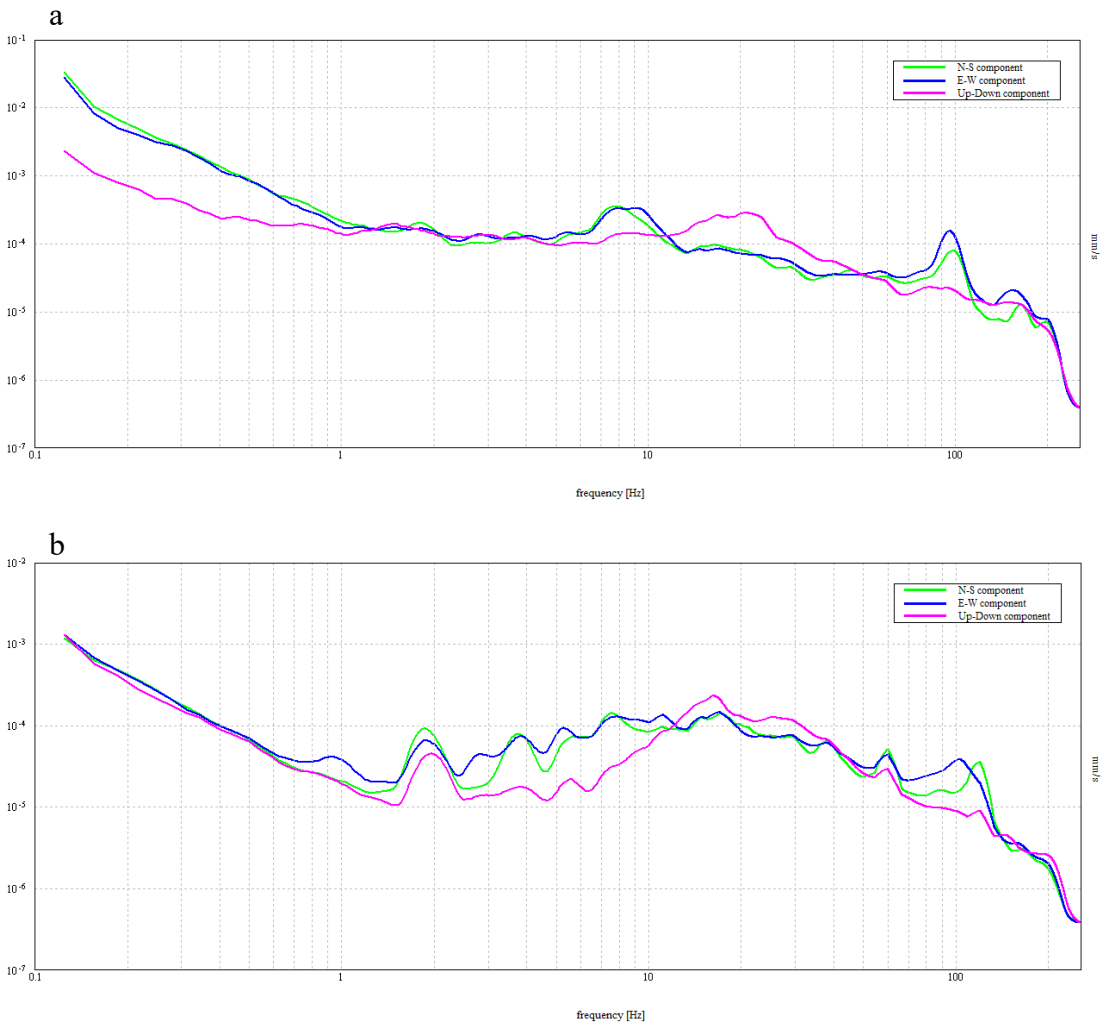

Figure C-72 MIZ Quad Site 4 site, Test 4, concrete (a), grass (b)

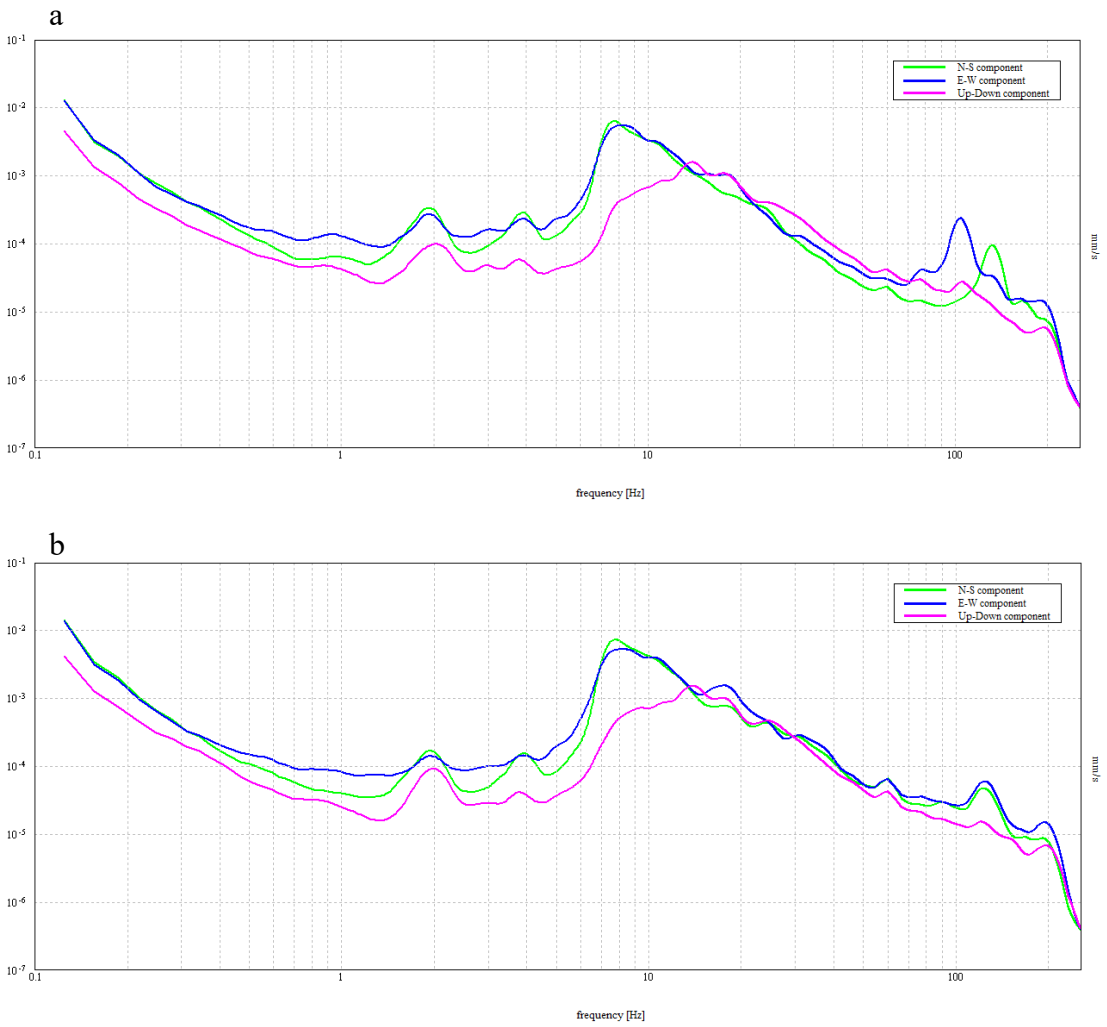

Figure C-73 MIZ Quad Site 4 site, Test 5, concrete (a), grass (b)

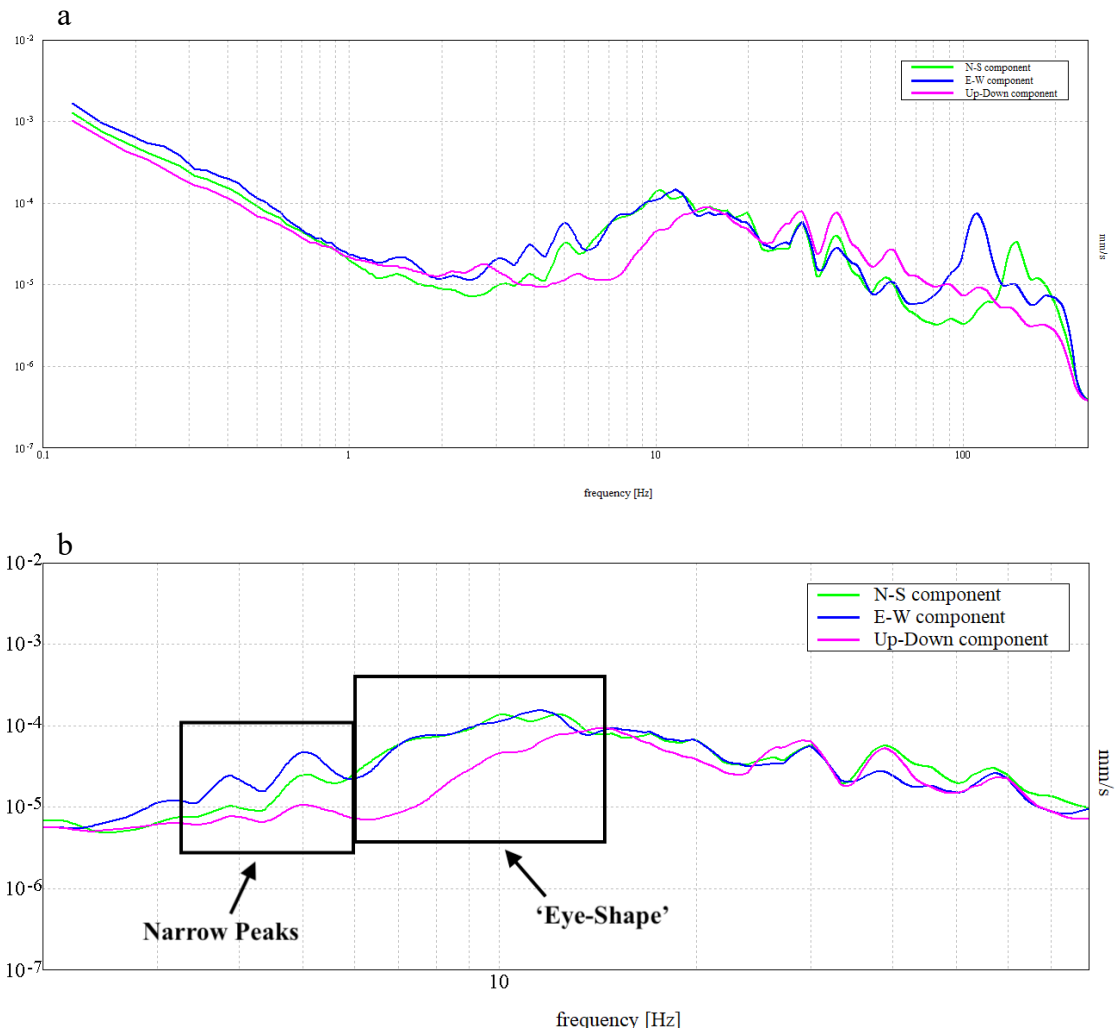

Figure C-74 MIZ Quad Site 4 site, Test 6, concrete (a), grass (b)

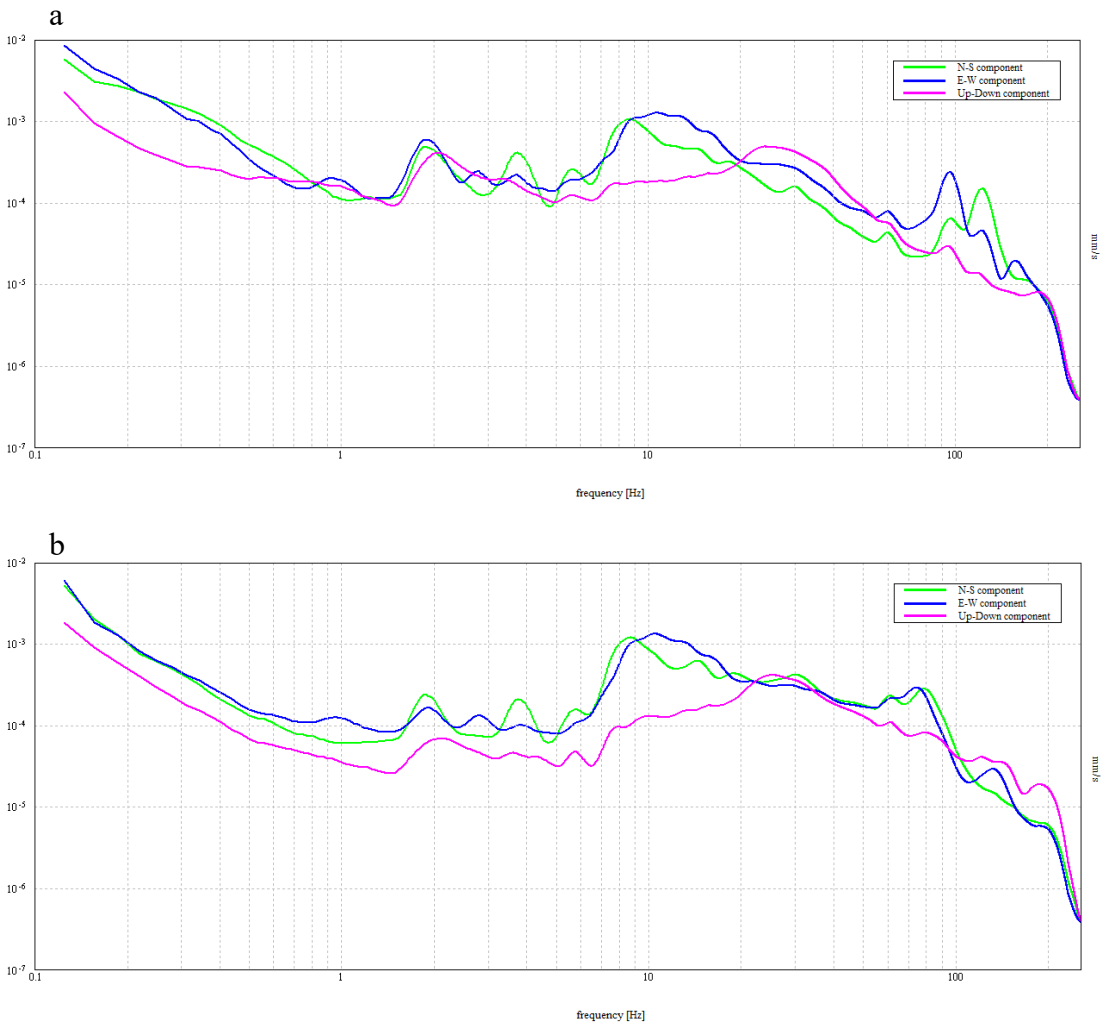

Figure C-75 MIZ Quad Site 5 site, Test 1, concrete (a), grass (b)

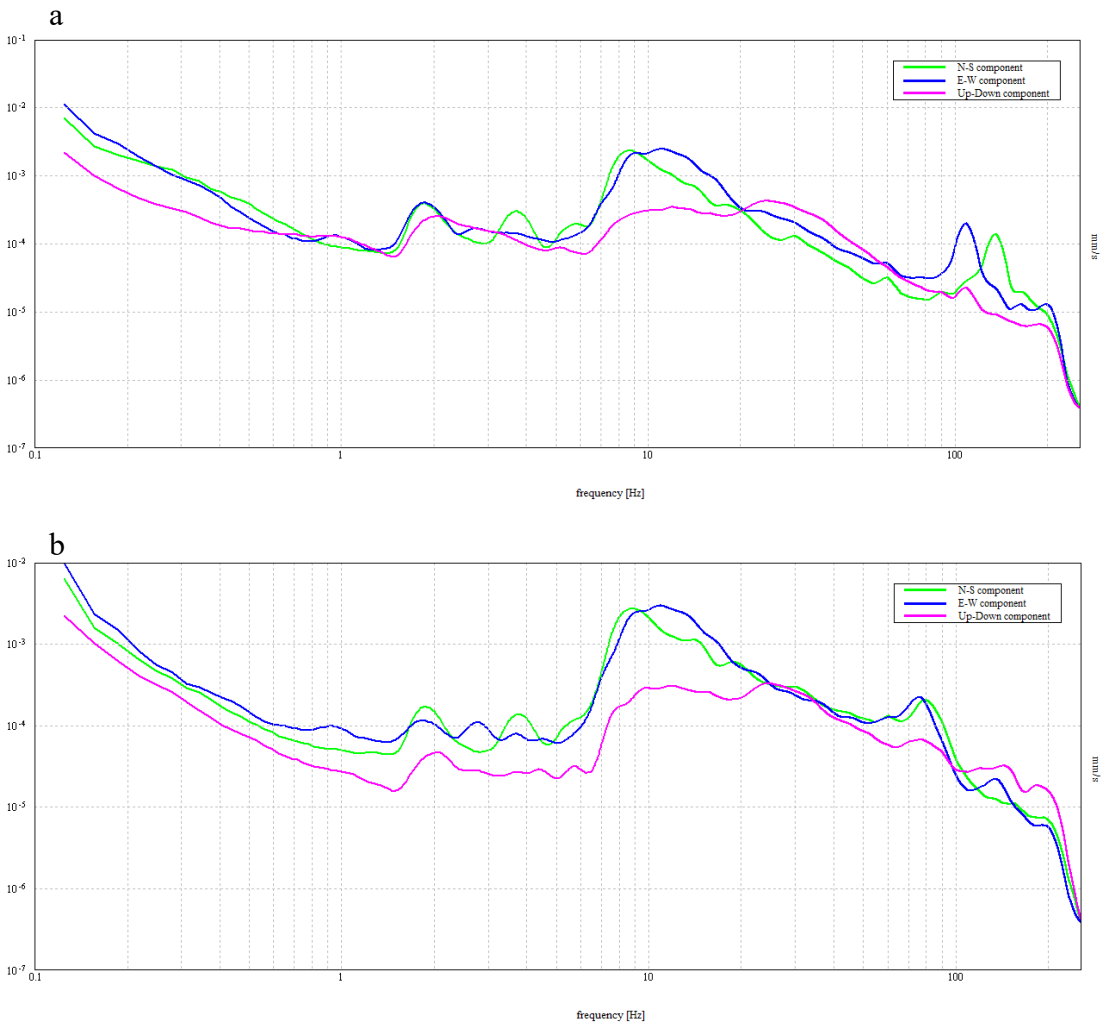

Figure C-76 MIZ Quad Site 5 site, Test 2, concrete (a), grass (b)

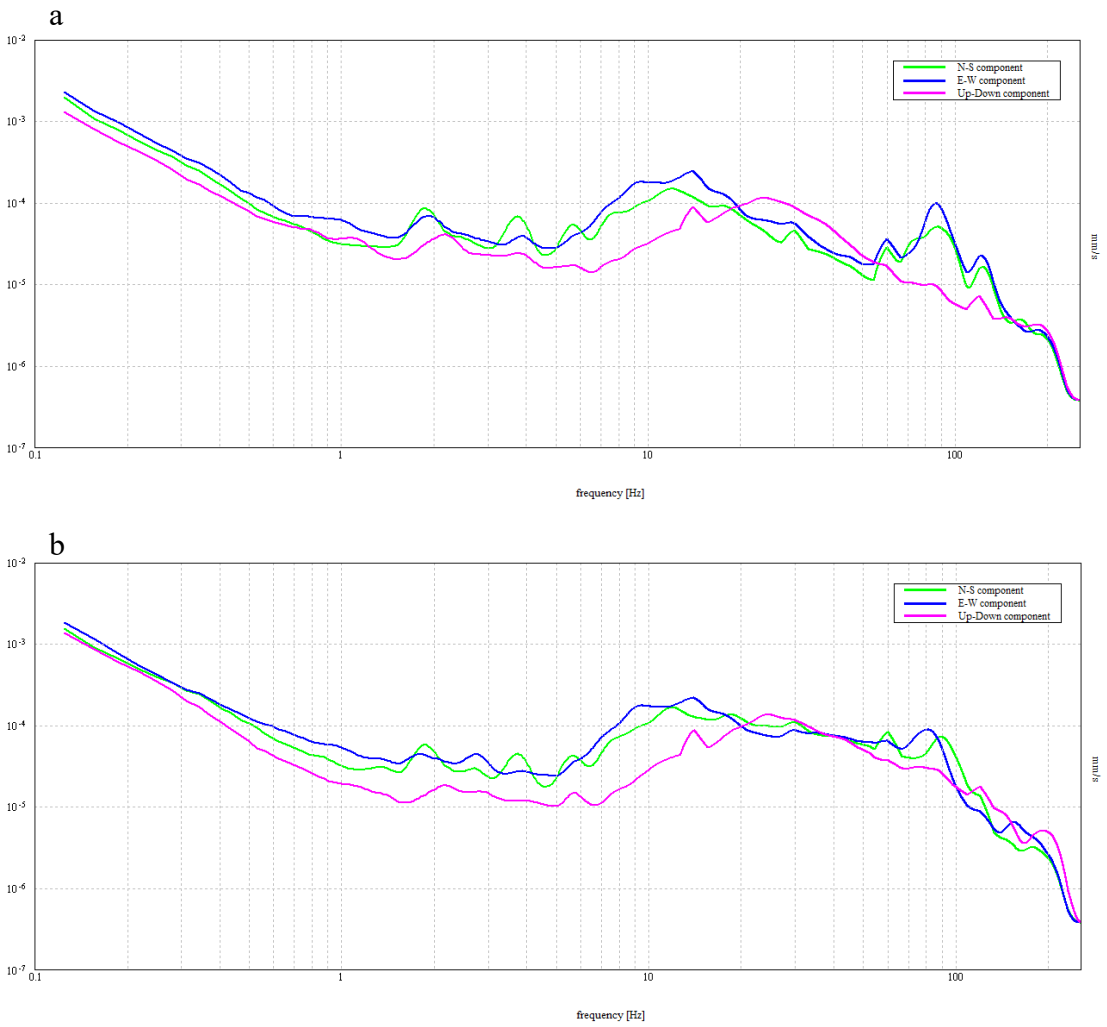

Figure C-77 MIZ Quad Site 5 site, Test 3, concrete (a), grass (b)

APPENDIX D

Time Rec

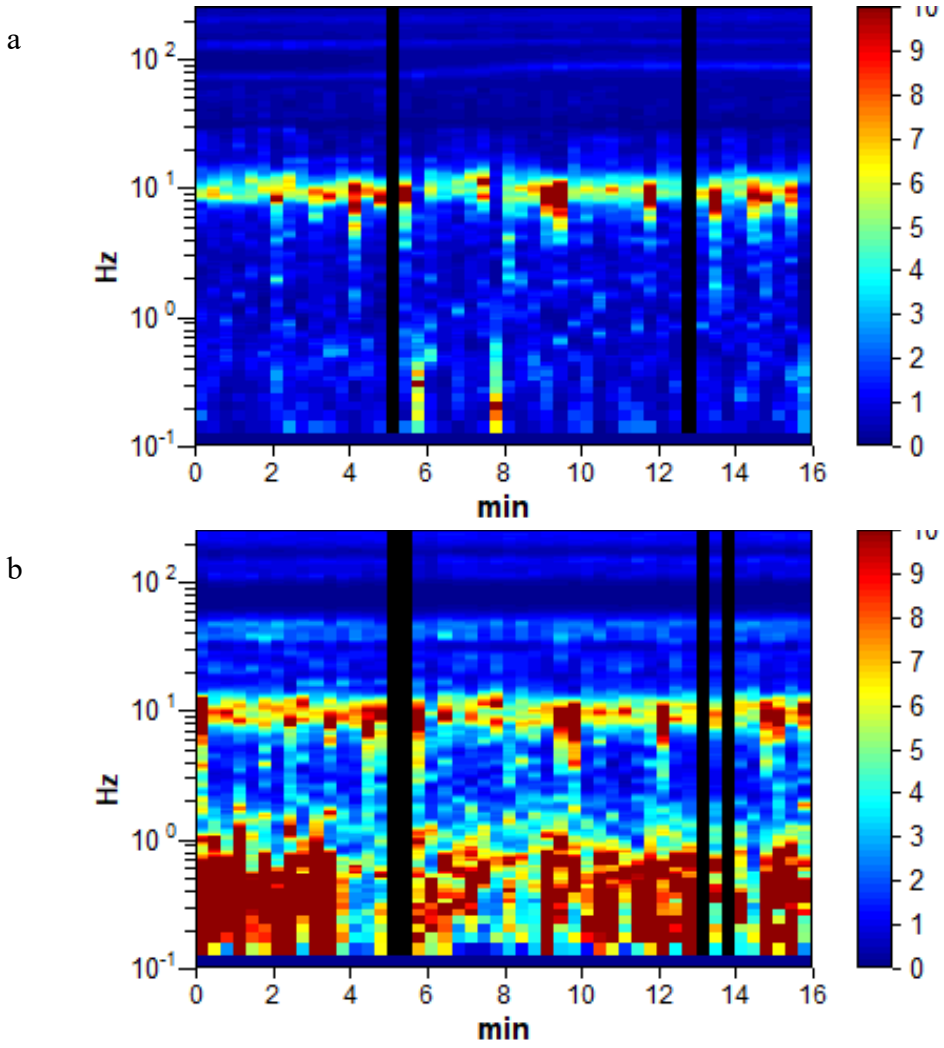

Figure D-1 Animal Hospital 1 site, Test 1, concrete (a), grass (b)

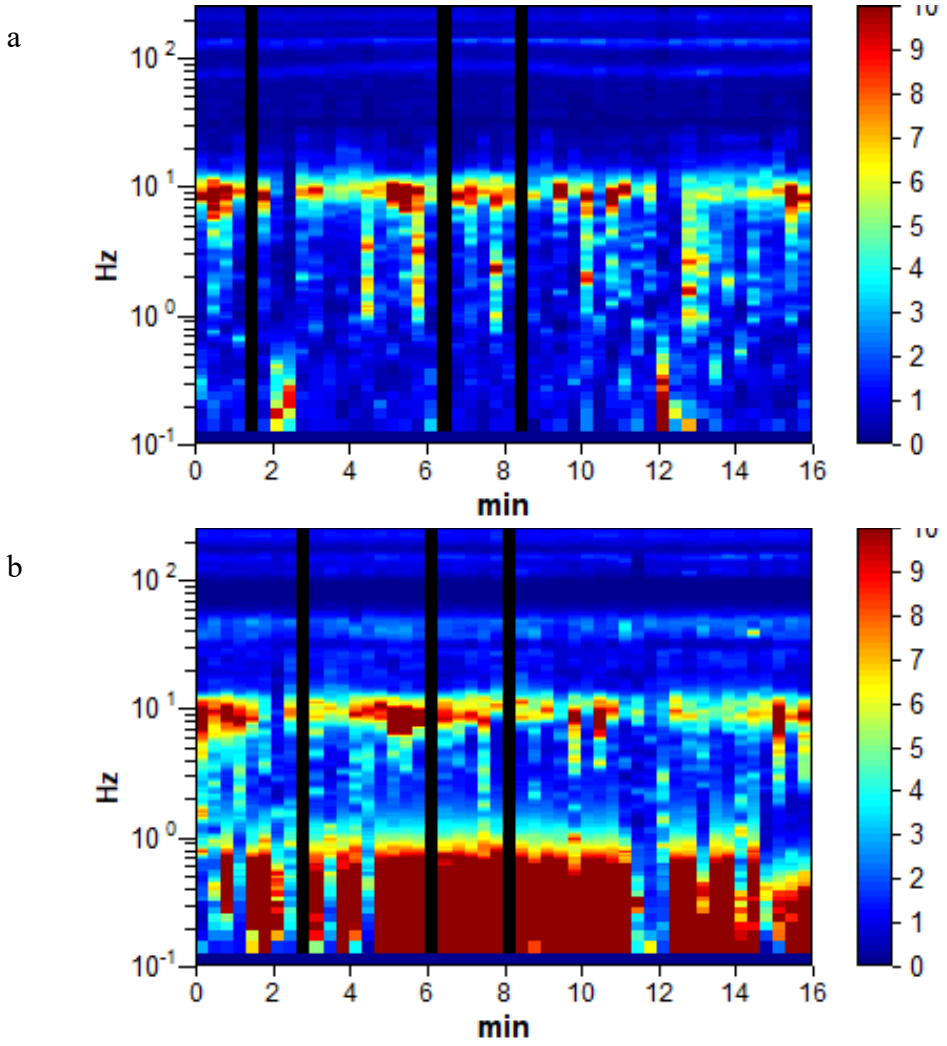

Figure D-2 Animal Hospital 1 site, Test 2, concrete (a), grass (b)

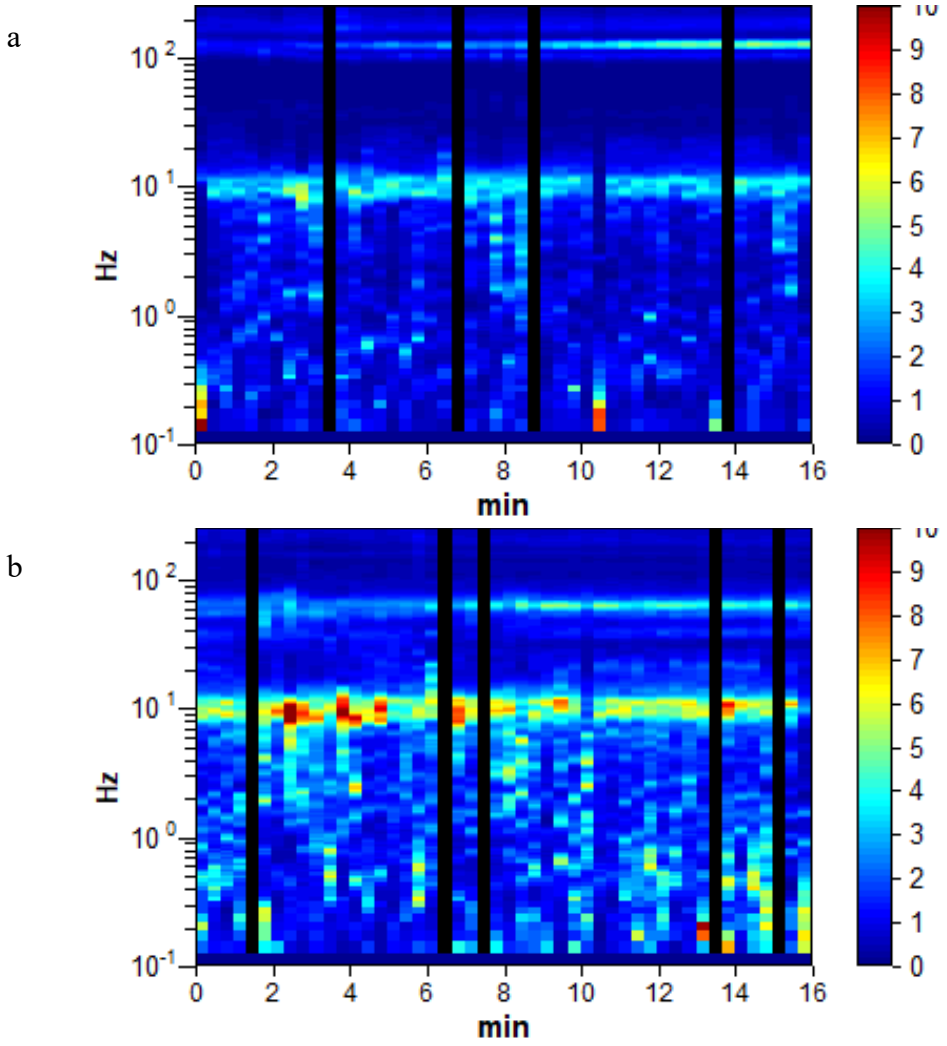

Figure D-3 Animal Hospital 1 site, Test 3, concrete (a), grass (b)

a

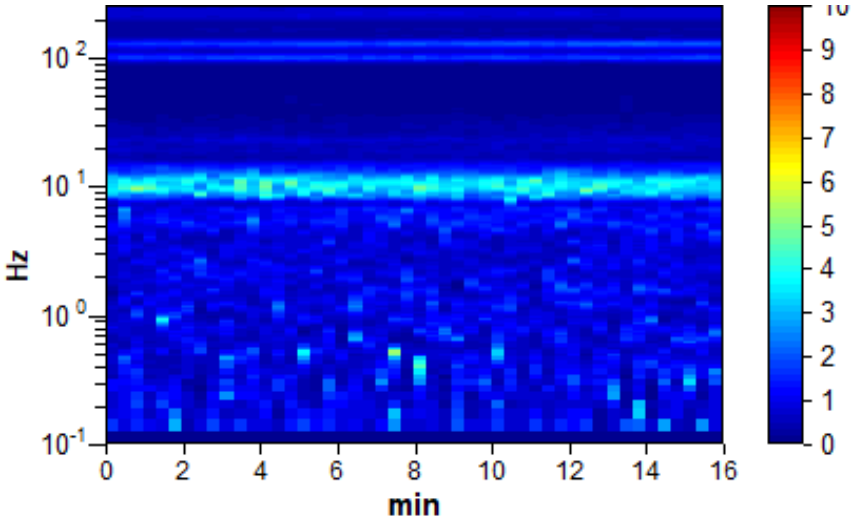

b

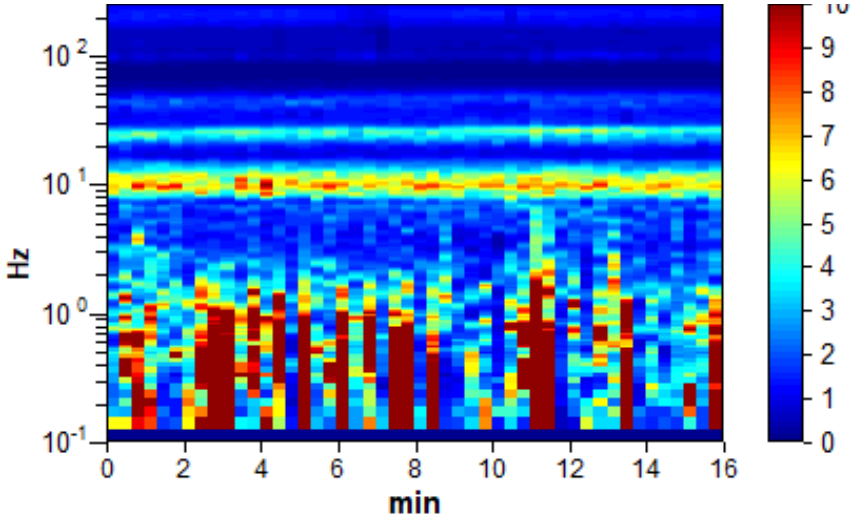

Figure D-4 Animal Hospital 1 site, Test 4, concrete (a), grass (b)

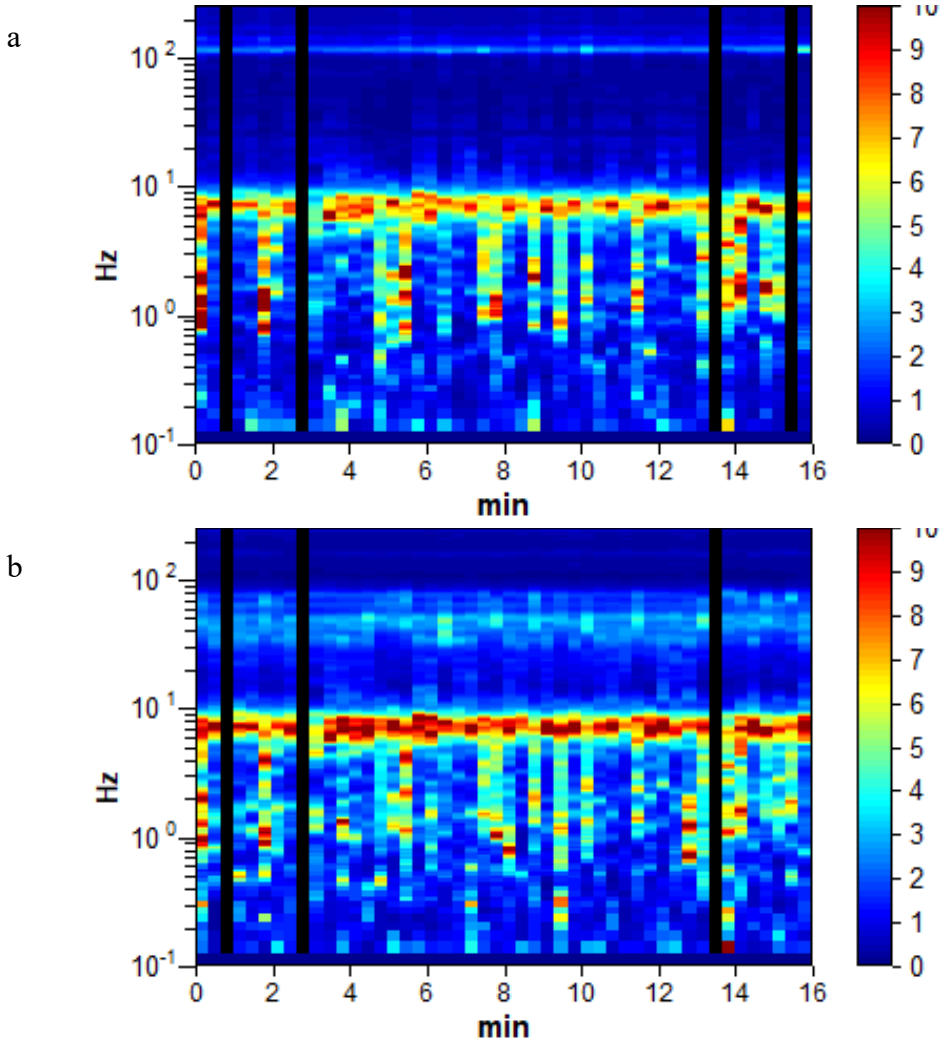

Figure D-5 Animal Hospital 2 site, Test 1, concrete (a), grass (b)

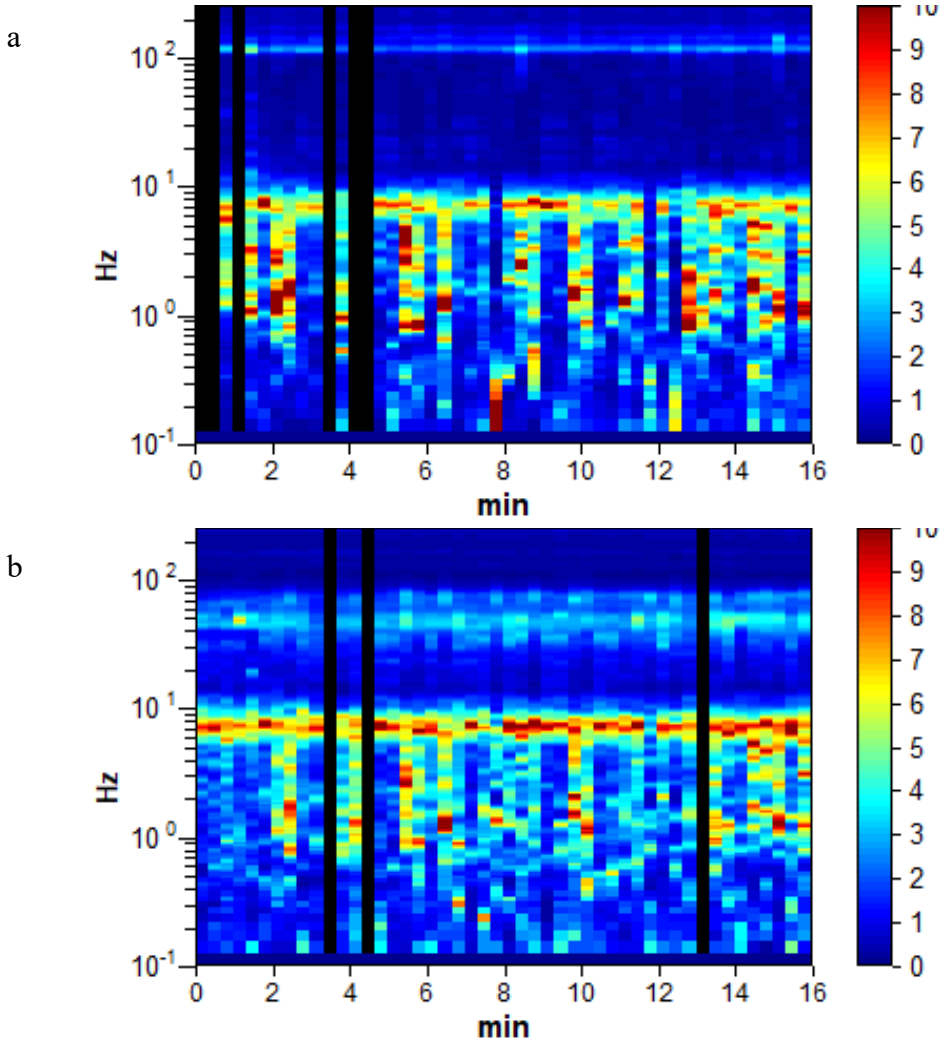

Figure D-6 Animal Hospital 2 site, Test 2, concrete (a), grass (b)

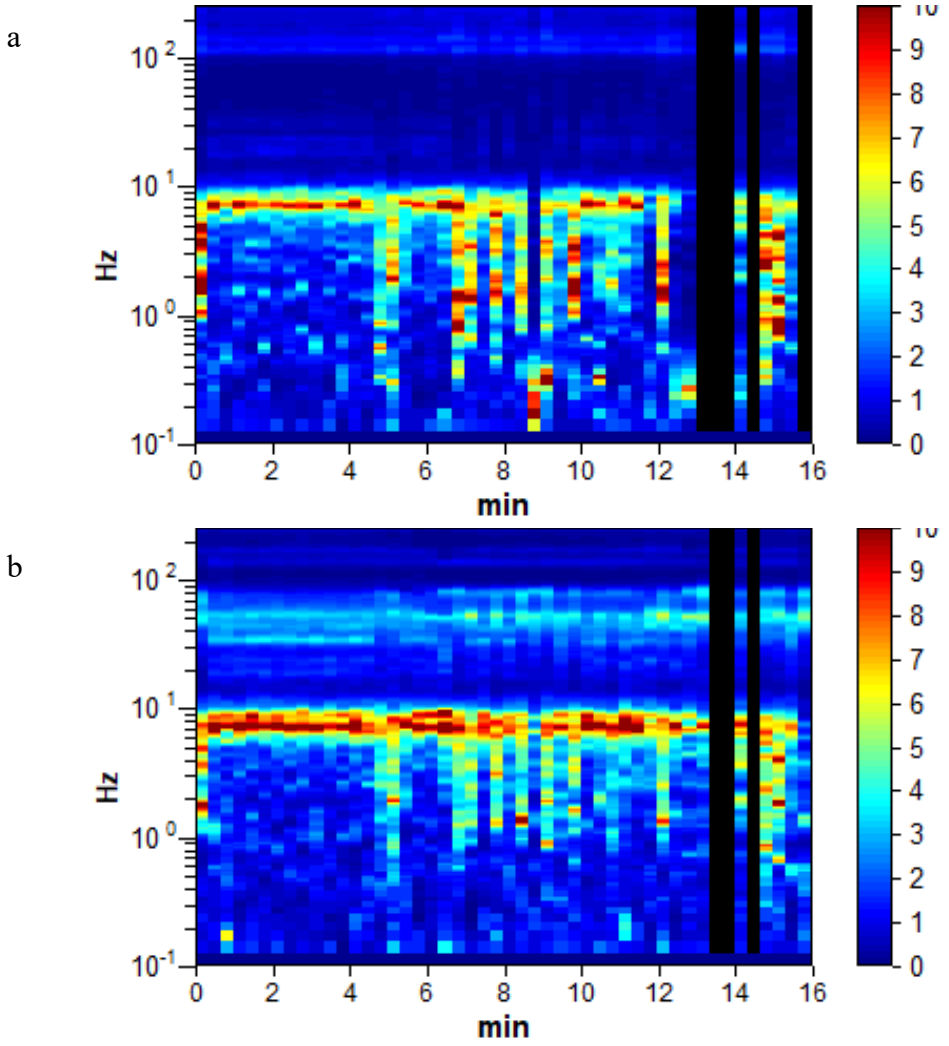

Figure D-7 Animal Hospital 2 site, Test 3, concrete (a), grass (b)

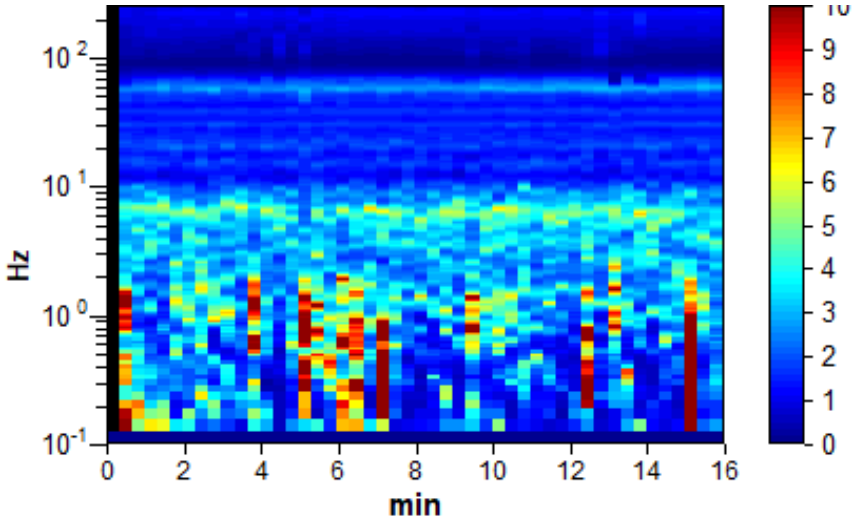

Figure D-8 Ellis Library BH-01 site, Test 1, grass

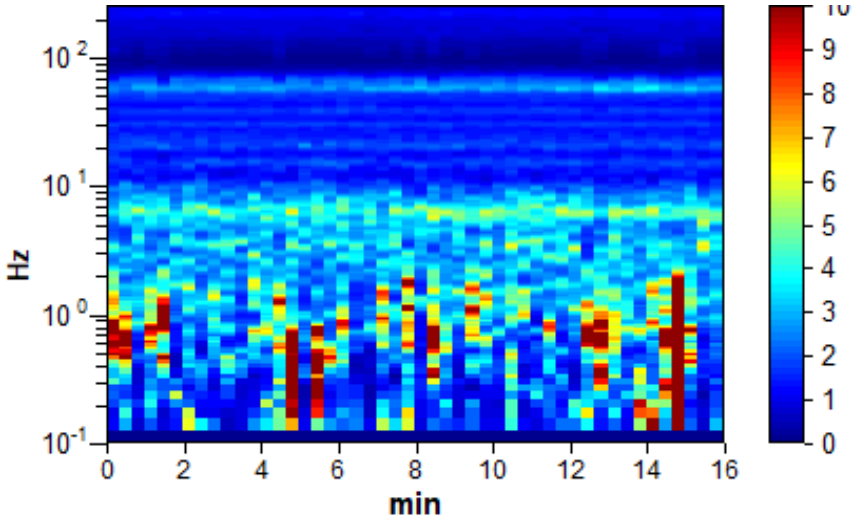

Figure D-9 Ellis Library BH-01 site, Test 2, grass

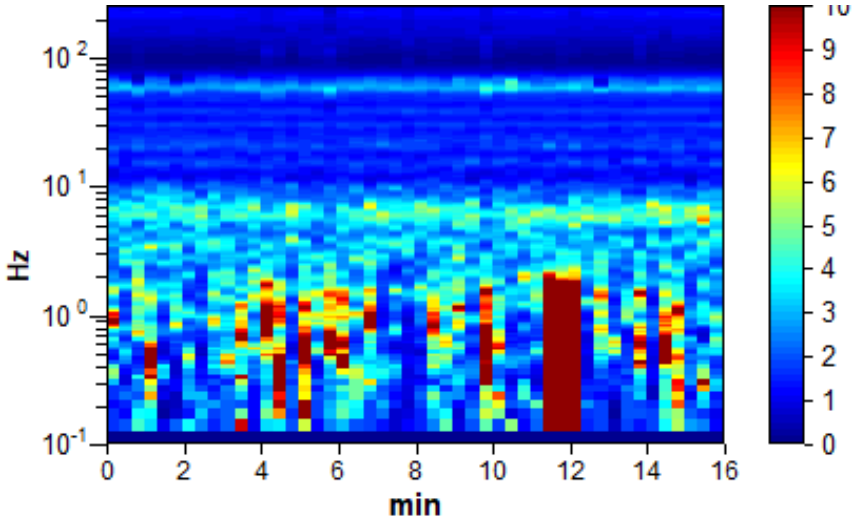

Figure D-10 Ellis Library BH-01 site, Test 3, grass

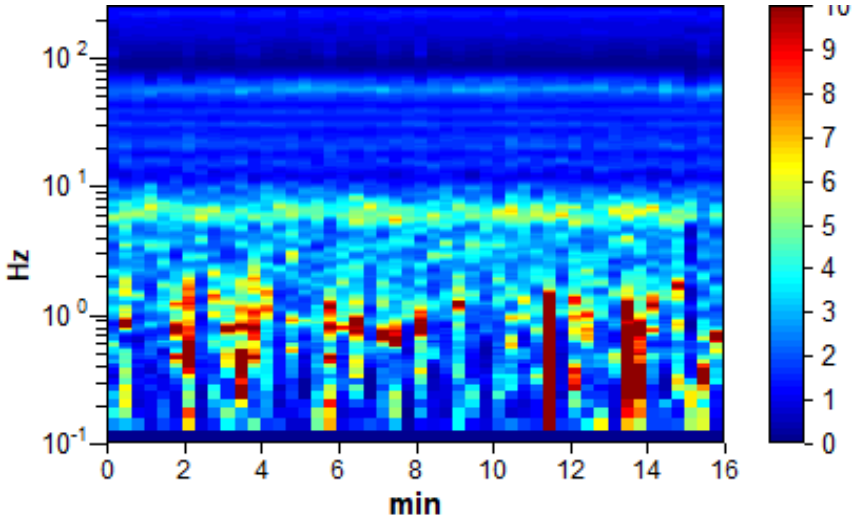

Figure D-11 Ellis Library BH-01 site, Test 4, grass

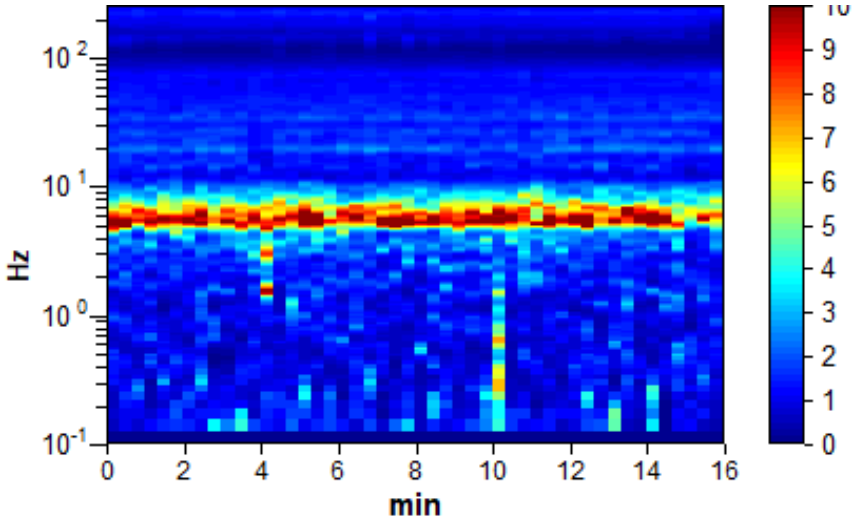

Figure D-12 Ellis Library BH-01 site, Test 5, grass

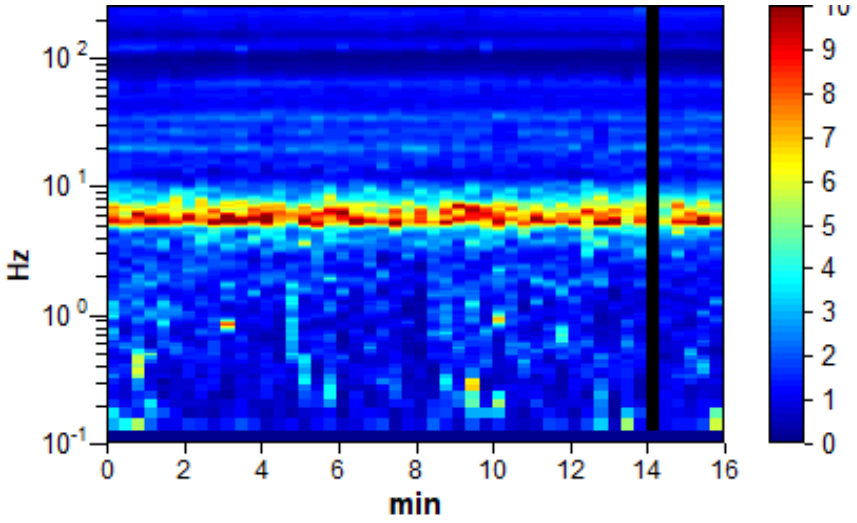

Figure D-13 Ellis Library BH-01 site, Test 6, grass

a

b

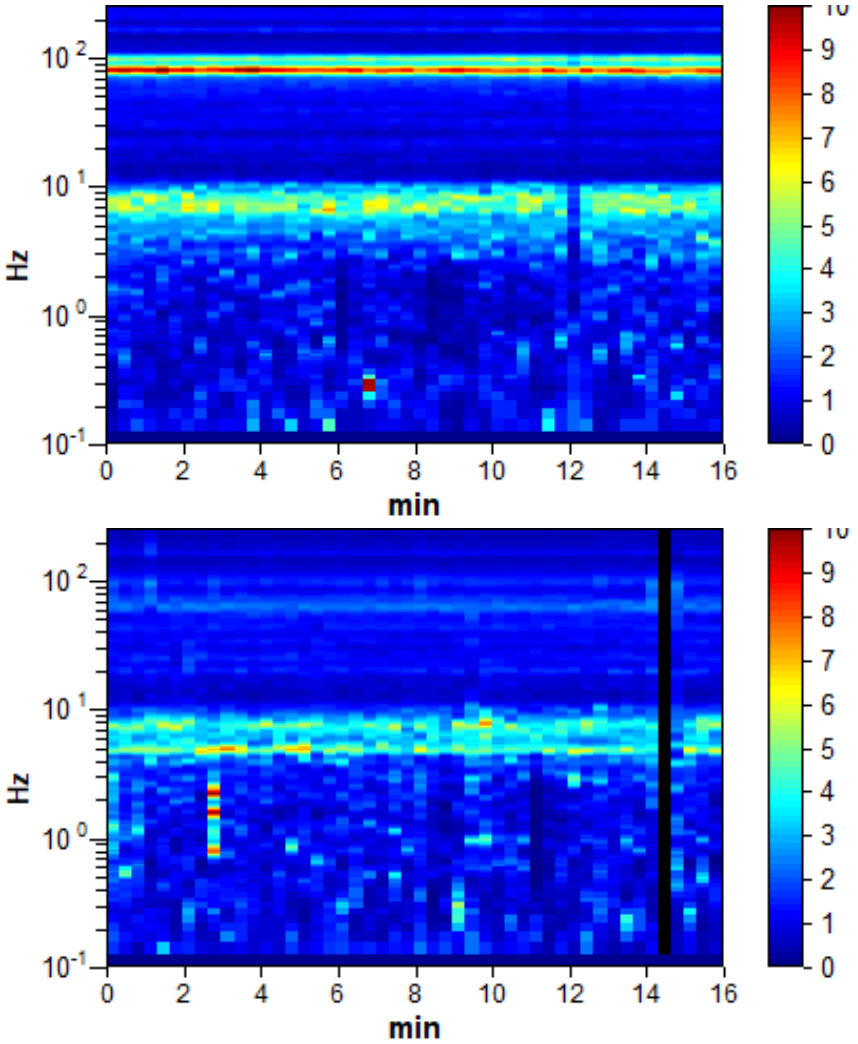

Figure D-14 Ellis Library BH-03 A site, Test 1, concrete (a), grass (b)

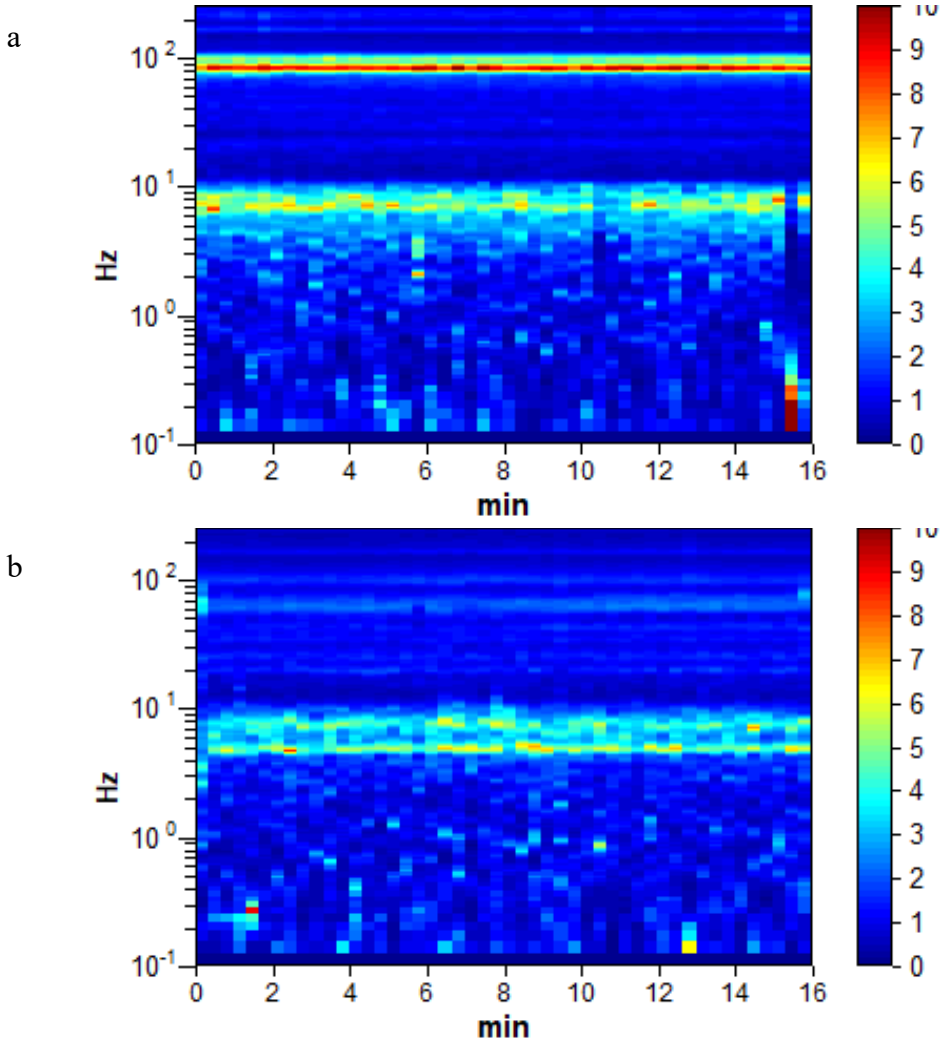

Figure D-15 Ellis Library BH-03 A site, Test 2, concrete (a), grass (b)

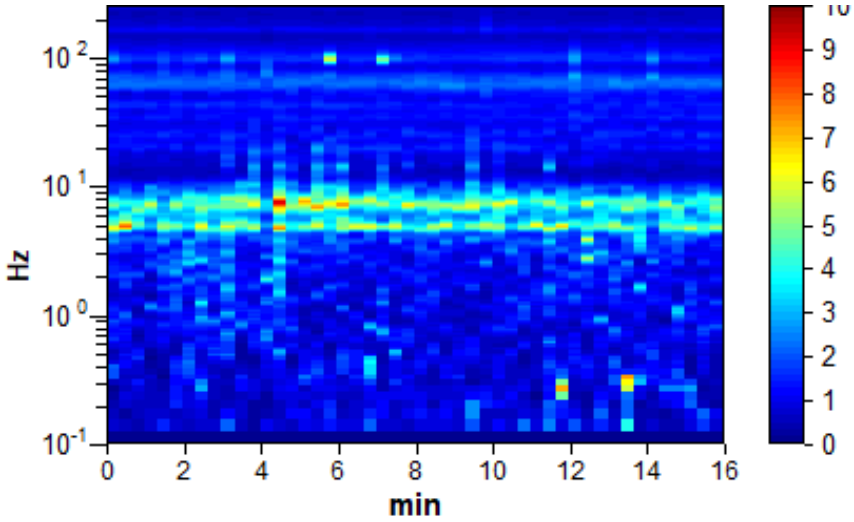

Figure D-16 Ellis Library BH-03 A site, Test 3, grass

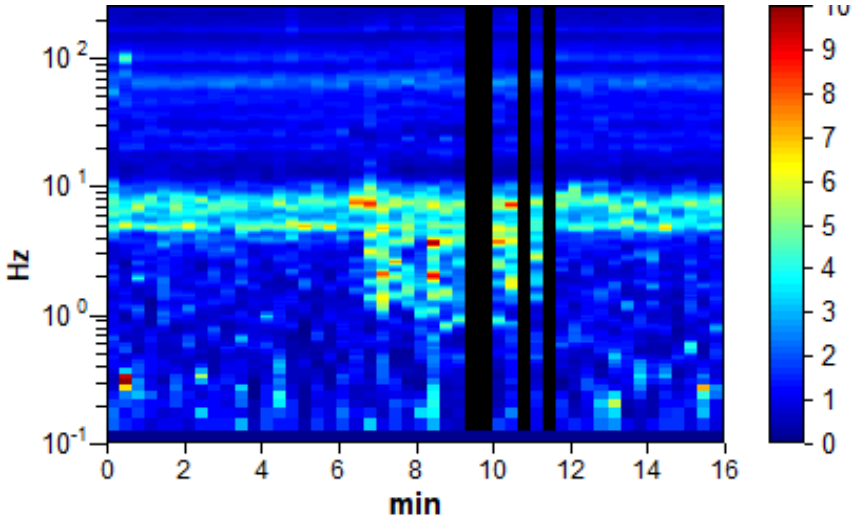

Figure D-17 Ellis Library BH-03 A site, Test 4, grass

a

b

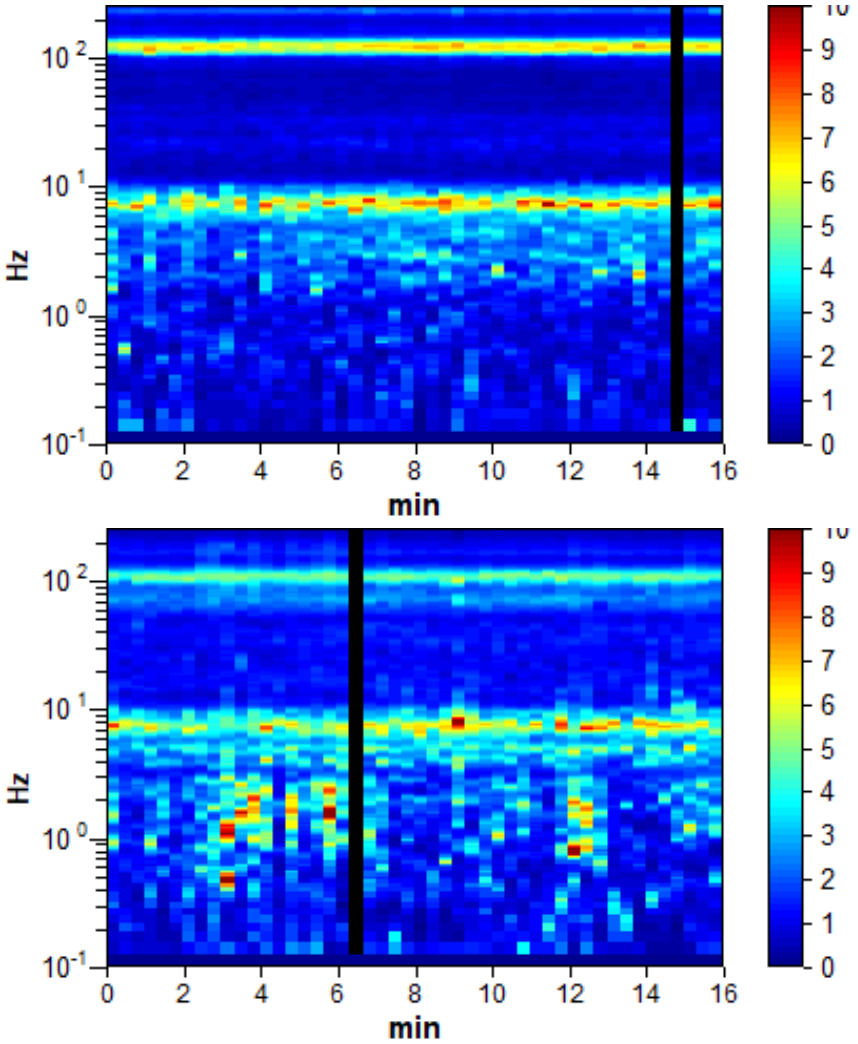

Figure D-18 Ellis Library BH-03 A site, Test 5, concrete (a), grass (b)

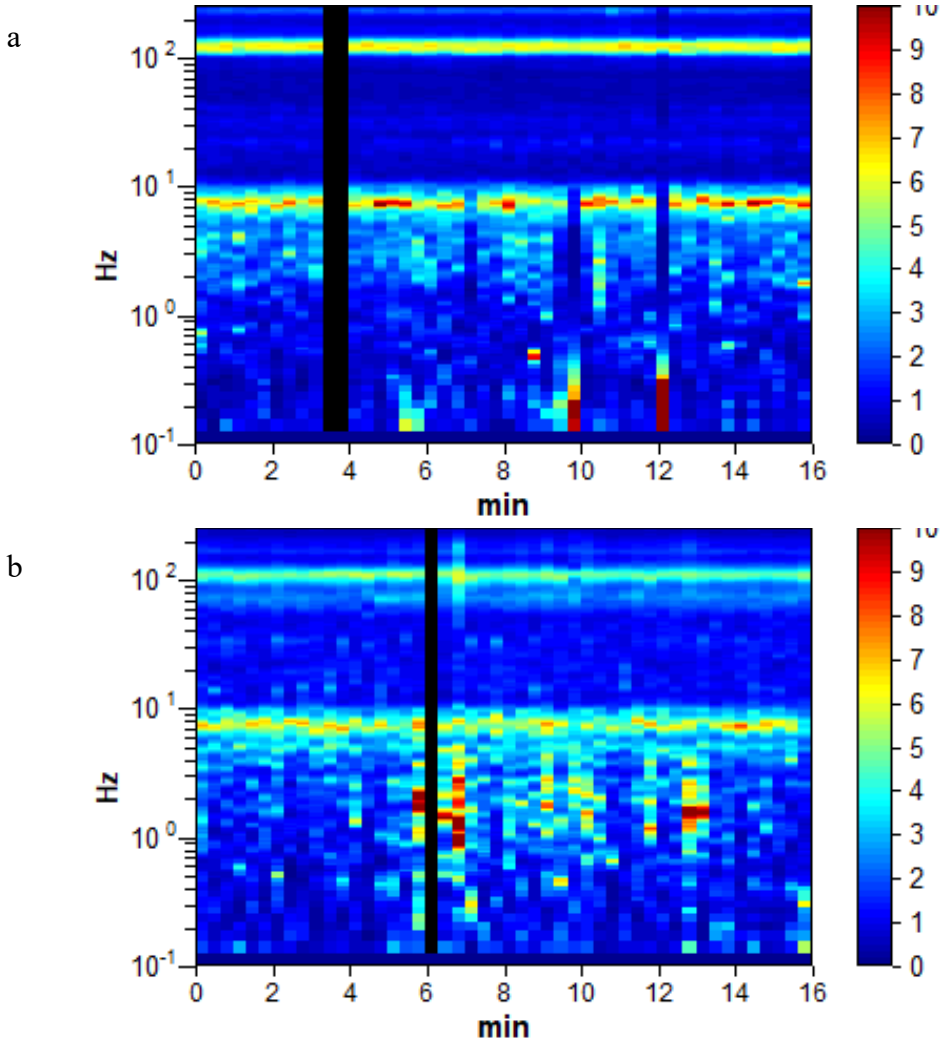

Figure D-19 Ellis Library BH-03 A site, Test 6, concrete (a), grass (b)

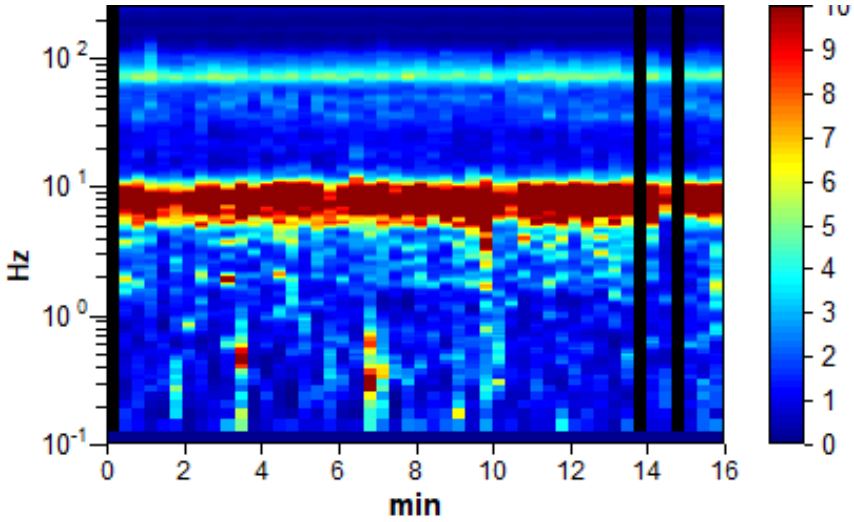

Figure D-20 Ellis Library BH-03 B site, Test 1, grass

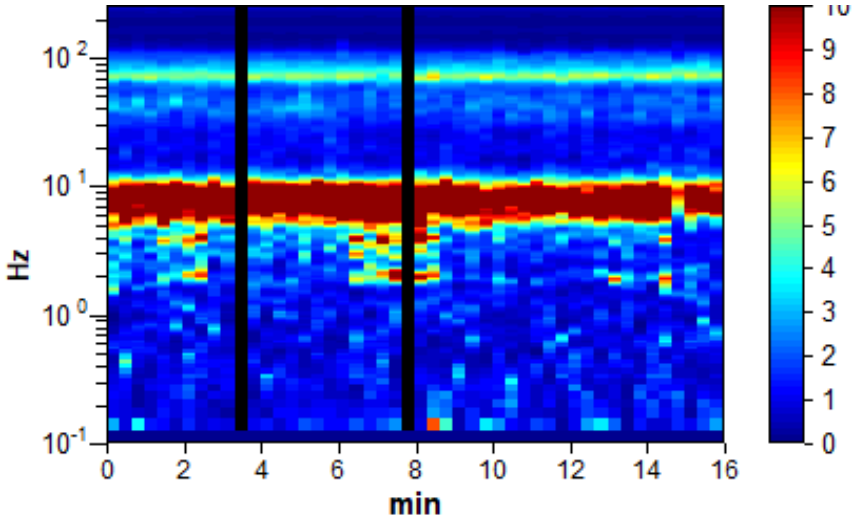

Figure D-21 Ellis Library BH-03 B site, Test 2, grass

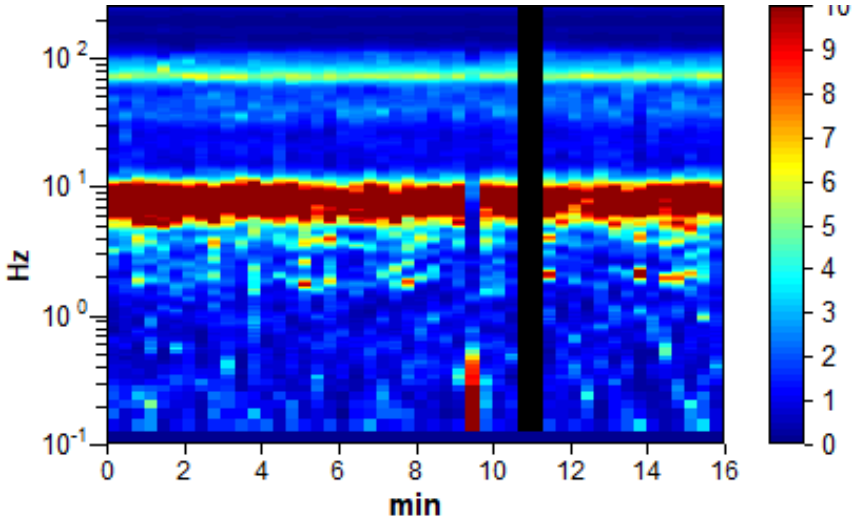

Figure D-22 Ellis Library BH-03 B site, Test 3, grass

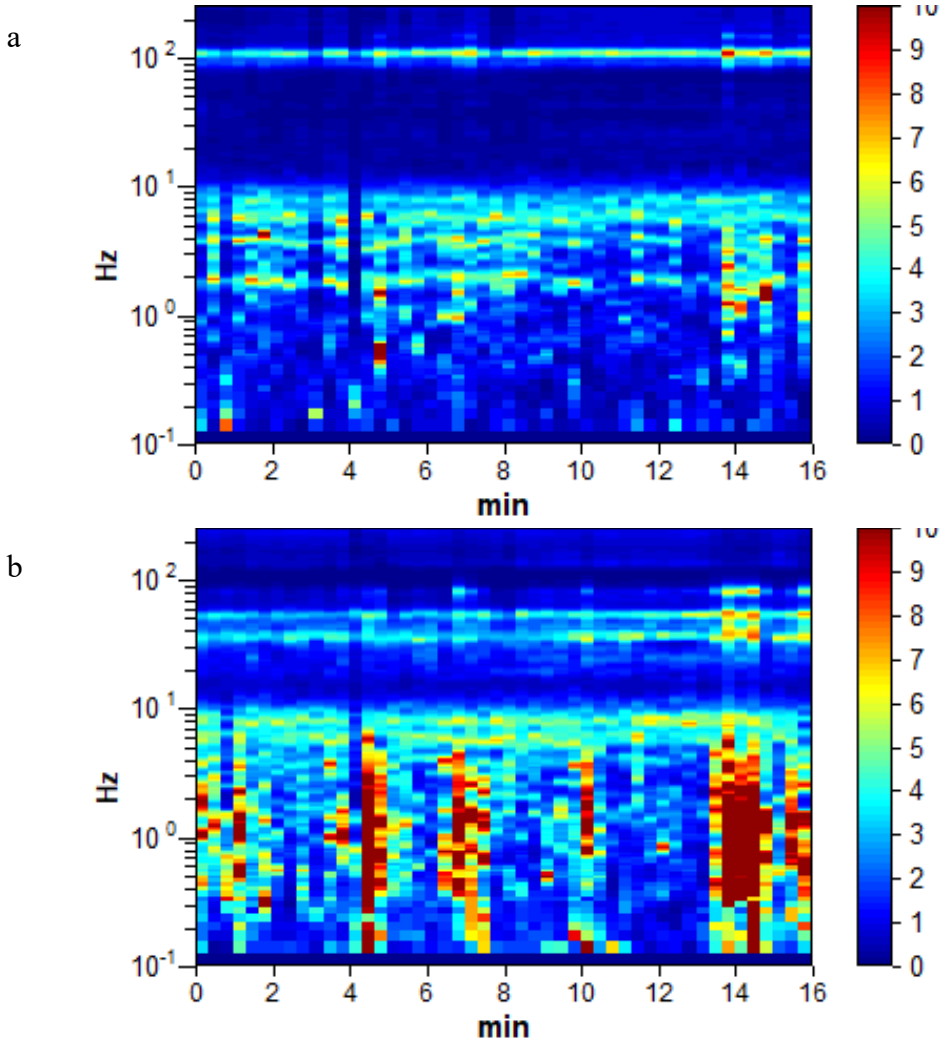

Figure D-23 Journalism B-06 A site, Test 1, concrete (a), grass (b)

a

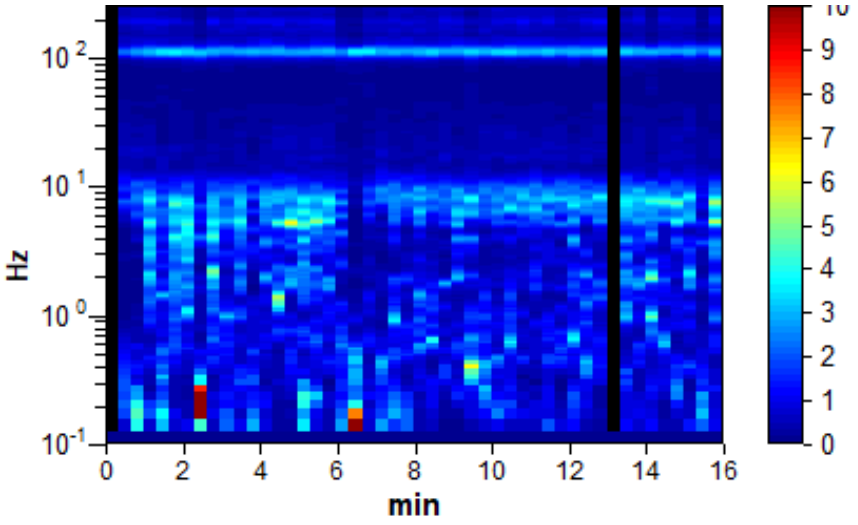

b

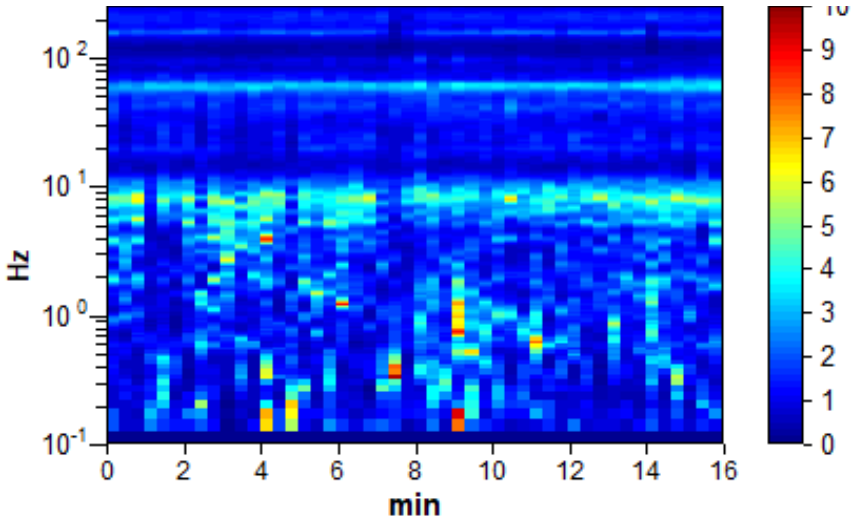

Figure D-24 Journalism B-06 A site, Test 2, concrete (a), grass (b)

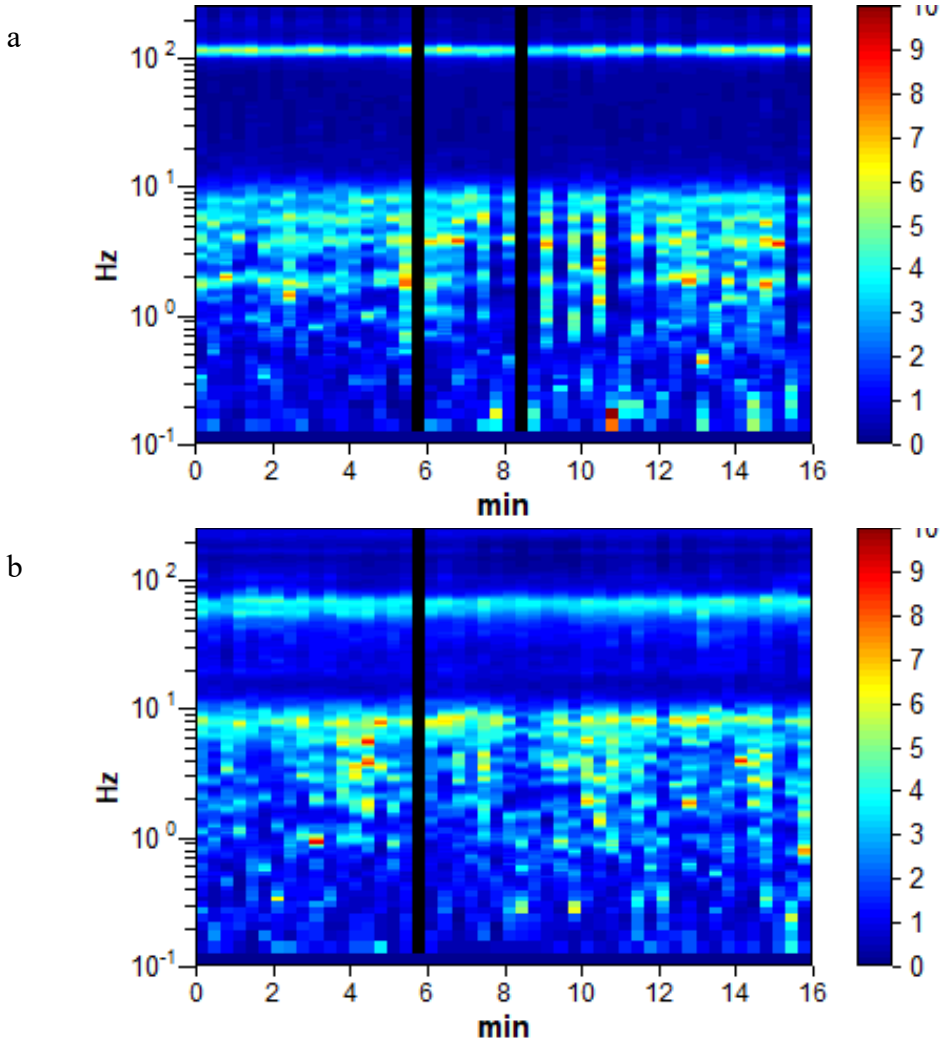

Figure D-25 Journalism B-06 A site, Test 3, concrete (a), grass (b)

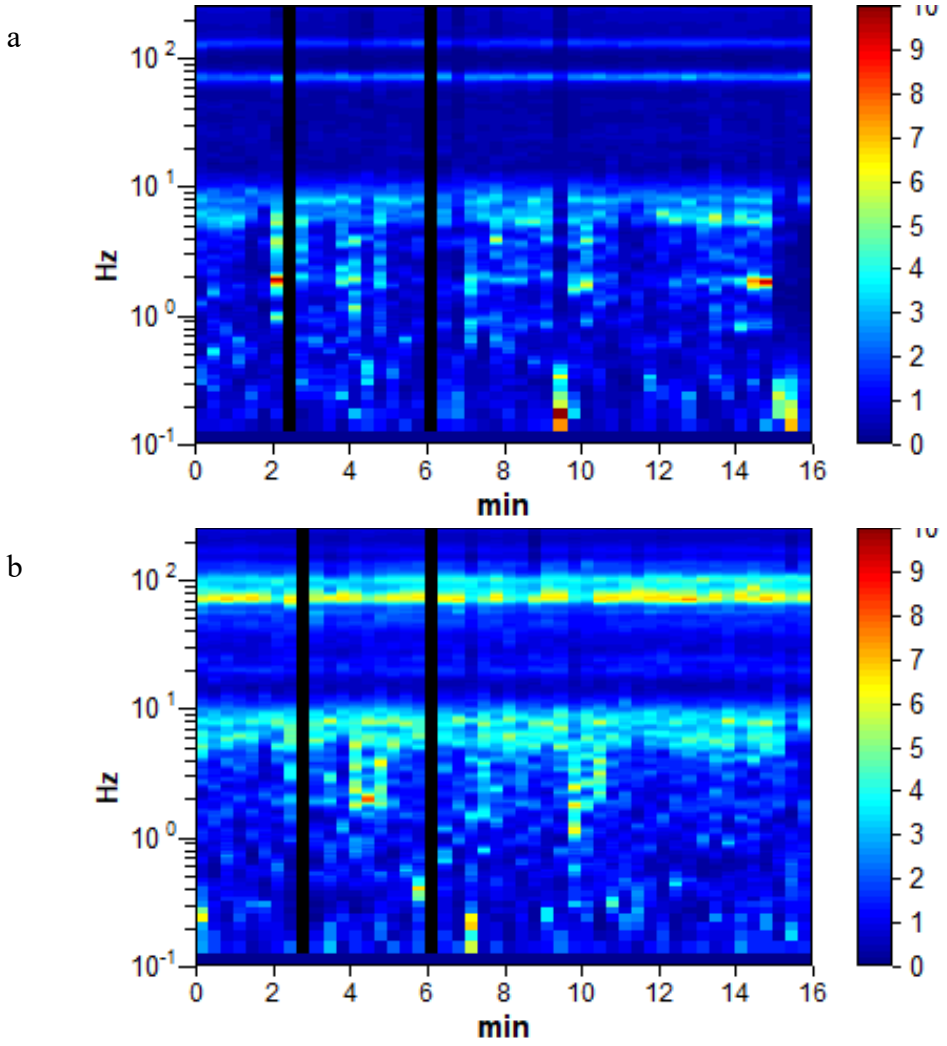

Figure D-26 Journalism B-06 A site, Test 4, concrete (a), grass (b)

a

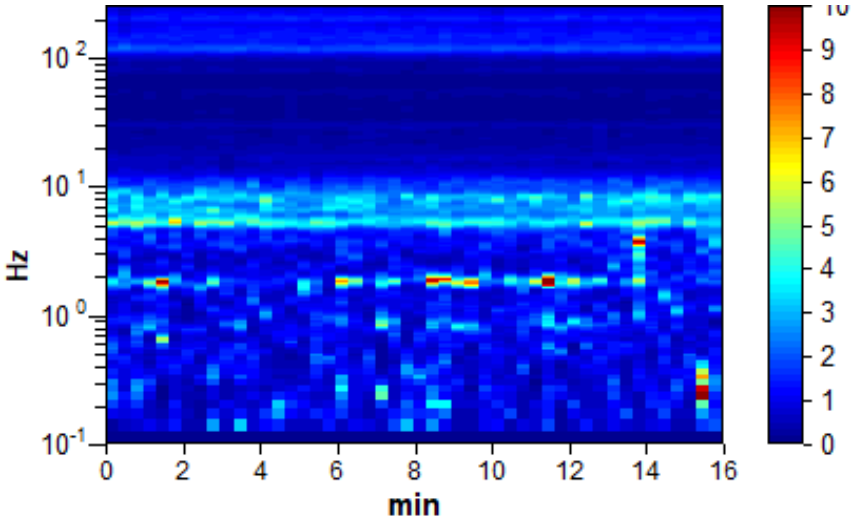

b

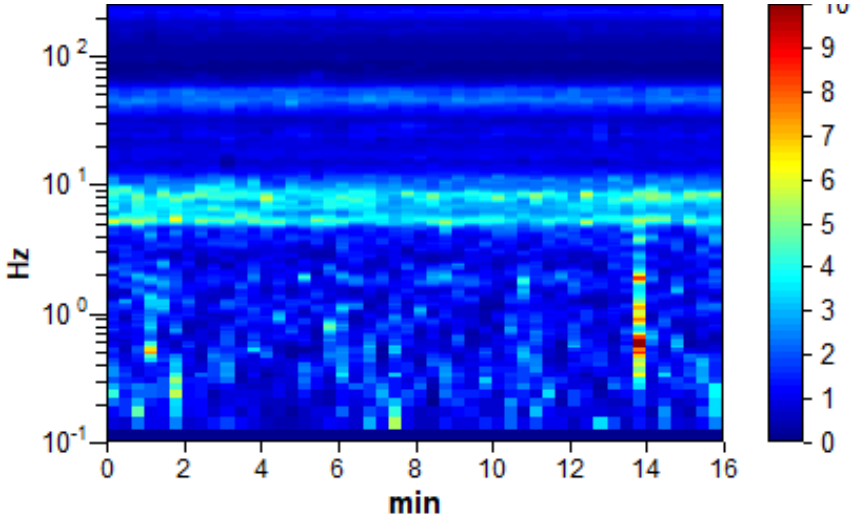

Figure D-27 Journalism B-06 A site, Test 5, concrete (a), grass (b)

a

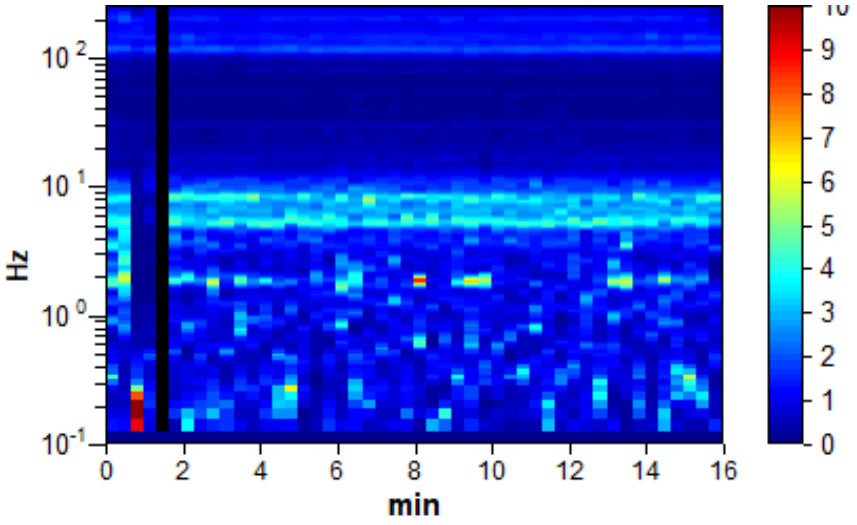

b

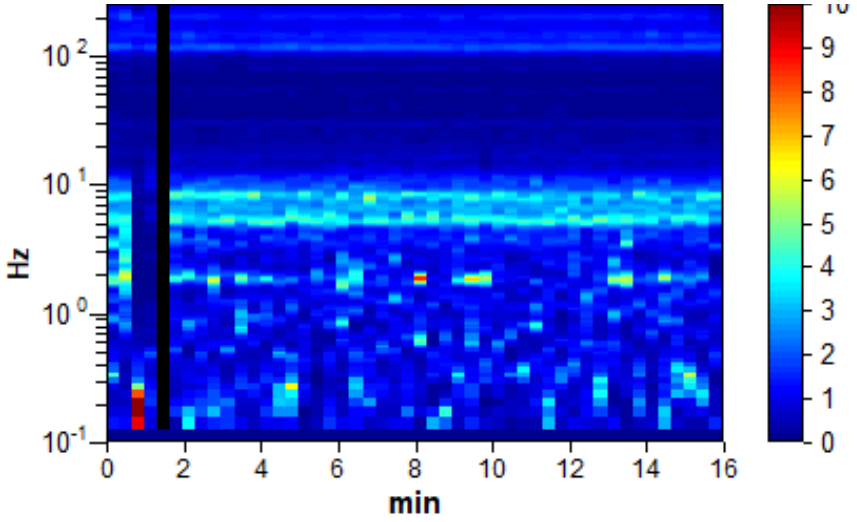

Figure D-28 Journalism B-06 A site, Test 6, concrete (a), grass (b)

a

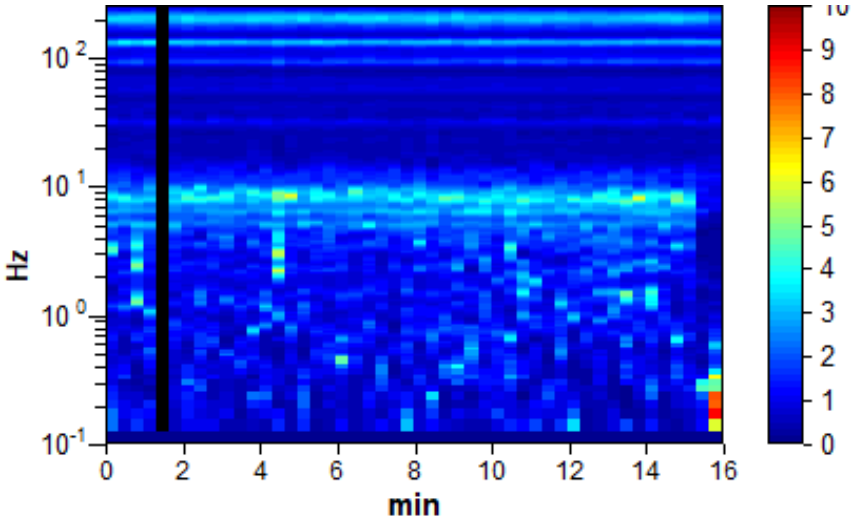

b

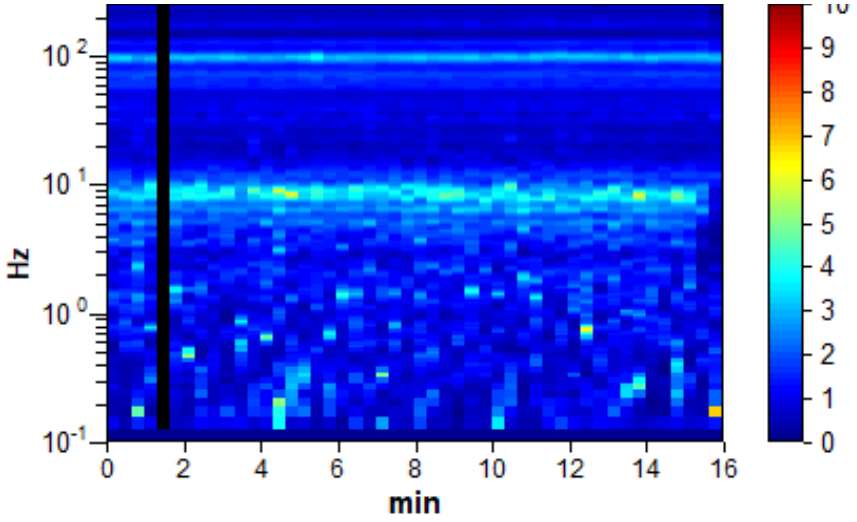

Figure D-29 Journalism B-06 B site, Test 1, concrete (a), grass (b)

a

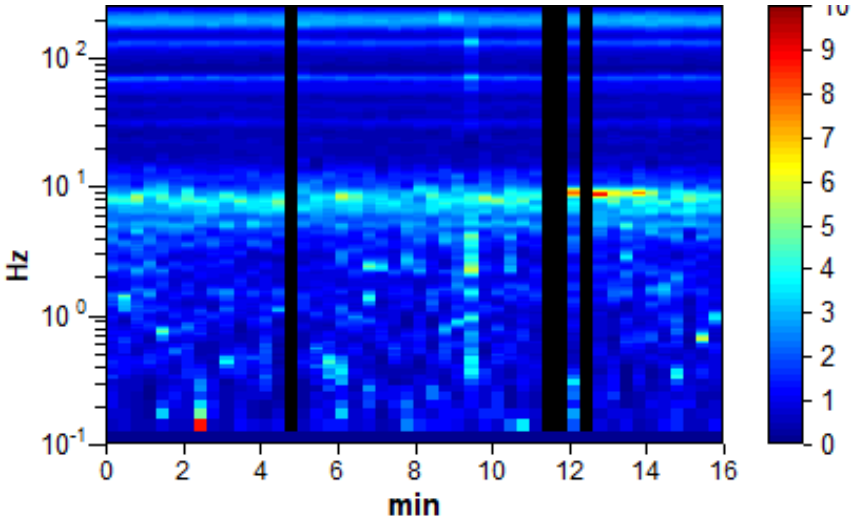

b

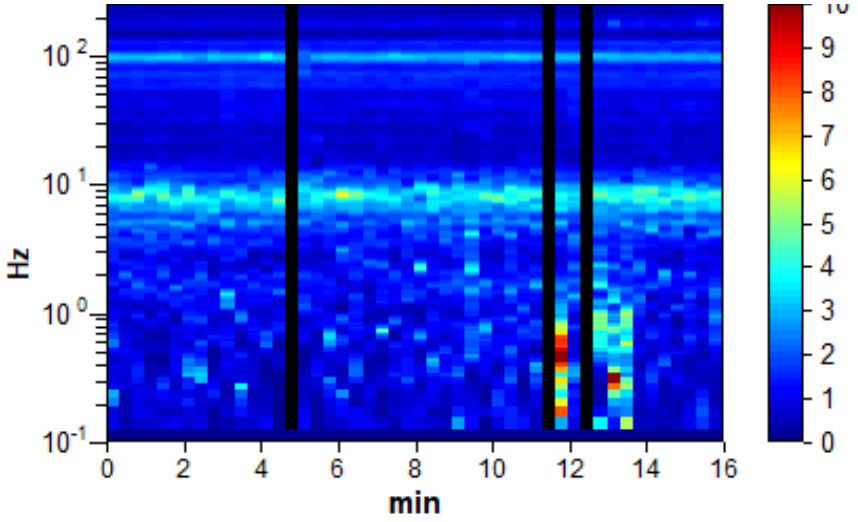

Figure D-30 Journalism B-06 B site, Test 2, concrete (a), grass (b)

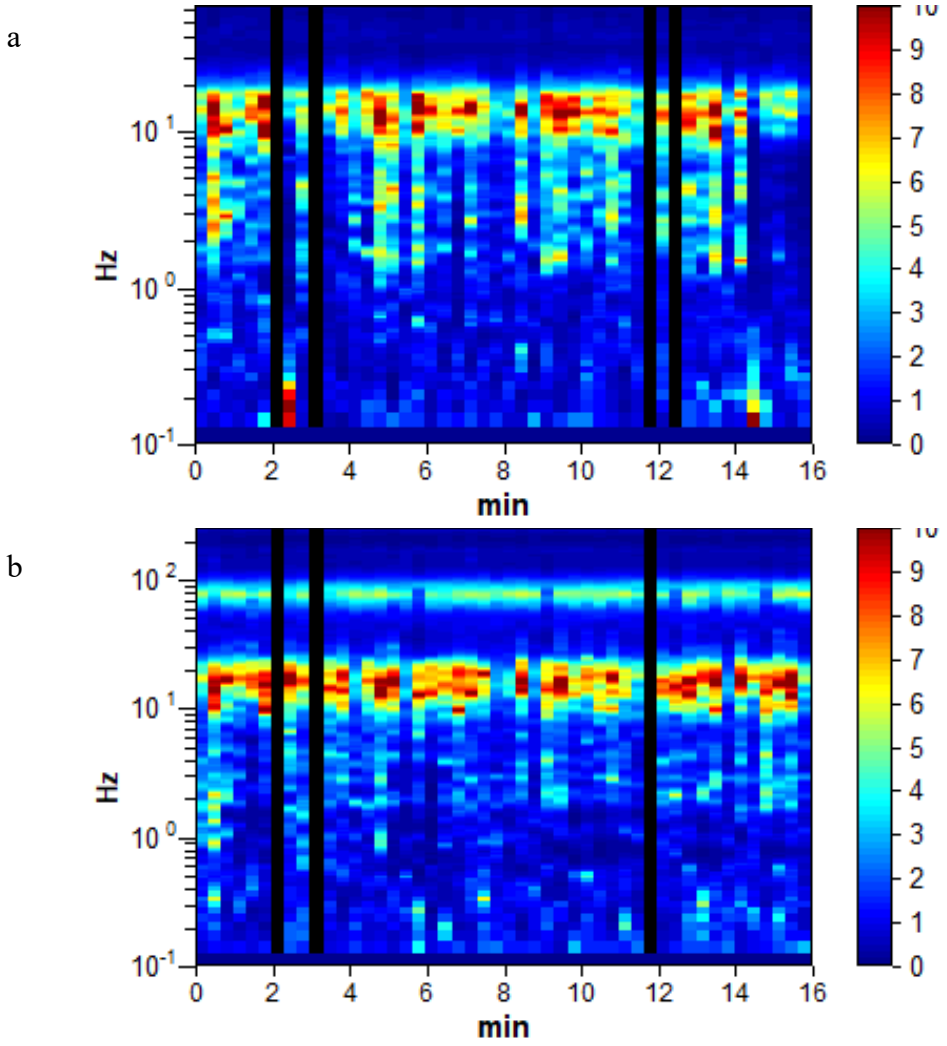

Figure D-31 Lee's Hall BH-08 site, Test 1, concrete (a), grass (b)

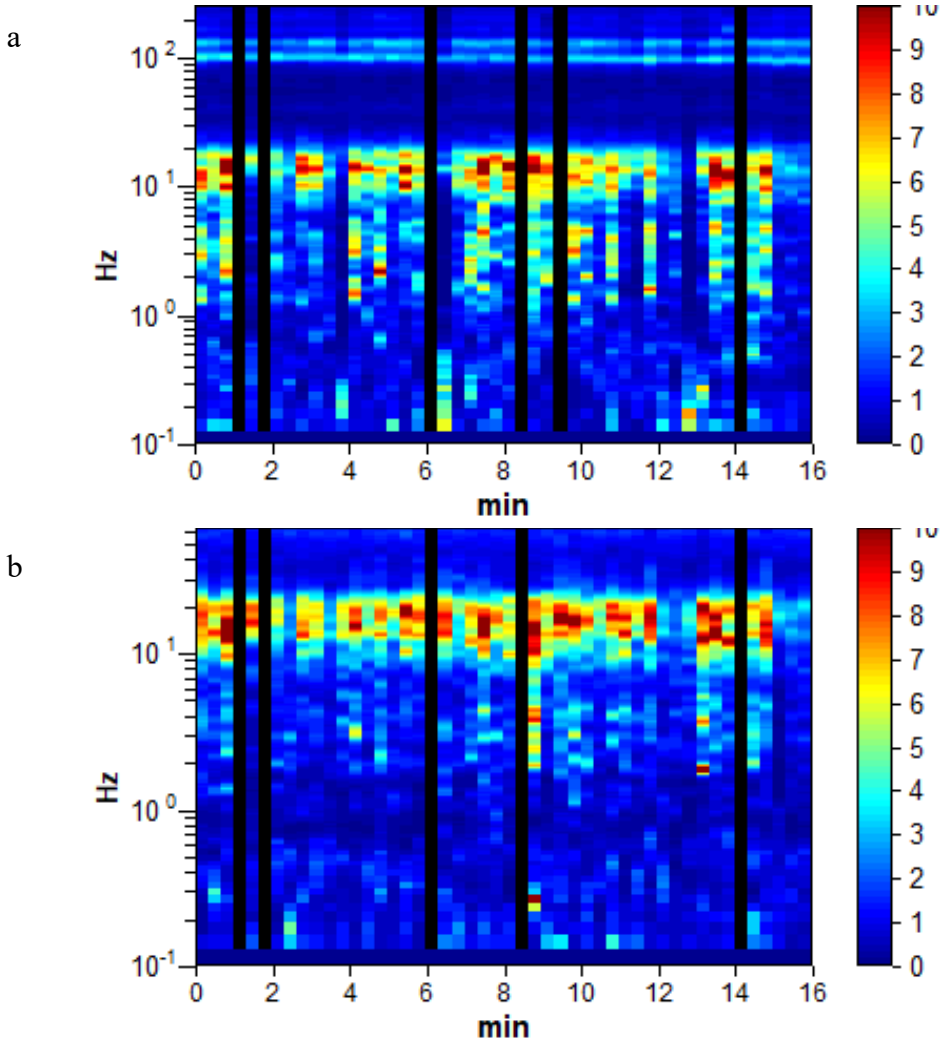

Figure D-32 Lee's Hall BH-08 site, Test 2, concrete (a), grass (b)

a

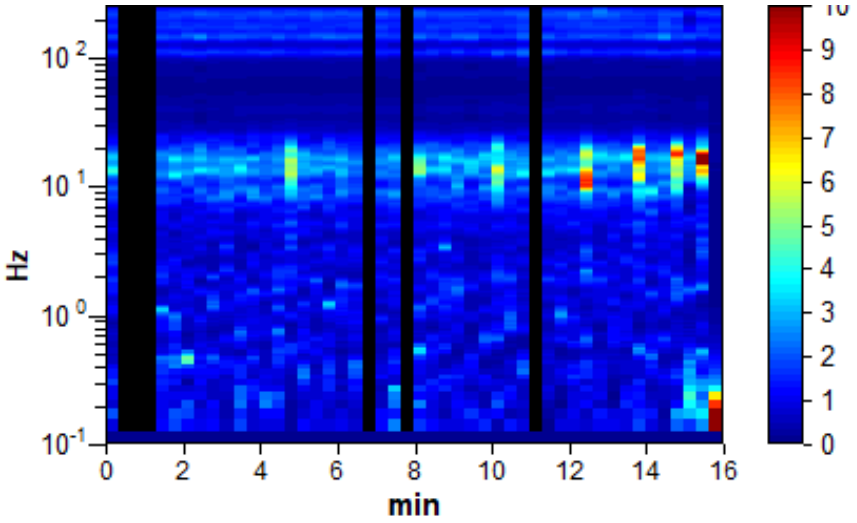

b

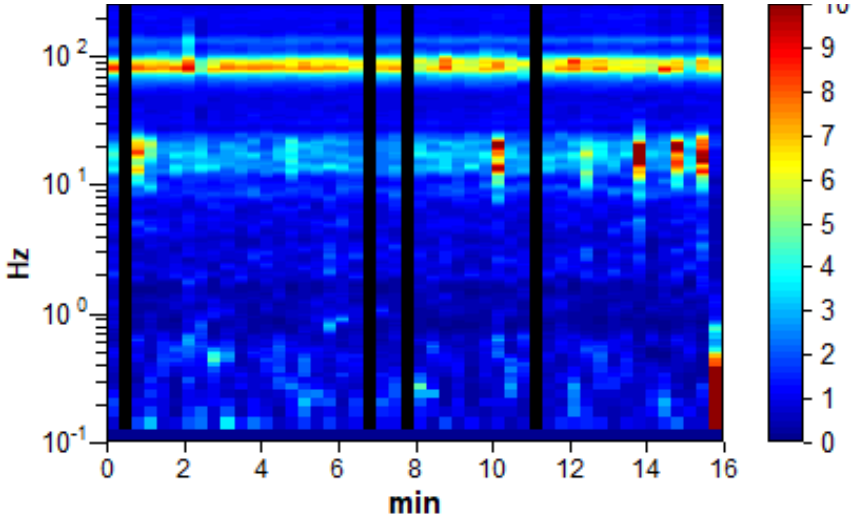

Figure D-33 Lee's Hall BH-08 site, Test 3, concrete (a), grass (b)

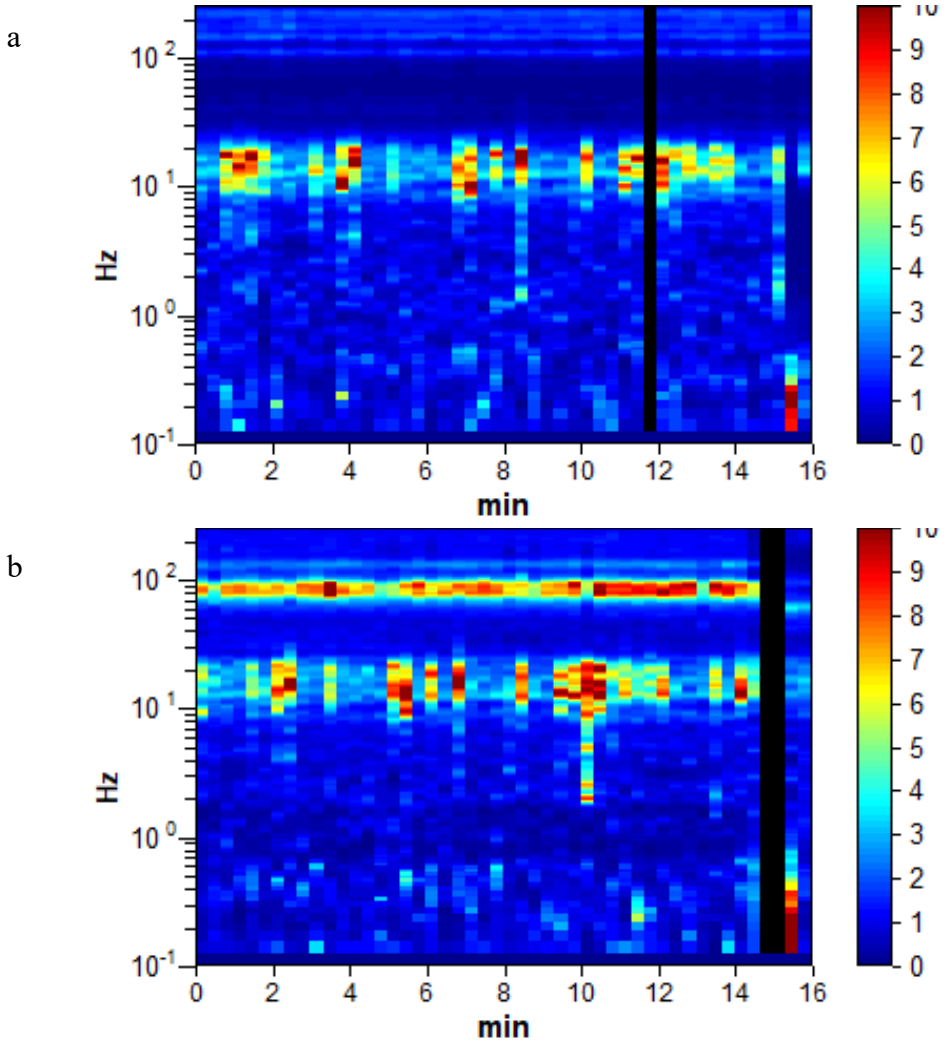

Figure D-34 Lee's Hall BH-08 site, Test 4, concrete (a), grass (b)

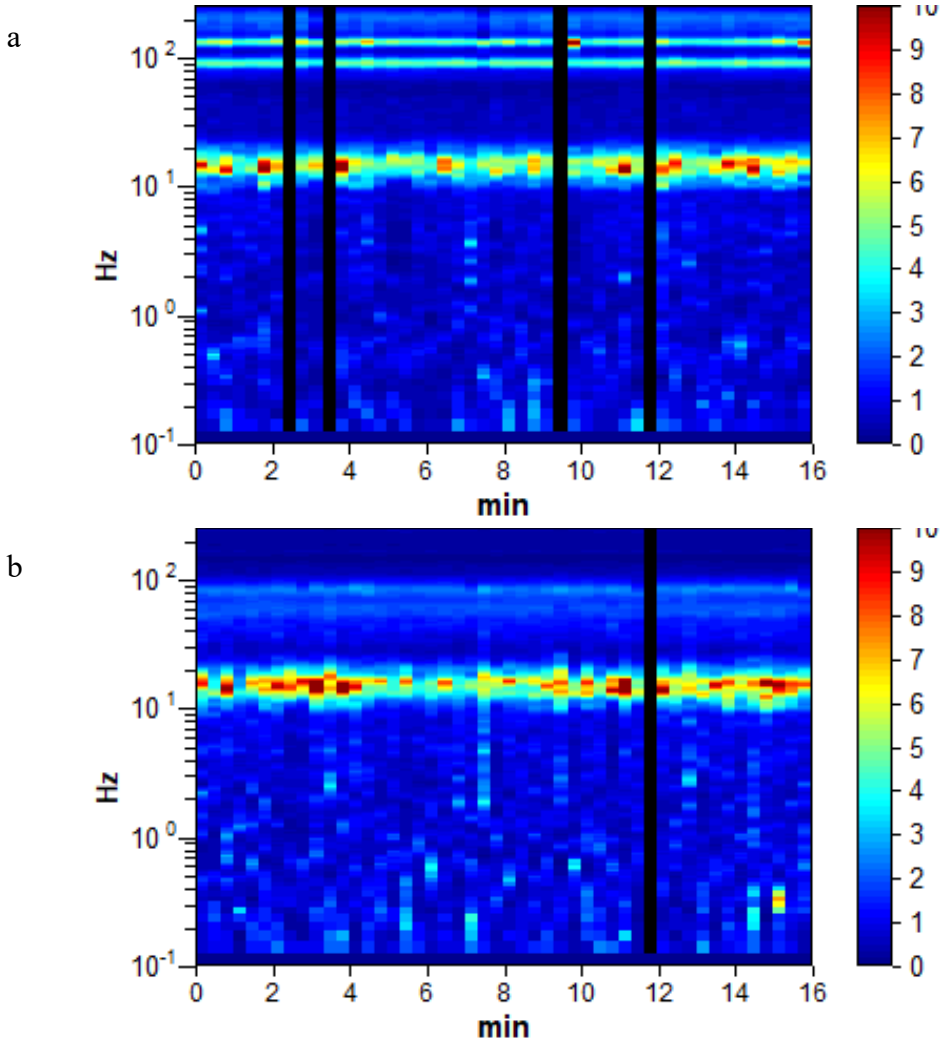

Figure D-35 Lee's Hall BH-18 site, Test 1, concrete (a), grass (b)

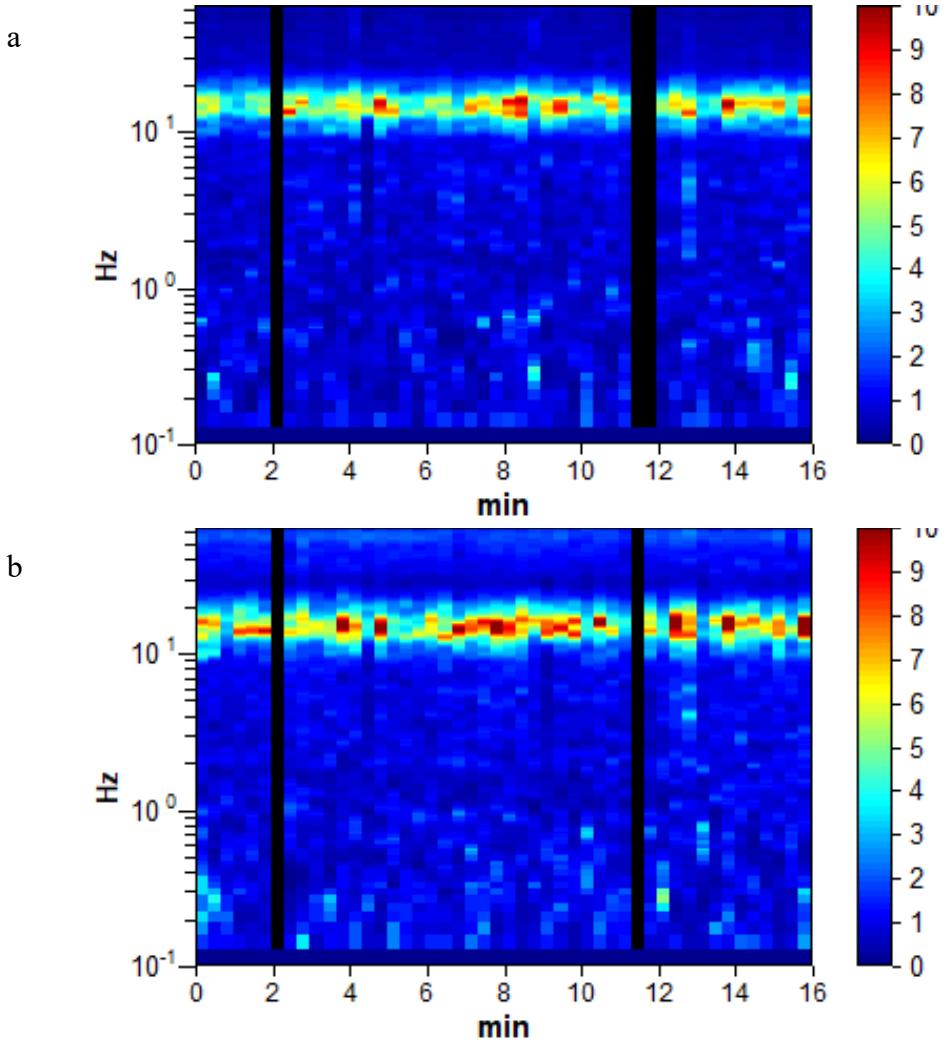

Figure D-36 Lee's Hall BH-18 site, Test 2, concrete (a), grass (b)

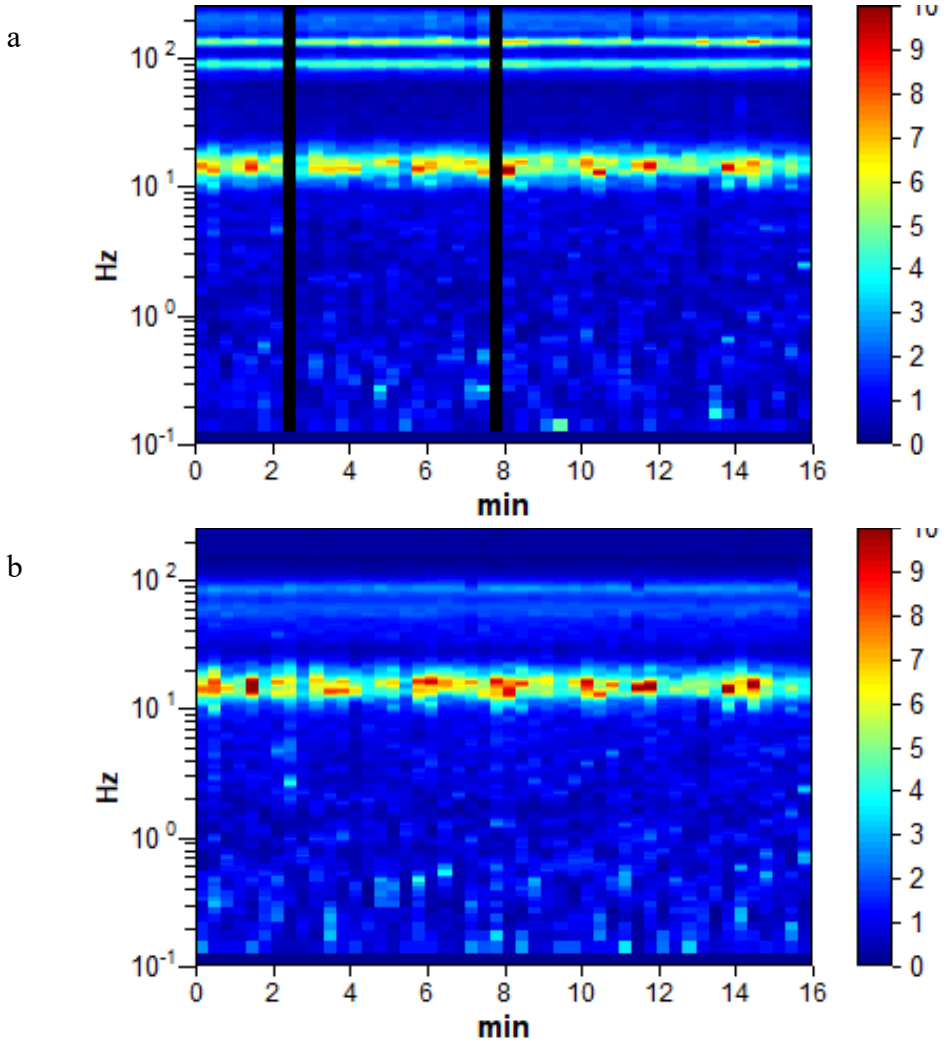

Figure D-37 Lee's Hall BH-18 site, Test 3, concrete (a), grass (b)

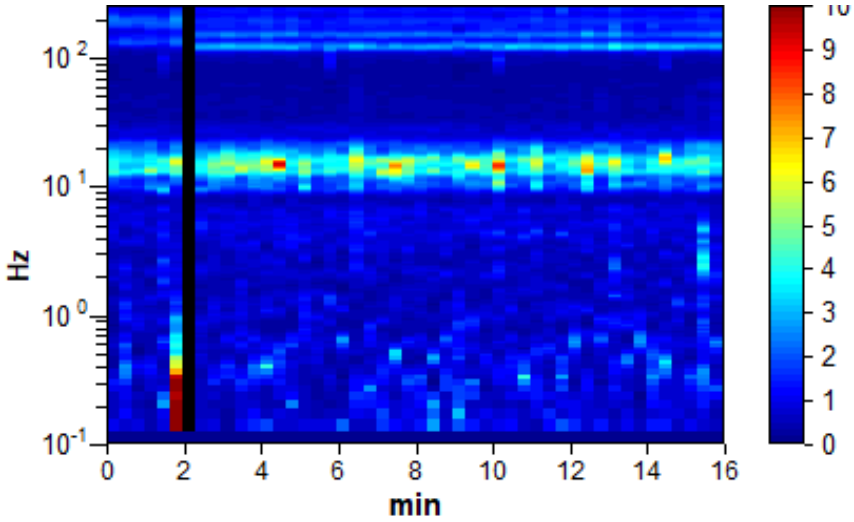

Figure D-38 Lee's Hall BH-18 site, Test 4, concrete

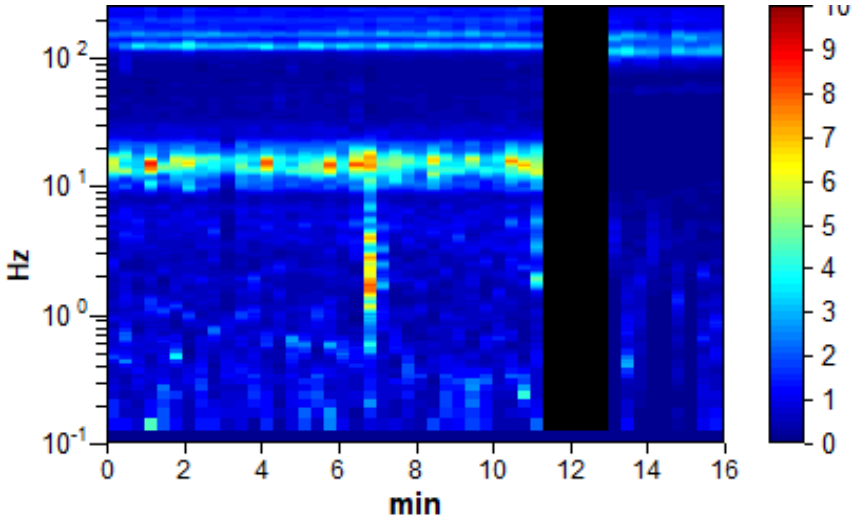

Figure D-39 Lee's Hall BH-18 site, Test 5, concrete

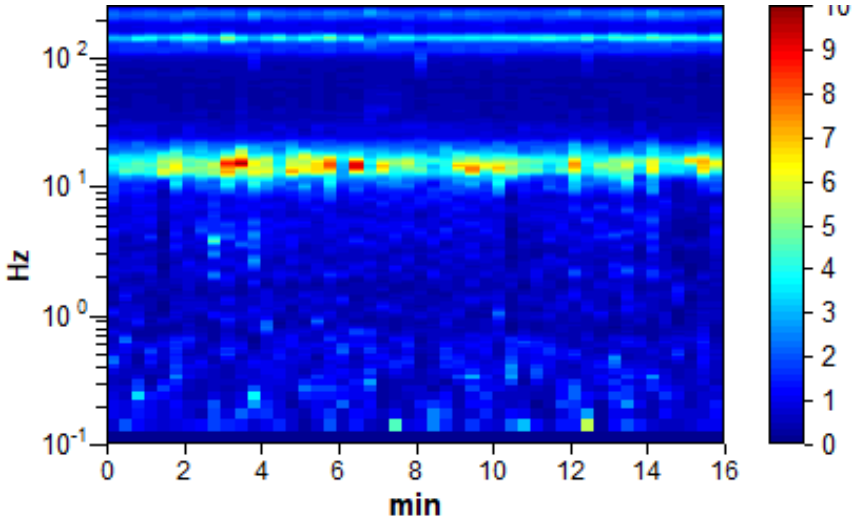

Figure D-40 Lee's Hall BH-18 site, Test 6, concrete

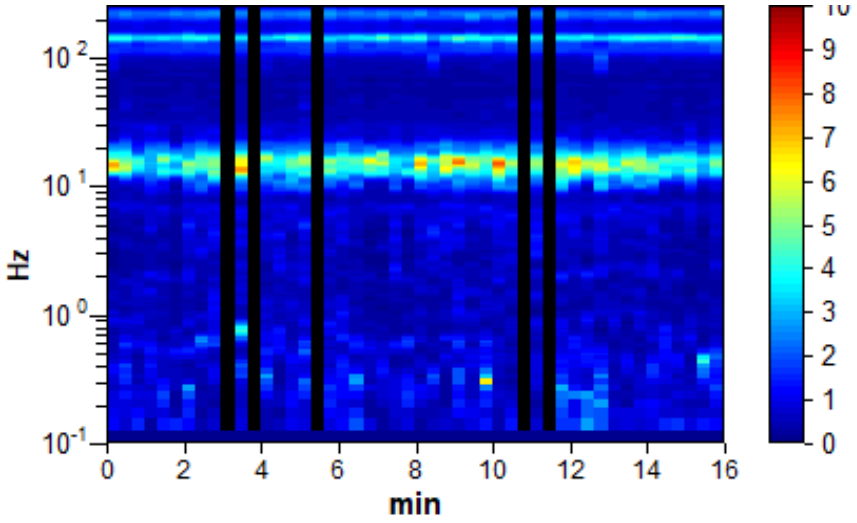

Figure D-41 Lee's Hall BH-18 site, Test 7, concrete

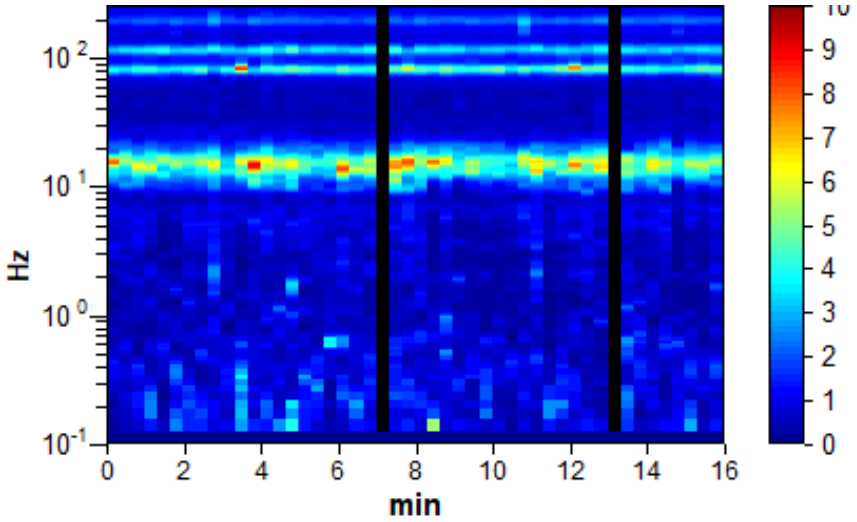

Figure D-42 Lee's Hall BH-18 site, Test 8, concrete

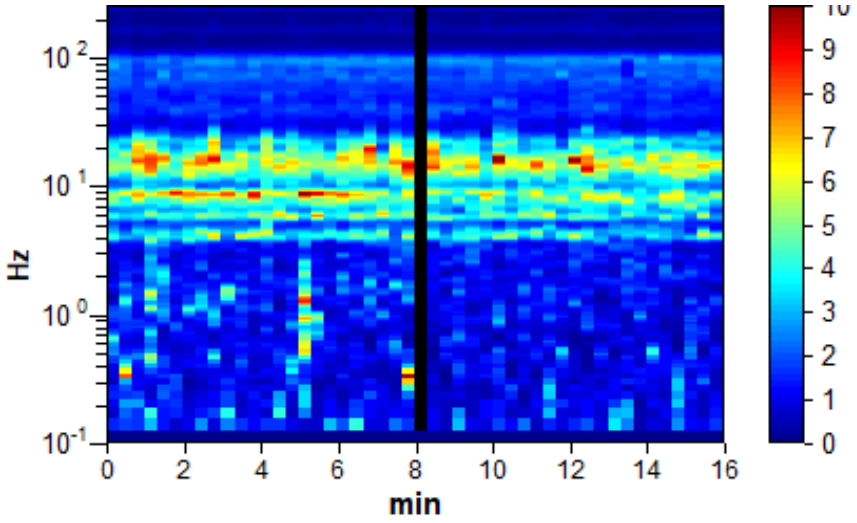

Figure D-43 Lee's Hall Selected site, Test 1, grass

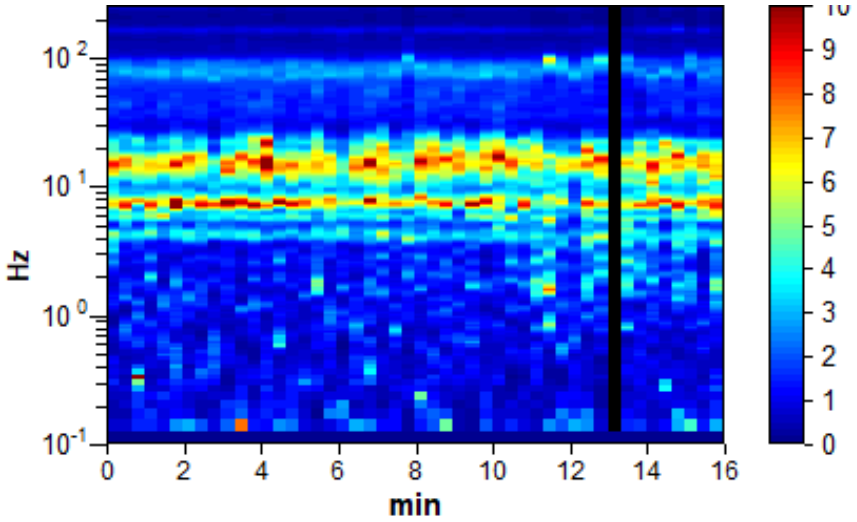

Figure D-44 Lee's Hall Selected site, Test 2, grass

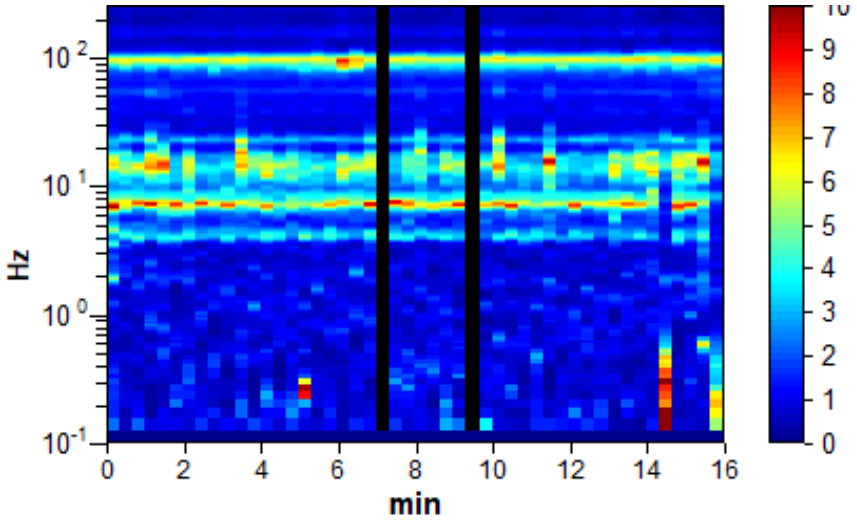

Figure D-45 Lee's Hall Selected site, Test 3, grass

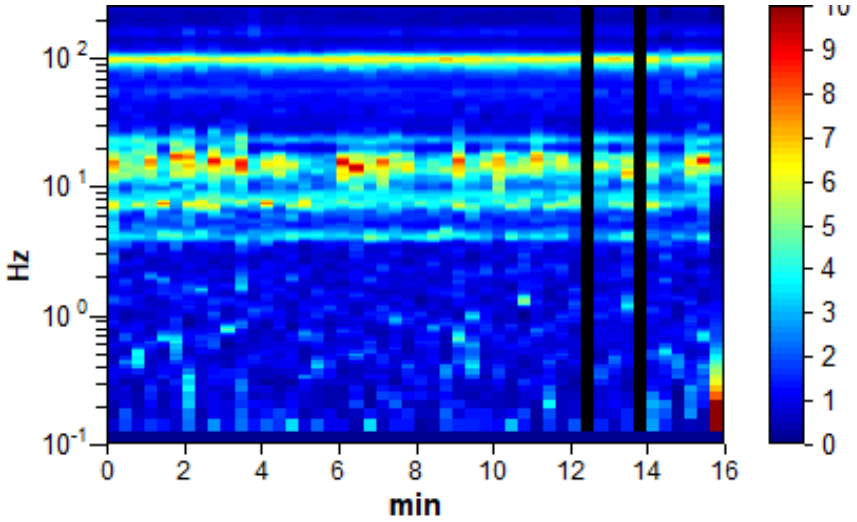

Figure D-46 Lee's Hall Selected site, Test 4, grass

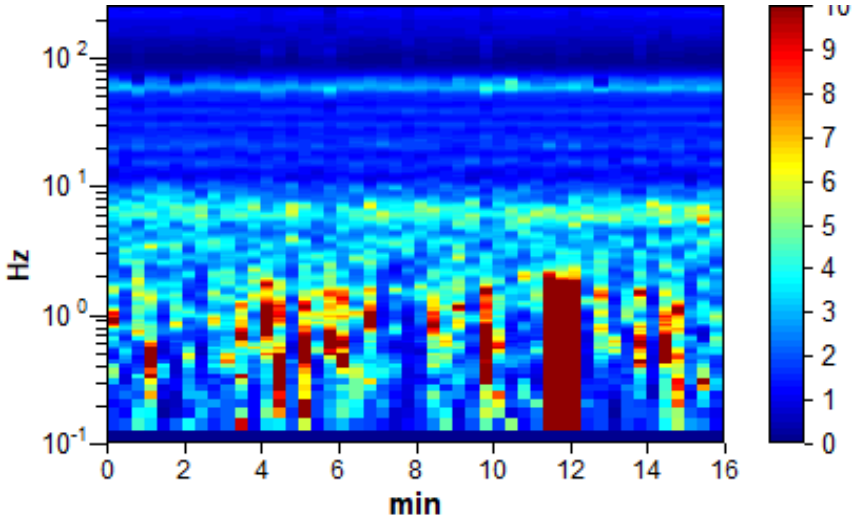

Figure D-47 Lee's Hall Selected site, Test 5, grass

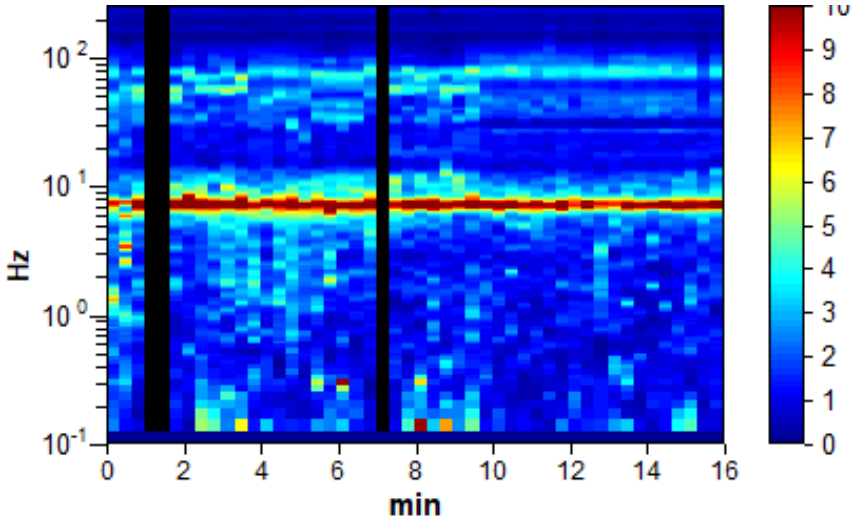

Figure D-48 MIZ Middle Quad site, Test 1, grass

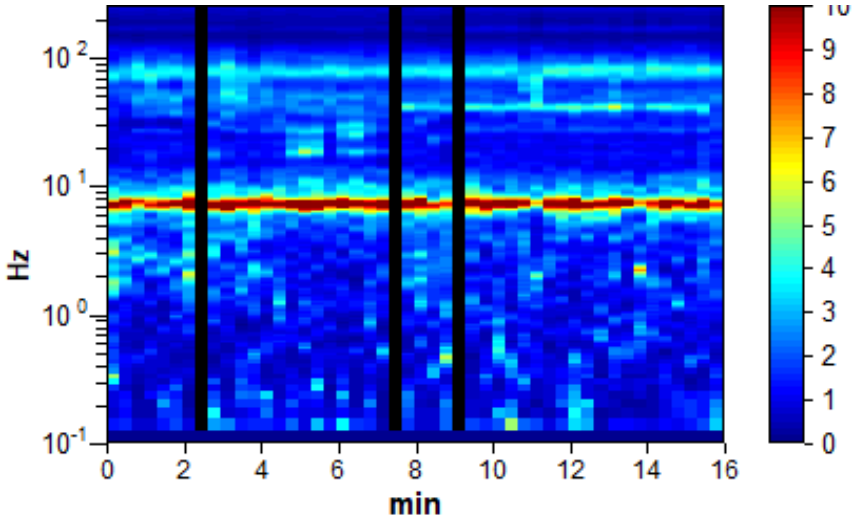

Figure D-49 MIZ Middle Quad site, Test 2, grass

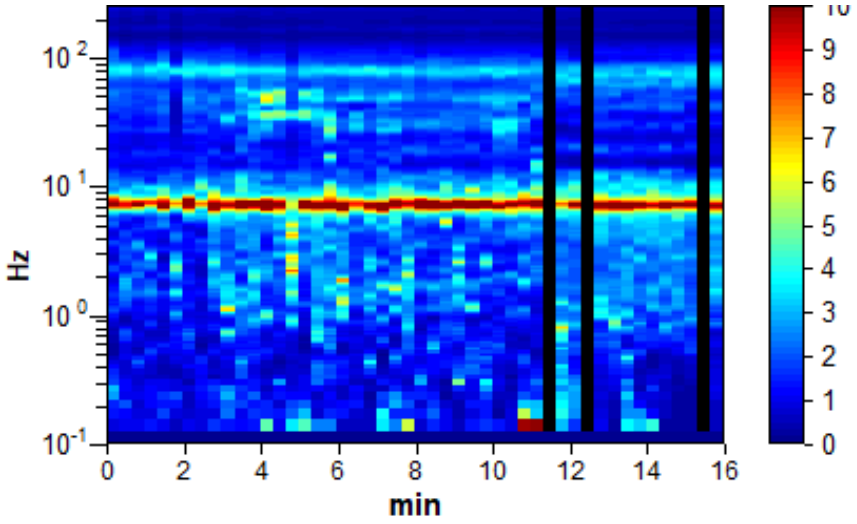

Figure D-50 MIZ Middle Quad site, Test 3, grass

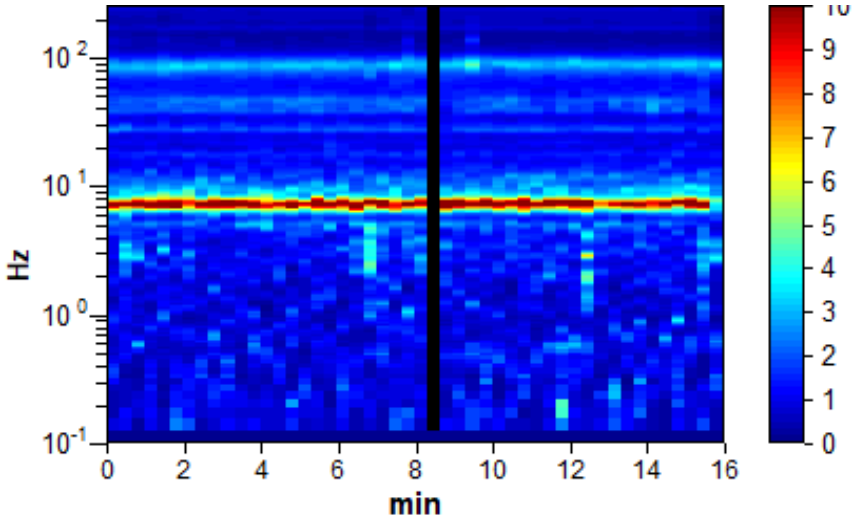

Figure D-51 MIZ Middle Quad site, Test 4, grass

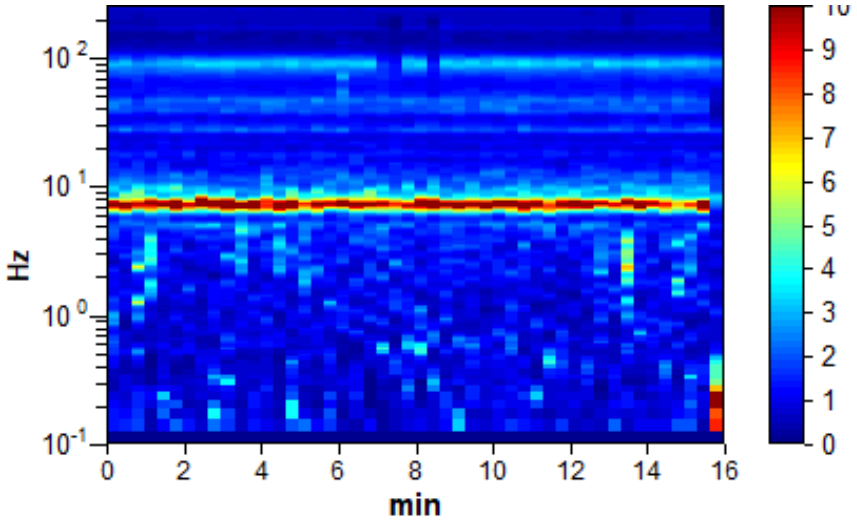

Figure D-52 MIZ Middle Quad site, Test 5, grass

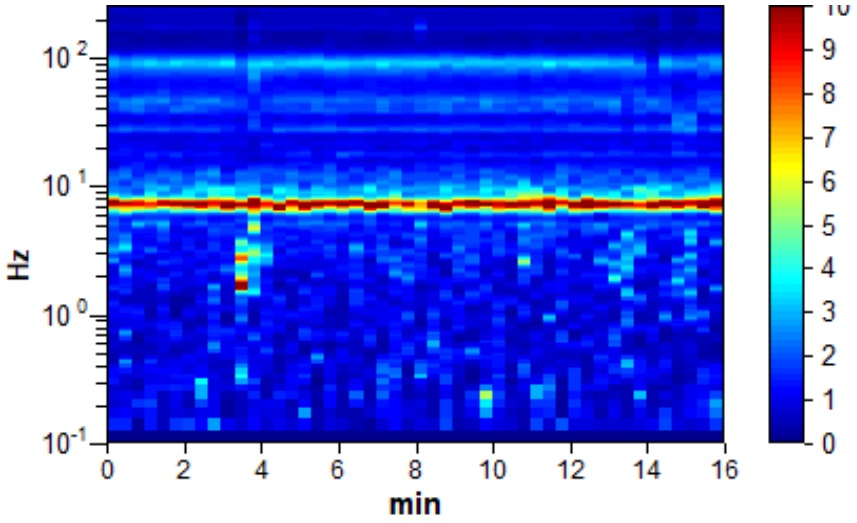

Figure D-53 MIZ Middle Quad site, Test 6, grass

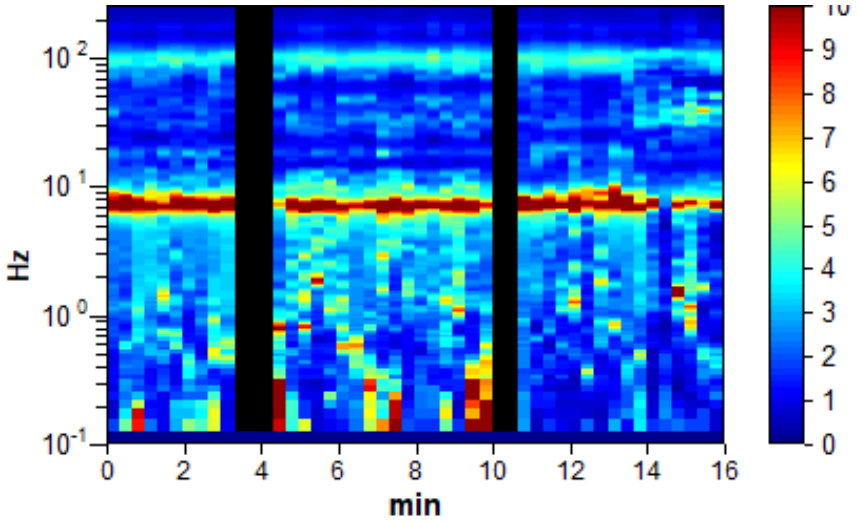

Figure D-54 MIZ Middle Quad site, Test 7, grass

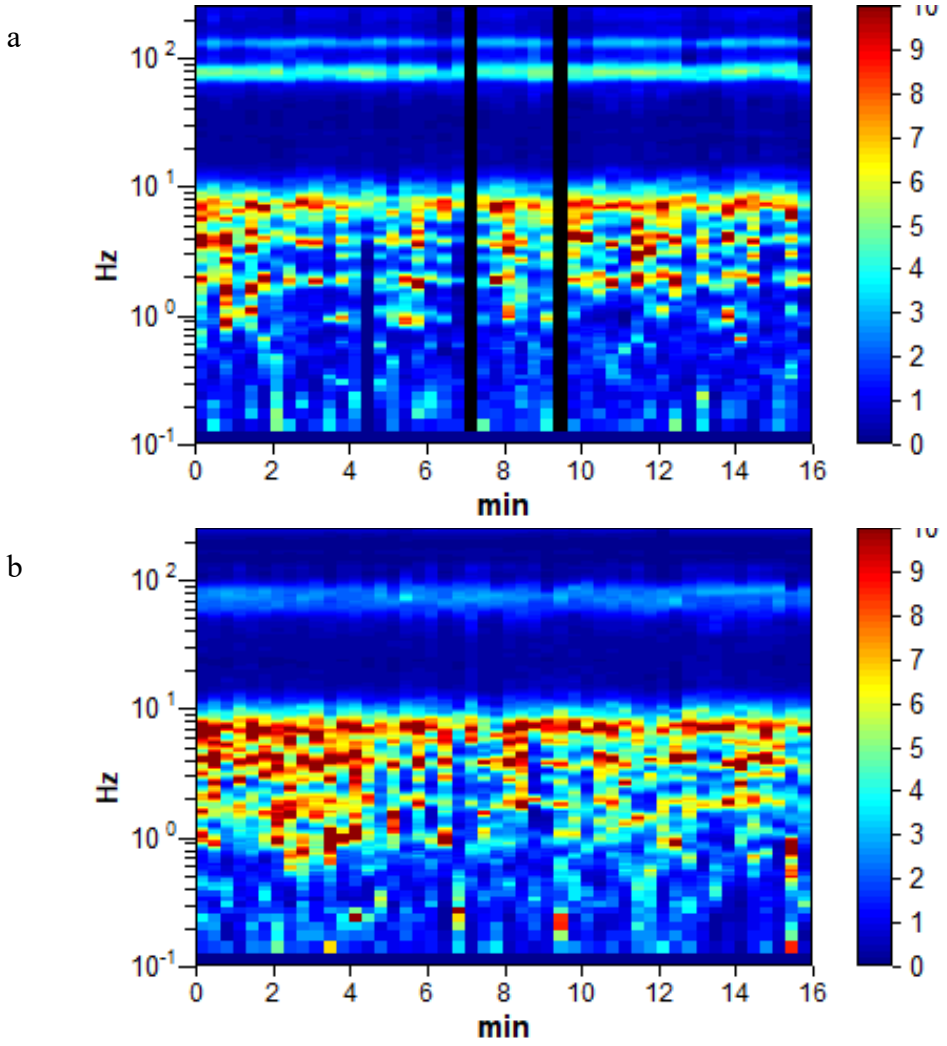

Figure D-55 MIZ Quad Site 1 site, Test 1, concrete (a), grass (b)

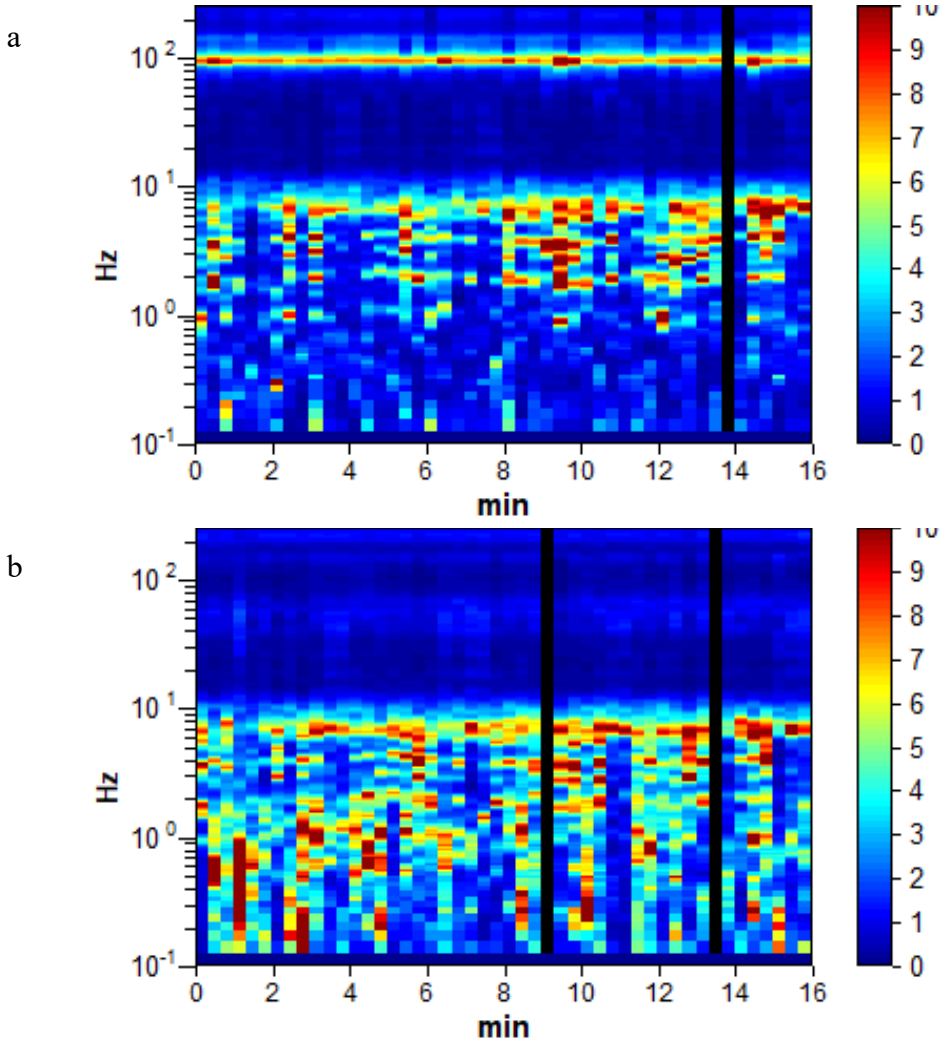

Figure D-56 MIZ Quad Site 1 site, Test 2, concrete (a), grass (b)

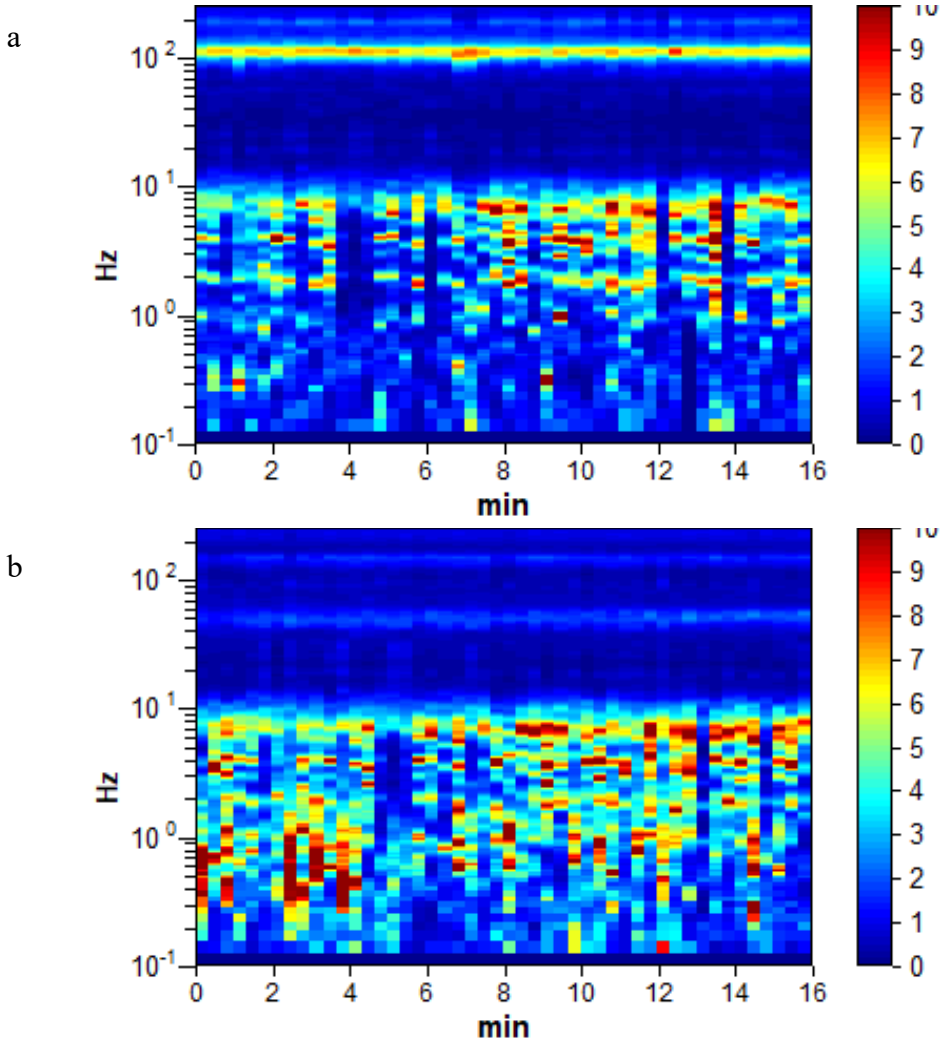

Figure D-57 MIZ Quad Site 1 site, Test 3, concrete (a), grass (b)

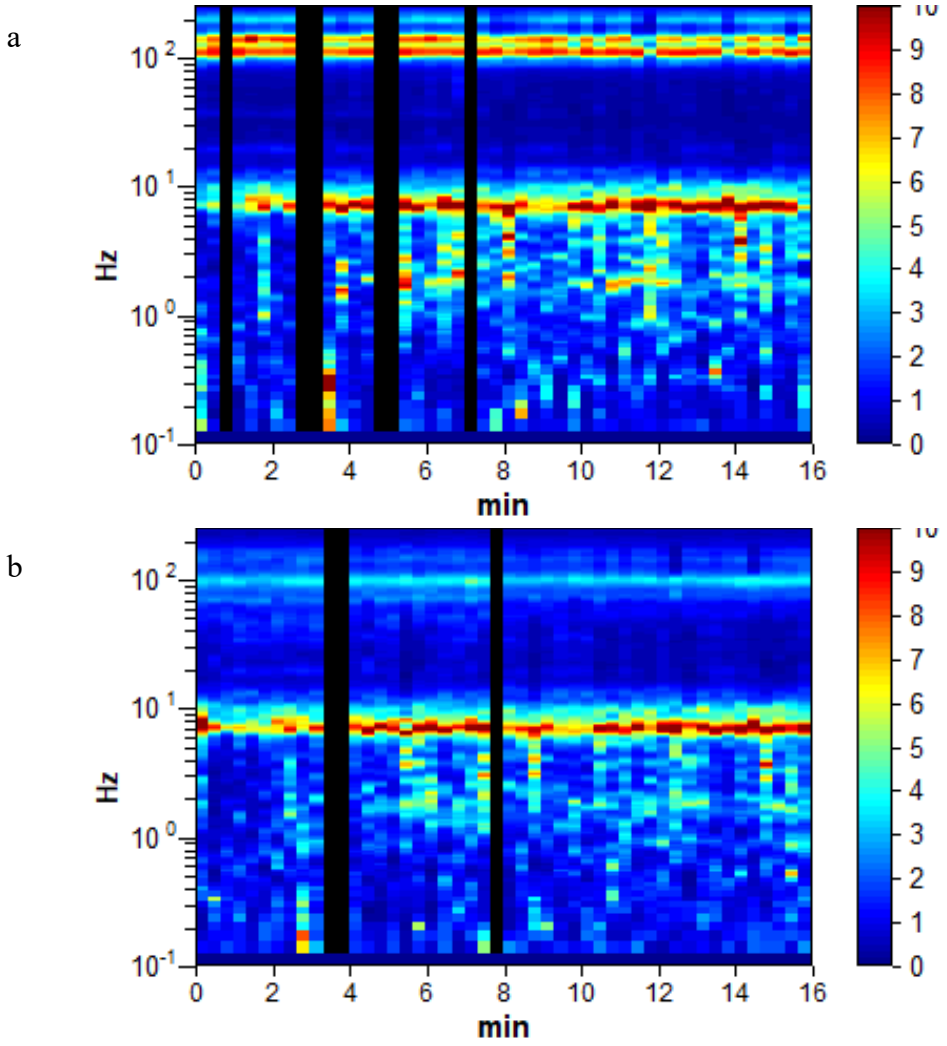

Figure D-58 MIZ Quad Site 1 site, Test 4, concrete (a), grass (b)

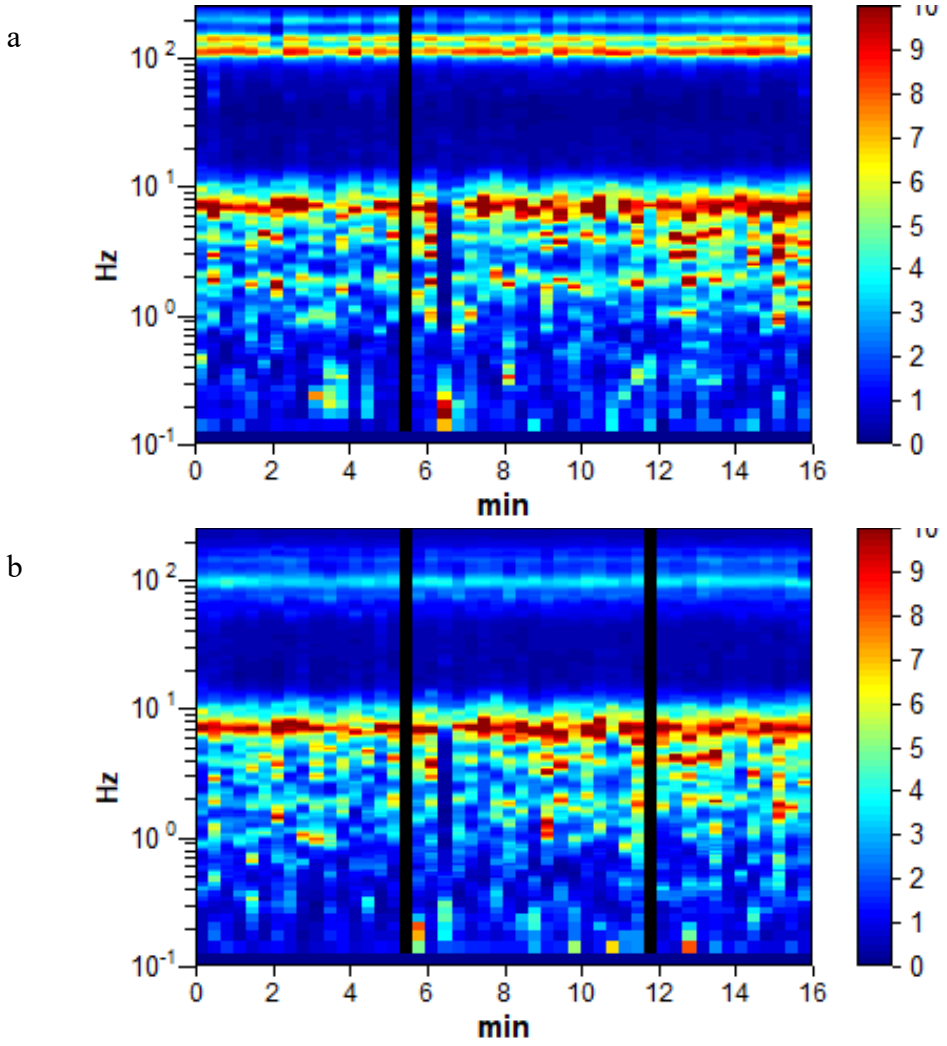

Figure D-59 MIZ Quad Site 1 site, Test 5, concrete (a), grass (b)

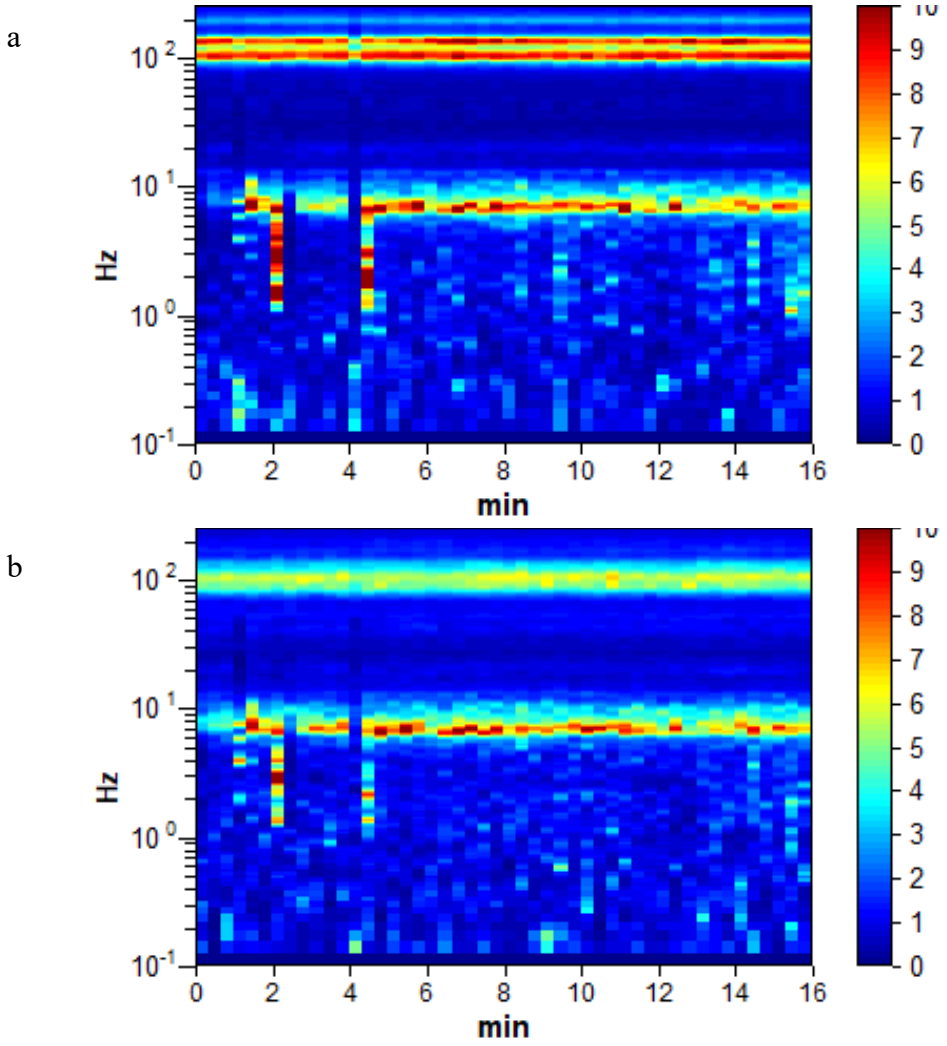

Figure D-60 MIZ Quad Site 1 site, Test 6, concrete (a), grass (b)

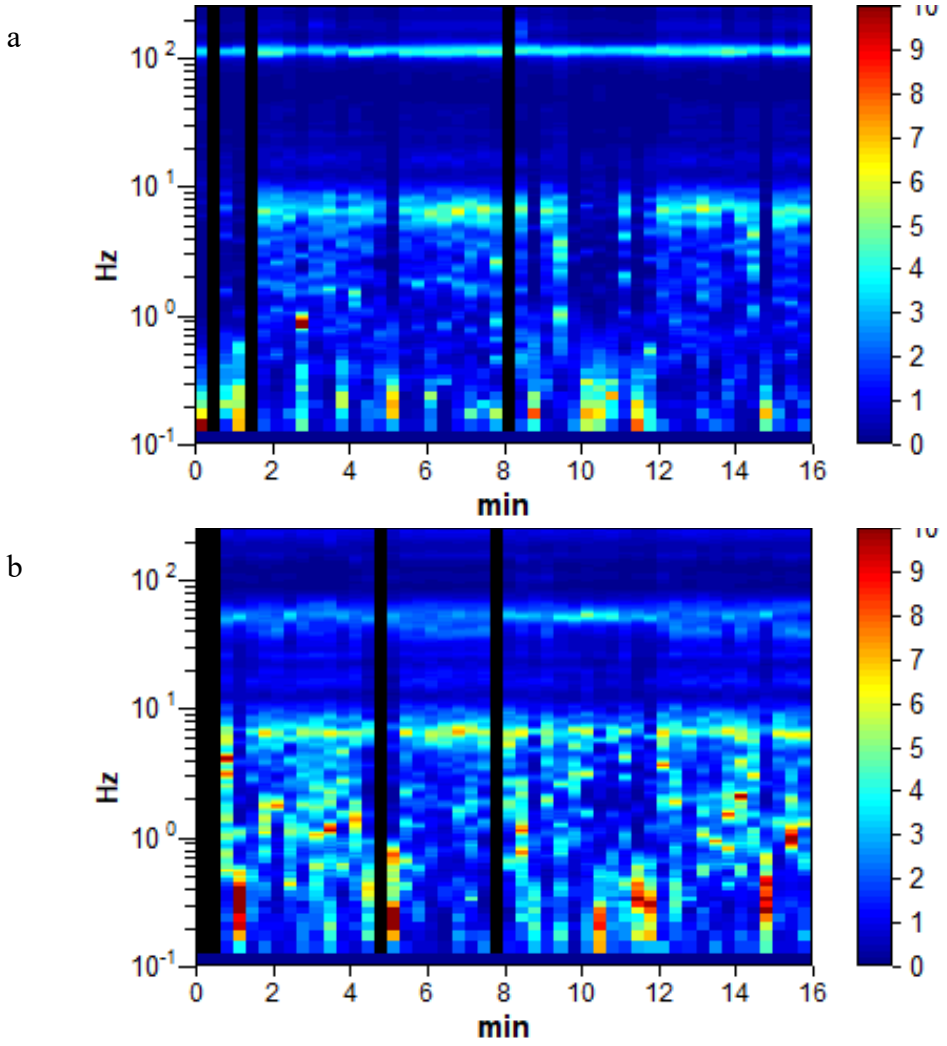

Figure D-61 MIZ Quad Site 2 site, Test 1, concrete (a), grass (b)

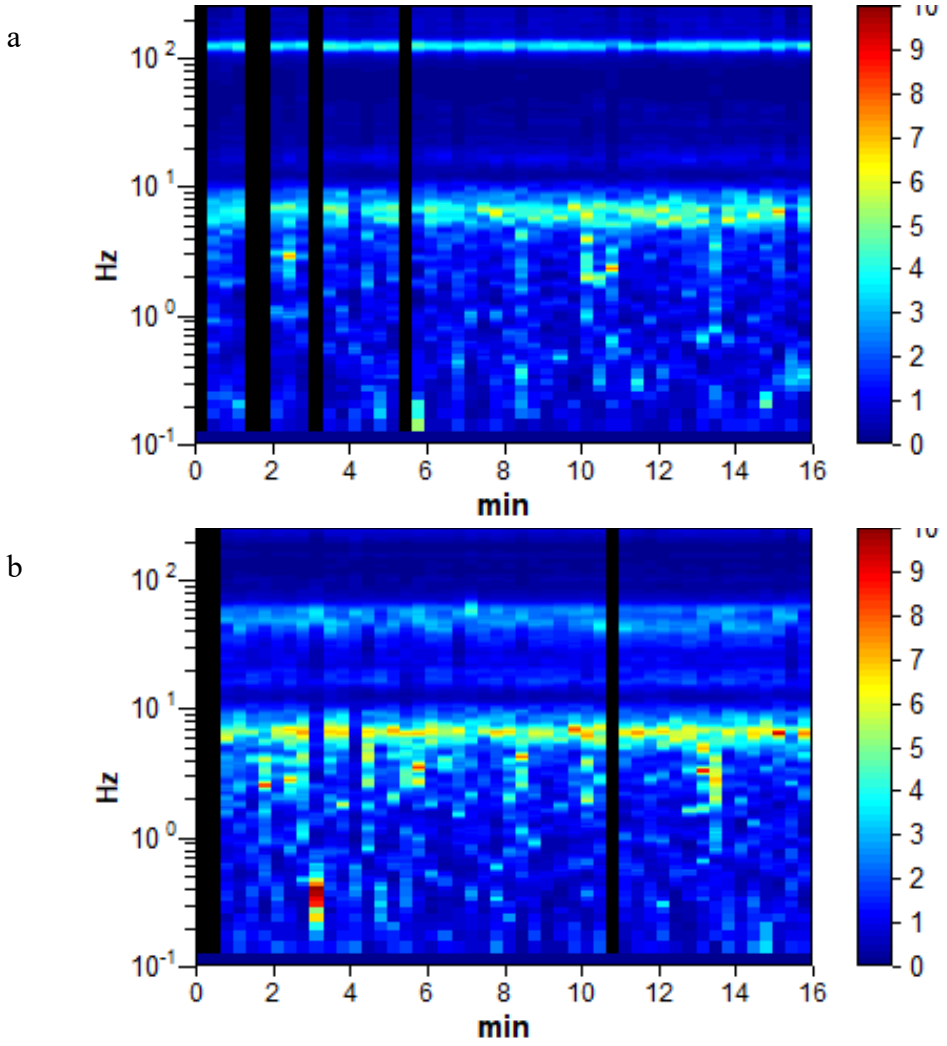

Figure D-62 MIZ Quad Site 2 site, Test 2, concrete (a), grass (b)

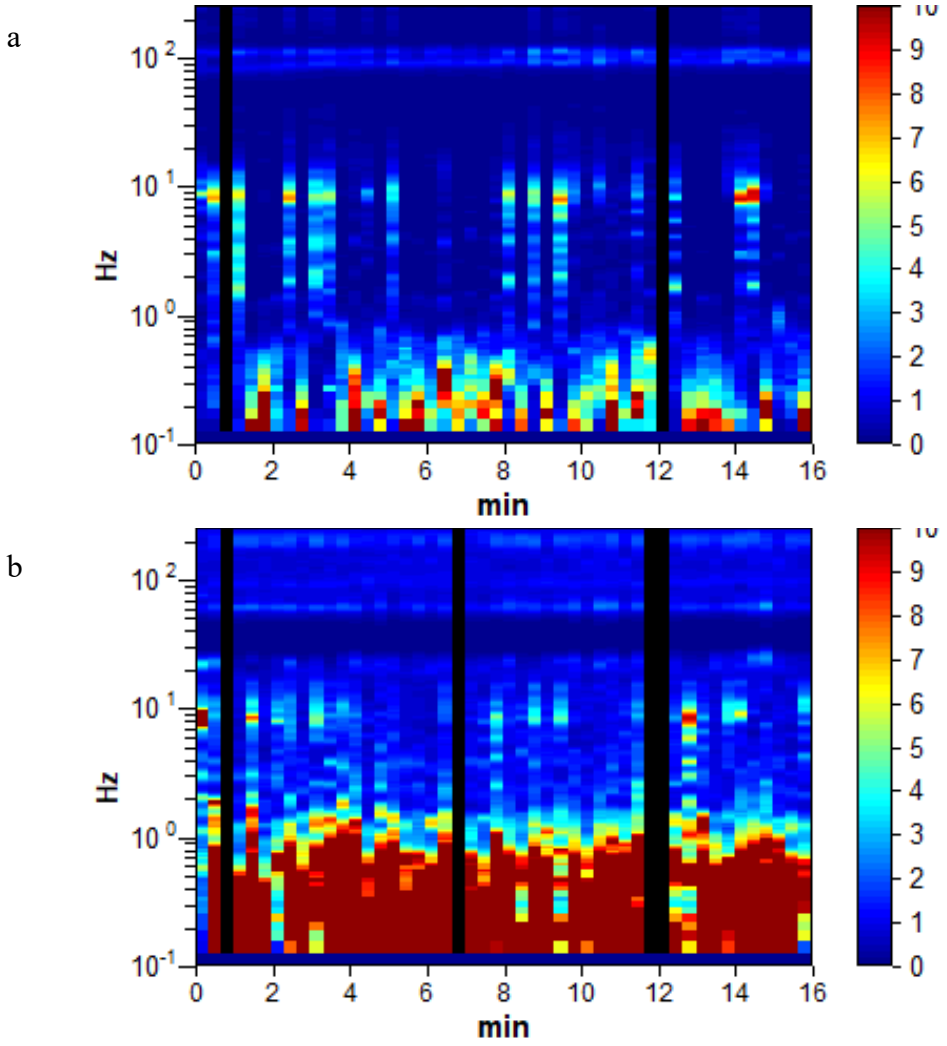

Figure D-63 MIZ Quad Site 3 site, Test 1, concrete (a), grass (b)

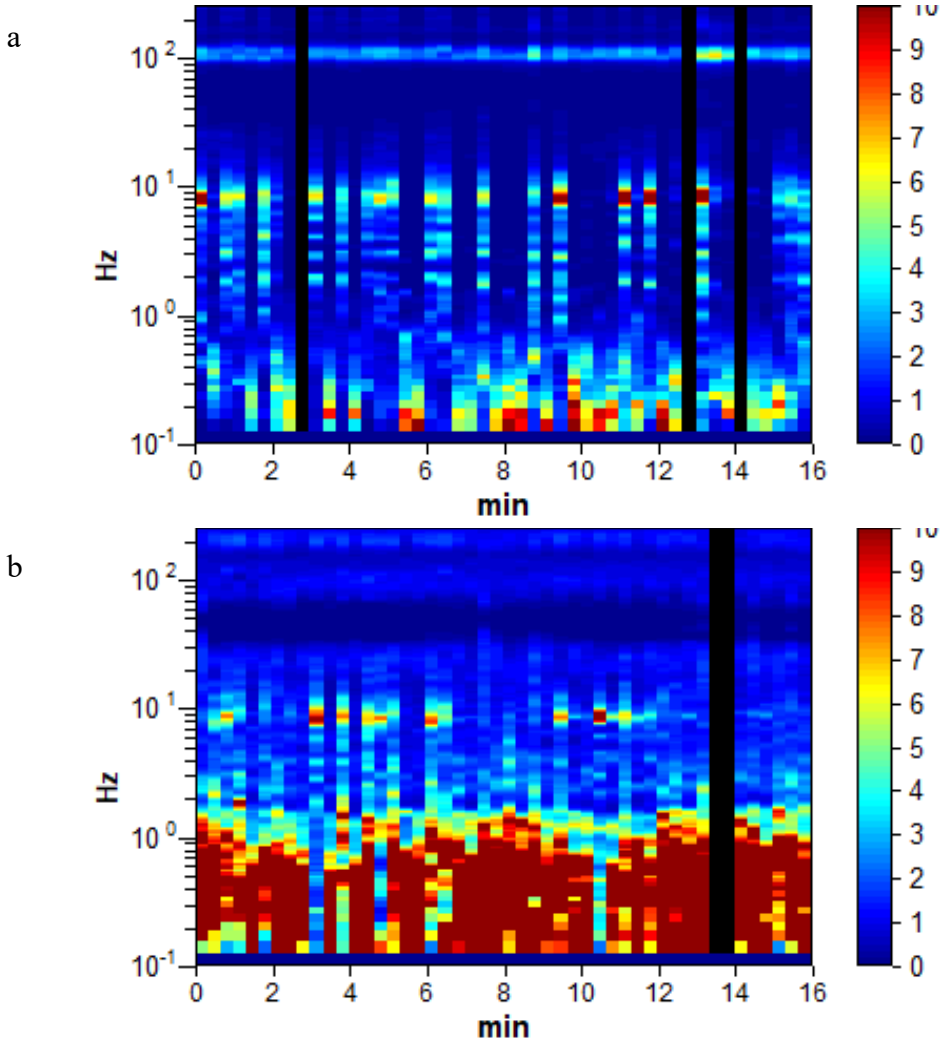

Figure D-64 MIZ Quad Site 3 site, Test 2, concrete (a), grass (b)

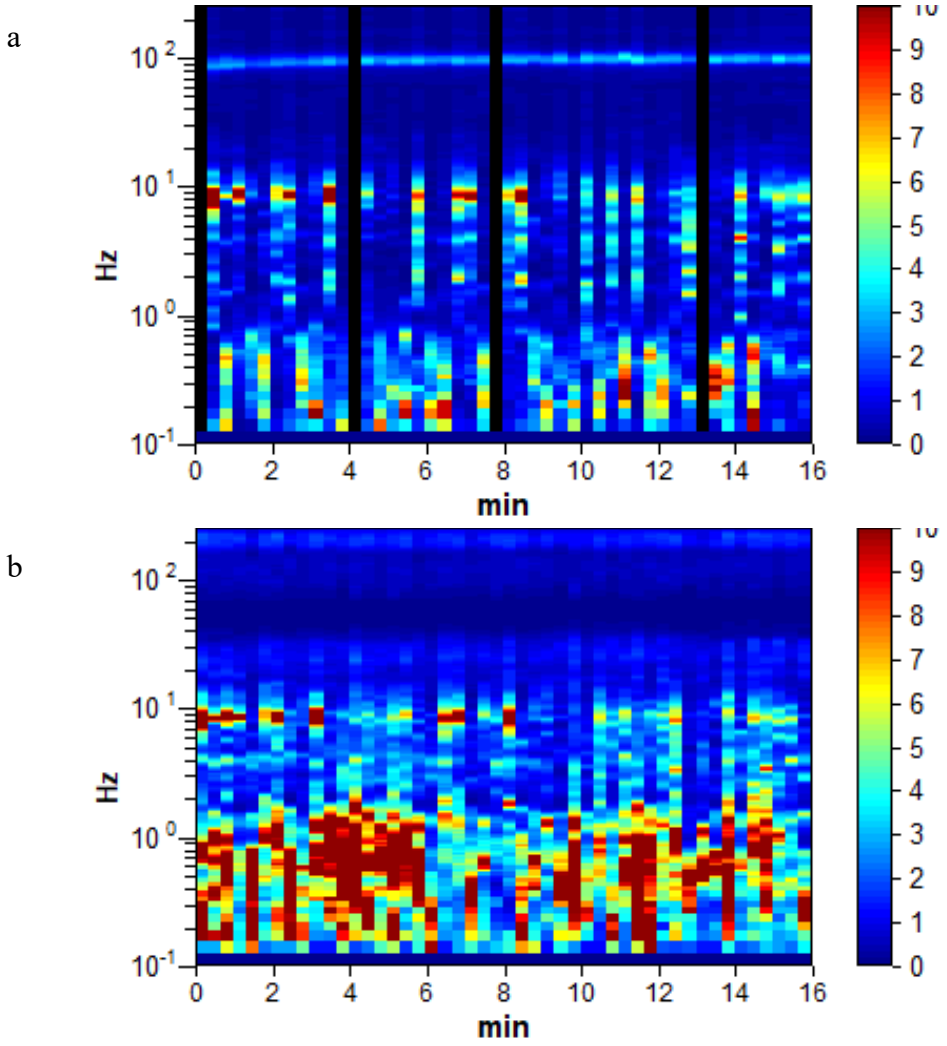

Figure D-65 MIZ Quad Site 3 site, Test 3, concrete (a), grass (b)

a

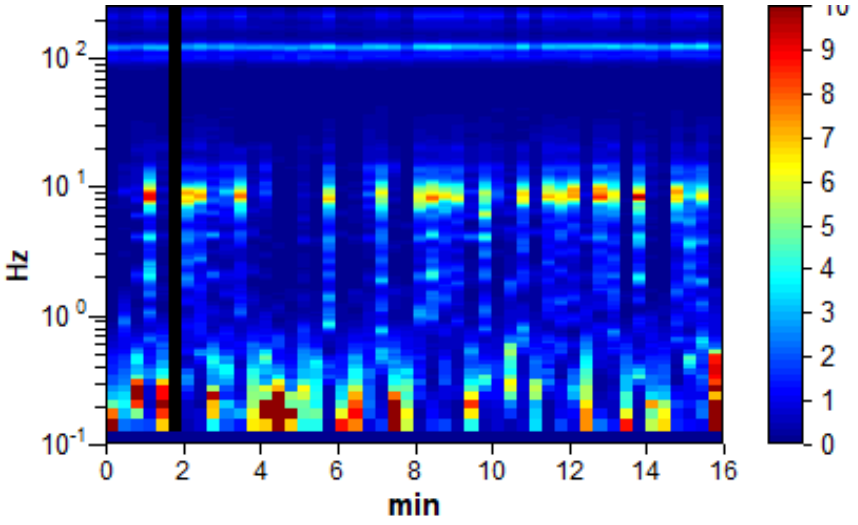

b

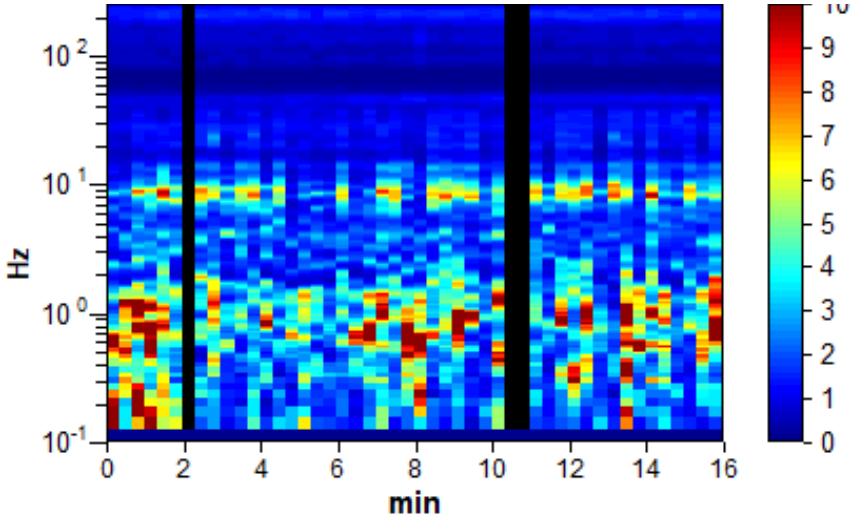

Figure D-66 MIZ Quad Site 3 site, Test 4, concrete (a), grass (b)

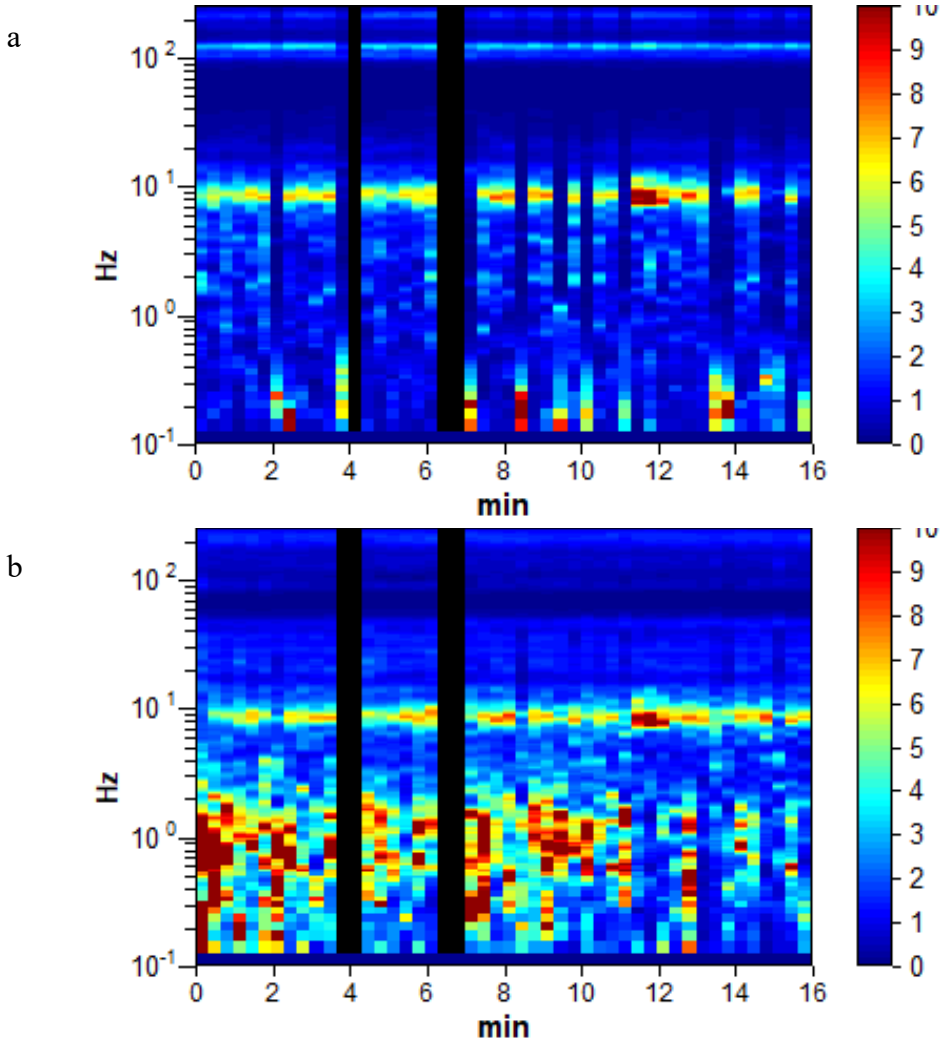

Figure D-67 MIZ Quad Site 3 site, Test 5, concrete (a), grass (b)

a

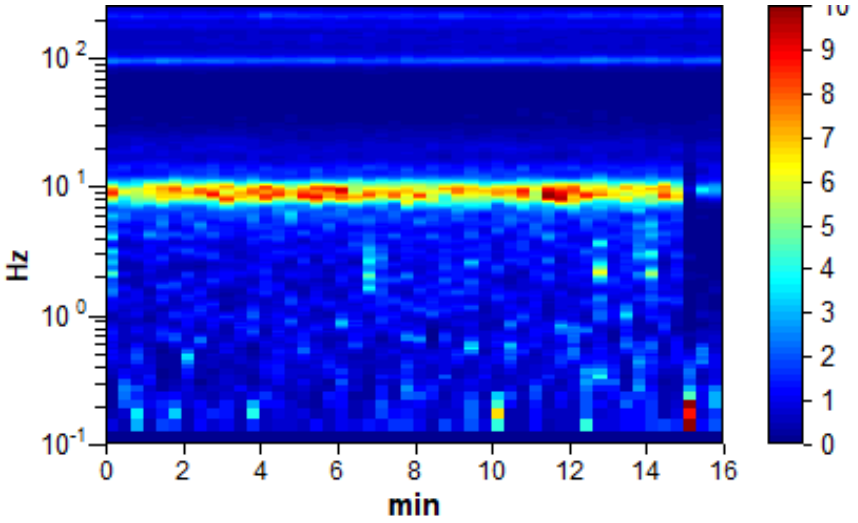

b

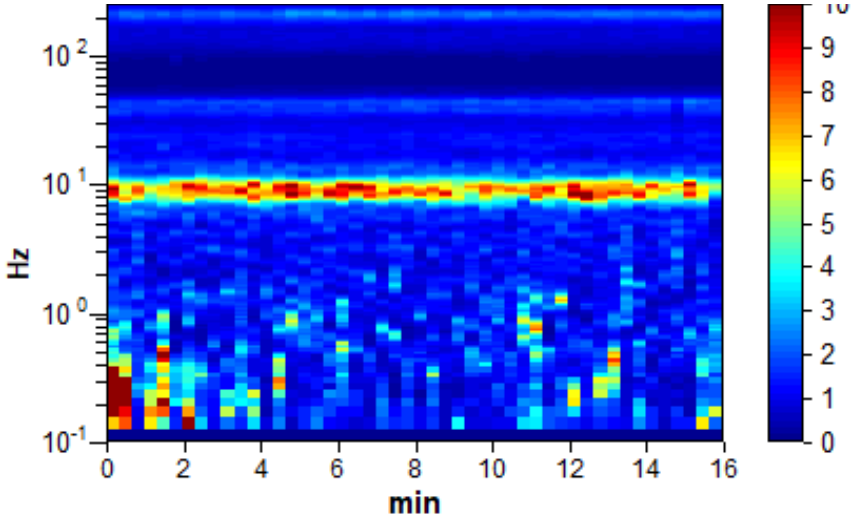

Figure D-68 MIZ Quad Site 3 site, Test 6, concrete (a), grass (b)

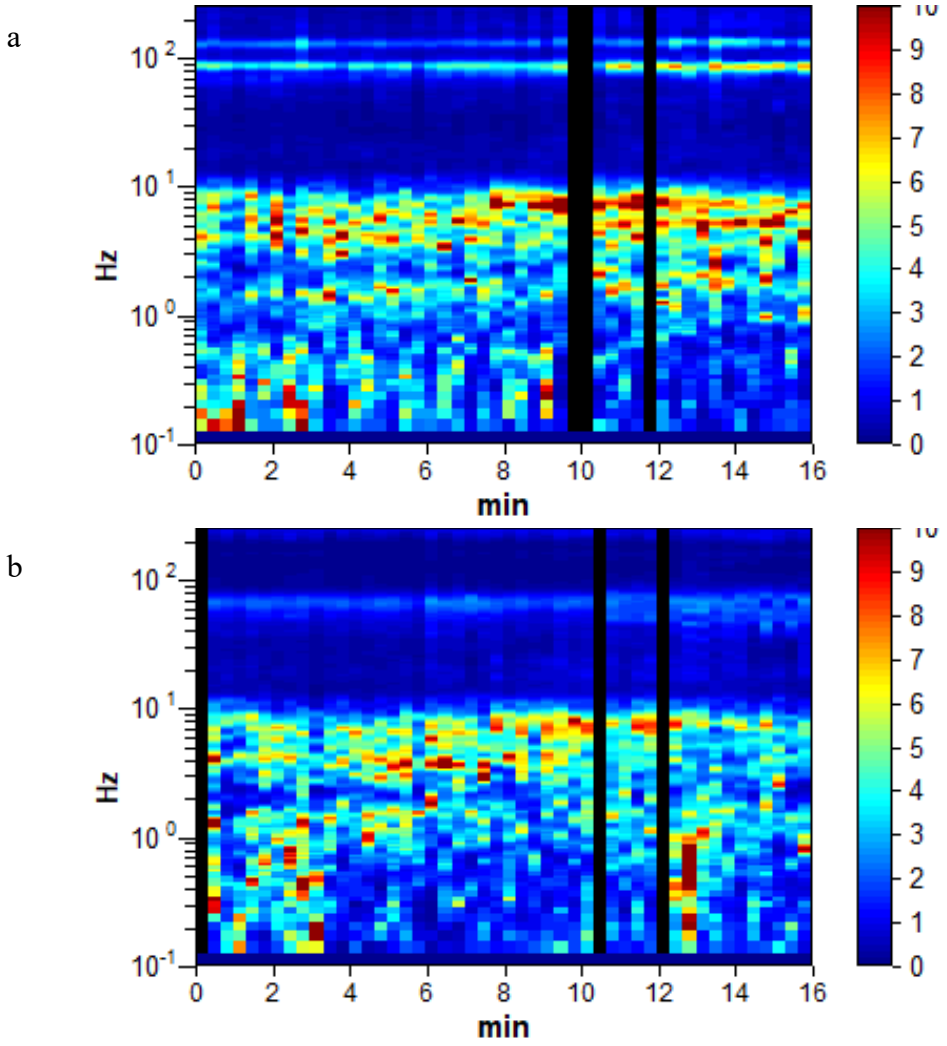

Figure D-69 MIZ Quad Site 4 site, Test 1, concrete (a), grass (b)

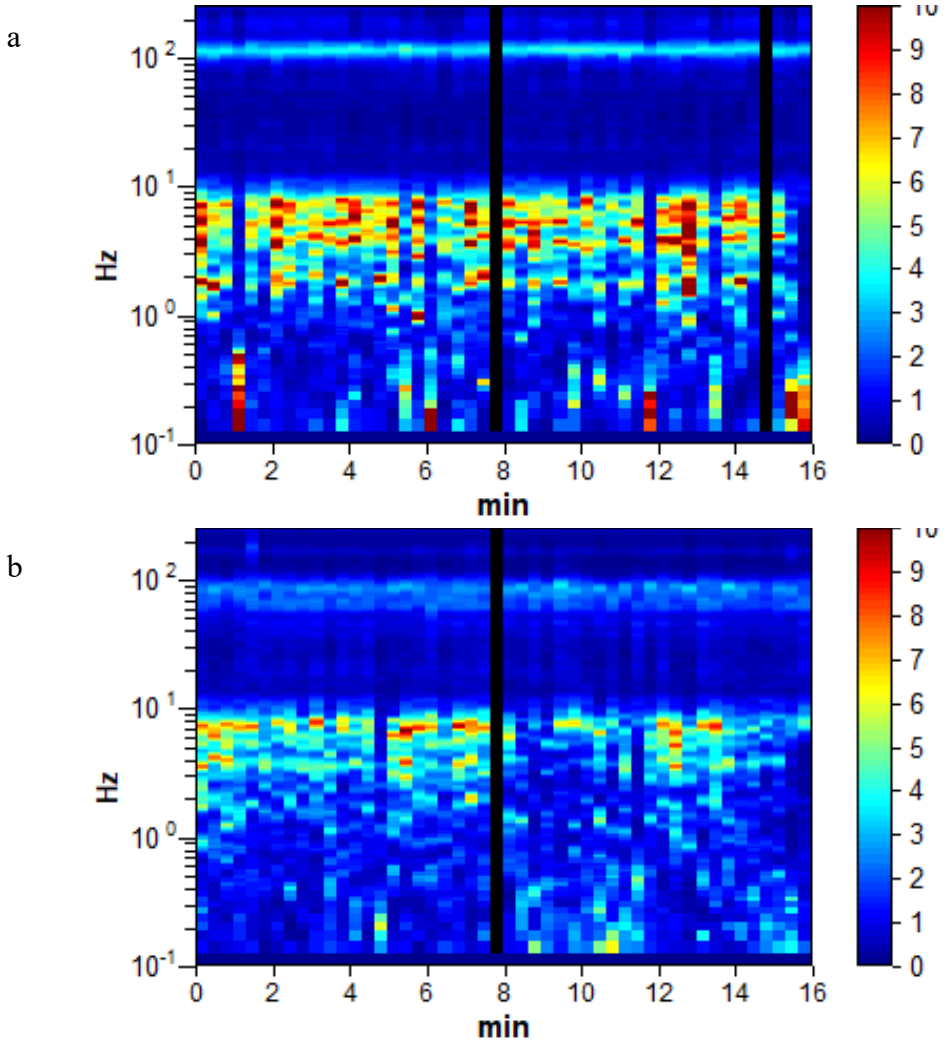

Figure D-70 MIZ Quad Site 4 site, Test 2, concrete (a), grass (b)

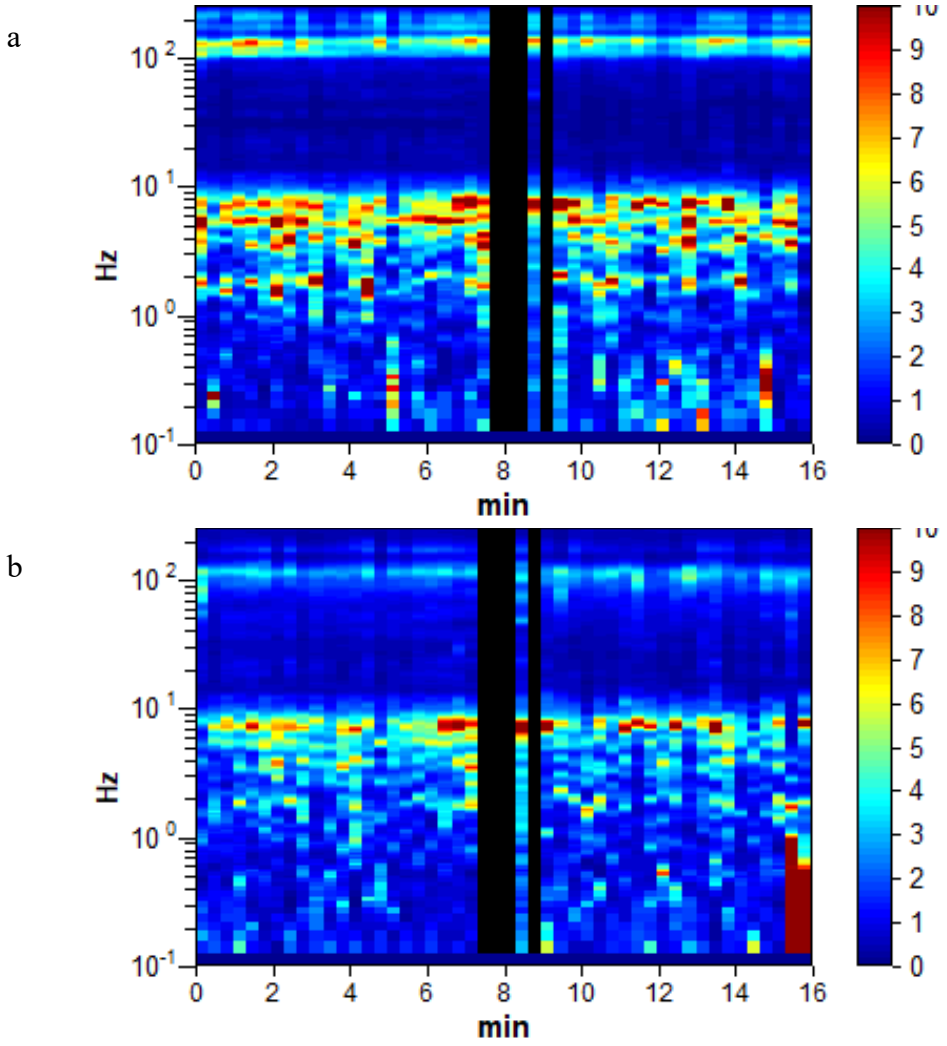

Figure D-71 MIZ Quad Site 4 site, Test 3, concrete (a), grass (b)

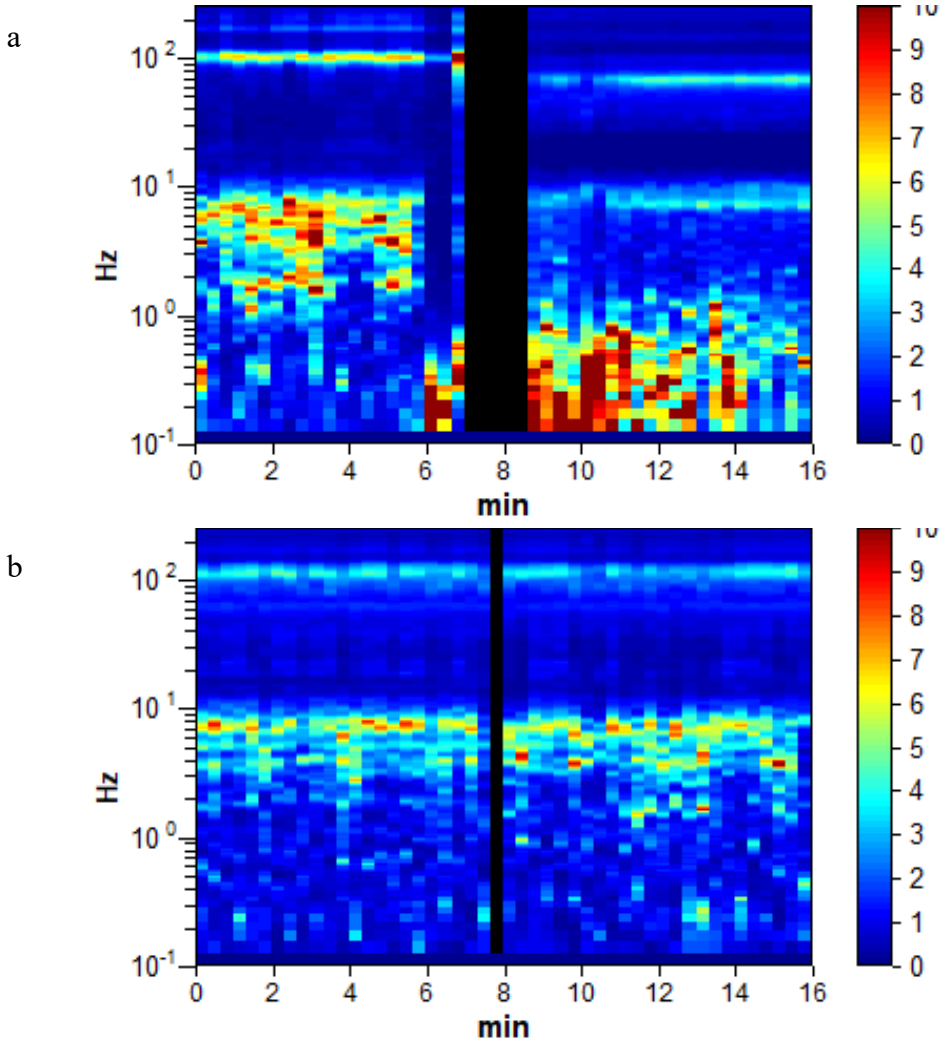

Figure D-72 MIZ Quad Site 4 site, Test 4, concrete (a), grass (b)

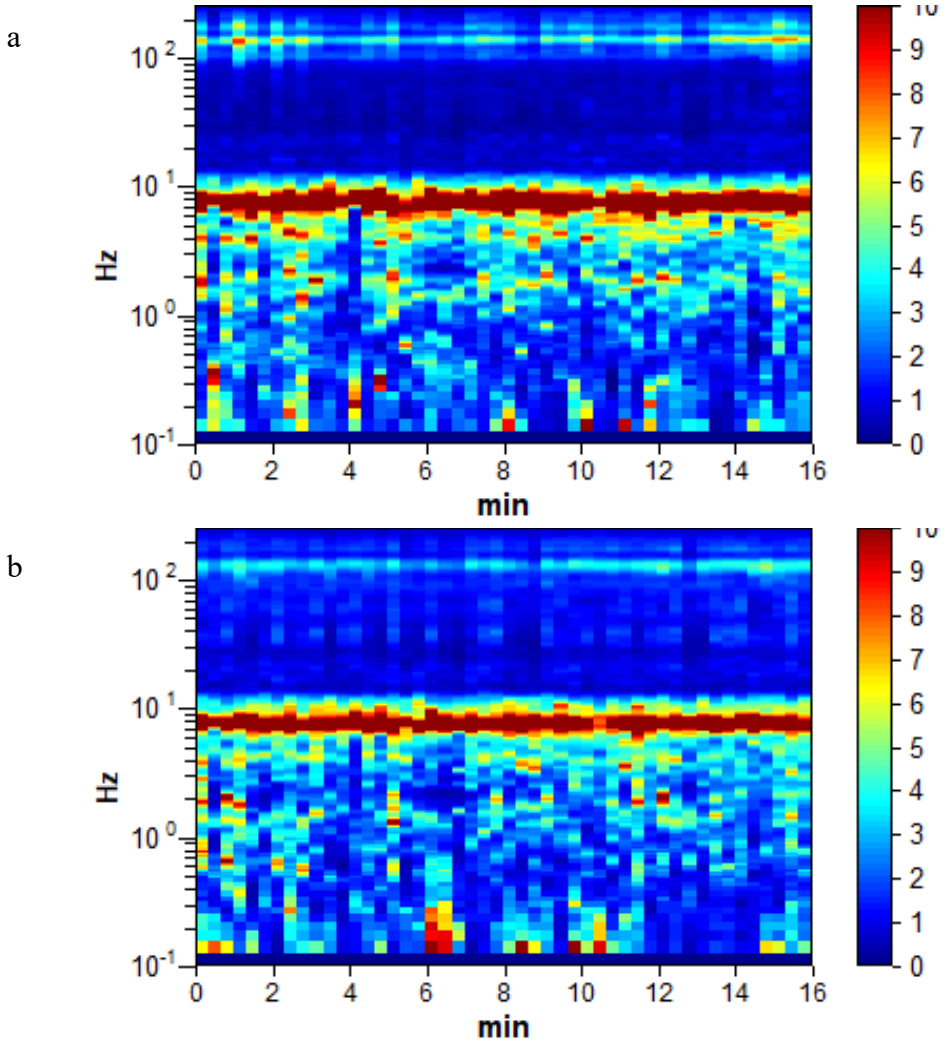

Figure D-73 MIZ Quad Site 4 site, Test 5, concrete (a), grass (b)

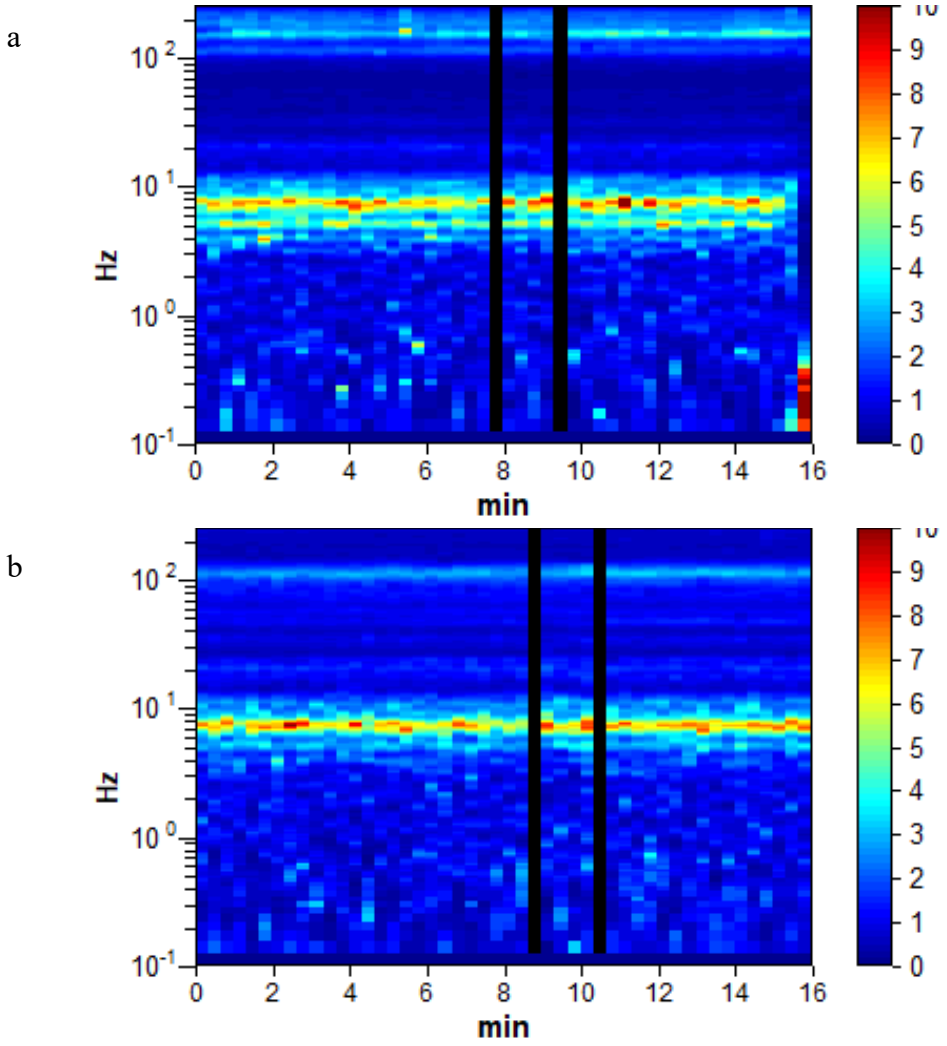

Figure D-74 MIZ Quad Site 4 site, Test 6, concrete (a), grass (b)

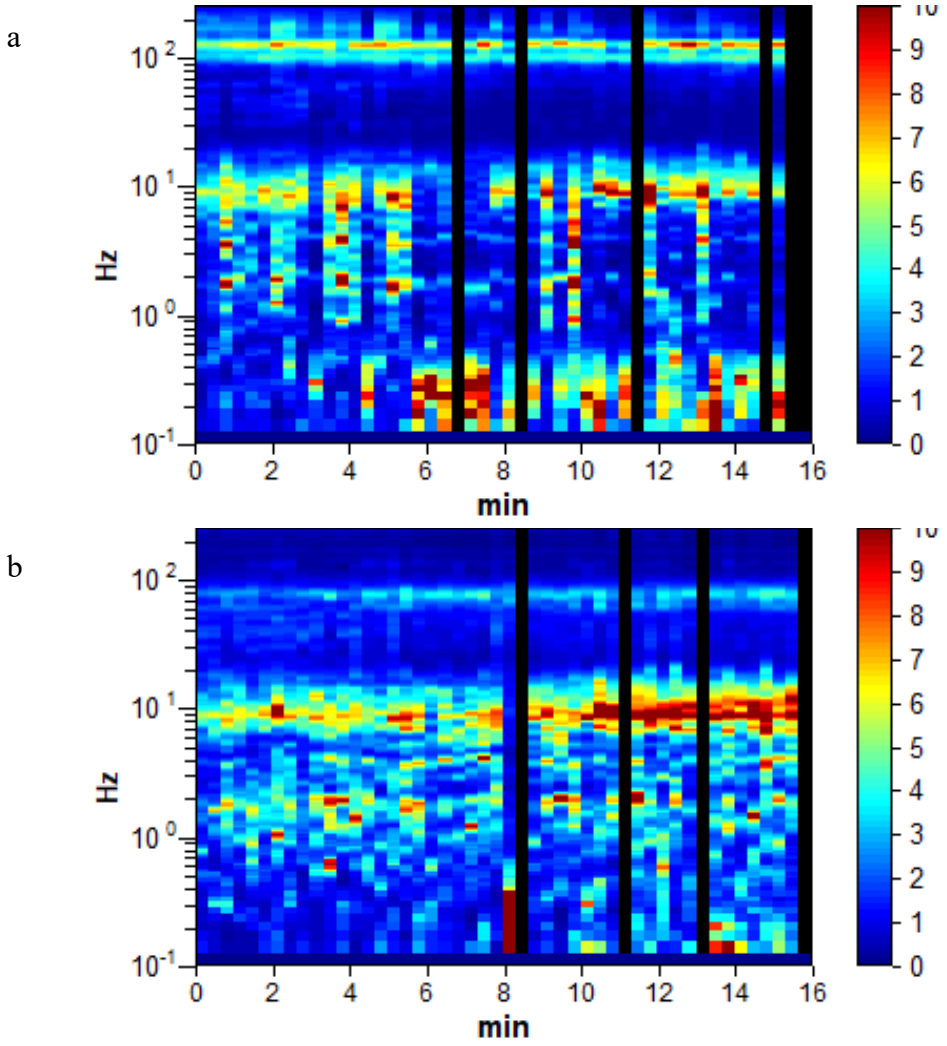

Figure D-75 MIZ Quad Site 5 site, Test 1, concrete (a), grass (b)

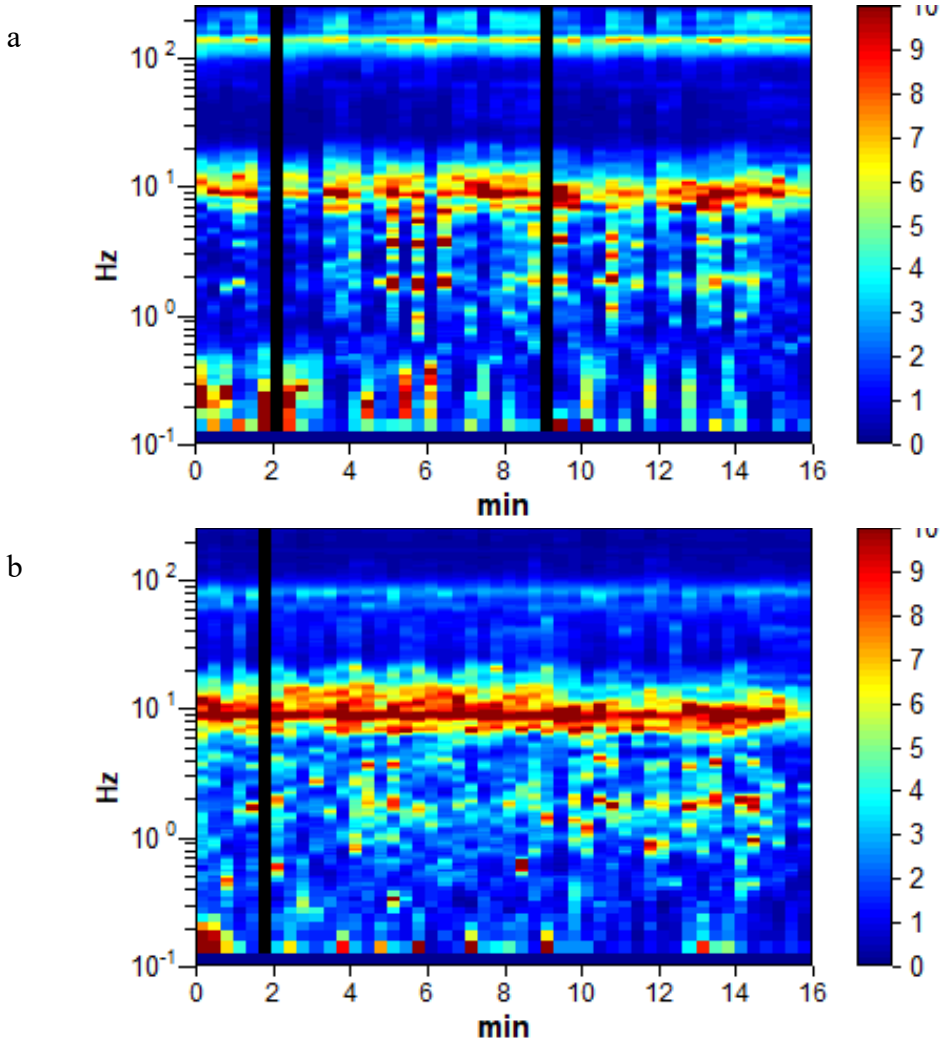

Figure D-76 MIZ Quad Site 5 site, Test 2, concrete (a), grass (b)

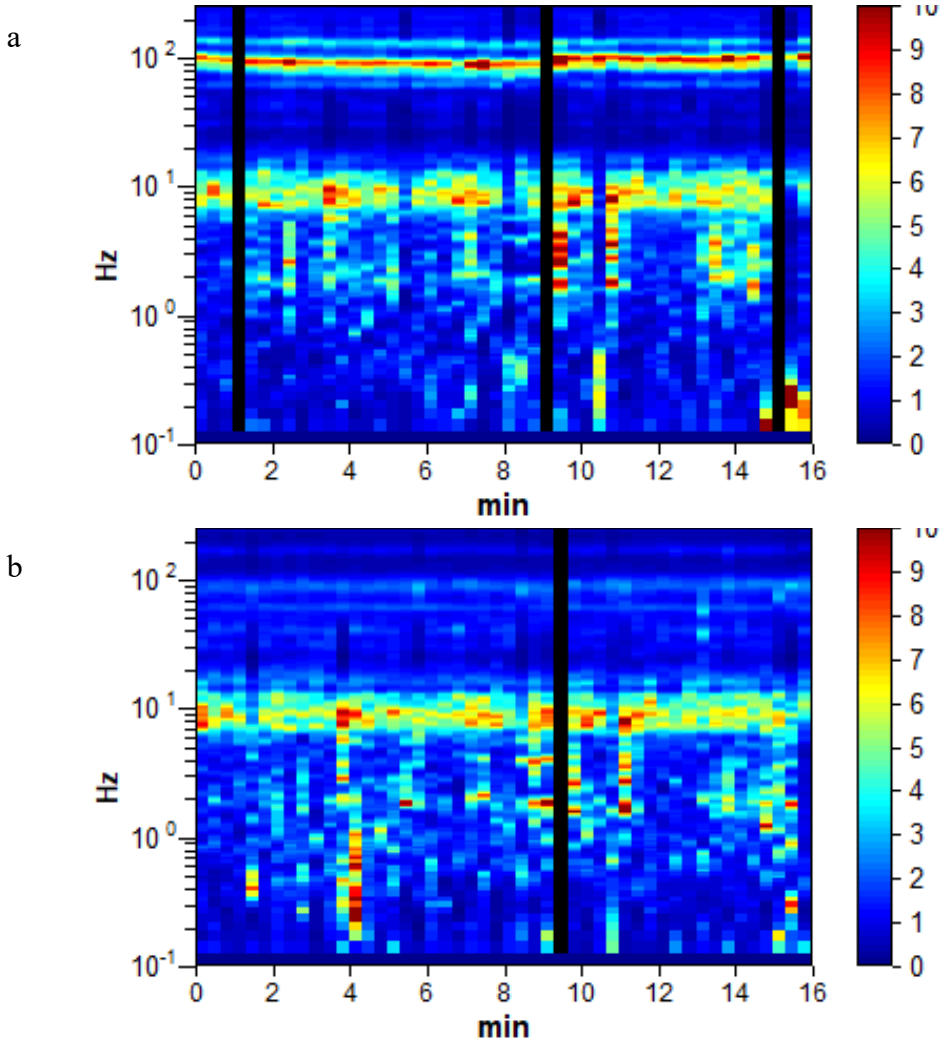

Figure D-77 MIZ Quad Site 5 site, Test 3, concrete (a), grass (b)

APPENDIX E

Figure E-1: Aerial Image of Animal Hospital 1 and 2 Location and Construction Locations

Figure E-2 a & b: Animal Hospital 1 Acquisition Images

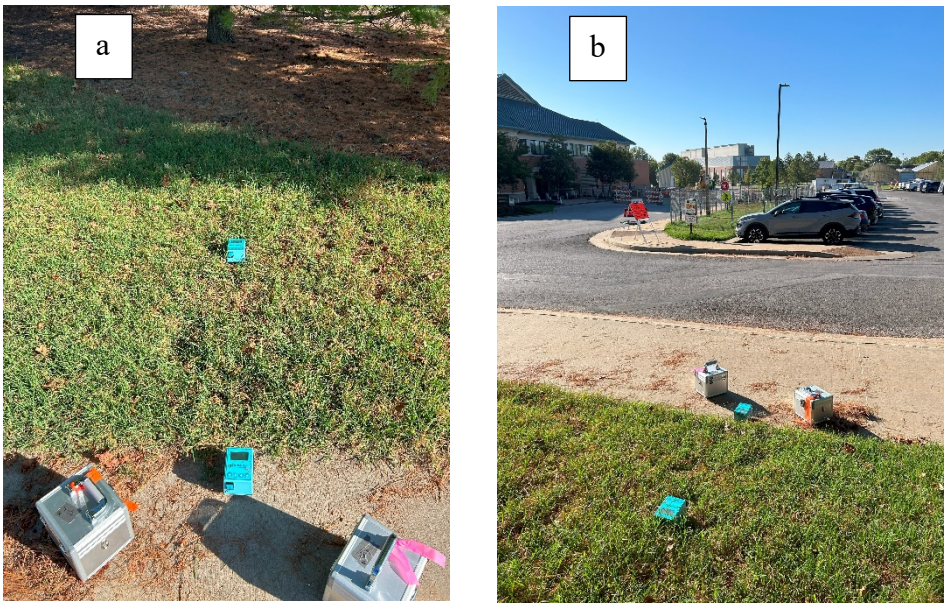

Figure E-3 a & b: Animal Hospital 2 Acquisition Images

Figure E-4: Aerial Image of Ellis Library BH-01, Ellis Library BH-03 A and Ellis Library BH-03 B Locations

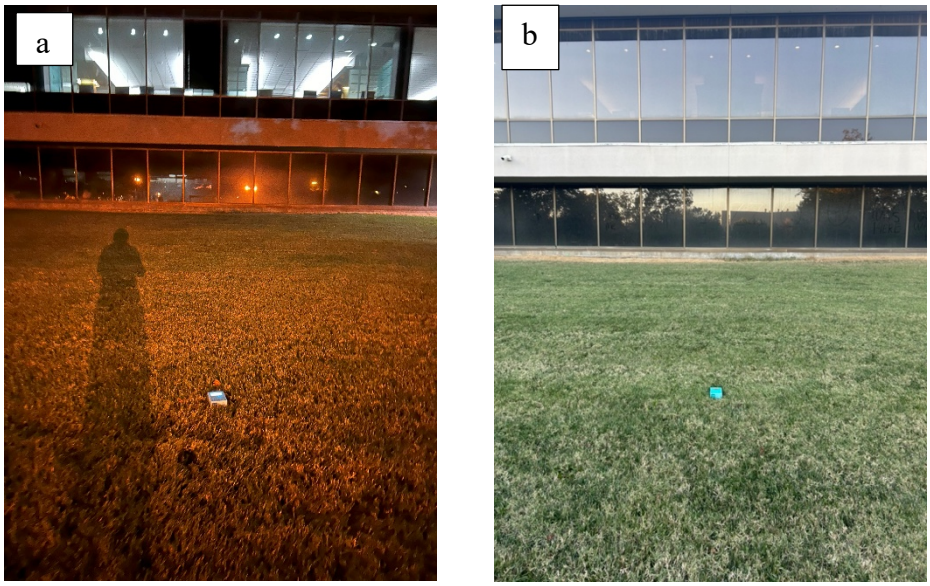

Figure E-5 a & b: Ellis Library BH-01 Acquisition Images

Figure E-6: (a) Ellis Library BH-03 A (b) Ellis Library BH-03 B Acquisition Images

Figure E-7: Aerial Image of Journalism B-06 A and Journalism B-06 B Locations

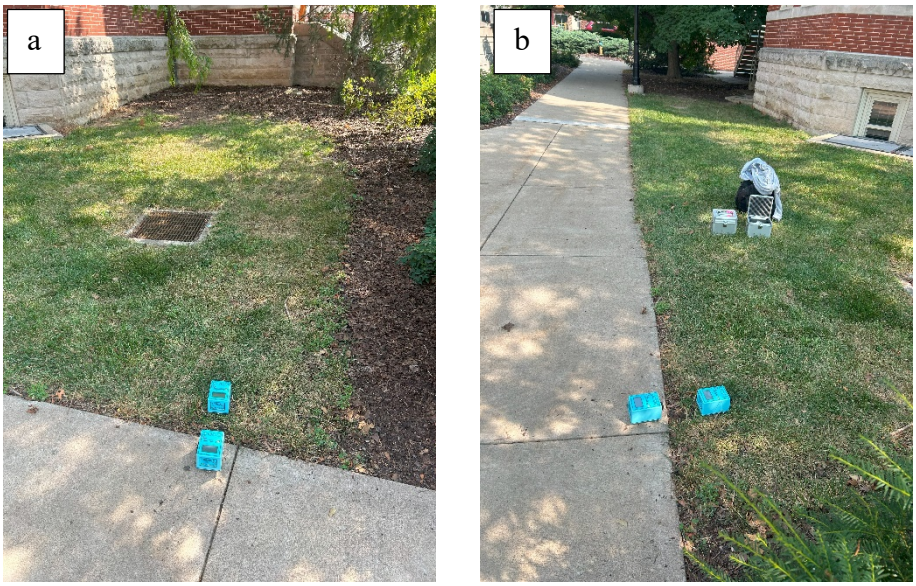

Figure E-8 a & b: Journalism B-06 A Acquisition Images

Figure E-9: Journalism B-06 B Acquisition Images

Figure E-10: Aerial Image of Lee's Hall BH-08, Lee's Hall. BH-18, and Lee's Hall Selected Locations

Figure E-11 a & b: Lee's Hall BH-08 Acquisition Images

Figure E-12 a & b: Lee's Hall BH-18 Acquisition Images

Figure E-13 a & b: Lee's Hall Selected Acquisition Images

Figure E-14: Aerial Image of MIZ Quad Site 1, MIZ Quad Site 2, MIZ Quad Site 3, MIZ Quad Site 4, MIZ Quad Site 5 Locations

Figure E-15:a & b: MIZ Quad Site 1 Acquisition Images

Figure E-16 a & b: MIZ Quad Site 2 Acquisition Images

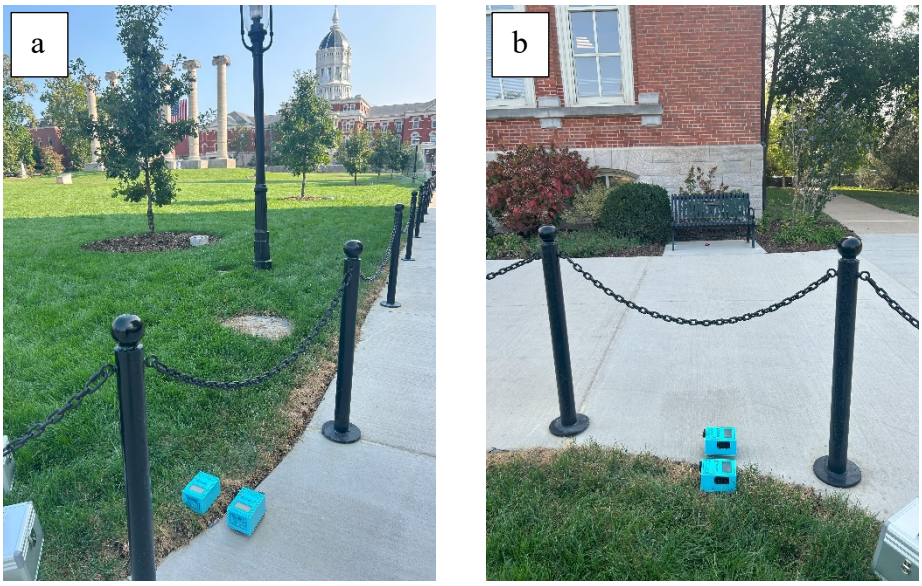

Figure E-17 a & b: MIZ Quad Site 3 Acquisition Images

Figure E-18 a & b: MIZ Quad Site 4 Acquisition Images

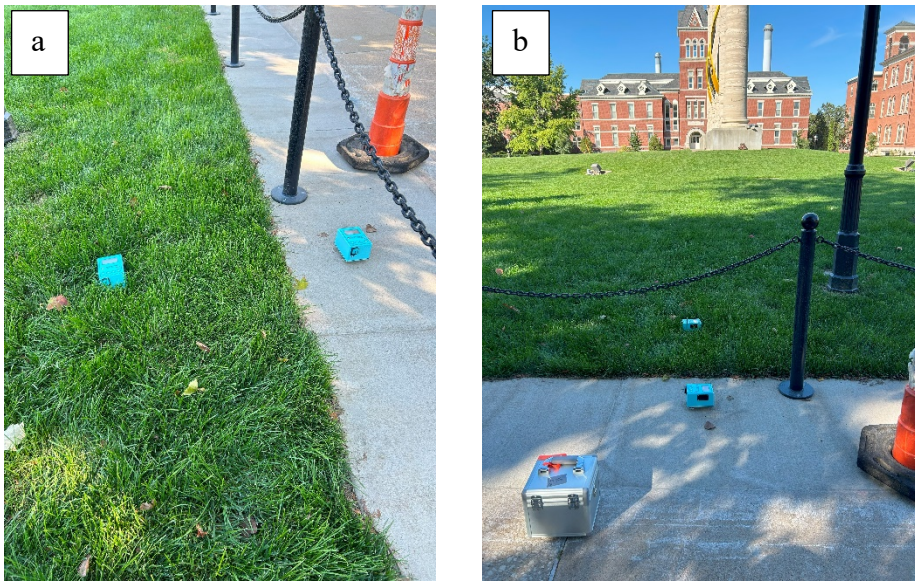

Figure E-19 a & b: MIZ Quad Site 5 Acquisition Images

Figure E-20: Aerial Location of MIZ MiddleQuad and Construction Location

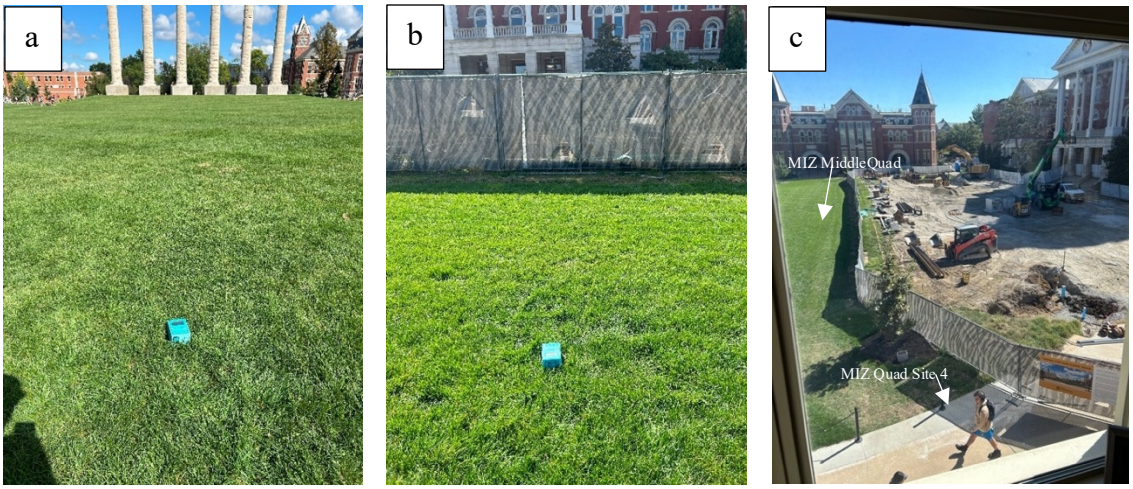

Figure E-21 a, b & c: MIZ MiddleQuad Acquisition Images

APPENDIX F

Table F-1: Site and Field Observations Notes

Research Observation Notes Heavy = almost constant of the time record or > 20 instances Moderate = content over a short duration of time record or > 3, < 20 instances Low = Very short duration of time record, < 3 instances	
MIZ Quad Site 1 (1) 09/09/24	Heavy foot traffic. 1 skateboarder. 3 bikes. 3 cars. 2 scooters. 72 F. Sunny. Little wind. 11:50 am.
MIZ Quad Site 2 (1) 09/09/24	Moderate foot traffic. 1 skateboarder. 80 F. Sunny. Little to no wind. 4:51 pm
MIZ Quad Site 3 (1) 09/09/24	Moderate foot traffic. Some walked close to instrument. 80 F. Sunny. Little wind. 4:28 pm
MIZ Quad Site 4 (1) 09/10/24	Moderate foot traffic. Construction noise. Watering grass. 81 F. Sunny. Little wind. 1:50 pm
MIZ Quad Site 1 (2) 09/09/24	Low foot traffic. 80 F. Sunny. Little to no wind. 5:19 pm
MIZ Quad Site 3 (2) 09/10/24	Low foot traffic. 83 F. Sunny. Light wind. 2:36 pm
Journalism B-06 A(1) 09/10/24	Low foot traffic. Sunny 84 F. Little to no wind. 3:19pm
Journalism B-06 A (2) 09/11/24	Low traffic. Talking near. 9:17 am. Sunny. 69 F. Little mind
MIZ Quad Site 3(3) 09/11/24	Moderate foot traffic. Sunny. 79 F. 11:01 am.
MIZ Quad Site 1 (3) 09/11/24	Low foot traffic. Sunny 79 F. Light wind. 11:22 am. 2 cars
Journalism B-06 A (3) 09/11/24	Moderate to heavy foot traffic. Sunny. 82 F. Little wind. 11:42
MIZ Quad Site 4 (2) 09/11/24	Low foot traffic. No construction. 80 F. No wind. 7:16 pm
MIZ Quad Site 2 (2) 09/11/24	Low foot traffic. 77 F. 7:46 pm
Journalism B-06 A (4) 09/11/24	Low foot traffic. Dog running 76 F. 8:08 pm
MIZ MiddleQuad (1) 09/30/24	Orange Tromino, 11:54 am construction noise. 2 people walk by at beginning. 76 F partition 17
MIZ MiddleQuad (2) 09/30/24	Orange Tromino, Partition 18 12:12 pm 77F people walking by at 36 secs. Big boom at 9 minutes 30 sec

MIZ MiddleQuad (3) 09/30/24	Orange Tromino, Partition 19 12:30 pm 78F most equipment shut off less noise. 2 trucks showed up at 3 minutes. More equipment turned on at 12 minutes
MIZ Quad Site 4 (3) 09/30/24	1:15 pm. Both Construction noise over the duration of record
MIZ Quad Site 4 (4) 09/30/42	7:15 pm. Both. No construction noise present moderate foot traffic throughout record
MIZ MiddleQuad(4) 09/30/24	7:36 partition 22 quiet no traffic. 75 F. 9 minute 5 seconds someone walks by
MIZ MiddleQuad (5) 09/30/24	7:53 partition 23. Quiet no traffic 74 F.
MIZ MiddleQuad (6) 09/30/24	8:09 Partition 24. Quiet. Person and dog at 4 minutes 5 secs
Ellis Library BH-03 A (1) 10/01/24	4:35 am. Partition 7. Orange grass. Pink. Concrete. 64 F quiet
Ellis Library BH-03 A (2) 10/01/24	4:59 am. Partition 25. 64F
Ellis Library BH-03 A (3) 10/01/24	Partition 26 orange 5:16 am. Cars become present at 4 minutes 5 seconds. 64F trash getting thrown out and door opening and closing around 12 minutes
Ellis Library BH-03 A (4) 10/01/24	Partition 27 orange partition 26 pink(think failed). 5:39 am. Some cars. Garage truck at 6 minutes 52 seconds. Loud noise and raving up at 9 minutes 9 sec until 9 minutes 33 sec. 9 min 51 sec boom. 10 minute 11 sec raving and boom until 10 min 32 sec. Leaving at 11 min 20 sec
Ellis Library BH-01 (1) 10/01/24	6:01 am partition 28 quiet
Ellis Library BH-01 (2) 10/01/24	6:22 am partition 29 quiet breeze
Ellis Library BH-01 (3) 10/01/24	6:40 am partition 30 quiet breeze
Ellis Library BH-01 (4)	7:00 am partition 31 quiet
MIZ Quad Site 4 (5) 10/01/24	9:45 am heavy foot traffic construction noise 62F
MIZ MiddleQuad (7) 10/01/24	10:10 am breeze. 62F 4 minutes big drop from something chock the ground partition 33
MIZ Quad Site 5 (1) 10/01/24	Partition 34 both. 10:31 am. 62 F. Construction noise present in distance. Person walk by at 3 minutes and 4 minutes dog right by it at 8 minutes
MIZ Quad Site 5 (2) 10/01/24	Partition 35 both. 10:58 am. Construction noise present in distance. Moderate Foot traffic. No foot traffic fro 7 minutes to 10 minutes

MIZ Quad Site 5 (3) 10/01/24	Partition 36 both. 5:32. No construction noise in distance. Person walked by 6 minute 22 sec and runners at 4 minute 70F 8 minutes. 9 minutes 2 seconds to 20 sec 9 min 52 sec
Animal Hospital 1 (1) 10/02/24	Partition 37 both. 8:37 am. 48 F constitution noise. Cutting. Generators throughout time
Animal Hospital 1 (2) 10/02/24	Partition 38 both. 8:54 am 48 F. Construction noise. Generators throughout time
Animal Hospital 2 (1) 10/02/24	Partition 39 both. 9:19 am 3 car and 1 minute to 3 minutes. Heavy car traffic
Animal Hospital 2 (2) 10/02/24	Partition 40 both. 9:38 am heavy truck at 3 minutes 35 sec. Heavy car traffic
Lee's Hall Selected (1) 10/02/24	Partition 41 orange grass 10:20 am building occupied
Lee's Hall Selected (2) 10/02/24	Partition 41 pink partition. 10:39 am
Lee's Hall BH-08(1) 10/02/24	Partition 42 both. 5:19 pm 73 F. Traffic south and west on position
Lee's Hall BH-08 (2) 10/02/24	Partition 43 both. 5:37 pm. Traffic to the west and south
Lee's Hall BH-18 (1) 10/02/24	Partition 44 both. 5:59 pm. Traffic west and south
Lee's Hall BH-18 (2) 10/02/24	Partition 45 both. 6:17 pm traffic west and south
Lee's Hall BH-18 (3) 10/02/24	Partition 46 both 6:34 pm
Animal Hospital 2 (3) 10/02/24	Partition 48 both7:47 pm. 63 F. No construction noise less car traffic 13 minutes foot traffic
Animal Hospital 1 (3) 10/02/24	Partition 50 both. 9:00 pm 5 minutes heavy equipment started running. Generators at 7 minutes
Journalism B-06 A (5) 10/17/24	Partition 19 both. Orange grass. Pink concrete. 6:11 am. 35 F. Springers running on quad
Journalism B-06 A (6) 10/17/24	Partition 20 both. 6:35 am. 35 F quiet
Ellis Library BH-03 A (5) 10/17/24	Partition 21 both. 5:02 pm 67 F car traffic and foot traffic
Ellis Library BH-03 A (6) 10/17/24	Partition 22 both 5:32 pm 67 F car and foot traffic
Ellis Library BH-03 B (1) 10/17/24	Partition 23 orange 5:44 pm 65 F car and foot traffic

Ellis Library BH-01 (5) 10/17/24	Partition 23 pink 5:58 pm. 65 F foot traffic light 12 paces from building. 13 paces from stump
Ellis Library BH-03 B (2) 10/17/24	Partition 24 orange 6:01 pm. Car and foot traffic 65 F
Ellis Library BH-01 (6) 10/17/24	Partition 24 pink. 6:34 pm. Foot traffic 64 F
Ellis library BH-03 B (3) 10/17/24	Partition 25 orange 6:17 pm. 65 F
Lee's Hall BH-08 (3) 10/18/24	Partition 26 both. 6:20 am 41 F car traffic in first 2 minutes. Car at 12 min 50 sec. Bike at 15 minute 28 sec
Lee's Hall BH-08 (4) 10/18/24	Partition 27 both 6:37 am car traffic in throughout collection. Close car at 12 min 25 sec
Lee's Hall BH-18 (4) 10/18/24	Partition 28 pink. 6:59 am. 41 F. Large E-W noise at 1-2 min
Lee's Hall Selected (3) 10/18/24	Partition 28 orange 7:00 am. 41 F unoccupied
Lee's Hall BH-18 (5) 10/18/24	Partition 29 pink. 7:17 am 41 F. Truck at 6 min. Failed. Women picked up devices
Lee's Hall Selected (4) 10/18/24	Partition 29 orange 7:35 am 41 F unoccupied
Lee's Hall BH-18 (6) 10/18/24	Partition 30 pink. 7:35 am 41 F
Lee's Hall BH-18 (7) 10/18/24	Partition 31 pink 7:51 am 41 F
Lee's Hall Selected (5) 10/18/24	Partition 30 orange 7:54 am 41 F. Occupied
Lee's Hall BH-18 (8) 10/18/24	Partition 32 pink 8:09 am 42 F
MIZ Quad Site 3 (4) 10/21/24	Partition 33 both 7:48 am 49 F foot traffic first 2 minutes
MIZ Quad Site 3 (5) 10/21/24	Partition 34 both 8:05 am 49 am. 2 min 27 sec person walking by. Bike and person with wheel barrel at 4 min 25 sec. Vehicle at 6 min 50 sec.
MIZ Quad Site 1 (4) 10/21/24	Partition 35 both. 8:25 am 50 F
MIZ Quad Site 1 (5) 10/21/24	Partition 36 both. 8:35 am 50 F. foot traffic
Animal Hospital 1 (4) 10/23/24	Partition 37 both 4:09 am. 54F. Quiet
MIZ Quad Site 3 (6) 10/23/24	Partition 38 both 4:39 am. 55 F. Quad sprinklers going off on the other side of quad
MIZ Quad Site 1 (6) 10/23/24	Partition 39 both. 5:01 am 54 F quad sprinklers at a distance
MIZ Quad Site 4 (6) 10/23/24	Partition 40 both. 6:02 am 54 F. At 6 min 57 sec large noise far away. Sounded like interstate. Runner at 9 minute 9 sec. Equipment star up at 10 min 35 sec

Journalism B-06 B (1) approximately 27 feet 10/23/24	Partition 41 both. 6:36 am 53 F. Sprinklers on quad. Truck on road at 2 minutes. Pedestrian wants on quad sidewalk at 6 minutes. Sprinklers stop at 8 minutes. Bike at
Journalism B-06 B (2) approximately 27 feet 10/23/24	Partition 42 both. 6:53 am. 53 F. Garage truck on road at 5 min 30 sec. Collecting garbage at 10 min 16 sec